



THE UNIVERSITY *of* EDINBURGH

This thesis has been submitted in fulfilment of the requirements for a postgraduate degree (e.g. PhD, MPhil, DClinPsychol) at the University of Edinburgh. Please note the following terms and conditions of use:

This work is protected by copyright and other intellectual property rights, which are retained by the thesis author, unless otherwise stated.

A copy can be downloaded for personal non-commercial research or study, without prior permission or charge.

This thesis cannot be reproduced or quoted extensively from without first obtaining permission in writing from the author.

The content must not be changed in any way or sold commercially in any format or medium without the formal permission of the author.

When referring to this work, full bibliographic details including the author, title, awarding institution and date of the thesis must be given.

**Controls on and the effect of Extensional Fault
Evolution in a Transected Rift setting, Northern North
Sea**



Ryan M. Williams

School of Geoscience

2012

Declaration

The results of this thesis have not been submitted for the examination of any other degree or qualification. The observations and conclusions presented in this volume are the results of my own studies except where cited or acknowledged otherwise.

Ryan M. Williams

Edinburgh 2012

Abstract

The East Shetland Basin is a superb natural laboratory in which to study the role that normal fault growth and linkage has in determining petroleum prospectivity. Use of several high density 3D seismic volumes and over 250 boreholes permits key aspects of the Late Jurassic rift and its Permo-Triassic precursor to be analysed and its role on hydrocarbon trap formation, reservoir distribution and migration determined. The regional interpretation has revealed the generation of a North Sea archipelago of Upper Jurassic islands, the role of relay ramps in controlling syn-rift sediment dispersal patterns and the impact of normal faults of the later episode crossing and offsetting those generated by the earlier phase. The uplift, erosion and meteoric flushing of Upper Jurassic and older strata within the exposed fault blocks could potentially have huge consequences for the Brent play by enhancing reservoir properties and hence, help identify new play opportunities down-dip of major structures. Fault control on sediment dispersal can also be documented in a more localized study on the Cladhan Field, the site of a pronounced basin-margin relay ramp. This recent discovered set of syn-rift density flows illustrates how the development and distribution of depositional gradients and transport pathways form subtle play types. The Cladhan area is just one of several locations throughout the East Shetland Basin where the interaction of multiple rift phases is influential in the structural feedback after the Upper Jurassic rifting event. The delicate interaction and reactivation of underlying structural trends creates a series of multi-tiered fault block systems which can define several aspects of a petroleum system, depending upon the strike, polarity and level of reactivation of faults from one rift to another. The observations of fault growth and linkage in the Northern North Sea may provide generic lessons that help in determining petroleum prospectivity in other hydrocarbon rift basins (e.g. E. Africa and the N. Atlantic seaboard of North America)

Acknowledgements

This project was created in partnership with John Underhill and the primary sponsors Valiant Petroleum and EnQuest. John has been an unending well of help and advice throughout the project and his contribution of ideas and endurance have been extremely helpful over the past four years. To him I am forever indebted.

The support I have received from both sponsors has been enormously valuable. I would like to thank Valiant Petroleum for their generous financial and logistic support of the project and for the release of the bulk of the 3D seismic data volumes. In particular, I acknowledge Justin Morrison, Richard Morgan, Ruth Hamilton and Tim Chapman, all of whom have helped make the project possible. The late Rupert Hoare and his company, Schlumberger WesternGeco is thanked for providing access to the additional 3-D seismic volume strategically located over the Cladhan-Pobie area. The seismic interpretation was carried out using SMT's Kingdom software on workstations housed in The University of Edinburgh's seismic interpretation laboratory. Supporting well data was kindly made available through the Common Data Access (CDA) portal, permission for the use of which was granted by Malcolm Fleming. The School of Geosciences' Computer Officers, Chris Place and Magnus Hagdorn are acknowledged for their support of the seismic facility during the course of the study.

Undertaking this project in the seismic laboratory of the Grant Institute has only been as good as the people within it. The support and advice from all the students who have worked in this room during my time here has made my working life even more enjoyable. Special thanks go to Rachel Jamieson, Kirsten Hunter, Suzannah Toulmin and Gustavo Guariguata whose

assistance and constant supply of support, suggestions and Haribo have helped me retain some sanity throughout the project.

The submission of this thesis will no doubt be a great relief to all my family especially my mother and father Denise and Michael Williams, who now no longer have to put up with my endless talk about work. Their never-ending belief and encouragement has guided me through my entire university life and for this I am forever grateful. Finally immeasurable thanks go to Suzanne Aitken for putting up with my constant supply of Geology related problems and the occasional sport related injury, without you by my side I would probably still be writing the introduction.

Table of Contents

Volume 1

CONTROLS ON AND THE EFFECT OF EXTENSIONAL FAULT EVOLUTION IN A TRANSECTED RIFT SETTING, NORTHERN NORTH SEA.....	I
DECLARATION.....	II
ABSTRACT	III
ACKNOWLEDGEMENTS	IV
LIST OF FIGURES.....	X
CHAPTER 1 INTRODUCTION	1
1.1 RATIONALE.....	1
1.2 AIMS OF THIS THESIS	2
1.3 STRUCTURE OF THESIS.....	3
CHAPTER 2 STRUCTURE AND DEVELOPMENT OF A RIFT PROVINCE.....	5
2.1 DEVELOPMENT AND EVOLUTION OF EXTENSIONAL SYSTEMS.....	5
2.1.1 <i>Wilson Cycle</i>	5
2.1.2 <i>Crustal Stretching</i>	8
2.1.3 <i>Major Faulting</i>	11
2.1.4 <i>Minor Faulting</i>	16
2.1.5 <i>Pure and Simple Shear Topography</i>	17
2.2 FAULT GROWTH AND FAULT LINKAGE OF INDIVIDUAL FAULTS.....	22
2.3. CONTROLS ON SEDIMENTATION IN A RIFT PROVINCE	28
2.3.1 <i>Pre-Rift Sedimentation and Controls and Architecture</i>	29
2.3.2. <i>Pre-Rift to Syn-Rift Transition</i>	30
2.3.3 <i>Syn-Rift Sedimentation and Controls and Architecture</i>	31
2.3.4. <i>Syn-Rift to Post-Rift Transition</i>	36
2.3.5 <i>Post-Rift Sedimentation and Controls and Architecture</i>	37
2.4 RIFT CONTROLS ON PETROLEUM SYSTEMS	39
2.4.1 <i>Source</i>	39
2.4.2 <i>Migration</i>	40
2.4.3 <i>Reservoir</i>	45
2.4.4 <i>Trap</i>	47
2.4.5 <i>Seal</i>	48
2.4.6 <i>Timing</i>	51

CHAPTER 3 DEVELOPMENT AND EVOLUTION OF THE NORTHERN NORTH SEA BASIN.....	53
3.1 BASIN SETTING AND LOCATION	53
3.2 EXTENSIONAL STRUCTURES OF THE VIKING GRABEN AND EAST SHETLAND BASIN	54
3.2.1 Initial basin setting – post Caledonian Orogeny.....	54
3.2.2 Late Permian – Early Triassic Rifting event.....	56
3.2.3 Middle Triassic – Lower Jurassic Intra-rift subsidence	58
3.2.4 Middle Jurassic Doming event.....	59
3.2.5 Upper Jurassic – Lower Cretaceous Rifting event.....	63
3.2.6 Lower Cretaceous – Tertiary Post Rift Thermal Subsidence.....	68
3.2.7 Structural Summary	72
3.3 STRATIGRAPHY	72
3.3.1 Permian	74
3.3.2 Triassic	78
3.3.3 Jurassic	88
3.3.4 Cretaceous	103
3.3.5 Tertiary	108
3.4 EXPLORATION HISTORY	112
CHAPTER 4 DATA AND METHODS.....	116
4.1 SEISMIC DATA	116
4.1.1 Acquisition	117
4.1.2 Processing	118
4.1.3 Calibration and Interpretation	120
4.1.4 Seismic interpretation tools.....	124
4.1.5 Seismic dataset list	125
4.2 BOREHOLE DATA	139
4.2.1 Geological Samples.....	140
4.2.2 Geophysical Well Logs	141
CHAPTER 5 CONTROLS ON AND CONSEQUENCES OF RIFT TRANSECTION.	148
5.1 INTRODUCTION	148
5.2 STUDY AREA	149
5.3 EVIDENCE OF A TRANSECTED RIFT	153
5.3.1 Type 1 Rifting; same fault strike, full fault plane reactivation and same fault polarity	
156	

5.3.2	<i>Type 2 Rifting; same fault strike, partial fault plane reactivation and opposed fault polarity.</i>	186
5.3.3	<i>Type 3 Rifting; oblique fault strike, partial fault plane reactivation and variable fault polarity</i>	213
5.3.4	<i>Type 4 Rifting; perpendicular fault strike, partial fault plane reactivation and mixed fault polarity</i>	245
5.4	EFFECTS OF TRANSECTING RIFTS	290
5.5	CONCLUSIONS	300

Volume 2

CHAPTER 6 EVIDENCE FOR AND CONTROLS ON UPPER JURASSIC ISLAND		
ARCHIPELAGO FORMATION		303
6.1	INTRODUCTION	303
6.2	STUDY AREA	305
6.3	EFFECTS OF JURASSIC RIFTING	309
6.3.1	<i>Seismic Interpretation</i>	310
6.3.2	<i>Biostratigraphic Analysis</i>	325
6.3.3	<i>Sedimentological Analysis</i>	333
6.4	EFFECTS AND CONSEQUENCES OF ISLAND FORMATION	335
6.4.1	<i>Island Archipelago Erosion in the East Shetland Basin</i>	336
6.4.2	<i>Meteoric leaching</i>	342
6.5	CONCLUSIONS	357
CHAPTER 7 ROLE OF BASEMENT STRUCTURE AND NORMAL FAULT		
PROPAGATION IN GOVERNING SYN-RIFT SEDIMENT DISPERSAL		360
7.1	INTRODUCTION	360
7.2	CLADHAN AND TERN-EIDER RIDGE	361
7.2.1	<i>Seismic data and well calibration</i>	362
7.3	PERMO-TRIASSIC RIFTING	370
7.4	JURASSIC RIFTING	377
7.5	REACTIVATION OF PERMO-TRIASSIC FAULTS IN THE UPPER JURASSIC	381
7.6	UPPER JURASSIC SEDIMENTARY DISPERSAL PATTERNS	388
7.6.1	<i>Cause of the anomalies</i>	397
7.6.2	<i>Sedimentary dispersal analogues</i>	410
7.7	INFLUENCE OF UNDERLYING STRUCTURAL PATTERNS	416

7.8	DROWNING OF THE POBIE PLATFORM.....	423
7.9	EOCENE FAULT REACTIVATION.....	429
7.10	CONCLUSIONS	433
CHAPTER 8 DISCUSSION AND IMPLICATIONS		435
8.1	INTRODUCTION	435
8.2	RELEASE FAULTING VS. REACTIVATION	437
8.3	REGIONAL RESPONSES	442
8.3.1	<i>East Shetland Basin Response</i>	442
8.3.2	<i>North Sea Response</i>	446
8.4	GENERIC CONSEQUENCES.....	451
8.4.1	<i>Offshore Newfoundland</i>	452
8.4.2	<i>Kenya-Sudan, East African Rift</i>	457
CHAPTER 9 CONCLUSIONS		468
CHAPTER 10 REFERENCES.....		473
CHAPTER 11 APPENDIXES		487
APPENDIX 1 - REGIONAL SURFACES.....		488
	<i>Sea Bed Structure Map</i>	489
	<i>Top Balder Formation Structure Map</i>	490
	<i>Top Cretaceous Structure Map</i>	491
	<i>Top Plenus Marl Structure Map</i>	492
	<i>Top Cromer Knoll Formation Structure Map</i>	493
	<i>Base Cretaceous Unconformity Structure Map</i>	494
	<i>Top Brent Group Structure Map</i>	495
	<i>Top Dunlin Group Structure Map</i>	496
	<i>Base Syn-Rift 1 Structure Map</i>	497
	<i>Post-Rift Package 2; Sea Bed to Base Cretaceous Unconformity Isochron</i>	498
	<i>Syn-Rift Package 2; Base Cretaceous Unconformity to Top Brent Group Isochron</i>	499
	<i>Intra-Rift; Top Brent Group to Top Dunlin Group Isochron</i>	500
	<i>Rift Package 1; Top Dunlin Group to Base Syn-Rift 1 Isochron</i>	501

List of Figures

Figure 2-1 Wilson cycle (Whitmeyer et al. 2007)	6
Figure 2-2 Wilson cycle (Whitmeyer et al. 2007)	7
Figure 2-3. Rifting model illustrating how stretching can change the heat flow within a basin (Roberts and Yielding 1994).....	9
Figure 2-4. Rifting models that can be generated by the presence of a mantle plume (Burke and Dewey 1973).....	11
Figure 2-5. The illustration of footwall uplift and hangingwall subsidence in normal faults (Yielding 1990)	12
Figure 2-6. Illustration of the flexural cantilever model (Kusznir 1991)	13
Figure 2-7. Flexural cantilever model explained within different scenarios, such as singular or multiple fault domains (Roberts and Yielding 1994).....	15
Figure 2-8. The shape and dimensions of a normal fault (Watterson 1986) ...	17
Figure 2-9. Illustrating the "pure shear" model in diagram (a) and the "simple shear" model in diagram (b) (Wernicke 1985).....	18
Figure 2-10. The classic Basin and Range analogue is observed in the Western United States where extension has created a series of structural features depending upon the length of time an area has been in extension. This diagram illustrates three locations within the Basin and Range evolution history that is observed in US Basin and Range Province. (a) Is an undeformed location where little or no stretching has occurred. (b) Is the initiation of a large scale normal fault that cuts deep into the seismogenic layer. (c) Illustrates the decollement of small scale planar normal faults onto the underlying detachment surface. (d) shows that the rate of extension is so great that the uplifting asthenosphere come so close to the surface and may induce magmatic activity (Wernicke 1985).	19
Figure 2-11. Illustration on fault patterns from varying extensional models. (A) Illustrates the fracture pattern developed by a radial fracture pattern. (B)	

illustrates the fracture pattern relating to a basin and range style of extension (east-west) (Stewart 1971).	20
Figure 2-12. Illustrating the method of growth and eventual linkage between multiple faults to generate a much large fault system (Fraser 2003). In plan view (1) it possible to see the overlapping of two individual faults prior to linkage. The 3D model (2) then illustrates how the relay ramp location that was once a structural low is uplifted to generate a structural high.....	23
Figure 2-13. Illustration of fault growth and linkage and the resultant generation of accommodation space (Gawthorpe 2000)	24
Figure 2-14. . Illustrating the structural geometry of a normal fault with hangingwall release faults, to accommodate hangingwall subsidence (Destro 1995).	25
Figure 2-15. The possible structures that can be formed as a direct result of release faulting. The contours are to show height with 1 being the highest and 5 the lowest (Destro 2003).	26
Figure 2-16. The orientation of release faults relates back to the geometry of the initial parent fault as shown in A and B. The greater curve on the parent fault will illustrate a more oblique release fault pattern. The displacement and orientation of release faults can also play an important role in forming channels and turbidite systems within the extensional basin (Destro 2003)..	27
Figure 2-17 Illustration of varying alluvial fan depositional models. A) Highlights the development of alluvial fans in a late stage syn-rift infill, whereas, B) shows the progressive infill of syn-rift accommodation space by marginally-derived alluvial deposits (Fordham et al, 2010).....	32
Figure 2-18. Sediment distribution at a relay ramp (Roberts and Yielding 1994)	33
Figure 2-19. The evolution and linkage of rift parallel faults and the subsequent sedimentation (Gawthorpe and Leeder 2000).....	34

Figure 2-20. Illustrating the change from the syn-rift active stretching to thermally driven subsidence in the post-rift setting (Kyrkjebø 2004)	36
Figure 2-21. The generation and varying unconformity types within a rift province (Kyrkjebø 2004). Areas in grey indicate the underlying pre-rift sediments that have been cut by the unconformity in black.	37
Figure 2-22. Illustrating post-rift on-lap and infill (Schlische 1999)	38
Figure 2-23. illustrating how faulting plays a major role in the generation of a source kitchen (Burley 1993; Husmo 2003).....	39
Figure 2-24. Allan diagram illustrating the potential overlapping and migration of fluids from one stratigraphic unit to another vis a fault plane (Allan 1989). The lower (hangingwall) green unit crosses the footwall (upper) of the red horizon, generating a leak point between the two units...	41
Figure 2-25. Various models to show fluid flow properties along fault planes (Yielding 1997).....	42
Figure 2-26. Illustrating the variation in faulting types that can effect fluid flow within a reservoir (Knipe 1998).....	43
Figure 2-27. This illustrates the offset that can be achieved by release faulting, which shows the effect it can play on reservoir performance (Stewart 2001).	44
Figure 2-28. Diagram illustrating the variation in reservoir quality across the Ganymede Field. A is a top structure map identifying the good and poor reservoir locations and B illustrates the variation in reservoir thickness and its relationship to reservoir quality (A and B after Leveille, 1997)	45
Figure 2-29. The role of faulting in determining reservoir quality and potential productivity (Leveille 1997)	46
Figure 2-30 Seismic section through the Alwyn Field illustrating a typical Northern North Sea trap. In this instance multiple reservoirs are found at varying levels within the structure (Underhill. 2003).....	47
Figure 2-31. The tilted fault block of the Brent Field, where two separate reservoirs have been produced from (Taylor 2003)	48

Figure 2-32. Structural disposition, outline of the Murchison field shape (Warrender 1991).....	49
Figure 2-33. The Dunbar Field is an example of fault bounding reservoir compartmentalisation. This may occur where the reservoir units are not juxtaposed across the fault plane or a high shale smear content is present along the fault plane (Ritchie 2003)	50
Figure 2-34. Evidence of structural inversion south of Wytch Farm led to the remigration of hydrocarbons in the initial hangingwall locations prior to the formation of the large scale monocline, The only locations in which hydrocarbons are found are the unreactivated tilted fault blocks to the north (Underhill and Stoneley 1998)	52
Figure 3-1. Map illustrating the general structural trends observed in the Northern Sea, with the East Shetland Basin highlighted in red (Zanella and Coward 2003).....	53
Figure 3-2. The structural evolution from the Devonian to the early Permian (Coward 2003).....	55
Figure 3-3. The structural evolution and the opening of the North Sea through the Triassic (Goldsmith 2003).....	57
Figure 3-4. Illustrating some of the structural highs created by the Permo-Triassic rifting event (Færseth 1998).....	58
Figure 3-5. Illustrating the thickness of Triassic sediment in the Northern North Sea and ESB (Ziegler 1982).....	59
Figure 3-6. Illustrating the effect of uplift and erosion due to the Aalenian doming in the Central North Sea (Underhill and Partington 1993)	60
Figure 3-7. Regional onlap map to illustrate the overall effect of uplift and erosion from the Aalenian doming event in the Central North Sea (Underhill, 1993).	61
Figure 3-8. Showing what occurred as a result of the Doming in the Central North Sea in the Middle Jurassic (Underhill 1998).....	62

Figure 3-9. Fault patterns form the second phase of rifting in the North Sea (Zanella and Coward 2003).....	64
Figure 3-10. Illustrating footwall degradation and structurally down dip prospects (Zanella and Coward 2003).....	65
Figure 3-11. Illustration of how the underlying faults may play a role in effecting the overlying fault patterns (Tomasso 2008). Block A indicate the Early Triassic, B is illustrative of the mid -Triassic and C illustrates the structures present by the Base Cretaceous.	67
Figure 3-12. Map to illustrate the Cretaceous rifting located in the West of Shetland (Dean 1999).	68
Figure 3-13. Diagram illustrating Lower Cretaceous syn-rift packages within the West of Shetland area (Dean 1999).....	69
Figure 3-14. Maps illustrating the shift in depocentres from the Cretaceous to the Paleocene in the West of Shetland (Dean 1999).....	70
Figure 3-15. Subsidence curve for the Northern North sea, taking into account Palaeocene uplift and Eocene subsidence relating to the Iceland plume generation (Nadin 1995).	71
Figure 3-16. Permian lithostratigraphic column of the North Sea (Glennie 2003)	75
Figure 3-17. Deposition of all Permian sediments in the North Permian Basin (Glennie 2003)	76
Figure 3-18. Development of the proto-Atlantic and initial Viking Graben (Glennie 2003)	77
Figure 3-19. Lithostratigraphy of the Triassic in the Northern North Sea (Goldsmith 2003)	80
Figure 3-20. illustrating the subdivision of the Statfjord formation within the Banks Group (Fisher 1998).....	82
Figure 3-21. illustrating the distribution of the three members which make up the Statfjord formation (Goldsmith 2003)	83

Figure 3-22. Demonstration of the inter-linking channels which make up the fluvial units of the Statfjord Formation (Goldsmith 2003).	85
Figure 3-23. Illustration of the parallel Middle Jurassic Brent Group and Statfjord Formation reservoir sandstones (Taylor 2003).	87
Figure 3-24. Lithostratigraphy of the Lower and Middle Jurassic (Richards 1990)	89
Figure 3-25. Schematic diagram showing the Brent Group orientation in the East Shetland Basin (Richards 1992).....	91
Figure 3-26. Sedimentological model for the deposition of the Brent Group sediments (Hampson 2004).....	94
Figure 3-27. Diagram illustrating the transgressive/ regressive nature of the Brent Delta (Helland-Hansen 1992).....	95
Figure 3-28. Overview of the Upper Jurassic rift related sequence stratigraphy (Rattey and Hayward, 1993)	96
Figure 3-29. A stratigraphic column illustrating the deposition of sediments relating to the Magnus Sandstone Formation (Morris 1999)	99
Figure 3-30. Sediment distribution diagrams for the Magnus Sandstone formation. A) Isopach for the latest Kimmeridgian; B) Isopachs for Early Volgian and C) Isopachs for mid Volgian. (Morris 1999). The Magnus Field is outlined in solid black.	101
Figure 3-31. Stratigraphy of the Upper Jurassic (Fraser 2003).....	102
Figure 3-32. Cretaceous stratigraphy (Copestake 2003)	104
Figure 3-33. Upper Cretaceous deposition patterns (Surlyk 2003)	106
Figure 3-34. Lithostratigraphy of the Upper Cretaceous (Surlyk 2003)	107
Figure 3-35. Lithostratigraphy of the Tertiary sediments in the Northern North Sea (Jordt 1995)	108
Figure 3-36. Lithostratigraphy of the Montrose and Moray Group sediments (Ahmadi 2003)	109
Figure 3-37. Lithostratigraphy of the Stronsay Group (Jones 2003)	110

Figure 3-38. Lithostratigraphy of the Westray and Nordland Groups (Fyfe 2003)	111
Figure 3-39 A= observation of buried highs IMF (Fraser 2003) B=Observation of Northern north sea buried highs (Erratt 1999)	113
Figure 3-40. Improvement of understanding through available data from wells (Brennand 1998)	114
Figure 4-1. illustrating the issue that may require processing in collecting seismic data (Sheriff 1983).....	119
Figure 4-2. Illustrating the generation of background noise in seismic data (Sheriff 1983).	119
Figure 4-3. Illustration of a synthetic seismograms and how it is used to tie variable sets of data to accurately pick the change in rock facies in the subsurface (Becquey 1979).	122
Figure 4-4. Illustration of how the velocity variations in sediments can create seismic induced features (Underhill 2008).	123
Figure 4-5 Highlighted in red is the limits of the 3D Cladhan seismic dataset.	127
Figure 4-6 Highlighted in purple is the limits of the 3D Don SW+NE seismic dataset.	128
Figure 4-7 Highlighted in light green is the limits of the 3D Hudson seismic dataset.	129
Figure 4-8 Highlighted in dark green is the limits of the 3D Hutton seismic dataset.	130
Figure 4-9 Highlighted in light blue is the limits of the 3D M07 seismic dataset.	131
Figure 4-10 Highlighted in brown is the limits of the 3D N07 seismic dataset.	132
Figure 4-11 Highlighted in grey is the limits of the 3D Murchison Small seismic dataset.	133

Figure 4-12 Highlighted in maroon is the limits of the 3D Murchison Large seismic dataset.	134
Figure 4-13 Highlighted in dark blue is the limits of the 3D Tern-Eider seismic dataset.	135
Figure 4-14 Highlighted in grey is the limits of the 3D Tern-Spec seismic dataset.	136
Figure 4-15 Highlighted in teal is the limits of the 3D West Don-Thistle seismic dataset.	137
Figure 4-16 Highlighted in yellow is the limits of the 3D Western Geco 210/11 PreSTM 2008 seismic dataset.	138
Figure 4-17 Full acreage of the 12 3D seismic datasets used within this study.	139
Figure 5-1 Regional map illustrating the large scale structural geology that is present within the East Shetland Basin (Edited from Fraser et al. 2003).	150
Figure 5-2. Map illustrating the 4 areas of interest. Area 1, Highlighted in red, Tern-Eider Ridge. Area 2, highlighted blue, Cormorant to Brent. Area 3, Highlighted purple, Pobie platform. Area 4, Highlighted yellow, Causeway to Statfjord North.	151
Figure 5-3. Stratigraphic column illustrating the tectonic evolution of the Northern North Sea and the relevant sedimentary rifting phase (Zanella 2003).	155
Figure 5-4. Base map illustrating the study area (red) and a series of seismic sections to constrain seismic interpretation.	159
Figure 5-5 Illustrating the synthetic seismogram for well 210/25a-9.	160
Figure 5-6 Seismic line 1-1 is a NW-SE trending seismic line that runs through the northern section of the Tern-Eider Ridge study area.	161
Figure 5-7 Seismic line 1-1 shows significant offset between the Top Brent Group across the western limit of the Tern-Eider Ridge. As the offset of both	

the Brent and the Base syn-rift 1 are equal it is likely that this fault is purely an Upper Jurassic fault.	162
Figure 5-8 Seismic line 1-2 is NW-SE oriented line that runs through the central area of the Tern-Eider Ridge study area.	163
Figure 5-9 seismic line 1-2 shows significant offset between both the Top Brent Group and the Basement horizons. As the offset between the Basement horizon is greater than the Brent offset it suggests that a Permo-Triassic fault has reactivated in the upper Jurassic. The north-western edge of the seismic section illustrates the western limit of the East Shetland Basin.	164
Figure 5-10 Seismic line 1-3 is a NW-SE oriented line in the southern section of the Tern-Eider Ridge area.	165
Figure 5-11 Seismic line 1-3 further illustrates the western rift shoulder of the East Shetland Basin. The southeast section of the seismic line shows no offset along the Permo-Triassic fault which illustrates no Upper Jurassic offset and thus has not reactivated in the second rifting phase. The footwall of the TER also contains an upper Jurassic thrust.	166
Figure 5-12 Seismic line 1-4 is a SW-NE oriented line located in the hangingwall of the Tern-Eider Ridge.	167
Figure 5-13 Seismic line 1-4 shows in the south-western location an increased thickening section in syn-rift 1 and a post-rift thermal sag basin to the northeast, which relates to the Upper Jurassic rifting event.	168
Figure 5-14. Seismic line 1-5, an uninterpreted seismic section across to footwall of the Tern-Eider Ridge.	169
Figure 5-15. Seismic line 1-5, interpreted seismic section illustrating the topographic structures over the Tern-Eider Ridge.	170
Figure 5-16. Top Basement (pre-rift) map illustrating the overall combined effects of both sets of rifting events. This map illustrates two separate depocentres along the Tern-Eider Ridge.	173

Figure 5-17. Top Brent Group structure map illustrating the NE-SW orientation of the Upper Jurassic rifting event.	174
Figure 5-18. Top Base Cretaceous structure map illustrating the depo-centres created by the Upper Jurassic rifting event.	175
Figure 5-19 Illustrating the evolution of fault systems from the Permo-Triassic (A) through to the Upper Jurassic (B+C). Diagram (D) highlights the area where the two fault systems overlap and reactivate through time.	176
Figure 5-20. BCU to Top Basement marker bed illustrating the overall thickness trends identified through a combination of the two rifting events that occurred in the Permo-Triassic and upper Jurassic.	179
Figure 5-21 Initial syn-rift section between a Permo-Triassic marker bed and the Top Brent Group sediments, illustrating a large depocentre to the SW of the Tern-Eider Ridge.....	180
Figure 5-22. Base Cretaceous to top Brent Group isochron map illustrating depocentres that were created and filled by Humber Group sediments during the Upper Jurassic rifting event which is the second rift phase observed in the Tern-Eider Ridge area.	181
Figure 5-23. Fault displacement-length plot showing the offset of the Permo-Triassic and Upper Jurassic pre-rift sediments along the western edge of the Tern -Eider Ridge. The black line represents the overall displacement of both rifting events and relates to the economic basement. The red line illustrates the displacement of the top Brent Group sediments, which are the pre-rift to the Upper Jurassic rifting event and records fault movement solely for this stretching event. By subtracting the Upper Jurassic faulting from the overall displacement it is possible to generate the initial Permo-Triassic Displacement, this is illustrated here by the green line.....	182
Figure 5-24 illustrates the method of vertical relay planing. This shows how two faults react and interlink with the same sense of throw and polarity...	184
Figure 5-25. Box diagram for the structural evolution of Type 1 rifting.	185

Figure 5-26 Seismic cross-section from Tomasso et al (2008) illustrating the presence of an underlying Permo-Triassic fault.....	187
Figure 5-27 Area 2 study area and seismic lines used within this study.	189
Figure 5-28 Synthetic seismogram generated for well 211/27-9.....	190
Figure 5-29. Seismic line 2-1 illustrates large scale tilted fault blocks throughout the East Shetland Basin. It is further possible to see a continual thickening of the basement pick (cyan) from west to east.	191
Figure 5-30. Seismic line 2-2, illustrates a thickening of Permo-Triassic sediments from west to east across the section. The thickest sections of these sediments are found in the current footwall highs relating to the Upper Jurassic rifting event.	192
Figure 5-31 Seismic Line 2-3 is an N-S oriented line over the western section of the study area.	193
Figure 5-32 Seismic Line 2-3 illustrates a relatively thin covering of Mesozoic sediments above the Basement horizon.....	194
Figure 5-33 Seismic Line 2-4 is an N-S oriented line located within the centre of the study area.	195
Figure 5-34 Seismic Line 2-4 illustrates an increased amount of Mesozoic sediment present above the metamorphic Basement.	196
Figure 5-35 Seismic Line 2-5 is an N-S oriented line in the eastern location of the study area.....	197
Figure 5-36 Seismic Line 2-5 illustrates the thickest section of Mesozoic sediments can be situated to the furthest east of the dataset. Here a thick covering of Triassic and Jurassic sediments are located in the footwall to a large scale Upper Jurassic normal fault	198
Figure 5-37. Top Base Cretaceous top structure map.	201
Figure 5-38. Top Brent Group structure map illustrating significant structural highs and lows from the Upper Jurassic rifting event.....	202
Figure 5-39. Top Permo-Triassic structure map.	203

Figure 5-40. Complete thickness isochron from BCU to Permo-Triassic illustrating a significant thickness in the tectonostratigraphic megasequence package under the Brent Field.	206
Figure 5-41. Top Brent Group to Top Permo-Triassic isochron map illustrates an easterly thickening wedge.	207
Figure 5-42. Top BCU to Top Brent Group isochron map shows westerly thickening wedges of the Upper Jurassic (Syn-Rift 2) sequences.	208
Figure 5-43. Schematic illustration of the evolution of Type two multiphase rifting.	210
Figure 5-44. Box diagram for the structural evolution of Type 2 rifting.	211
Figure 5-45. Study area 3 outline and orientation of seismic lines used in the study.	214
Figure 5-46 synthetic seismogram for well 210/24a-5.	215
Figure 5-47 Seismic Line 3-1 is the furthest south of the three seismic lines, here the Pobie Platform can be imaged along with the terrace areas to the NE and SW.	216
Figure 5-48 Seismic Line 3-1 the reactivation of the old Caledonian trending Pobie Fault can be observed although it is in the footwall to the Upper Jurassic normal fault.	217
Figure 5-49 Seismic Line 3-2 is located within the central location of the three seismic sections, here the Pobie Platform is not present but the rift shoulder is located further to the NW.	218
Figure 5-50 Seismic Line 3-2 illustrates two large terrace blocks that have formed in the Upper Jurassic. The terrace block to the NW has a significantly larger section of Mesozoic sediments within it as this was a hangingwall location during the initial Permo-Triassic rifting event.	219
Figure 5-51 Seismic Line 3-3 is furthest north of the three sections and illustrates reactivation of an initial fault plane.	220

Figure 5-52 Seismic Line 3-3 highlights the Upper Jurassic thrust fault that forms as a result of a space issue due to the western bounding and Tern-Eider Ridge extensional faults.....	221
Figure 5-53. Top Jurassic top structure map illustrating the structural high relating to the western limit of the East Shetland Basin which also contains the Unst Basin.	224
Figure 5-54. Top Brent Group structure map illustrates the Cladhan area relay ramp to the east of the Pobie Platform. The thrust fault highlighted in earlier seismic lines can also be imaged to the north of the Cladhan area. ..	225
Figure 5-55. Top Basement structure map highlights two Permo-Triassic basins which appear to be cross cut by the Upper Jurassic rift bounding fault.	226
Figure 5-56. Top Upper Jurassic to Permo-Triassic isochron map highlighting the NE-SW oriented depocentres to the north and the N-S oriented depocentres relating to the Cladhan area to the south.	229
Figure 5-57. Top Upper Jurassic to Top Brent Group isochron shows the greatest amount of thickening to be found in the Cladhan relay ramp area and a thinning of section over the hangingwall of the upper Jurassic thrust fault.....	230
Figure 5-58. Top Brent to Permo-Triassic isochron map shows the thickest Permo-Triassic sediments to be located in the depocentres that were highlighted in the Top basement structure map. It appears that the depocentres seem to thicken to the SW and die out to the NE suggesting this initial fault could be further observed to the SW in to the Unst Basin.....	231
Figure 5-59. Isochron between the Top Balder and Top Jurassic over the Pobie Platform illustrating the accommodation space generated by the Upper Jurassic rifting event.	233
Figure 5-60. Uninterpreted section illustrating the extensionally derived thrust fault located to the SW of the Tern-Eider Ridge.	235

Figure 5-61 Seismic section illustrating the extensionally derived thrust fault which is located to the SW of the Tern-Eider Ridge.	236
Figure 5-62 The East – West section shows a series of NNE-SSW oriented faults which are present within the basement material of the Pobie Platform. The strike of these faults is the same to that of the faults which create the hydrocarbon fields on the Tern-Eider Ridge.....	238
Figure 5-63. Top Structure map of ancient NNE-SSW oriented faults in the Pobie Platform.	239
Figure 5-64 Schematic illustration of the development of Type 3 rifting	241
Figure 5-65. Box diagram for Type 3 rifting.	242
Figure 5-66. Box diagram evolution of a transected rift block. (A) Initial undeformed state. The initial fault (B) is identified with a red plane separating the block into an initial footwall and hangingwall scenario. The second rifting phase (C) identified in green cuts these two blocks into four and again forming a new relative footwall and hangingwall. By merging the two faults systems together it is possible to identify each of the blocks has a unique evolution	244
Figure 5-67. Map illustrating the localised study area and seismic lines used in this location.....	247
Figure 5-68 synthetic seismogram for well 211/18-6.....	248
Figure 5-69. Seismic line 4-1 is the furthest NW of the three strike lines in this study.....	249
Figure 5-70. Seismic line 4-1 illustrates a series of NW-SE trending faults cross cutting into the footwall of an Upper Jurassic fault.	250
Figure 5-71. Seismic line 4-2 is a central strike line through the study area.	251
Figure 5-72. Seismic line 4-2 illustrates the large scale Tornquist trending faults cross cutting into the Caledonian trending Upper Jurassic footwall and is responsible for creating the Thistle (west) and the Murchison (east) Fields.	252

Figure 5-73. Seismic line 4-3 is the furthest southeast of the three strike lines with the majority of the section located in the hangingwall to the large scale Upper Jurassic Normal fault.....	253
Figure 5-74. Seismic line 4-3 illustrates the large cross cutting fault of a Tornquist trend which has been cross cut by the Upper Jurassic Normal fault. This NW-SE trending fault would have originally been the same fault that bounds the Thistle Field to the NE, but as it is in the hangingwall it creates the Dunlin Field.....	254
Figure 5-75 Seismic Line 4-4 is a dip line that is situated to the far SW of the study area and passes through the Osprey and Dunlin Fields. Here the Osprey Field can be observed in the centre of the seismic section forming an Upper Jurassic structural high.	256
Figure 5-76 Seismic Line 4-4 highlights the syn-rift 1 thickness variation across the reactivated Caledonian oriented normal fault.	257
Figure 5-77 Seismic Line 4-5 is also situated to the SW of the dataset and passes through the Thistle Field.	258
Figure 5-78 Seismic Line 4-5 illustrates that the Thistle location has been a structural high through both the Permo-Triassic and Upper Jurassic rifting events.	259
Figure 5-79 Seismic line 4-6 is a relatively central line that passes through the Murchison Field.....	260
Figure 5-80 Seismic line 4-6 illustrates a large scale fault to the SE of the section is the Caledonian trending fault which bound the field. This structural feature was also a structural high through both the Permo-Triassic and Upper Jurassic rifting events.	261
Figure 5-81 Seismic line 4-7 passes through the graben location between the Murchison Field and the Statfjord Nord Field to the NE.....	262
Figure 5-82 Seismic line 4-7 illustrates two sub-dividing sections of the multi-tiered fault block can be imaged in this section. Both of these sections were	

located in the hangingwall low to a Tornquist trending fault in the Permo-Triassic rifting event but the area to the NW with a thinner covering of Mesozoic sediments is situated in the footwall to the Upper Jurassic normal fault. The area to the SE on the other hand has been in the hangingwall location in both rifting event.	263
Figure 5-83 Seismic Line 4-8 is situated to the far NE of the study area and passes through the Statfjord Nord Field.....	264
Figure 5-84 Seismic Line 4-8 illustrates that the Thistle and Murchison Fields was also a structural high through both rifting events.....	265
Figure 5-85. Base Cretaceous structure map illustrates a series of highs and lows relating to reactivated faults in the Upper Jurassic.	268
Figure 5-86. Top Brent Structure Map highlights the hydrocarbon fields that have formed as a result of Upper Jurassic faulting.....	269
Figure 5-87. Base Syn-rift 1 structure map shows the initial Permo-Triassic depo-centres that were in place prior to Upper Jurassic rifting.	270
Figure 5-88. BCU to Base Syn-rift 1 isochron map shows the location of the depo-centres for both rifting events throughout the study area.....	273
Figure 5-89. Brent Group to Base Syn-rift 1 isochron map illustrates the reactivation of the Caledonian and Tornquist faults in the Permo-Triassic.	274
Figure 5-90. BCU to Top Brent Group isochron map illustrates the structural features that were generated in the Permo-Triassic rifting event. This includes the structural lows located to the SW and NE of the Murchison Field.....	275
Figure 5-91 Schematic diagram of the evolution of Type 4 rifting.	278
Figure 5-92. Box diagram of Type 4 rifting around the Murchison Field.....	279
Figure 5-93 Seismic line from Young et al illustrating thickening of Lower Jurassic Dunlin sediments against the jog fault. This would suggest that an older Permo-Triassic fault is in place to cause this thickening (Young et al 2001).	282

Figure 5-94 Illustrates two isochron maps used in the Young et al paper to explain the depocentre evolution through time. On these maps the underlying Permo-Triassic Tornquist trending faults have been superimposed on and match up with the Upper Jurassic depo-centre (Young et al 2001).	283
Figure 5-95. Well section through the Thistle and Murchison Fields show a subtle difference in thickness between the stratigraphic units corresponding to separate rift sequences. The numbers in black represent the depth (ft), whereas the figures in red represent thickness. Here it is possible to see a thickening within the footwall of these fields a thickening trend can be observed in the graben area, which suggests that faulting must have been active prior to the upper Jurassic.	285
Figure 5-96 Illustrating Triassic thickening against the Dunlin/Hutton fault system (Johnson & Stewart 1985).	287
Figure 5-97. Structural evolution variables for the Murchison Field. A illustrates the underlying Tornquist trending Triassic faults (Blue). B illustrates the evolution of the Murchison Field by Young et al. (2001), with the field forming through relay-ramping of overlapping normal faults and subsequent release faults forming in the footwall of this new, longer fault. C illustrates the formation of the Murchison Field with the aid of reactivating the underlying Triassic faults. It may have been possible for the upper Jurassic fault to propagate past the NE edge of the Murchison Field, but once the Triassic fault began to move again the fault strand became abandoned. D highlights a top structure map of the Brent Group around the Murchison Field.	288
Figure 5-98. A Top Brent Group map illustrating the Halibut High study area highlighted in the red box.	293

Figure 5-99. An S-N well correlation through the Halibut High area illustrating an increase in Statfjord Formation sediment thickness across the NW-SE Permo-Triassic fault.....	295
Figure 5-100. Maps illustrating the structure of the Northern North Sea and the effects of the underlying Caledonian trend. The highlighted box illustrates the possible extremity of the Tern-Eider ridge and associated strcutures (Lee and Hwang 1993; Coward 2003).....	297
Figure 5-101. Map illustrating the overall structural trends observed throughout the whole of the Greater North Sea area. The Caledonian Trend (red) and the Tornquist Trend (green) cross and intercept over the East Shetland Basin, which results in the multiple styles of cross-rifting throughout the basin (edited after Underhill (1998)).....	299
Figure 6-1. Map illustrating the location of seismic coverage and the regional structures effecting the area (Copestake 2003).....	305
Figure 6-2. Study area for the study of an Upper Jurassic island archipelago	306
Figure 6-3. Map illustrating the effect of Quaternary erosion on the SW coast of Norway (Jackson 2004).	309
Figure 6-4. Interpreted seismic cross section of the East Shetland Basin illustrating a series of tilted fault blocks which form large hydrocarbon fields such as the Cormorant, Hutton and Brent Fields.	312
Figure 6-5. Well log cross section over the Brent Field. Possible to see the eroded section of the Brent Group sediments and image the sediments below seismic resolution.	313
Figure 6-6. Brent field illustrating the erosion that can affect the up-dip location of the reservoir unit (edited from (Taylor 2003)). The crossed hatch Brent section is the areas that have been eroded away (sub-crop), whereas in the lower image the blue arrows indicate areas of onlap (supra-crop).....	315

Figure 6-7. Map illustrating the possible location of islands by seismic mapping of a pre-rift and syn-rift isochron.....	316
Figure 6-8. Top structure and time thickness (isochron) map of the Cromer Knoll Group. Here it is possible to identify thickening depo-centres in the late stage of the Upper Jurassic rifting event	319
Figure 6-9. Map of the Top Plenus Marl. Areas in white are areas of non-deposition suggest either an erosive surface was present or that the surface is on-lapping to a structurally high feature, which may be above sea level. The lower map illustrating the thickness of the Plenus Marl and it thinning out onto the structural highs such as the Tern-Eider Ridge.	320
Figure 6-10. Well 211/29-4 illustrates an erosion surface between the Lower Jurassic Dunlin Group and Upper Cretaceous sediments, suggesting an island formed during the Upper Jurassic and eroded sediments of Middle and Lower Jurassic age and prevented deposition through the Upper Jurassic and Lower Cretaceous.....	322
Figure 6-11. Illustration of the sub-crop over the Brent Field (Struijk and Green 1991).....	324
Figure 6-12. Chronostratigraphic break down of the Middle and Upper Jurassic (Cox 1990).	326
Figure 6-13. Maps illustrating the erosion surfaces observed within biostratigraphic and composite logs throughout the study area. Only the significant structural highs such as the Pobie Platform, Penguin Ridge and Brent Field show erosion in Kimmeridgian times, whereas erosion was observed throughout the basin in the Bathonian Callovian and Oxfordian times.	328
Figure 6-14. Map illustrating the biostratigraphic breaks in the sedimentary record due to erosion in the East Shetland Basin	330

Figure 6-15. Overlaying the biostratigraphic data on top of the Base Cretaceous Unconformity to top Brent isochron map illustrates the potential location for island locations.....	332
Figure 6-16 highlighting the development of the Magnus Sandstones Formation (Shepard 1991).....	338
Figure 6-17. Illustration of two types of secondary reservoirs over the Snorre Field. Generation of down-dip detached sands (orange) and back shed attached sands, which could possibly for oolitic sediments (yellow) (Dahl and Solli 1993).....	339
Figure 6-18 schematic diagram of the varying environments created by the Upper Jurassic rifting.....	340
Figure 6-19. Illustration of the erosion that may occur to the Upper Jurassic sediments as a result of footwall uplift close to or above sea level (Yielding 1992).	341
Figure 6-20. Illustration of sediment dispersal patterns as a result of footwall uplift segmentation and fault propagation (Underhill 1994).	342
Figure 6-21 Illustrating feldspar grain dissolution. Evidence from well 211/27-A28 located within the Hutton Field highlight a feldspar grain (F) has been partially dissolved due to meteoric leeching (Scotchman et al 1989)...	343
Figure 6-22 Evidence of feldspar grain dissolution in the Huldra Field, Northern North Sea (Bjorlykke 1998). The dissolution of feldspar grains can significantly increase porosity within reservoir units.	344
Figure 6-23. Map illustrating boreholes which have potassium concentration logs and can be used for the study of meteoric leaching.	346
Figure 6-24 A series of seismic lines have been generated to illustrate the effects of meteoric leaching in the East Shetland Basin. By using a suite of well logs which include Gamma Ray, Potassium Concentration and Bulk Density it is possible to see the change in porosity depending upon the location of each well.	348

Figure 6-25 Evidence from the Cormorant Field of reservoir enhancement due to meteoric leeching at the fault crest.	349
Figure 6-26 Seismic and well section through the Brent Field. The improvement of reservoir quality in the up-dip locations of a tilted fault block are again observed here.	350
Figure 6-27 Seismic and well section through the Magnus and West Don Fields and also through the structure known as the Halibut High.	351
Figure 6-28 seismic and well section illustrating the change in porosity values from the northern edge of the Tern-Eider Ridge to the Causeway Field	352
Figure 6-29. Illustration of kaolin morphologies over the Cormorant Field. Left: illustrates vermiform kaolin. Right: regular blocky Kaolin found down dip of the Cormorant Field (Wilkinson 2006).	356
Figure 7-1. Semi-regional basin map showing the locations of the Unst and East Shetland Basins along with large scale normal faulting. Highlighted in black is the study area which is covered by a series of 3D seismic datasets and the insert in red highlights the location of the Cladhan Field (Platt 1995, Sterling Resources, 2012).	362
Figure 7-2 Highlighted in red is the Cladhan 3D seismic data volume and in blue is the Tern-Eider Ridge 3D seismic data volume extent.....	364
Figure 7-3 Synthetic seismogram for well 210/29a-3 illustrating the tie from the borehole to the seismic data within the Cladhan study area.	366
Figure 7-4. Well correlated section through the Cladhan seismic dataset....	367
Figure 7-5. Seismic line from the Pobie Platform (west) through to the basinal area to the east.	368
Figure 7-6. The seismic line illustrates a large terrace area to the east of the Pobie Platform. The eastern edge of the Pobie Platform has been heavily eroded; it is possible that the eroded material may have been re-deposited down-dip of the large scale normal fault.....	369

Figure 7-7. Platforms and basins created by Permo-Triassic rifting (Goldsmith 2003).	371
Figure 7-8 Previous research illustrate the Tern-Eider Ridge may have once been a much larger laterally continuous structural feature (Lee and Hwang 1993).	372
Figure 7-9. Initial shape and size of the Unst Basin in the Triassic compared to what it looks like after the Upper Jurassic rifting event (Zanella 2003). ..	373
Figure 7-10. Top Cretaceous map illustrating the NE-SW orientation of the Tern-Eider Ridge and Pobie fault.	374
Figure 7-11 Uninterpreted seismic section through the southern limits of the Tern-Eider Ridge.	375
Figure 7-12. Seismic cross section illustrating a thickening package of Permo-Triassic sediments in the hangingwall to the western edge of the Tern-Eider Ridge.	376
Figure 7-13. Top Brent Group structure map illustrating the north-south orientation of the Upper Jurassic faults and some of the structural features that form as a result. Over the Cladhan area a relay ramp forms where two Upper Jurassic North-South orientated normal faults overlap and do not link through faulting. This creates a terraced area, which separates the Pobie Platform high with the East Shetland Basin area.	378
Figure 7-14. West-East seismic section through the Cladhan study area.	379
Figure 7-15. Seismic line illustrating the role of N-S orientated Upper Jurassic faults. This seismic line illustrates how the seismic volume can be subdivided in to different structural domains. From West to East the section can be divided into the Unst Basin – Pobie Platform– Cladhan Terrace – Cladhan Relay-Ramp – East Shetland Basin. The faults highlighted in red are the Permo-Triassic faults including the reactivated Pobie Fault.	380
Figure 7-16. Top Brent Group structure map illustrating the reactivation of the NE-SW faults in the Upper Jurassic. The Pobie Fault and the Tern-Eider	

Ridge illustrates major fault movements in the Upper Jurassic which do not have an orientation N-S, but retains their NE-SW orientation from the older Permo-Triassic rifting event.	382
Figure 7-17 Uninterpreted seismic section through the Pobie fault.	384
Figure 7-18. Cross section through the Pobie Fault and on to the Pobie Platform. It is possible to identify two separate thickening packages, relating to the two individual rifting events (Pink relates to Permo-Triassic faulting and the orange wedge to the fault reactivating in the Upper Jurassic.	385
Figure 7-19. Graph showing the displacements between the Permo-Triassic and Upper Jurassic pre-rift sediments along the western edge of the Tern – Eider Ridge. The black line represents the overall displacement of both rifting events and relates to the economic basement. The red line illustrates the displacement of the top Brent Group sediments, which are the pre-rift to the Upper Jurassic rifting event and records fault movement solely for this stretching event. By subtracting the Upper Jurassic faulting from the overall displacement it is possible to generate the initial Permo-Triassic Displacement, this is illustrated here by the green line.	387
Figure 7-20. Varying sediment responses relating to the development of a half graben system in the Permo-Triassic rift system (Leeder and Gawthorpe 1987).	389
Figure 7-21. Well Log 210/29a-3 illustrating the erosional unconformity (highlighted in red) over the Pobie Platform and the lack of Cretaceous sediments deposited over the Middle Jurassic Brent Group sediments.	391
Figure 7-22. Diagram illustrating the erosion of the Brent Group sediments on the Pobie Platform and potential re-deposition into the terraced and basin areas in the Cladhan area.	393
Figure 7-23. Mapping of the amplitudes identified within the seismic data and undertaking amplitude extraction on the horizon makes it possible to	

identify a potential submarine fan, sourced from the SW, towards the Pobie Platform.	394
Figure 7-24. Basic illustration of how thinly bedded sediments can influence the seismic response of the surrounding sediment (Simm, 2009).....	395
Figure 7-25. Cartoon illustrating a reservoir confidence map. Areas in green illustrate a 90% chance of finding effective reservoir, orange ranging from 90-10% and red below 10%. The evidence for this is determined by well logs and distance from the source area, which in this case is the Pobie Platform.	396
Figure 7-26 zoomed in section illustrating the two bright spots that can be correlated to two separate channel sands found in well 210/29a-4	398
Figure 7-27 The synthetic seismogram for well 210/29a-4 further illustrates the effect of the channel sediments.....	399
Figure 7-28 Seismic section highlighting the bright-spots that are indicative of the Upper Jurassic channel sediments.	400
Figure 7-29 Biostratigraphic analysis undertaken by Sterling resources to date the sand channel sequences.	401
Figure 7-30 A stratigraphic template for the North Sea highlighting where the Sequence 1, 2A and 2B sands fit into the depositional environment (Partington et al 1993).....	402
Figure 7-31 Amplitude extraction maps of the Lower (S1) and Upper (S2A+B) channel sands. The amplitude extraction map for the Sequence 1 sand channels was undertaken by creating a measurement window below the Mid-Magnus Shale of 20ms, where the largest negative reflection is measured. A similar window of 20ms was created above the Mid-Magnus shale to measure the Sequence 2A and 2b channel sands.....	403
Figure 7-32 case study from onshore Greenland illustrating the different deposition style deepening on varying source points (Surlyk 1987).....	405

Figure 7-33 Schematic diagram illustrating the evolution of the channel sediment distribution over the Cladhan relay ramp due to fault growth. A – Illustrates the ribbon like channel sands which formed in the early stages of the Cladhan Terrace. B – As the Cladhan faults grew, the footwall uplift deflected the channel sands down a relay ramp. C – The final stage of channel development relates to the ponding of sediment in the footwall highs. Here the channels were unable to reach the basin area and ponded over the footwall.....	406
Figure 7-34 Pressure data from well 210/29a-4. Two separate pressure trends can be observed within the two sandstone sequences. The pressure system identified in sequence 2A and 2B appears to be in communication to the sea level and increase steadily with depth. But, the pressure system identified in Sequence 1 sandstones is significantly over-pressured.....	408
Figure 7-35 Schematic diagram illustrating the inverted clast stratigraphy of the Jurassic and Triassic sediments from the Pobie Platform on to the Cladhan Terrace through the Upper Jurassic.	409
Figure 7-36 Illustration of the Brae and Miller Fields accompanied with a generalized cross section of the fields (Rooksby 1991).....	411
Figure 7-37 Diagrammatic illustration of the varying types of sedimentation that can occur around a fault plane location in the Helmsdale area (Wignall & Pickering, 1993).	412
Figure 7-38. Illustration of sediment dispersal patterns as a result of footwall uplift segmentation and fault propagation (Underhill 1994).	413
Figure 7-39. Restoration work upon the Top Brent horizon illustrates a missing section of Brent Group sediments over the Pobie Platform. An estimated 3 million cubic meters of sediment has been eroded from the eastern edge of the Pobie Platform. This figure was generated by measuring the eroded area and applying a simplified depth conversion model to the missing section to generate a depth of scour. The volumes also took into	

consideration the shape of the eroded area which in this case was triangular.	415
Figure 7-40 Uninterpreted seismic section in the hangingwall of the Cladhan Terrace.....	417
Figure 7-41 Seismic cross-section illustrating the generation of compaction driven lows in the Triassic sediments to aid the direction of flow for Upper Jurassic submarine fans.....	418
Figure 7-42. Top Brent Group dip map, illustrating the reactivation of an underlying Permo-Triassic fault in the hangingwall area of Cladhan.....	421
Figure 7-43. Seismic cross section illustrating the reactivation of an old Permo-Triassic fault in the basin area of Cladhan.	422
Figure 7-44 well 210/19-3 illustrating the presence of Upper Cretaceous (draping) sediments over the East Shetland Platform.....	425
Figure 7-45. Base Tertiary map illustrating the existence of the Pobie Platform at Cretaceous times and the partial covering of polygonal faulting at this layer by redeposited sediments form the structural high to the west.....	427
Figure 7-46. Top Brent time structure map, illustrating areas which have been eroded down through the Brent Group on the footwall high that is the Pobie Platform. The cross-hatched area is where Brent Group sediments are not present over the platform.....	428
Figure 7-47. Top Balder Formation. Identification of small scale faulting (Black) above the East Shetland Platform fault.....	430
Figure 7-48. Top Balder dip map illustrating faults within the Balder level. The faults orientated E-W are compaction related polygonal faults, whereas the N-S faults are related to the slipping of Paleogene sediments.....	431
Figure 7-49. Seismic section showing the lack of linkage between of the two sets of faults and the decollement of the Balder level faults in the Base Tertiary/ Upper Cretaceous.	433

Figure 8-1. Schematic illustration of the petroleum systems in the East Shetland Basin. The bars in blue are the timing of the petroleum elements in the initial Permo-Triassic rifting event where the red blocks are illustrating the Upper Jurassic rifting event and the resulting petroleum system elements (Buley 1993; Jones 2003).	436
Figure 8-2. Fault polygons indicating the orientation of faults that generate the Murchison Field.	440
Figure 8-3. Structural evolution variables for the Murchison Field. A illustrates the underlying Tornquist trending Triassic faults (Blue). B illustrates the evolution of the Murchison Field by Young et al. (2001), with the field forming through relay-ramping of overlapping normal faults and subsequent release faults forming in the footwall of this new, longer fault. C illustrates the formation of the Murchison Field with the aid of reactivating the underlying Triassic faults. It may have been possible for the upper Jurassic fault to propagate past the NE edge of the Murchison Field, but once the Triassic fault began to move again the fault strand became abandoned. D highlights a top structure map of the Brent Group around the Murchison Field.	441
Figure 8-4. Seismic section over the Halibut High illustrating the thickness variation over the structural high that is related to the interaction of underlying fault systems that have been cross cut by a later rifting event. .	443
Figure 8-5. Illustration of the Top Basement structure map within the East Shetland Basin. This map encapsulates the effects of faulting in all of the rifting events that has occurred in the basin from the Permo-Triassic through to the Upper Jurassic rifting event. Within this area Caledonian trending faults are illustrated in yellow, Tornquist trending faults in red and purely Upper Jurassic faults in pink.	444

Figure 8-6. Top Basement structure map illustrating the breached relay ramp locations due to the interaction of the Caledonian (orange) and Tornquist (red) faults.	445
Figure 8-7. Geological cross section through the Norwegian Johan Sverdrup Field which is found in the hangingwall to a normal fault which has reactivated through multiple rift phases. Evidence form this geological section show thickening packages in the hangingwall to the major fault in the Upper Jurassic, Triassic and the Permian Rotliegend sections suggesting the fault has been active in more than one phase of rifting. This fault is oriented NW-SE and aligns with the Tornquist trend suggesting that it is a long lasting trend of weakness (Lundin 2012).	448
Figure 8-8. Illustrates the structural configuration of the multi-tiered fault block system around the Johan Sverdrup Field (Lundin 2012).	449
Figure 8-9. Diagram illustrating the tectonic setting of the Heidrun Field, which illustrates at least two rifting events separated by an intra-rift section (Ramnarine 2011).	450
Figure 8-10. Structural history of the Offshore Newfoundland area (Hubbard 1985).	454
Figure 8-11. Localised study of the faulting linkage and evolution through the Mesozoic (Hubbard 1985).	456
Figure 8-12. Regional map of Africa illustrating the location of the mobile belts located within the basement of the continent (Ebinger 1994).	458
Figure 8-13. Structural evolution of the Eastern limb of the East African Ridge western limb (Ebinger 1994).	459
Figure 8-14. Seismic interpretation across the southern Anza Graben illustrating a series of structural features that range from shallow to deep within the seismic. The deep structures are related to older Basement and Cretaceous stretching events. The shallow events relate to the Holocene	

rifting, although some reactivation of faults has occurred in this most recent stretching phase (Morley 1999).	460
Figure 8-15. Seismic section oriented SW-NE through the southern Anza graben illustrating a combination of cross cutting faults (Morley 1999).	461
Figure 8-16. Cartoon illustrating the structural configuration that can be generated by the interaction of two perpendicular rift systems. The Tertiary Ethiopian Rift arm faults are illustrated in blue and the Cretaceous Anza Graben faults are depicted in red. By simplifying the model down it illustrates the locations of primary traps which were highs in both rifting events (H/H).....	462
Figure 8-17. Diagram illustrating the formation of a transverse fold as seen in the South Lokichar Basin (Morley 2002).	463
Figure 8-18. Seismic line parallel to the Anza Graben illustrating the formation of a transverse fold in the hangingwall to a Cretaceous normal fault (Morley 2002).	465

Chapter 1 Introduction

1.1 Rationale

It has been previously well documented that the Northern North Sea has undergone several plate tectonic cycles and intra-plate rifting phases. Within the East Shetland Basin it is possible to see the widespread transecting effects of these multiple phases of stretching. The interaction, reactivation and transecting of normal faults from one rifting phase to another are extremely valuable in determining petroleum prospectivity. Transecting can be defined as *“divided by cutting across”* and can be applied within these geological constraints by analysing the crosscutting nature of multiple rift events.

The most recent rifting phase in the Upper Jurassic defines the majority of the structural traps, kitchen source areas and through its post-rift (drift) subsidence has also dictated maturation and migration pathways that make the East Shetland Basin such a prolific petroleum basin. Thus, if the location, strike and polarity of normal faults in this rifting phase is predetermined by a previous rifting phase this could open up a new wave of exploration prospectivity in a declining mature basin.

The interaction of transected rifts could create long-standing structural highs which could undergo high levels of erosion. This erosion could result in the deposition of density driven flows that may become prospective if filled with hydrocarbons. This may also affect the location of a reservoir and or the size of a potential prospect. If a reservoir is located over a tilted fault block and it eroded away, the most prospective location would be either behind the crest of the block or down-dip across the fault plane. The nature of this erosion is also of great importance as large scale erosion is normally reserved for subaerial exposure. If this is so meteoric waters would enter the underlying

substratum and result in a flushing effect and alter the composition of the underlying formations.

All of these aspects can be studied in depth with high quality 3D seismic datasets that have accumulated over the past 60 years of hydrocarbon exploration. With a blanket covering of seismic data it is not only possible to observe new areas in detail, but also put them within the regional picture. This in turn will be supported by the vast catalogue of well logs, biostratigraphic and sedimentological logs which will add another dimension into the investigation. By including all these varying types of data in a regional context it will be possible to identify the role of underlying structures and their effects on and control on petroleum systems relating to a later rift system.

1.2 Aims of this Thesis

The primary objectives of this thesis are to analyse the effects of extensional faulting and the evolution of faults in the transected rift basin of the Northern North Sea. The study of and documentation of evidence of rift transection and the resulting structural feedback will be obtained with the use of high density 3D seismic datasets accompanied by over 250 wells, whereby three specific topics can be addresses:

- **Controls on and consequences of rift transection in the East Shetland Basin, Northern North Sea.**
- **Evidence for and controls on Upper Jurassic island archipelago formation**
- **Role of basement structure and normal fault propagation in governing syn-rift sedimentation and dispersal**

1.3 *Structure of Thesis*

This thesis documents the rationale, background understanding of rift basins and the evolution of the Northern North Sea. Individual research chapters illustrate the procedures and methods aimed at answering the thesis aims mentioned above with a later chapter identifying the localised and global consequences of multi-phase cross rifting.

Chapter 2 introduces the development and evolution of a rift system on both a large and small scale. This section explains the role normal faulting plays on rifting and how the growth and linkage of normal faults of individual faults is crucial in the evolution of a rift basin. The rifting plays a determining factor on sedimentation, supply and dispersal and is addressed here. Normal faulting is therefore key in understanding a petroleum system and the effect of faulting on each element of the petroleum system is further described.

The details of Chapter 3 are focused on the development and evolution of the Northern North Sea. This chapter includes sections which cover structural and sedimentology evolution through geological time through multiple rift phases in the Northern North Sea. Further information is given on the petroleum systems in the major basins and the effects of faulting on migration routes in the East Shetland Basin. Chapter 4 illustrates the varying types of data that are used in hydrocarbon exploration and how each of these data types are acquired and utilised.

Chapter 5 is the first results chapter and illustrates the effects and controls on transected rifts. This section uses individual areas of the East Shetland Basin which have varying structural evolutions to illustrate how multi-phase rifting events interact and reactivated depending upon the strike and

polarity of normal faults from the initial rifting event to the most recent rifting event.

Chapter 6 is a regional study based on the Upper Jurassic rifting event and how the reactivation of existing faults accompanied with new normal faults and how the growth and linkage of these faults form an island archipelago system. By defining the processes upon which an island forms, it is possible to observe the exposed areas with the use of seismic, biostratigraphic and sedimentological data. These defined island locations are then highlighted and used to illustrate how the formation of an island archipelago can drastically affect a petroleum system.

The final results chapter (7) is focused around the Cladhan area and investigates the role underlying basement faults have on sediment dispersal in later rifting events. The reactivation and interaction of existing faults play a crucial role in determining the location and orientation of Upper Jurassic syn-rift density flows.

The results from each of these chapters are brought together in Chapter 8 where the implications for multi-phase cross rifting are discussed. The regional concepts and the generic implications of cross rifting are illustrated in other cross rifting basins located around the world.

Chapter 9 contains the concluding comments for the thesis as a whole. Here the major points and findings highlighted in the earlier results chapters are emphasized. The references for the research undertaken here is located within chapter 10 and additional information is located within the appendixes in chapter 11.

Chapter 2 Structure and Development of a Rift Province

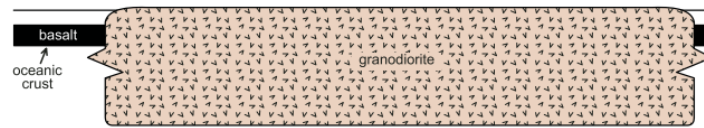
2.1 Development and Evolution of Extensional Systems

2.1.1 Wilson Cycle

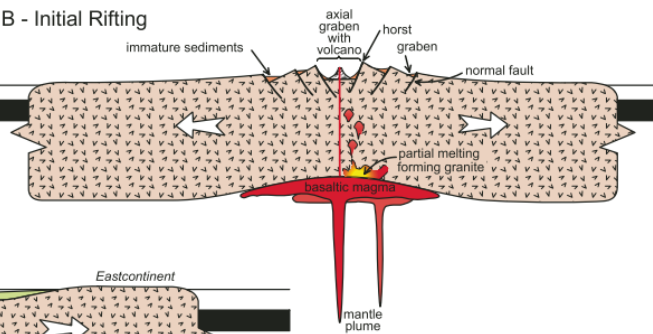
The Wilson Cycle can be defined as a multiple phase evolution of an ocean basin from opening to closure. The initial theory was published by John Tuzo Wilson from whom the cycle gets its name. His original theory that was published in 1996 suggests a six stage evolution process by which an ocean basin may be generated and then restored back to its original environment. More recent studies such as Whitmeyer et al. (2007) not only support the initial work by Wilson but also add three extra stages to take into account more recent discoveries about Wilson Cycles, as illustrated in Figures 2-1 and 2-2.

The 9 stage evolution of a Wilson Cycle as defined by Whitmeyer et al. (2007) start with a stable continental craton. This stable craton is then subject to an initial rifting event, this could be triggered by an underlying hotspot or mantle plume. The third stage of the Wilson Cycle involves the development of the rift basin from the rift to drift phase. This can include the development of a trilete rift system. The next stage of the cycle shows the initial continental craton has developed into a full ocean basin with a central ridge driving sea floor spreading and ridge push. The growth of the sea floor spreading ridge can advance to an island arc development once an initial subduction zone has formed. This subduction event may occur by the ridge push and the divergent continental margins moving at variable rates. This stage of the Wilson cycle is the start of the closure phase to the previously developed ocean basin.

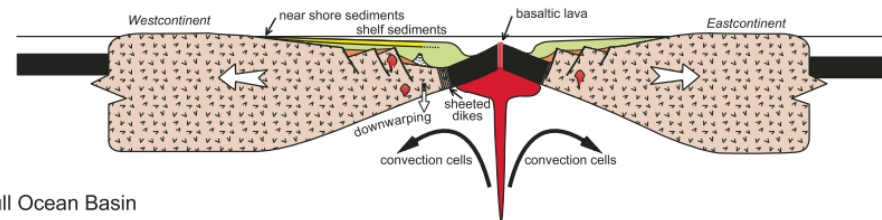
Stage A - Stable Continental Craton



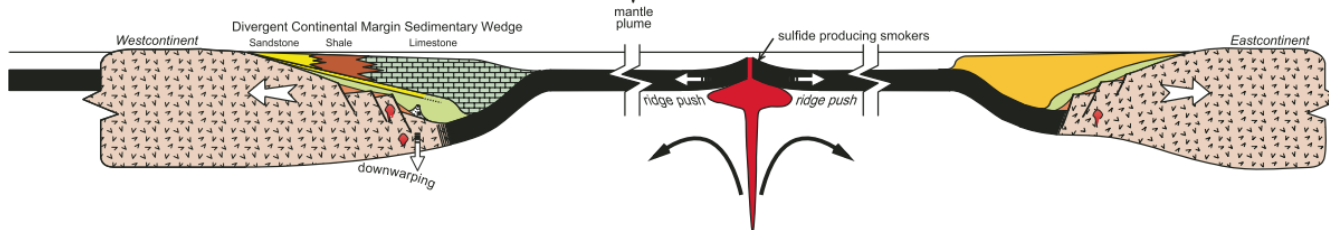
Stage B - Initial Rifting



Stage C - Early Ocean Basin Formation



Stage D - Full Ocean Basin



Stage E - Island Arc Development

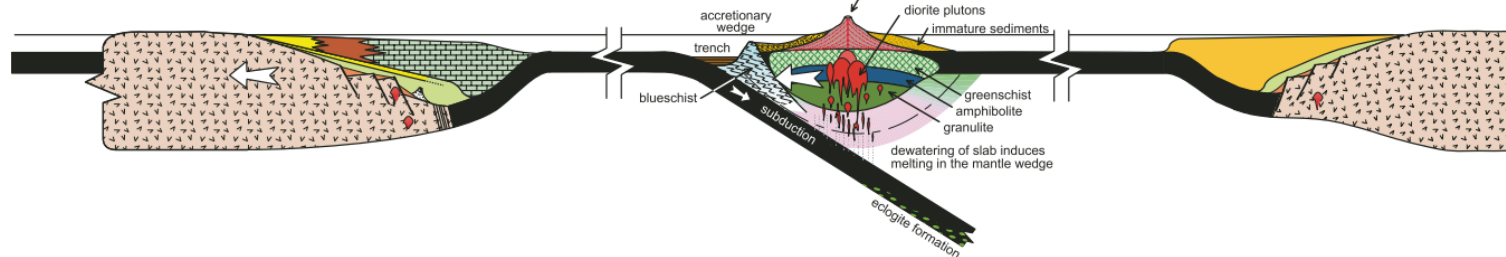


Figure 2-1 Wilson cycle (Whitmeyer et al. 2007)

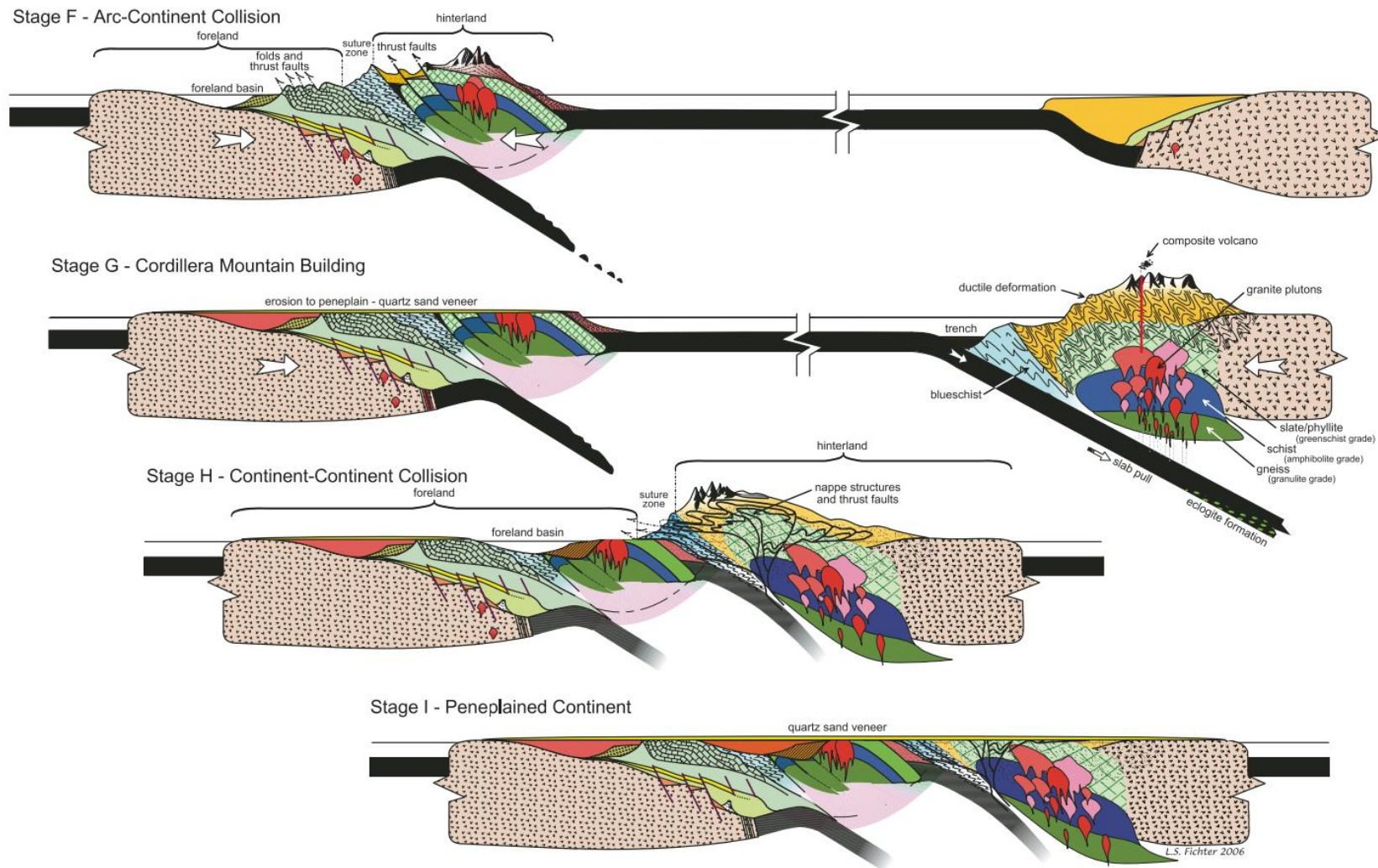


Figure 2-2 Wilson cycle (Whitmeyer et al. 2007)

The development of the island arc leads to the first collisional event in the Wilson Cycle. This Arc-Continent collision event generates a foreland basin in the previous continental segment and a series of thrust faults in the arc section of the newly formed continent. The seventh stage of the Wilson Cycle involves subduction which leads to cordillera mountain building in the opposing continent. Eventually the remaining oceanic crust is subducted and the Wilson Cycle enters into its second collision event. This event is continent-continent collision and generates a series of nappe structures and thrust faults within the collisional area. Now the initial stable continental craton has opened and closed it goes through a prolonged period of erosion and is termed a Peneplain continent. This process from start to finish is estimated to take ~500Ma per cycle (Whitmeyer et al. 2007).

2.1.2 Crustal Stretching

Continental break up initially occurs through rifting in an intra-cratonic location where stretching forces result in the thinning of continental lithosphere (Burke and Dewey 1973). From evidence in the stratigraphic record, it is possible to identify that the generation of a rift province initiates with extensive normal faulting and subsidence (McKenzie 1978). The extensional faulting and consequential thinning of the lithosphere results in the passive up-welling of hot asthenospheric mantle (Roberts and Yielding 1994). This is best illustrated using the McKenzie model, which assumes that the stretching of the continental lithosphere is geologically instantaneous.

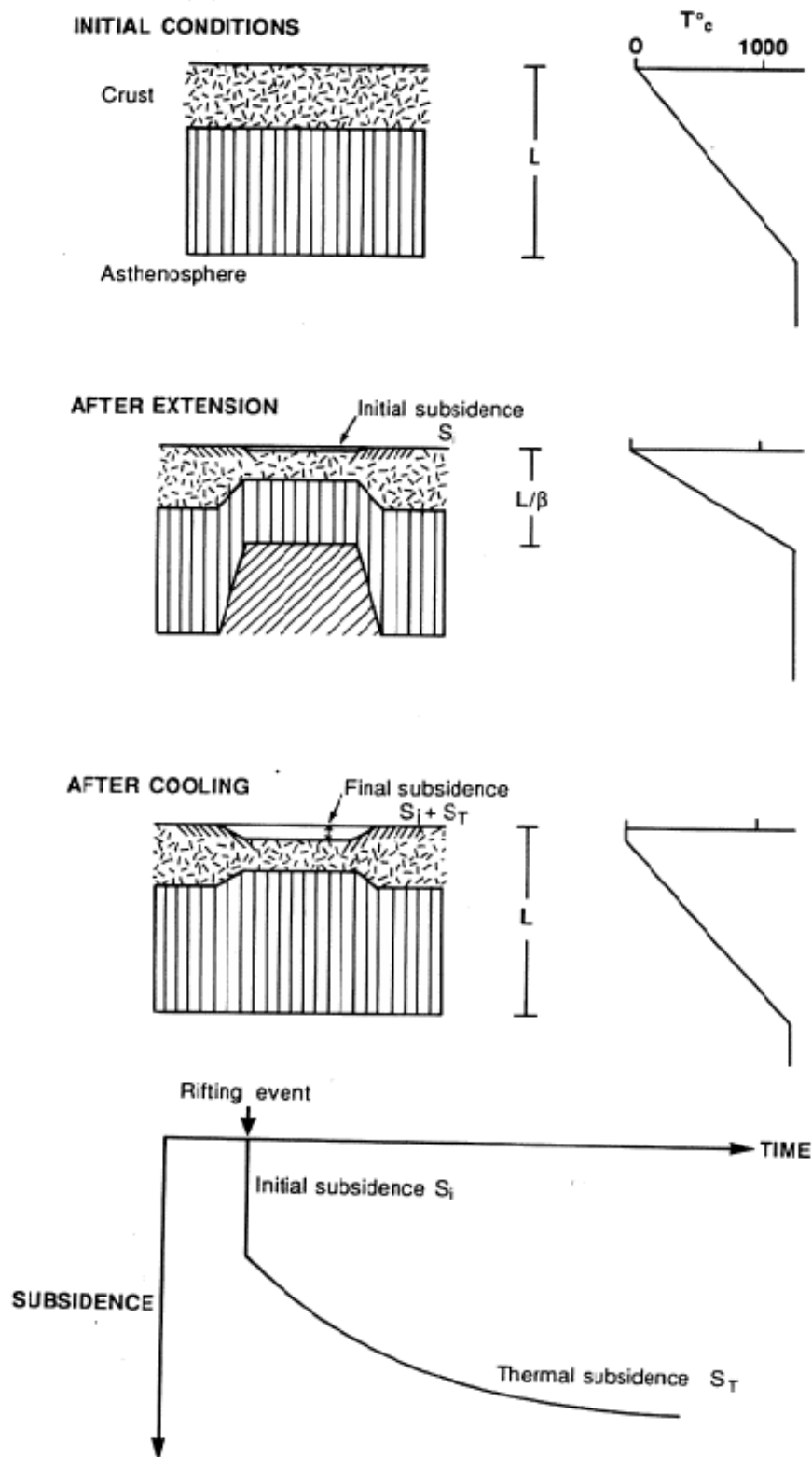


Figure 2-3. Rifting model illustrating how stretching can change the heat flow within a basin (Roberts and Yielding 1994)

The McKenzie model (Figure 2-3) is extremely useful in explaining the presence of sag basins which appear un-deformed directly above rift provinces or tilted fault blocks during subsequent unfaulted (post-rift) phase of subsidence (Roberts and Yielding 1994). The basis of this theory is that after an instantaneous stretching event, the asthenosphere will effectively rise up to cause a small period of uplift. As the asthenosphere cools, (as it is closer to the surface) the reduction of heat in the system results in a period of subsidence until the Mohorovičić discontinuity (moho) is returned to a deeper (original) position between the lithosphere and asthenosphere (McKenzie 1978). It is during the period of asthenospheric cooling that the overlying, undeformed thermal sag basins are generated above a faulted rift system (Roberts and Yielding 1994).

If thinning of the continental crust is extreme it may be possible for the asthenosphere to up-well by adiabatic decompression. This will result in an initial uplift and volcanism prior to the generation of a triple-junction, highlighted in Figure 2-4 (Burke and Dewey 1973). The additional rupturing of the continental lithosphere by extensional faulting can be accelerated by the uplifting from the hot asthenosphere. This can further lead to the generation of three rift arms which meet at roughly 120° to one another to create a triple-junction. Commonly, one of these rift arms fails to develop forming an aulacogen whilst generating two active rift arms (Burke and Dewey 1973). These rift arms can form by either active or passive rifting. Active rifting relates to the melting of the lower lithosphere by direct (vertical) forces, such as up-welling asthenosphere. In contrast, passive rifting is related to the stretching and thinning of the lithosphere by opposing (lateral) forces such as subduction or trench-pull (Fitton 1983).

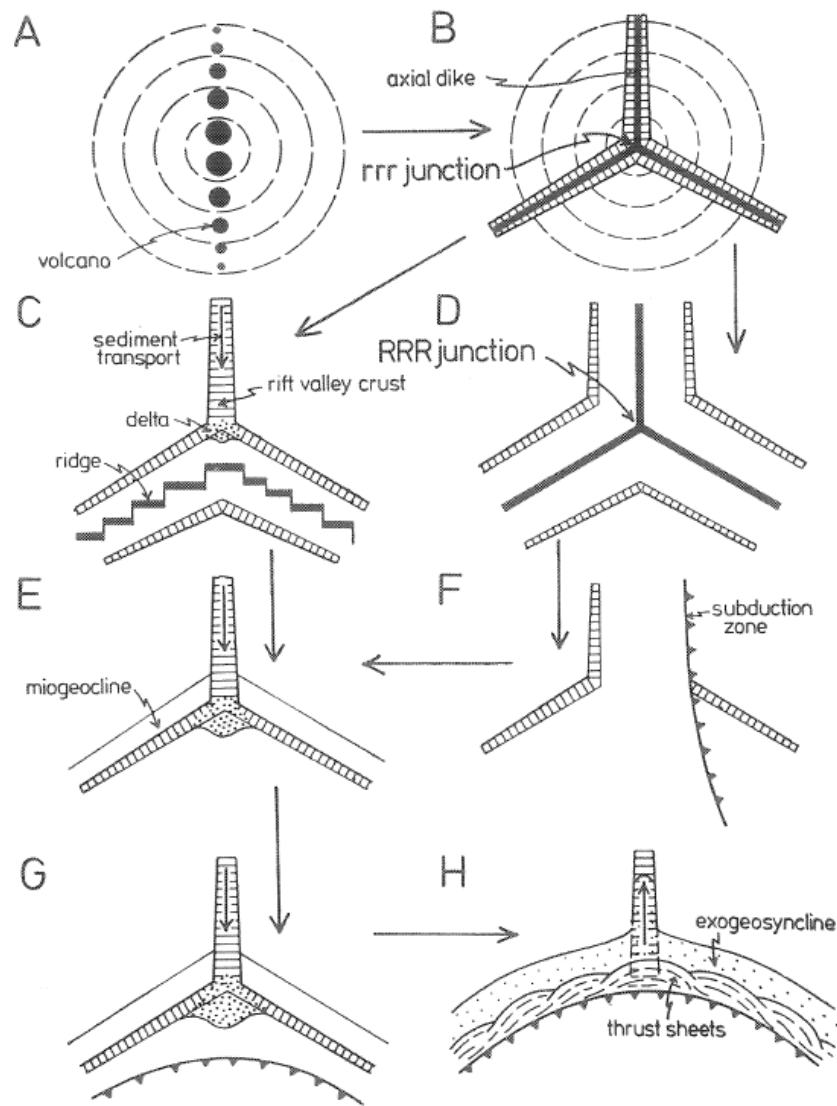


Figure 2-4. Rifting models that can be generated by the presence of a mantle plume (Burke and Dewey 1973)

2.1.3 Major Faulting

The instantaneous event mentioned in McKenzie (1978) is commonly extensional normal faulting (Figure 2-5). These can be primary controlling factors in the generation of sedimentary basins and can be separated into two categories, major faults and minor faults (Roberts and Yielding 1994). In this section only the major faulting event will be discussed.

Major faulting can be defined as large scale planar faults which cut completely through the seismogenic layer (Roberts and Yielding 1994). From the study of earthquake data and the instantaneous faulting, it has been possible to identify that deformation occurs on two different timescales. The first is the initial co-seismic and post-seismic deformation for an individual event. The second is related to much more long-term isostatic responses to repeated deformation events (Roberts and Yielding 1994).

Co-seismic deformation is directly related to the amount of footwall uplift and hangingwall subsidence a fault generates. This is strongly associated with the steepness of an individual fault plain (Roberts and Yielding 1994). The steeper the fault plain is the greater the footwall uplift is generated. If a normal fault is exactly vertical the uplift and subsidence either side of the fault would be equal (Roberts and Yielding 1994).

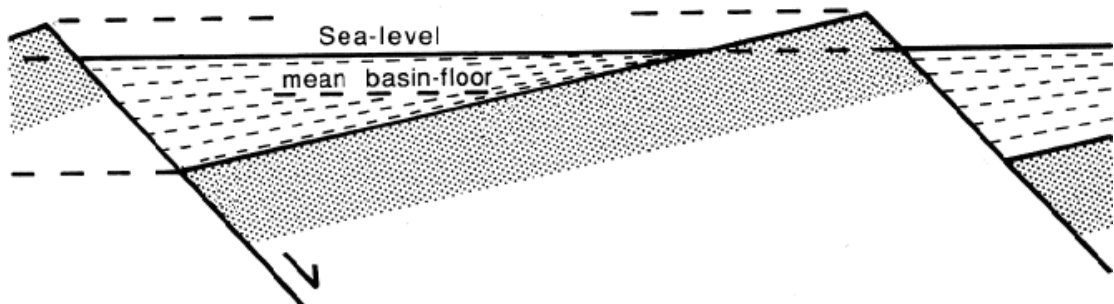


Figure 2-5. The illustration of footwall uplift and hangingwall subsidence in normal faults (Yielding 1990)

The amount of footwall uplift generally accounts between 10-20% of the throw on a normal fault, as the sediments respond in a purely elastic manner to the slip of a fault (Roberts and Yielding 1994).

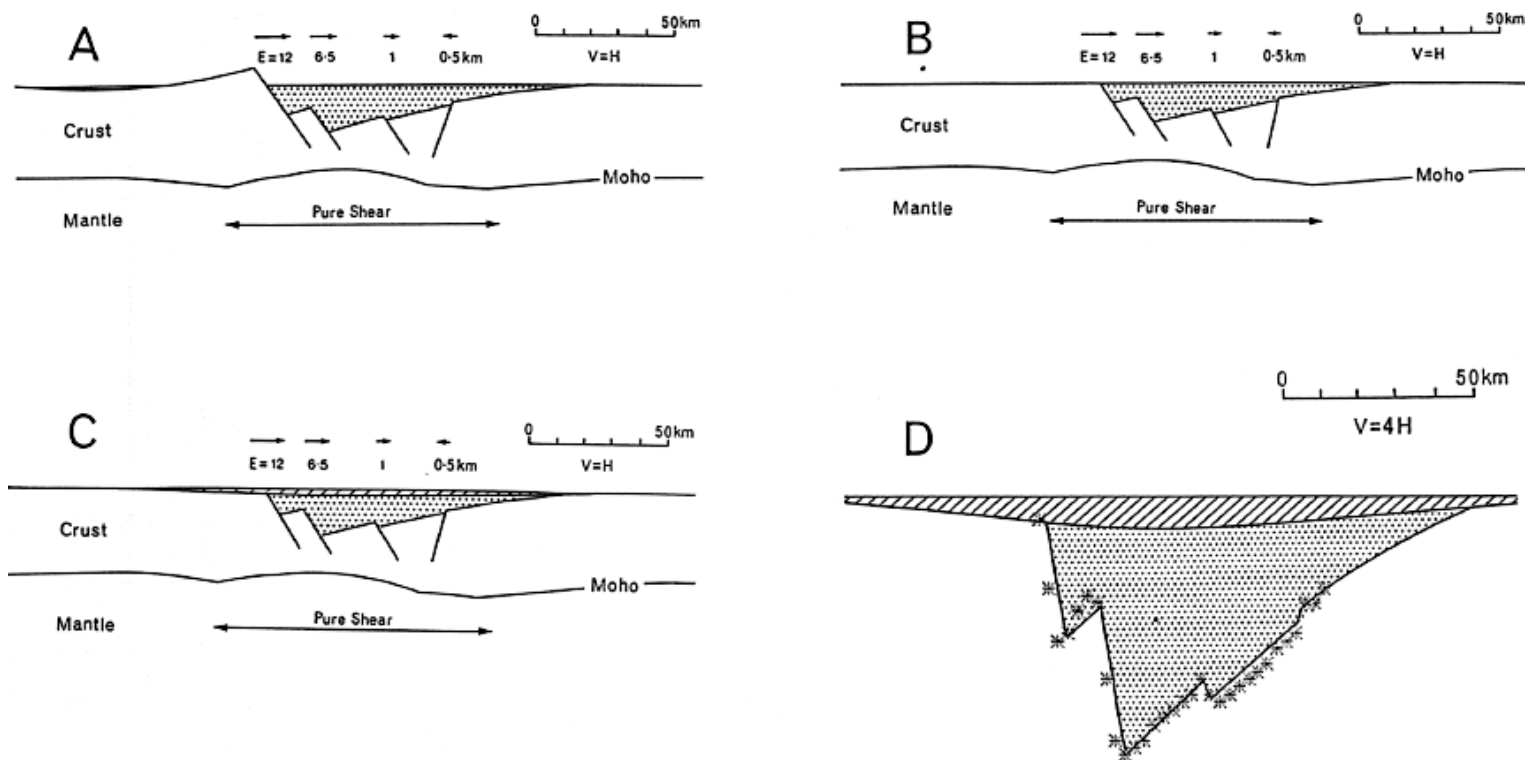
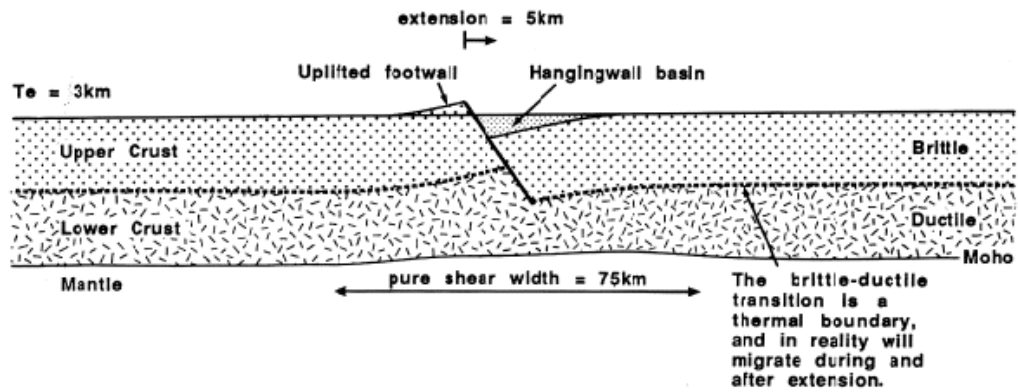


Figure 2-6. Illustration of the flexural cantilever model (Kusznir 1991)

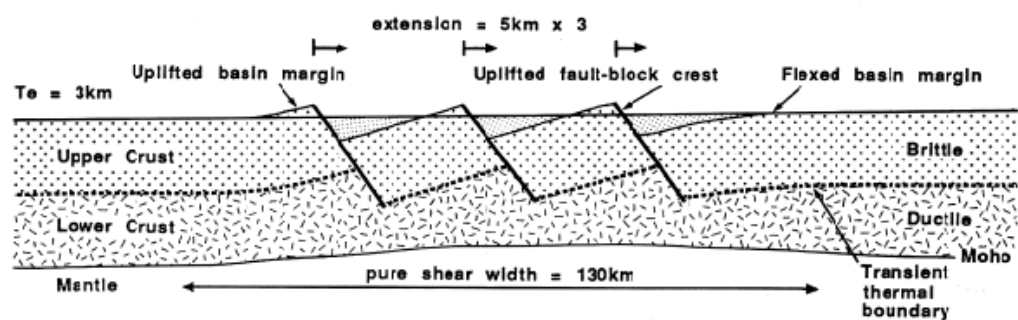
Post-seismic events relate to the elastic strain built up through faulting. This often results in post-seismic rebound. Post-seismic rebound tries to restore isostatic equilibrium within the lithosphere after a faulting event (Cohen 1981; Badley 1988; Roberts and Yielding 1994). This is achieved by trying to equalise the asymmetric, co-seismic movement across a fault. For a normal fault where the majority of the throw is related to subsidence, the area around the fault undergoes a period of uplift (Roberts and Yielding 1994). The long-term response major scale faults can be explained by the flexural-cantilever model (Figure 2-6).

This accommodates the initial syn-rift sedimentation in the rifting area, where co-seismic and post-seismic events occur along with the up-welling of the hot/buoyant asthenosphere (Roberts and Yielding 1994). Once the uplifted area begins to lose energy and the up-welling asthenosphere begins to cool, the faulted area begins to go into thermal subsidence (Kusznir 1991). This suggests an additional subsidence event which covers both the initial fault hangingwall but also the fault footwall. As erosion and subsidence engulfs the peak of the hangingwall, deposition can now begin over the crest of the fault. This deformation can also occur over a series of normal faults, such as domino faulting. This suggests that in a single fault it may be possible for one fault to deform as a footwall to one fault, but as the hangingwall to another fault, illustrated in Figure 2-7 (Roberts and Yielding 1994). This will then play a major role in the amount of asthenosphere that will rise up due to faulting.

a) Single fault model



b) Multiple fault model



c) Multiple fault model, includes erosion and thermal subsidence

(Time elapsed since rift = 150ma)

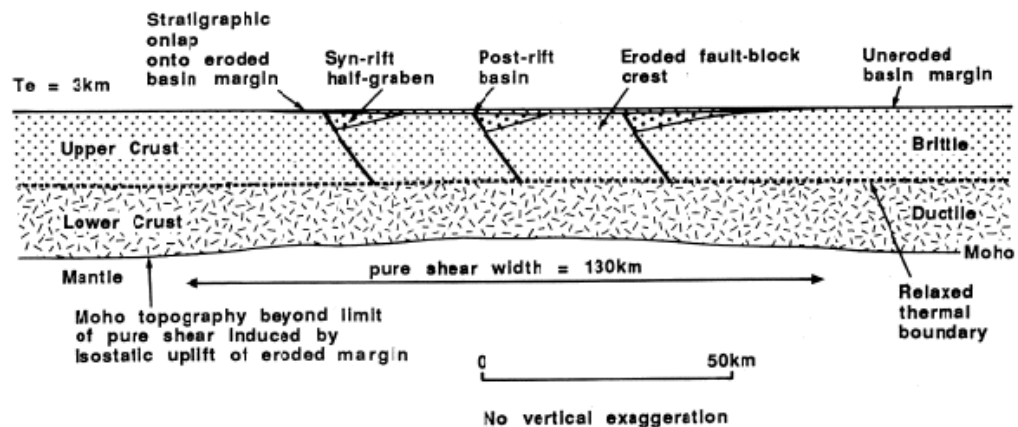


Figure 2-7. Flexural cantilever model explained within different scenarios, such as singular or multiple fault domains (Roberts and Yielding 1994)

2.1.4 Minor Faulting

Minor extensional faulting is described as faults which maybe both planar and listric in appearance and are contained within the seismogenic layer. These types of faults do not generate the same amount of topographic loads compared to the major faults, thus, isostasy is not as much of an issue (Roberts and Yielding 1994). There is, however, a significant difference between listric and planar faults.

Planar faults have generally a high dip angle and form simple structures such as horsts and grabens. Horsts and grabens form when planar normal faults form in opposite directions, but, if the faults occur with the same sense of dip they can generate structures that resemble fallen dominoes and are referred to as tilted fault blocks. Listric faults on the other hand have a sense of rotation about their slip, which results in the fault plane decreasing in dip angle with depth. These faults form where an area of detachment is down with depth and creates structures such as rotated fault blocks and roll-over anticlines.

Although the major faults account for the largest throws on faults their numbers are insignificant compared to that of the minor faults. Since minor faults significantly outnumber major faults they cannot be ignored when discussing the evolution of a rift province. The ellipse of a normal fault is described by Watterson (1986) and illustrates the lateral and vertical extent of a fault's limits (Figure 2-8). Although minor faults do not have as much throw as major faults their understanding within a rift system in terms of generation of structural highs for a petroleum system is still majorly important. It must be mentioned that any rift interpretation sees the end-product of extension, not how it evolved to look like the end product.

In an extensional province such as a continental basin, it is common for smaller normal faults to grow and interact with one another or in fact die out during the rifting event. As these smaller faults interact and link together the length and throw on the overall fault increases, thus playing a much larger role in the basin than originally thought (Roberts and Yielding 1994).

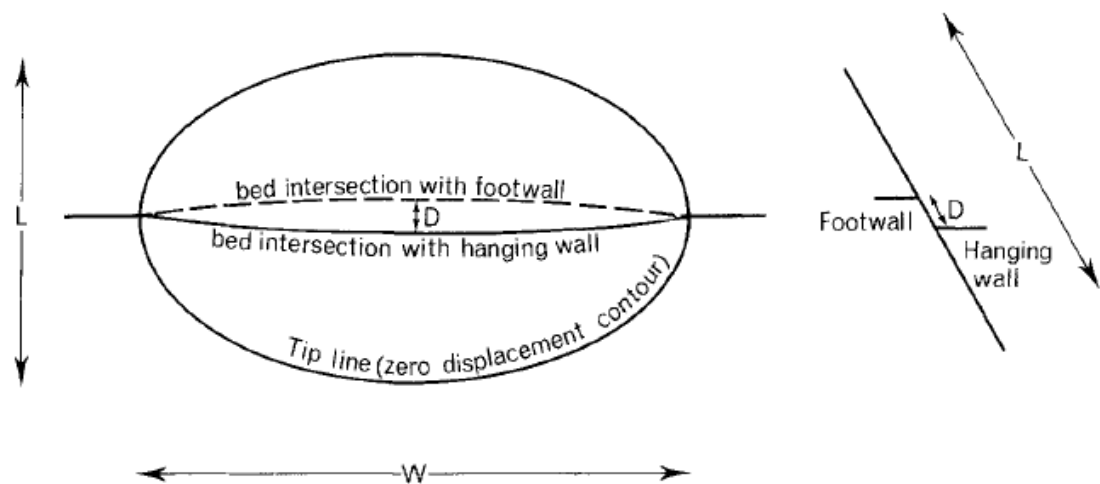


Figure 2-8. The shape and dimensions of a normal fault (Watterson 1986)

A classic example of the linkage and growth of minor faults playing a major role on determining a hydrocarbon field generation and preservation can be observed along the Strathspey-Brent-Statfjord fault system. Here it is possible to see the extent to which minor faulting can create large extensional structures, with significant throw to generate structural highs and generate basins deep enough to form kitchen areas, from which hydrocarbons can migrate from.

2.1.5 Pure and Simple Shear Topography

The result of large scale extensional faulting leads to a topography that resembles overlapping dominos or books on a book shelf. Nowhere is this better exemplified than in the western USA.

The geometry of low angle fault planes, many of which links with volcanism in an extensional belt led a Basin and Range setting to it being used as an example where low angle detachment controlled lithospheric and crustal deformation occurs (Figure 2-9).

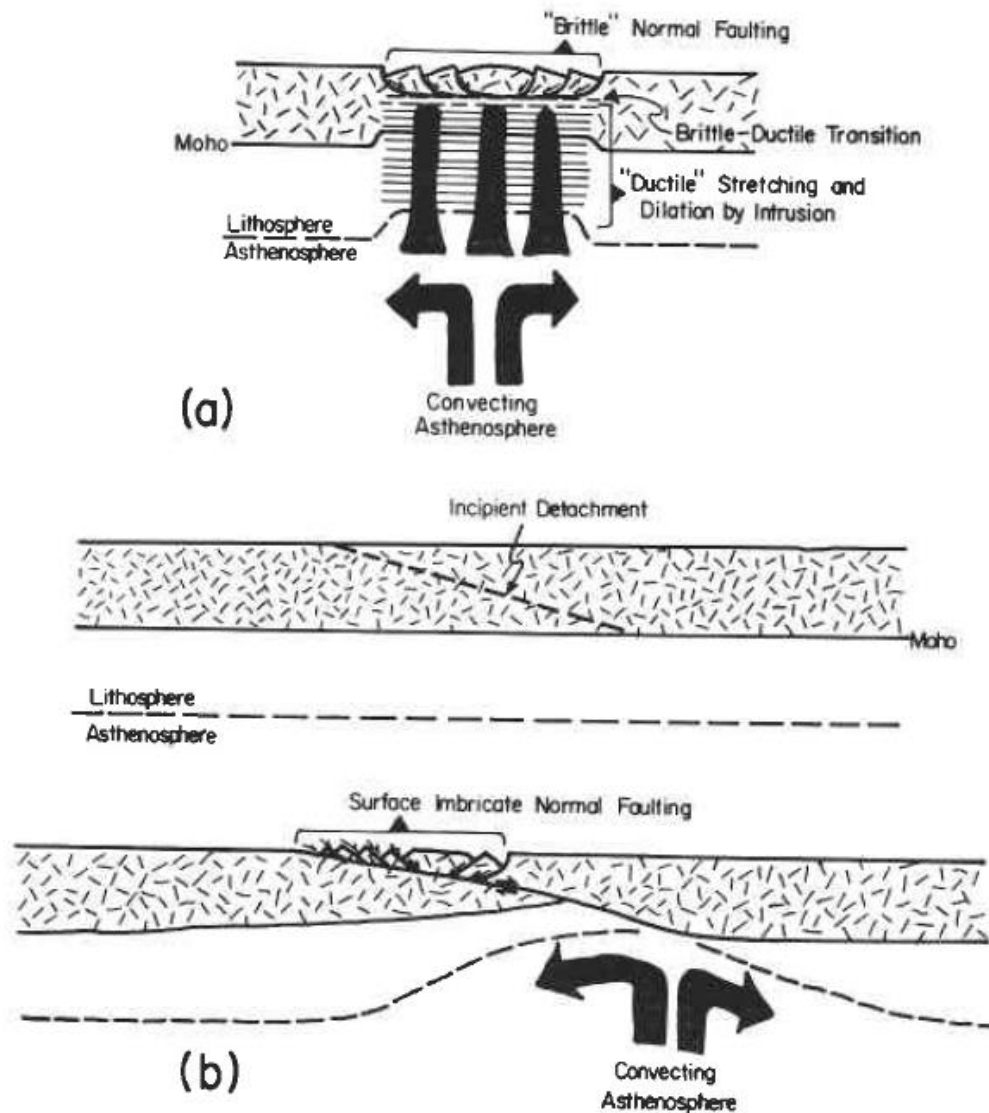


Figure 2-9. Illustrating the "pure shear" model in diagram (a) and the "simple shear" model in diagram (b) (Wernicke 1985).

This is commonly a combination of large scale faults which cut the seismogenic layer accompanied with a series of smaller scale faults which may detach upon a deep seated detachment layer (Sonder 1999).

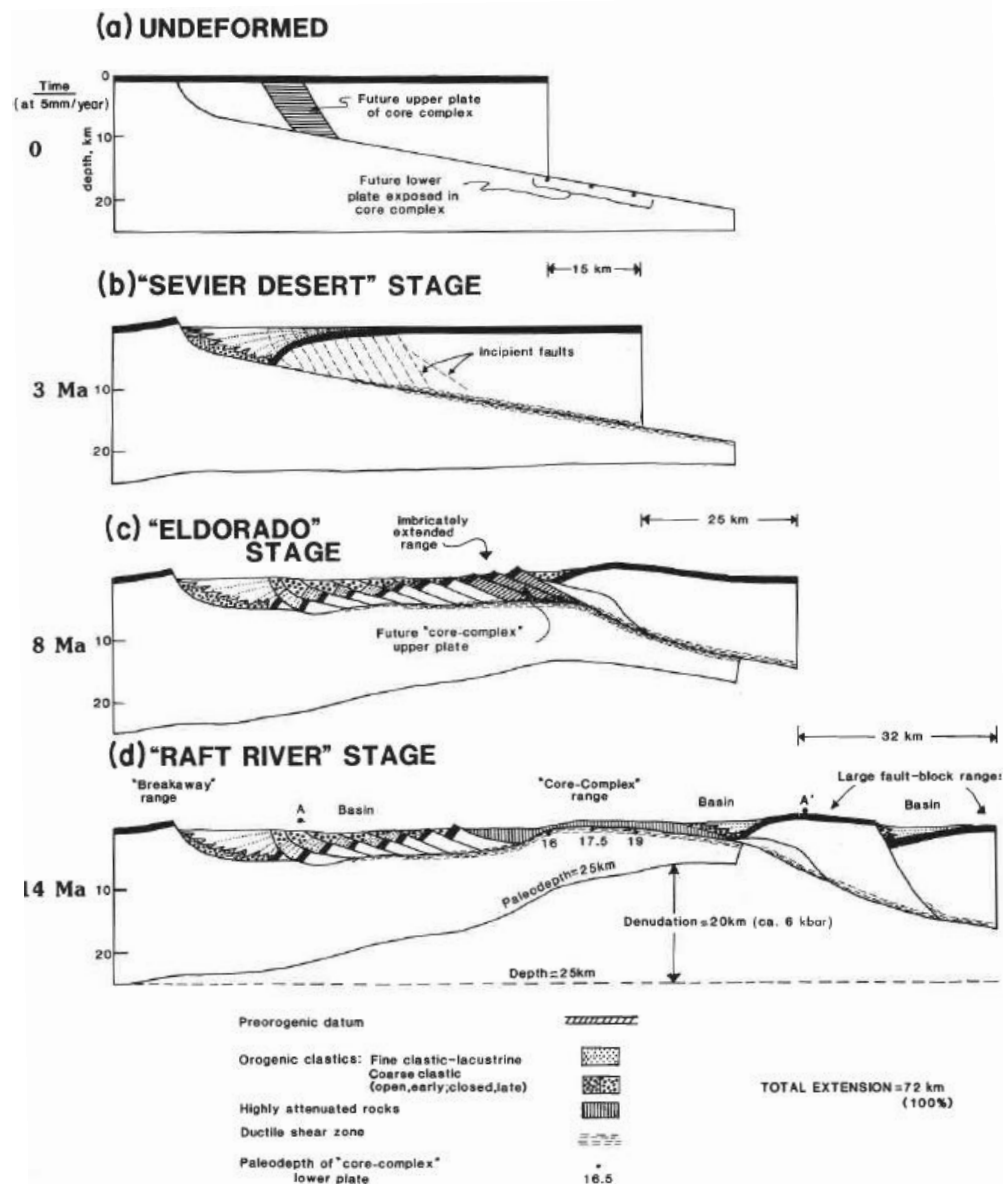


Figure 2-10. The classic Basin and Range analogue is observed in the Western United States where extension has created a series of structural features depending upon the length of time an area has been in extension. This diagram illustrates three locations within the Basin and Range evolution history that is observed in US Basin and Range Province. (a) Is an undeformed location where little or no stretching has occurred. (b) Is the initiation of a large scale normal fault that cuts deep into the seismogenic layer. (c) Illustrates the decollement of small scale planar normal faults onto the underlying detachment surface. (d) shows that the rate of extension is so great that the uplifting asthenosphere come so close to the surface and may induce magmatic activity (Wernicke 1985).

The structural evolution and interaction of both listric and planar faults is extremely important in the evolution of a rift basin. By planar faults penetrating down onto a listric slip surface or detachment zone this will

enhance block rotation and aid uplift of the footwall of many normal faults (Figure 2-10). The generation of these large rotated blocks over a thinning crust may also lead to small scale magmatism if the stretching rate (β factor) is great enough.

The generation of a Basin and Range style of extension could be of extreme importance in terms of rifting. The block rotation observed in a Basin and Range environment accounts for large movement along low angle normal faults. It could further explain the presence of magmatic materials in post rift stages or in between rifting phases. The generation of horst and graben structures that detach on a deep seated decollement zone could be directly related to a Basin and Range environment (Stewart 1971).

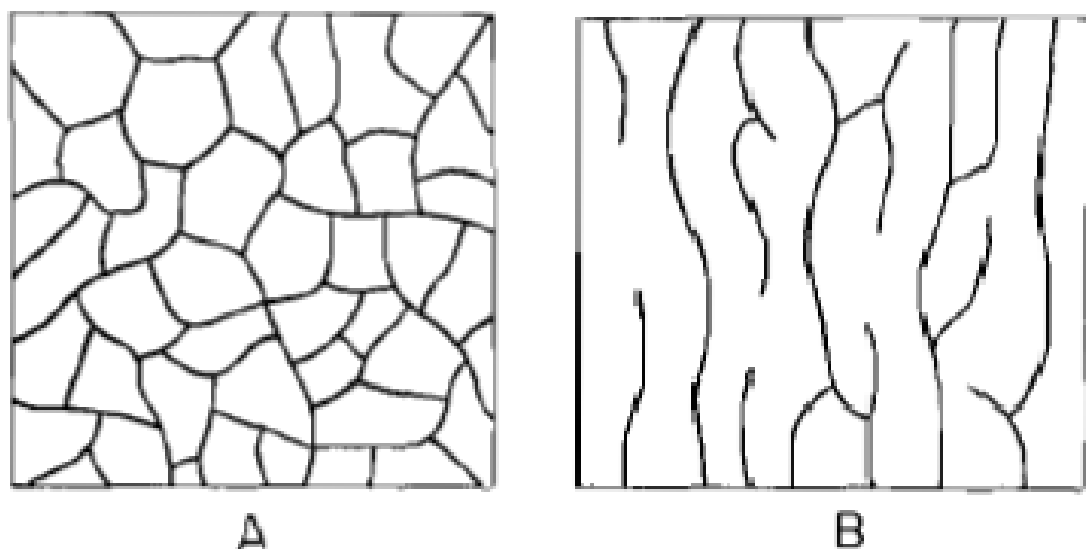


Figure 2-11. Illustration on fault patterns from varying extensional models. (A) Illustrates the fracture pattern developed by a radial fracture pattern. (B) illustrates the fracture pattern relating to a basin and range style of extension (east-west) (Stewart 1971).

A product of basin and range style faulting is the strong alignment of normal faults from the faulting event (Figure 2-11). By having a strong alignment of normal faults it makes it more likely for faults to link and grow. This is essential in any hydrocarbon basin as it is the primary factor in determining

structural traps and source kitchen areas. The evolution of planar normal faults in a brittle crustal environment which detach on to a lower plastically deformable layer often represented by large scale listric faults could be essential in developing a hydrocarbon basin (Stewart 1971). The interaction and linkage of brittle and ductile deformation within the Earth's crust as normal faults at depth is important in defining structural features within a basin.

A basin and range evolution can be compared to that of a rift basin as both are large scale plate tectonic processes and both of these systems are bound laterally by large scale extensional faults. The primary difference being that a rift basin is bound by planar faults and a basin and range by listric fault(s). The rift basin will create a series of horst and grabens within the rift shoulders with smaller scaled planar fault in areas of high stretching, whereas, a basin and range locality will produce evenly spaced planar faults that will detach on the under lying listric fault(s). As stretching continues with both rifting events, tilted fault blocks will appear in the rift basin to accommodate the additional stretching. The basin and range will also produce rotated fault blocks, but these will eventually become over rotated and appear at shallow angles, but with significant offset. This dissimilarity in deformation between systems can lead to significant variations in structural features being generated between basins. A strong structural understanding of a basin's evolution and type as noted in this section can be the difference in determining the types of structural patterns that are likely to be present within a set data type. Although the two types of basins are similar in the early stages of evolution a Basin and Range environment will eventually become so stretched that the metamorphic core complexes are exhumed which is the key difference between the two basin types.

2.2 *Fault Growth and Fault linkage of Individual Faults*

The effect faulting has in the North Sea can be observed on a small scale in terms of flow between grains and on a much larger scale, in terms of determining the deposition of the sediments and forming structural traps. The role of fault growth and linkage in the basin generally refers to the much larger scale and relates to fault migration and basin formations, but also effects fluid flow between rocks at the fault plain.

Fault linkage can be described as the amalgamation of two or more previously isolated depo-centres over which migration of deposition move to the centre of the new longer strand, as shown in Figures 2-12 and 2-13 (McLeod 2000). Work has been undertaken by McLeod (2000) on the Strathspey-Brent-Statfjord (SBS) fault array in the Northern North Sea, East Shetland Basin, and shows that the faults grow through radial propagation and linkage of fault segments. This work, along with that done by (Dawers and Underhill 2000) shows vast variations within the fault length diagrams for individual faults. However, when the sums of the fault arrays are added together, a smooth curve showing a decrease in displacement the further away from the depo-centre maximum is observed. In the SBS fault system, it is possible to see two major groups of faults. One set are the long lived faults which relate to the growths of the major half graben structure, whilst, the second set are much smaller and are found in the hanging wall of the major fault (McLeod 2000). These smaller faults die out relatively early into the formation of the rift. It is possible to interpret these faults as the abandoned fault tips, which once defined the sub-basins before the faults became hard linked (Dawers and Underhill 2000; McLeod 2000). The growth and linkage of the faults in terms of activity and cessation generally trend from south to north in the Statfjord fault and can be interpreted to the fault sequence as a whole (Dawers and Underhill 2000). This is shown by the use of isopach

maps of the Oxfordian-Kimmeridgian, which indicate subsidence in the southern part of the Statfjord fault and then the development of a new depocentre to the north east (Dawers and Underhill 2000). The growth of these faults occur due to an increased activity around the fault tips, which results in the incorporation of the fault tip as a part of the northward migrating fault until it becomes linked with the next major fault system (Dawers and Underhill 2000).

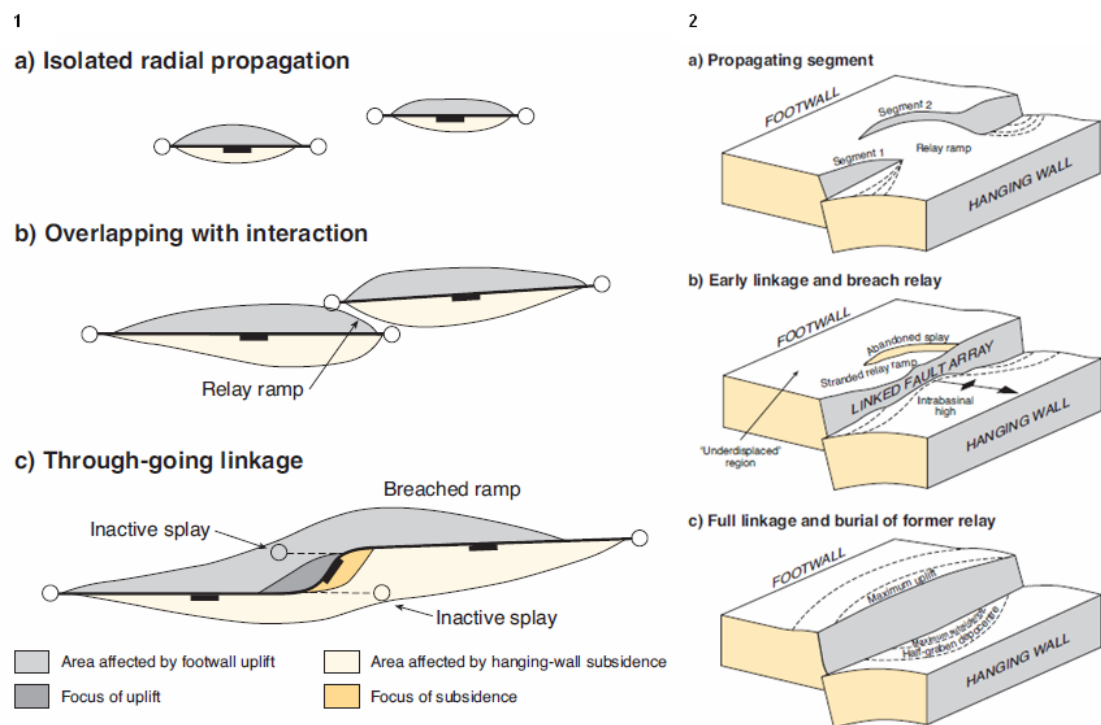


Figure 2-12. Illustrating the method of growth and eventual linkage between multiple faults to generate a much large fault system (Fraser 2003). In plan view (1) it possible to see the overlapping of two individual faults prior to linkage. The 3D model (2) then illustrates how the relay ramp location that was once a structural low is uplifted to generate a structural high.

Strathspey-Brent-Statfjord release faulting can play a major role in controlling petroleum migration in and around a hydrocarbon field. A release fault often forms due to the variation in displacement along a listric normal fault (Destro 1995). These tend to form adjacent to the initial "parent" fault and die out into the hangingwall or footwall (Destro 2003). The majority of release faults form as a direct result of bending stresses in

listric normal faults and accommodate the increase in throw along a fault (Destro 1995; Destro 2003).

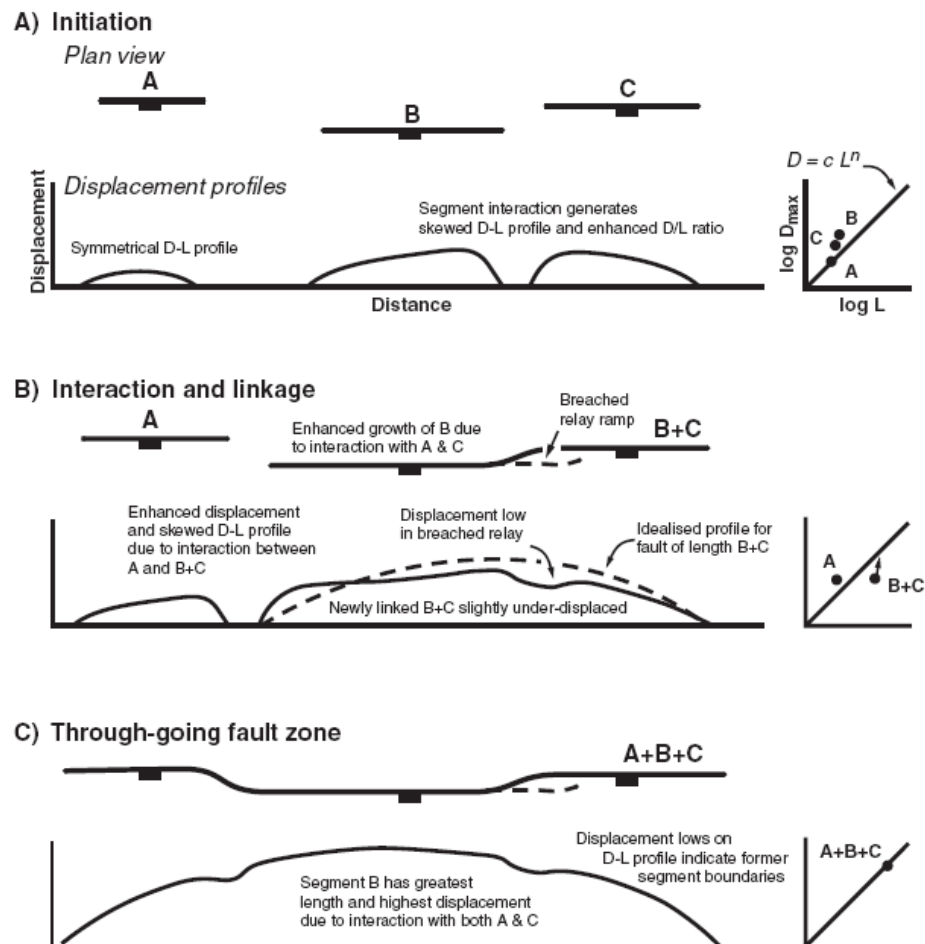


Figure 2-13. Illustration of fault growth and linkage and the resultant generation of accommodation space (Gawthorpe 2000)

An ideal illustration of a hangingwall release fault is demonstrated in Figure 2-14. Although the majority of research in release faulting has been undertaken in hangingwall faults it is still plausible for this to occur in the footwall of faults as the uplift which occurs in the footwalls may also illustrate similar structural patterns (Destro 2003). Release faults do not cut normal fault planes or connect distinct normal faults, they form solely to accommodate differential fault movement and die out in the hangingwall or footwall of normal faults (Destro 2003).

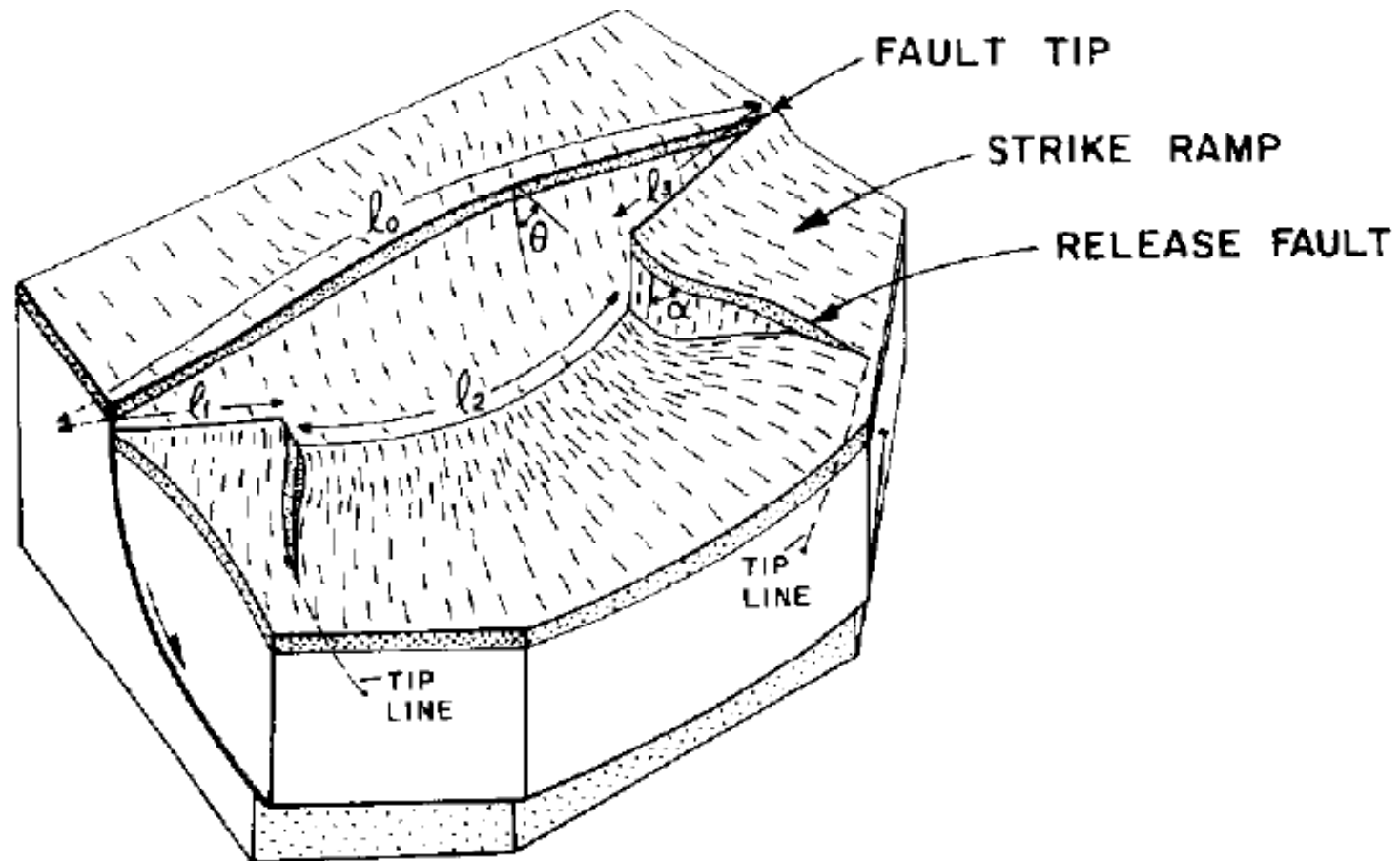


Figure 2-14. . Illustrating the structural geometry of a normal fault with hangingwall release faults, to accommodate hangingwall subsidence (Destro 1995).

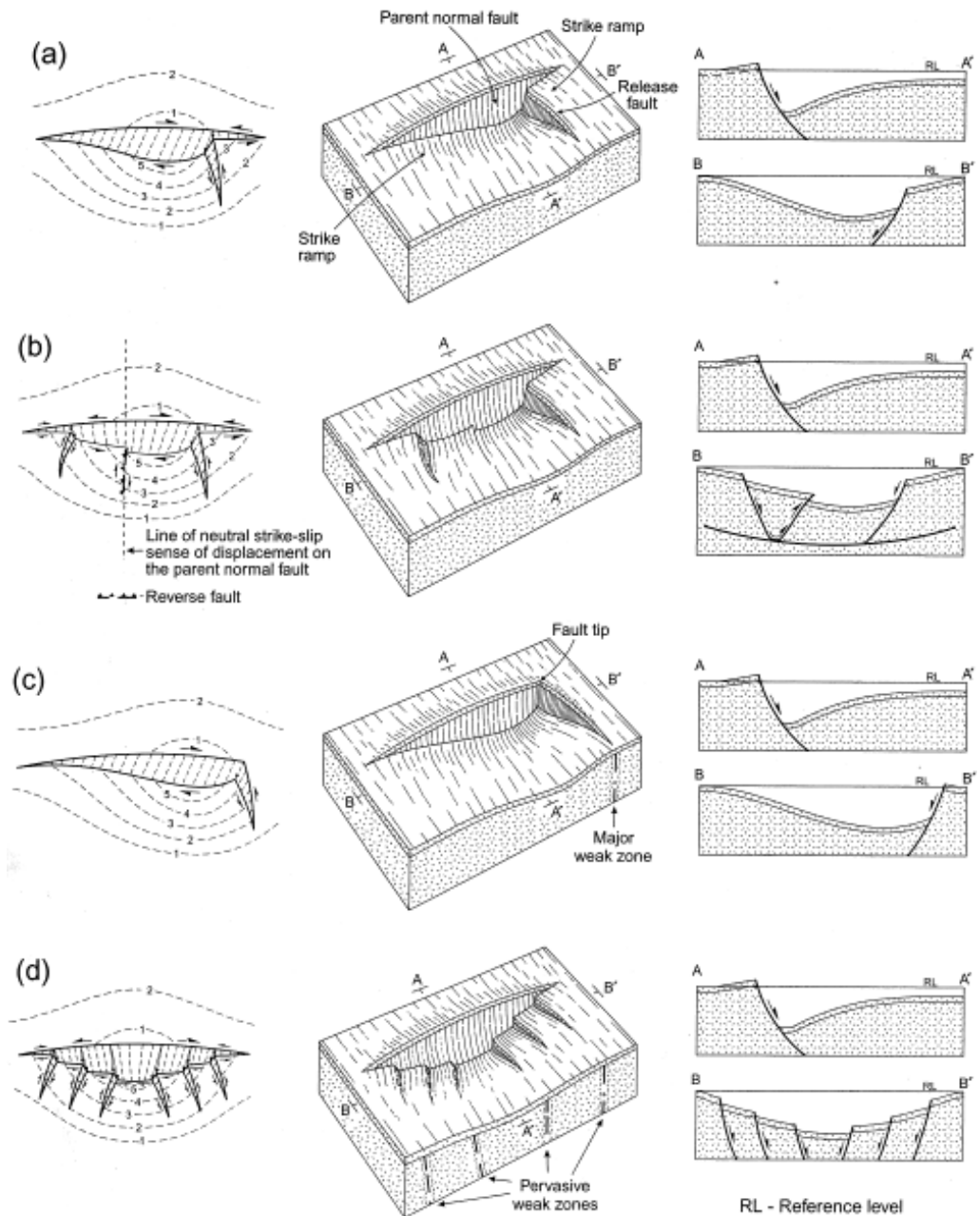


Figure 2-15. The possible structures that can be formed as a direct result of release faulting. The contours are to show height with 1 being the highest and 5 the lowest (Destro 2003).

Some of the subtle structures that can form due to release faulting and are illustrated in Figure 2-15. This illustrates that the release faults form to accommodate the large offset that is often observed towards the centre on major normal faults. The illustrations in Figure 2-16 highlight that the shape of the “parent” fault is directly represented in the orientation of the

associated release faults. The Figure 2-16 illustrates that a fairly straight fault, with minimum curvature will form release faults which are almost perpendicular to the parent fault. Whereas the more curved the parent fault is the more oblique the release faults will form relative to the parent fault (Destro 2003).

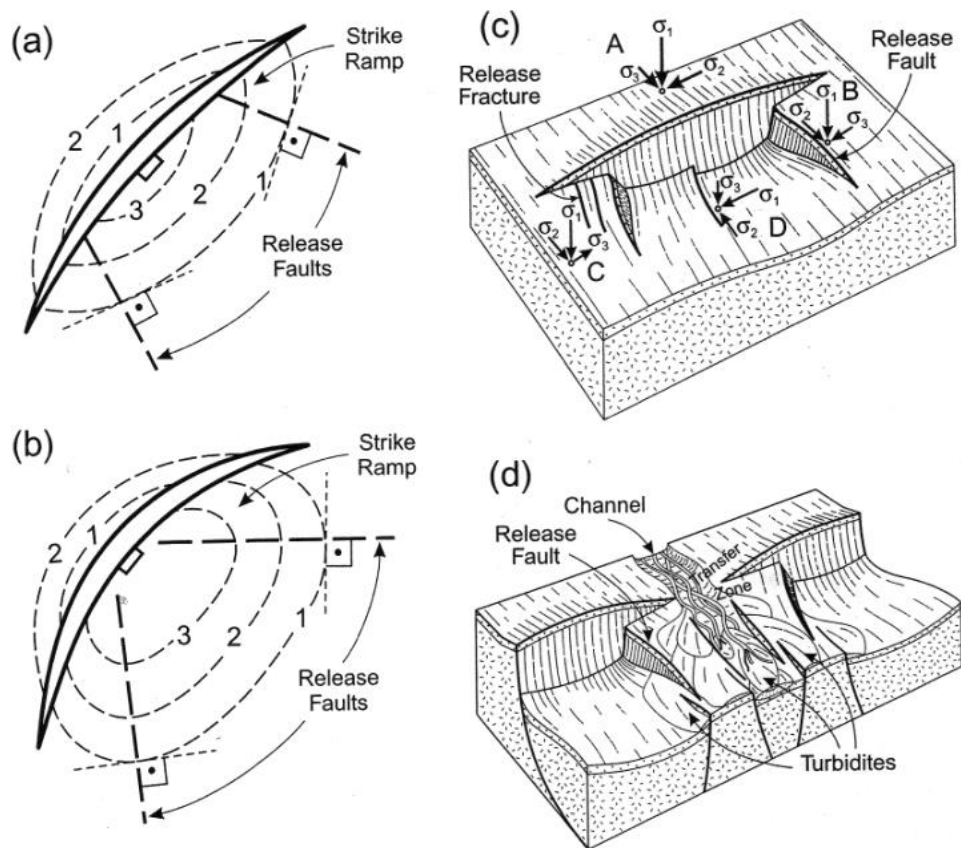


Figure 2-16. The orientation of release faults relates back to the geometry of the initial parent fault as shown in A and B. The greater curve on the parent fault will illustrate a more oblique release fault pattern. The displacement and orientation of release faults can also play an important role in forming channels and turbidite systems within the extensional basin (Destro 2003).

With the faults illustrated, it is clear to see that the enhancement of a hangingwall deposition centre or increase in footwall uplift can play a major role in reservoir interpretation. This could range from an increase in higher quality reservoir rock, to greater erosion of the reservoir rock respectively.

These faults may also play a major role in basin dynamics, as they can influence hydrocarbon migration and the development of turbidity currents to fill distant depo-centres (Destro 2003). The sealing capacity of these faults will also play an important role in hydrocarbon migration. If the faults are sealing then this may lead to reservoir compartmentalisation or blocking of hydrocarbon migration pathways. Although these ideals are primarily based in the hangingwall sides of faults, the ideas have recently extended into the footwall, where similar structures albeit with smaller throws also exist.

2.3. *Controls on Sedimentation in a Rift Province*

Now that a continental rift system has been defined as an elongate extensional tectonic event in which the entire lithosphere has been modified, it is possible to identify individual rifts and how they affect sedimentation (Lambiase 1995; Olsen 1995).

An individual rift province can be defined as a fault bounded basin in which footwall uplift and hangingwall subsidence occur. This generates structural features and accommodation space during a phase of extension (Lambiase 1995; Schlische 1999). The generation of a rift province and the development of basin architecture is strongly influenced by the complex interaction and evolution of fault propagation, fault linkage and the subsequent change in the drainage pattern within a rift basin (Gawthorpe and Leeder 2000). A rift province can be separated into three main structural phases, which determine sedimentation and structural architecture. These are the pre-rift, syn-rift and post-rift sequences, each of which has an individual character to sedimentation and structural tendencies (Prosser 1993). The primary controls of sedimentation in a rift province depend upon three factors;

accommodation space, sediment influx and water depth, with the final factor being heavily influenced by climate.

2.3.1 Pre-Rift Sedimentation and Controls and Architecture

Pre-rift architecture is commonly composed of basement material and the most recent set of lithified sediments that were deposited prior to the rifting event. This description indicates that the pre-rift environment is not driven by tectonic events, such as faulting, thus structural features are sparse. Any structural features that are present during the deposition of pre-rift sediments are generally inferred to have occurred in an earlier rifting event. This can be observed in the Northern North Sea where earlier Permo-Triassic highs are generated and are not completely buried, and thus determine deposition patterns in the Upper Jurassic rifting event. As most of these sediments deposited in this phase of rifting are unfaulted, the majority of the beds are deposited evenly over the basin area with thickening patterns deduced from any underlying structural features.

The controls on sedimentation through this phase are purely related to sediment flux and climate. If sediment supply is low then the current accommodation space will fill in over a long period of time, but, if the sediment influx is high, then the accommodation space will fill much quicker and could lead to the cannibalisation of already deposited sediment. The climate within the pre-rift also has a determining factor on sedimentation. Within environments that are dry and have a low water level it is possible to see that the majority of sedimentation is related to alluvial fans from existing highs. In wetter environments fluvial channels or deltas maybe the driving factor in sedimentation (Fordham et al. 2010).

2.3.2. Pre-Rift to Syn-Rift Transition

The boundary between the pre-rift and syn-rift can be identified as a sudden change in sedimentation. With the onset of rift come the generation of major structural features such as rift shoulders and depo-centre generation. The generation of rift shoulders plays a major role in determining sedimentation within the rift province in the early stages of the syn-rift stage (Gawthorpe, Sharp et al. 1997). The uplift and subsequent tilting of the shoulders generates a set of relative highlands which can deflect fluvial channels and clastic input into the basin area. This dramatically reduces the amount of sediment flux into a basin and thus affects the sedimentation within the newly generating half-graben.

The generation of the half-grabens associated with rift provinces usually affect the sedimentation pattern by a rapid increase in accommodation space. This subsequent drowning of the pre-rift strata and reduction of clastic input into the rift basin and may result in lacustrine deposits to form throughout the initial stages of syn-rift tectonic phase if water is readily available.

A key structural feature that is often found within the pre-rift to syn-rift transition is a doming event. This doming event directly relates to an underlying upwelling mantle plume which is often the precursor to active rifting. As seen in the North Sea (Underhill & Partington. 1993) the uplift relating to this doming event can lead to extreme erosion and sediment reworking.

2.3.3 Syn-Rift Sedimentation and Controls and Architecture

The majority of the structural features relating to a rift system are generated during the syn-rift sedimentation. The syn-rift is determined by the initial sign of faulting and rupturing of the continental crust by extensional processes. It is this faulting which leads to the generation of a rift system, which in-turn produces a series of structural features associated to the rifting. As mentioned earlier, a rift province is fault bounded, and it is this major basinal fault, which generates the first two structures in the basin. The two major structures generated by the extensional faulting are the rift shoulders and the adjacent basin depocentres (Lambiase 1995). The rift shoulders define the outermost limit of the rift and undergo footwall uplift. Often the rifts are asymmetrical and only one bounding fault is present. This leads to the generation of a half graben structure, but, if two bounding faults are present opposite to one another a full graben structure can form (Lambiase 1995). It is these half grabens where the major depo-centres are located where the greatest amount of accommodation space is generated (Schlische 1999).

The deposition within this newly generated accommodation space is purely dependent on sediment supply and climate. During the syn-rift sedimentation phase the faults are continuously moving and thus continuously generating accommodation space. If sediment flux is outpaced by accommodation space throughout this faulting phase then the basin will eventually end up underfilled, when the post-rift rift phase initiates.

The generation of this accommodation space directly leads to regional uplift of the rift shoulders and the basin area. This isostatic rebound is directly related to the generation of accommodation space in the hangingwall as, the accommodation space is filled with generally less dense material

(sediment/air/water) than that of the existing pre-rift and basement rocks (Lambiase 1995). This uplift of the rift shoulders may also be eroded, but due to the tilted block shape, the drainage pattern of sediment maybe deflected away from the rift basin (Roberts and Yielding 1994). There may also be local sediment input into the hangingwall directly from the footwall. This commonly occurs in the formation of alluvial fans, especially in dry climates.

In areas where little or no axial drainage is present, sedimentation is dominated by alluvium deposits (Figure 2-17). This is a direct response to climate conditions and drainage patterns. In wetter climates where axial drainage is present alluvial deposition do not dominate sedimentation, but, where the climate is more extreme and is significantly dryer alluvial deposits dominate sedimentation (Fordham et al. 2010).

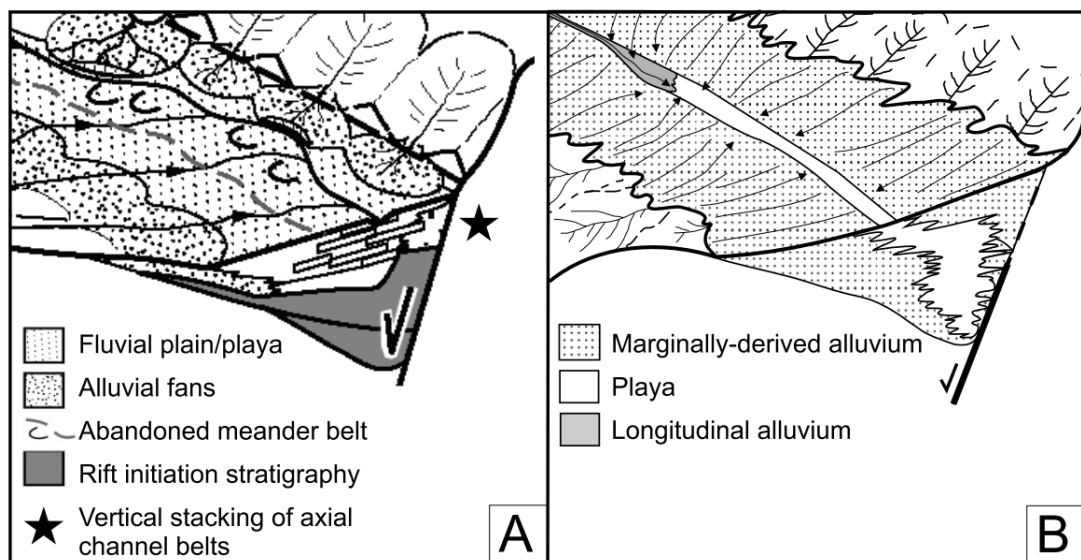


Figure 2-17 Illustration of varying alluvial fan depositional models. A) Highlights the development of alluvial fans in a late stage syn-rift infill, whereas, B) shows the progressive infill of syn-rift accommodation space by marginally-derived alluvial deposits (Fordham et al, 2010).

With the rift basin areas of the half grabens it is possible to generate a series of rift parallel faults, which in-effect generate a series of pseudo-basins

(Lambiasi 1995). Rift parallel faults are generally formed due to the continual stretching of the lithosphere beyond the initial faulting event (McKenzie 1978). The increase stretching factor leads to the increased demand of the normal extensional fault. These faults can lead to the burial of sediments into the oil and gas windows, if the stretching factor is high enough. Not all of the faults within the basin are parallel to the bounding faults. It is possible to get perpendicular faults which are termed transfer faults. The generation of transfer faults can produce a four sided, fault bounded basin (Lambiasi 1995). Transfer faults are often generated to aid in either uplift or subsidence. Transfer faults are generally found in the basinal areas opposed to the uplifted areas.

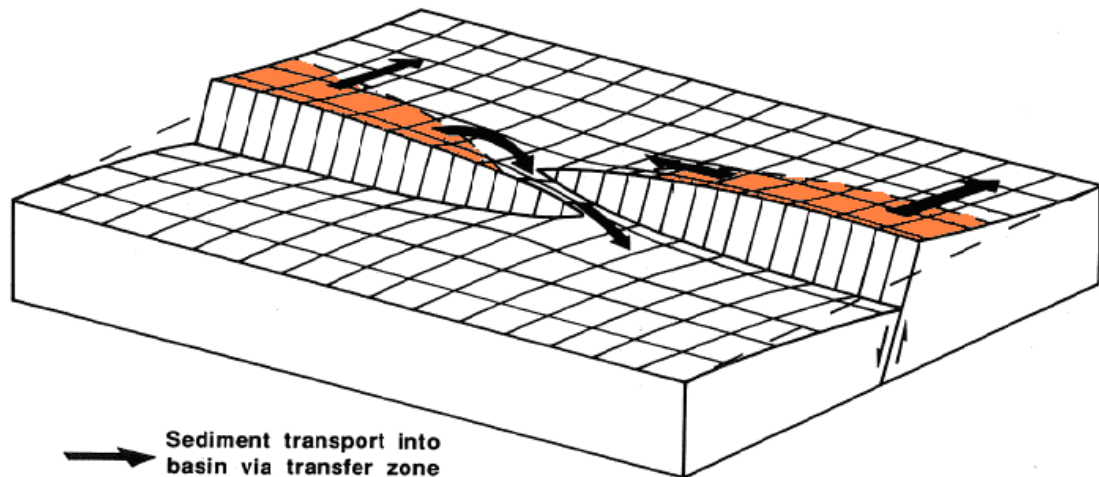


Figure 2-18. Sediment distribution at a relay ramp (Roberts and Yielding 1994)

The main process of sediment supply down-dip of the fault scarp is through relay ramp locations (Gawthorpe 1993). Relay ramps occur where fault tips are within close proximity and act as a sediment transfer zone due to their low lying structural topography (Figure 2-18). These sediments are generally fluvial or alluvial in nature. Again the location of these relay ramps are depicted by fault growth and linkage. If two faults grow enough and a relay ramp becomes breached, then the topographic low evolves into a structural high and deflects the sediment transfer zone laterally along the fault length

(Figure 2-19). The growth and linkage of faults naturally lead to an increase in fault throw. This throw and potential loading of the hangingwall will generate block rotation to the associated footwall.

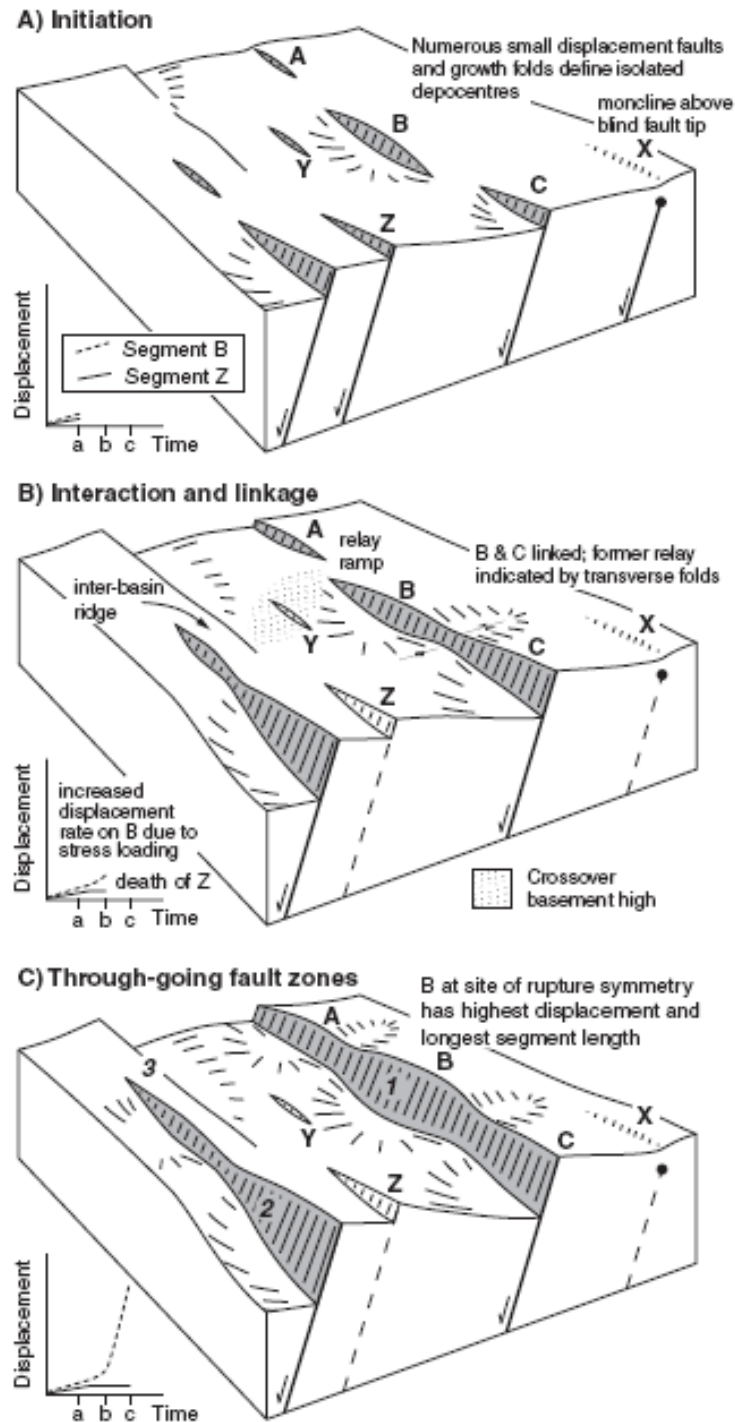


Figure 2-19. The evolution and linkage of rift parallel faults and the subsequent sedimentation (Gawthorpe and Leeder 2000)

The latest stage of syn-rift structures generated in a rift system is fault block rotation. Fault block rotation can heavily influence sedimentation dispersal and depo-centre locations. The rotation of normal faults causes footwall uplift on the smaller scale rift parallel fault which again can generate erosion and influence sediment dispersal. The uplift may also reduce the amount of accommodation space available due to the localised uplift relating to the rotation of the rift parallel fault block. These sediments are more likely to be deposited laterally along the rift rather than down-dip towards the axis of the basin. Although some of this sediment must migrate down the fault scarp, the majority of the eroded material is transported away from the footwall towards depo-centres in subsequent hangingwall synclines towards the rift shoulders.

An important factor within the syn-rift phase of deformation relates to the environment prior to rifting. It is possible through rifting that an environment can transform from terrestrial to marine due to extension. This dramatic change in environment will have a huge effect on sedimentation and the dominant sedimentation process. If an area is located within an arid environment prior to rifting the primary sedimentary process is alluvial fans from existing structures and the small scale drainage rivers. If this environment was then transformed into a marine dominated location, the transition from one to the other will also be recorded within the sedimentary record. The influx of fluvial sediments, which may progress into deltaic setting before being drowned and onset of marine based sedimentation will be recorded.

2.3.4. Syn-Rift to Post-Rift Transition

The transition from syn-rift sedimentation to post-rift sedimentation is commonly dominated by a single truncation event. The primary control on the development of an unconformity within the rift province is directly related to the change of extension from active fault controlled stretching to the initiation of thermal subsidence (Kyrkjebø 2004). This generates a tectonically influenced onlapping onto the underlying syn-rift sediments, due to the alteration in depocentre location; from locally fault derived depocentres to the main regional axial depocentre location (Figure 2-20). The unconformity type is directly dependent upon the structural location within a rift province (Kyrkjebø 2004).

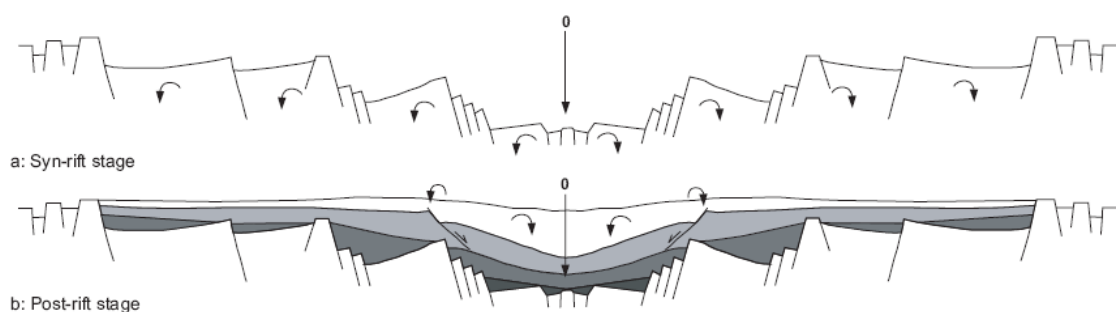


Figure 2-20. Illustrating the change from the syn-rift active stretching to thermally driven subsidence in the post-rift setting (Kyrkjebø 2004)

In the platform areas of a rift province which are commonly depicted as the rift shoulders a clear angular unconformity is present, where the tilted footwall has been eroded away due to either submarine or subaerial exposure as illustrated in Figure 2-21 (Kyrkjebø 2004). Within the half graben and rift margin areas, which are normally rift parallel fault, multiple phases of block rotation or sea/ lake level changes, generates a series of composite unconformities, which merge into one major unconformity.

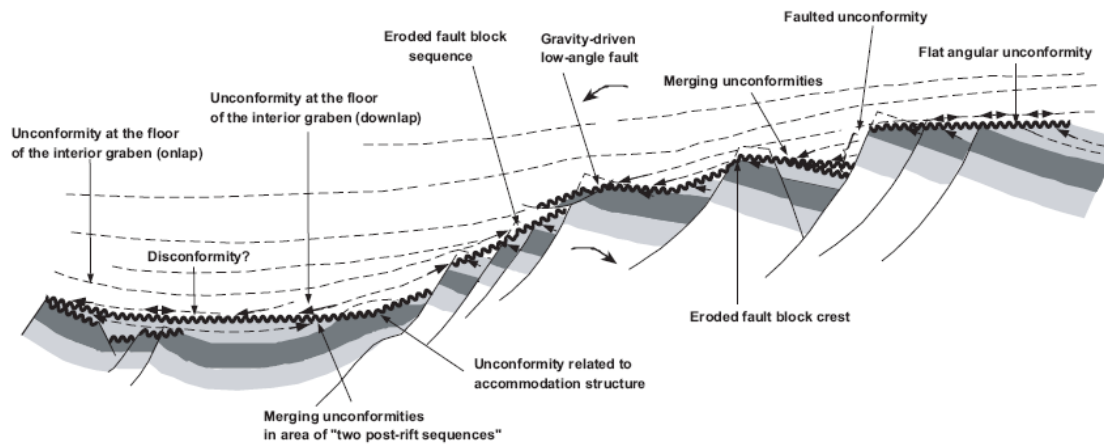


Figure 2-21. The generation and varying unconformity types within a rift province (Kyrkjebø 2004). Areas in grey indicate the underlying pre-rift sediments that have been cut by the unconformity in black.

It is within these areas that particularly deep levels of erosion may occur, depending upon the rheology of the sediments. This similarly occurs by the rotation bringing the sediments up to potentially a subaerial environment and the erosion of the fault crest (Kyrkjebø 2004). The subsequent erosion of the fault crest leads to the deposition of the eroded material into the subsequent boundary fault hangingwall located behind the rift parallel fault (Roberts and Yielding 1994). Within the basin floor of the rift province a disconformity is more likely to form as faulting and uplift is less intense (Kyrkjebø 2004).

2.3.5 Post-Rift Sedimentation and Controls and Architecture

The post-rift architecture of a rift province is similar to the pre-rift structures as no tectonic movements take place during this phase of rifting. The post-rift phase, solely relates to the thermally driven basinal sag related to the rifting event. As the lithosphere slowly begins to sink over the axis of the rift a large saucer-shaped depression occurs over the entire basin. This

prolonged period of subsidence leads to the eventual drowning of many of the structural highs generated in the earlier syn-rift faulting event.

The change to thermal subsidence does not however mean the termination of accommodation space generation, although the focus for subsidence changes onto a more regional scale, rather than a localised driven subsidence in the syn-rift. Now that the rift axis is the focus for subsidence, a basin wide tectonically driven onlap surface is developed on the underlying syn-rift sediments (Kyrkjebø 2004).

This subsequent onlap and increase in accommodation space leads to the drowning of many if not all of the structures that were created during the syn-rift extensional phase (Figure 2-22). This can only happen if sediment input does not decrease. In some instances it may be possible for sediment influx to increase due to the eventual drowning of the plateau areas, or by external forces causing uplift and erosion into the already existing rift basin.

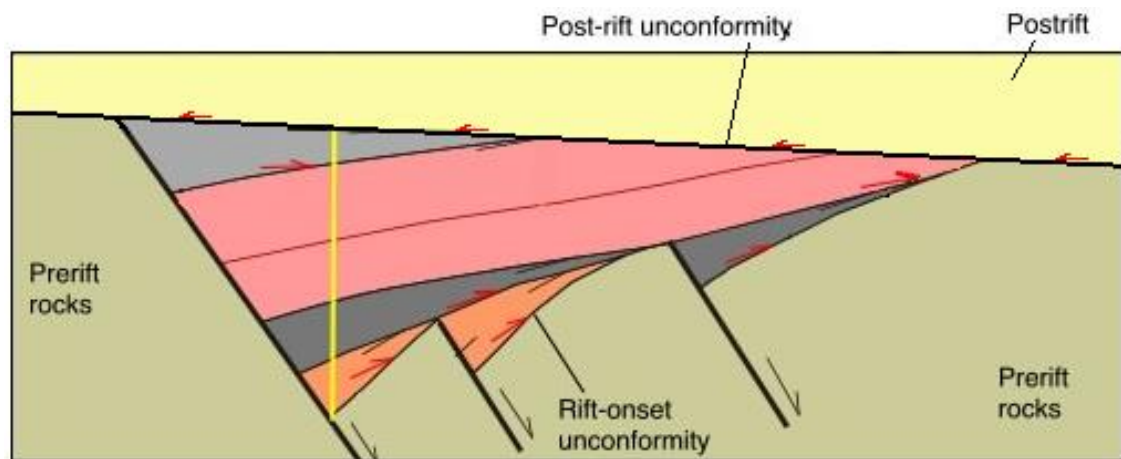


Figure 2-22. Illustrating post-rift on-lap and infill (Schlische 1999)

2.4 Rift Controls on Petroleum systems

The trapping and production of hydrocarbons rely on six major petroleum system elements being successful; these are source, migration, reservoir, trap, seal and timing. Without all of the jigsaw pieces being in place, it will not be possible to produce hydrocarbons from the subsurface. The role of fault growth and fault linkage plays an important role in all six elements mentioned above.

2.4.1 Source

The source is one of the key elements of any hydrocarbon system, as it is here where the production of hydrocarbons occurs. For the source rock to reach the maturation window in the North Sea, there has to be another force acting than simply burial subsidence. This is where faulting plays an important role in determining a source rock kitchen area.

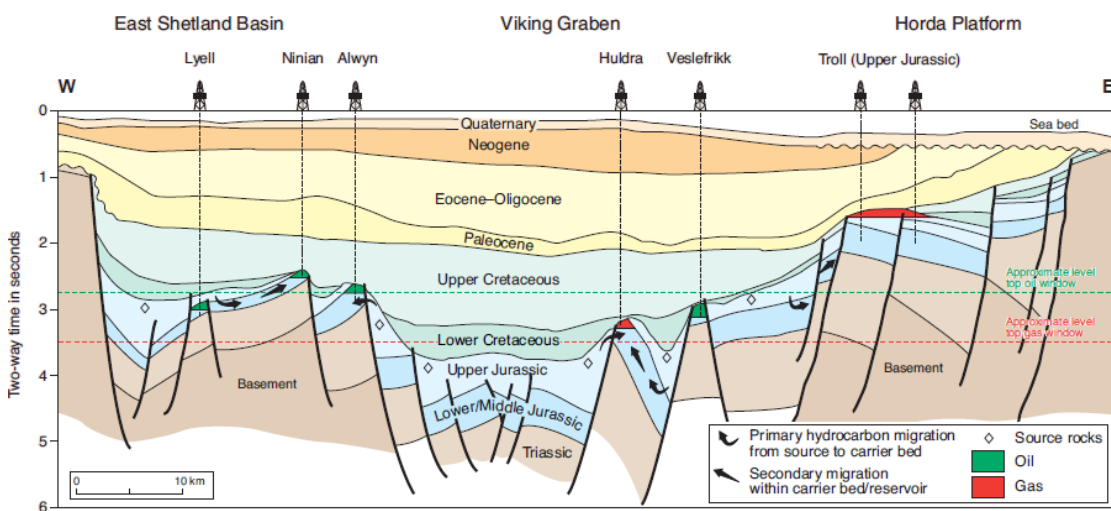


Figure 2-23. illustrating how faulting plays a major role in the generation of a source kitchen (Burley 1993; Husmo 2003).

The importance of the source rock in a regular Brent Group play involves the Kimmeridge Clay Formation (KCF) which is stratigraphically above the reservoir unit needs to be brought down below the reservoir to reach maturity. A reservoir unit is also needed above this area for the hydrocarbons to migrate into. This is best achieved in the Northern North Sea with extensional faulting within the seal-reservoir pairing of the Kimmeridge Clay Formation-Brent Group (Figure 2-23).

2.4.2 Migration

The migration of hydrocarbons from a kitchen area to a trap is key to the trapping and storing of hydrocarbons. Faults can play an important role in assisting and hindering the migration of hydrocarbons. Fault migration can occur by hydrocarbons using the fault plane as a conduit to bypass a potential seal overlying the carrier beds. It must also be noted that faulting can have the reverse effect and prevent the flow of hydrocarbons or in fact compartmentalise a potential reservoir rock. Work undertaken by Yielding (1997) shows that there are generally four ways in which fault sealing can effect migration within a petroleum system:

a) Reservoir juxtaposition

Reservoir juxtaposition; this is best shown with the use of Allan diagrams (Figure 2-24), which show the displacement of the high porosity and permeability reservoir rock against a low permeability rock. The lower permeability rock will have a much higher entry pressure and reduce the possibility of fluid flow across the fault plane. This can play a key role in identifying spill points in structures and migration across fault planes. Where sand prone units overlap across the fault plane it may be possible for migration of hydrocarbons to occur.

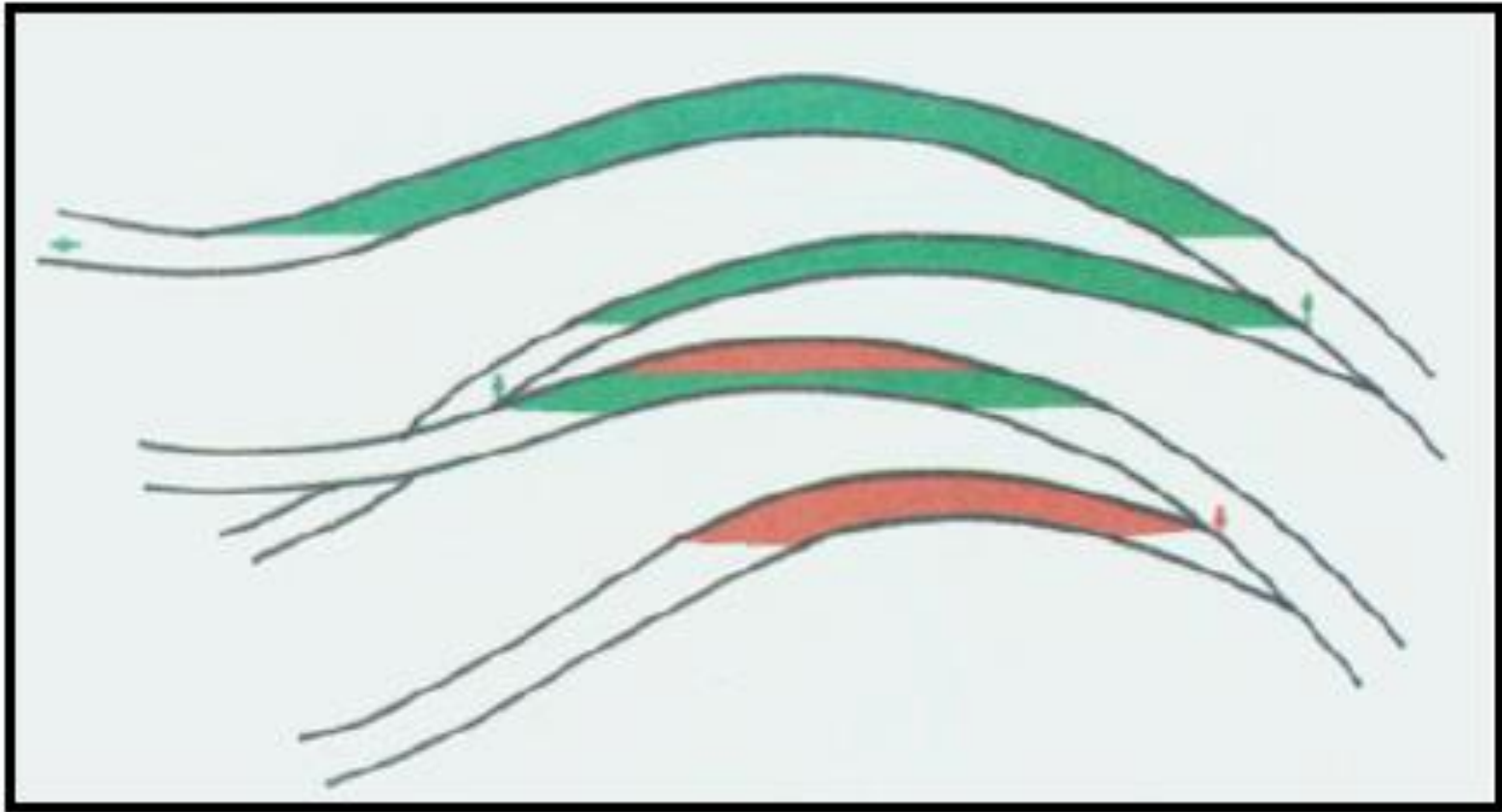


Figure 2-24. Allan diagram illustrating the potential overlapping and migration of fluids from one stratigraphic unit to another vis a fault plane (Allan 1989). The lower (hangingwall) green unit crosses the footwall (upper) of the red horizon, generating a leak point between the two units.

b) Clay/ Shale smear

Clay/ Shale smear; can be sub-divided into three separate factors, Clay Smear Potential (CSP), Shale Smear Factor (SSF) and Shale Gauge Ratio (SGR). Each one of the factors measures the change in entry pressure along the fault plane/zone, relating to the thickness of the source bed and the amount of displacement within the fault plane/zone. These are all shown in Figure 2-25.

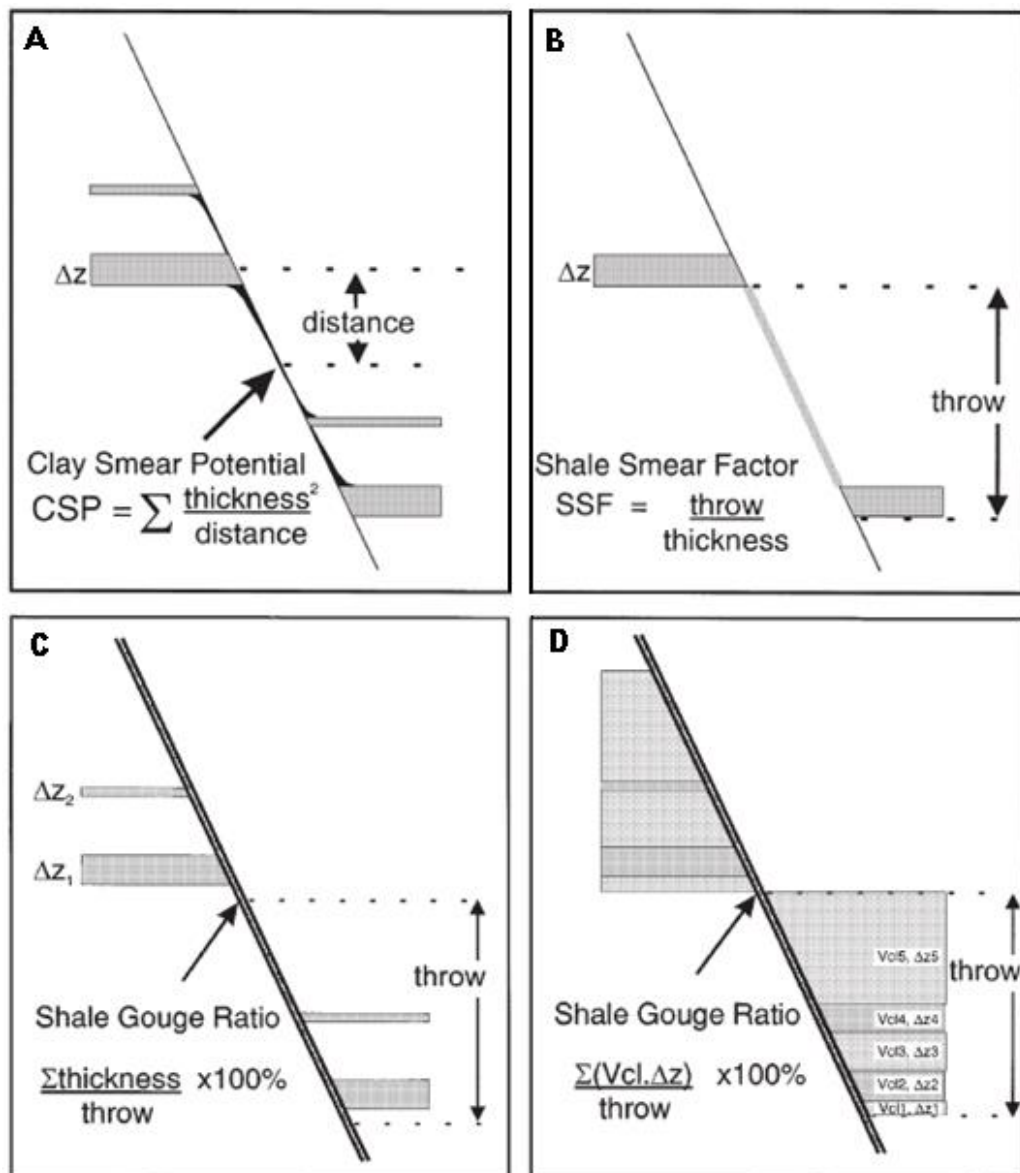


Figure 2-25. Various models to show fluid flow properties along fault planes (Yielding 1997)

c) Cataclasis

Cataclasis; the breaking up and crushing of grains from the hanging wall and footwall sections of a fault zone. The introduction of smaller grains into a high porosity rock, will significantly reduce the pore space in the fault damage zone. The reduction in pore space results in an increase in fluid entry pressure, and increase the likelihood of the fault acting as a sealing fault. This is primary the case in clean quartz arenite where the zones are often referred to as granulation seams. This is particularly important in the aeolian reservoirs of the Southern North Sea.

d) Cementation

Cementation; within an already existing fault plane fluid flow may already exist. If the water compositions change suddenly, it may result in an increase in cementation along the fault zone. This cementation may reduce the porosity and increase the fluid entry pressure or completely remove the porosity and create a hydraulic seal across the fault plane.

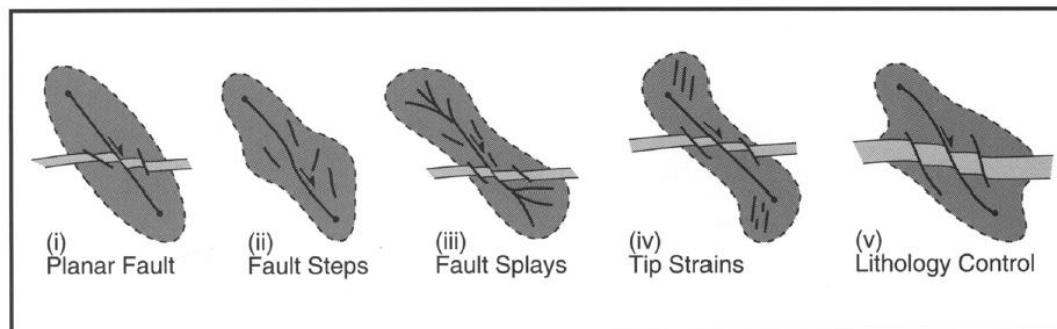


Figure 2-26. Illustrating the variation in faulting types that can effect fluid flow within a reservoir (Knipe 1998)

Most of the models mentioned above are based on simple planar fault models. In reality this is not always the case and the fault plane is much more complicated. Fault plain/zones can be described in one of five ways which are shown in Figure 2-26 (Knipe 1998). Each of the fault planes must

be treated independently from the other one, as each plane/zone may react differently to fluid flow changes (Figure 2-27).

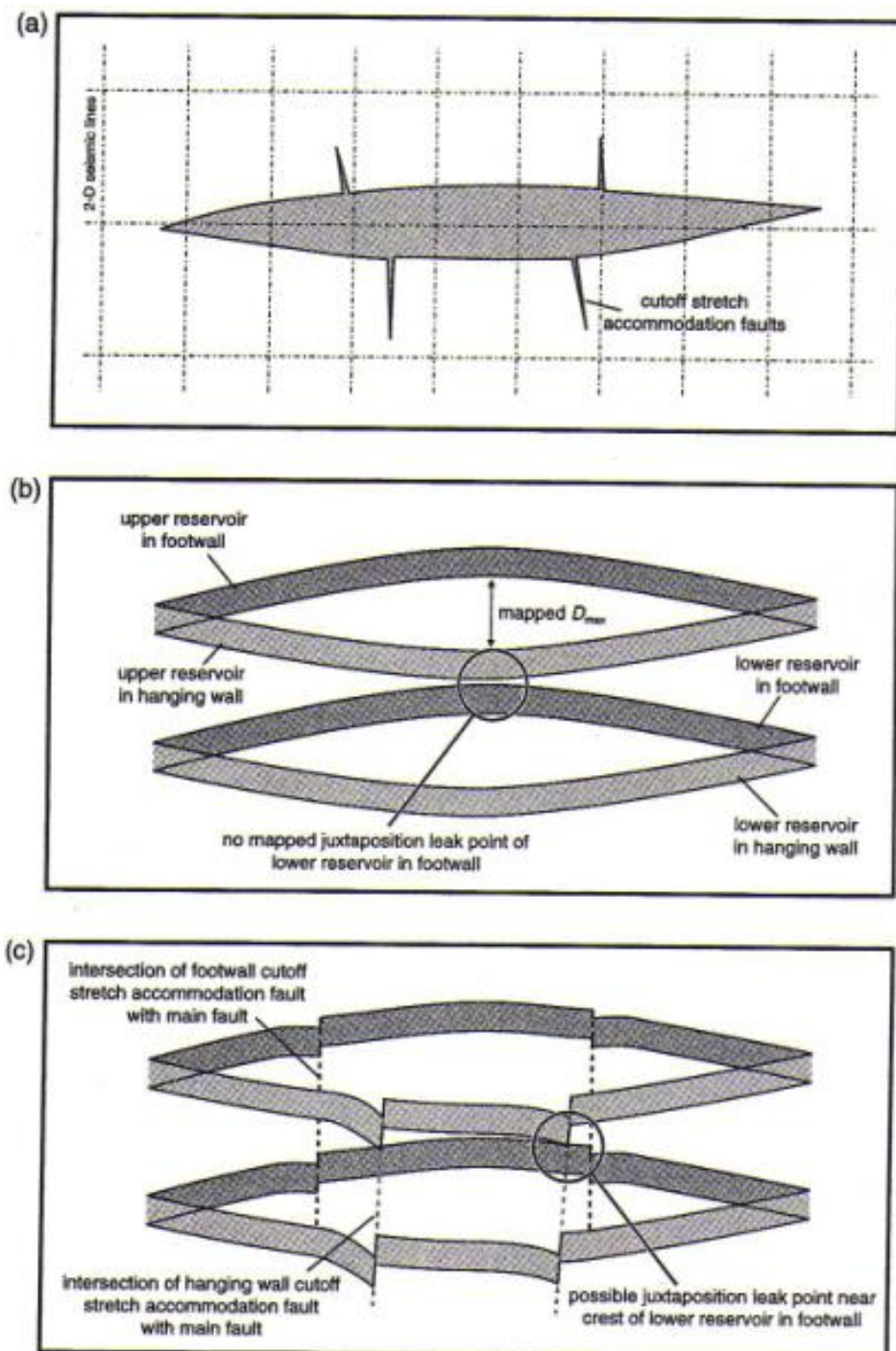


Figure 2-27. This illustrates the offset that can be achieved by release faulting, which shows the effect it can play on reservoir performance (Stewart 2001).

2.4.3 Reservoir

The deposition of a reservoir rock and its properties can also be heavily influenced by faulting. A prime example of this is in the Southern North Sea and the reservoir quality variation of the Lower Permian Rotliegend Group in the Jupiter Fields, where reservoir quality varies considerably between fault blocks (Leveille 1997). Over the Ganymede field it is possible to see reservoir quality variations across fault blocks relative to reservoir thickness. As illustrated in Figure 2-28 the Ganymede Field has a reservoir thickness varying from 400-700 feet, which is a direct result of faulting and deposition and re-faulting (inversion).

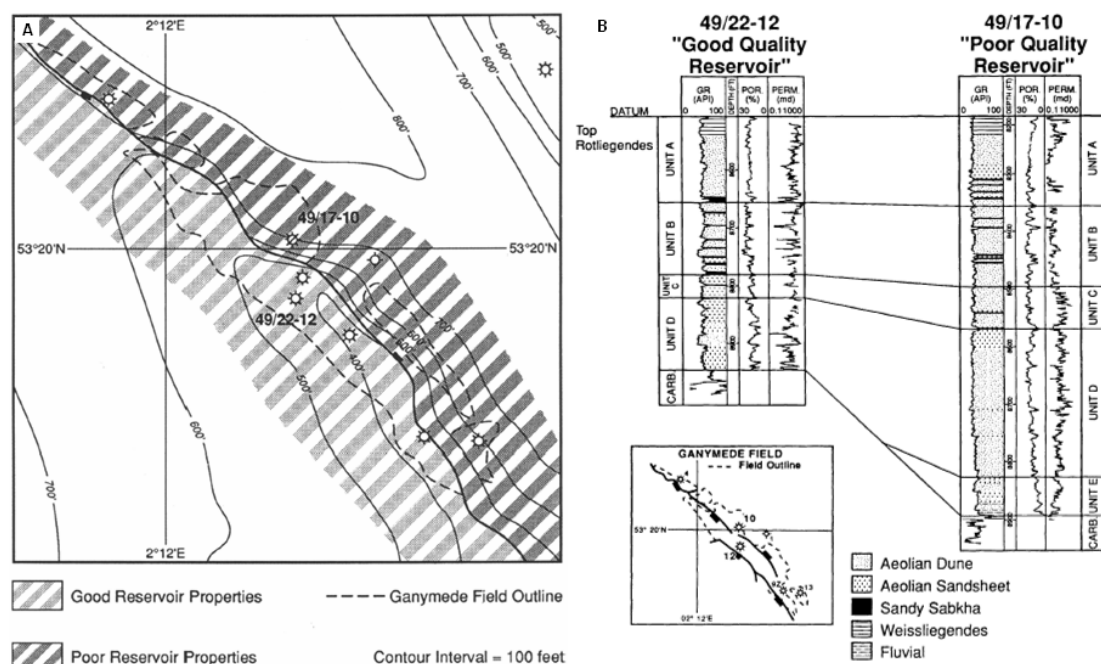


Figure 2-28. Diagram illustrating the variation in reservoir quality across the Ganymede Field. A is a top structure map identifying the good and poor reservoir locations and B illustrates the variation in reservoir thickness and its relationship to reservoir quality (A and B after Leveille, 1997)

The hanging wall section of the field comprises of the thicker but poorer section of the field, where as the footwall section of the field has a much thinner but has a much higher reservoir quality. This is resultant of

pervasive illitisation and compaction during the Jurassic. Although the quality of the reservoir is determined by diagenesis the thickness of the reservoir is primarily determined by faulting. The thick sediment is generated by syn-sedimentary deposition, i.e. more sediment deposited where the greater amount of accommodation space is available. When inversion occurs during the Tertiary the deeper thicker poor quality reservoir is brought back up to make a structural trap along with the footwall high generated by the Jurassic rifting. This results in the juxtaposition of thick poor quality reservoir and thin good quality reservoir across a fault plane (Figure 2-29). It must be noted that this could only happen due to the role of normal faulting and inversion.

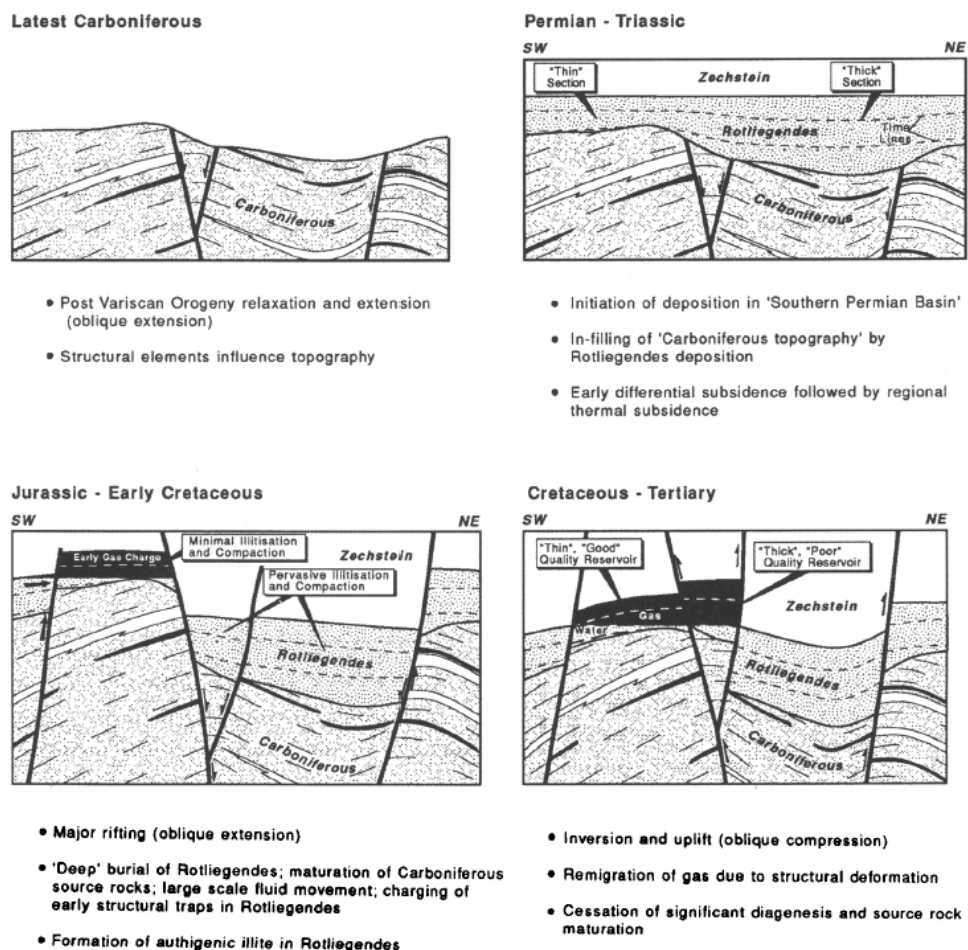


Figure 2-29. The role of faulting in determining reservoir quality and potential productivity (Leveille 1997)

2.4.4 Trap

The trap type commonly associated with the Northern North Sea is fault blocks which have been generated by normal faulting (Figure 2-30). Up to 70% of the oil-equivalent resources discovered in the northern North Sea is trapped within fault block traps (Spencer and Larsen 1990). The Northern North Sea has undergone two separate rifting events, an initial Permo-Triassic rift which generated a series of N-S and NNE-SSW trending faults. The secondary stretching phase began in the Upper Jurassic shortly after the deposition of the Brent Group, which is the primary reservoir in the East Shetland Basin. This earlier rifting event in the Triassic had an opposite sense of throw to that of the later Upper Jurassic faults (Tomasso 2008). It is thought that during the Upper Jurassic rifting event the underlying Triassic faults may reactivate. These rifting events form a series of tilted/ rotated fault blocks for the hydrocarbons to migrate into.

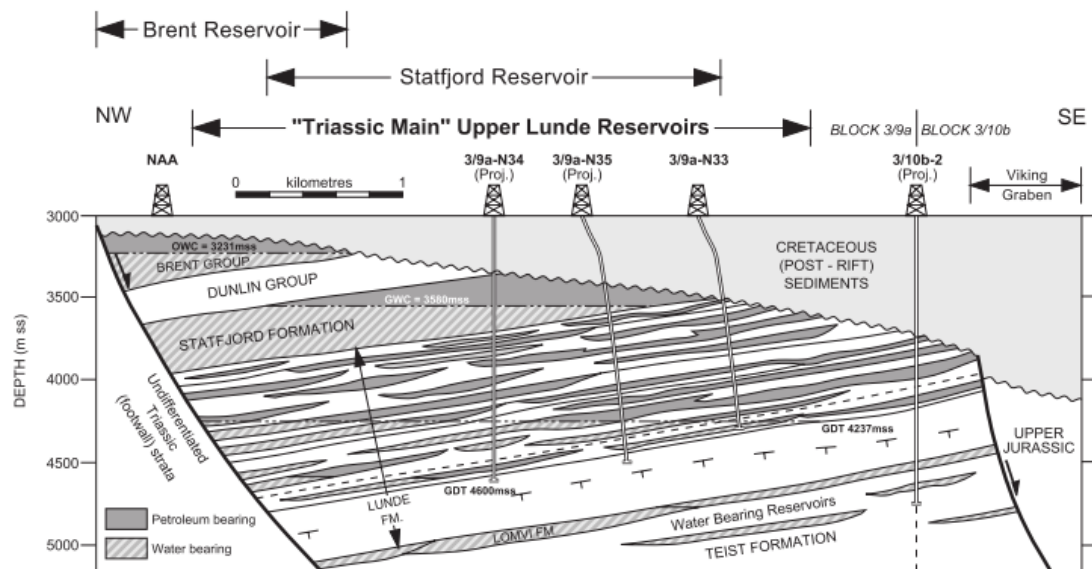


Figure 2-30 Seismic section through the Alwyn Field illustrating a typical Northern North Sea trap. In this instance multiple reservoirs are found at varying levels within the structure (Underhill. 2003).

In some instances it is possible to identify areas where both Jurassic and Triassic reservoir rocks have been drilled in the footwalls of large normal faults (Figure 2-31). Both sets of reservoir rocks have producible amounts of hydrocarbons trapped within the structural closure. This is illustrated in the Brent Field where both the Upper Jurassic Brent Group and the Upper Triassic Statfjord group contain producible hydrocarbons.

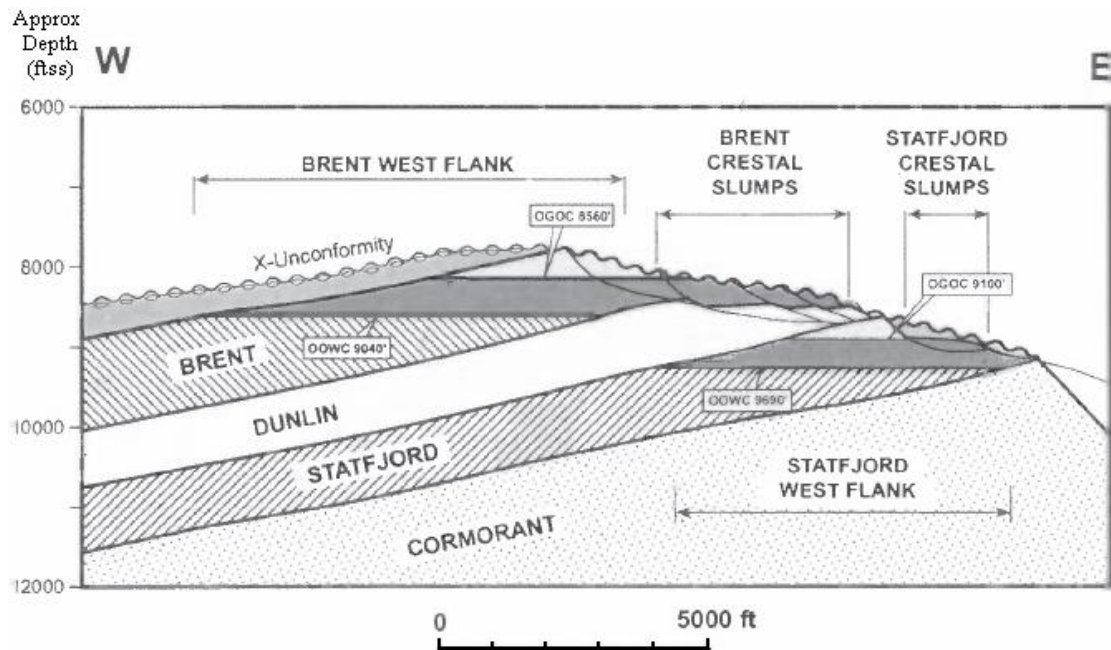


Figure 2-31. The tilted fault block of the Brent Field, where two separate reservoirs have been produced from (Taylor 2003)

2.4.5 Seal

The primary seal that forms most reservoirs is a top seal. This is commonly in the form of a shale layer where permeability is low enough to prevent the accumulation and preservation of hydrocarbons. Although this covers the upper limit of a reservoir it is quite common for the lateral extent of a prospect to be fault bounded. The role of fault sealing is a crucial part of the generation of a hydrocarbon prospect. Faulting can in fact be the limiting

factor to the prospect and/ or compartmentalise a potential field. In most cases the main seal to a hydrocarbon trap is overlying sediments, which have a pore entry pressure higher than that of the pressure in the reservoir. Again, this might be caused by the faults generating a fault gouge or clay smear factor whereby the pressure in the reservoir is not great enough for the fluid to flow through or past it. In other cases, such as in the Murchison Field the faulting will define the shape and size of the structure.

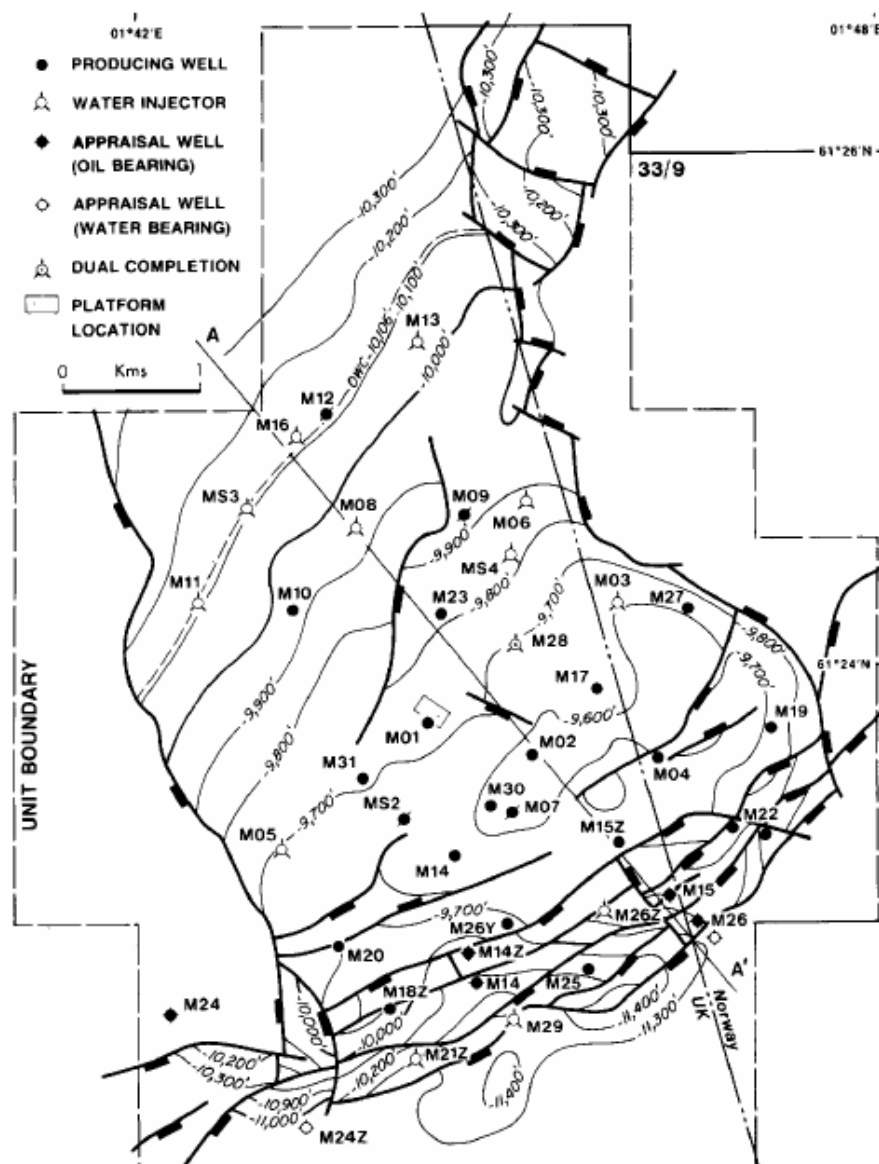


Figure 2-32. Structural disposition, outline of the Murchison field shape (Warrender 1991)

In the Murchison Field the faulting identified on the NE, SE and SW limits of the field are of such a magnitude that the reservoir rock (Brent Group) is juxtaposed against other groups of sediments (Heather Group and/ or Kimmeridge Clay Formation) where hydrocarbon migration is not possible, as illustrated in Figure 2-32 (Warrender. 1991). Another example is seen in the Dunbar Field, where the faulting is so extreme it compartmentalises the field into several sections with their own oil-water-contacts (Figure 2-33). This occurs by a series of sealing faults separating the reservoir rock into different panels. Reservoir compartmentalisation is commonly identified by there being no pressure or fluid connectivity between the two fault separated reservoir sections. If all the reservoir blocks were connected then only one oil-water-contact would be expected with one pressure value observed.

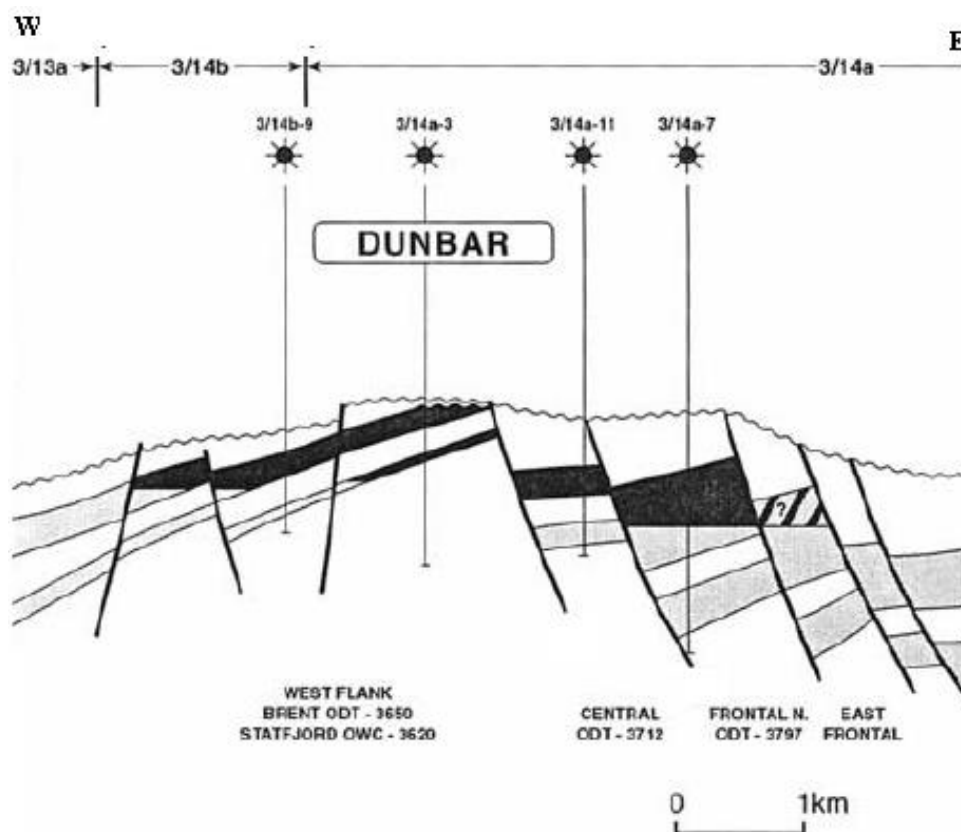


Figure 2-33. The Dunbar Field is an example of fault bounding reservoir compartmentalisation. This may occur where the reservoir units are not juxtaposed across the fault plane or a high shale smear content is present along the fault plane (Ritchie 2003)

These are examples of fault sealing and acting as a barrier to flow, but not all faults are sealing. It can be possible for hydrocarbons to flow across faults as long as the pore entry pressure is not too high for fluid flow to continue. This often occurs where low clay content rocks are faulted against one another, so fluid flow is not inhibited as much. The presence of fine grains such as clays can drastically reducing porosity and permeability and thus acts as a baffle to flow as opposed to a barrier (sealing fault).

2.4.6 Timing

The timing of events in the process of hydrocarbon maturation to trapping is the most important component of all. If the generation of hydrocarbons occurs prior to a trap forming then it is not possible to store hydrocarbon. The same could be said about trap generation occurring after migration and trapping of hydrocarbons in an existing trap. This would result in a re-migration of hydrocarbons and a high possibility of hydrocarbon leakage. This is what occurred on the Dorset coast (Figure 2-34), where a tilted fault block system was in place and exposed to a later inversion event. Hydrocarbons had been trapped and stored against southerly dipping normal faults, which generated a series of tilted normal faults (Underhill and Stoneley 1998). Once the Tertiary inversion event had happened and some normal faults had reactivated with a reverse throw, there was the re-migration of hydrocarbons and the re-generation of structural traps.

The reactivated faults generated much larger monocline traps compared to the initial tilted fault block traps. As the hydrocarbons were already in place prior to the reshaping of the traps, during the uplift the hydrocarbons migrated away from the new traps along the existing and new fault plain,

thus leaving the new larger structures dry and the small old structures filled (Smith and Hatton 1998).

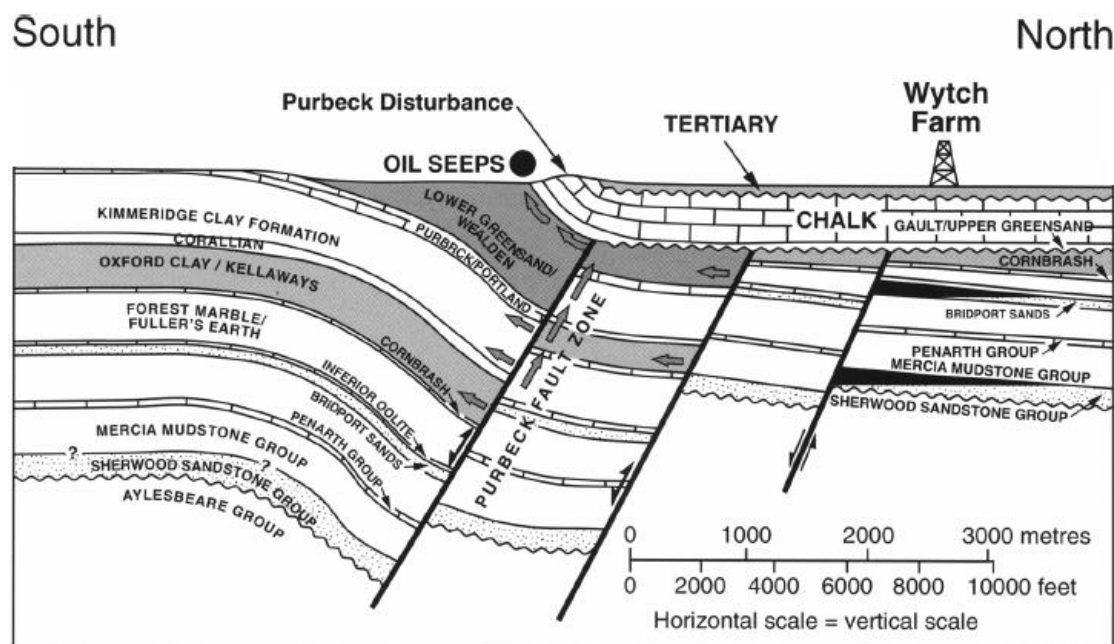


Figure 2-34. Evidence of structural inversion south of Wytch Farm led to the remigration of hydrocarbons in the initial hangingwall locations prior to the formation of the large scale monocline, The only locations in which hydrocarbons are found are the unreactivated tilted fault blocks to the north (Underhill and Stoneley 1998)

What this illustrates, is that no matter what part of a hydrocarbon prospectivity you are investigating, faulting can play an important role in determining the final outcome. This makes the mature hydrocarbon province which is the northern North Sea an ideal area for research. This excellent example of a natural laboratory has a vast extent of data in many forms. A comprehensive coverage of both 2D and 3D seismic data accompanied with copious amounts of well data ranging from core to wireline logs makes this research possible.

Chapter 3 Development and Evolution of the Northern North Sea Basin

3.1 Basin Setting and Location

The East Shetland Basin (ESB) highlighted in Figure 3-1, is an area of extremely high hydrocarbon production situated between Scotland and Norway.



Figure 3-1. Map illustrating the general structural trends observed in the Northern Sea, with the East Shetland Basin highlighted in red (Zanella and Coward 2003).

Exploration had been undertaken since 1976, when the first licence block became available and is still active today. Many of the major hydrocarbon fields have been discovered, with several smaller fields still in the early stages of exploration. This thesis will discuss the role that fault growth and linkage plays in determining possible migration route issues, reservoir compartmentalisation and how this may affect reservoir management.

3.2 Extensional Structures of the Viking Graben and East Shetland Basin

The structural events that occur within the Northern North Sea have been well documented in recent years, and a comprehensive review of the Brent Province has been written by Yielding et al. (1992). These authors discussed the major structural trends which occur towards the formation and deposition of the Brent Group and the trapping geometries for hydrocarbons. It is possible to identify six major structural phases which have occurred during the formation of the Viking Graben and East Shetland Basin.

3.2.1 Initial basin setting – post Caledonian Orogeny

The basement to the Mesozoic sediments in the Northern North Sea is determined by the underlying structural pattern of the Caledonian Orogeny as seen in Figure 3-2 (Zanella and Coward 2003). This generated a series of basins and structural highs within the Northern North Sea which played an important role in determining sedimentation and deposition models throughout the Mesozoic.

The Caledonian fault blocks and granites generated a series of obdurate structures, which underpinned many of the structural highs within the Northern North Sea. These can then play an important role in compaction rates and the generation of stratigraphic traps within the basin. Some granite batholiths can determine the orientation of overlying faulting and redirect the fault lineation (Donato 1981; Zervos 1987).

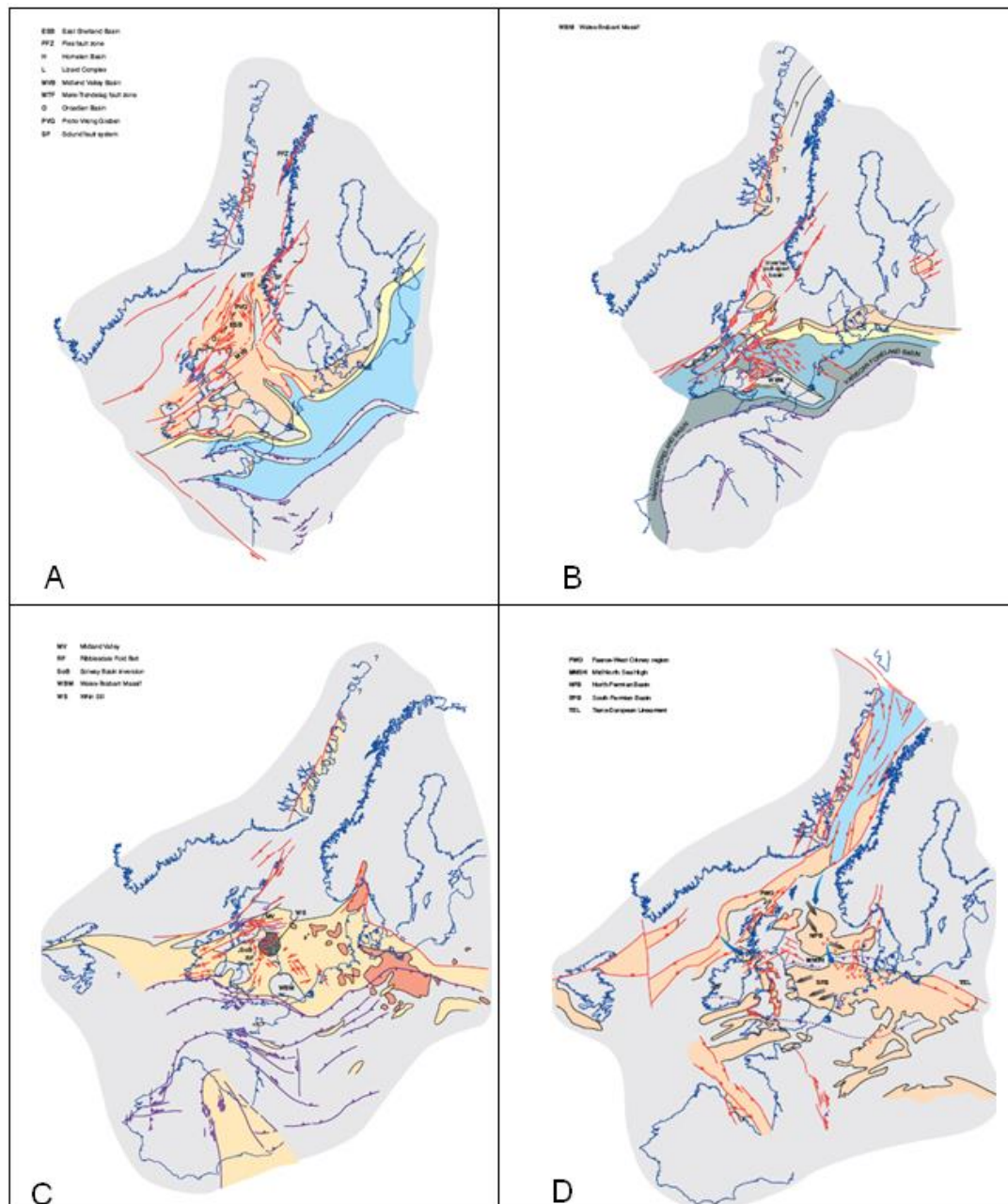


Figure 3-2. The structural evolution from the Devonian to the early Permian (Coward 2003)

It is suggested that once deposition of Permian sediments began in the northern basin that no major faulting was controlling the depositional patterns. The basins were created as a direct result of the underlying Caledonian Orogeny and structural flexure of the continental crust.

3.2.2 Late Permian – Early Triassic Rifting event

There is some controversy of dating the initial faulting in the Permo-Triassic rifting event. It has been documented that the trigger for the formation of the initial Viking Graben was the opening of the Proto-Atlantic Ocean to the north, between the UK, Scandinavia and Greenland, highlighted in Figure 3-3 (Glennie 1995). It is thought that this rifting propagated South to form a complex N-S orientated series of grabens and half grabens (Fisher 1998; Goldsmith 2003).

The rifting between Greenland and the UK/ Scandinavia has been well perceived to be occurring by the Middle Permian, which, fully supports the idea that rifting in the Northern North Sea could have established by the late Permian (Glennie 1995).

Other authors such as Ziegler (1982) have suggested that the first stage of rifting in the Northern North Sea is restricted solely to the Triassic. It has been noted that the top of the syn-rift sediments in the Triassic rifting event is bound within the Teist Formation, which is of Lower Triassic age. This would indicate that the period of rifting if contained solely to the Triassic, would initiate at the onset of the Triassic and end by the end of the Lower Triassic (Færseth 1995; Færseth 1996). This would leave only a short period of time to generate the large long lasting structures observed in the subsurface (Figure 3-4).

Work that has been undertaken from Roberts (1995) suggests that the stretching factor in the Triassic is lower than that of the Upper Jurassic rifting event. This would imply that the initial rifting event must have initiated prior to the onset of the Triassic to generate such significant structures in the Northern North Sea, such as the Tern-Eider Ridge (Fraser 2003).

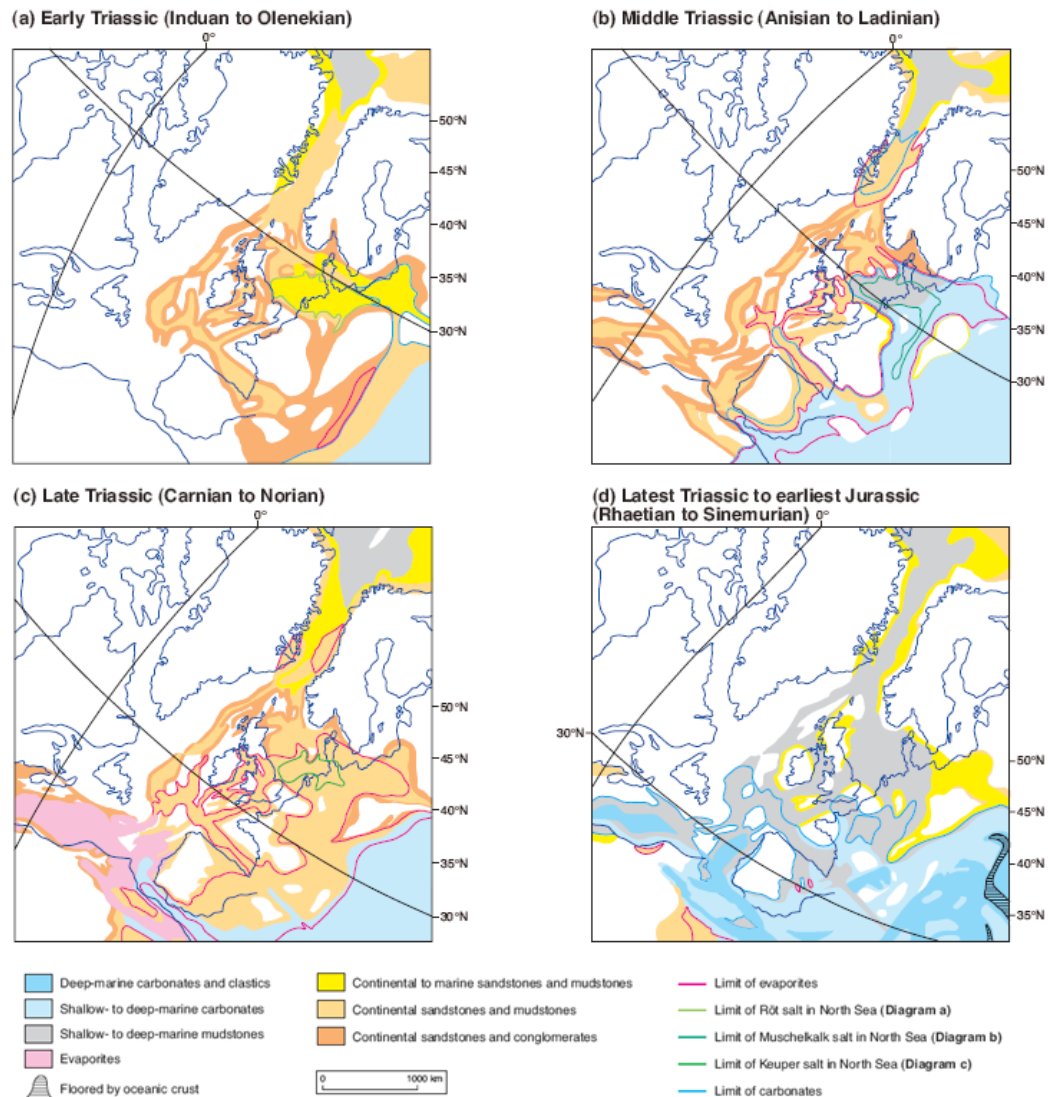


Figure 3-3. The structural evolution and the opening of the North Sea through the Triassic (Goldsmith 2003).

The generation of the Triassic N-S orientated major faults played an important role on the distribution and thickness of sediments (Roberts 1995). This also generated an original line of weakness of overlying sediments and

structures to deform against. This is observed with the main graben development observed in the Upper Jurassic rifting event with the reactivation to some of the initial Permo-Triassic faults.

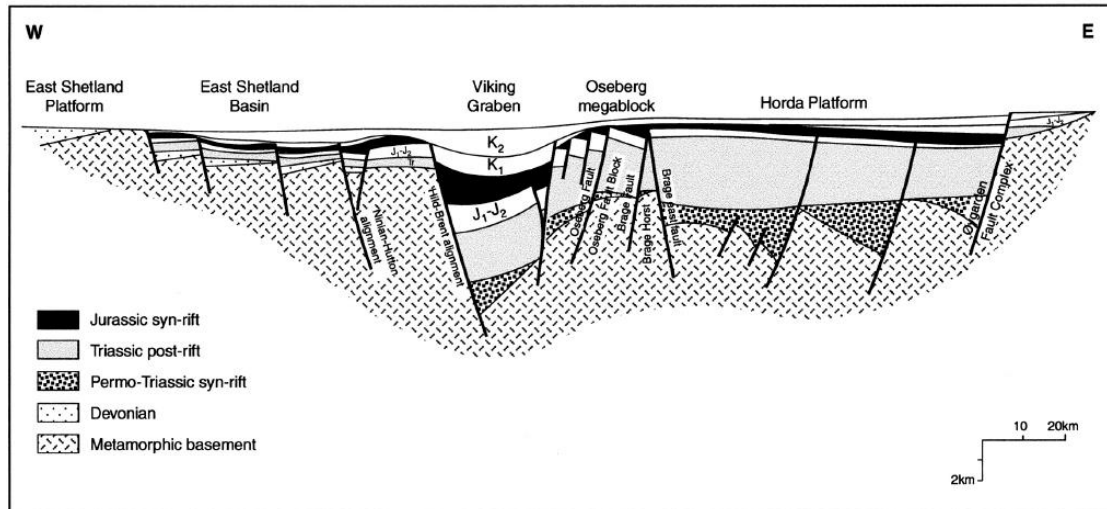


Figure 3-4. Illustrating some of the structural highs created by the Permo-Triassic rifting event (Færseth 1998)

3.2.3 Middle Triassic – Lower Jurassic Intra-rift subsidence

The Middle Triassic to Middle Jurassic can be best described as a period of intra-rift subsidence and a map illustrating its deposition can be seen in Figure 3-5. This is a combination of the Permo-Triassic post-rift phase and the Upper Jurassic pre-rift phase (Ravnås 2000). Commonly this period of time has been regarded as a period of post-rift thermal subsidence relating to the earlier Permo-Triassic rifting event (Steel 1993). Further studies illustrate that this is not the case, as the overlying sediments do not conform to a strictly thermally subsiding basin.

The majority of subsidence was controlled by lithospheric extension, but block rotation also played a valuable role in the subsidence and uplift within the basin (Steel 1993; Fisher 1998; Ravnås 2000). Towards the Middle

Jurassic, most of the block rotation had ceased and the basin was dominated by thermal subsidence prior to a major doming event, in the Lower Middle Jurassic, in the Central North Sea.

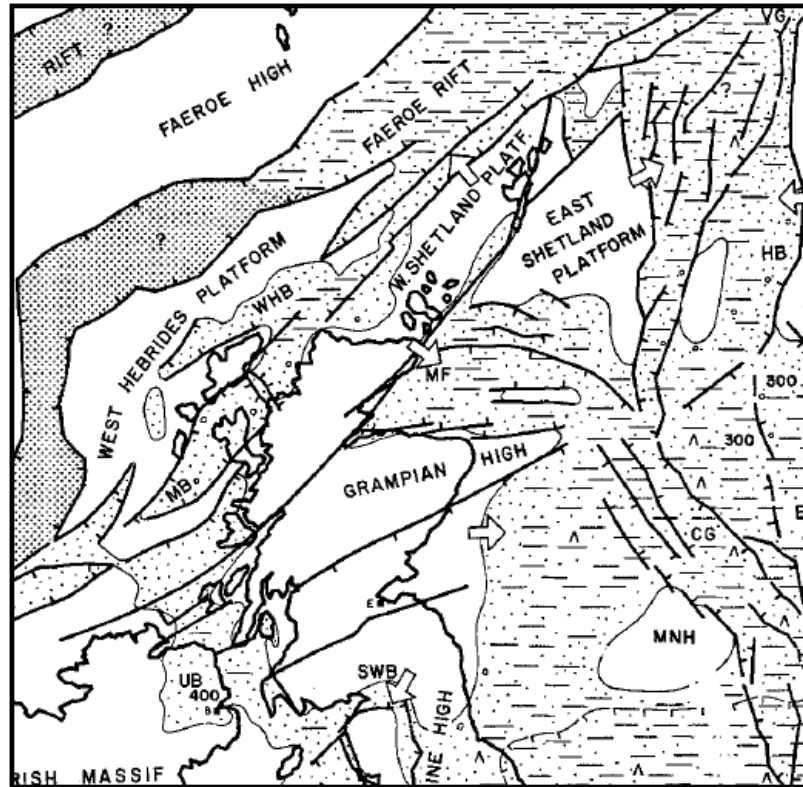


Figure 3-5. Illustrating the thickness of Triassic sediment in the Northern North Sea and ESB (Ziegler 1982).

3.2.4 Middle Jurassic Doming event

The Middle Jurassic in the North Sea is structurally dominated by the presence of a plume generated dome over the central North Sea area, which is highlighted in Figure 3-6 and 3-7 (Underhill and Partington 1993). This generated a structure known as the Aalenian North Sea Dome (Husmo 2003). This doming event led to the uplift and erosion of the recently deposited Lower and Lower Middle Jurassic sediments. In some areas close to the centre of the dome, Middle Jurassic sediments are deposited straight on top of Triassic sediments (Underhill and Partington 1993). This erosion surface is

called the Mid-Cimmerian Unconformity, and can be mapped throughout the majority of the North Sea.

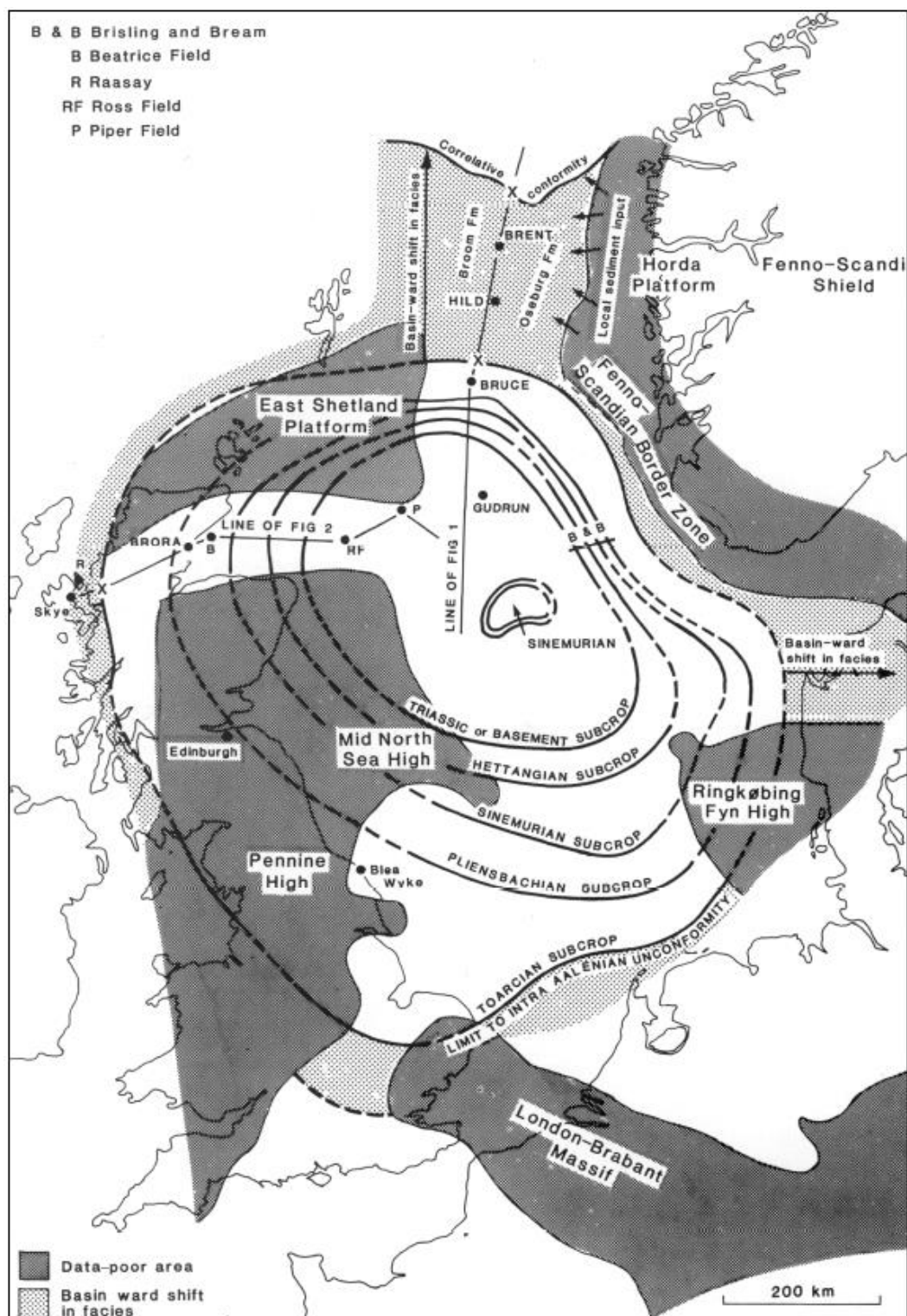


Figure 3-6. Illustrating the effect of uplift and erosion due to the Aalenian doming in the Central North Sea (Underhill and Partington 1993)

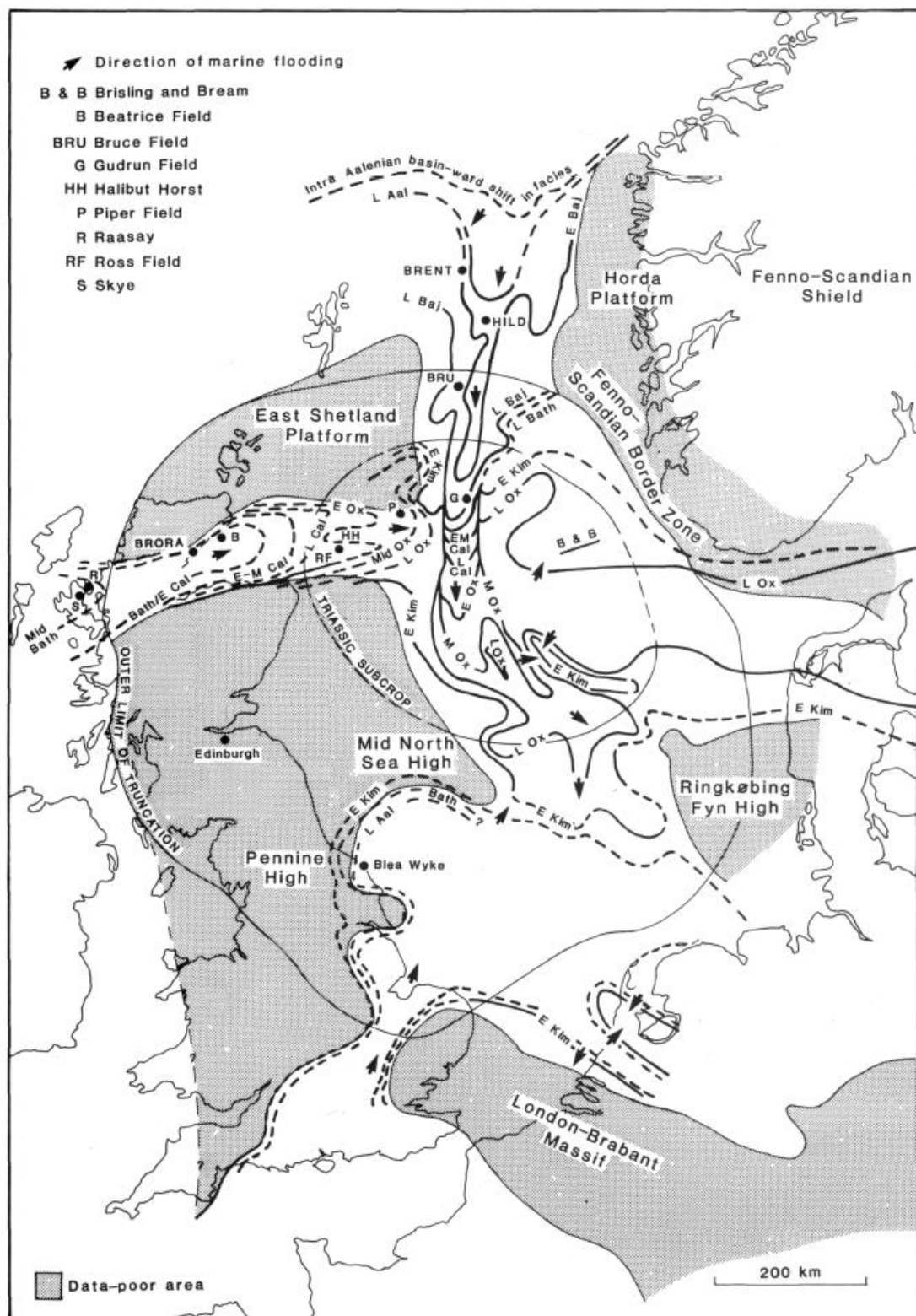


Figure 3-7. Regional onlap map to illustrate the overall effect of uplift and erosion from the Aalenian doming event in the Central North Sea (Underhill, 1993).

Some of the extrusive magmatic products from this dome have been drilled through in the Forties province. The evidence from core and cuttings

suggests that the Aalenian North Sea Dome extruded a mildly undersaturated alkali basalt (Latin 1990). Further work suggests that the magmatic material was extruded into small bodies of water, which suggests the extrusive event was close to sea level (Latin 1990).

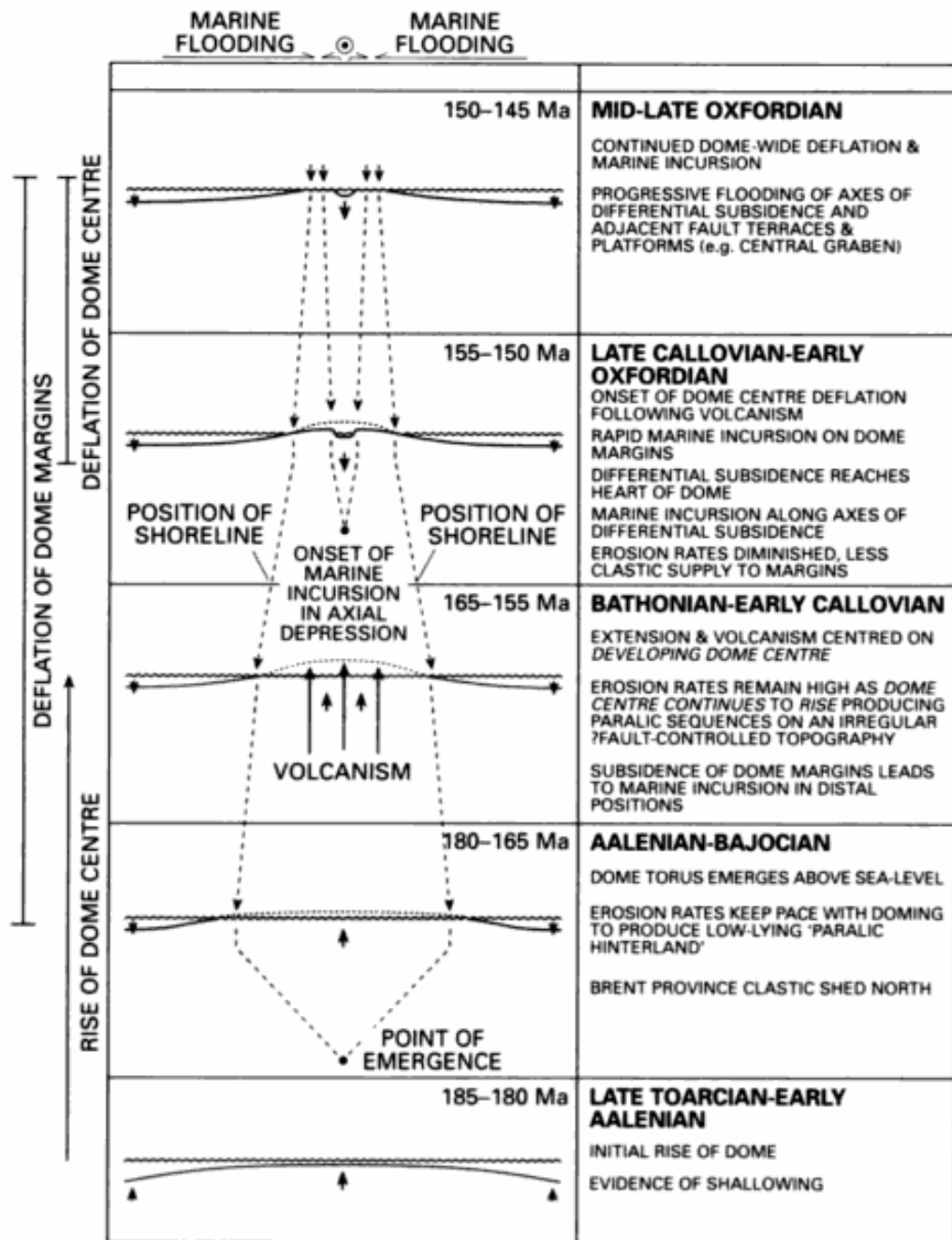


Figure 3-8. Showing what occurred as a result of the Doming in the Central North Sea in the Middle Jurassic (Underhill 1998).

It is generally thought that the deflation of the dome in the Oxfordian made it possible for marine incursion to occur and the deposition of the main reservoir unit in the Northern North Sea, the Brent Sandstone Group (Figure 3-8). As deflation increased over the basin, dispersion of sediments to the outer parts of the basin ceased and marine incursion could eventually occur over the centre of the plume event (Underhill and Partington 1993). Shortly after the deflation of the Aalenian North Sea dome, rifting ensued throughout the North Sea. This generated the main structural trends observed in the Northern North Sea today.

3.2.5 Upper Jurassic – Lower Cretaceous Rifting event

The onset of the second phase of extensional rifting occurred in the North Sea shortly after the deposition of the Brent Group sediments in the early Bathonian. The epicentre to the rifting is based around the deflating Aalenian dome in the central North Sea. It is at this location where a triple junction of three rift arms is located, as shown in Figure 3-9. An in depth review of plume-generated triple junctions is observed within Burke and Dewey (1973).

The main structures to the triple junction, are three separate rift arms, termed the Viking Graben (N-S), Moray Firth Graben (E-W) and the Central Graben (NW-SE). It has been possible to date the faulting in these rift arms to two separate phases. The first of these rift arms to subside was the Viking Graben, which reactivated along a plain of weakness which was generated by the underlying Permo-Triassic rift event (Færseth 1997; Zanella and Coward 2003).

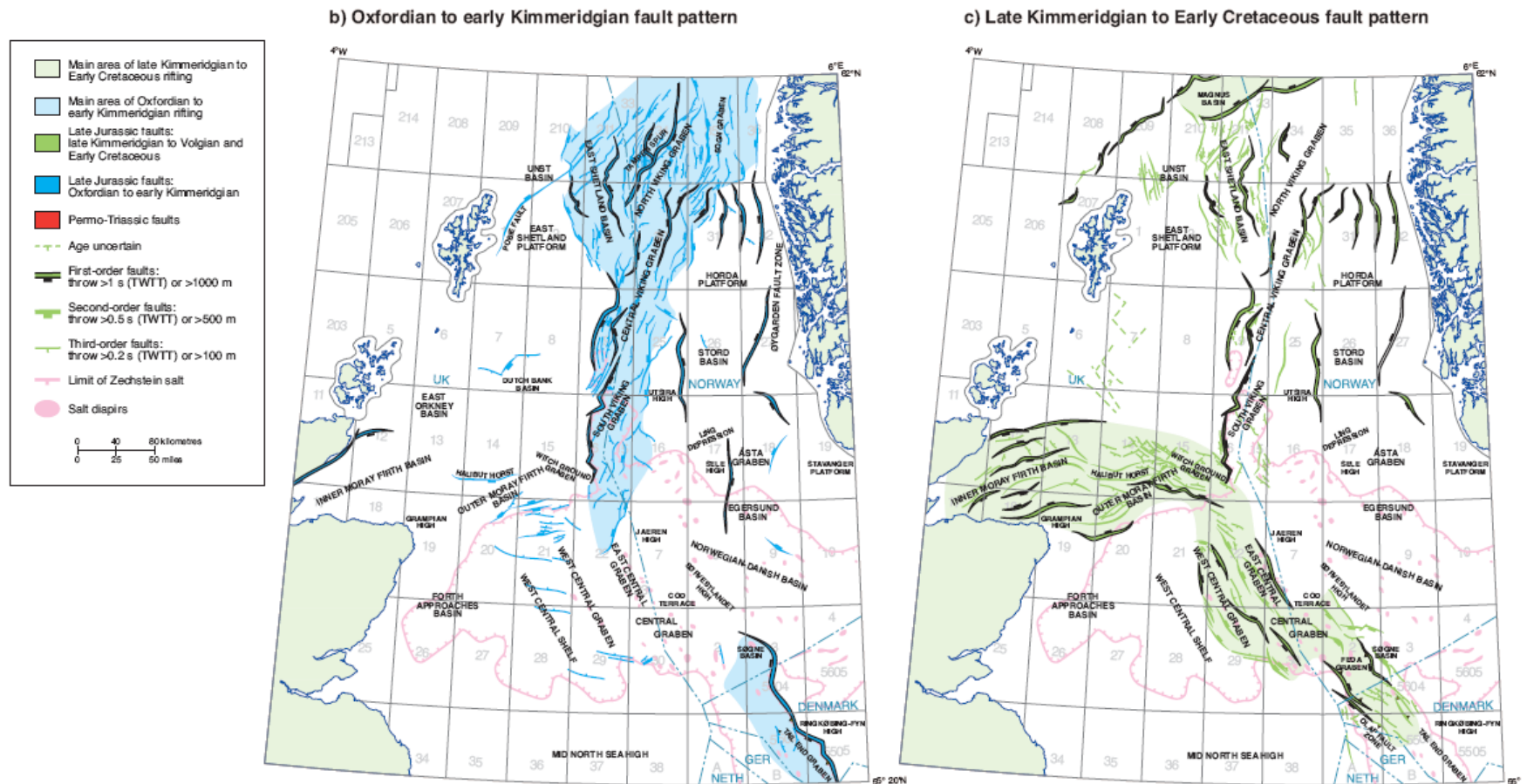


Figure 3-9. Fault patterns form the second phase of rifting in the North Sea (Zanella and Coward 2003).

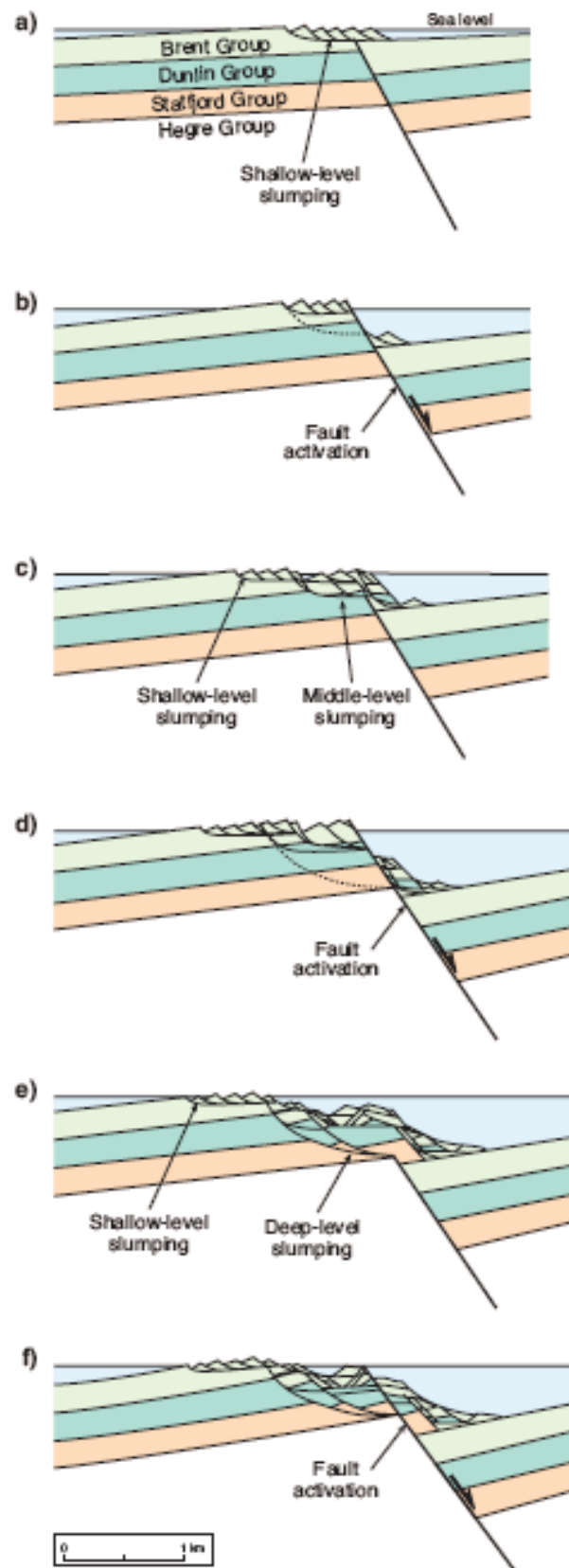


Figure 3-10. Illustrating footwall degradation and structurally down dip prospects (Zanella and Coward 2003)

The second phase of rifting related to the Upper Jurassic rifting event is the onset of subsidence in the Moray Forth and Central Graben areas. It must also be noted that in this second phase of extension, new faults and old faults continued to move in the Northern North Sea.

The second rift event in the Viking Graben takes place with an increased stretching magnitude, compared to the earlier Permo-Triassic rifting event. Stretching peaked in the Oxfordian-Kimmeridgian, Upper Jurassic. It is thought that during the Upper Jurassic rifting event the underlying Triassic faults may have reactivated. This shows a shift in depocentres from the existing Triassic hangingwall to later on the Triassic footwall in the Upper Jurassic rifting event (Figure 3-11). This earlier rifting event in the Triassic, in areas had an opposite sense of throw to that of the later Upper Jurassic faults (Tomasso 2008).

This second phase of stretching formed the main structural traps for the Brent province. A typical cross-section of an Upper Jurassic faulting phase will show wedge shaped packages of infill sediments, within a tilted-fault block topography.

The faulting continued through to the earliest stages of the Lower Cretaceous. There is potential that during the Lower Cretaceous when fault blocks are rotating and generating localised uplift, the main reservoir unit (the Brent Sandstone Group) was brought up to or potentially above sea level (Figure 3-10). This may have a major effect on the reservoir quality of the Brent and also the thickness of the Brent sediments over the crests of rotated normal faults. This is illustrated in the Statfjord Field, where the footwall degradation occurs to the tilted Brent Group sediments (Gibbons 2003; Zanella and Coward 2003). This uplift and erosion also generates structurally down dip prospects from the large normal faults.

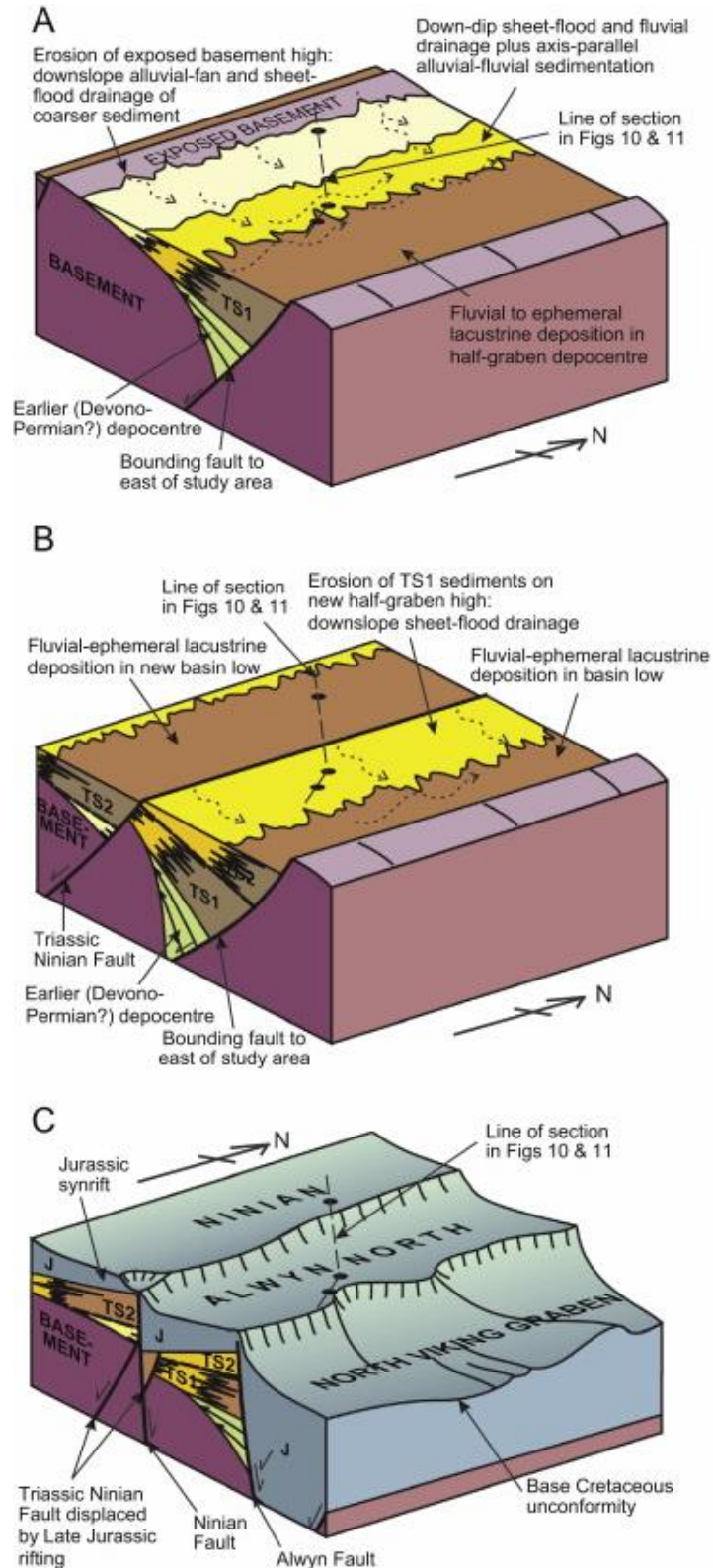


Figure 3-11. Illustration of how the underlying faults may play a role in effecting the overlying fault patterns (Tomasso 2008). Block A indicate the Early Triassic, B is illustrative of the mid –Triassic and C illustrates the structures present by the Base Cretaceous.

3.2.6 Lower Cretaceous – Tertiary Post Rift Thermal Subsidence

The rocks found within this phase of deposition are related to the post-rift infill of the Upper Jurassic rifting phase (Bowman 1998). This is a more conventional period of lithospheric subsidence, unlike the earlier Middle Triassic –Middle Jurassic intra rift event. Over the structural highs, there is in some cases, a period of erosion. This is related to fault block rotation and the subsequent uplift. However, other large scale rifting events do occur west of the East Shetland Basin.

To the west of the Shetland Islands, the Cretaceous saw a period of active rifting (Figure 3-12). This rifting is thought to have originated in the northeast towards Norway and had spread to the southwest and eventually linked with the opening North Atlantic.

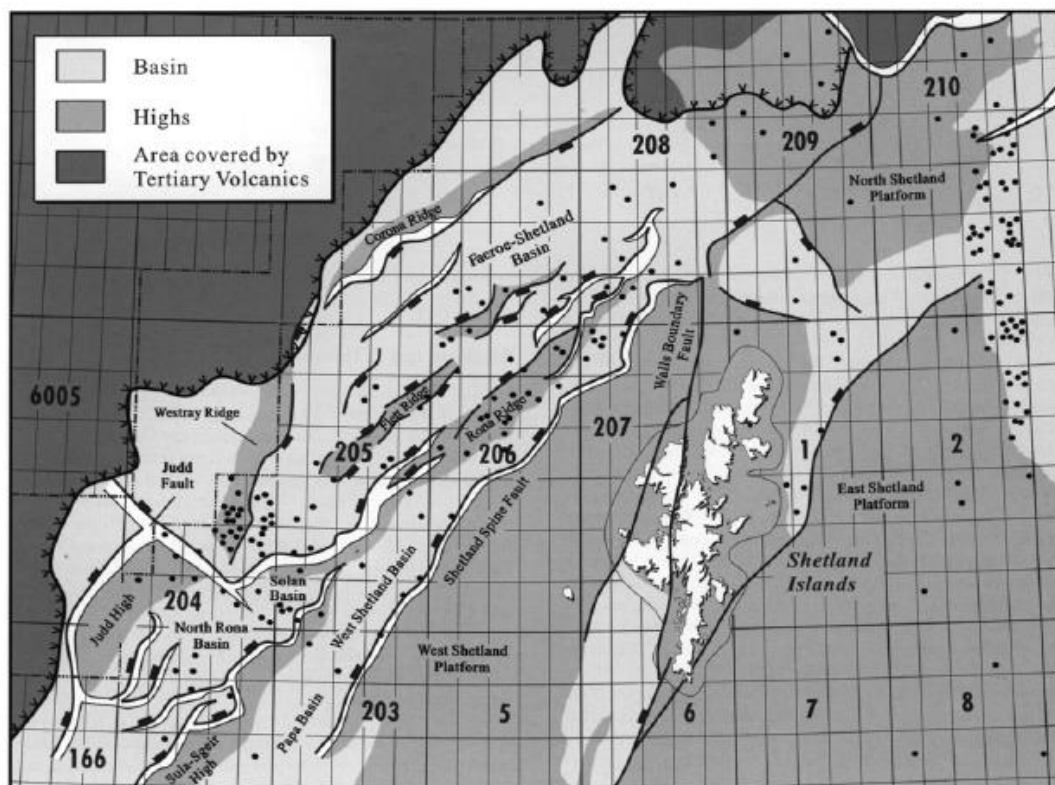


Figure 3-12. Map to illustrate the Cretaceous rifting located in the West of Shetland (Dean 1999).

The Lower Cretaceous syn-rift sediments show large resemblance to the Northern North Sea syn-rift packages, which suggest deposition was taking place whilst the faults were active, as shown in Figure 3-13.

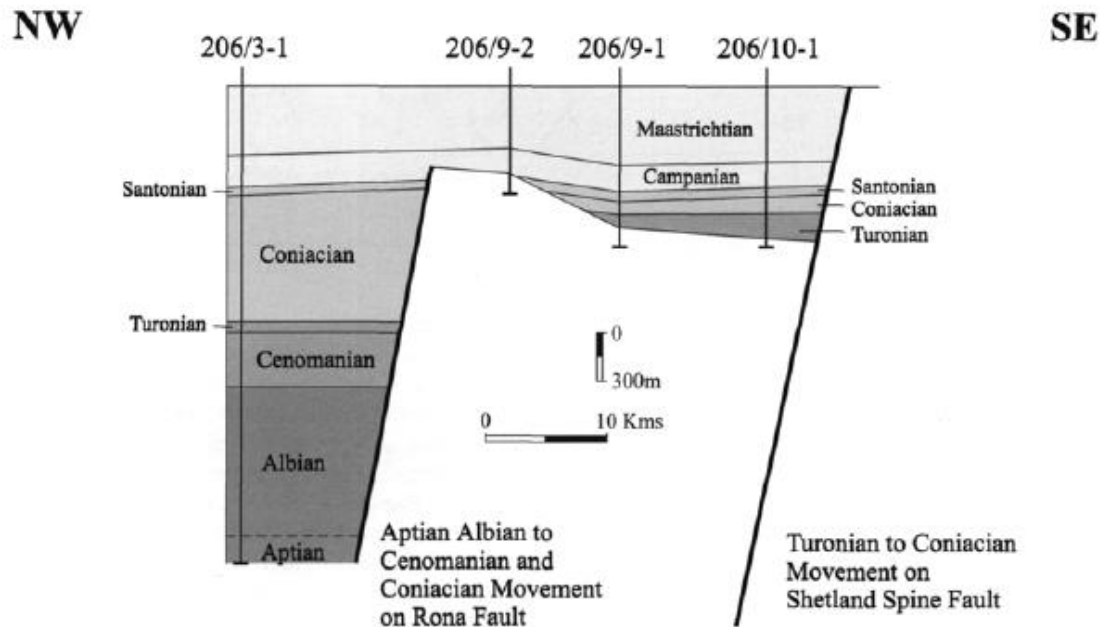


Figure 3-13. Diagram illustrating Lower Cretaceous syn-rift packages within the West of Shetland area (Dean 1999).

These active faults grew towards the southwest and by the Paleocene (Figure 3-14) subsidence is aided by North Atlantic faults to the south; hence a slight change in orientation between the two sets of faults. Although these structures are not confined to the North Sea, their formation is very similar to that of the Permo-Triassic and Upper Jurassic fault systems observed in the North Sea. In the East Shetland Basin 3km of sediment is estimated to be deposited during this subsidence period, whereas in the axis of the Viking Graben an estimated 5km of sediment is expected. Subsidence in the basin is thought to outpace the sedimentation rate and resulting in a deep water basin. The formation of the Iceland mantle plume did however affect the sedimentation rates (Figure 3-15).

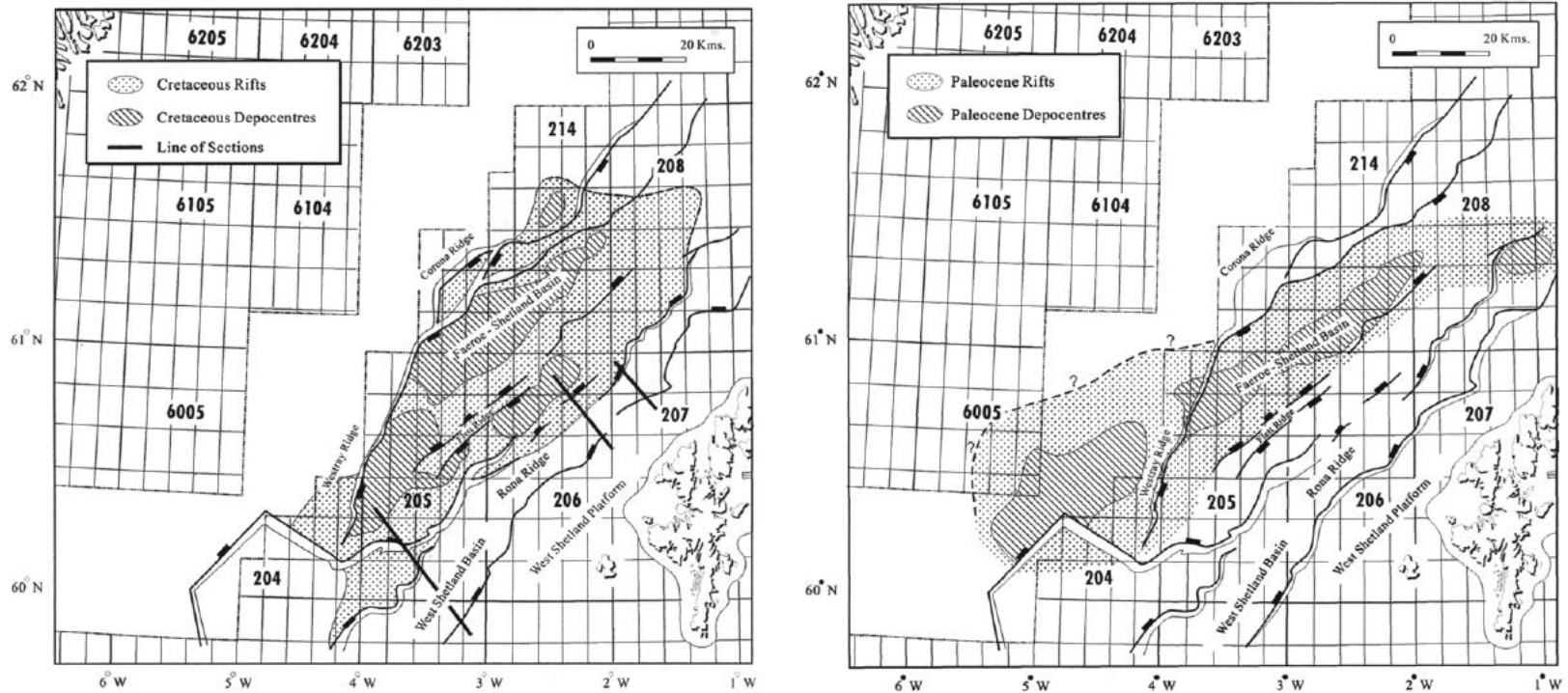


Figure 3-14. Maps illustrating the shift in depocentres from the Cretaceous to the Paleocene in the West of Shetland (Dean 1999).

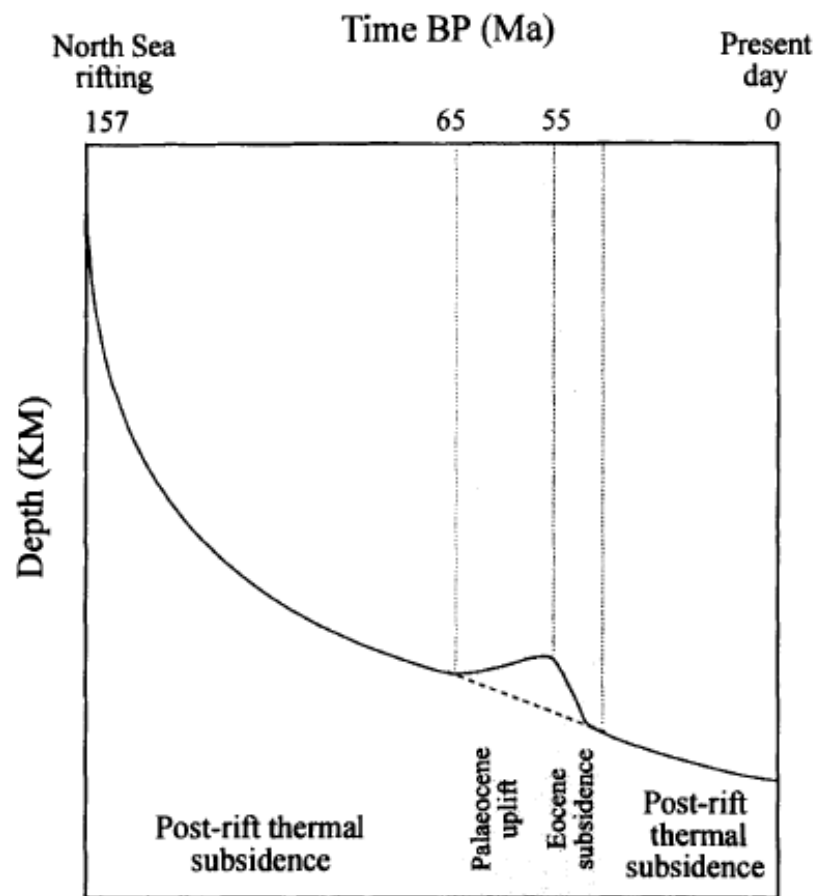


Figure 3-15. Subsidence curve for the Northern North sea, taking into account Palaeocene uplift and Eocene subsidence relating to the Iceland plume generation (Nadin 1995).

The East Shetland Basin and the Northern North Sea post rift subsidence as a result was not as straight forward as initially implied. The occurrence of the Iceland mantle plume resulted in a regional uplift, tilting, erosion and re-deposition of sediments within the basins. The appearance of the mantle plume does match up with the subsidence anomaly observed within the East Shetland Basin (Jordt 1995; Nadin 1995; Bowman 1998). Other far-field stresses relating to uplift in the Tertiary relate to the Northern Atlantic opening which is thought to have impacted a regional easterly tilt on to the basin. Both of these structural events are thought to play a crucial role in

determining the location of coarse clastic sediments within a predominantly mud-prone depositional environment.

3.2.7 Structural Summary

Although these regional structural trends apply to the basin, some smaller scale structural events also occurred within the basin prior to and during the Brent deposition. The initial faulting in the Triassic not only caused tilting of the basement rocks but also had an after effect on compaction rates of the Brent Group. In the areas where the Triassic sediments are thickest, greater amounts of compaction can occur and generate further accommodation space for the deposition of the Brent Group. This means that even where faults have not moved; there should still be a significant variation in the Brent Group thicknesses. If some faults did initiate during the deposition of the Brent Group then they will have localised effects on thickness. The second rifting phase in the Upper Jurassic not only caused an increase in hanging wall sediments, but also caused thinning of footwall sediments by uplift and erosion (Odinsen 2000). This shows that along with the three major structural events governing the basin there are four other regional structural trends that apply to the deposition of the Brent Formation. These are Triassic thermal subsidence, renewed post-Triassic faulting, differential compaction rates and localised thinning and thickening due to Upper Jurassic faulting.

3.3 Stratigraphy

The majority of the sediments deposited within the East Shetland Basin are Mesozoic in age, with a Carboniferous and Permian basement (Færseth

1996). After the initial faulting episode in the Triassic (which may have later reactivated), monotonous sandstone-mudstone sequences were deposited in the half graben environment (Tomasso 2008). These continental sediments are then overlain by the coastal deposits of the Banks Group and then by the marine Lower Jurassic Dunlin Group. This major transgression could imply that the sedimentation rate was not keeping pace with subsidence rates, which may have reversed during the deposition of the Brent Group (Yielding 1992). The Middle Jurassic Brent Group derives its name from the fivefold sub-division which was modified and formalised by Deegan (1977). The five sub-divisions are made up of the Broom, Rannoch, Etive, Ness and Tarbert Formations. It is widely thought that the depositional environment of the Brent is a regressive-transgressive wedge as shown in Figure 3-25 (Brown 1987). Within the initial four formations of the Brent Group (Broom – Ness), a northward prograding (regressive) delta can be identified. The Tarbert Formation (and in some areas the Upper Ness Formation) shows a relative rise in sea level, which results in the deposition of transgressive marine sediments (Richards 1992). The Brent Group sedimentary source is thought to be related to the thermal doming event, which occurred to the south prior to Brent Group deposition (Underhill and Partington 1993; Underhill 1998).

This transgression continued into the Upper Jurassic when the second phase of rifting occurred during the deposition of the Heather Formation and the Kimmeridge Clay Formation. The Kimmeridge Clay Formation was deposited in a deep marine environment and is the major source rock for the Northern North Sea (Milne and Brown 2003). Locus of extension migrated basin-ward shortly after the Kimmeridgian, faulting in the East Shetland Basin was arrested and the basin went into a period of thermal subsidence, where infill sediments of Cretaceous and Tertiary age are found up to 5Km thick in the axis of the Viking Graben (Yielding 1992; Cowie 2000).

A full review of the sedimentary basins and setting for the Northern North Sea and the East Shetland Basin is located below.

3.3.1 Permian

The Northern North Sea in Permian times was heavily influenced by the underlying tectonic events of the Caledonian Orogeny which had a large effect on sedimentation (Kent 1975). This resulted in the majority of the Lower Permian Rotliegend Group sediments missing either through erosion or through non-deposition (Figure 3-16).

The youngest Permian sediments found in the Northern North Sea belong to the Auk Formation (Kent 1975). These sediments were laid down in a broad, shallow basin in which aeolian sediments could be deposited (Figure 3-17). The base of the Auk Formation is depicted by a conglomerate unit, which suggests an earlier fluvial flooding event. Some of the pebbles within the conglomerate have a basaltic texture, which is related to the erosion of the underlying Caledonian Orogeny (Trewin 2003). In the uppermost unit of the Rotliegendes it is possible to identify slumping and subaqueous reworking, which suggests flooding of the dune sediments, prior to the deposition of the globally widespread Kupferschiefer Formation as shown in Figure 3-18 (Glennie 2003).

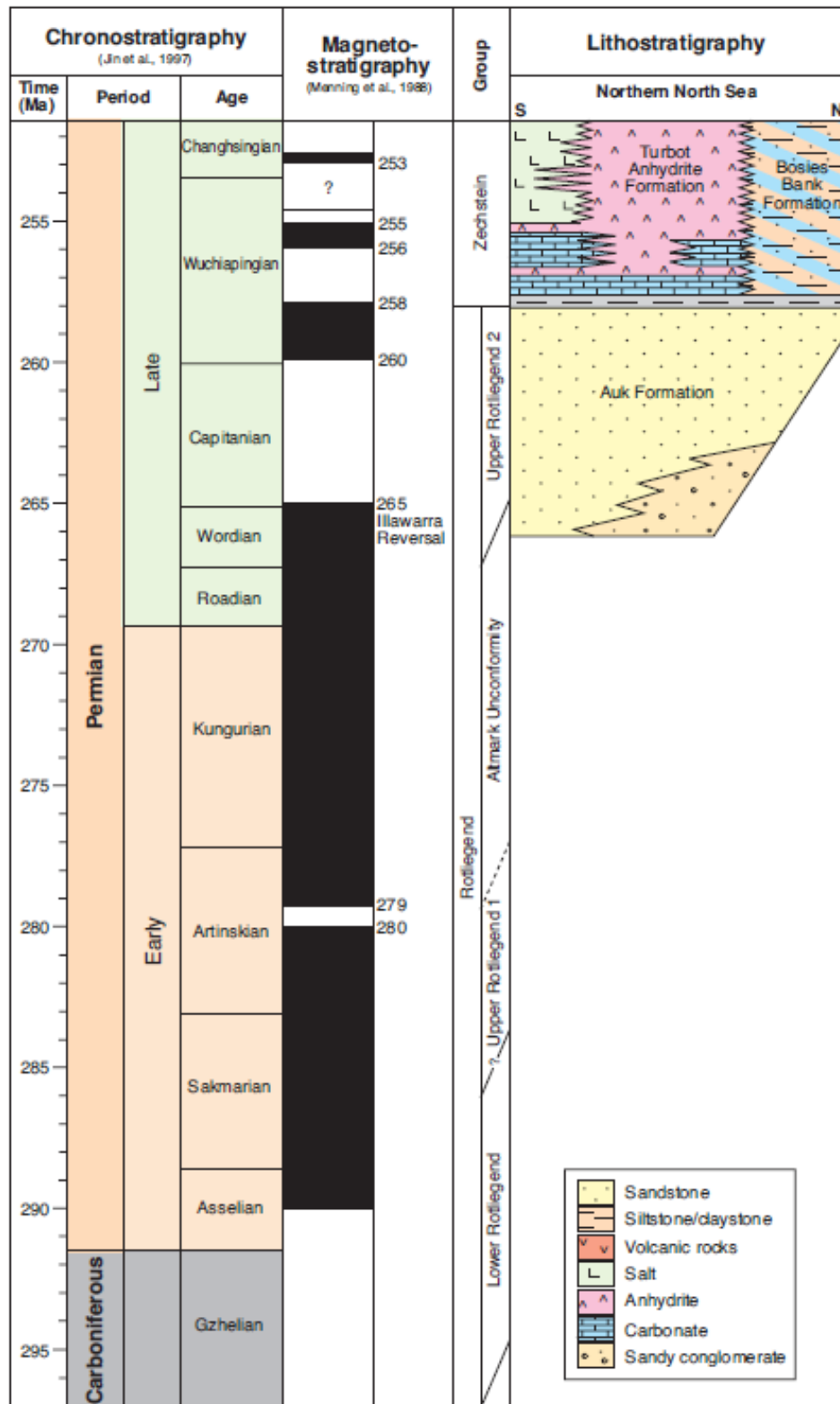


Figure 3-16. Permian lithostratigraphic column of the North Sea (Glennie 2003)

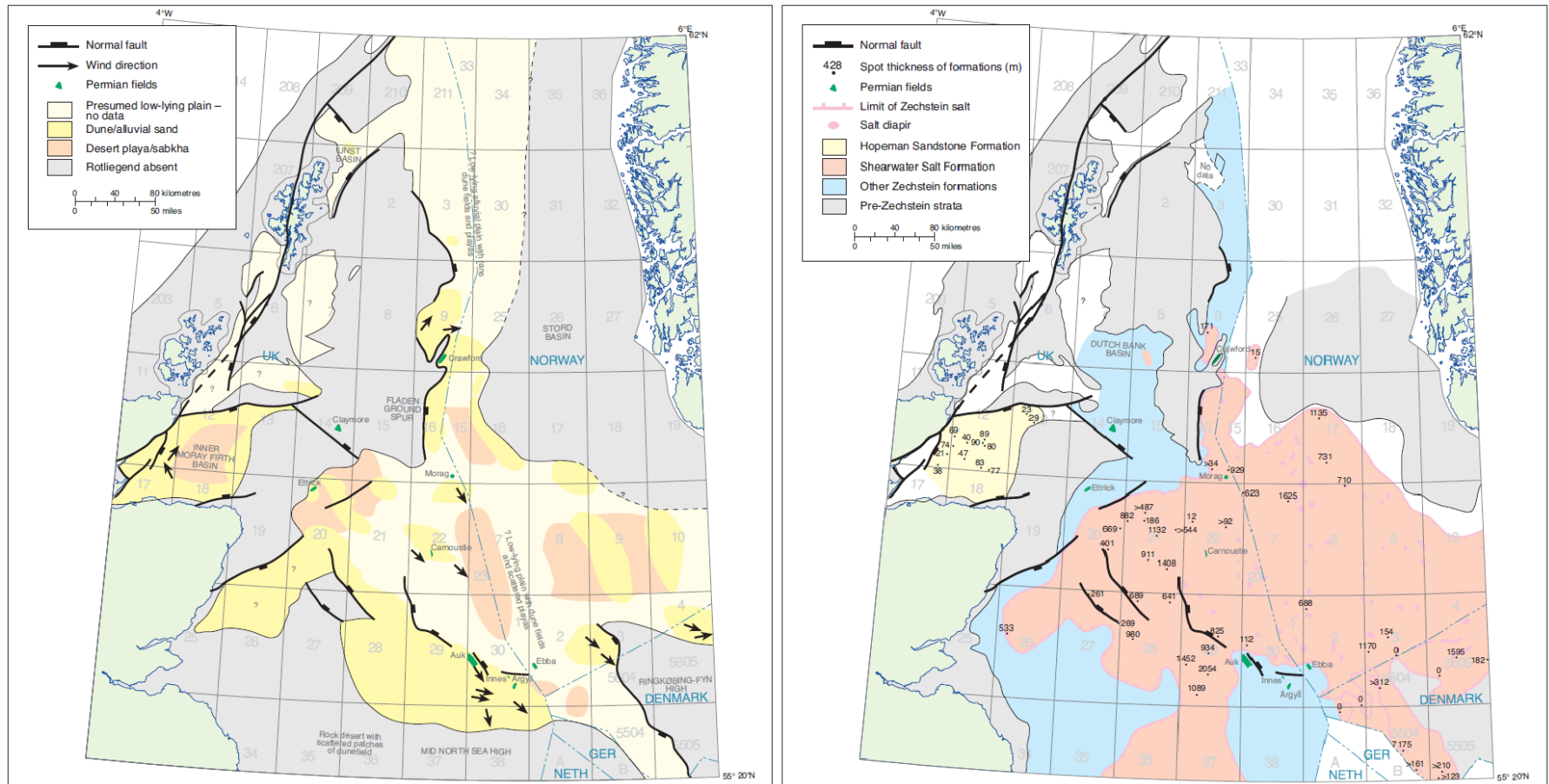


Figure 3-17. Deposition of all Permian sediments in the North Permian Basin (Glennie 2003)

The Upper Permian sediments in the Northern North Sea are represented by a basal Kupferschiefer Formation, which is overlain by the Halibut Carbonate Formation and the Turbot Anhydrite Formation (Glennie 2003). The Kupferschiefer is generally an organic rich shale which illustrates the flooding of the earlier continental environments in the Lower Permian, within an anoxic environment. Like all the Zechstein cycles, the first sequence to be deposited is a carbonate layer; in this case it is the Halibut Carbonate Formation. This limestone dominated rock also has traces of thin shales throughout, which have been later dolomitised. This subsequently led to the evaporative drawdown cycle which is commonly associated to the Zechstein sub-groups. In the Northern North Sea this is represented by the Turbot Anhydrite Formation (Glennie 2003). Some clastics are evident within the basin and are related to the localised inflow of fresh water from the north (Taylor 1998).

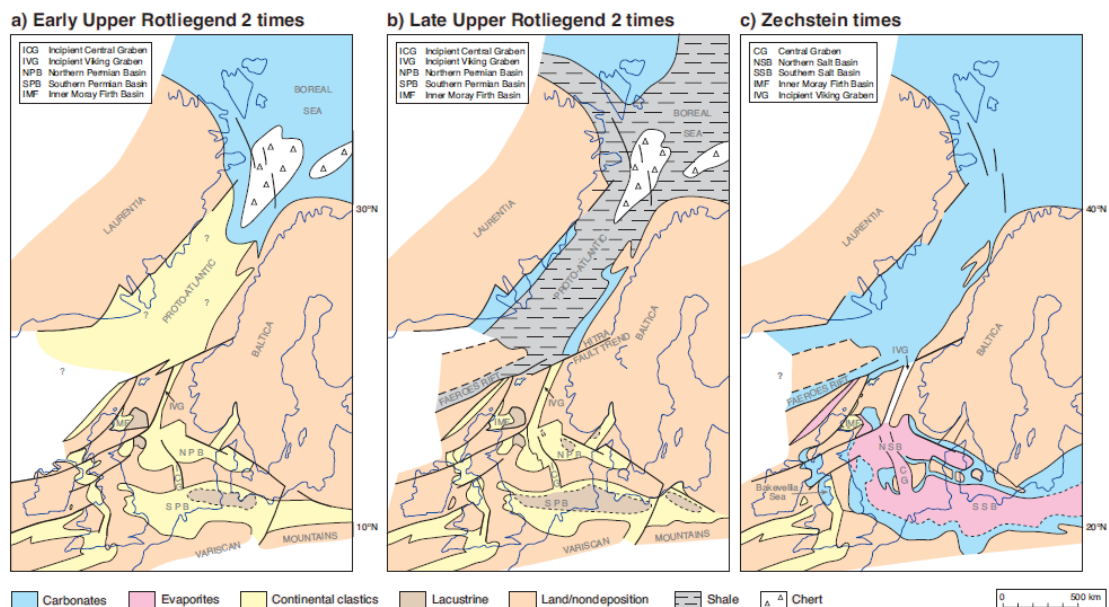


Figure 3-18. Development of the proto-Atlantic and initial Viking Graben (Glennie 2003)

The transition to deposition of evaporite and carbonate sequences in the Northern North Sea relates to the opening of the Proto-Atlantic to the north

and the influx of fresh water. The rifting to the north is potentially related to the late Permian – early Triassic rifting which occurred in the Northern North Sea. This initial extension and thinning led to the original development of the Viking Graben, in which fresh water could flow into the Northern Permian Basin (Glennie 2003).

These sediments and underlying Carboniferous sediments, make up the basement for the majority of the Northern North Sea prior to the late Permian – early Triassic rifting event (Fisher 1998).

3.3.2 Triassic

The early Triassic sedimentation was determined by the on-going rifting event which initiated in the late Permian. This was thought to produce a series of complex half grabens during the development of the rift in the early Triassic which then underwent thermal subsidence in the middle to later Triassic (Frostick 1992; Steel 1993). In some areas this generated up to 1000m of Triassic sediments but in others where erosion is evident, no Triassic sediments are deposited and the overlying Jurassic is deposited directly on to Permian strata (Ravnås 2000).

The end of the Permian and the onset of the Triassic saw the end of marine based deposition and a return to a more non-marine fluvial dominated environment as illustrated in Figure 3-19 (Fisher 1998). The Triassic sequence is almost completely made up of continental red beds, with non-marine, aeolian, sabkha, lacustrine and alluvial-fan deposits present in a predominantly arid environment (Frostick 1992; Fisher 1998; Ravnås 2000). The climate in which the sediments were deposited also plays a key role in determining sedimentation processes.

The dry, arid climate of the early Triassic is replaced with a general upward wetting transgression throughout the Triassic. The lack of water based accommodation space throughout the Triassic leads to the dominance of alluvial fan deposits which may be populated by the occasional fluvial channel (Fordham, 2010). As the environment became wetter throughout the later stages of the Triassic the primary depositional force was that of fluvial channels. This transition from terrestrial to marine environments through the Triassic reaches its maximum in the Lower Jurassic with the onset of purely marine based sediments. With this noted it is possible to see that the Northern North Sea Triassic sediments can be broadly separated into four formations that make up the Hegre Group.

The majority of the Hegre Group consists of the Cormorant Formation which is the structural high equivalent of three subdivided basinal formations, the Teist Formation, Lomvi Formation and the Lunde Formation. The Cormorant Formation terminology is generally restricted to structural highs in the UK sector, where definition between the finer formations becomes too difficult. Both of these definitions are overlain by the Statfjord Formation, which straddles the Triassic – Jurassic boundary (Fisher 1998). For this study, the Triassic Hegre Group will be sub-divided into the Teist Formation, Lomvi Formation and the Lunde Formation.

The Teist Formation is the lowermost unit in the Hegre Group and consists predominantly of interbedded sandstones, conglomerates and siltstones (Frostick 1992). One of the key components of the Teist Formation is that it contains the top unit of the syn-rift infill of the Permian – early Triassic rifting event (Ravnås 2000). As these sediments are partially deposited in a syn-rift environment, it is possible to observe wedge shaped thickening packages in the early stages of the Teist Formation. These were thought to have been predominantly continental in origin (Fisher 1998).

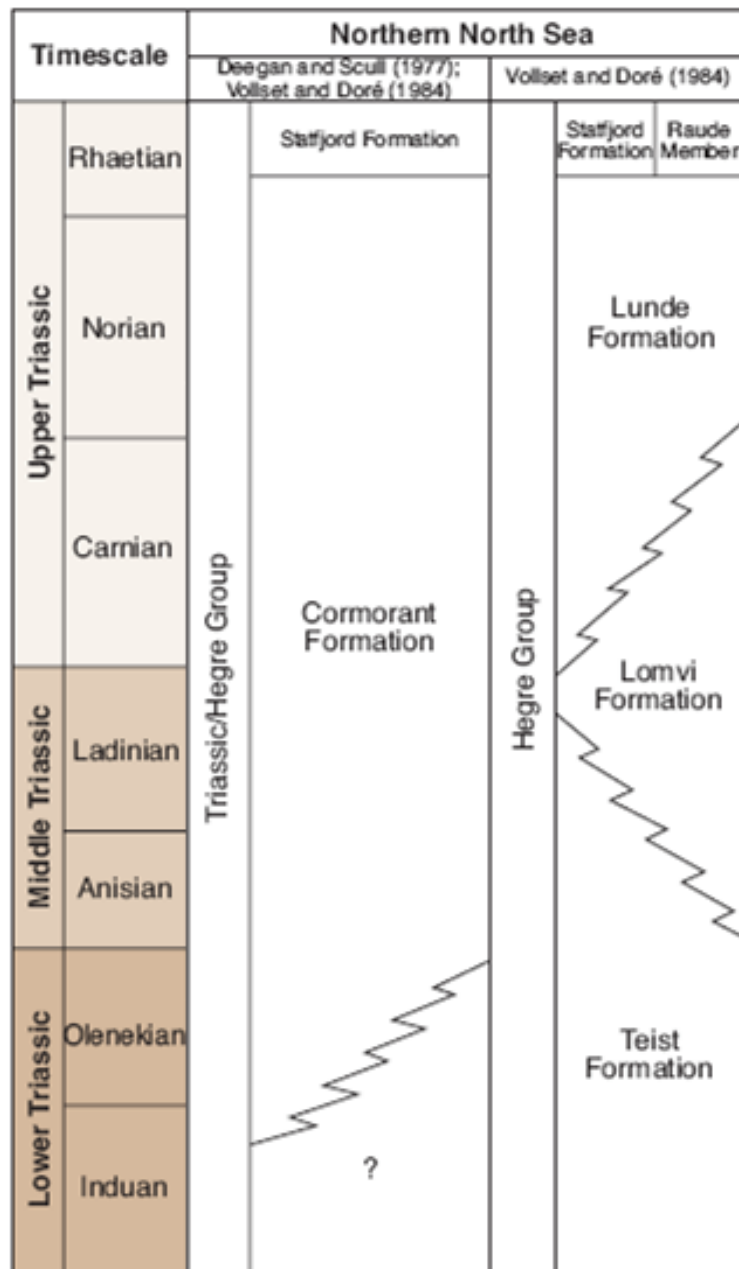


Figure 3-19. Lithostratigraphy of the Triassic in the Northern North Sea (Goldsmith 2003)

The Lomvi Formation is deposited in within a post-rift environment, where tilted fault blocks play an important role in the generation of accommodation space (Steel 1993). These sediments are mainly fine-coarse grained sandstones, which are thought to be fluvial in origin. The basal unit of the Lomvi Formation is a relatively pure sandstone although some kaolinite is found in upper sections (Frostick 1992; Fisher 1998). The uppermost unit of

the Lomvi Formation which marks the beginning of the Lunde Formation is a thick claystone unit (Fisher 1998). This is thought to be related to a period of subsidence and then uplift due to block rotation from the underlying rift faulting (Steel and Ryseth 1990).

The Lunde Formation which correlates to the upper unit of the Cormorant Formation is also deposited in a post-rift, thermally subsiding basin environment (Ravnås 2000). There is some variability in the relative thickness of the Lunde Formation due to post-Triassic erosion. This may be related to the uplift and doming effect in the Middle Jurassic (Frostick 1992). The majority of these sediments are lacustrine and fluvial in nature, which has generated a series of mottled claystones and marly units (Fisher 1998). In the middle and upper units of the Lunde Formation it is possible to see bioturbation of the sandy members (Steel and Ryseth 1990). The transition from the Lomvi Formation up into the Statfjord Formation is commonly observed as an upward coarsening succession.

It is generally accepted that the Hegre Group is topped by the Banks Group, which straddles the Triassic – Jurassic boundary (Goldsmith 2003). The boundary between the Triassic and the Jurassic is generally picked upon the first down hole occurrence of the terrestrial palynomorphs *Riccisporites Tuberculatus* and *Ovalipollis Pseudoalatus*, which are both of Rhaetian age (Steel and Ryseth 1990). Within the Banks Group is the Statfjord Formation, which is generally described as arkosic sandstones with inter-bedded shales and siltstones and a potential reservoir unit within the Northern North Sea (Steel and Ryseth 1990; Richards 1993; Fisher 1998; Ravnås 2000).

The Statfjord Formation can generally be subdivided into three main members (Figure 3-20). The three units are known as the Raude member, Eiriksson Member and the overlying Nansen Member and their deposition

patterns are shown in Figure 3-21 (Deegan 1977; Gibbons 2003). In many instances the uppermost unit (Nansen Member) is often separated away from the Statfjord Formation and is its own individual formation within the Banks Group and is solely of Jurassic age. Over the East Shetland Basin, the Statfjord Formation reaches a maximum thickness of over 300m (Richards 1993).

Series	Stage	Lithostratigraphy				
		Beryl Embayment	E Shetland Basin	Norway Viking Graben		
L JURASSIC	SINEMURIAN	BANKS GP	NANSEN FM	NANSEN FM		
	HETTANGIAN		STAT-FJORD FM	STAT-FJORD FM	Eiriksson Mbr Raude Mbr	STATFJORD FM
UPPER TRIASSIC	RHAETIAN	HERON GROUP	Harris Mbr	CORMORANT FM	LUNDE FM	HEGRE GROUP
	NORIAN		Lewis Mbr			
	CARNIAN					

Figure 3-20. illustrating the subdivision of the Statfjord formation within the Banks Group (Fisher 1998).

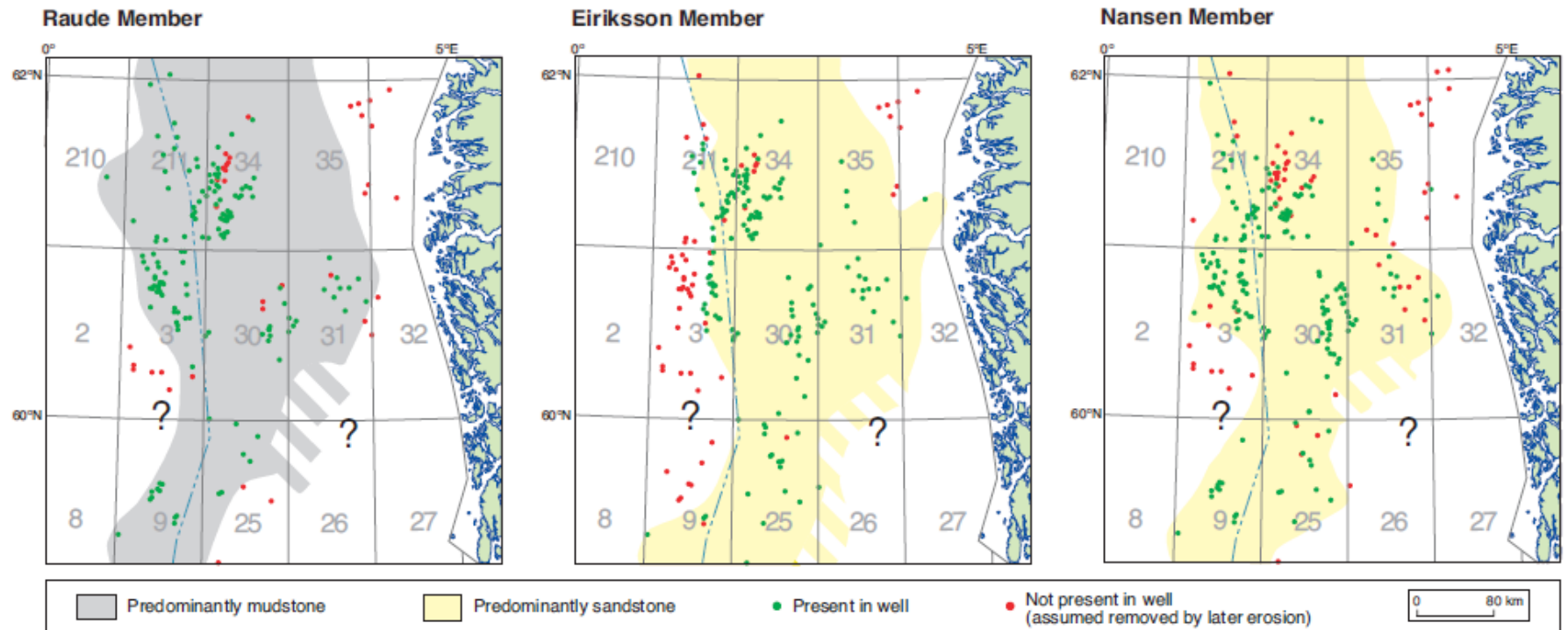


Figure 3-21. illustrating the distribution of the three members which make up the Statfjord formation (Goldsmith 2003)

The base of the Statfjord Formation is very hard to define as no major break or change in sedimentation is observed (Gibbons 2003). The only change from the underlying Cormorant Formation and the Statfjord Formation is a gradual input of coarse sandstones into the basin (Morton 1993). This is a gradual change from the argillaceous facies associated to the underlying Cormorant Formation and the varying channel types are shown in Figure 3-22 (Richards 1993).

The overall pattern from the deposition of the Raude Member to the Nansen Member shows an increase in clastic and sand dominated sediments which further illustrates an upward wetting trend through the Triassic to the Jurassic (Morton 1993). This is illustrated above, where the Raude Member is depicted as being primarily mud-dominated, whereas the Nansen Member is sandstone dominant.

Raude Member and Eiriksson Member

Although the Raude and Eiriksson Members are two separate stratigraphic units they are both very similar in composition and depositional environment. The Raude and Eiriksson Members are often depicted as predominantly heterogeneous fluvial red bedded sandstones (Morton 1993; Gibbons 2003). The Lower Raude Formation is often more shaley than the overlying units. This represents a major transgressive event in which the fluvial domain could dominate the depositional sequences (Fisher 1998). This is down to the tectonic environment the units are located within. The Statfjord formation is generally deposited within a post-rift environment and is generally subsiding after the Permo-Triassic rifting event. It is only when sedimentation keeps up pace or outpaces subsidence that the more coarse proximal sediments are deposited over the finer distal sediments of the Cormorant Group.

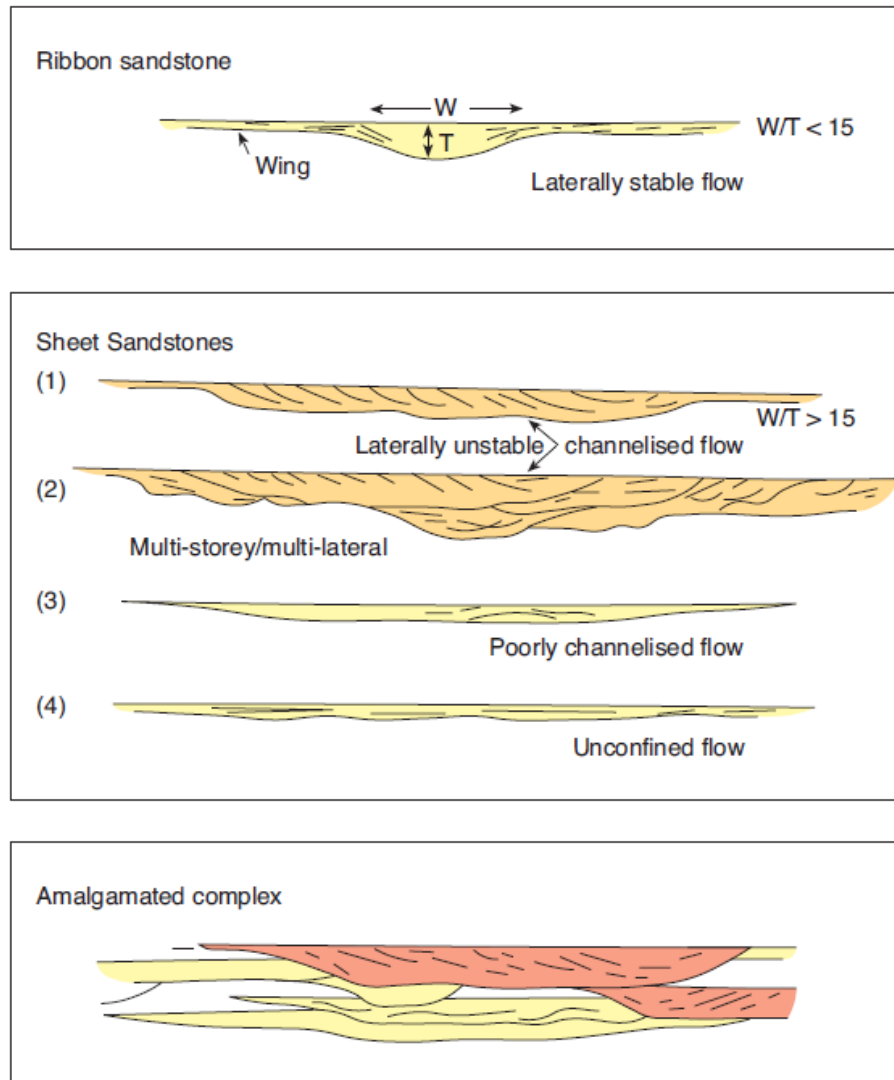


Figure 3-22. Demonstration of the inter-linking channels which make up the fluvial units of the Statfjord Formation (Goldsmith 2003).

The Raude and Eiriksson Members are generally expressed as fluvial dominated sediments (Richards 1993). The majority of these fluvial sediments can be described as heterolithic sandstones, siltstones and mudstones which are occasionally cross-bedded and are fine to very coarse in nature (Høimyr 1993; Richards 1993; Fisher 1998). This is interpreted by several authors (Deegan 1977; Chauvian 1980; Kirk 1980; Skarpnes 1980; Høimyr 1993), that the Raude and Eiriksson Members are deposited as part of a braided river system.

The major issue with fluvial dominated reservoirs is channel sand connectivity, where porosity and permeability are highest. As illustrated above, it is possible to generate three defining sandstone bodies. As the Raude and Eiriksson members are interpreted as braided streams it is more likely that the reservoir sandstones will form either as a sheet sandstone or as an amalgamated complex (Goldsmith 2003). With these types of channel sandstones, it is possible to generate more laterally continuous sand bodies. One issue could be the destruction and cannibalisation of good reservoir quality and replacing it with poorer quality sand due to the eroding nature of the base of the river system, as seen in an amalgamated complex. With the inter-bedded siltstones and mudstones, the Raude and Eiriksson members have a relatively poor reservoir quality but show a distinct coarsening and an increased input of clastic material above the clay and mud dominated Cormorant Group. In some areas coal seams are found to be up to 3.5 m in thickness, in the upper most parts of the Eiriksson formation (Richards 1993).

Nansen Member

As earlier mentioned, in some areas the Nansen Member can be removed from the Statfjord Formation and given its own stratigraphic title within the Banks Group. The Nansen Member has generally been described as a shallow-marine deposit by Deegan and Scull (1977), but has also been interpreted as a fan delta by Richards (1991) and a more fluvial dominated system by Kirk (1980), Chauvin & Valachi (1980) and Skarpnes *et al.* (1980).

These marine based sediments relate to the marine transgression which took place in the Early Jurassic (Richards 1993). It was this subsequent rise in sea-level which led to the deposition of shallow-marine dominated deposits in the Nansen Member. The Nansen Member is described as a fine to coarse grained well sorted sandstone, which is occasionally calcite-cemented. It is

this calcite cementation which made the unit so distinguishable and correlative across the Northern North Sea basin (Richards 1993). It has also been suggested by that horizontal and vertical burrowing had been distinguished in the Nansen member with some wave ripple lamination (Røe and Steel 1985).

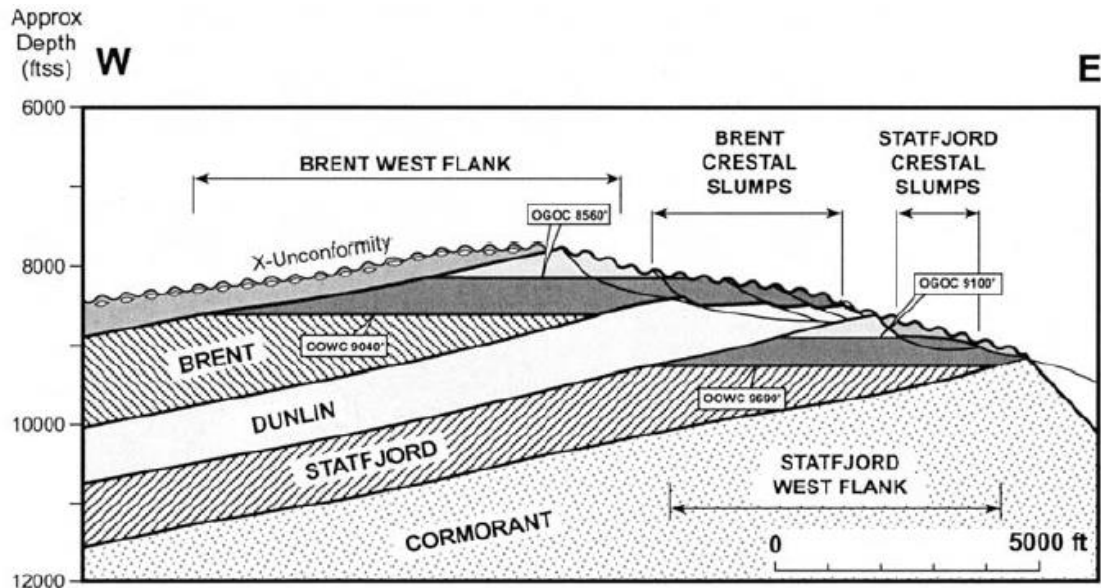


Figure 3-23. Illustration of the parallel Middle Jurassic Brent Group and Statfjord Formation reservoir sandstones (Taylor 2003).

As the Nansen Member is dominated by well-sorted, fine to coarse grained sandstone units with occasional fine beds of siltstones, the reservoir quality is much higher than the underlying Raude and Eiriksson members. This is illustrated in the giant oil fields of the Northern North Sea, such as the Brent and Statfjord fields, where the primary reservoir is the Middle Jurassic Brent, but the Statfjord Formation acting as a secondary reservoir, parallel to the overlying Brent succession (Figure 3-23). This makes the hydrocarbon prospectivity of a significant structural high in the Northern North Sea so appetising. The prospect of discovering not just one but two major hydrocarbon fields within the one geological structure illustrates why the Northern North Sea is such a densely explored hydrocarbon basin.

The top of the Nansen Member illustrates a sudden drowning of the shallow marine sandstones and inter-bedded siltstones of the Banks Group to the mudstones of the overlying Dunlin Group (Richards 1993).

3.3.3 Jurassic

As noted above the lowermost unit of the Jurassic is the Banks Group which also makes up the uppermost units in the Triassic. A major transgression occurred towards the end of the Banks Group and resulted in the drowning of the sand prone fluvial-deltaic environment (Purvis 1995; Ravnås 2000).

The Jurassic can be separated into 3 major groups (Figure 3-24), which depict a change in depositional environment from, marine-deltaic-marine. The Lower Jurassic is made up of the Dunlin Group, which indicates the initial drowning of the Triassic sediments and deposition of predominantly mudstones and siltstones. These were laid down in a thermally subsiding post-rift environment (Richards 1991). The Middle Jurassic is dominated by the Brent Group, which consists of the main reservoir in the Northern North Sea, the Brent Group. The Upper Jurassic is dominated by another marine transgression and the deposition of the mudstone and shaley Humber Group.

The Dunlin Group can be separated into 4 mudstone or siltstone dominated formations. These are the Amundsen Formation, Burton Formation, Cook Formation and the Drake Formation.

The Amundsen Formation is the lowermost unit and is representative of fully marine conditions after a period of deposition in a shallow marine environment at the base of the Jurassic (Richards 1990). The majority of the

mudstones and siltstones show signs of bioturbation and some coarsening up sequences towards its base (Underhill 1998).

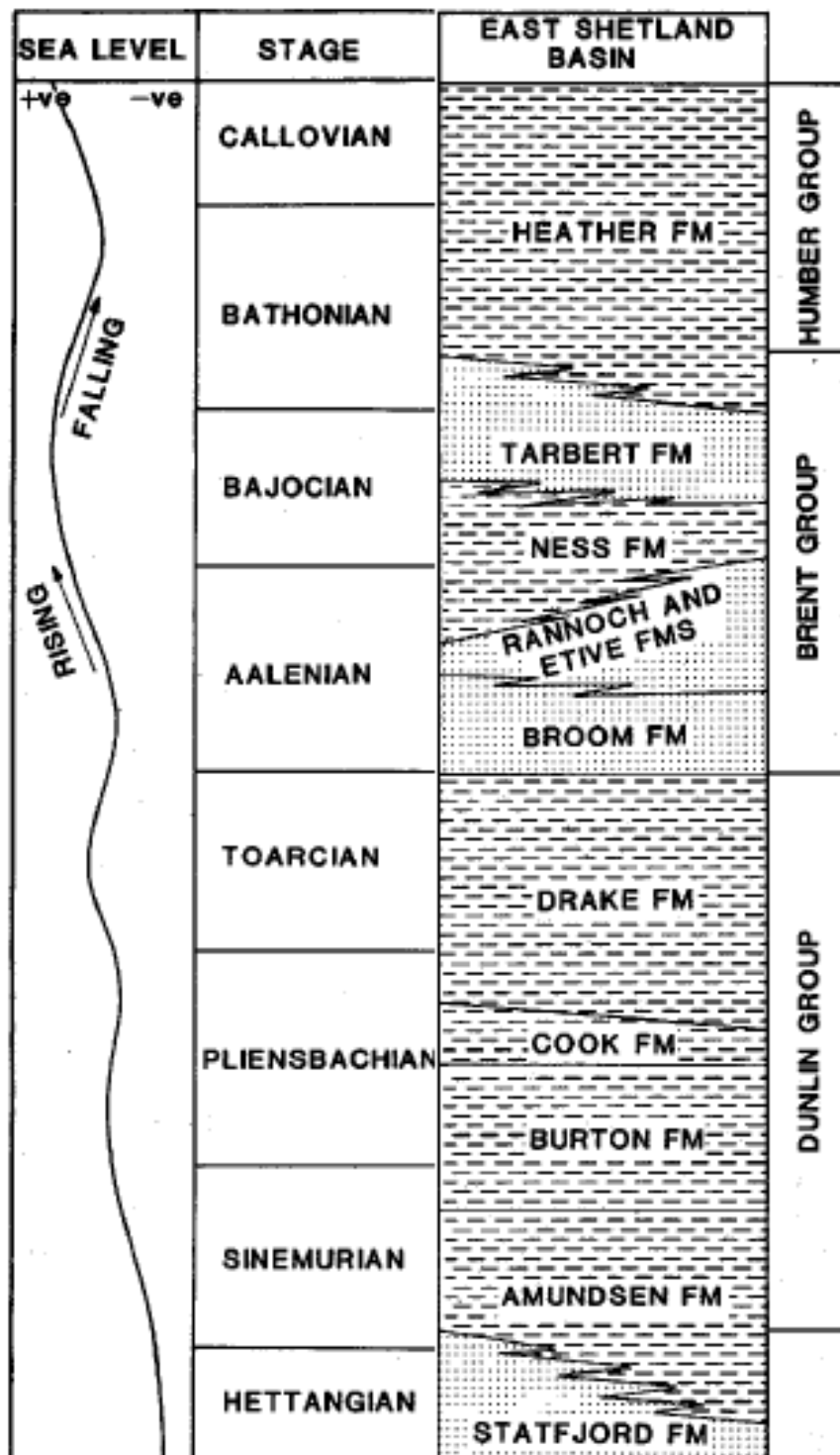


Figure 3-24. Lithostratigraphy of the Lower and Middle Jurassic (Richards 1990)

The Burton Formation is very similar to the underlying Amundsen Formation, but one major difference is the lack of bioturbation within the mudstone units. This suggests that both formations have an offshore marine origin, which is dominated by mudstones and occasional millimetre thick sandstone beds (Richards 1990; Underhill 1998).

The Cook Formation is a more sand prone-unit which is encased within mudstones of the underlying and overlying Burton and Drake Formations (Underhill 1998). These sandbodies are interpreted as prograding shallow marine sandstone, which were deposited at a low point within a period of eustatic sea level rise (Richards 1990). The upper and lower sections of the Cook Formation show both upward coarsening within the units and a relative cleaning in the sands (Underhill 1998).

The uppermost formation of the Lower Jurassic is the Drake Formation. This formation has previously been termed the “shale member” as no sandstones are present within the formation, and it is encased by sandstone both below (in the Cook Formation) and above (with the Brent Group). The uppermost unit of this section is usually missing, due to the uplift and erosion relating to the Mid Cimmerian Unconformity in the Middle Jurassic (Underhill 1998). It must also be noted that the Dunlin Group acts as a top seal to the underlying Triassic reservoirs and stratigraphically compartmentalises the underlying Statfjord Formation and the overlying Brent Group.

The appearance of the Mid Cimmerian Unconformity is usually accepted as the boundary between the Lower and Middle Jurassic sediments. This unconformity is related to the doming and volcanism that occurred in the central North Sea at the trilete rift arm junction (Leckie 1982). This doming and uplift plays an important role in the deposition of the Middle Jurassic Brent Group.

The development of the Brent Group indicates a period of shallowing and the deposition of non-marine fluvio-deltaic sediments. The Brent Group is described as a prograding delta system which can be sub-divided into five major formations (Figure 3-25 and 3-26).

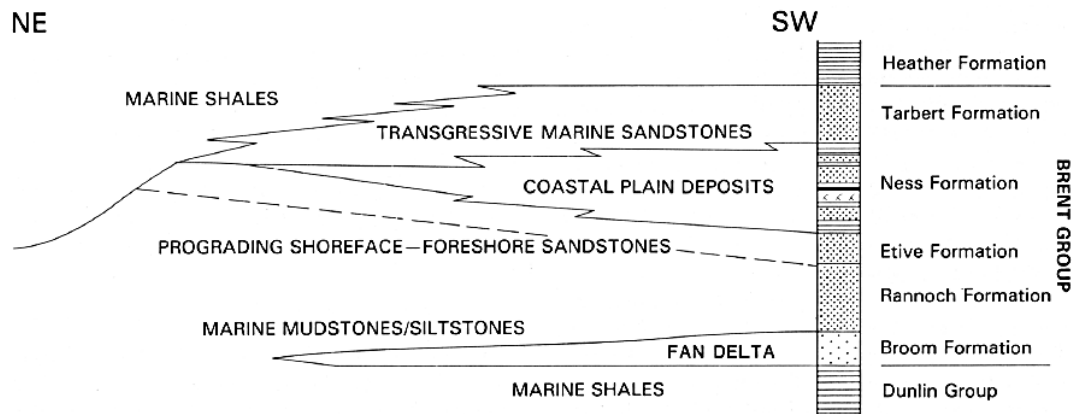


Figure 3-25. Schematic diagram showing the Brent Group orientation in the East Shetland Basin (Richards 1992)

Although the Brent Group sediments are among the most documented sediments in the North Sea, they are still some of the most misconstrued. Although five formations are defined (Broom, Rannoch, Etive, Ness and Tarbert Formations (Deegan 1977)), the interpretations can still be rather controversial. In response to this a palynographic model was generated by Graue (1987), who are able to sort the Brent Group into four distinct bio-zones. Other issues surrounding the Brent Group relate to its source and accurately describing it into a sedimentary system.

The first of the major discussions that surround the Brent Group is the source of the sediments. It was strongly believed by many authors that the source was derived by a thermal doming event which occurred at the earliest during the Middle Jurassic (Underhill and Partington 1993; (Underhill 1994)). This uplift event in the Central North Sea resulted in erosion of older sediments that subcrop the mid Cimmerian unconformity leading to progradation and

deposition along the axis of the Viking Graben. Other theories of sediment provenance relate to heavy mineralogy studies of the Brent sediments. These indicate a source origin from the basin marginal areas (Richards 1992). After heavy mineral and isotope analysis of the Brent sediments, it is possible to suggest that the Brent Group has multiple source areas. These were river systems which drained far to the West of the Brent provenance in the UK sector and far east as the Norwegian Brent provenance. These also contain the northward draining river system from the doming event in the Central North Sea (Hampson 2004).

Another uncertainty associated with the Brent Group is the type of sedimentary system it belongs to. The general consensus is that the Brent Group is part of a prograding deltaic system, although evidence from Alexander (1992) suggests that the Brent Group is part of a prograding coastal plain.

The base of the Brent Group is the Broom Formation. This is the most controversial of all since there is evidence of shallow to deep water descriptions of the Broom Formation (Richards 1992). The most legitimate explanation for the variation in facies within the Broom Formation is that it is part of a fan delta system, which relates to sedimentary infill from the uplifted rift margins (Cannon 1992). It was described by Graue (1987) that the Broom Formation in the UK sector may be an equivalent of the Oseberg Formation, observed in Norwegian sector of the Northern North Sea. The base of the Broom Formation in recent years has been identified as a sequence boundary which shows regional angular truncation.

The overlying Rannoch and Etive Formations constitute the main marine to coastal progradational phase of the Brent delta (Richards 1992). The Rannoch Formation is made up of several overall coarsening up sequences

with a sudden increase in grain size at the Formations top (Cannon 1992). The Rannoch Formation is generally interpreted as a full shore-face sequence which progrades in front of the Brent delta. This is interpreted to be deposited within a storm-wave-dominated environment (Cannon 1992; Richards 1992).

The Etive Formation is very similar to the upward-coarsening sediments of the Rannoch Formation, but is comprised of coarser sediments. The medium grained sandstones in the Etive Formation are topped by an in situ coal development (Cannon 1992). The base of the Etive is generally composed of beach deposits and passes up into barrier and back-barrier sediments.

The Ness Formation is a major reservoir in the Brent Group, as it has a higher porosity and permeability in its sand rich layers. It is possible to sub-divide the Ness Formation into three units. The Lower Ness Unit comprises of siltstones, which are likely to have formed in a lagoon to lower delta front environment (Richards 1992). The Middle Ness Unit is comprised of a widespread organic shale, which would have formed in an open lagoon setting (Cannon 1992). The Upper Ness Unit dominantly formed in a delta top or coastal plain environment and has higher sand: shale ratio than the other units within the Ness Formation (Cannon 1992; Richards 1992). Overall, the Ness Formation shows the progradation of coastal plain sediments and lagoonal sediments to a fluvial dominated upper delta plain sequence. The top of the Ness Formation and base of the Tarbert Formation indicates another sequence boundary with a widespread erosional truncation and missing sediments from the Upper and Middle Ness Units (Hampson 2004). Although no sequence boundaries are identified within the Rannoch, Etive and Ness Formations, several high frequency sequences are clearly identified (Hampson 2004).

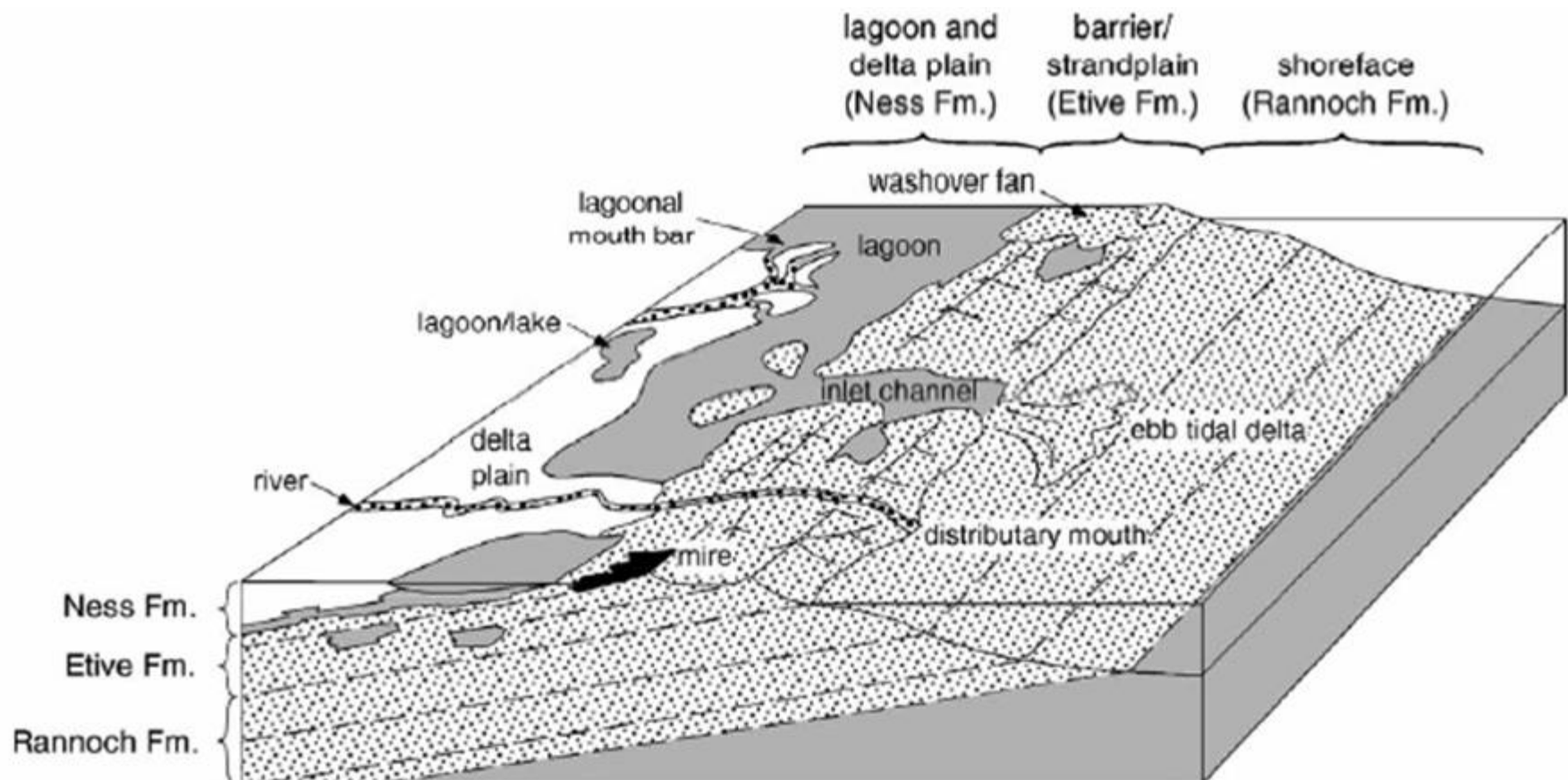


Figure 3-26. Sedimentological model for the deposition of the Brent Group sediments (Hampson 2004)

The upper most unit of the Brent Group, the Tarbert Formation, can be identified as the start of a transgressive phase of retreat. These are identified by large erosional lag deposits found at its base, these are overlaid by fine to medium grained sandstones (Cannon 1992; Richards 1992). A review of the structural and sedimentological evolution of the Tarbert Formation is discussed by Davies (2000) and identifies several sedimentological intervals within the Tarbert formation.

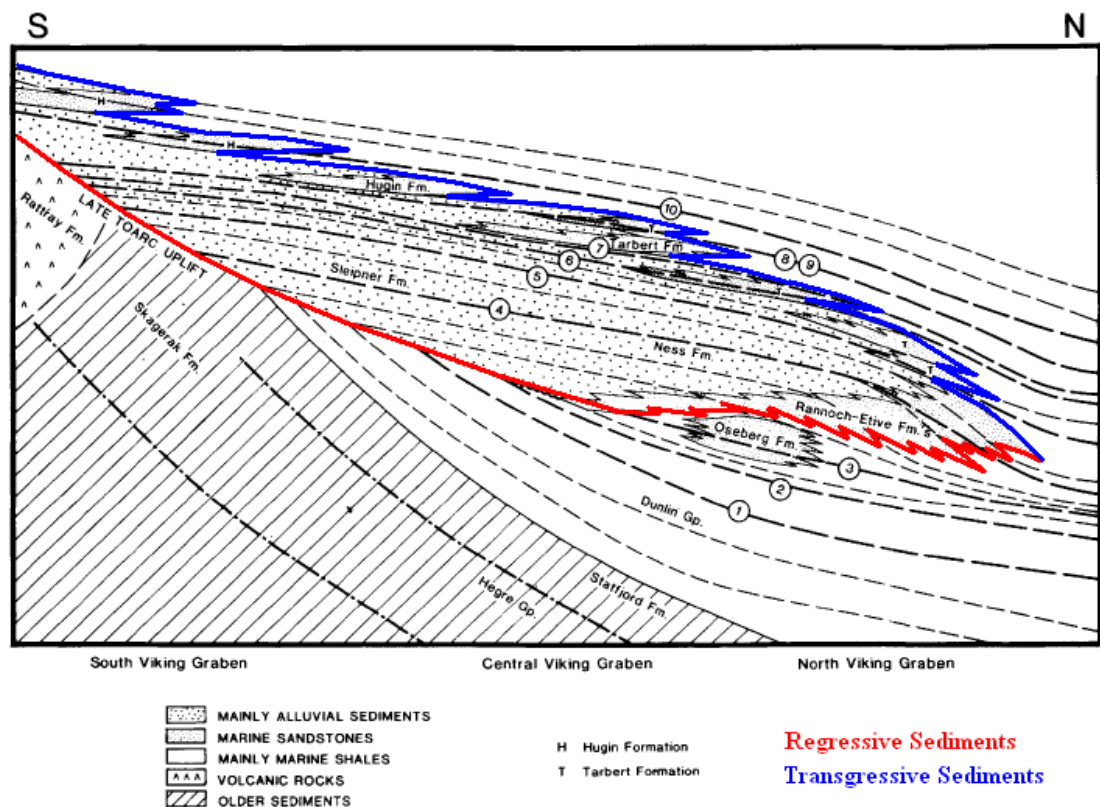


Figure 3-27. Diagram illustrating the transgressive/ regressive nature of the Brent Delta (Helland-Hansen 1992).

In summary the Brent Group is often described as a regressive – transgressive wedge (Figure 3-27), which as a whole can be separated into three major sections as described above. The base is made up of the Broom Formation which is best described as a deltaic fan deposit. This is then overlaid by the prograding delta front and coastal plain deposits, which consist of the Rannoch, Etive and Ness Formations. The final section of this

wedge is the transgressive top which consists mainly of the Tarbert Formation.

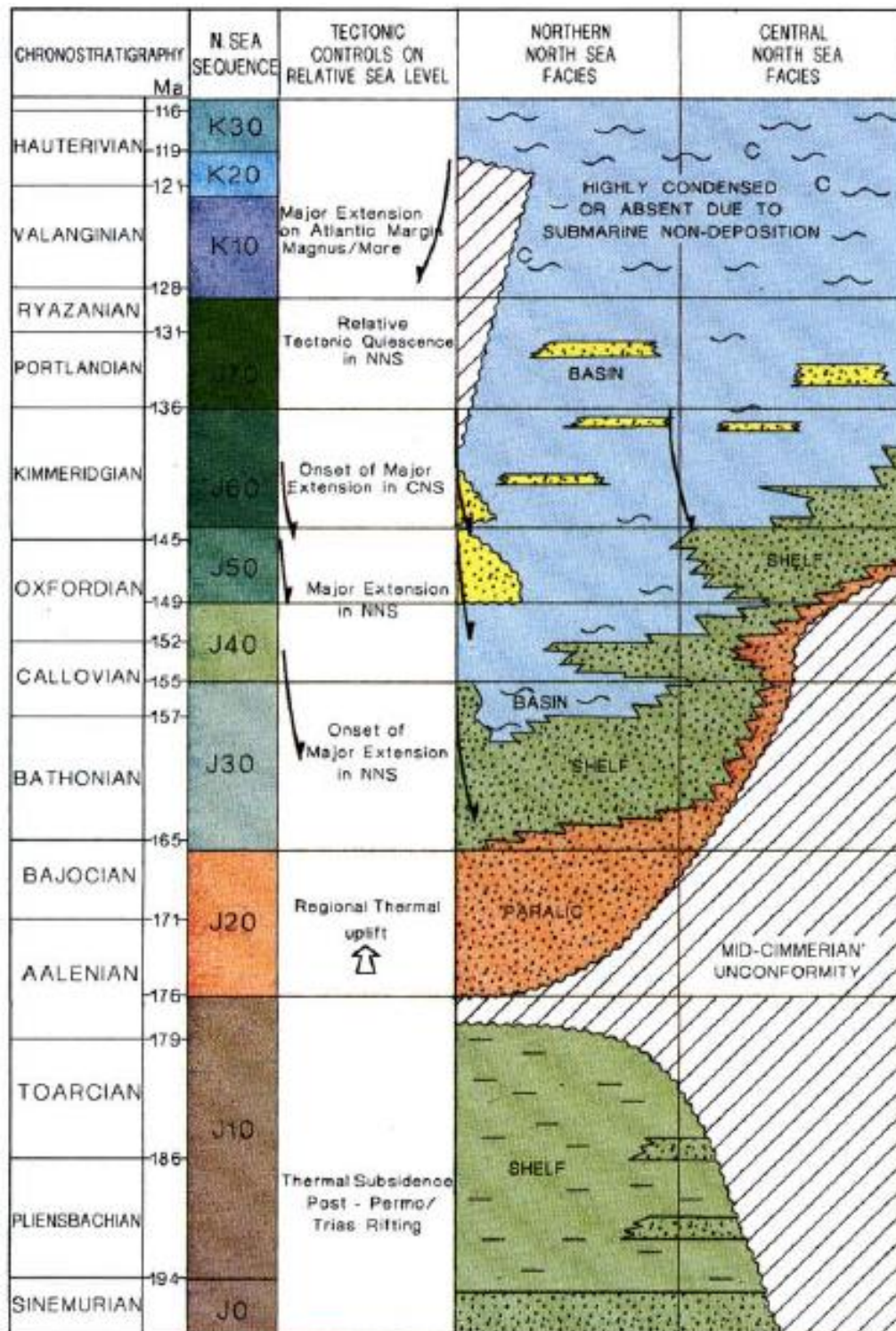


Figure 3-28. Overview of the Upper Jurassic rift related sequence stratigraphy (Rathey and Hayward, 1993)

The transgression and drowning of the Brent sediments led to the deposition of sediments back into the marine realm. This drowning is related to the opening up of the North Sea rift province, which initiated in the Late Jurassic (Leckie 1982). This transgression led to the deposition of the shale dominated Humber Group, where the Heather Formation straddles the boundary between the Middle and Upper Jurassic sediments as shown in Figure 3-28 (Underhill 1998).

The Humber Group contains two major formations, both of which are silt and mud rich but both have distinctive characteristics (Figure 3-29). It is thought that one of the reasons (along with the generation of a rift province) for the drowning of the Brent delta was that sediment supply could not keep pace with subsidence rates (Ravnås 2000). This caused a transition from the sandstone dominant Brent Group to the more silt rich Heather Formation. This was deposited within a syn-rift environment and the generation of tilted fault blocks led to the development of significant fault scarps and degradation on the top of the tilted fault blocks (Underhill 1998).

With subsidence still out pacing sedimentation, the Northern North Sea saw the deposition of the Kimmeridge Clay Formation. This is an extremely important formation within the Northern North Sea for two reasons. Firstly, the Kimmeridge Clay Formation is the primary source rock in the Northern North Sea, and secondly, it is the seal for the majority of reservoirs in the Northern North Sea. The claystones that make up the Kimmeridge Clay Formation were deposited in an anoxic environment which enhances the preservation of organic material (Underhill 1998). This accompanied with the lack of sediment supply, led to the deposition of an exceptional widespread source rock in the Northern North Sea.

The Kimmeridge Clay Formation is not completely mud rich. In some areas such as the Magnus Field it is possible to identify the deposition of a deep-water marine fan, which acts as a reservoir unit (Dawers and Underhill 2000). This is termed the Magnus Sandstone Formation and is thought to be derived from the East Shetland Platform.

The Late Jurassic Magnus Sandstone Formation (MSF) as illustrated in Figure 3-29 was deposited after the Brent Group and within the Kimmeridge Clay Formation, Late Jurassic (Shepherd 1991), as a part of the Humber Group. The Humber Group is deposited as a direct result of the drowning of the Brent Group and a continued transgression. This transgressive phase led to the deposition of the Heather Formation and the overlying mudstone rich, Kimmeridge Clay Formation, in which the Magnus Sandstone Formation is deposited (Dawers and Underhill 2000).

The Magnus Sandstones were deposited on submarine slopes, the attitude of which were related to the underlying basin depocentre axis which in turn was controlled largely by on-going rifting and syn-sedimentary footwall uplift (Shepherd 1991; Underhill 1998). The uplift that is related to the tilted fault blocks is not only responsible for erosion but also sediment redistribution, often through fault overlapping zones which form extensional relay ramps (Underhill 1998).

The MSF sediments which constitute the fan sediments are made up of high density turbidity currents, which are often fine to coarse grained and usually 2m thick (Shepherd 1991). The MSF turbidity currents have a high net: gross (commonly up to 0.9) and are surrounded by the likely source rock for the area the Kimmeridge Clay Formation (MacGregor 2005).

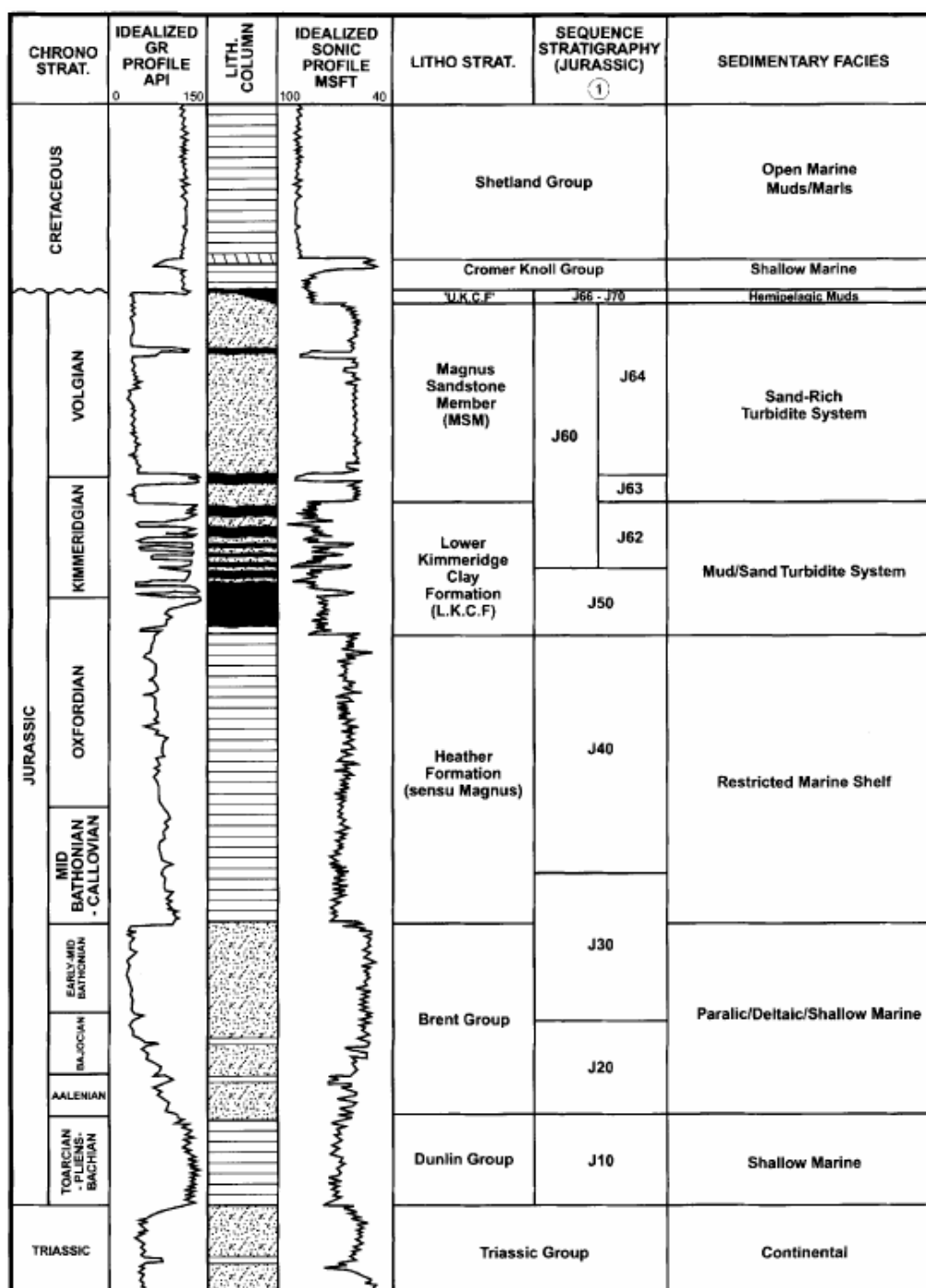


Figure 3-29. A stratigraphic column illustrating the deposition of sediments relating to the Magnus Sandstone Formation (Morris 1999)

It is possible to identify some inter-bedded mudstones and siltstones layered between the sandstone units along with some regionally continuous shale layers as shown in Figure 3-31 (Shepherd 1991). The original interpretation of the fan sediments were divided into three major units, with the Magnus

Sandstone Formation being the primary reservoir with a low net: gross mudstone based turbidity current at its base, the Lower Kimmeridge Clay Formation (Shepherd 1991; Warren and Smalley 1994). Within the MSF sediments four distinct lobes can be identified and are separated by interbedded mudstones (Warren and Smalley 1994). The interpretation of four lobes was built up by using the initial well and core data that was gathered. In 1995 after further drilling and more core data was made available it was possible to identify five other layers with the Magnus Sandstone Formation, with the use of biostratigraphic data (Partington 1993; Morris 1999).

With the aid of biostratigraphic data it was possible to identify three major deposition phases which make up the MSF deposits. The first of these three events was dated to have occurred during the latest Kimmeridge.

This formed a single marine fan which was sourced from the northwest and was deposited in the depo-centre of the faulted system Figure 3-30. The second phase of deposition formed in the Early Volgian where two depo-centres have been located either side of the Brent High. The final deposition phase occurred shortly after with a similar deposition pattern but the eastern depo-centre is controlled by further faulting (Morris 1999).

This indicates the evolution of the turbidity currents over time and how the distribution was initially controlled by structural activity which was occurring as the sediments were being deposited (Morris 1999). The channelling of sediment dispersal as seen here in hangingwall lows is a prime example of how coarse clastic material is transported into deep marine mud prone areas.

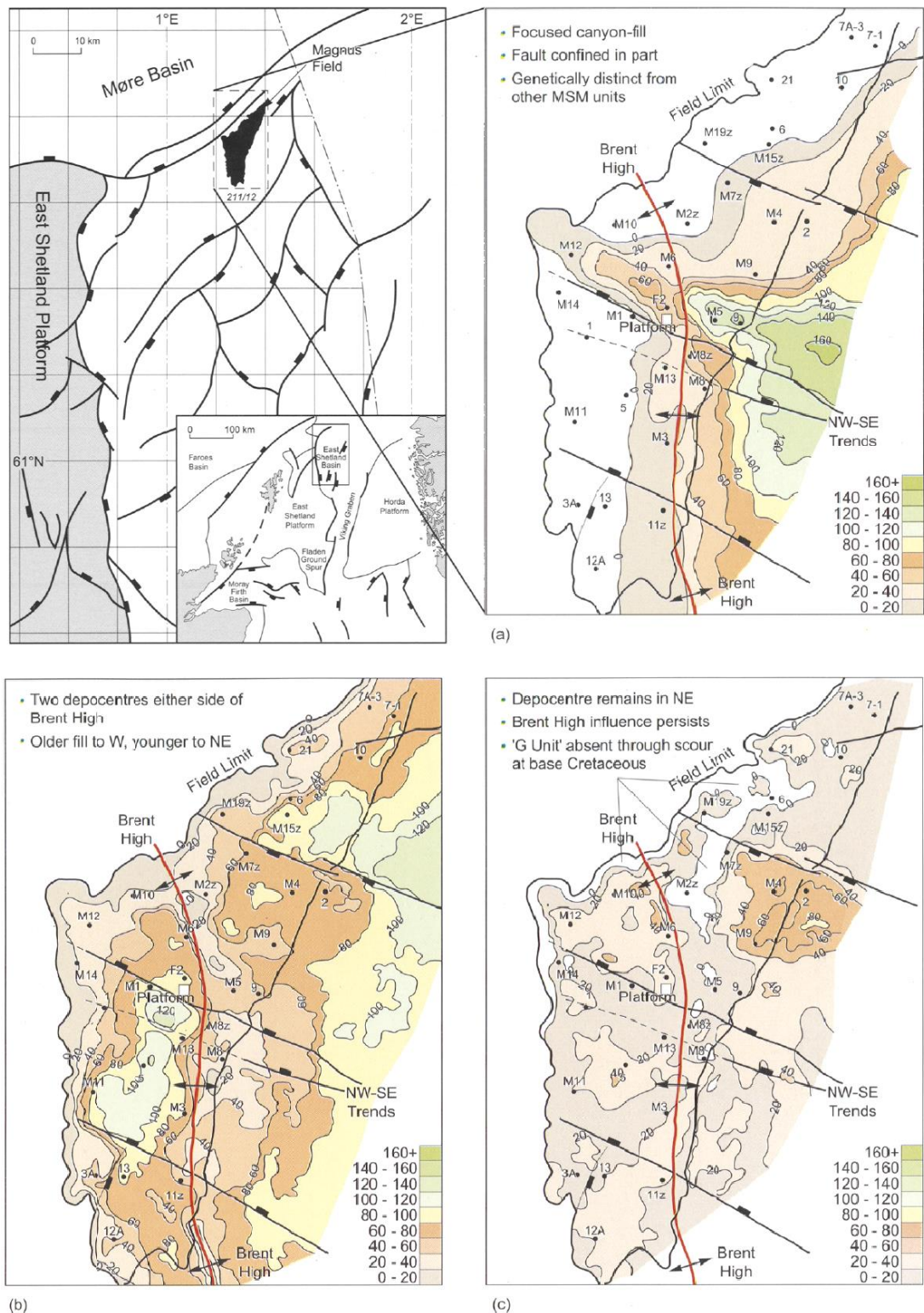


Figure 3-30. Sediment distribution diagrams for the Magnus Sandstone formation. A) Isopach for the latest Kimmeridgian; B) Isopachs for Early Volgian and C) Isopachs for mid Volgian. (Morris 1999). The Magnus Field is outlined in solid black.

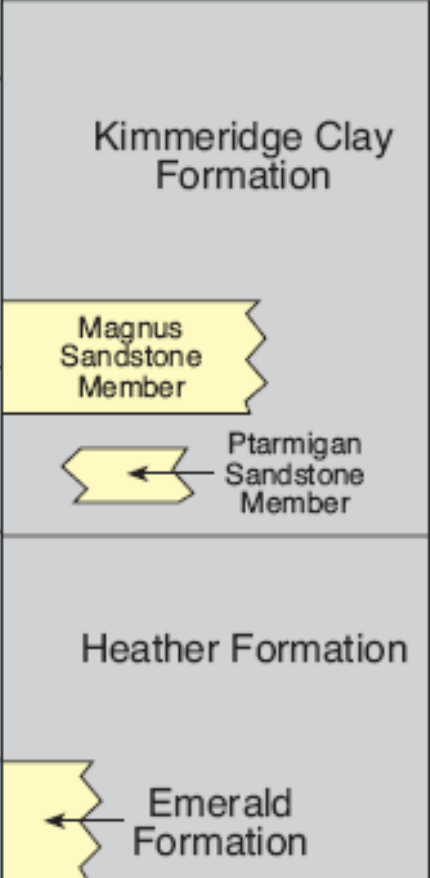
Chrono-stratigraphy		Northern North Sea	
System/ series	Stage	East Shetland Basin	
Cretaceous	Valanginian	Cromer Knoll Group	
	Ryazanian		
Upper Jurassic	Volgian		
	Kimmeridgian		
	Oxfordian		
Middle Jurassic	Callovian	Emerald Formation	
		Humber Group	

Figure 3-31. Stratigraphy of the Upper Jurassic (Fraser 2003)

The Magnus Sandstone Formation forms large stratigraphic pinch-out traps, which have formed by a period of erosion in the Lower Cretaceous. The lateral extent of the reservoir is determined by deposition patterns; both a lateral and vertical seal is formed by the overlying Kimmeridge Clay formation. If the top of the Kimmeridge Clay formation is eroded by Upper

Jurassic uplift, a top-seal can still be formed by the overlying Lower Cretaceous mudstones (Warren and Smalley 1994).

The uppermost sections of the Kimmeridge Clay Formation often show signs of erosion. This is related to the late Cimmerian Unconformity which occurs in several areas over the North Sea as either an erosional, angular or disconformity depending upon the amount of uplift generated by block rotation related to the Middle Jurassic rifting event (Copestake 2003).

3.3.4 Cretaceous

The Cretaceous is marked by a major unconformity which has often been termed the late Cimmerian Unconformity or the Base Cretaceous Unconformity. The generation of this unconformity is related to the block rotation from underlying faulted blocks, and a general shallowing that occurs in the North Sea (Rawson and Riley 1982; Copestake 2003). The shallowing is not just related to the uplift of tilted fault blocks, but also as a reduction in subsidence rates and the progressive infill of sediments. It is clear to see that the unconformity episode wasn't a singular event but a series of unconformities, which cut into one another to emphasize the erosive nature of the unconformity (Copestake 2003). It is important to mention that the structures that were generated in the Upper Jurassic rifting event were under-filled come the Cretaceous (Oakman 1998). A possible reason for the under-filled nature of the basins, is related to the failed dome in the Central North Sea, which could have caused over-deepening and further creation of accommodation space (Oakman 1998).

Chrono-stratigraphy		Sequence stratigraphy		Northern North Sea	
Series	Stage			UK Viking Graben	
				North	South
Upper Cretaceous				Chalk/Shetland Group	
Lower Cretaceous	Albian	K60		Rødby Formation	
		K55		Carrack Formation	
		K50		Skiff Sst Mbr	
	Aptian	K45		Fischschiefer Bed	
		K40			
	Barremian	K30	K38	Munk Marl Bed	
			K36		
			K34		
			K32		
	Hauterivian	K20		'End of the World Sands'	
	Valanginian	K10	K14		
			K12		
	Ryazanian	J70		Valhall Formation	
Upper Jurassic				Kimmeridge Clay Formation	

Figure 3-32. Cretaceous stratigraphy (Copestake 2003)

The Cretaceous in general can be subdivided into two major chronostratigraphic groups (Figure 3-32 and 3-34). The Lower Cretaceous is referred to as the Cromer Knoll Group and the Upper Cretaceous is termed the Shetland Group. The Cromer Knoll Group sediments are dominated by siliciclastic strata, whereas, the Shetland Group sediments are mainly claystones and argillaceous marls (Leckie 1982; Oakman 1998).

The Lower Cretaceous Cromer Knoll Group saw the beginning of a prolonged post-rift thermal subsidence, which led to the generation of a broad synclinal basin over the rift arm of the Viking Graben in the Northern North Sea (Leckie 1982). The Cromer Knoll Group can be separated into three formations, the Valhall Formation, Carrack Formation and the Rødby Formation.

The basal unit to the Cromer Knoll Group is the Valhall Formation. This formation is deposited prior and posts the minor unconformities relating to the major Base Cretaceous Unconformity. This results in coarse clastic sediments being deposited within a predominantly marine environment. The majority of the sediments are calcareous claystones and marls (Copestake 2003). In the upper sections of the Valhall Group it is possible to identify the Fischchiefer Bed, which has a total organic carbon content of up to 12.7%. This bed, although it is thin is capable of generating large quantities of hydrocarbon (Copestake 2003).

The Carrack Formation overlies the Valhall formation and consists of poorly calcareous, hemiplegic claystones. Within other basins in the North Sea, several reservoir sandstone units are deposited. In the Moray Firth area, the Halibut Horst is heavily eroded due to uplift, which generates the Captain Sandstone Member (Copestake 2003). Whereas, in the Northern North Sea area, more marine dominated sediments are deposited on the gradually subsiding basin.

The upper formation of the Cromer Knoll Group is the Rødby Formation, which is dominated by pelagic carbonates, marls and calcareous claystones. These were the last sediments to be deposited prior to the onset of the Chalk Sea which was dominant in the Southern North Sea (Kent 1975; Surlyk 2003). This led to the eventual drowning of all the structural highs in the North Sea

such as Upper Jurassic footwall highs which were close to or above sea level during the Cretaceous period. This may have played an important role on reservoir quality in the exposed sediments.

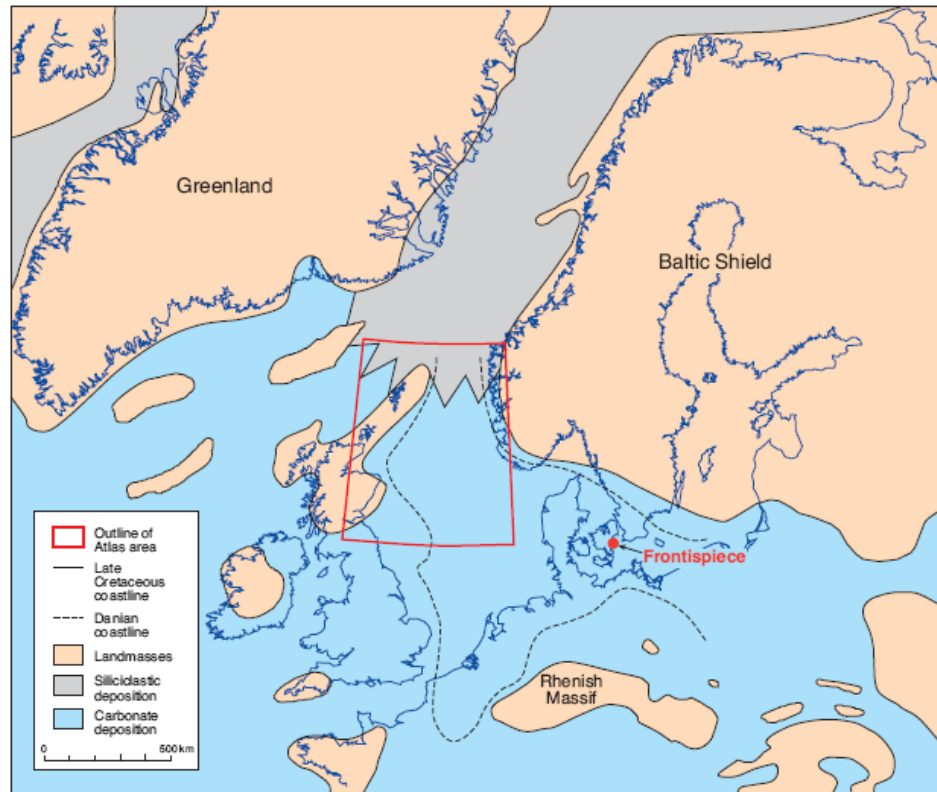


Figure 3-33. Upper Cretaceous deposition patterns (Surlyk 2003)

The Upper Cretaceous saw a further deepening of the North Sea, especially in the Northern North Sea. It has been proposed that the over-deepening in the Northern North Sea is the reason why no carbonate material is recorded in the Shetland Group (Oakman 1998). In the Southern North Sea the Shetland Group is termed the Chalk Group and is represented by thick continuous deposition of Chalk, as seen along the southern coast of England. Whereas, in the subsiding basin of the Northern North Sea siliciclastic and clay dominated sediments are present as shown in Figure 3-33 (Surlyk 2003). The continual thermal subsidence related to the Upper Jurassic rifting event may have resulted in the sea bed in the Northern North Sea being too cold and below the carbonate compensation level (Leckie 1982).

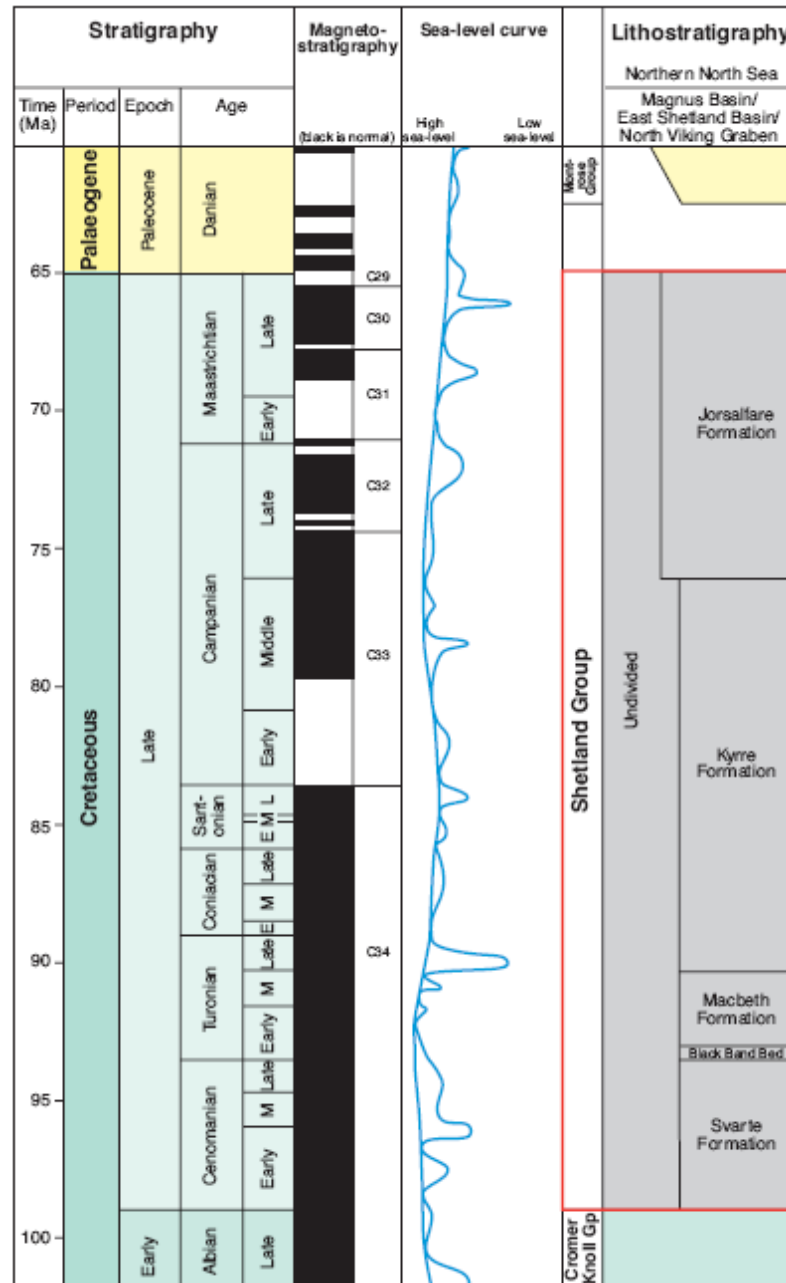


Figure 3-34. Lithostratigraphy of the Upper Cretaceous (Surlyk 2003)

The deposition of marl and silty sediments continued throughout the Upper Cretaceous and it is possible to subdivide the Shetland Group into five main formations, but for the purpose of this research the subdivision is not required.

3.3.5 Tertiary

The Tertiary sediments like the Cretaceous sediments are laid down in an unfaulted subsiding basin. This is continual thermal subsidence related to the Upper Jurassic rifting event (Kent 1975; Erratt 1999; Jordt 2000). In general terms the Tertiary sediments are made up of marine clastics which are predominantly fine grained to shaley with reservoir sandstones present within the Palaeocene and Pliocene (Kent 1975).

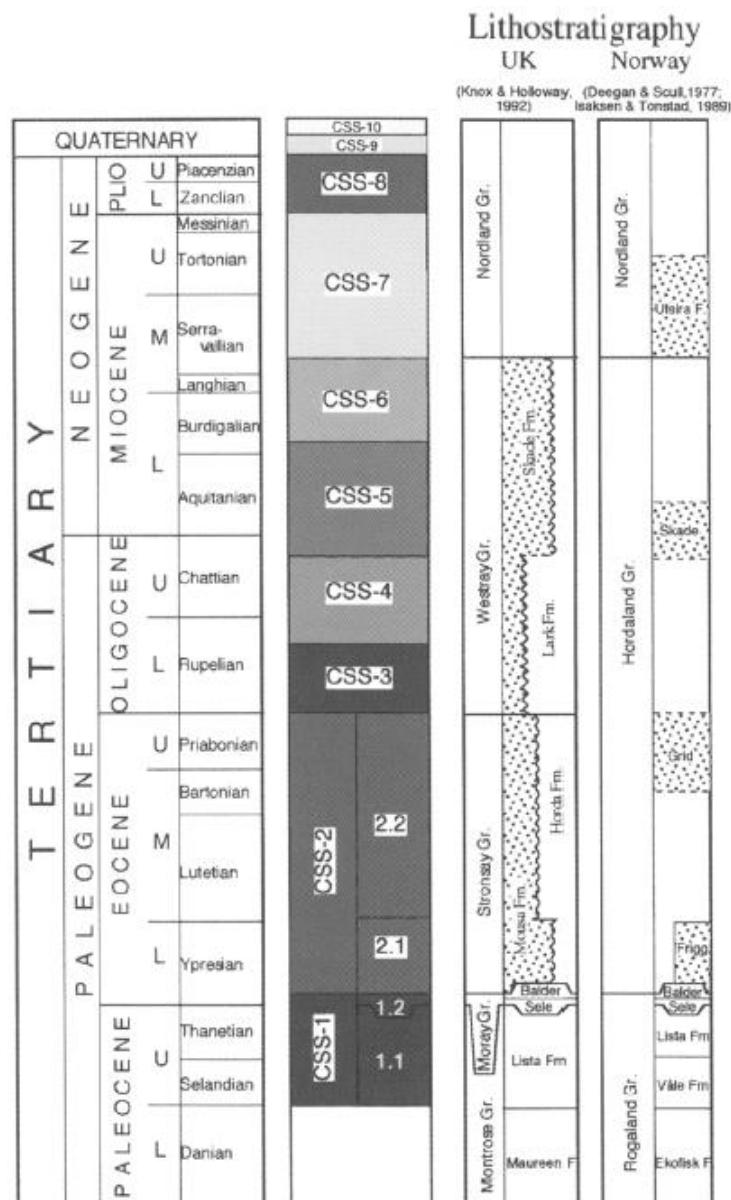


Figure 3-35. Lithostratigraphy of the Tertiary sediments in the Northern North Sea (Jordt 1995)

The Tertiary sediments can be separated into five major groups (Figure 3-35), which roughly correlate to Tertiary Epochs. These are the Montrose Group (Figure 3-36), Moray Group (Figure 3-36), Stronsay Group (Figure 3-37), Westray Group (Figure 3-38) and the Nordland Group (Figure 3-38). Each of these Groups can be sub-divided into separate formation, such as the Balder Formation of the Moray Group, which is depicted as a tuff deposit. These tuffs are correlated to the continental break up phase in the North Atlantic between Greenland and Europe (Bowman 1998; Ahmadi 2003).

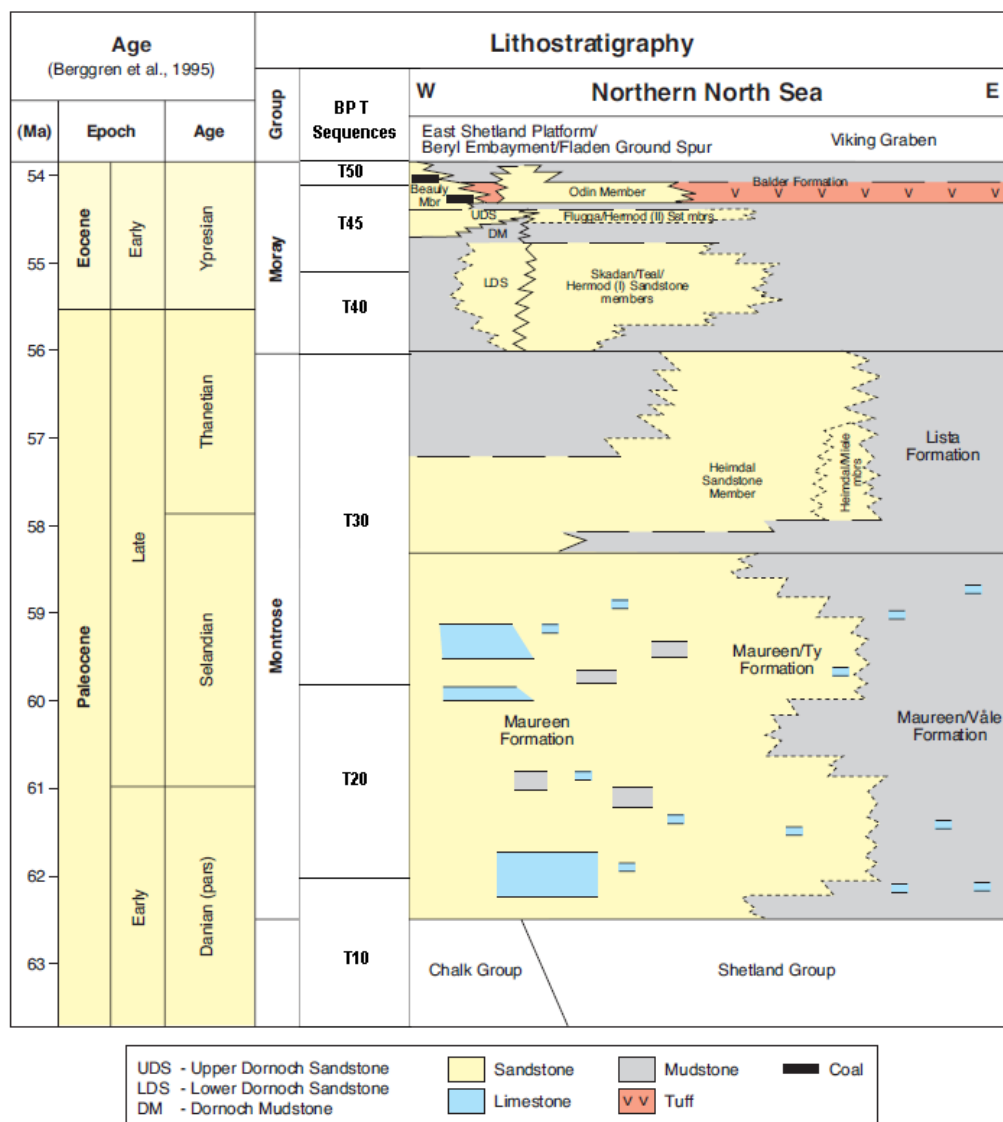


Figure 3-36. Lithostratigraphy of the Montrose and Moray Group sediments (Ahmadi 2003)

Timescale			Sequence stratigraphy		Lithostratigraphy								
Ma	Epoch/age		Magneto- chrono- strat	BP genetic seq strat Jones and Milton (1994)	Knox and Holloway (1992)								
31	Oligocene	Early	C12		Westray Group								
32													
33	Eocene	Late	Priabonian	C13	T90	T98	Stromsøy Group	Mousa Formation (shelf sandstone) Horda Formation (basinal mudstone) H3	Grid Sandstone Member				
34													
35													
36													
37		Bartonian	C17	C18						T96	T94	H2	
38													
39													
40													
41		Lutetian	C19	C20						T92	T84	T82	H1
42													
43													
44													
45													
46													
47	Early	Ypresian	C21	T80	T70	T60	Moray Group	Beauly Fm Balder Fm					
48													
49													
50													
51	Late	Thanetian	C22	T60/ 70	T50	T45	T40	Mont-rose	Lista Fm				
52													
53													
54													
55	Paleocene			C23									
56													

Figure 3-37. Lithostratigraphy of the Stromsøy Group (Jones 2003)

This volcanic activity also uplifted the western edge of the UK, which led to widespread erosion of the uplifted areas. This uplift and erosion led to deposition of clastic material, such as deltaic and sub-marine fan complexes in the deep basins of the Northern North Sea in the Tertiary (Bowman 1998). Once the rifting event was successfully complete in the North Atlantic, there was a reduced rate of uplift and erosion. This restricted the amount of clastic input into the Tertiary basins from the Eocene onwards (Bowman 1998; Jordt 2000).

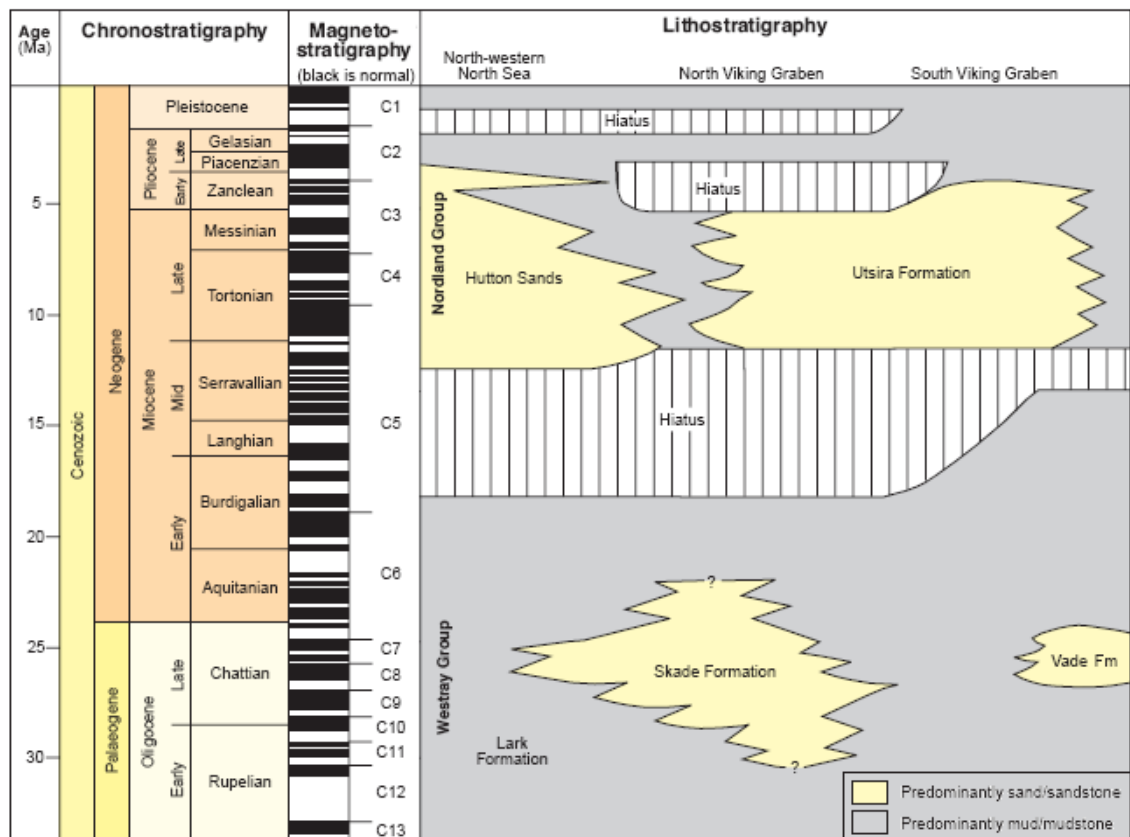


Figure 3-38. Lithostratigraphy of the Westray and Nordland Groups (Fyfe 2003)

The uppermost units of the Tertiary belong to the Nordland Group. These sediments in areas are very sand rich, although they have been deposited in a deep-marine environment. This is related to turbidite deposits, which can be sourced from the marginal areas within the basins. These sands along with others deposited throughout the Tertiary are widely assumed to have

significant value in hydrocarbon exploration. Several discoveries are being developed from Tertiary reservoirs in the UK sector of the Northern North Sea, such as the Frigg and Alba Fields (Jones 2003).

3.4 *Exploration History*

The East Shetland basin is an area of extremely high hydrocarbon production situated between Scotland and Norway (Figure 3-39). The continental shelf of Northwest Europe situated between the United Kingdom, Norway, Denmark, Germany, Netherlands, Belgium and France has been the scene for hydrocarbon exploration for over 160 years. The first case of exploration was with the mining of Boghead coal in the Midland Valley of Scotland for the generation of oil-shales (Brennand 1998).

The initial offshore exploration occurred in 1958 once the territorial rights to mineral resources below the seabed had been agreed; meanwhile onshore exploration had been on-going for several decades. The Wietze Field was discovered in 1859 near Hanover, northern Germany and continual exploration of salt domes and anticlines led to the discovery of a further 70 fields (Brennand 1998). The earliest onshore UK exploration well in the east of England found gas in the Eskdale anticline within Zechstein dolomites. Although drilling began in 1930 in the south of England where oil seeps were known to occur, the Kimmeridge oilfield was not discovered until 1973 (Brennand 1998).

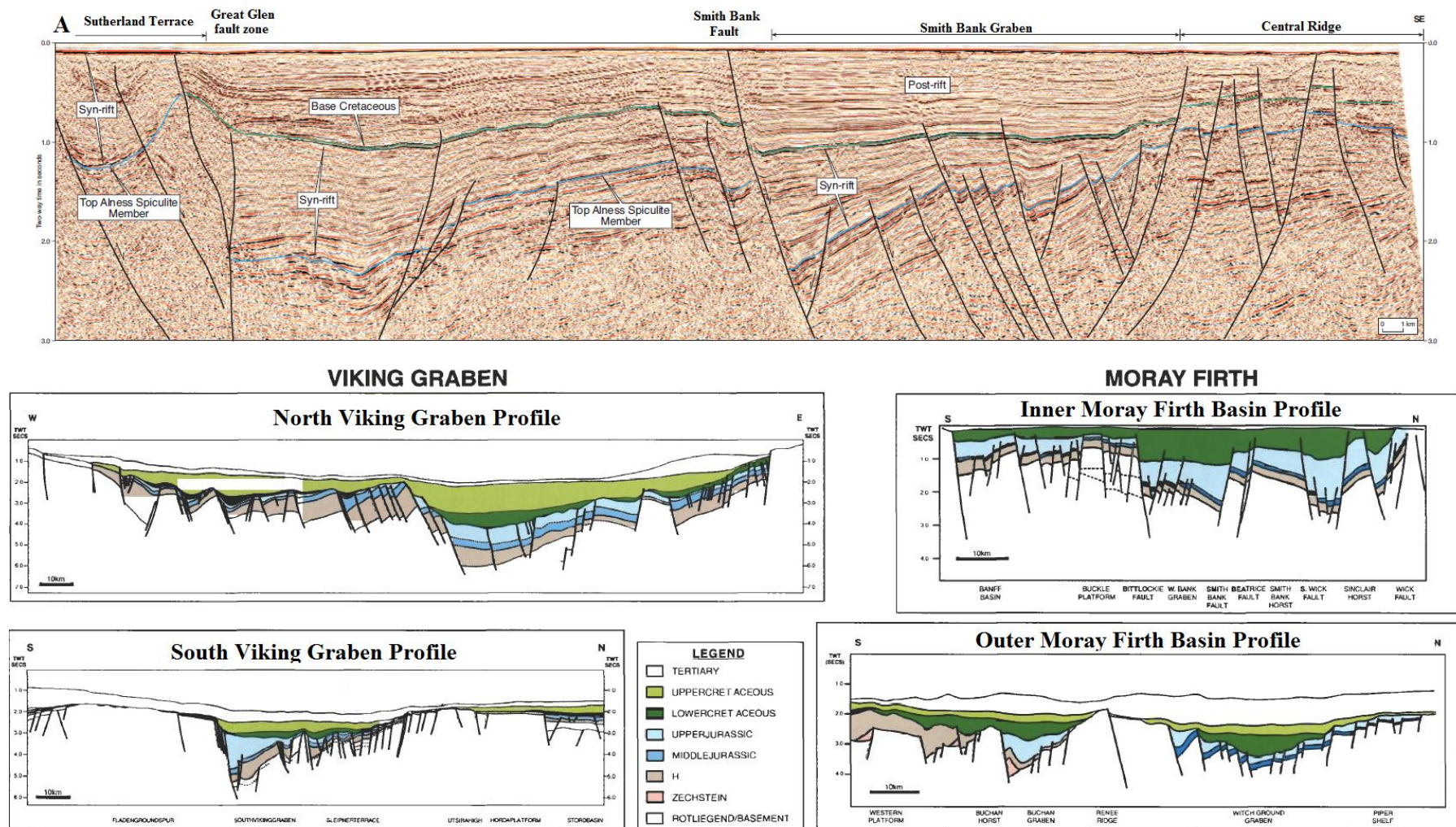


Figure 3-39 A= observation of buried highs IMF (Fraser 2003) ,B=Observation of Northern north sea buried highs (Erratt 1999)

With discoveries being found on both sides of the Southern North Sea it was only logical that other large discoveries will be found in between the two areas. This led to the exploration of the Southern North Sea, which boomed in the 1960's. The first UK offshore well was drilled in 1964 on the Mid North Sea High. With the continual drilling of prospects in the Southern North Sea it was only a matter of time before exploration spread northwards.

With the enhancements in 2D seismic data in the late 1960's it was now possible to identify the extent of prospective fields more precisely (Figure 3-40). By the 1970's exploration had spread up to the Northern North Sea and the use of 2D and 3D seismic datasets showed buried highs which were considerable larger than any field found in the Southern North Sea (Brennand 1998).

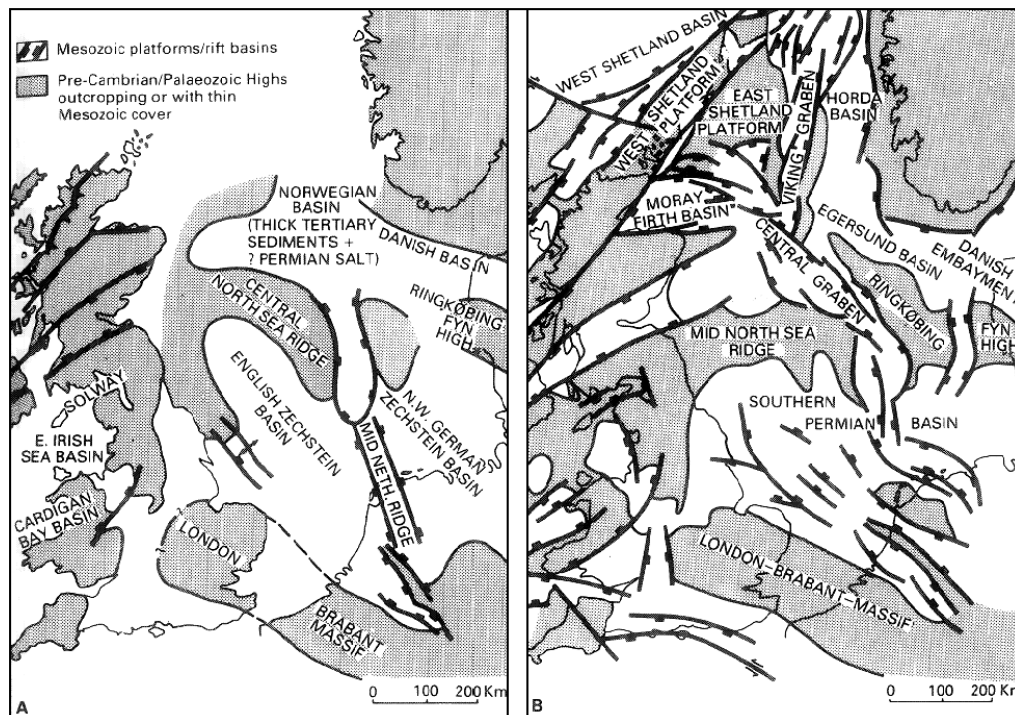


Figure 3-40. Improvement of understanding through available data from wells (Brennand 1998)

The first oil field to be discovered in the Northern North Sea was the Brent Field in 1971 (Taylor 2003). The discovery of oil bearing sands of deltaic origin in the Jurassic led to extensive exploration in the succeeding years which led to the discovery of further Jurassic aged fields.

The persistent discovery of enormous oil fields in the Northern North Sea led to the continual drilling of wells in the area. Along with the drilling and seismic data being processed, a greater amount of information was being produced. This led to a better understanding of the subsurface and how it has evolved over geological time.

After 50 years of continuous exploration and development in the Northern North Sea the seismic datasets and well results have built up an extensive library of resources available to undertake this project. The merged seismic database that was made available to this thesis along with the copious amounts of well data in both log and core form gives the ideal opportunity to investigate outstanding issues within the basin.

Chapter 4 Data and Methods

Before the advent of seismic data prospective sites for drilling were primarily determined by visible surface expression, such as anticlines, where hydrocarbons could accumulate over geological time due to their lower density and propensity to rise. With the use of geophysical methods, however, the quest for hydrocarbons moved into areas where no surface expressions are visible. The use of seismic, gravity and magnetic data supported by borehole data enabled geologists and geophysicists to identify the nature and attitude of the rock in the deep subsurface (Nettleton 1976).

Following the discovery of the Groningen Field in North Holland in 1959 the search for hydrocarbons was extended into the Southern North Sea in the early 1960's after significant oil and gas discoveries on the east coast of England and the west coast of Holland respectively. The idea being that, if hydrocarbons are found in structural closures below land, hydrocarbons should be found in similar structures below the southern North Sea. With the advancements made in hydrocarbon exploration, generally more than one source of data is used to quantify the potential location of stored hydrocarbons. The types of data more commonly used in hydrocarbon exploration are seismic data, borehole data and a combination of gravity and magnetic data. Each of these data types has its own unique way of aiding the interpretation of the underlying subsurface.

4.1 *Seismic Data*

The seismic dataset methods of interpretation are generated on the measurement of travel times of artificially induced elastic waves that are sent

into the ground and reflect off horizons of acoustic impedance (due to changes in density and/or velocity) (Nettleton 1976). The improvement in seismic data in the last 30 years has significantly improved hydrocarbon exploration and field appraisal.

The ability to look deep into the subsurface with a good degree of certainty has aided in the ability to identify much smaller more complex structures that may not have been identified earlier on. The improvement in 3D seismic volumes and the generation of time-lapse 4D seismic data over an earlier shot seismic area further enables the ability to enhance reservoir evaluation and reservoir character. The generation of seismic data for exploration purposes can be sub-divided into three key sections.

4.1.1 Acquisition

The acquisition of seismic data is undertaken by a seismic vessel (in the marine realm) which has a specially mounted source gun attached to the rear of the ship which acts as the seismic source. Accompanying this source gun are streams of geophones to record the refracted and reflected waves which return back to the surface (Nettleton 1976). The seismic source for marine seismic is normally an air-gun, which creates a pulse of acoustic energy which escapes in all directions. When the acoustic energy hits the sea-bed, depending on the angle of impact the wave will either reflect back to the surface towards the geophones or refract deeper into the subsurface (Sheriff 1982).

The waves will eventually return to the surface, the deeper the waves penetrate, the longer it takes for them to return. When the waves return, they are recorded by a series of geophones, which record the wave travel

times. It is these wave travel times which are then processed and interpreted as the subsurface (Nettleton 1976; Sheriff 1982). Each recorded wave consists of individual wavelets which measure the acoustic impedance between the reflected or refracted waves across a geological surface. The impedance kick is determined by the rocks density and wave velocity. As a wave crosses a bed boundary the change in rock will also have a change in density (either positively or negatively) and as a result have a change in wave velocity. It is this impedance which is processed to generate the seismic data record.

The frequency of the sound wave is crucial in the acquisition of any seismic dataset. Whenever seismic data is shot the frequency is of great importance as the lower the frequency the greater the penetration of sound wave, but, the lower the resolution. As the resolution of a formation is determined by the frequency of a sound wave and the internal velocity of the rock, if the frequency of the wave is too small some of the smaller formations may not be identified. This is crucial in the Northern North Sea where more subtle traps are now being targeted and a high resolution is required. But, if the frequency isn't high enough then the waves might not penetrate the subsurface deep enough to reflect and refract of the desired formation, thus, the frequency of a sound wave is generally a balancing act between the depth of penetration versus the required resolution, which is relating to the trap type, size and depth/ location.

4.1.2 Processing

The aim of seismic processing is to manipulate the recorded time data into an image that may be used to interpret the sub-surface structure (Figure 4-1). This often involves velocity analysis, noise reduction, stacking and migration.

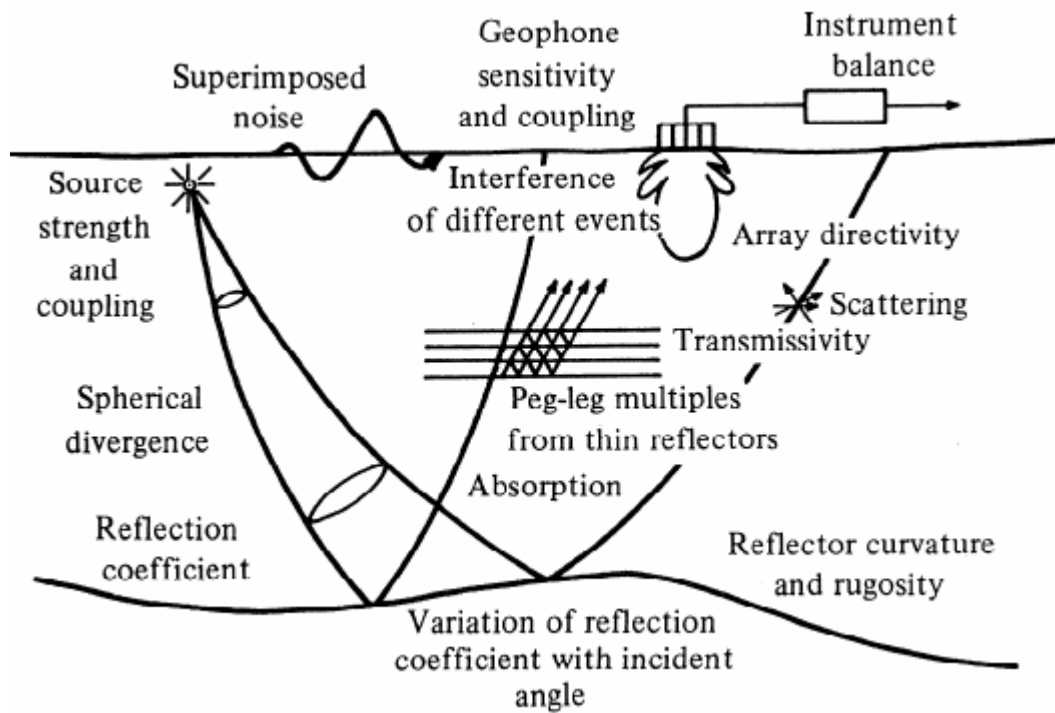


Figure 4-1. illustrating the issue that may require processing in collecting seismic data (Sheriff 1983).

One of the biggest issues with seismic data processing is additional background noise which is generated by the reflection of waves on their return to the surface. As illustrated in Figure 4-2, this background noise will only hamper interpretation of the seismic data.

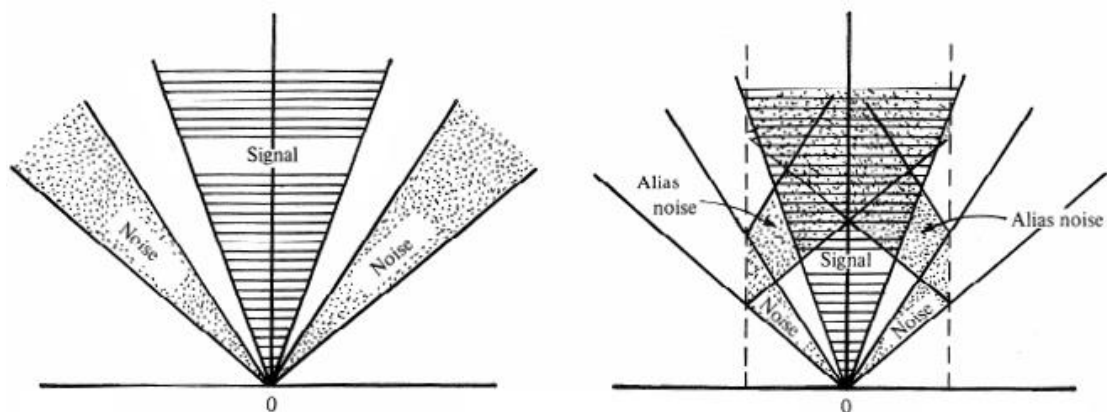


Figure 4-2. Illustrating the generation of background noise in seismic data (Sheriff 1983).

This means it is crucial that background noise cut down to a minimum. This noise issue can also be illustrated prior to migration processing. Migration processing helps identify the true character of the wavelet once aligned alongside several other wavelets. Stack-migration can significantly reduce the noise effect and reduce multiple energy thus aiding in the ability to interpret seismic data. It is processes such as these which significantly aid petroleum prospectivity and exploration in the deep subsurface.

It is possible however, to undertake amplitude variation with offset (AVO) which can be used to indicate that some formations can change in seismic response depending up on the distance between shot point and receiver. This is often used to identify hydrocarbon fluids and other rock properties. An example of this would be a gas filled sandstone unit would show an increase in amplitude with increasing offset, whereas, a coal formation would show a decrease in amplitude with increasing offset. As a result it may be possible to generate a near and far stacked offset datasets for a detailed comparison and further aid in identifying hydrocarbons.

4.1.3 Calibration and Interpretation

Seismic data is the measurement of travel times of waves, to calibrate this data to the rock record it needs to be converted into depth. The calibration of seismic data for interpretation comes directly from velocity logs which are often generated during the well test phase after drilling has ceased. The velocity log takes into account the internal velocity speeds within each rock unit and associates a set depth with a set time. This can then be used once the horizons have been configured to specific depths, to convert the depths into time. These top surface locations can then be placed within the seismic

volume at each well position at a specific time, relevant to its depth in the subsurface.

One method of tying the well data to the seismic data is with the use of a seismic seismogram. This is a one dimensional model of acoustic energy that can be used to provide a tie between changes in subsurface properties within both seismic and borehole data. By using the Zero-Phase Wavelet that is used in the seismic a synthetic trace can be calculated and is compared to the well trace and acoustic impedance, as shown in Figure 4-3.

Ideally a copy of the Zero-Phase Wavelet should appear when the well trace transfers from one lithology type to another. This can be further backed up with other well logs such as the sonic and density logs, which can be used to illustrate the acoustic impedance. All these pieces of information should align to give a good well tie to a formation top.

The only problem with generating a synthetic seismogram is that it can only be accurately created from a well. If seismic interpretation is then taken from this log and it does not tie with a well top in another well a miss-tie occurs. The only way to account for this miss-tie is to undertake a time shift so that all the seismograms from each borehole tie on the seismic (Ziolkowski 1998). Other issues that occur with the use of synthetic seismograms relates to variation in wavelet from trace to trace and that the seismic is generally processed from well logs, which might not accurately tie (Ziolkowski 1998). Once the well tops can be identified it is possible to undertake seismic interpretations throughout the seismic volume. Once this process is complete it is important to depth convert the seismic data to see the true structures and to reduce any of the effects of seismic.

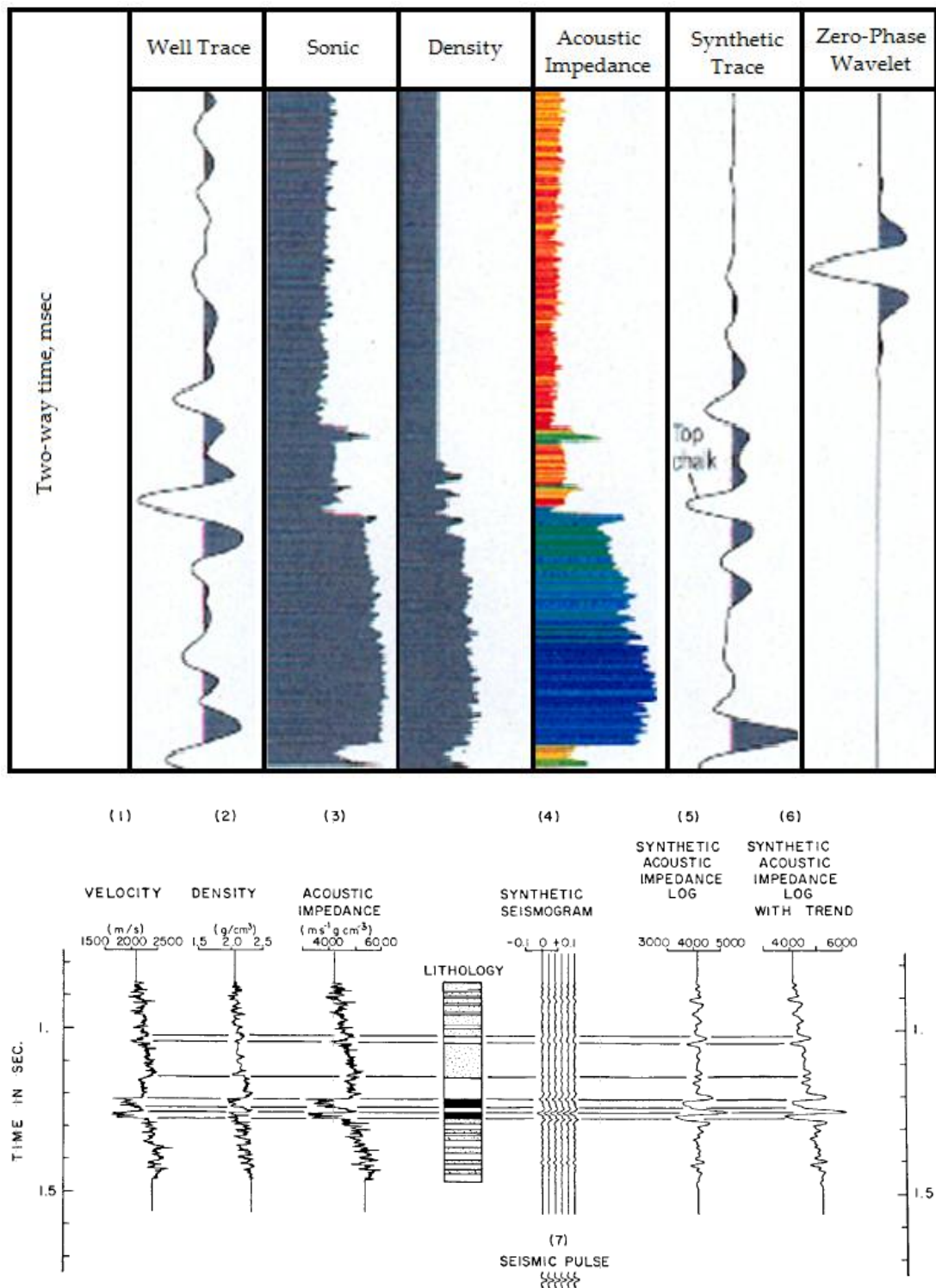


Figure 4-3. Illustration of a synthetic seismograms and how it is used to tie variable sets of data to accurately pick the change in rock facies in the subsurface (Becquey 1979).

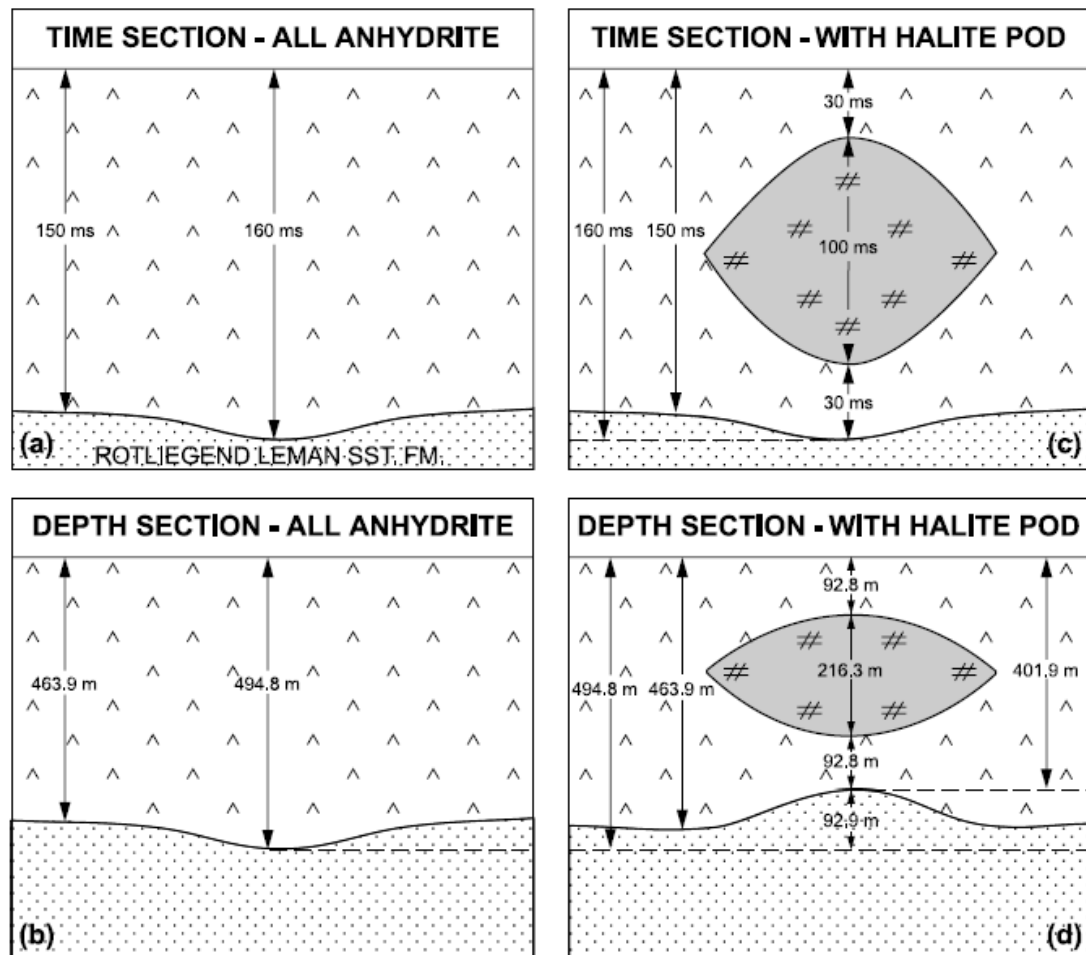


Figure 4-4. Illustration of how the velocity variations in sediments can create seismic induced features (Underhill 2008).

Depth conversion is undertaken by separating the seismic interpretation into a series of horizons that are parted by sedimentological boundaries. Each of these sediment packages has a different rheology due to varying amounts of compaction and composition, thus they have different internal velocities. By allocating an internal velocity for each package it will be possible to reduce and seismic push-up or pull-down effects created by varying thickness of sediments with the true geology being revealed.

This is observed in the Southern North Sea where Upper Permian Pods of halite are deposited within an anhydrite body (Figure 4-4). Without accounting for the halite pods and just assuming a constant velocity through

this section would give a seismic push down effect, when actually a high is actually present. This is extremely important as seen in the Southern North Sea as the underlying sediments are the Lower Permian Rotliegend Leman Sandstone Formation, which is the primary reservoir, thus, interpreting the bulk rock amount for prospect analysis may be incorrect.

4.1.4 Seismic interpretation tools

The introduction of 3D seismic data in 1975 was a significant breakthrough in the quest for hydrocarbons. With the ability to observe the subsurface in three dimensions more accurate models and a better understanding of a petroleum system can be generated. Since then quality of seismic data and computer imaging has increased even further. This project used the Seismic Micro-Technology (SMT) Kingdom software which has the ability to image the seismic subsurface in three dimensions.

One benefit of 3D seismic data is the vast quantity of data acquired as most datasets have a line spacing of 12.5 - 25m. By having such a close spacing of lines over a large area it is possible to create a time slice which is a visual representation of a set time through the seismic block. This is extremely useful in identifying thickening packages and fault locations within a basin. By digitising the seismic data in powerful interpretations it is possible to flatten seismic interpretations i.e. return the data to how it would have been shortly after deposition and give a snap shot of what the basin might have looked like in the past.

The seismic interpretation can also be put into structural evolution specific software such as Midland Valley's Move package and Badley Geosciences TrapTester software. Midland Valley specialise in structural restoration and

looking at how a specific basin may have structurally evolved and looking at what faults moved when. The Badley Geoscience software on the other hand can be used to analyse the effects of faulting at a reservoir scale and model the ability of hydrocarbon fluid flow along and across fault plane. By combining these two packages to a seismic interpretation it is possible to get a strong understanding of the structural evolution of a basin and how the faults affect the petroleum system.

4.1.5 Seismic dataset list

The study area for this thesis measures in total 5,499 Km² and is comprised of 12 3D seismic volumes, which are shown in Table 4-1 and Figures 4-5 – 4-17. These datasets range in size from 220km² to 2,640km² but all are equally important to blanket the East Shetland Basin in seismic data. In areas where the datasets overlap one another it is vitally important that the two sets of data match and no seismic miss-ties exist. These miss-ties occur when datasets are processed by different companies who use slightly different processing parameters. It is vitally important that these miss-ties are identified and adjusted so that the maps generated from the individual datasets match up and are not offset from one another.

Table 4-1 List of seismic dataset available throughout the East Shetland Basin.

Used Seismic Survey Name	Actual Seismic Survey name
Cladhan 3D Dataset	GE983F0002
Don SW+NE	BP933F0005
Hudson 3D Dataset	SH963F0002
Hutton 3D Dataset	CN903F0001 + CG963D2001
M07 3D Dataset	Mega Merge M07
N07 3D Dataset	Mega Merge N07
Murchison Small 3D Dataset	CG963D2004
Murchison Large 3D Dataset	-
Tern-Eider Ridge 3D Dataset	SH953F0001
Tern-Spec 3D Dataset	WG973F0002
West Don-Thistle Dataset	ET893F0001
Western Geco 210/11 PreSTM 2008 3D Dataset	-

Cladhan Information				
Area	295 Km ²			
Inline	Min	Max	Count	Spacing
	1233	1770	538	25m
Crossline	Min	Max	Count	Spacing
	676	2464	1789	12.5m
Dominant Frequency	16 Hz			
Resolution at Brent level	62m			
Polarity	European			

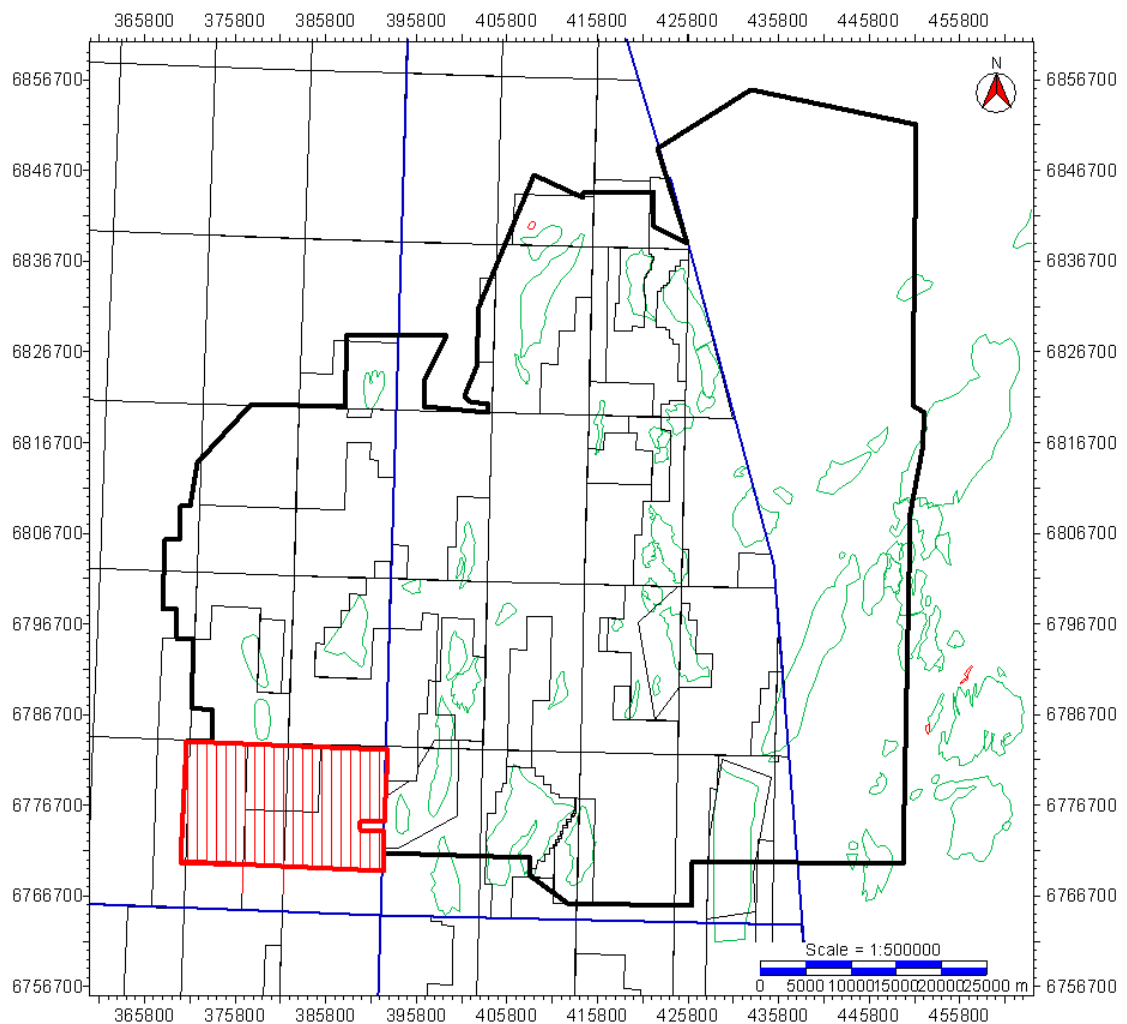


Figure 4-5 Highlighted in red is the limits of the 3D Cladhan seismic dataset.

Don SW+NE Information				
Area	281 Km ²			
Inline	Min	Max	Count	Spacing
	1000	3114	2115	25m
Crossline	Min	Max	Count	Spacing
	80	4991	4912	12.5m
Dominant Frequency	21 Hz			
Resolution at Brent level	43m			
Polarity	European			

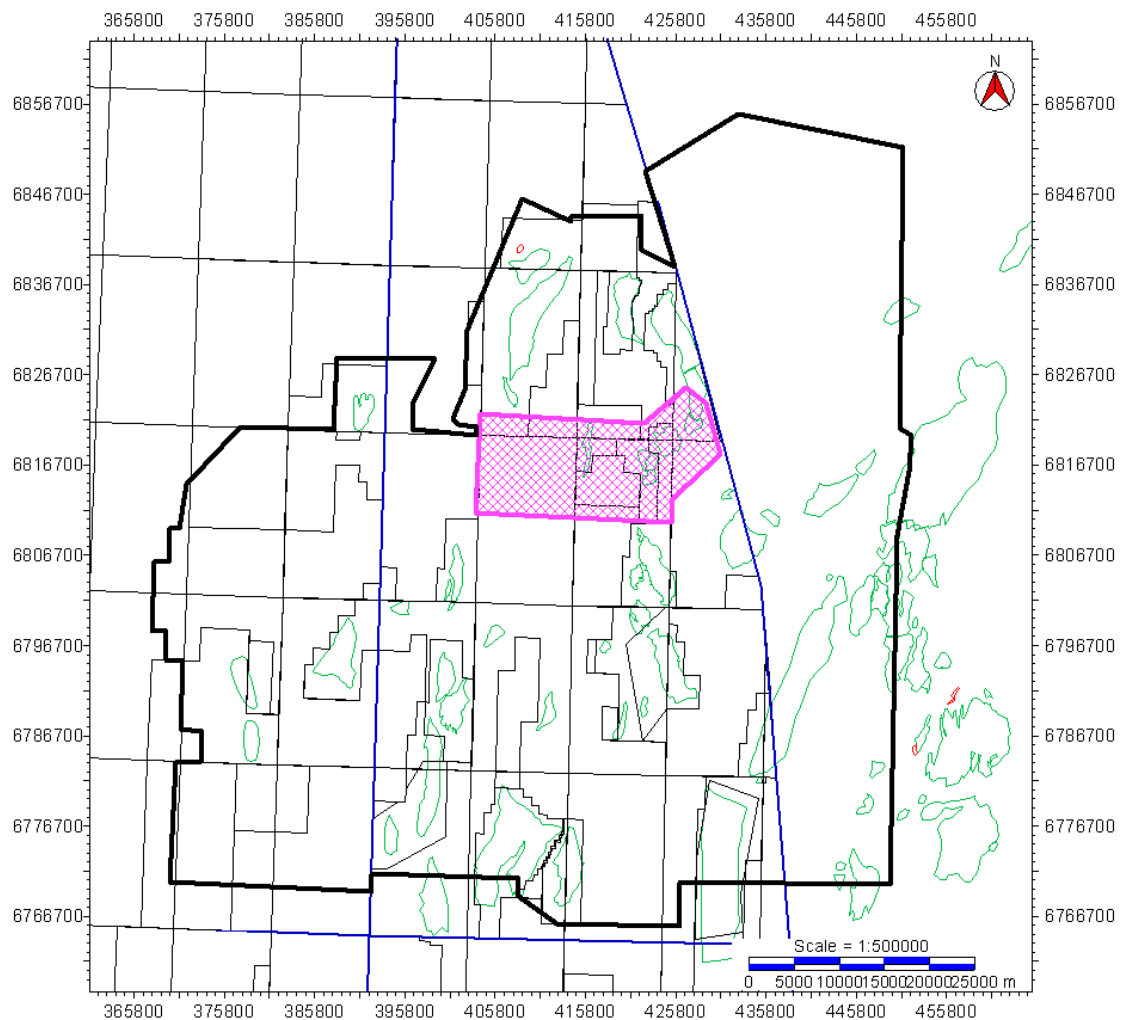


Figure 4-6 Highlighted in purple is the limits of the 3D Don SW+NE seismic dataset.

Hudson Information				
Area	530 Km ²			
Inline	Min	Max	Count	Spacing
	2230	4570	2341	12.5m
Crossline	Min	Max	Count	Spacing
	2270	7200	2466	12.5m
Dominant Frequency	16 Hz			
Resolution at Brent level	50m			
Polarity	European			

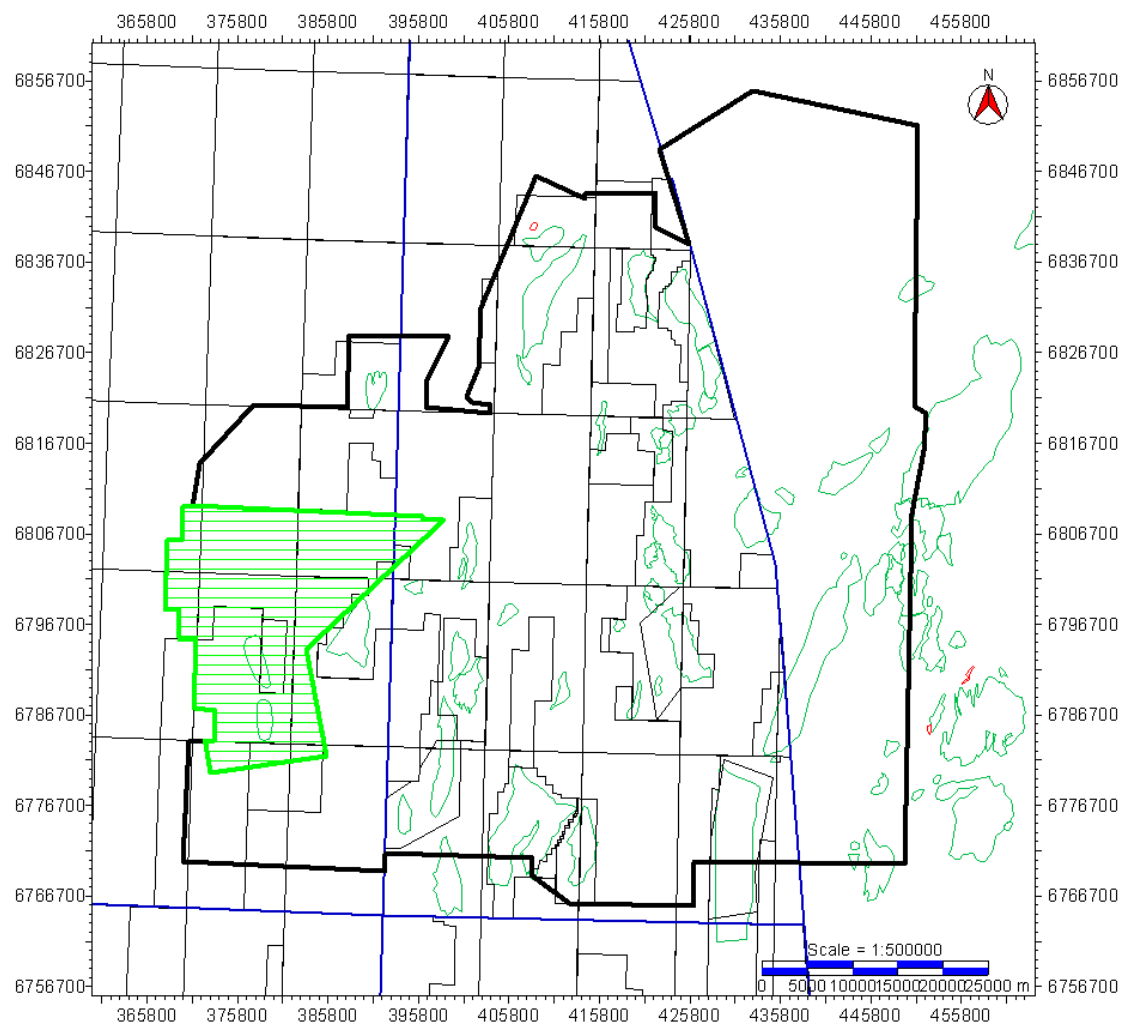


Figure 4-7 Highlighted in light green is the limits of the 3D Hudson seismic dataset.

Hutton Information				
Area	354 Km ²			
Inline	Min	Max	Count	Spacing
	2006	3692	1687	12.5m
Crossline	Min	Max	Count	Spacing
	300	2290	1991	12.5m
Dominant Frequency	16 Hz			
Resolution at Brent level	57m			
Polarity	European			

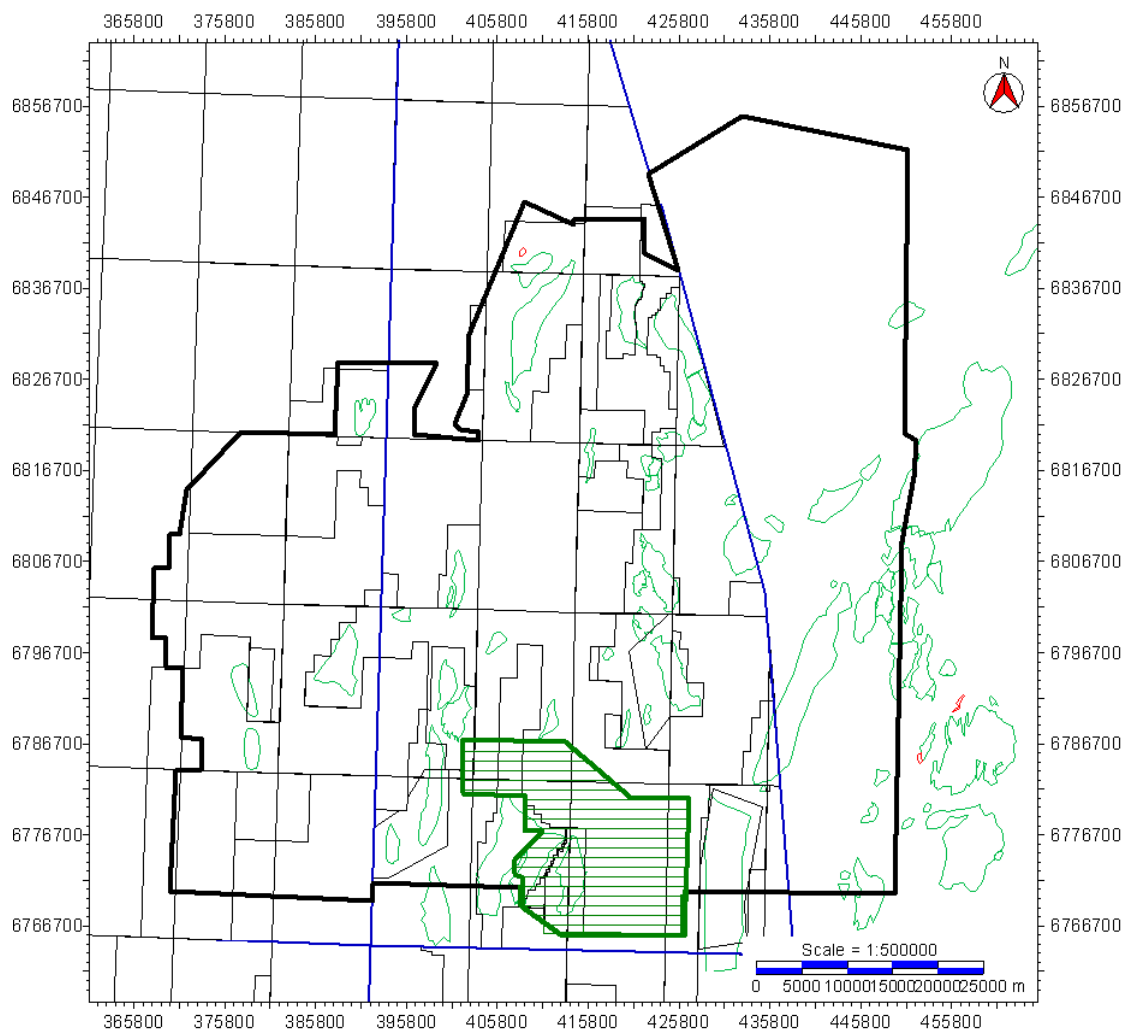


Figure 4-8 Highlighted in dark green is the limits of the 3D Hutton seismic dataset.

M07 Information				
Area	2,640 Km ²			
Inline	Min	Max	Count	Spacing
	10000	15000	1251	50m
Crossline	Min	Max	Count	Spacing
	16000	20000	1001	50m
Dominant Frequency	19 Hz			
Resolution at Brent level	55m			
Polarity	European			

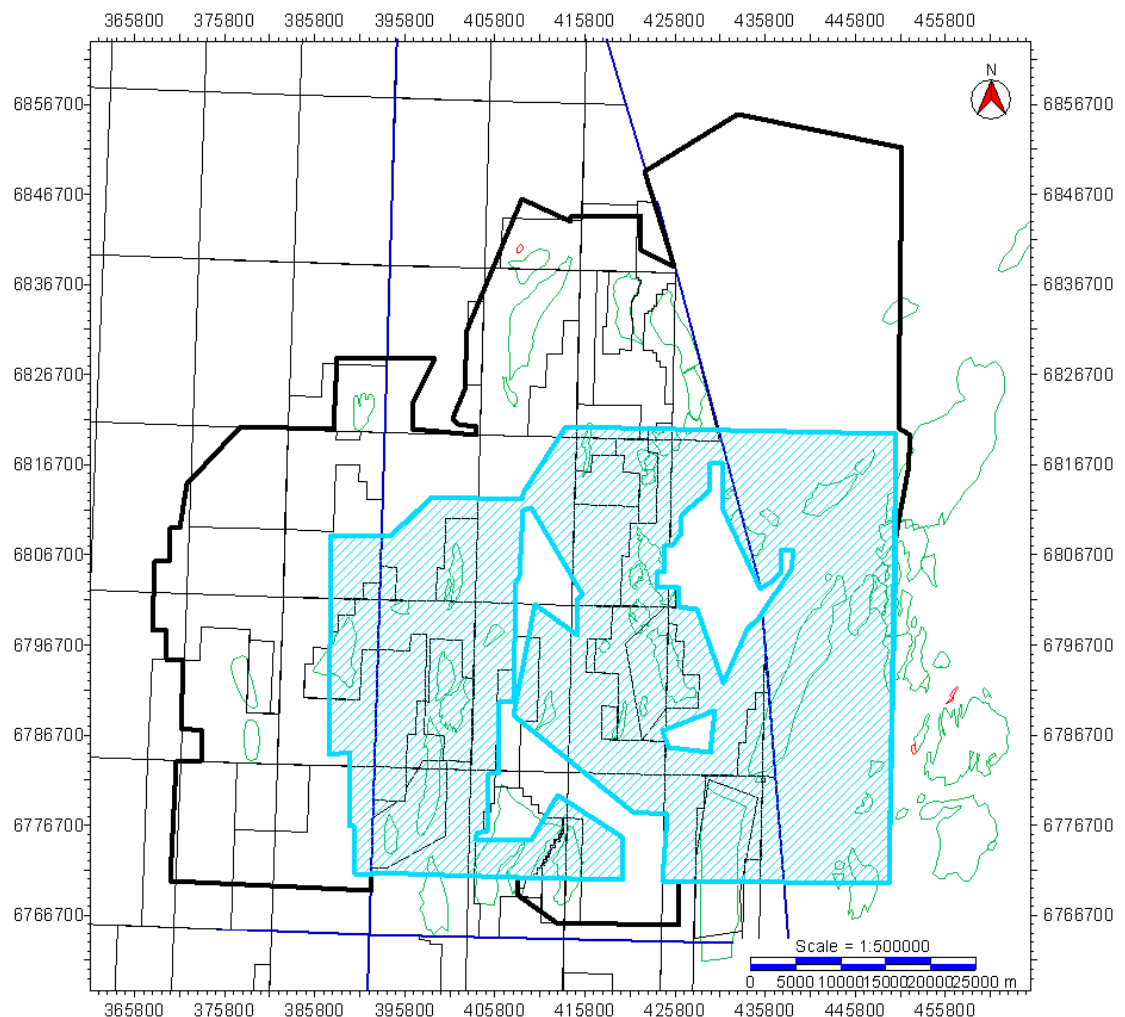


Figure 4-9 Highlighted in light blue is the limits of the 3D M07 seismic dataset.

N07 Information				
Area	1,315 Km ²			
Inline	Min	Max	Count	Spacing
	10000	15000	1251	50m
Crossline	Min	Max	Count	Spacing
	20000	24000	1001	50m
Dominant Frequency	20 Hz			
Resolution at Brent level	50m			
Polarity	European			

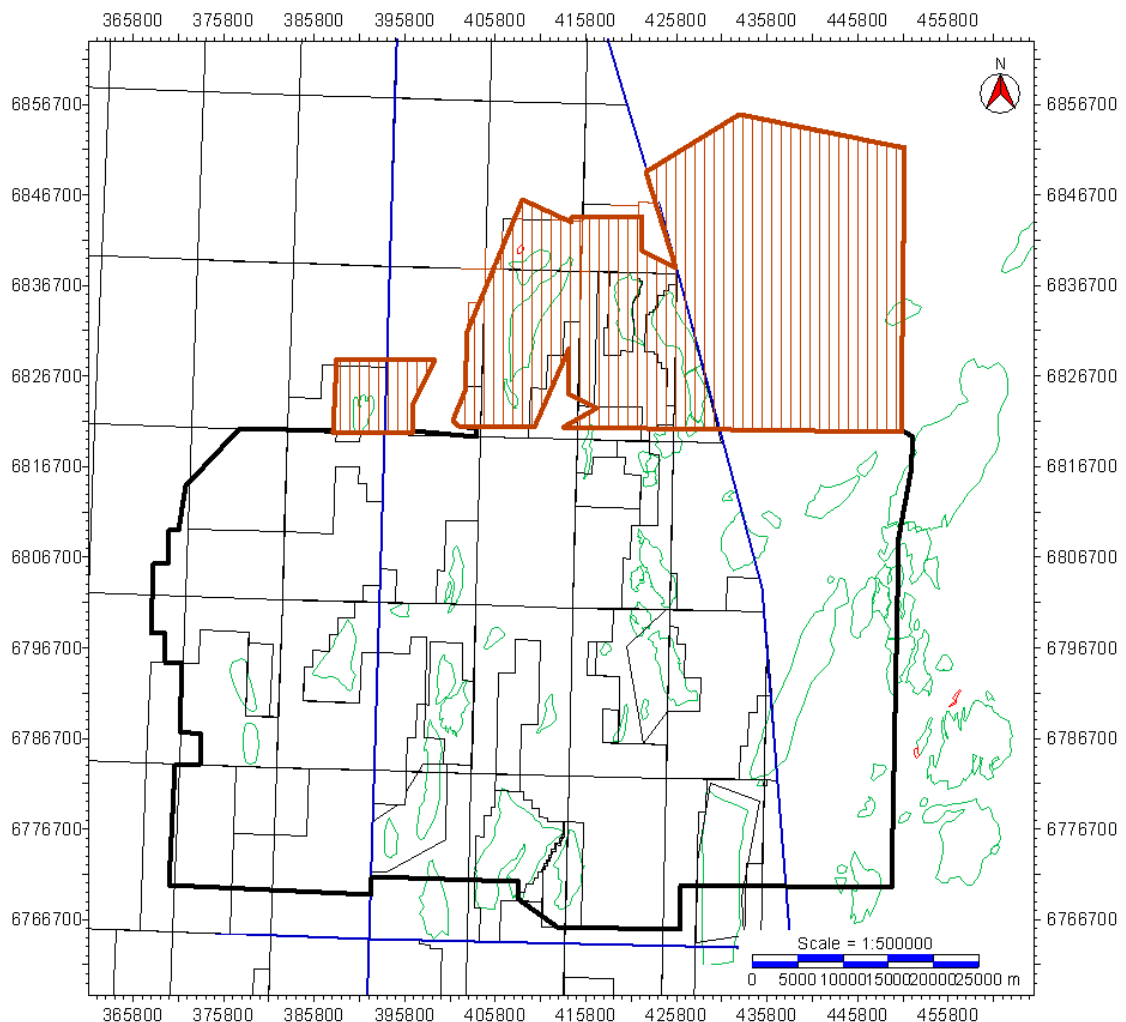


Figure 4-10 Highlighted in brown is the limits of the 3D N07 seismic dataset.

Murchison Small Information				
Area	263 Km ²			
Inline	Min	Max	Count	Spacing
	1970	3260	646	25m
Crossline	Min	Max	Count	Spacing
	2000	3760	881	25m
Dominant Frequency	20 Hz			
Resolution at Brent level	40m			
Polarity	European			

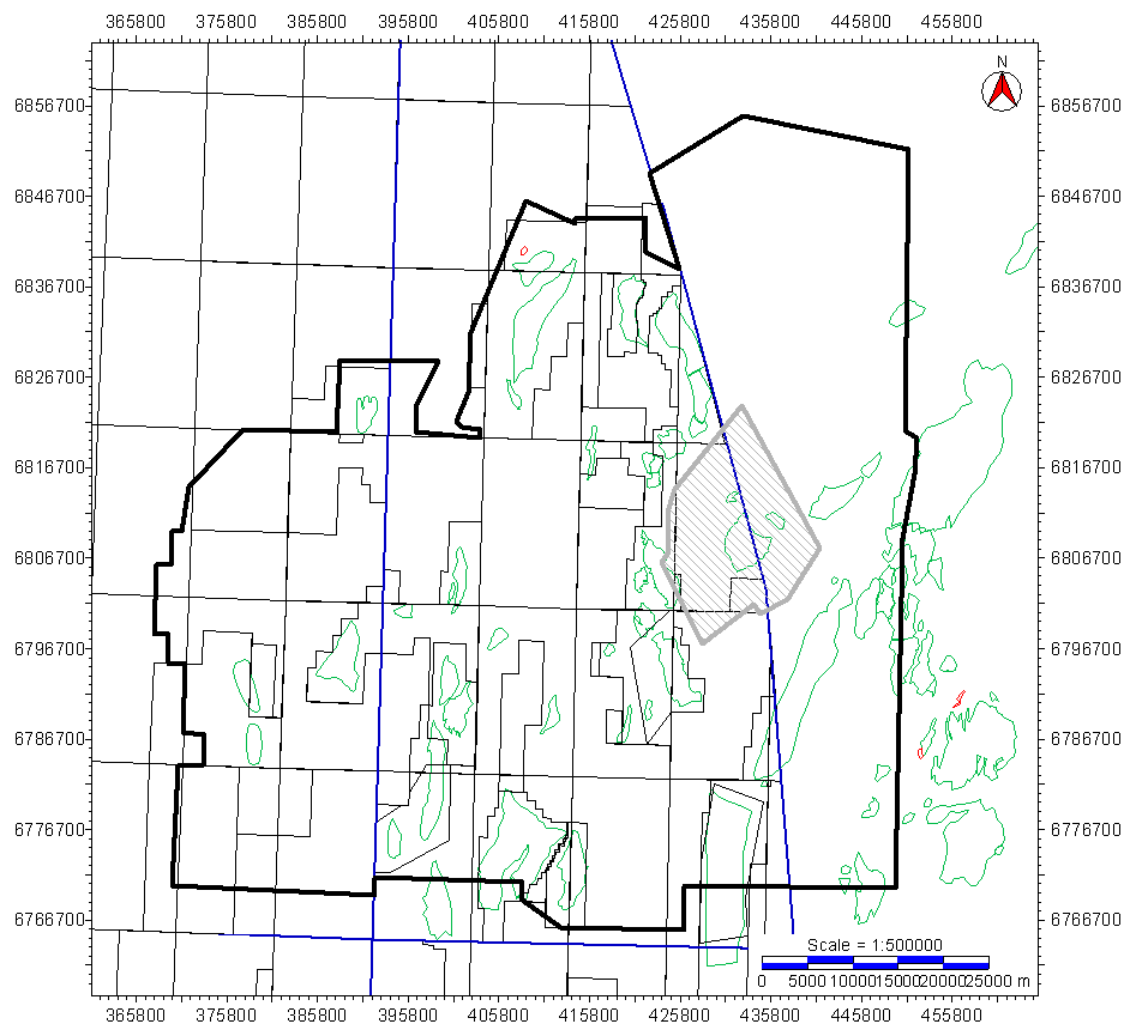


Figure 4-11 Highlighted in grey is the limits of the 3D Murchison Small seismic dataset.

Murchison Large Information				
Area	450 Km ²			
Inline	Min	Max	Count	Spacing
	133	1497	1365	18.75m
Crossline	Min	Max	Count	Spacing
	9513	11637	2125	12.5m
Dominant Frequency	16 Hz			
Resolution at Brent level	50m			
Polarity	European			

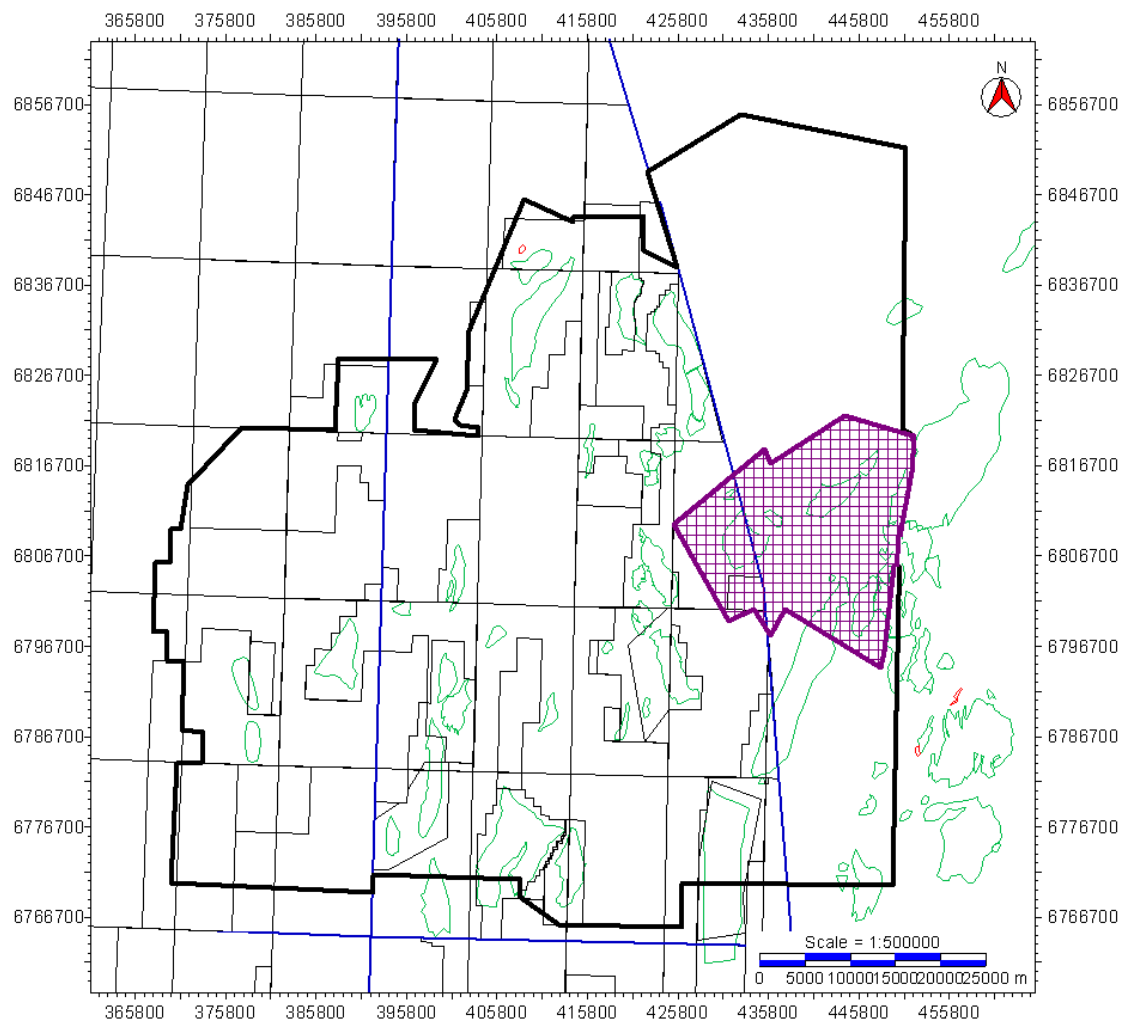


Figure 4-12 Highlighted in maroon is the limits of the 3D Murchison Large seismic dataset.

Tern-Eider Information				
Area	430 Km ²			
Inline	Min	Max	Count	Spacing
	1990	3289	1300	18.75m
Crossline	Min	Max	Count	Spacing
	661	5467	1603	18.75
Dominant Frequency	20 Hz			
Resolution at Brent level	46m			
Polarity	European			

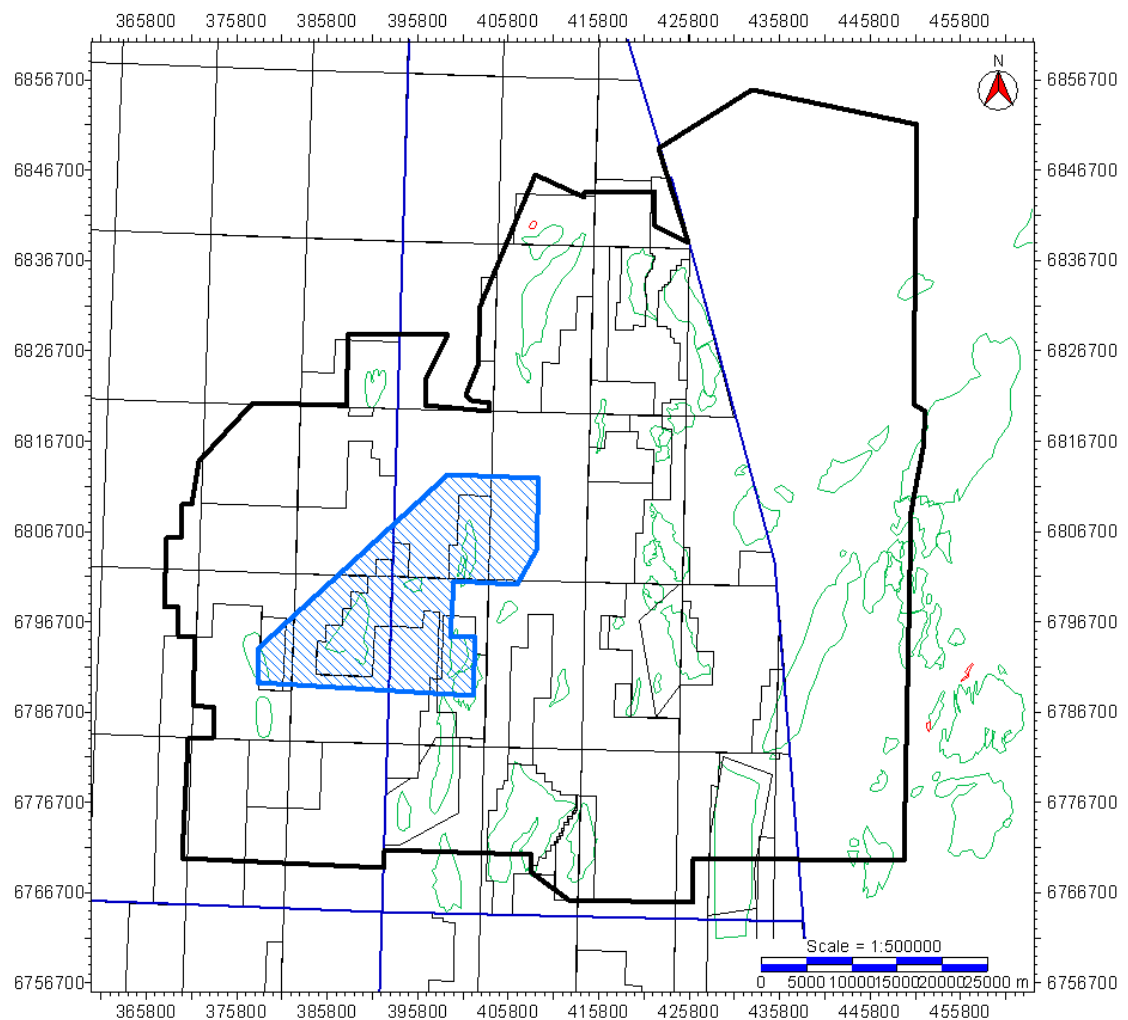


Figure 4-13 Highlighted in dark blue is the limits of the 3D Tern-Eider seismic dataset.

Tern-Spec Information				
Area	864 Km ²			
Inline	Min	Max	Count	Spacing
	556	1892	1337	25m
Crossline	Min	Max	Count	Spacing
	151	4535	4385	12.5m
Dominant Frequency	22 Hz			
Resolution at Brent level	45m			
Polarity	European			

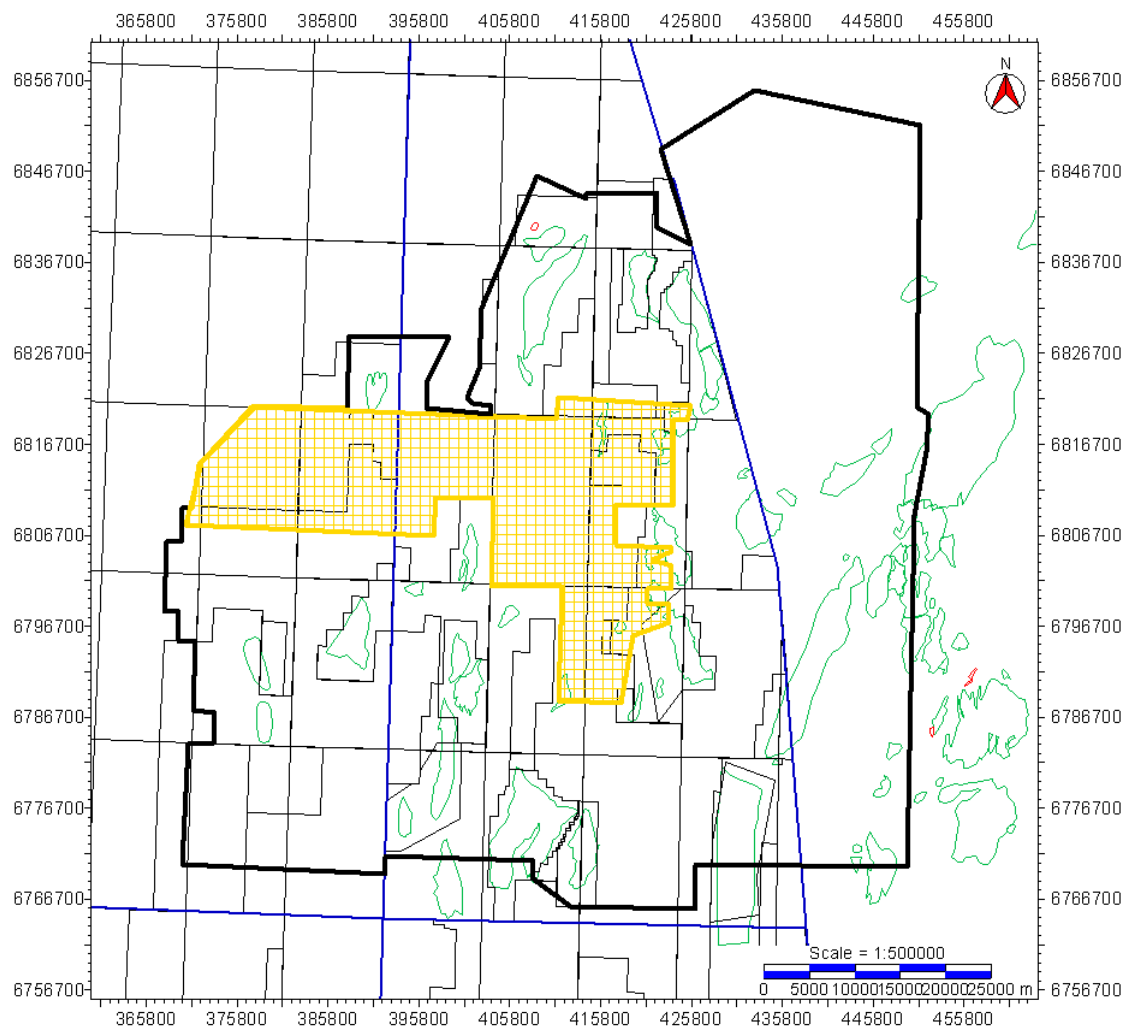


Figure 4-14 Highlighted in grey is the limits of the 3D Tern-Spec seismic dataset.

West Don to Thistle Information				
Area	220 Km ²			
Inline	Min	Max	Count	Spacing
	32	1080	1049	12.5m
Crossline	Min	Max	Count	Spacing
	380	2160	1781	12.5m
Dominant Frequency	25 Hz			
Resolution at Brent level	32			
Polarity	European			

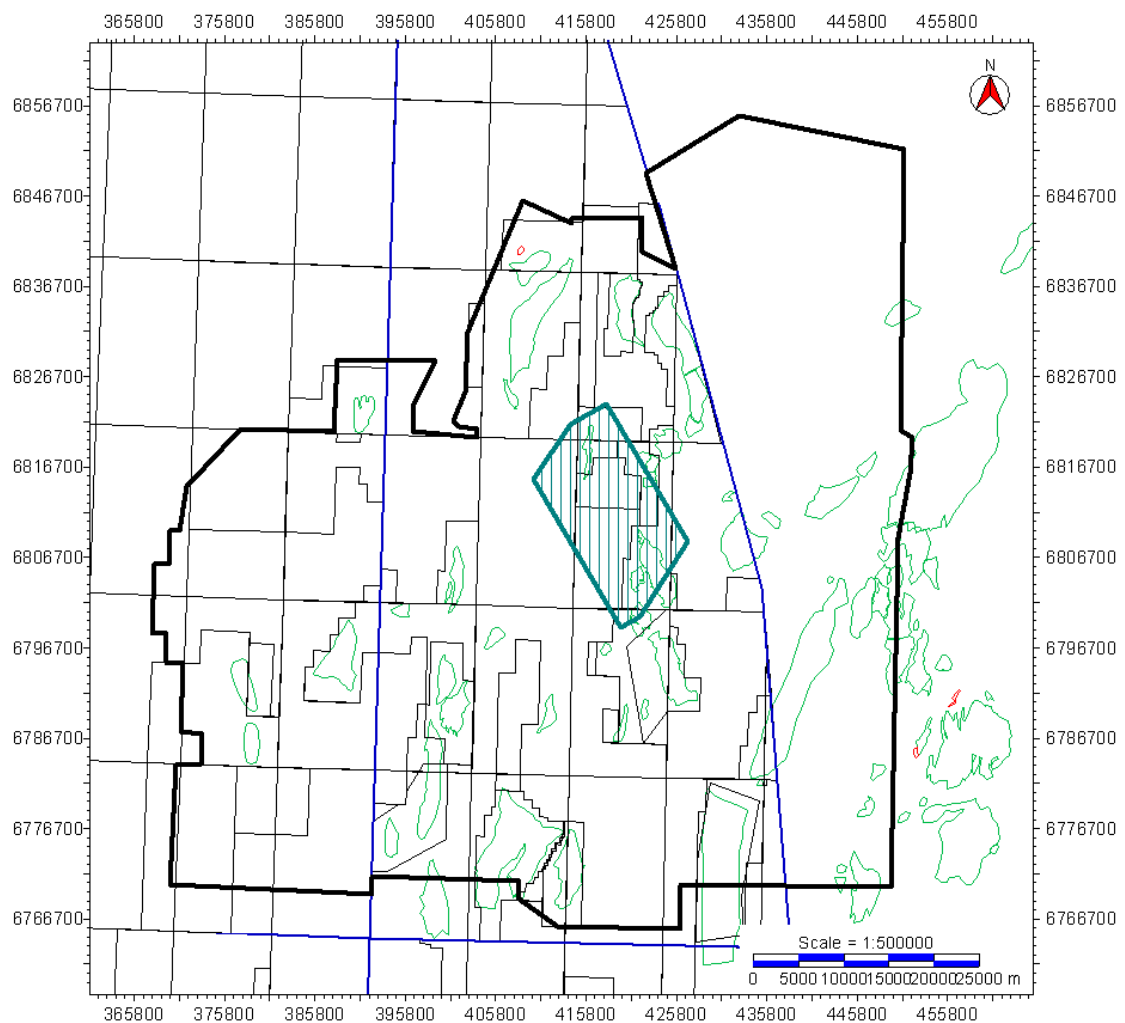


Figure 4-15 Highlighted in teal is the limits of the 3D West Don-Thistle seismic dataset.

Western Geco 210/11 PreSTM 2008 Information				
Area	724 Km ²			
Inline	Min	Max	Count	Spacing
	1000	2800	1801	25m
Crossline	Min	Max	Count	Spacing
	80	4570	4491	12.5m
Dominant Frequency	21 Hz			
Resolution at Brent level	56m			
Polarity	European			

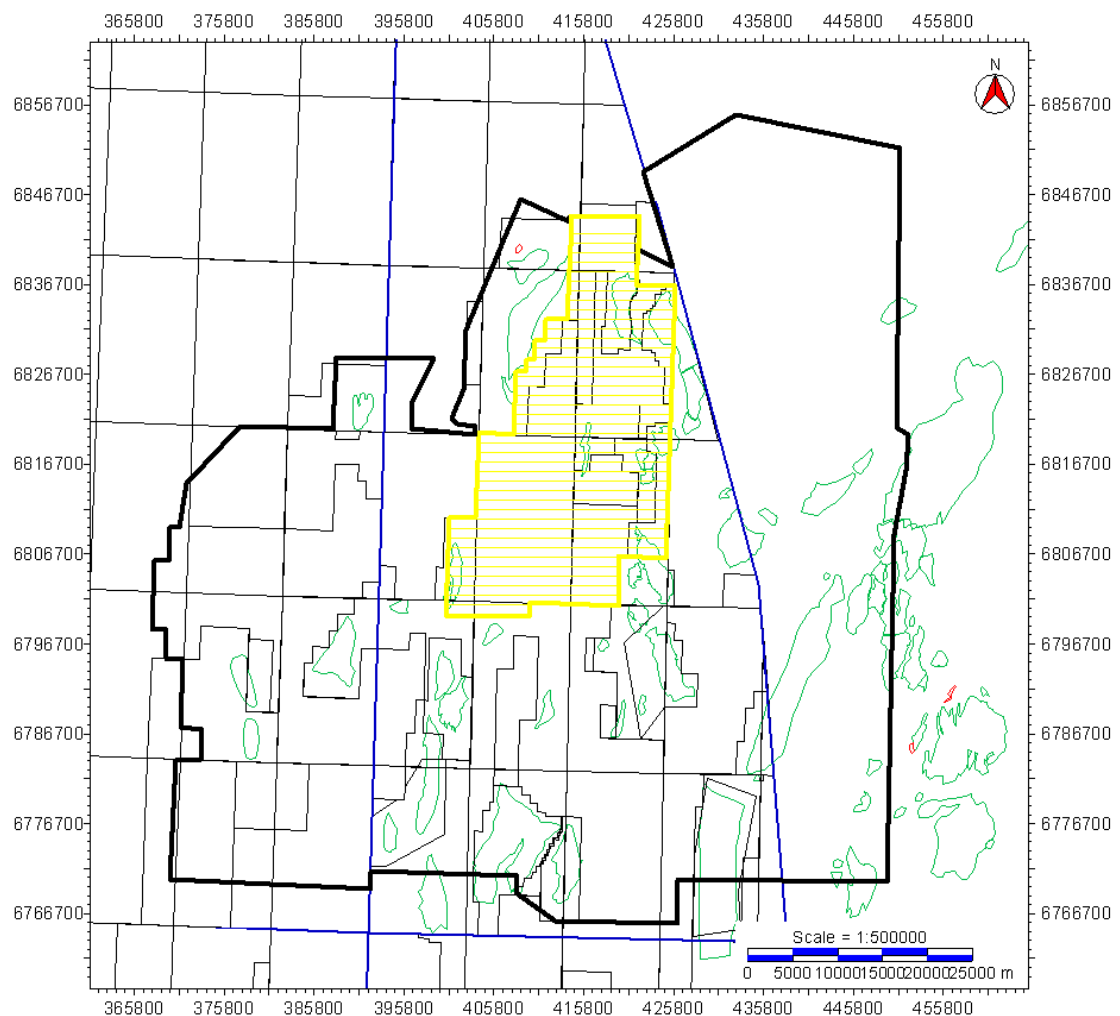


Figure 4-16 Highlighted in yellow is the limits of the 3D Western Geco 210/11 PreSTM 2008 seismic dataset.

Complete M

Area

5,499 Km²

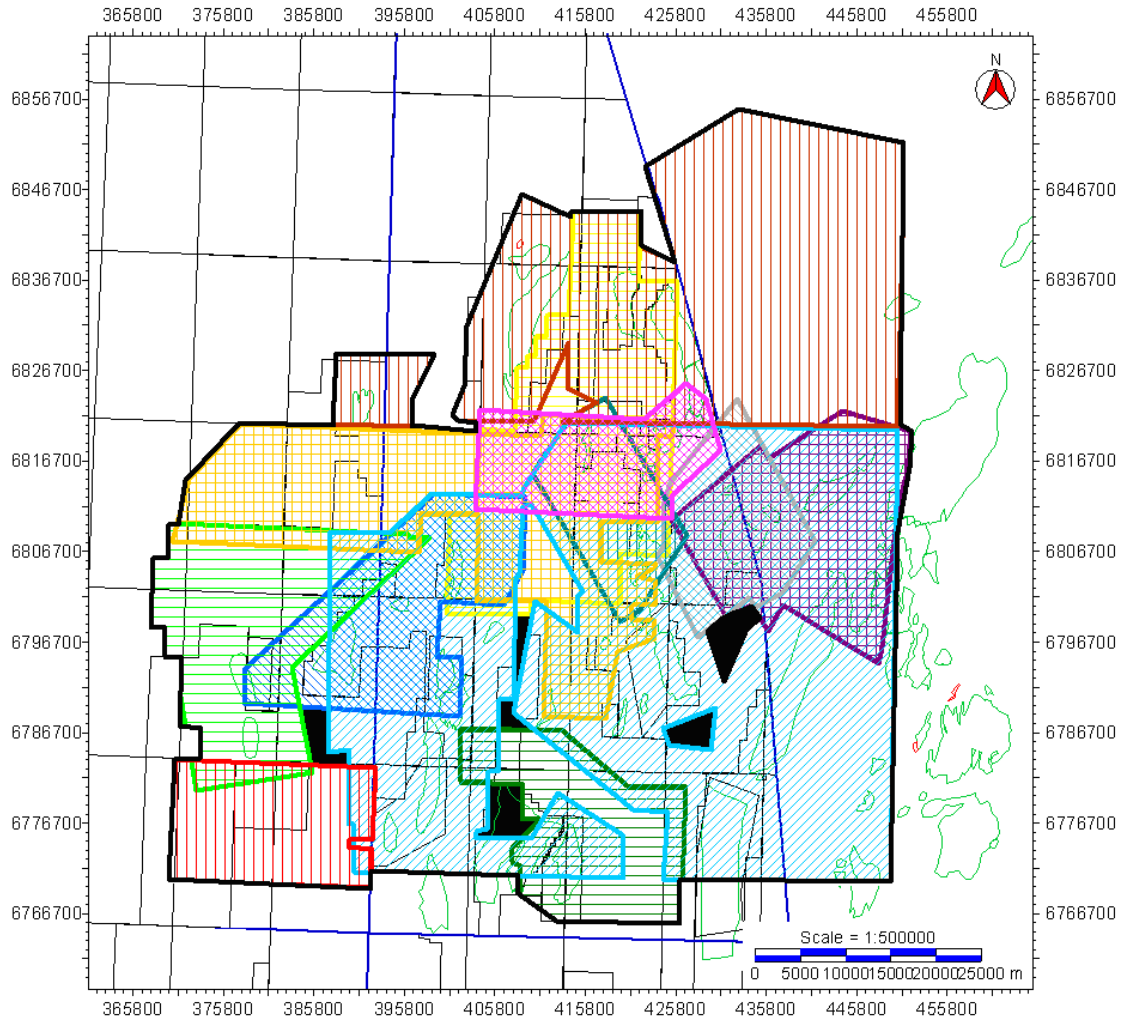


Figure 4-17 Full acreage of the 12 3D seismic datasets used within this study.

4.2 Borehole Data

As useful as seismic data is at viewing the geological subsurface, geophysical well logs are crucial in tying the time based seismic data to actual depth related structures. Borehole data can vary from a series of direct geological

samples to the production of geophysical well logs. Both of these data types are crucial to the interpretation of the subsurface.

4.2.1 Geological Samples

Geological samples are fragments, samples or sections of the borehole that have been removed for geological analysis. Cuttings are constantly being produced through the drilling process, but cannot be completely trusted as an exact subsurface description. The main issue with cuttings relates to the lag time from which the cuttings form at the well head and the moment at which they appear at the well surface. The cutting from other horizons will also mix with the new cuttings being generated, alas, the cutting can be used as a rough guide to what is being drilled, but results must be taken with a pinch of salt.

More accurate geological samples come in the form of coring and sidewall samples (sws). In both instances, a specific section of the borehole is needed for further in depth analysis. In the case of coring, a specific drill bit is attached that captures the rocks being drilled so that it can be brought to the surface and a series of tests can be undertaken. This test may vary from biostratigraphic analysis to potential permeability flow testing. Sidewall core sampling on the other hand relates to an area of the well that has not been cored but sedimentological samples are required. A side-wall gun is lowered to the specific level in the well and fires a group of small plugs into the desired horizon. Ideally, when the gun pulls the bullets from the horizon a sample of the borehole wall is retrieved, which can be brought to the surface for analysis.

Although geological samples are the best way to directly view the subsurface down a borehole, it is considerably more expensive than wire-line geophysical logs and thus often gets cut from an exploration drilling program.

4.2.2 Geophysical Well Logs

A geophysical well log can be described as the continuous recording of a geophysical parameter within a borehole (Rider 1996). These recordings can only take place on open hole borehole (prior to casing) so the results attained are more accurate. As noted above the process to gain core samples is an expensive process and is only really undertaken over key horizons, such as reservoir units. With this noted, this is the primary reason why geophysical well logs are required. Another advantage of well logs is that they are a continuous recording, which means they can fill in gaps that are missed by coring.

There are several different varieties of well logs available, each of which can be used to identify different properties within the subsurface. The most common of these well tests are Gamma Ray (GR), Sonic, Density, Neutron and Resistivity logs. The GR log actively measures the radioactivity of the formations in the subsurface. This is undertaken by measuring the amounts of Potassium, Thorium and Uranium in a set formation. This is often used for identifying rock type as the radioactive elements are often found in clay bearing sediments; whereas, sandstone units are generally void radioactive bearing elements. The Sonic log measures the ability to transmit sound waves and can be used to evaluate porosity. By combining the results of the GR and Sonic log it is possible to calculate the acoustic impedance of formations.

The Density log is used to calculate the density of a rock formation, including the grain matrix and that of the fluids contained within the pores of the formation. This too can be used to calculate a reservoirs potential porosity and the density of any bearing hydrocarbons, but primarily this is used as a lithology indicator. The Neutron log is predominantly a porosity identification log by measuring the amounts of hydrogen, which is water bearing formations, measures the amount of water content in the rock, thus the formations porosity. To get an accurate lithology and porosity reading for a set formation it is best to combine the Density and Neutron logs. Where the two logs cross over one another, i.e., an increase in density and a decrease in neutron porosity indicates sand prone sediments, if the overlap is significant this may indicate hydrocarbons (Rider 1996).

The Resistivity log was first invented to find hydrocarbons and it is still used in the same way today. A resistivity log is a measurement of a formations ability to conduct an electric current; areas with a high resistivity are inferred as hydrocarbon bearing as hydrocarbons are extremely resistive to an electric current, whereas, water is a great conductor and is thus less resistive (Rider 1996).

It is common of a single borehole to have a series of well tests undertaken so that crucial information such as lithology, porosity, permeability and hydrocarbon saturation can be measured and quantified by the overlap of information that each well test. For instance, the gamma log is primarily used to identify general lithology, but it can also be used to identify mineral identification and facies depositional environment which can also be identified with a self-potential (SP) log.

Listed below in Table 4-2 is a full account of well logs within the study area of the East Shetland Basin.

Table 4-2 Full list of wells available throughout this study. Well names listed in grey were not available in the public domain when this study was undertaken.

210/15	210/19	210/20	210/24	210/25
210/15-1	210/19-1	210/20-1	210/24-1	210/25-1
210/15-2	210/19-2	210/20-2	210/24-1A	210/25-2
210/15a-3	210/19-3	210/20-3	210/24-2	210/25-3
210/15b-4	210/19-4	210/20-3A	210/24a-3	210/25-3A
210/15a-5	210/19-4A		210/24a-4	210/25-3B
210/15a-6	210/-19-4B		210/24a-4A	210/25-3Z
			210/24a-5	210/25-4
			210/24a-6	210/25a-5
			210/24b-7	210/25c-6
			210/24a-8	210/25c-6A
			210/24a-9	210/25c-7
			210/24a-10	210/25b-8
			210/24a-10Z	210/25b-8Z
			210/24a-11	210/25a-9
			210/24a-11Z	210/25a-10
			210/24a-12	210/25a-10Z
			210/24a-12Z	
			210/24a-13	

210/29	210/30	211/07	211/08	211/11
210/29-1	210/30-1	211/07-1	211/08-1	211/11-1
210/29-2	210/30a-2	211/07a-2	211/08a-2	211/11-2
210/29a-3	210/30b-3	211/07a-3	211/08b-3	211/11a-3
210/29a-4	210/30a-4	211/07a-4	211/08c-4	211/11b-4
210/29a-4Y	210/30a-4X	211/07a-5	211/08c-4Z	211/11a-5
210/29a-4Z	210/30a-4Y	211/07a-5Z		211/11a-6
	210/30a-4Z	211/07a-6		

211/12		211/13		211/14
211/12-1	211/12a-13	211/13-1	211/13a-10	211/14-1
211/12-2	211/12a-14	211/13-2	211/13b-11	211/14-1Z
211/12-3	211/12b-15	211/13-3	211/13a-12	211/14-2
211/12-3A	211/12a-16	211/13-4	211/13a-13	211/14-2Z
211/12-4	211/12a-17	211/13-5	211/13a-13Y	211/14-3
211/12-5	211/12a-18	211/13-5A	211/13a-13Z	211/14-3Z
211/12-6	211/12a-19	211/13-6	211/13a-14	211/14-4
211/12-7	211/12a-19Z	211/13-7	211/13a-15	211/14-5
211/12-8	211/12a-20	211/13a-8	211/13a-15X	211/14-6
211/12a-9	211/12a-20Y	211/13a-8Z	211/13a-15Y	211/14-7
211/12a-10	211/12a-20Z	211/13a-9	211/13a-15Z	211/14-8
211/12a-11	211/12a-21	211/13a-9Z		211/14-9
211/12a-11Z	211/12a-22			
211/12a-12A	211/12a-23			

211/16	211/17	211/18		211/19
211/16-1	211/17-1	211/18-1	211/18-15	211/19-1
211/16-2	211/17a-2	211/18-2	211/18-16	211/19-2
211/16-3	211/17a-3	211/18-3	211/18a-17	211/19-3
211/16-4	211/17b-4	211/18-4	211/18a-18	211/19-4
211/16a-5	211/174A	211/18-4A	211/18a-19	211/19-5
211/16a-6		211/18-5	211/18a-20	211/19-6
211/16b-7		211/18-6	211/18a-21	211/19a-7
211/16b-7A		211/18-7	211/18a-22	211/19a-8
		211/18-8	211/18a-23	211/19a-9
		211/18-9	211/18a-24	
		211/18-10	211/18b-25	
		211/18-11	211/18a-26	

		211/18-12	211/18c-27	
		211/18-13	211/18a-28	
		211/18-14		

211/21		211/22	211/23	
211/21-1	211/21-10Y	211/22-1	211/23-1	211/23b-12
211/21-1Z	211/21-10Z	211/22-2	211/23-2	211/23b-12Z
211/21-2	211/21-11	211/22a-3	211/23-3	211/23a-13
211/21-3	211/21-12	211/22a-4	211/23-4	211/23a-13Z
211/21-3A	211/21-13	211/22b-5	211/23-5	211/23a-14
211/21-4	211/21-14	211/22a-6	211/23-6	211/23a-15
211/21-4A	211/21-14Z	211/22a-7	211/23-7	211/23a-16
211/21-5	211/21a-15	211/22a-7A	211/23-8	211/23b-17
211/21-6	211/21a-16	211/22a-8	211/23-9	211/23b-17Z
211/21-7	211/21a-17	211/22a-9	211/23b-11	211/23b-18
211/21-8	211/21a-17Z	211/22a-10		
211/21-9	211/21a-18			
211/21a-9Z	211/21a-19			
211/21-10	211/21a-20			

211/24	211/26	211/27	211/28	211/29
211/24-1	211/26-1	211/27-1	211/28-1A	211/29-1
211/24-2	211/26-2	211/27-1A	211/28-2	211/29-2
211/24-3	211/26-3	211/27-2	211/28-3	211/29-3
211/24-4	211/26-4	211/27-3	211/28-4	211/29-4
211/24-5	211/26-5	211/27-4	211/28-5	211/29-5
211/24a-6	211/26-5A	211/27-4A	211/28-6	211/29-6
211/24a-7	211/26-6	211/27-5	211/28a-7	211/29-7
	211/26-6A	211/27-5A		211/29-8A

	211/26-6B	211/27-6		211/29-9
	211/26-6Z	211/27-7		211/29-10
	211/26-7	211/27-8		211/29-10Z
	211/26-8	211/27-9		
	211/26a-9	211/27-10		
	211/26b-10	211/27-11		
	211/26-10Z	211/27-11Y		
	211/26a-11	211/27-11Z		
		211/27c-12		

211/30				
211/30-1				

Chapter 5 Controls on and Consequences of Rift Transection.

5.1 *Introduction*

The East Shetland Basin (Figure 5-1) has undergone multiple phases of rifting throughout geological time. The rifting in the Permo-Triassic and the Upper Jurassic (Coward 2003) is founded on a basement terrane that had already experienced deformation events prior to the development, evolution and destruction of the two-pronged Iapetus Ocean during the Early Proterozoic. Formation of the Caledonian collisional suture during Silurian-Devonian times was followed by orogenic collapse during the Devonian and rift-drift subsidence during the Carboniferous before being affected by the far-field effects of the Variscan collision results from closure of the Rheic Ocean in Southern Britain. Thus, this multi-rift province has buried structural weaknesses in several orientations, and depending upon the stress orientation of the next rift phase determines whether or not old trend reactivated or have been cross-cut. Basement lineations such as the Caledonian (NE-SW) and Tornquist (NW-SE) striking faults have acted as a long-lasting zones of weakness.

The N-S striking Viking Graben forms the northern rift arm of the triple North Sea rift system and is sited above/ upon the collage of buried structures. Its orientation and the component faults of the neighbouring East Shetland Basin (ESB) is N-S, and creates such large scale structures as the Brent Field. This suggests that the underlying NE-SW striking faults may have been reactivated in the Upper Jurassic. The idea of reactivation in the Northern North Sea is not a new theory. Work undertaken by Tomasso et al (2008) highlights Permo-Triassic trending faults which have been cross cut by

Upper Jurassic faults with a different fault polarity (dip). By mapping out the thickening packages of older rifting events, it has been possible to illustrate the cross-cutting nature of rift phases. The aim of this chapter is to try and decipher a series of fault models which are determined by the orientation of faults, fault polarity and the use of original fault patterns. By identifying these fault patterns it is possible to fully understand the structurally complex areas in the East Shetland Basin. This may give insights in to how some of the largest hydrocarbon fields may have evolved through time.

5.2 Study Area

To identify the role of multiple rifting events, the entirety of the seismic data is available for this project. Within this region, strategic areas of interest which have been studied in greater detail. The four individual study areas (Figure 5-2) have been selected to best illustrate the way in which fault lineaments and trends interact through geological time. In total seven 3D seismic volumes available have been used, along with the entire catalogue of well data found in the seismic volumes. These four sub-study areas have been selected to illustrate the varying ways in which transected rifts can be identified. Each of these areas has an individual structural feedback which can be used to illustrate the varying structural evolution of transecting rifts. The study areas use different seismic volumes and cover different North Sea blocks. The calibration of these seismic volumes has been possible using synthetic seismograms constructed from the well data that is available in each of the separate block. Table 1 lists the areas and what seismic volumes are used in its interpretation and what blocks the study area covers, thus what wells are being used.

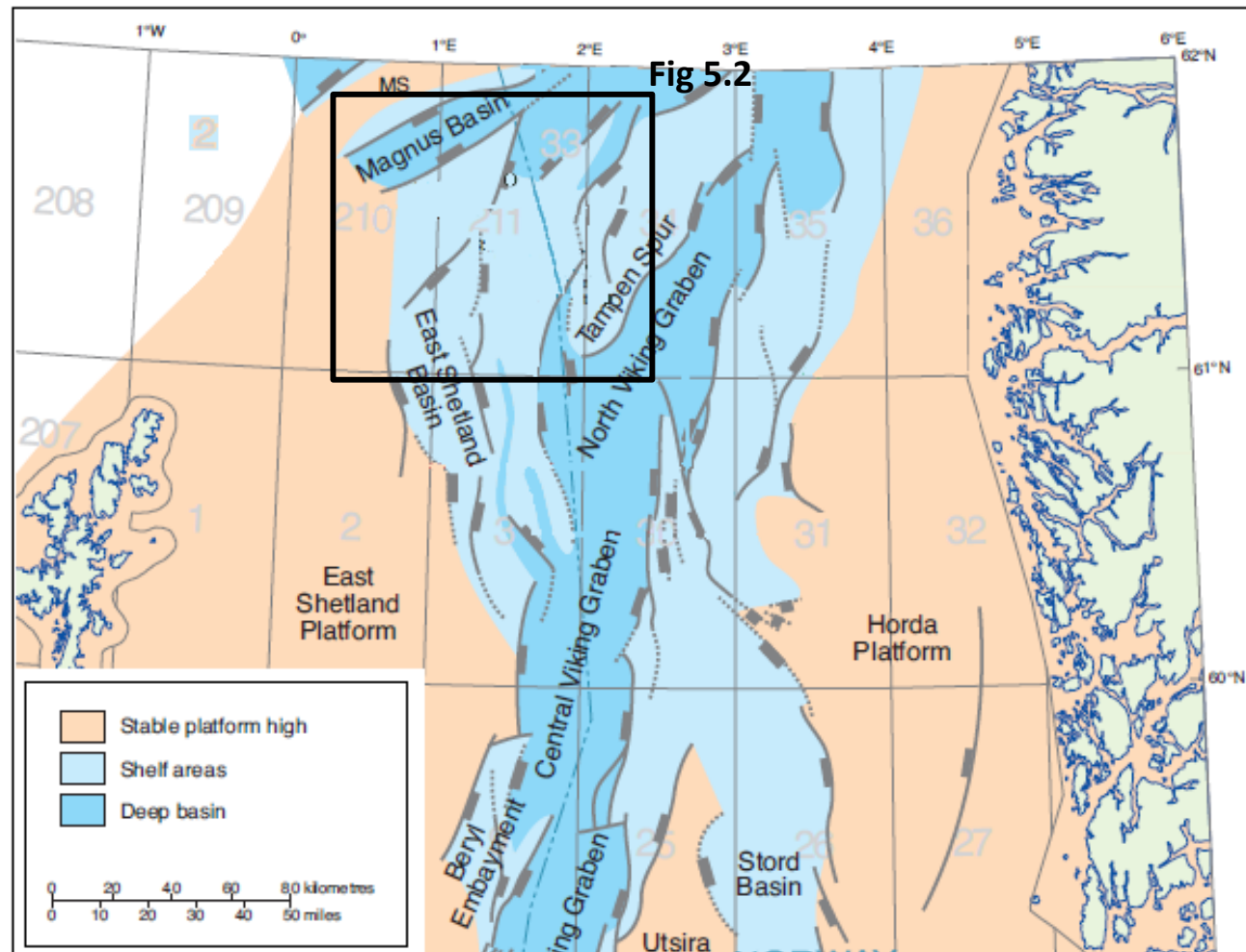


Figure 5-1 Regional map illustrating the large scale structural geology that is present within the East Shetland Basin (Edited from Fraser et al. 2003).

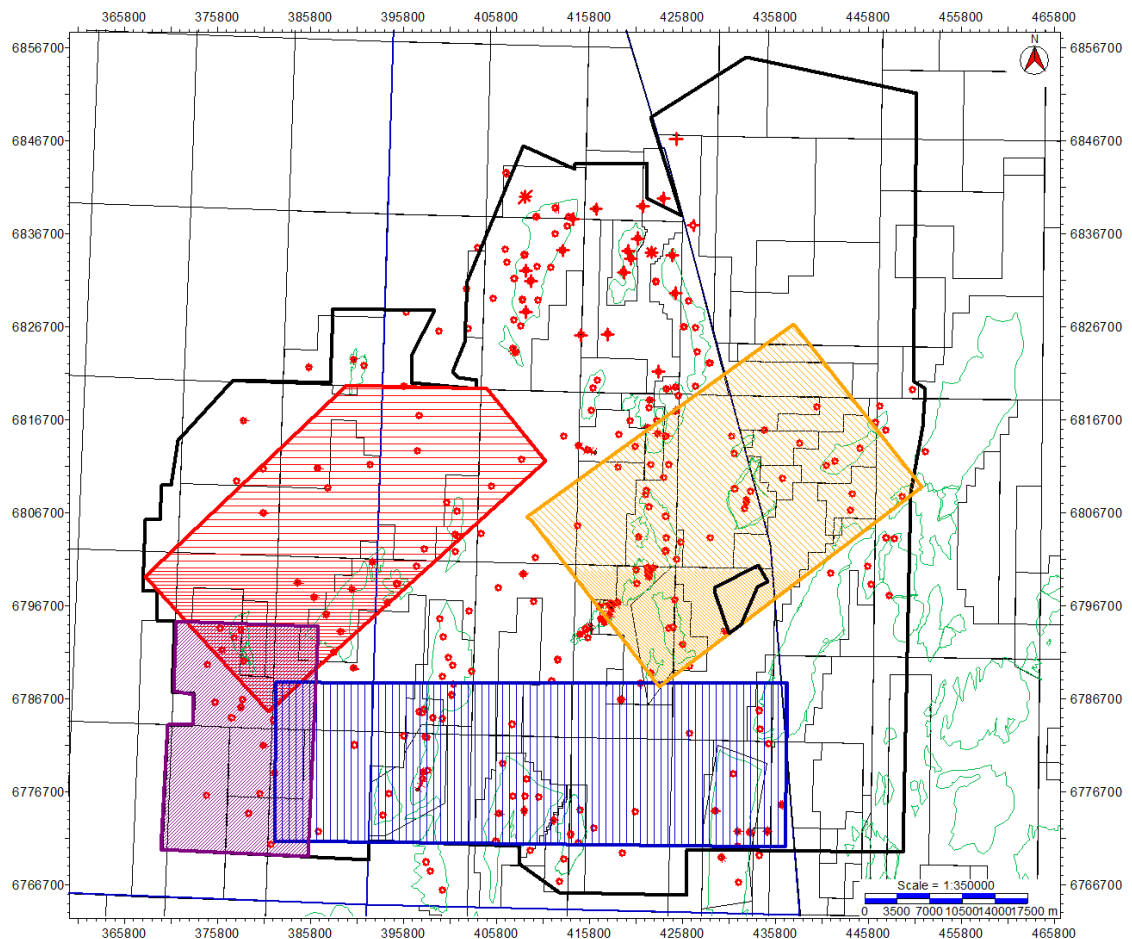


Figure 5-2. Map illustrating the 4 areas of interest. Area 1, Highlighted in red, Tern-Eider Ridge. Area 2, highlighted blue, Cormorant to Brent. Area 3, Highlighted purple, Pobie platform. Area 4, Highlighted yellow, Causeway to Statfjord North.

Synthetic seismograms were constructed for key wells where both sonic and density data were available. By accurately tying the seismic data to the borehole, it is possible to have more confidence with the horizon pick from well to well throughout the seismic. By generating a synthetic seismic trace along the borehole and comparing it to the actual seismic data, it may be possible to identify potential geobodies that may not have been identified in either borehole data or the seismic data. Throughout the study area, multiple horizons have been interpreted at different stratigraphic levels. A table illustrating the horizons that have been interpreted and the colour coding for them and the accompanying fault can be found in Table 2.

Table 5-1. List of data that was used in this chapter.

Area 1				
Seismic data	Hudson			
	Tern-Eider			
	Tern-Spec			
	X_Mega_m07			
Blocks	210/19	210/20	210/24	210/25
	211/16	211/21		

Area 2				
Seismic data	Cladhan			
	Hutton			
	X_Mega_m07			
	Hudson			
	Tern-Eider			
Blocks	210/25	210/30	211/21	211/22
	211/23	211/24	211/26	211/27
	211/28	211/29	211/30	

Area 3				
Seismic data	Cladhan			
	Hudson			
Blocks	210/24	210/25	210/29	210/30

Area 4				
Seismic data	Murchison Small			
	X_Mega_m07			
	X_Mega_n07			
	Tern-Spec			
Blocks	211/18	211/19	211/22	211/23
	211/24	33/6 (N)	33/9(N)	34/4 (N)
	34/7(N)			

Table 5-2 Highlights the horizons interpreted throughout the project and the colours which represent the different horizons and the varying faults (Zanella & Coward 2003).

Horizon Identification Table		
Stratigraphy	Age	Colour
Top Balder Formation	~55Ma	Red
Top Shetland Group	65Ma	Light Green
Top Cromer Knoll Formation	~99Ma	Dark Blue
Top Humber Group	~144Ma	Purple
Top Brent Group	~160Ma	Orange
Top Dunlin Group	~180Ma	Brown
Top Cormorant Group	~205Ma	Pink
Base Syn-rift 1	Estimated 250Ma	Cyan
Top Basement	~420Ma	Cyan

Fault Identification Table		
Rift system	Age	Colour
Permo-Triassic	255-240Ma	Red
Upper Jurassic	160-145Ma	Blue
Reactivated	255-145Ma	Black

5.3 Evidence of a Transected Rift

To analyse the effect of multiple rifting events, a series of well calibrated seismic horizons have been generated within the highlighted study areas and then used to make time thickness maps (isochrons) as shown in Figure 5-3. These isochrons can show the thickening trends of syn-rift sediments which relate to the movements and timing of normal faults and the generation of accommodation space. By mapping out the thickening trends at different geological times, it may be possible to see which faults moved when and in what orientation. Within the east Shetland basin four study areas have been highlighted which all show varying degrees of rift transection. These four

areas represent four different rifting types which vary in complexity from reactivation of an initial fault plane to complete cross cutting of faults. It has been possible to define the four models by analysing three aspects of the faults; the fault strike, fault dip polarity and fault plane reactivation. They are:

- | | |
|-----------------|--|
| Type 1 Rifting; | same fault strike, same fault polarity and full reactivation of existing fault planes. |
| Type 2 Rifting; | same fault strike, opposed fault polarity and partial fault plane reactivation. |
| Type 3 Rifting; | oblique fault strike, variable fault polarity and partial fault plane reactivation. |
| Type 4 Rifting; | perpendicular fault strike, mixed fault polarity and partial fault plane reactivation. |

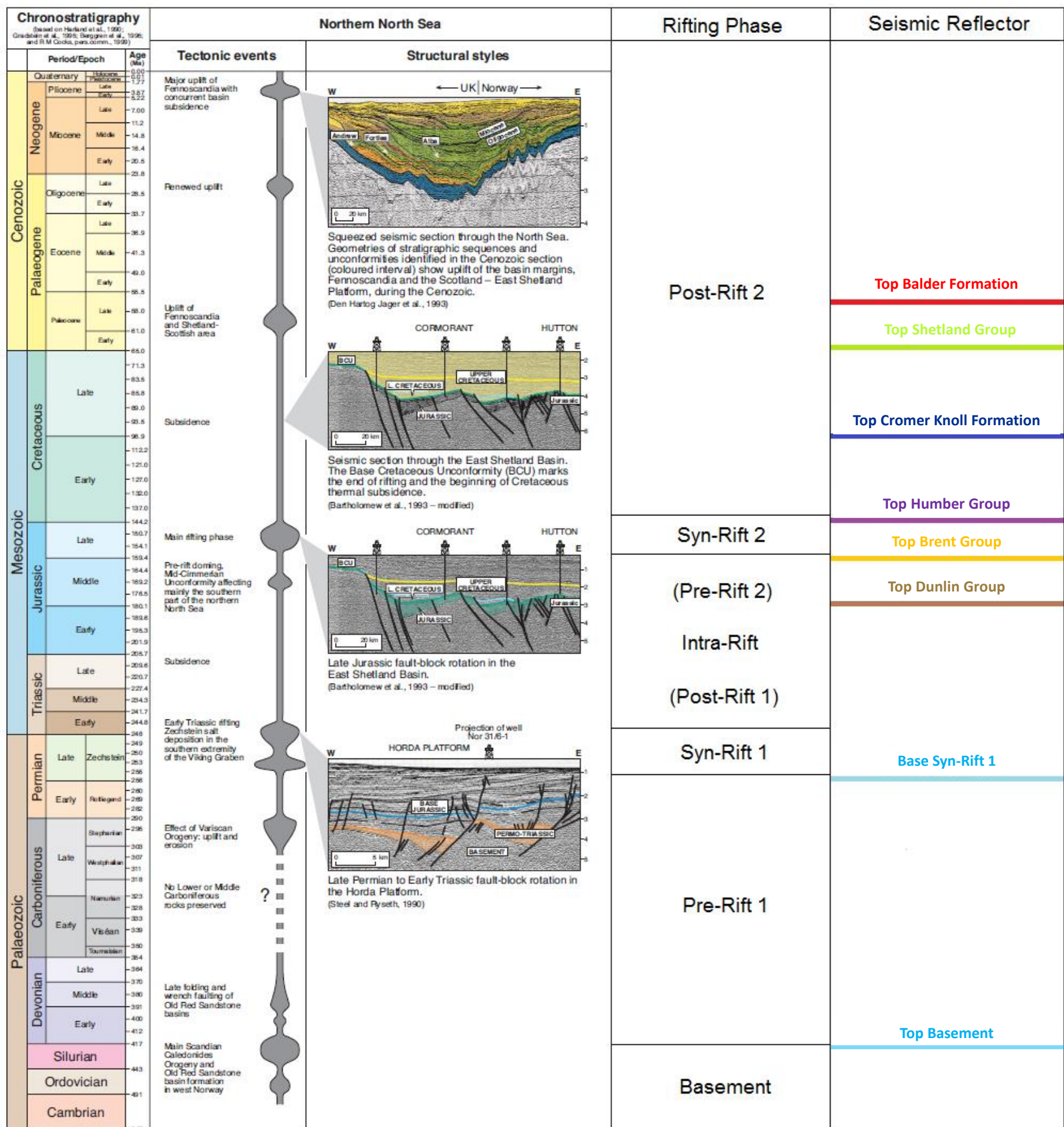


Figure 5-3. Stratigraphic column illustrating the tectonic evolution of the Northern North Sea and the relevant sedimentary rifting phase (Zanella 2003).

5.3.1 Type 1 Rifting; same fault strike, full fault plane reactivation and same fault polarity

The first of the rifting types that was observed in the East Shetland Basin is exemplified by the Tern-Eider Ridge (Figure 5-4). The Tern-Eider Ridge (TER) is a horst structure which contains the two hydrocarbon fields, Tern and Eider which gives the structure its name. The normal faults which create this structure are aligned NE-SW, which matches up with the underlying Caledonian fault orientation. This older fault trend can leave a zone of weakness that could lead to reactivation during later rifting events. The seismic mapping of a series of important horizons pertinent to the rifts evolution such as top pre/syn/post rift horizons can be used to indicate the potential reactivation of this older fault trend in the Permo-Triassic and Upper Jurassic.

In this location, the two rifting events have been identified and key reflectors have been picked to best illustrate the movement of faults through time. To illustrate this fault movement the horizons picks are the base syn-rift 1 (cyan horizon) which in this area has been configured as metamorphic (Gneissic) basement by several well penetrations. The top of syn-rift 1 package is identified as the Top Brent Group, which will also act as the base of syn-rift 2 package. The Base Cretaceous Unconformity will act at the top horizon for the syn-rift 2 package, thus completing the multiple rift packages of sediments.

A series of seismic lines have been generated and well tied with the use of synthetic seismograms (Figure 5-5) to best illustrate the cross-rifting that is present in the Tern-Eider area. Seismic lines 1-1, 1-2 and 1-3 are aligned perpendicular to the main structural trends to best show the faulting

observed in this area. Seismic lines 1-4 and 1-5 are parallel to the structures with line 1-4 located within the hangingwall of the main structures and line 1-5 in the footwall of the structures.

It is possible to see from seismic lines 1-1, 1-2 and 1-3 that the offset of the Brent Group varies along the length of the Tern-Eider Ridge. This variation relates to the Upper Jurassic rifting event. The structure as a whole tips out to the southwest and develops into the structural high to the northeast. A simple fault tip model suggests the largest offset should be located in the middle of the fault and the smallest towards the end of the fault, which is seen in the NE and SW areas respectively. However, this is evidently not the case with the Basement pick within the study area.

Seismic line 1-1 (Figure 5-6 and 5-7) is located in the NE of the study area and is close to the centre of the TER structure, which shows significant offset of the Top Brent horizon. There is also considerable offset in the Basement horizon, but, when the offset between the two horizons is measured there is very little difference between the two offset values. This suggests that this section of the TER is dominated by purely Upper Jurassic faulting and the offset is not influenced by the underlying Permo-Triassic faults.

Seismic line 1-2 (Figure 5-8 and 5-9) is located in the centre of the study area and is roughly parallel to seismic line 1-1, but is located further to the SW. This line also shows the continuation of the TER but, the offset between the top Brent horizon is less. This is related to the Upper Jurassic fault starting to die out. A major difference between seismic line 1-1 and 1-2 is the offset of the top Basement. Within line 1-2, it is possible to see a thickening package relating to an earlier phase of rifting below the Brent Group. This is related to the Permo-Triassic rifting event. This is the first instance where an underlying fault system looks to have reactivated in a later rifting event. It is

also important to point out the large scale fault that is located in the furthest NW location of the seismic line. This fault relates to the western limit of the Upper Jurassic rift system and bounds the basin area to the rift shoulders.

The final dip section is seismic line 1-3 (Figure 5-10 and 5-11) and is located to the SW of the study area. This location shows that the fault that generates the TER has now tipped out and as a result no offset is present within the top Brent Group horizon. The same cannot be said of the top Basement pick which now shows even more offset than in seismic line 1-2. As no faulting is observed in the Upper Jurassic, the Basement offset is entirely related to the Permo-Triassic rifting event. What is clear to see between these three dip lines is the evolution of the two rift systems along the length of the TER. Again the western limit of the East Shetland Basin can be observed with the presence of the basin bounding fault in the NW section of the seismic line. It must also be noted that a small thrust fault is located within the footwall of the Permo-Triassic fault and will be covered in the Type 3 rifting section.

Seismic line 1-4 (Figure 5-12 and 5-13) is the first of two strike lines, with this line being located within the hangingwall of the TER and seismic line 1-5 in the footwall of the TER structure. Although there is not as much structural feedback in line 1-4 as there is in the three previous dip lines, it is still possible to see the overall effect of the two rifting events. Seismic line 1-4 shows the continual thickening of syn-rift 2 package from SW to NE and the post-rift 2 thermal subsidence effects in the NE of the section. It may also be possible to see a slight thickening trend in the syn-rift 1 package in a south-westerly orientation.

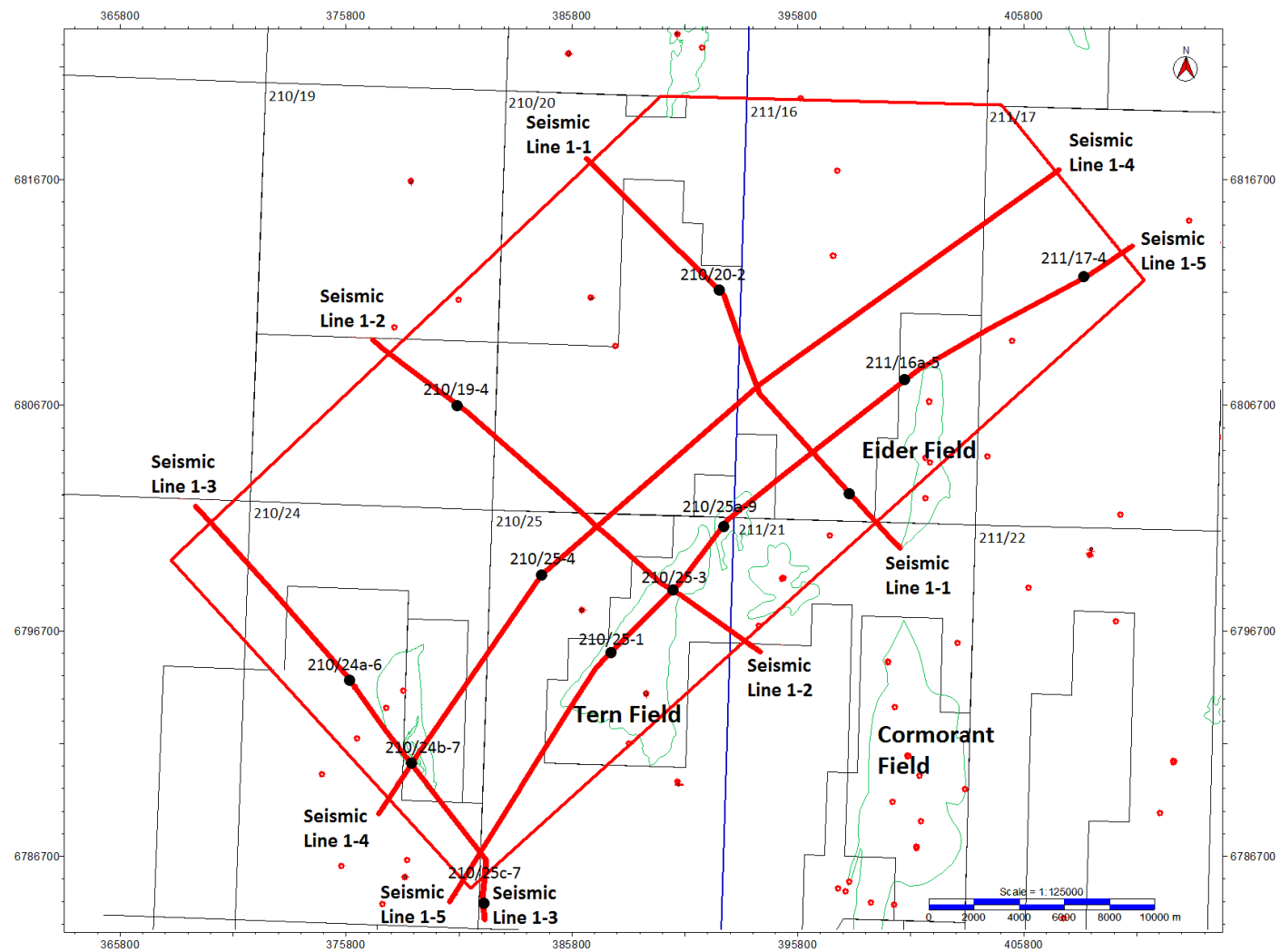


Figure 5-4. Base map illustrating the study area (red) and a series of seismic sections to constrain seismic interpretation.

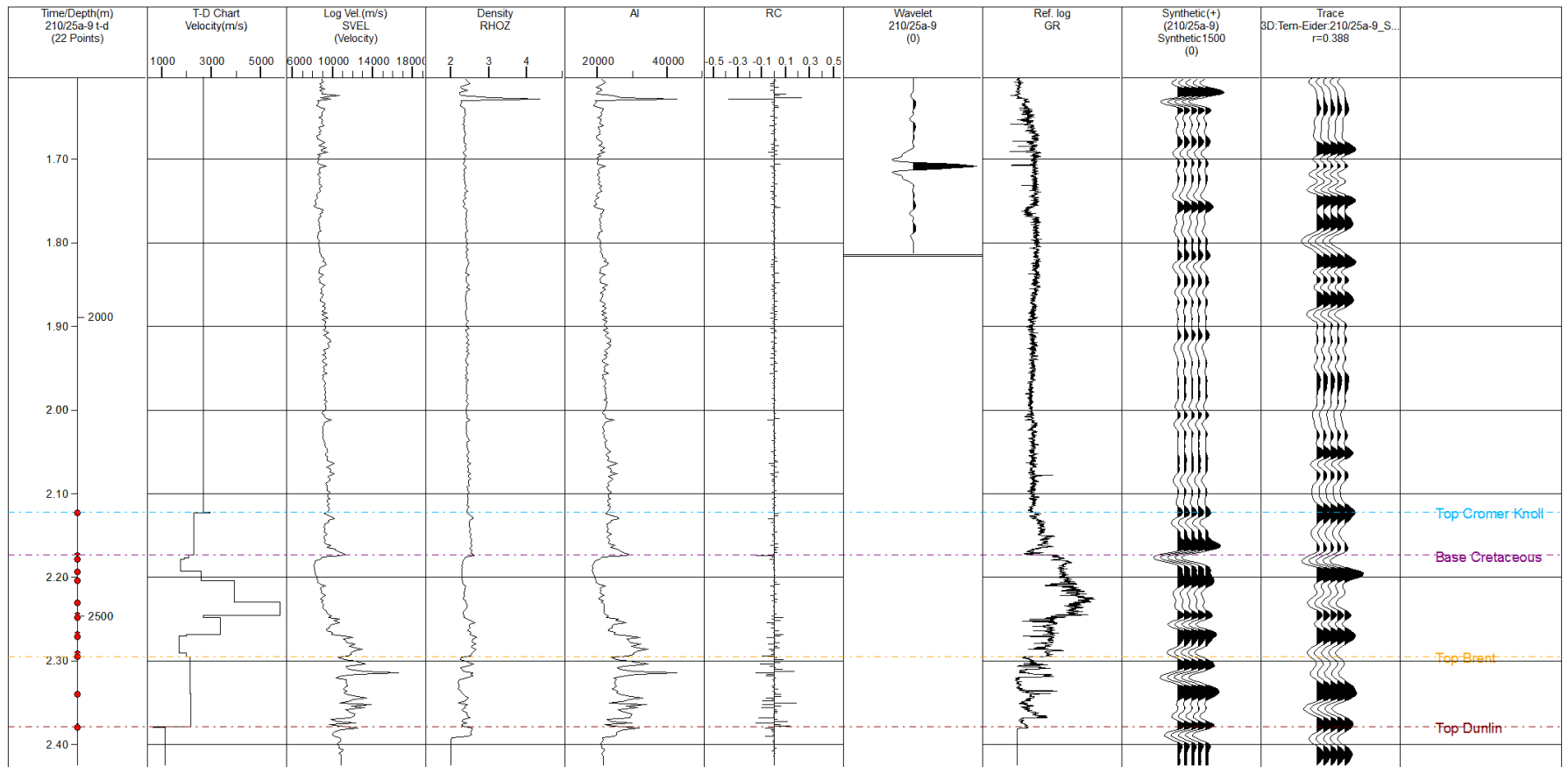


Figure 5-5 Illustrating the synthetic seismogram for well 210/25a-9

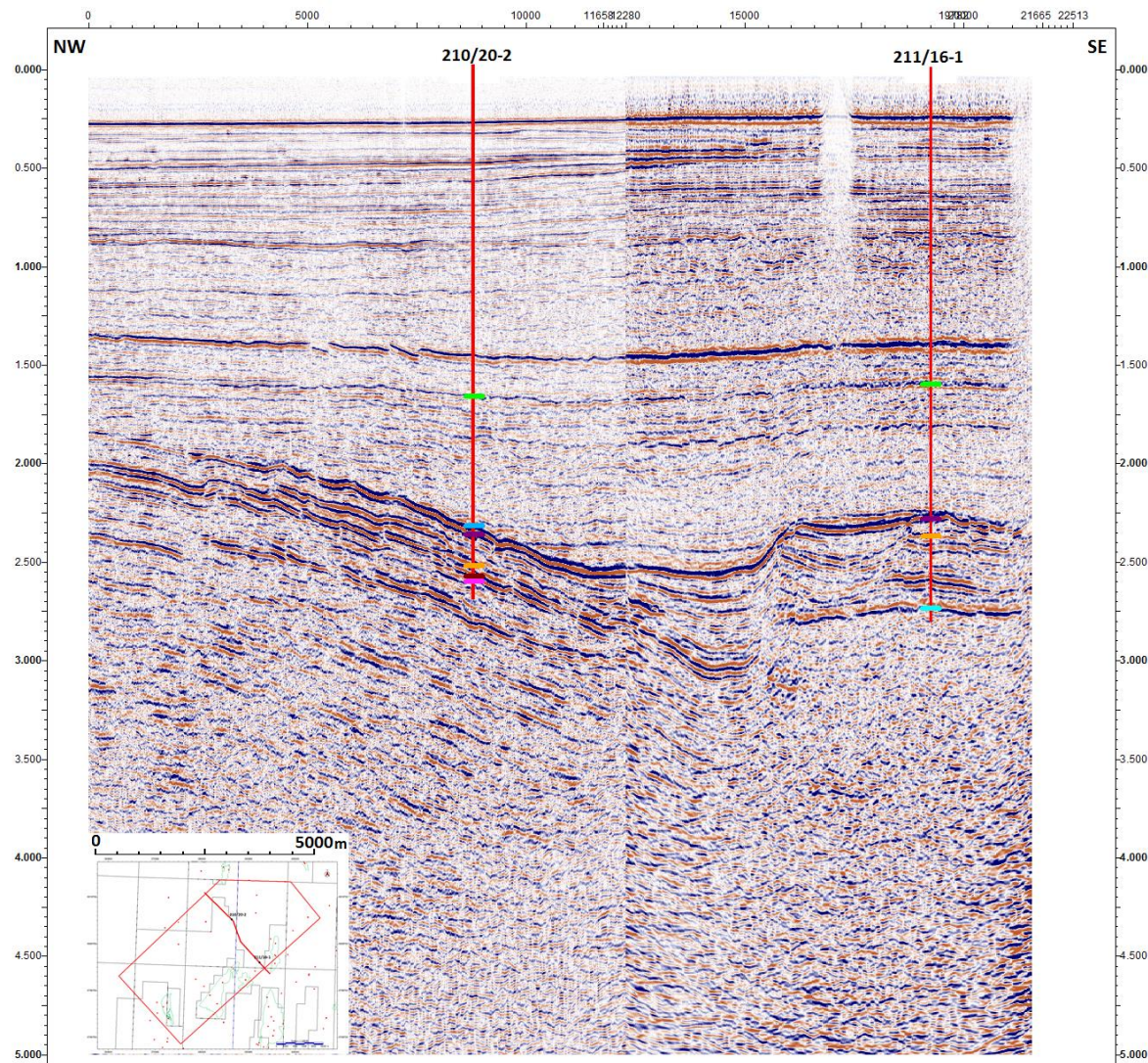


Figure 5-6 Seismic line 1-1 is a NW-SE trending seismic line that runs through the northern section of the Tern-Eider Ridge study area.

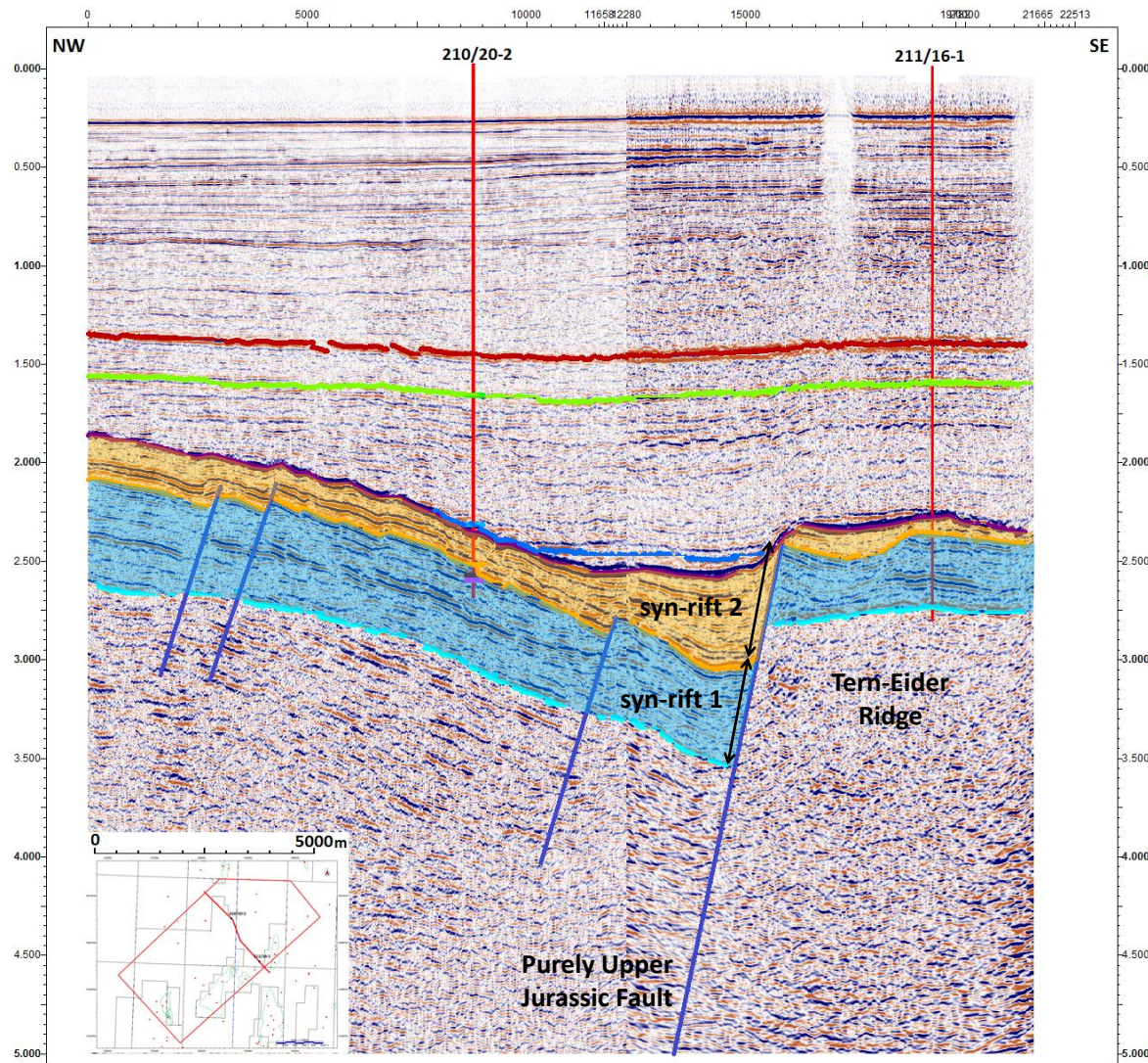


Figure 5-7 Seismic line 1-1 shows significant offset between the Top Brent Group across the western limit of the Tern-Eider Ridge. As the offset of both the Brent and the Base syn-rift 1 are equal it is likely that this fault is purely an Upper Jurassic fault.

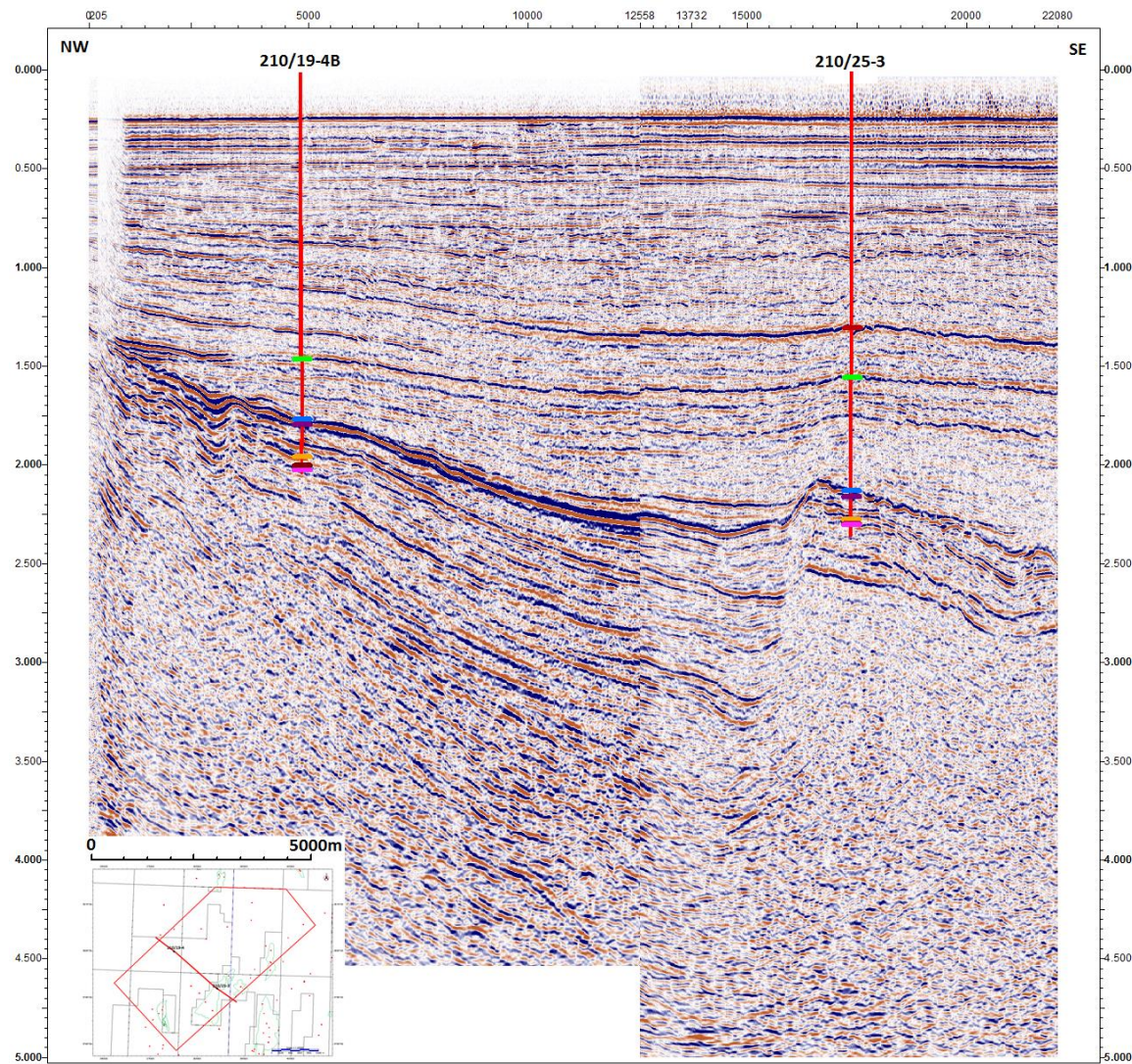


Figure 5-8 Seismic line 1-2 is NW-SE oriented line that runs through the central area of the Tern-Eider Ridge study area.

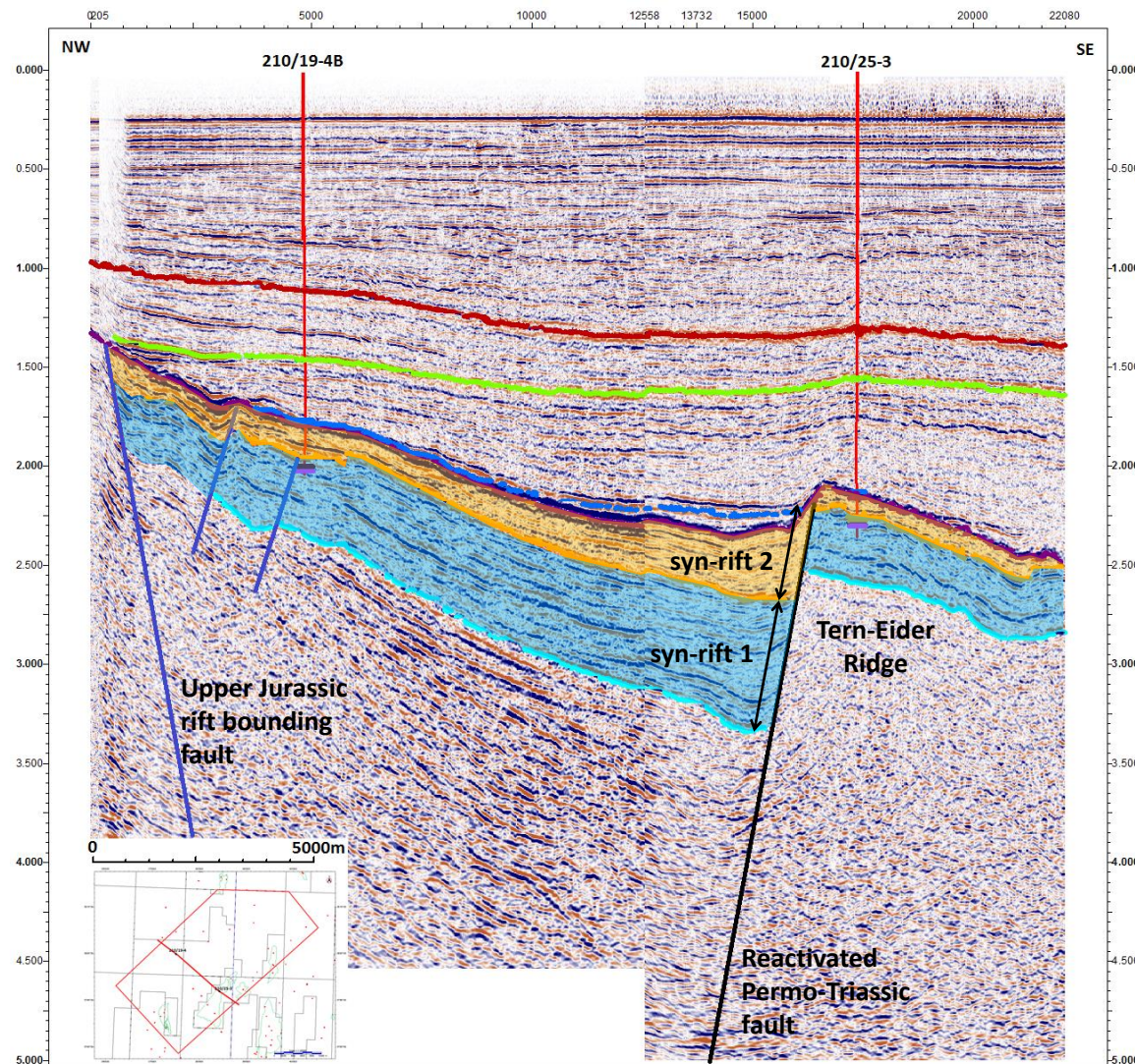


Figure 5-9 seismic line 1-2 shows significant offset between both the Top Brent Group and the Basement horizons. As the offset between the Basement horizon is greater than the Brent offset it suggests that a Permo-Triassic fault has reactivated in the upper Jurassic. The north-western edge of the seismic section illustrates the western limit of the East Shetland Basin.

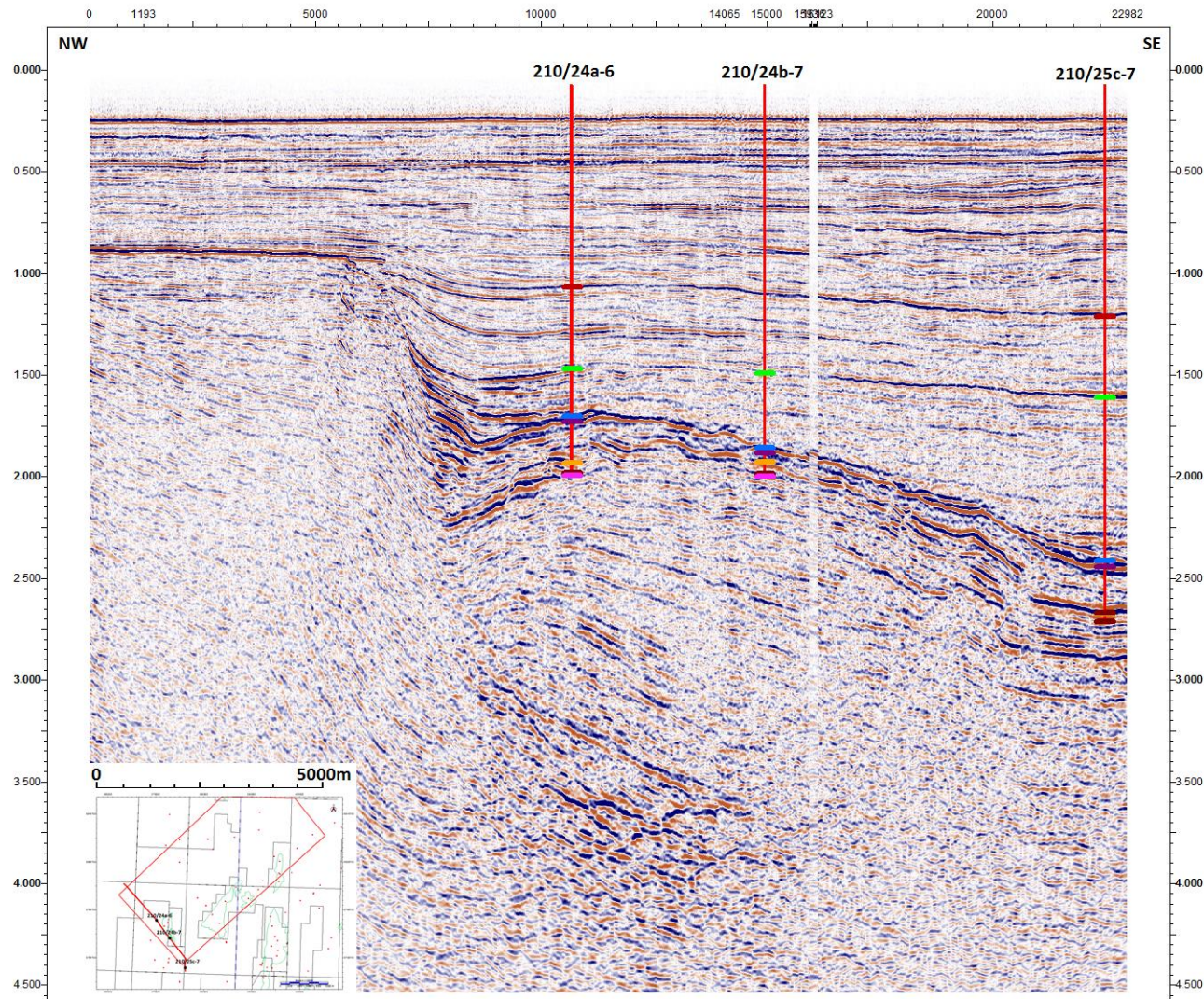


Figure 5-10 Seismic line 1-3 is a NW-SE oriented line in the southern section of the Tern-Eider Ridge area.

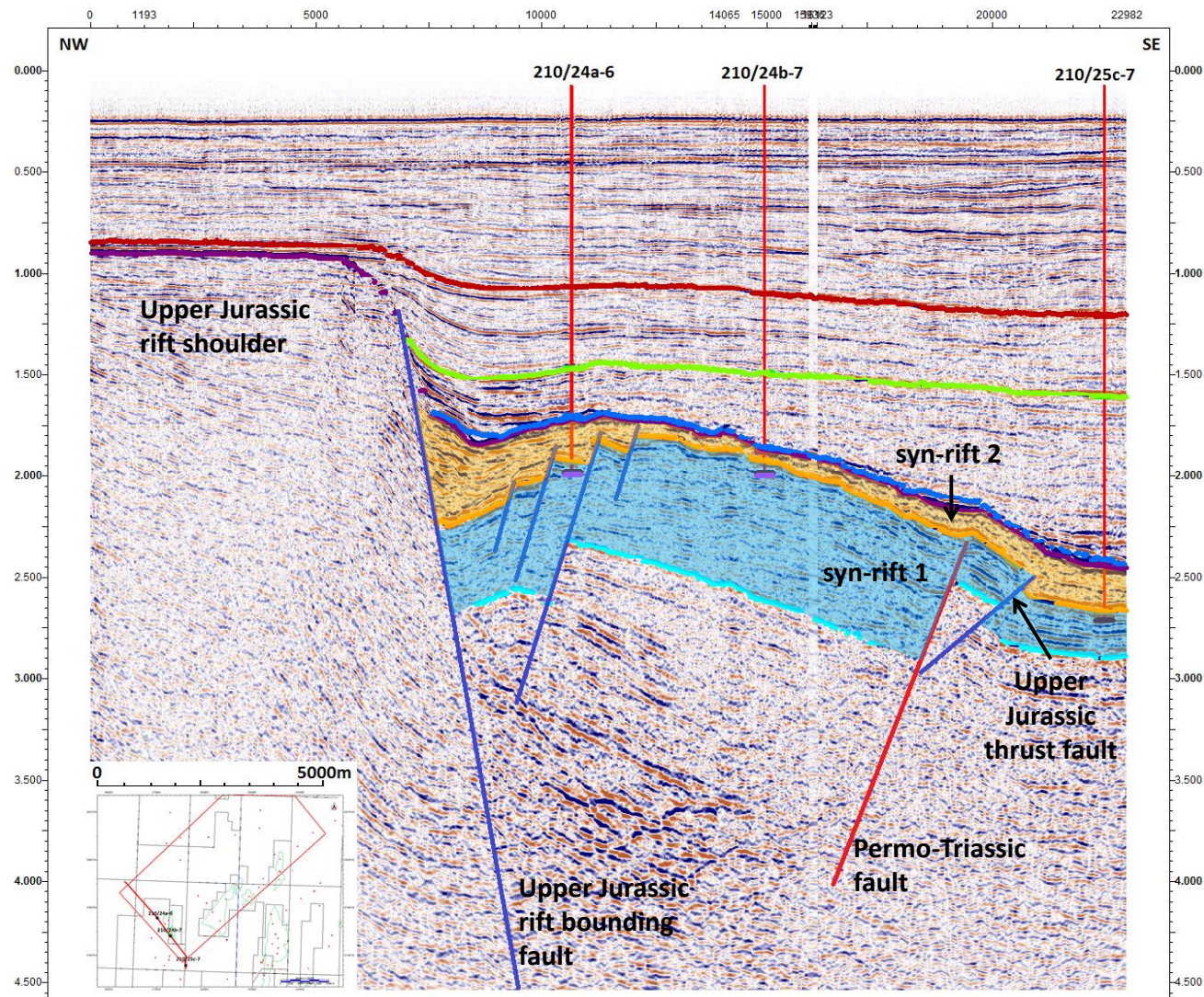


Figure 5-11 Seismic line 1-3 further illustrates the western rift shoulder of the East Shetland Basin. The southeast section of the seismic line shows no offset along the Permo-Triassic fault which illustrates no Upper Jurassic offset and thus has not reactivated in the second rifting phase. The footwall of the TER also contains an upper Jurassic thrust.

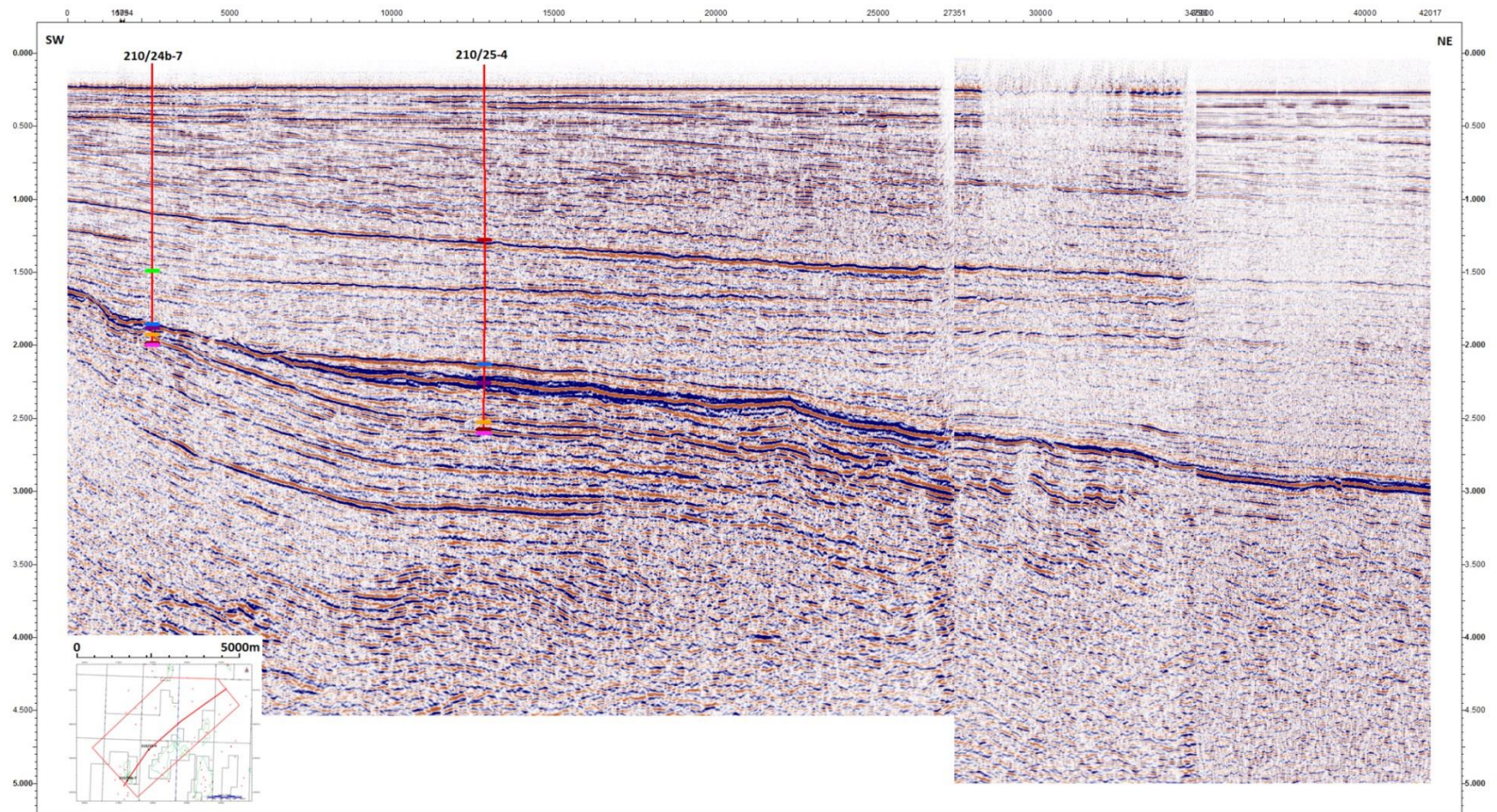


Figure 5-12 Seismic line 1-4 is a SW-NE oriented line located in the hangingwall of the Tern-Eider Ridge.

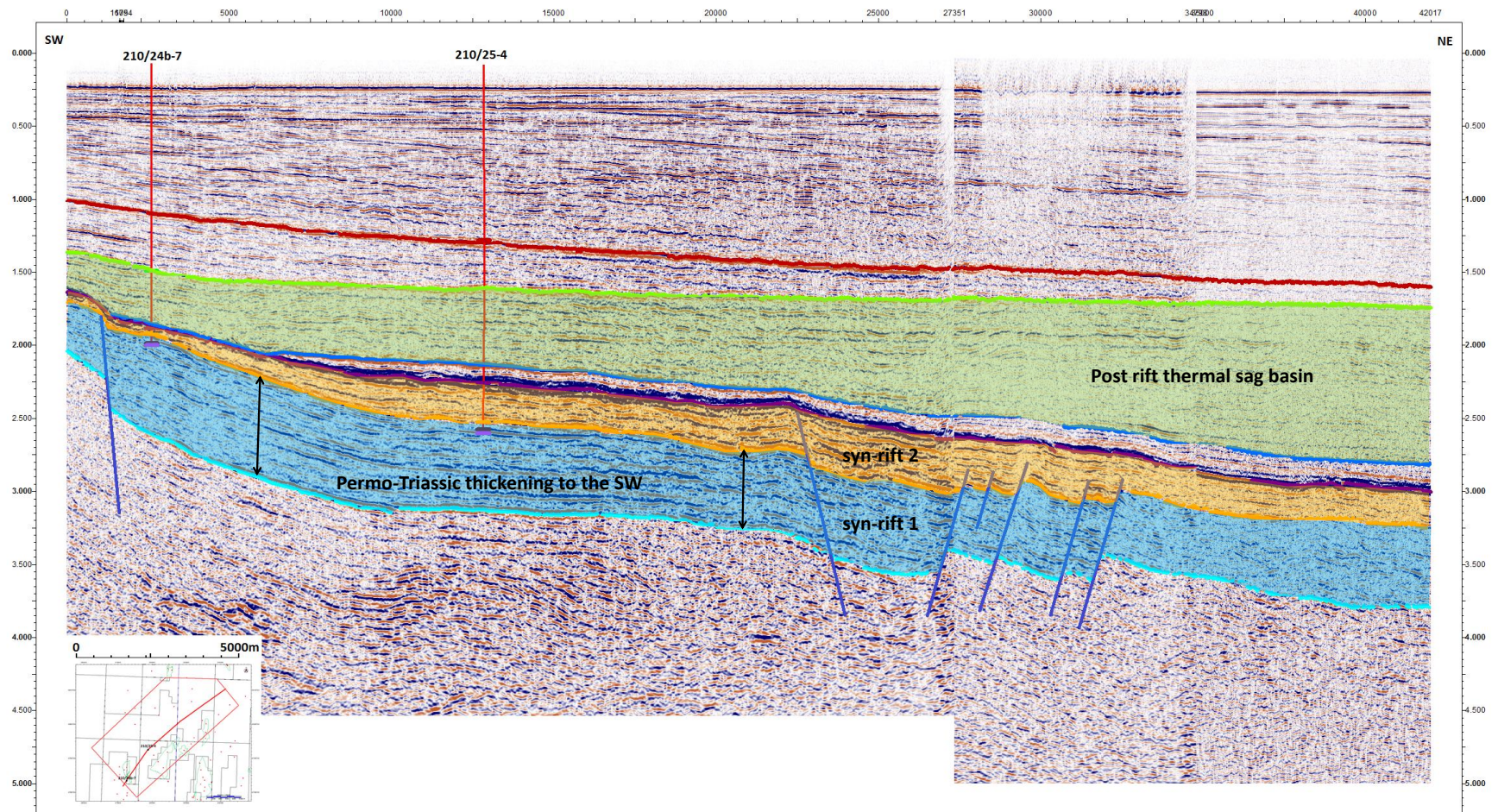


Figure 5-13 Seismic line 1-4 shows in the south-western location an increased thickening section in syn-rift 1 and a post-rift thermal sag basin to the northeast, which relates to the Upper Jurassic rifting event.

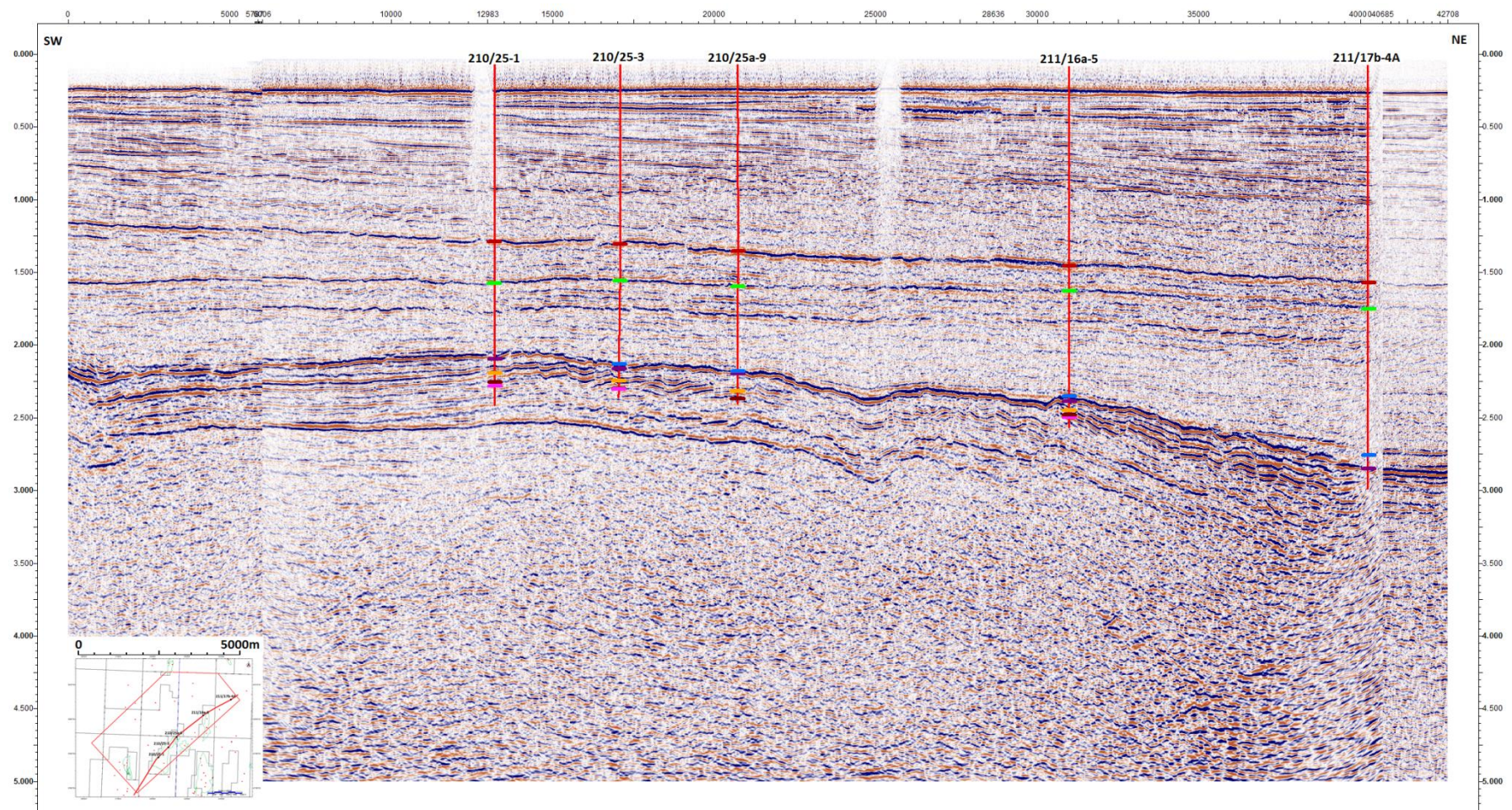


Figure 5-14. Seismic line 1-5, an uninterpreted seismic section across to footwall of the Tern-Eider Ridge.

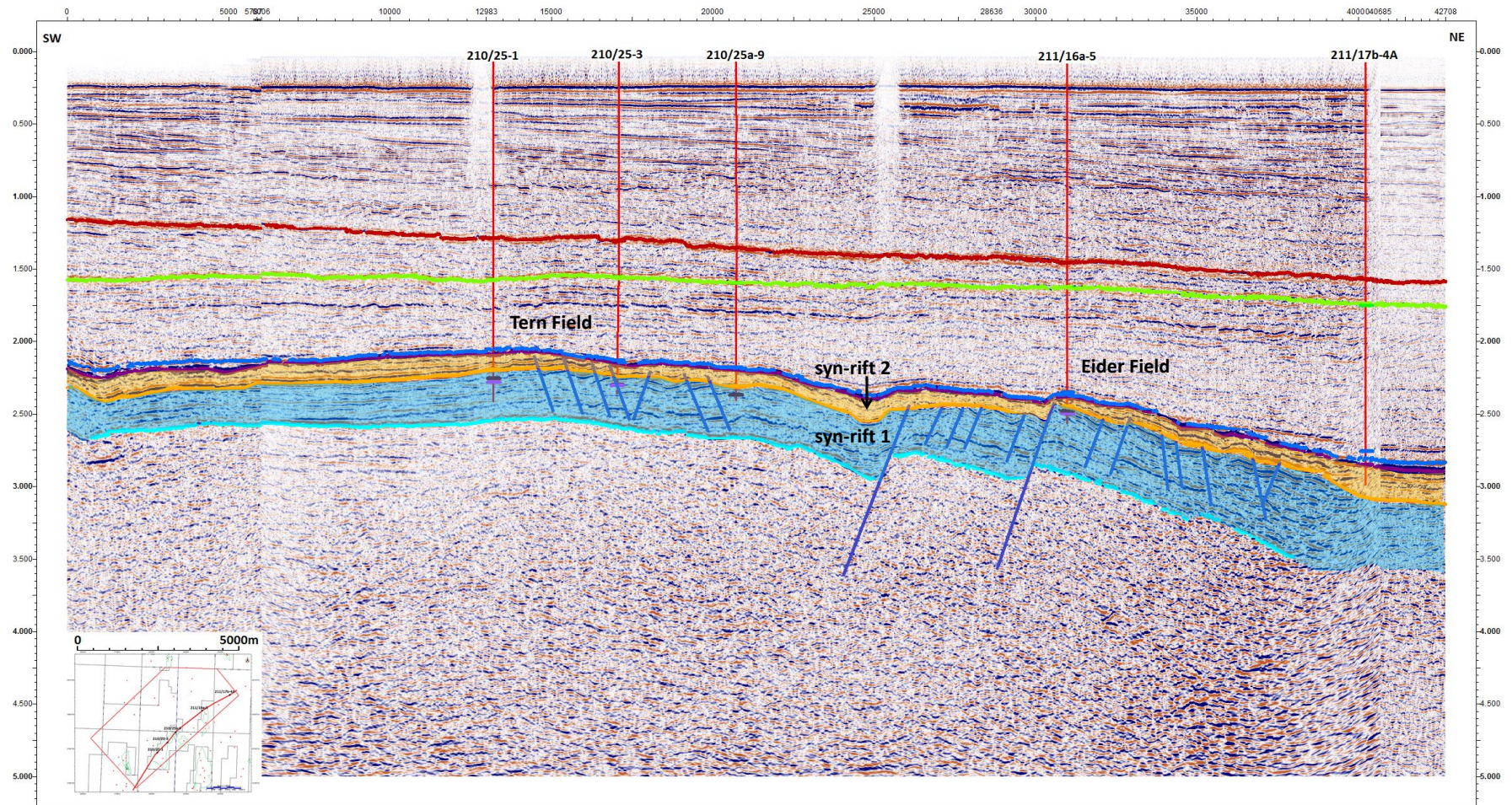


Figure 5-15. Seismic line 1-5, interpreted seismic section illustrating the topographic structures over the Tern-Eider Ridge.

The final seismic section is seismic line 1-5 (Figure 5-14 and 15) and is located in the footwall of the TER, which has a convex shape along the length of the structure. Within this section, it is possible to identify the two hydrocarbon fields over the structural high along with several other Upper Jurassic faults. These smaller normal faults run approximately N-S and their generation is covered in Type 3 rifting. Throughout this seismic section, it is possible to see a relatively thin covering of sediments between the basement horizon and the top Brent Group. This could be related to the elevated nature of the structure through two separate rifting events.

The seismic lines make it possible to see the differences that occur along strike sections of the TER area. The primary difference is the two thickening packages and the direction in which thickening occurs. This can be explained in more detail with the generation of top structure maps and isochron maps between the important horizons. The three top structure maps represent the top Basement, top Brent Group and Base Cretaceous Unconformity. As noted earlier, these three horizons represent key surfaces within the multi-rift system. The Top Basement structure map (Figure 5-16) illustrates the overall effects of both rifting events. This results in two depocentres located in different locations along the hangingwall of the NE-SW striking Tern-Eider Ridge. Potentially each of these depocentres relate to individual rifting events. A large depo-centre is located to the NE section of the study area which is an overprint effect of the Upper Jurassic rifting post-rift thermal subsidence associated with the rifting event. It was earlier mentioned that the Permo-Triassic faults appear to die out to the NE and any offset is related purely to the Upper Jurassic rifting event, which is observed here.

The Top Brent Group structure map (Figure 5-17) also illustrates the generation of a large scale normal faults that are aligned NE-SW. This

follows the same trend of the underlying Permo-Triassic faults. As this top structure map does not account for any offset relating to previous rifting events, it is possible to discriminate between what moved purely in the Upper Jurassic rifting event and what experienced in earlier (Permo-Triassic) rifting. Within this map it is again possible to see the post-rift thermal subsidence sag within the NE of the study area. It is further possible to see that the primary depo-centre to this fault is located within the centre of the TER. Along the crest of the Tern-Eider Ridge a series of N-S oriented faults are illustrated and bound the edge of the Tern and Eider Fields.

The Base Cretaceous top structure map (Figure 5-18) further emphasises the post-rift sag in the NE of the study area. As this is an unconformity event, there is very little to no offset observed throughout the structure map. It is however possible to identify the Tern-Eider Ridge and another significant high in the western edge of the study area. The fault identified in the seismic sections that make up the western rift shoulders of the Viking Graben can now be imaged within the BCU top structure map. It was not possible to illustrate this in the previous maps as there was no well data to tie to the interpretation over the high. The structure maps are also used to create time thickness maps which will be able to bring out the subtle changes in depo-centre locations within the Tern-Eider area.

The BCU to Top Basement isochron illustrates the structural trend of both the Upper Jurassic and Permo-Triassic rifting events. As noted in the Top Basement structure map two depo-centres can be identified which can be identified more clearly with this thickness map. The two syn-rift packages are located to the SW and the centre of the TER (Figure 5-19), whereas a significant post-rift thermal sag depocentre is located in the NE. These two depo-centres can however be separated out into individual rifting events, by looking at the isochron maps for the syn-rift 1 and syn-rift 2 packages.

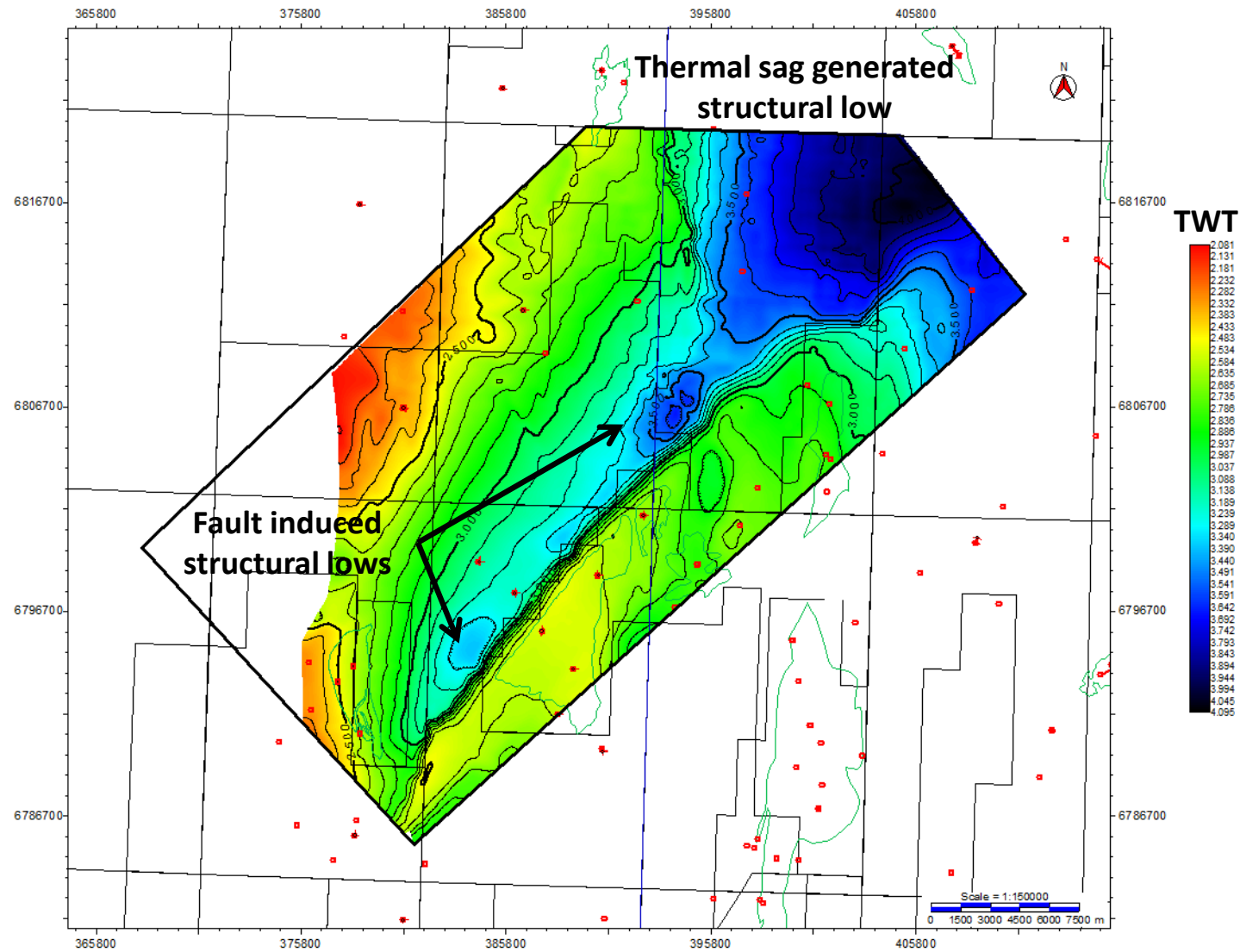


Figure 5-16. Top Basement (pre-rift) map illustrating the overall combined effects of both sets of rifting events. This map illustrates two separate depo-centres along the Tern-Eider Ridge.

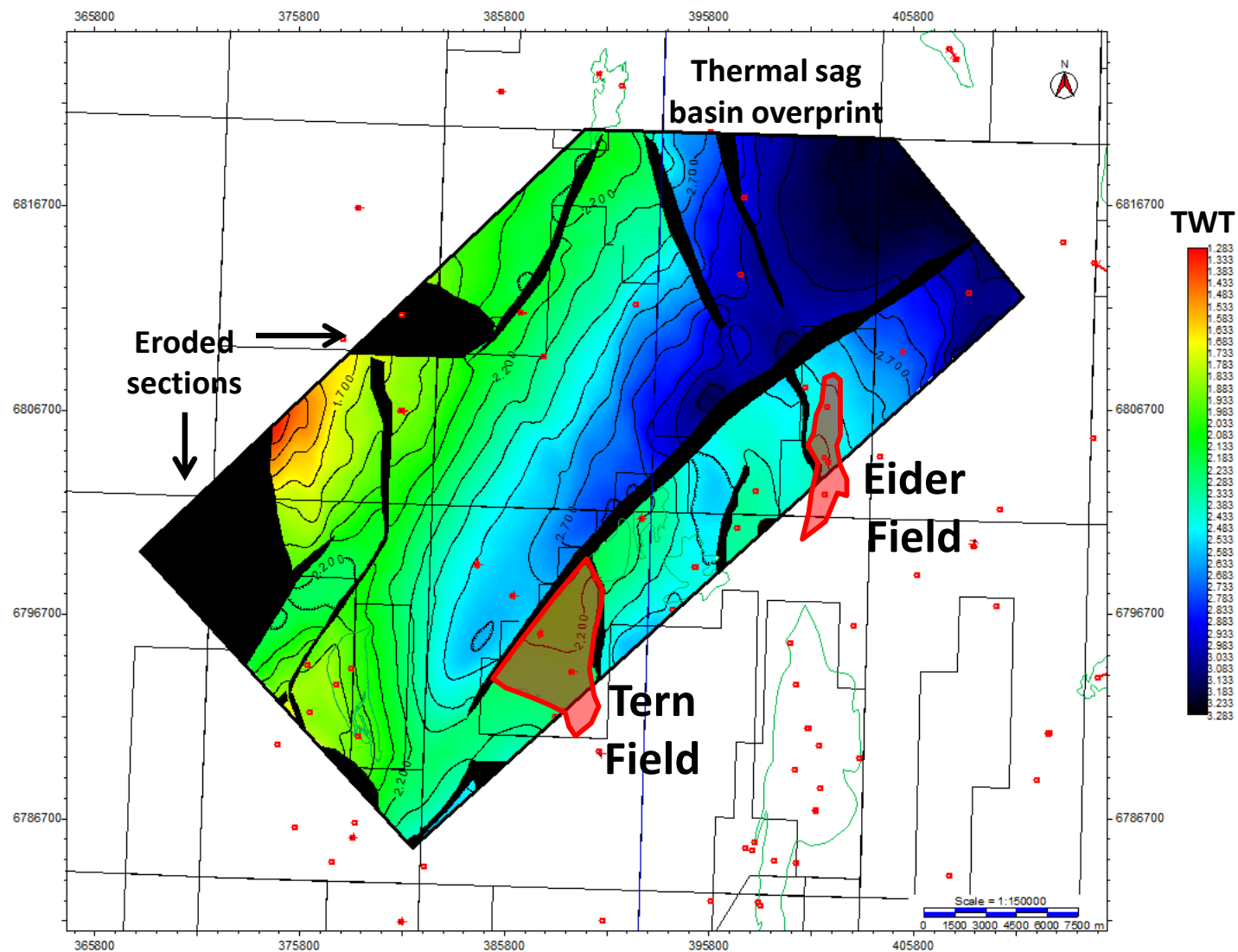


Figure 5-17. Top Brent Group structure map illustrating the NE-SW orientation of the Upper Jurassic rifting event.

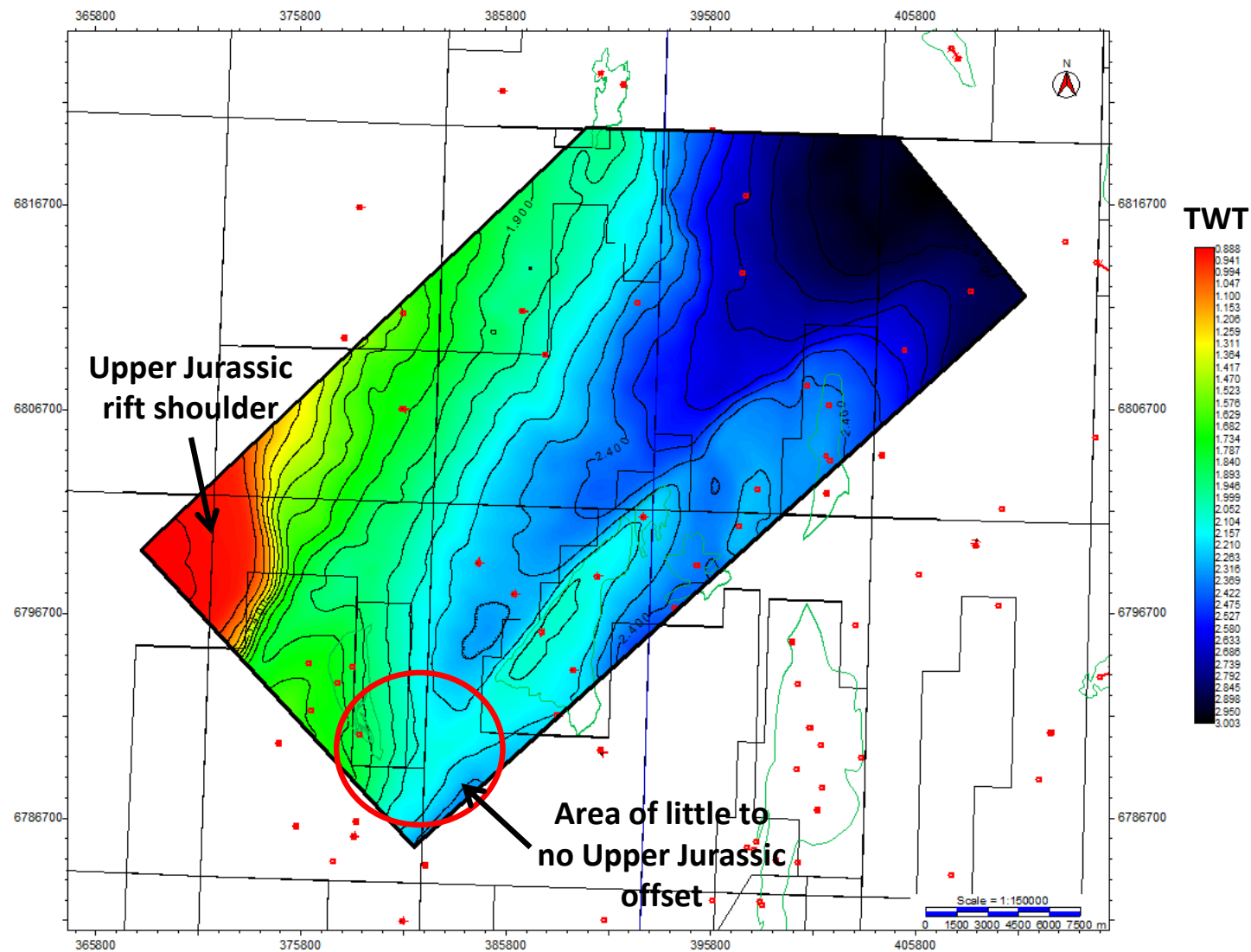


Figure 5-18. Top Base Cretaceous structure map illustrating the depo-centres created by the Upper Jurassic rifting event.

The syn-rift 1 thickness map (Figure 5-20) is generated by measuring the difference between the Top Basement reflector and the Top Brent horizon. By doing this it is possible to see what thickening trends were in-place prior to the Upper Jurassic rifting event. The evidence from this isochron shows that there was an original NE-SW oriented fault dipping towards the NW, in place to the SW of the existing Tern-Eider Ridge structure. This would suggest that the initial Permo-Triassic fault was of the same orientation and polarity to that of the Upper Jurassic faulting. The evidence from this map further illustrates that the Permo-Triassic fault tips out towards the centre of the TER structure and extends south-westerly. This thickening package accounts for the depo-centre located in the same area in the overall time thickness map.

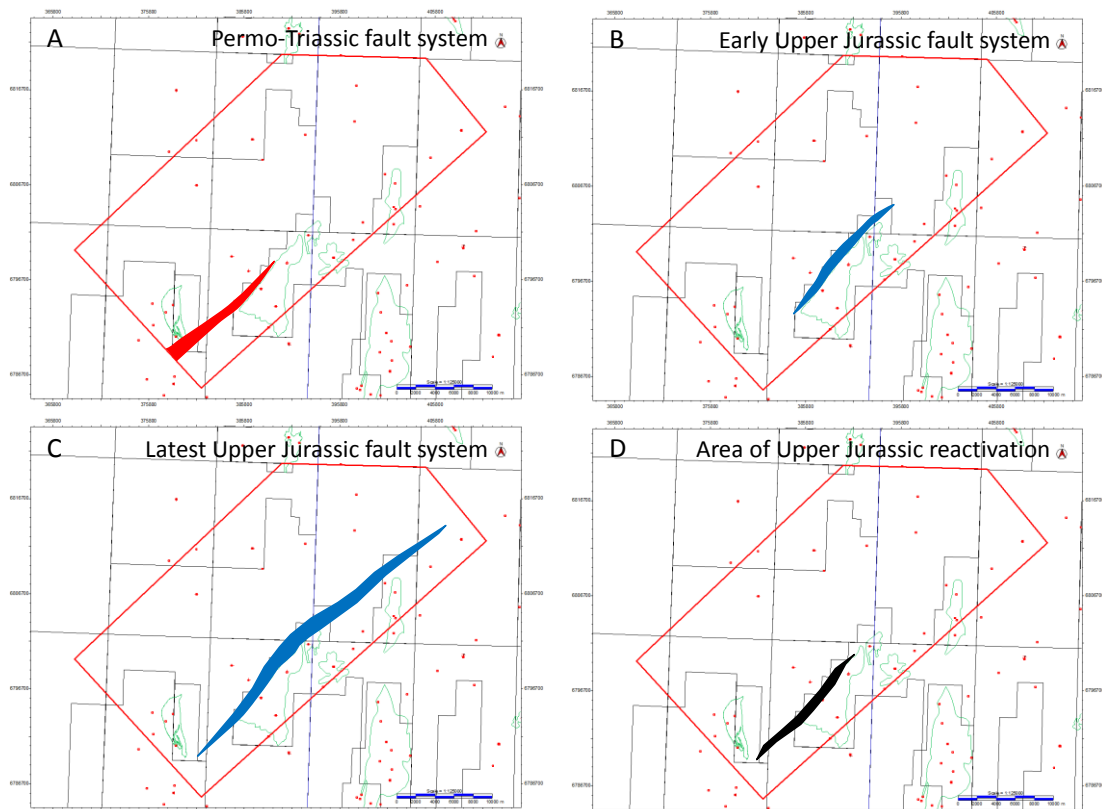


Figure 5-19 Illustrating the evolution of fault systems from the Permo-Triassic (A) through to the Upper Jurassic (B+C). Diagram (D) highlights the area where the two fault systems overlap and reactivate through time.

The Upper Jurassic syn-rift 2 package (Figure 5-21) responds directly to the Upper Jurassic faults and has been calculated by measuring the time gap between the Top Brent and the Base Cretaceous Unconformity horizons. Again a strong NE-SW oriented normal fault is present with a thickening section located within the centre of the TER, which is further NE than the depo-centre identified in the syn-rift 1 package.

This secondary depo-centre in the Upper Jurassic explains the appearance of a thickened section located on the overall isochron map. This suggests that the NE-SW fault that moved in the Permo-Triassic has reactivated in the Upper Jurassic. But, the position of the fault has changed laterally over time, potentially generating a vertical relay ramp (Figure 5-24). Vertical relay ramping occurs where a fault system forms in the same location to that of an older extinct fault system. This occurs within the Tern-Eider area where an underlying Permo-Triassic fault is in place, with a later Upper Jurassic fault occurring in the same orientation, polarity and location. As the second fault (Upper Jurassic) continues to grow with time the fault plane may eventually overlap with that of the older (Permo-Triassic) fault plane. As the new fault plane interacts with the older plane it may cause the older fault plane to reactivate and become part of the new (Upper Jurassic) fault system. As the faults have moved position laterally over time, there is a section of overlap between the two fault strands.

Between the two depocentres in the overall isochron map, a saddle area can be identified. This saddle area exhibits the results of both rifting events equally as it was not the location of a major depocentre in either rifting event, but an area of significant subsidence throughout time. The change in depocentre location is commonly depicted to fault linkage between two faults. This occurs throughout the East Shetland Basin and generates large topographic structures and deep lows which potentially form kitchen areas

for the generation and maturation of hydrocarbons. The faulting shows that two separate depocentres formed in two different times in two separate locations, illustrating the same fault has been reactivated through geological time.

By actively measuring the displacement of the Top Brent Group and the Top Basement, Figure 5-23 makes it possible to further show the multi-rift evolution of the Tern-Eider Ridge. It has been identified that the depo-centre to the SW is solely related to the Permo-Triassic and the depo-centre to the NE is relate to the Upper Jurassic rifting event.

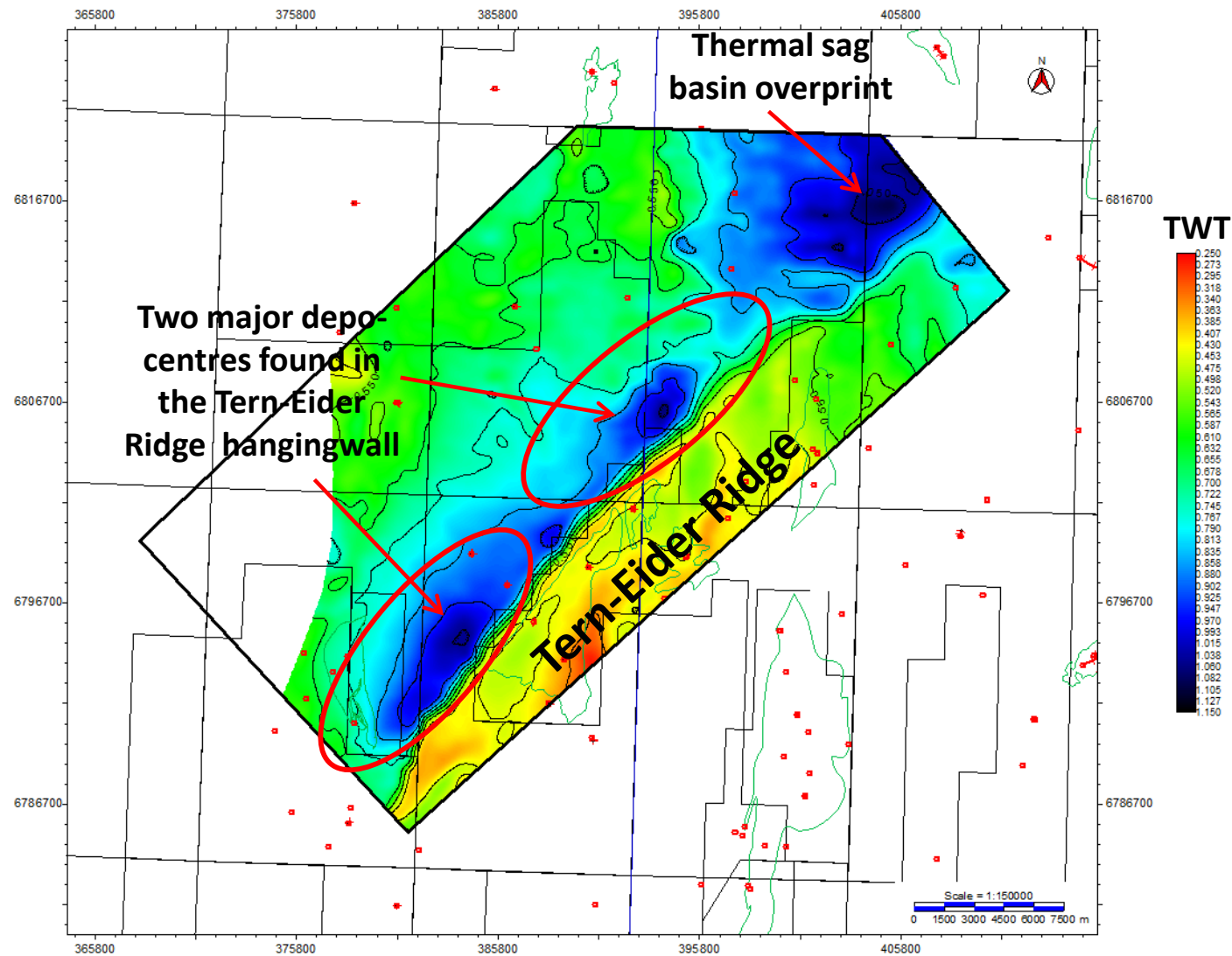


Figure 5-20. BCU to Top Basement marker bed illustrating the overall thickness trends identified through a combination of the two rifting events that occurred in the Permo-Triassic and upper Jurassic.

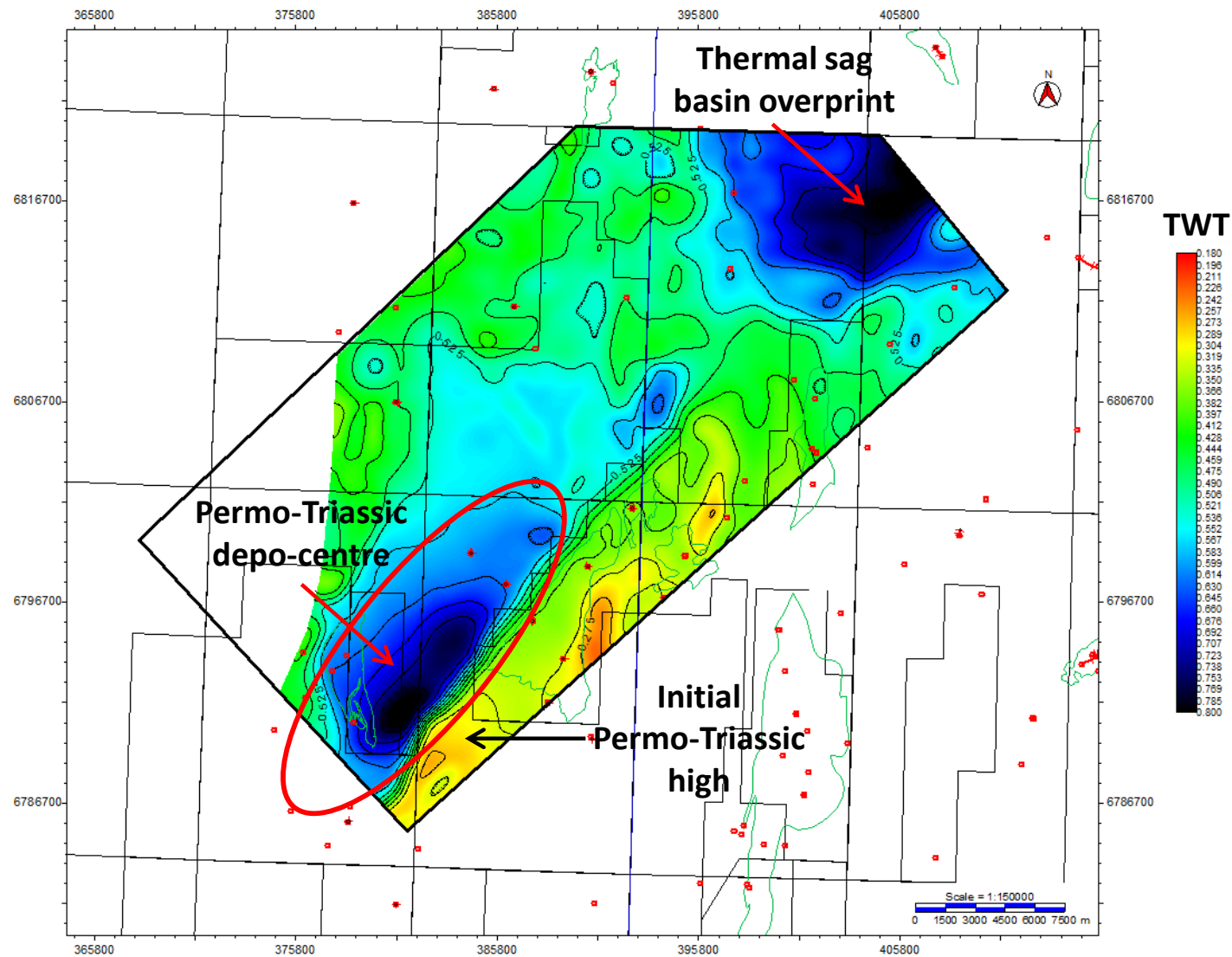


Figure 5-21 Initial syn-rift section between a Permo-Triassic marker bed and the Top Brent Group sediments, illustrating a large depocentre to the SW of the Tern-Eider Ridge.

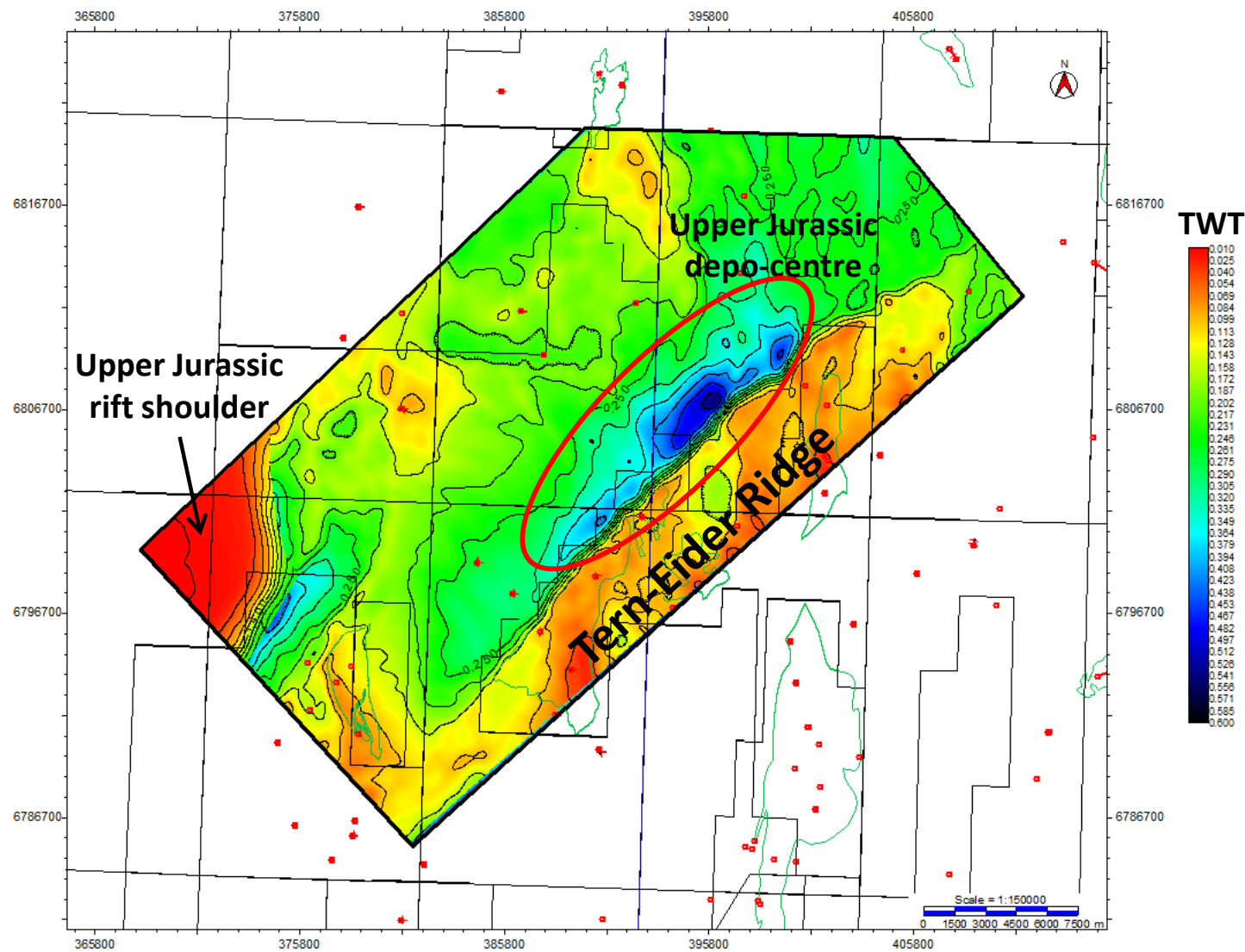


Figure 5-22. Base Cretaceous to top Brent Group isochron map illustrating depocentres that were created and filled by Humber Group sediments during the Upper Jurassic rifting event which is the second rift phase observed in the Tern-Eider Ridge area.

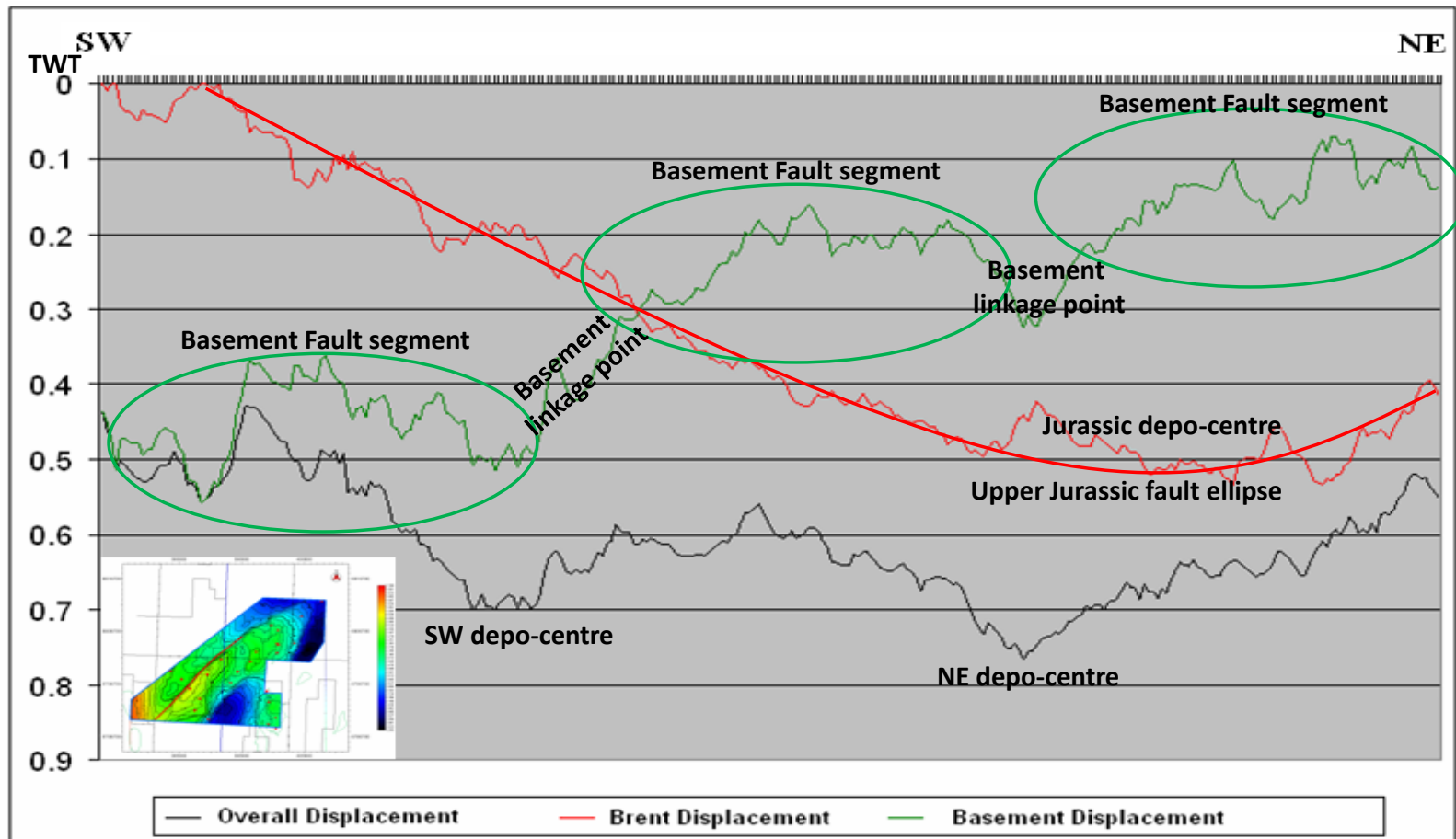


Figure 5-23. Fault displacement-length plot showing the offset of the Permo-Triassic and Upper Jurassic pre-rift sediments along the western edge of the Tern –Eider Ridge. The black line represents the overall displacement of both rifting events and relates to the economic basement. The red line illustrates the displacement of the top Brent Group sediments, which are the pre-rift to the Upper Jurassic rifting event and records fault movement solely for this stretching event. By subtracting the Upper Jurassic faulting from the overall displacement it is possible to generate the initial Permo-Triassic Displacement, this is illustrated here by the green line.

The results of the displacement analysis further backs up the idea of two depo-centres that have formed due to separate rifting events. As illustrated in seismic line 1-3 the SW section of the TER has little to no Upper Jurassic offset but significant Permo-Triassic offset. This evidence is reversed as you move NE along the Tern-Eider Ridge as the Permo-Triassic fault dies out and the Upper Jurassic fault begins to move. At the midpoint of the Tern-Eider Ridge, where the greatest effects of the Upper Jurassic rifting is evident, the thickness between the Top Brent Group to Top Basement either side of the fault is almost equal. This would suggest that the underlying Permo-Triassic fault has little or no impact on the Upper Jurassic faulting. By undertaking the displacement analysis it is also possible to identify more subtle information about the Permo-Triassic faulting. Along the length of the study it is clear to see three large fault segments which decrease in offset from SW to NE. Each of these segments is paired with a linkage point which could possibly have been a relay ramp location, thus showing the evolution of the underlying Permo-Triassic fault. The overall pattern of faulting in this study area suggests a structural domain that infers normal fault reactivation of the same fault strike, same fault polarity and re-use of the original fault plane.

The simplest type of multi-phase rifting is observed in the Tern-Eider Ridge area. Within this area Triassic trending faults have reactivated in the Upper Jurassic along the same fault strike, with the same fault polarity (dip) which leads to the re-use of an existing fault plane. This simple reactivation generally occurs along longstanding trends of weakness, which is observed in the Tern-Eider Ridge location. Although faulting is observed in the Triassic the trend upon which the fault initiated is that of an older Caledonian Trend. These deep seated trends of structural weakness reactivate during further rifting phases as seen in the Permo- Triassic and Upper Jurassic. Although the initial fault plane can be re-used the depo-centre, length and positioning of the reactivated fault may vary.

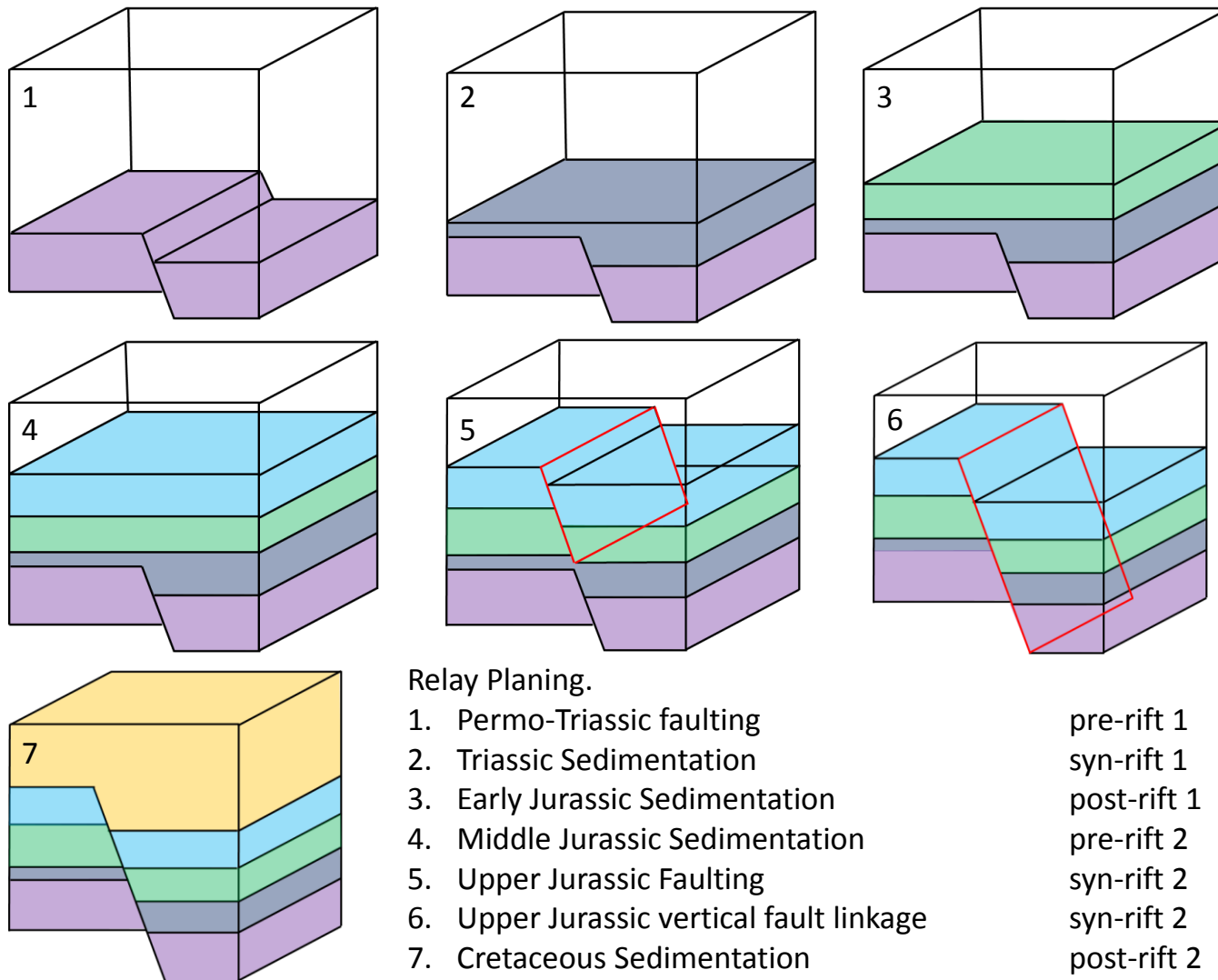


Figure 5-24 illustrates the method of vertical relay planing. This shows how two faults react and interlink with the same sense of throw and polarity.

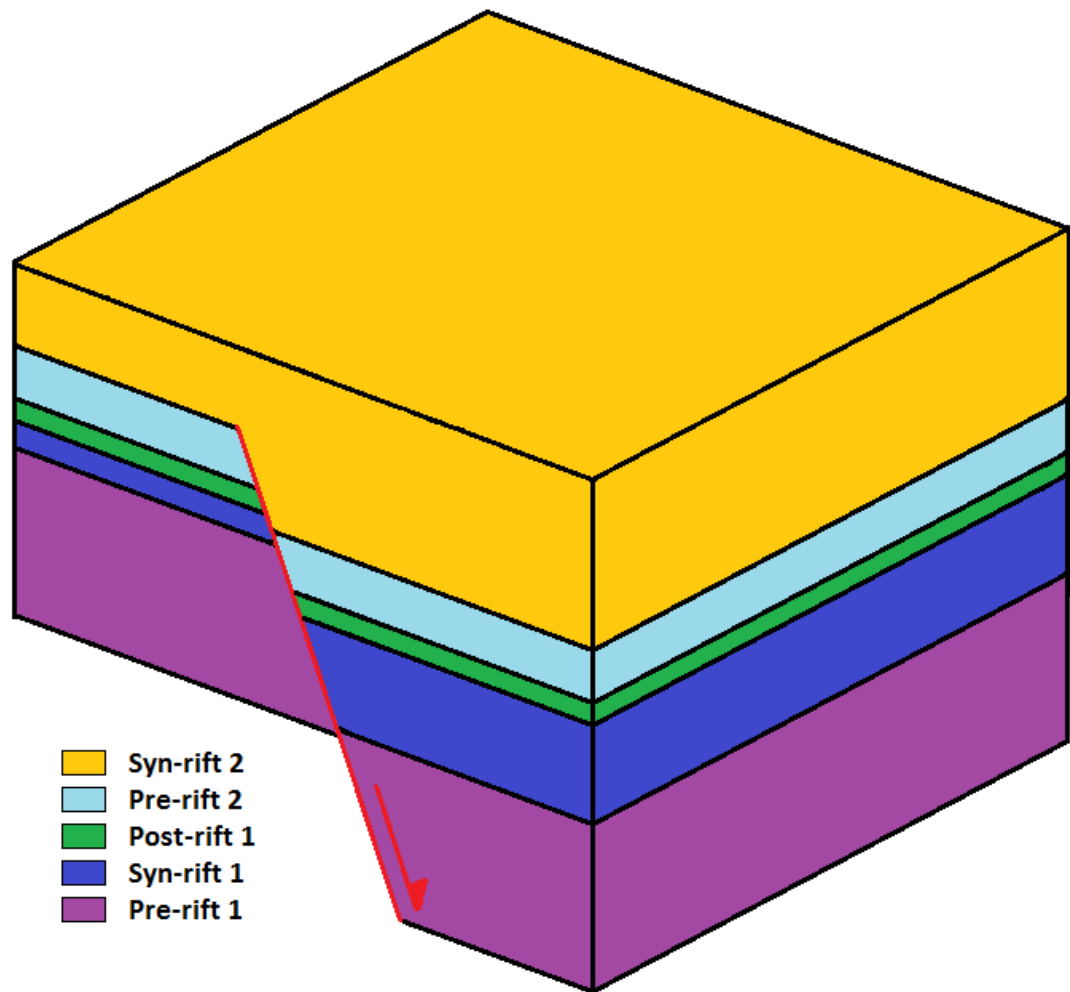


Figure 5-25. Box diagram for the structural evolution of Type 1 rifting.

The occurrence of Type 1 rifting (Figure 5-25) can be identified in the hanging wall of normal faults with a simple method. With the re-use of fault planes it should be possible to see two sets of thickening packages, with one beneath the other, separated by an intra-rift section. The intra-rift section will be composed of a combination of the post rift sediments from the initial rifting and the pre-rift sediments from the second phase of rifting. The second syn-rift package will then be covered by a thick secondary post rift section with structures relating to thermal subsidence. The identification of fault reactivation in this manner can be crucial in determining key components of a hydrocarbon system such as trap location, reservoir

distribution and hydrocarbon kitchen area location. A petroleum system issue with Type 1 fault reactivation is that the kitchen area might have been over deepened and any source rock may have been over cooked. This multi-phase rifting type can generate large laterally continuous structures as the reactivation of faults occurs along the same strike. This has been documented by Lee & Hwang (1993), who suggest that the Tern-Eider ridge could be a large structure that uses the Caledonian trend and the structure extends to the north-east into the Norwegian sector.

5.3.2 Type 2 Rifting; same fault strike, partial fault plane reactivation and opposed fault polarity.

The second type of structural configuration identified in having faults in multiple rifting events having the same fault strike, partial fault plane reactivation and opposed fault polarity. This type of rifting has been previously identified by Tomasso et al (2008), where it was possible to map out the underlying Permo-Triassic depo-centres in the footwalls of Upper Jurassic faults (Figure 5-26).

The study area between the Cormorant Field and the Brent Field lies in the southern and eastern sections of the East Shetland Basin study area (Figure 5-27). This location illustrates a series of tilted fault blocks, which form the large scale hydrocarbon fields. Between the Cormorant and Brent Fields lies the Hutton Field, this is also a footwall crest of large scale normal fault. The orientations of these faults are roughly N-S striking which associates them to the Upper Jurassic rifting event and the formation of the Viking Graben. Although the syn-rift thickening packages can be clearly observed in the Upper Jurassic Humber Group, which thicken west with the faults, an underlying thickening package can also be imaged of Permo-Triassic age,

which seem to thicken to the east. The mapping of key rifting related horizons such as the Base Syn-rift 1, Top Brent Group and the Base Cretaceous can be used to show the thickening relationship between potentially two separate rifting events.

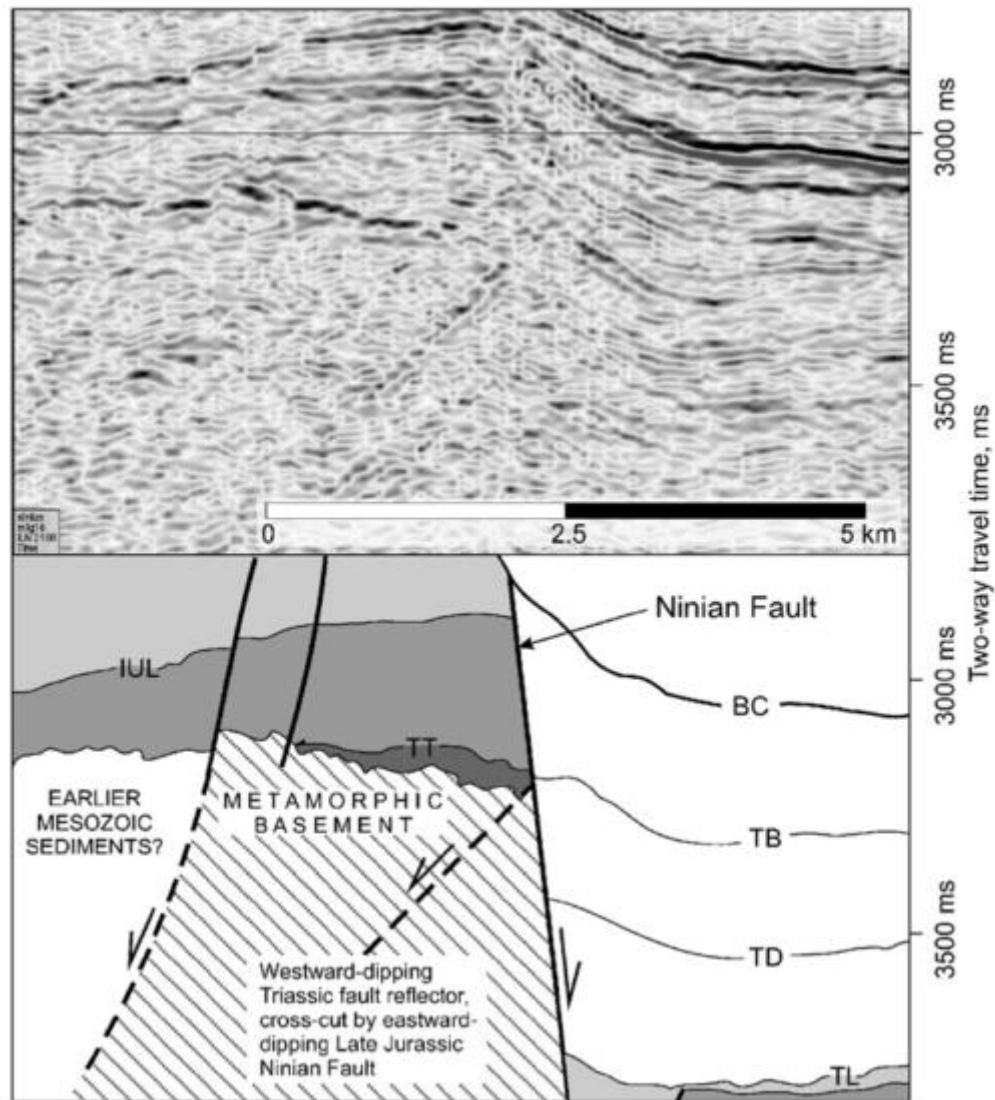


Figure 5-26 Seismic cross-section from Tomasso et al (2008) illustrating the presence of an underlying Permo-Triassic fault.

The Cormorant to Brent study area covers roughly 955Km² and used 5 separate 3D seismic surveys. Five seismic lines have been generated and tied with the used of synthetic seismograms (Figure 5-28) to best show the varying structural geology from one location to another.

The generation of well-tied arbitrary lines through these gives great insights to the evolution of the East Shetland Basin. Seismic lines 2-1 and 2-2 run perpendicular to the main structures (dip lines) and best show the effects of normal faulting. By looking at these two seismic lines, it is possible to identify large scale normal faults which penetrate deep into the subsurface. These large scale faults generate a series of tilted fault blocks which resembles books on a book shelf or dominoes on a table.

Seismic line 2-1 (Figure 5-29) is located in the southern section of the study area and runs from west to east. Throughout this seismic line, a series of easterly dipping normal faults can be observed, which creates the structural traps observed within the study area. Other features such as the eroded top of the fault blocks are observed within this section. This erosion is thought to have occurred due to the uplift associated to the footwall during rifting. In the down dip location of these footwall highs it is possible to see significant thickening packages associated to syn-rift 1, as illustrated west of the Cormorant Field. The syn-rift 2 package, however, is not as clearly observed. In the western section of the study area, the Base Syn-rift 2 horizon is defined as top Metamorphic Basement by five separate boreholes. As no wells east of the Cormorant Field penetrate the Metamorphic Basement, a marker horizon which is located at the base of the underlying syn-rift package has been interpreted. In the footwall of the Brent Field it is clear to see a significant syn-rift 2 thickening package which appears to thicken in an opposing direction to that of the current fault system. This suggests an older rift system may have been in place prior to the Upper Jurassic rifting event.

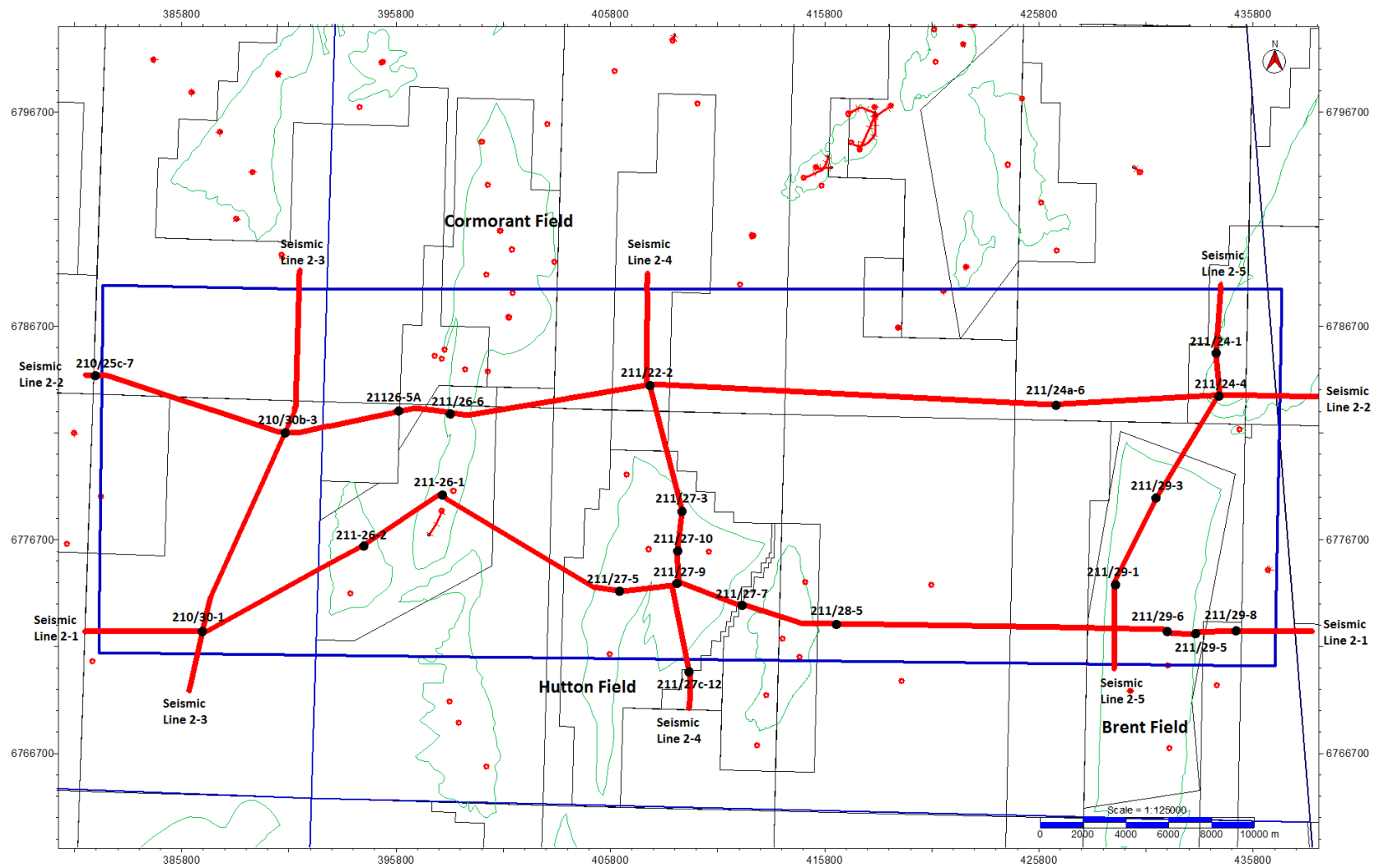


Figure 5-27 Area 2 study area and seismic lines used within this study.

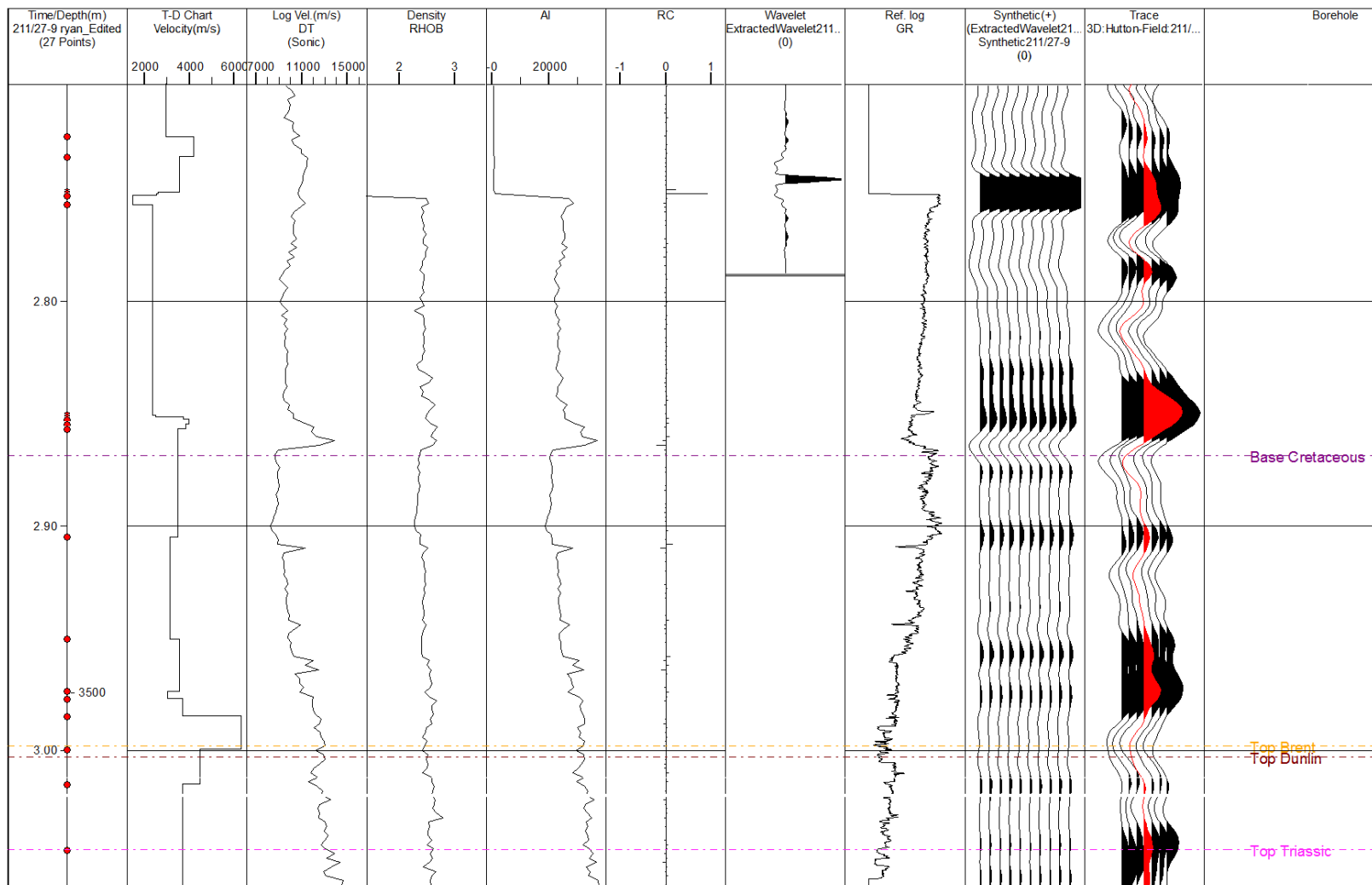


Figure 5-28 Synthetic seismogram generated for well 211/27-9.

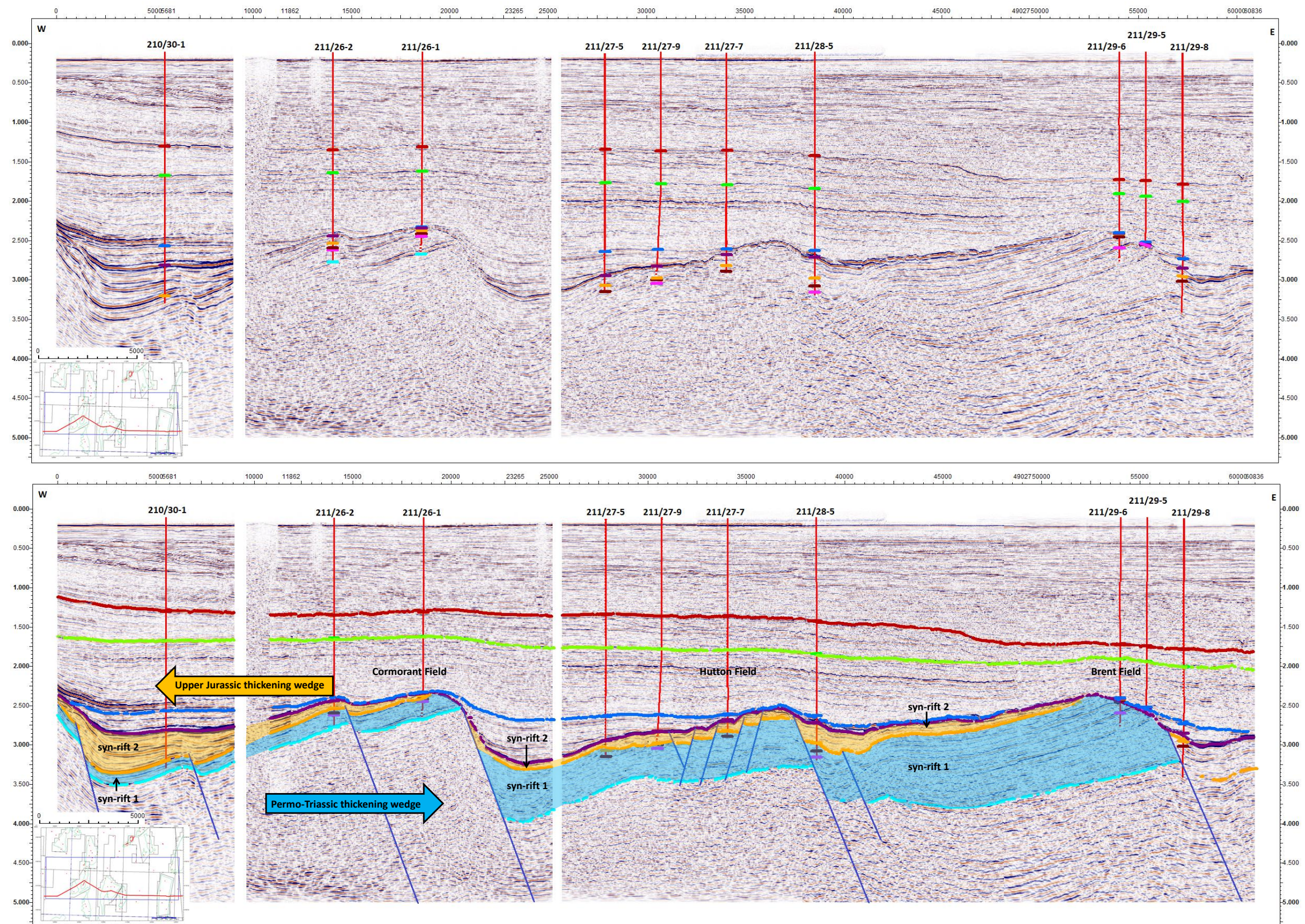


Figure 5-29. Seismic line 2-1 illustrates large scale tilted fault blocks throughout the East Shetland Basin. It is further possible to see a continual thickening of the basement pick (cyan) from west to east.

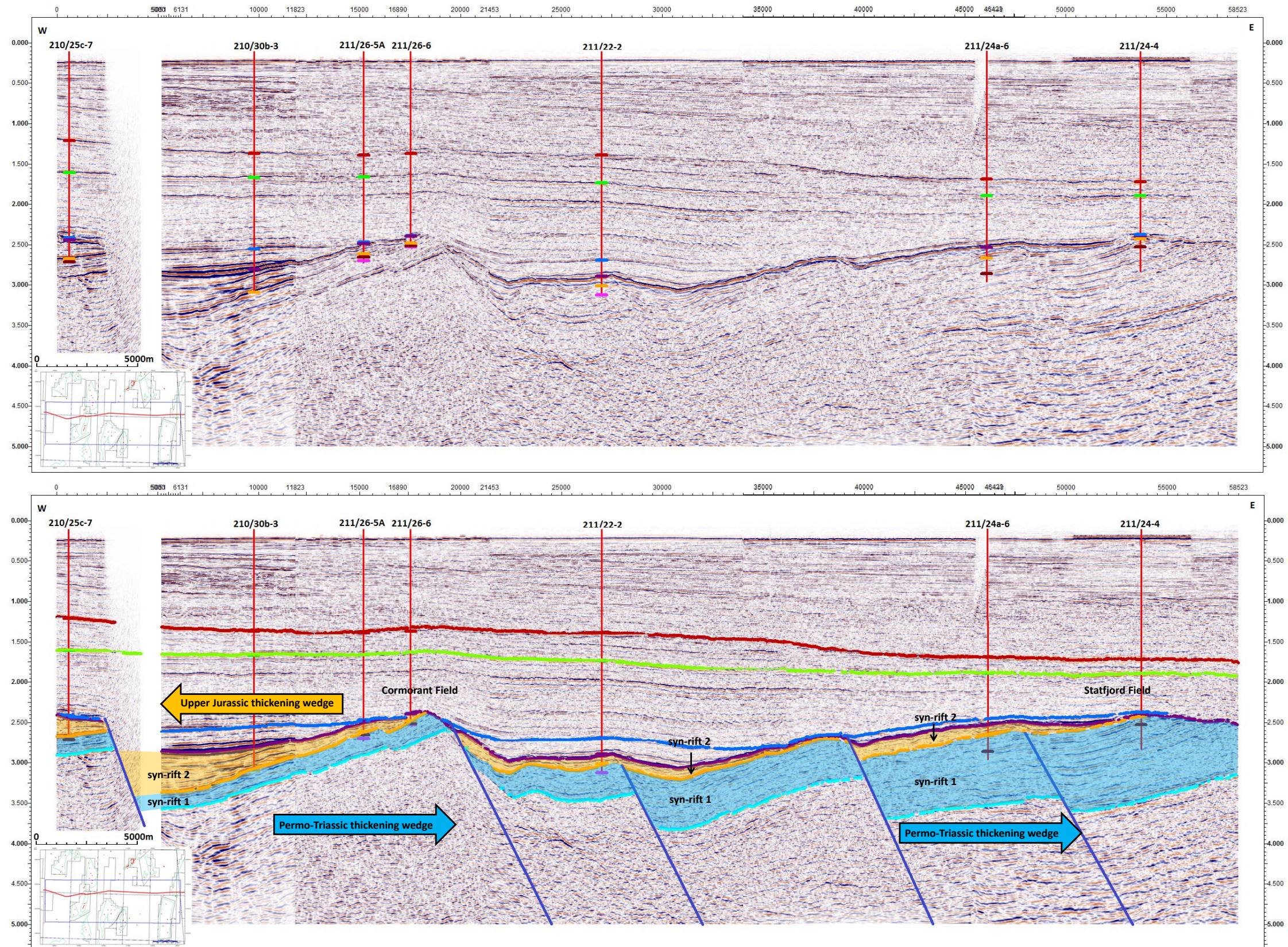


Figure 5-30. Seismic line 2-2, illustrates a thickening of Permo-Triassic sediments from west to east across the section. The thickest sections of these sediments are found in the current footwall highs relating to the Upper Jurassic rifting event.

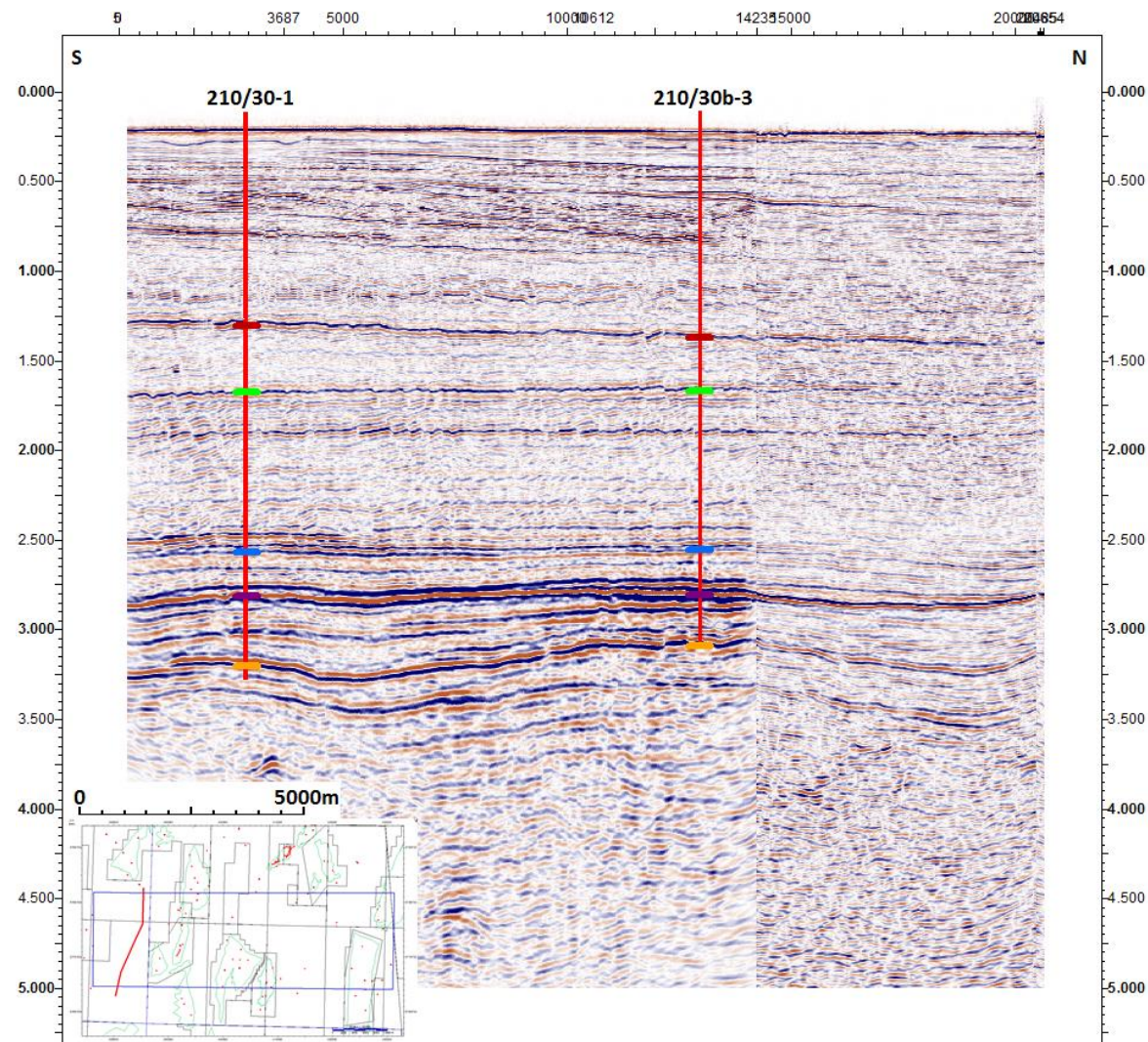


Figure 5-31 Seismic Line 2-3 is an N-S oriented line over the western section of the study area.

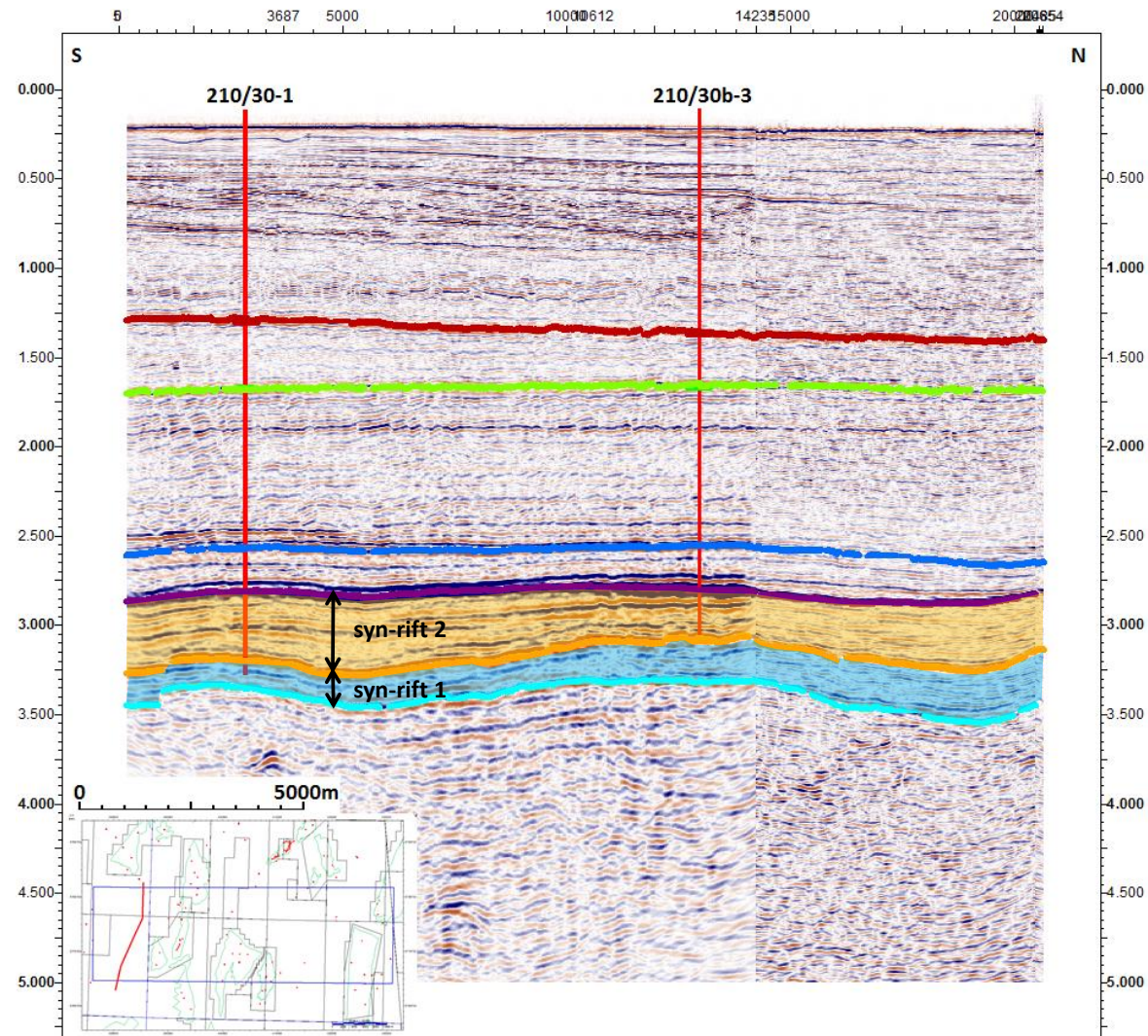


Figure 5-32 Seismic Line 2-3 illustrates a relatively thin covering of Mesozoic sediments above the Basement horizon.

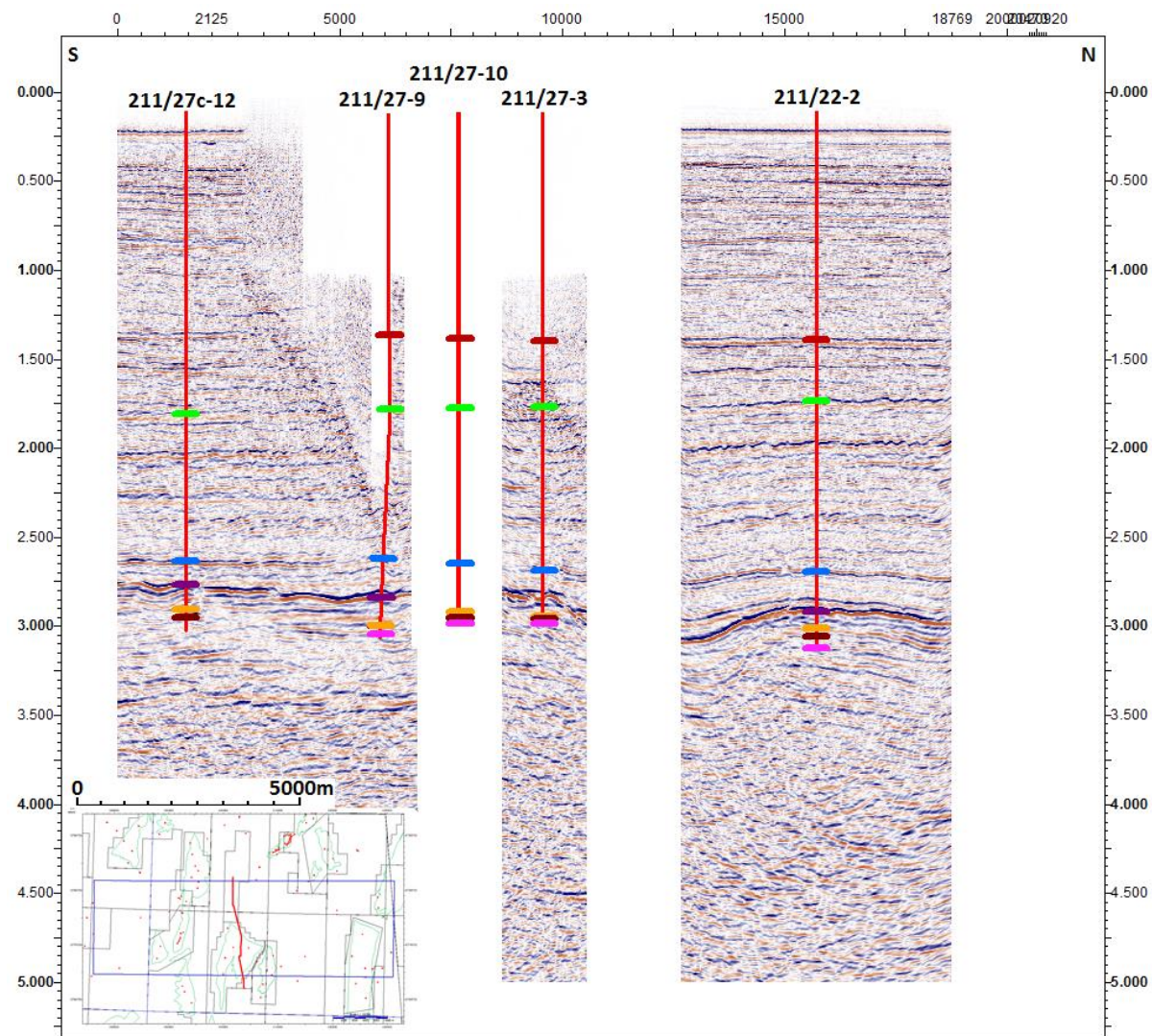


Figure 5-33 Seismic Line 2-4 is an N-S oriented line located within the centre of the study area.

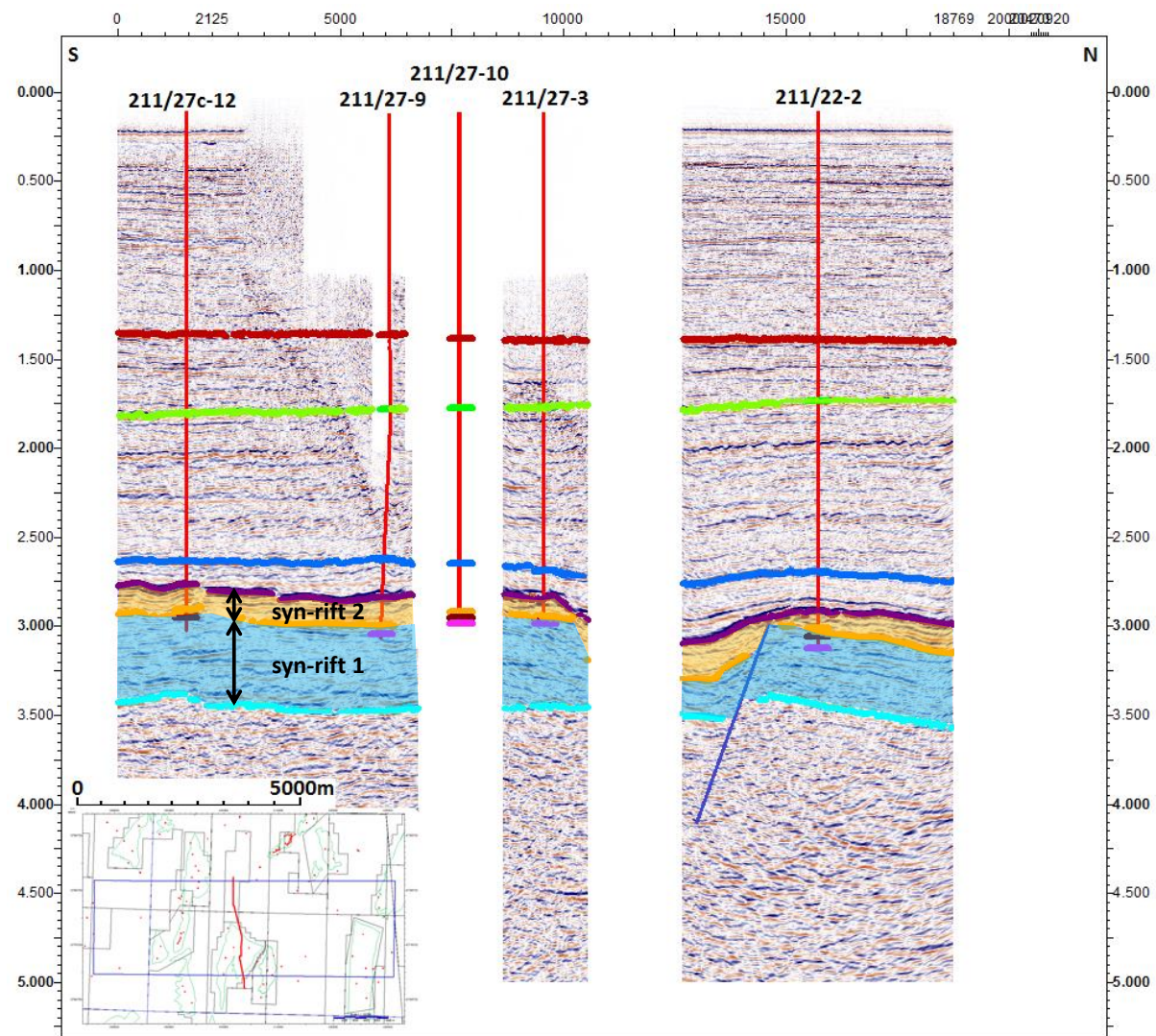


Figure 5-34 Seismic Line 2-4 illustrates an increased amount of Mesozoic sediment present above the metamorphic Basement.

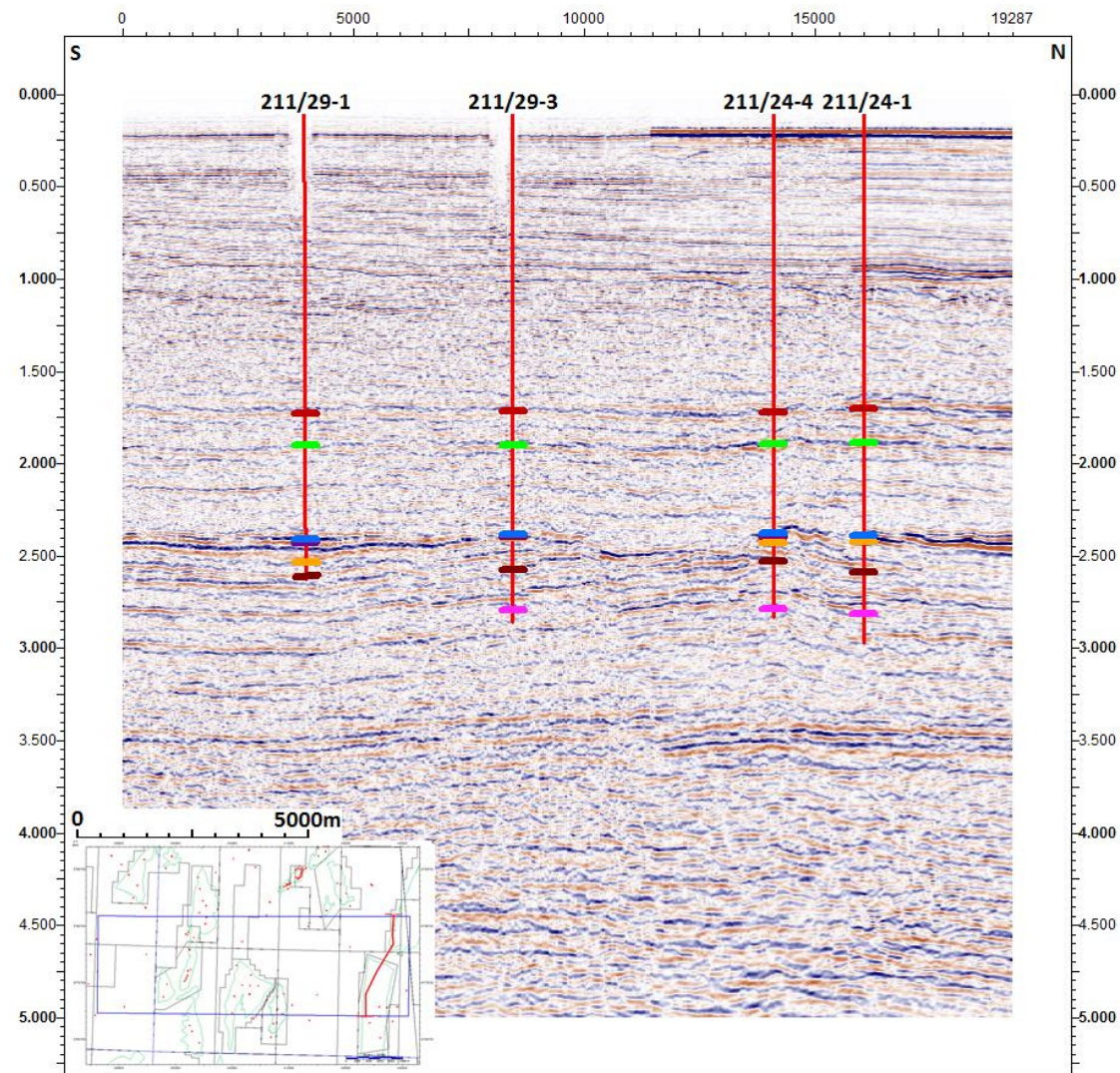


Figure 5-35 Seismic Line 2-5 is an N-S oriented line in the eastern location of the study area.

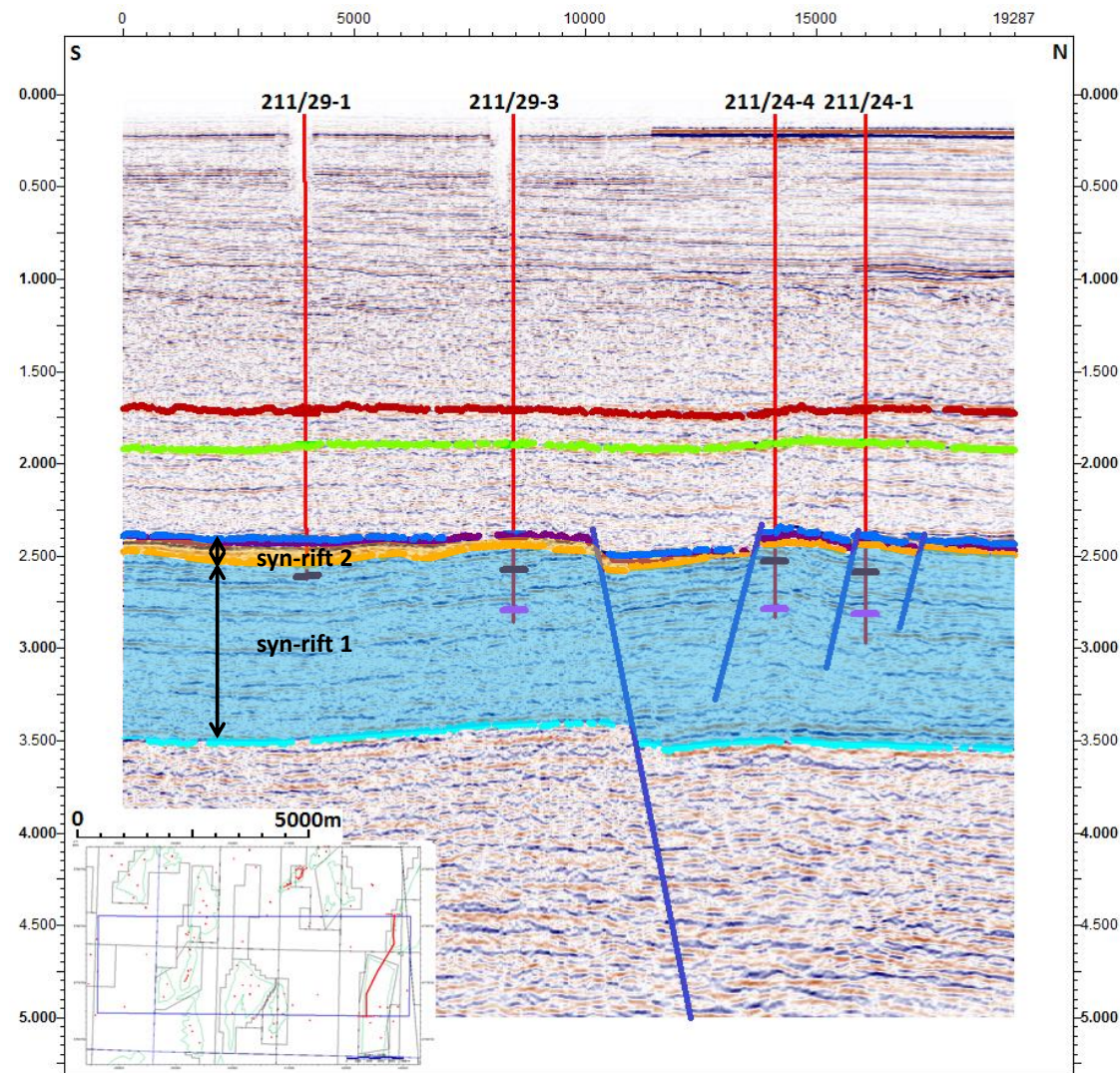


Figure 5-36 Seismic Line 2-5 illustrates the thickest section of Mesozoic sediments can be situated to the furthest east of the dataset. Here a thick covering of Triassic and Jurassic sediments are located in the footwall to a large scale Upper Jurassic normal fault

Seismic line 2-2 (Figure 5-30) also runs from west to east but is located in the northern section of the study area. This section also shows a series of easterly dipping faults relating to the Upper Jurassic rifting event, which also have the crests of their tilted fault blocks eroded away. The underlying thickening package, as noted in seismic line 2-1 appears to thicken in an opposing sense to that of the most recent rifting event. One feature that stands out here relates to the change in syn-rift 2 package thickness across the Upper Jurassic normal faults. Although this is a marker horizon, it is a distinct horizon that can be identified quite simply across faults. This would suggest that the location of the underlying faults is very similar to that of the Upper Jurassic rifting event.

Seismic lines 2-3, 2-4 and 2-5 are drawn parallel to the main structures and give snap shots in to the thickness variations from east to west. The aim of the three strike lines is to illustrate the delicate variations within sediment thickness between the two syn-rift packages from west to east.

Seismic line 2-3 (Figure 5-31 and 32) is located down dip of the Cormorant Field and is furthest west of the three strike lines. This seismic line illustrates an extremely thin syn-rift 1 package which is between the top Brent Group and the Gneissose Metamorphic Basement which underpins the East Shetland Basin. As this location is in the hangingwall to an Upper Jurassic fault it does show a significantly thick syn-rift 2 package, which consists of the Upper Jurassic Humber Group sediments.

Seismic line 2-4 (Figure 5-33 and 34) runs from south to north and is located over the Hutton Field, which is located in the centre of the study area. Within this seismic section a pair of Upper Jurassic faults are found which create a small scale graben feature. The southernmost fault is the bounding edge of the Hutton Field and defines the hydrocarbon field. It is also

possible to see an increased thickness within the syn-rift 1 package between the Brent Group and the Base-syn-rift 2 horizon. This is coupled with a thin covering of Humber Group sediments over the Upper Jurassic structural high. The pairing of the old-thick and new-thin syn-rift packages suggests that this location could have once been a hangingwall location in an initial rifting event, then a structural high in a second rifting event.

Seismic line 2-5 (Figure 5-35 and 36) is furthest east of the three south - north strike lines. As observed in seismic line 2-4 a series of normal faults can be identified that define the limits of hydrocarbon fields, in this case the southern section of the line covers the Brent Field and the north passes through the southern tip of the Statfjord Field. More similarities to section 2-4 are observed with the thick syn-rift 1 package and the thin syn-rift 1 package. As in the previous seismic line, this is the location of an extinct Permo-Triassic depo-centre that has been transformed into a structural high in the Upper Jurassic rifting event.

Although these seismic lines are a great insight into the underlying nature of subsurface, the generation of top structure maps and isochron maps will be make it possible to further identify the underlying nature of a multi-rift system.

Although a clear representation of the normal faults can be observed in the seismic sections, a more subtle review of the structural geology can be observed in the top structure maps generated for the selected horizons (Base Cretaceous, Top Brent Group and Top Basement). As all three structure maps adhere to the most recent rifting event, they are dominated by Upper Jurassic normal faulting. Although the three maps may appear are very similar at first, there are subtle differences that can be identified from map to map.

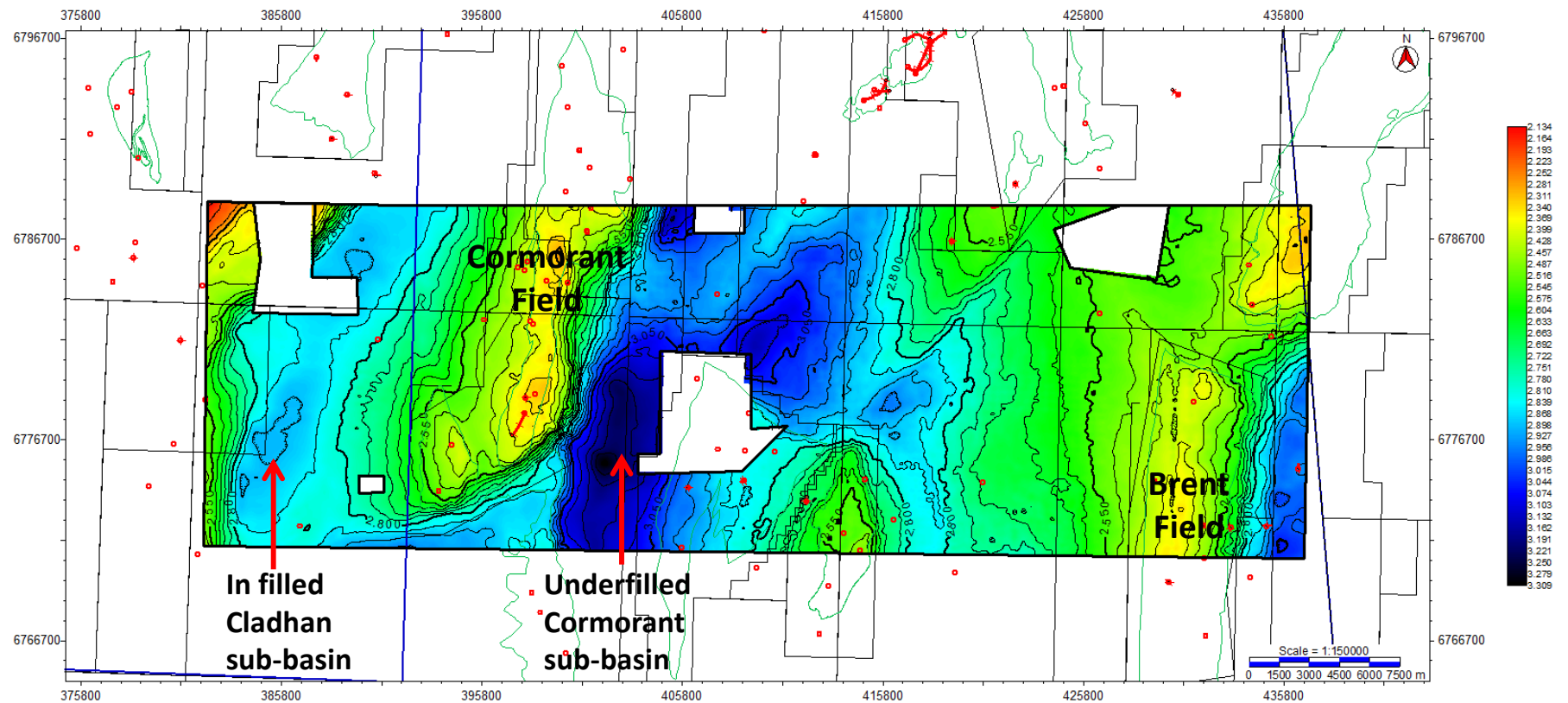


Figure 5-37. Top Base Cretaceous top structure map.

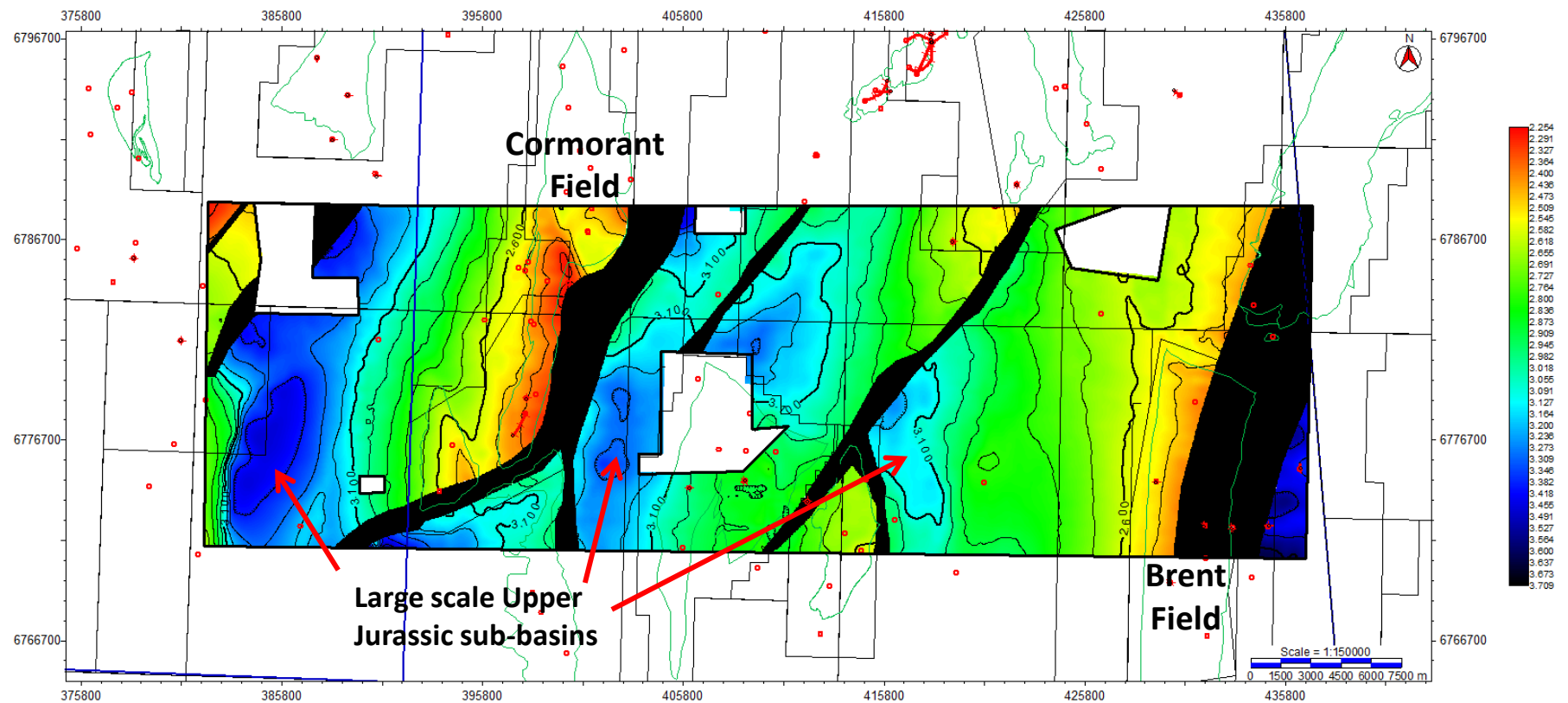


Figure 5-38. Top Brent Group structure map illustrating significant structural highs and lows from the Upper Jurassic rifting event.

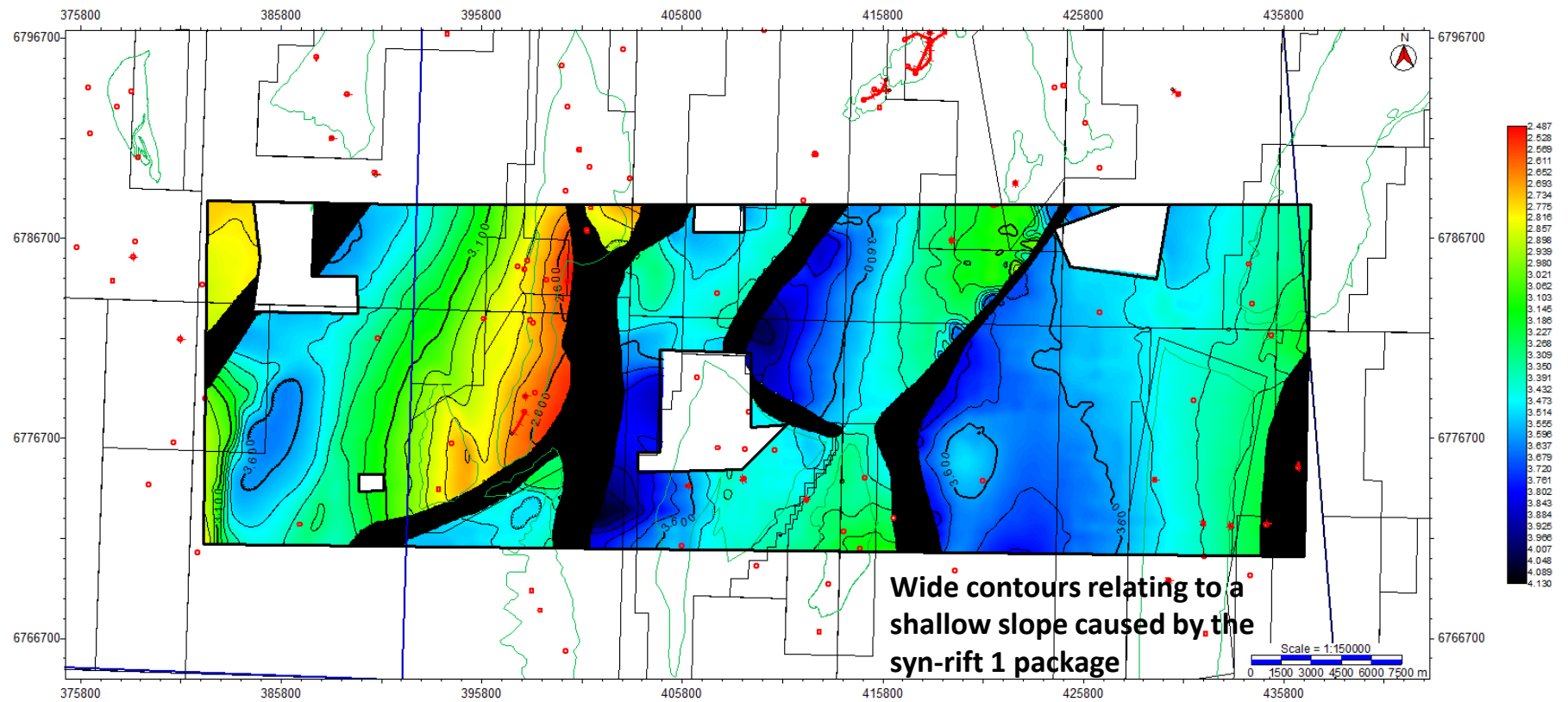


Figure 5-39. Top Permo-Triassic structure map.

The Base Cretaceous top structure map (Figure 5-37) is the top of syn-rift 2 package and shows evidence of the significant depo-centres that were created in the Upper Jurassic, which were still evident prior to the Cretaceous infill stage. Here major highs such as Cormorant, Hutton and Brent Fields are highlighted and all have a strong N-S lineament. It is possible to see that the Cladhan area west of the Cormorant Field has a relatively flat nature which suggests it is relatively infilled compared to the east of the Cormorant Field. This is further supported by Seismic line 2-1 which shows the infilled nature of the western depo-centre.

The Top Brent (Figure 5-38) structure map illustrates three significant structural highs. This relates to the three tilted fault blocks that make up this study area. Here the depo-centre that is infilled in the Cladhan area on the Base Cretaceous Unconformity map is clearly illustrated. In this map, the top Brent Group illustrates fairly constant contour spacing that is quite tightly spaced in the footwall of the normal fault. This would suggest an increased incline which is directly related to the Upper Jurassic rifting event. However, this is not seen in the Base Syn-rift 1 map.

The Base syn-rift 1 map (Figure 5-39) has a wider contour spacing especially over the Brent Field, where the greatest thickness of potential Permo-Triassic sediments is located. This shallower dip of the Base Syn-rift 2 horizon suggests that it is affected by a separate event. If it was all a part of the Upper Jurassic event it would have a similar contour spacing. The idea that it is related to a separate event is supported in seismic line 2-1 and 2-2 where the Base Syn-rift 1 horizon is less steep than that of the Upper Jurassic as it was over-deepened by being a subsiding hangingwall low location in the initial Permo-Triassic rift compared to an uplifted structural high in the Upper Jurassic rift.

As any underlying rifting event has been overwritten in the Upper Jurassic, the only way to identify these relic structures are thickness maps between the two sets of rift related sediments. As noted in Figure 5-3, each rifting event has its own set of pre-syn and post-rift sediments. By mapping out the syn-rift isochron maps for each rifting event makes it possible to identify the role of underlying faults that can no longer be imaged.

Having analysed the top structure maps, it is clear to see that the Upper Jurassic faults have generated a series of depo-centres which should thicken towards the fault in a westerly direction; this is also observed in seismic lines 2-1 and 2-2, where the Upper Jurassic Humber Group sediments thicken towards the faults. The overall time thickness map (Figure 5-40) which is generated between the BCU and Base Syn-rift 2 horizon on the other hand contradicts this assumption. The thickest sediments are found in the Brent Field location and thinnest sediments by the Cormorant Field. However, a series of smaller depo-centres are located to the far west of the dataset which seems to conform to the initial Upper Jurassic rifting model. Upon analysis of the syn-rift 1 (Brent Group to Base Syn-rift 1) sediment package (Figure 5-41) it is clear to see why this irregularity occurs. It must also be noted that the extremely thin sediment section located over the Cormorant Field is related to the erosion of Upper Jurassic sediments during the rifting event, which has caused an over thinning in this area. The general pattern that is observed in the syn-rift 1 is a general thickening package from west to east suggesting a separate set of older faults that control the sediment thickness patterns in the Permo-Triassic. This would explain the thickening trends that are observed throughout the seismic sections and top structure maps. The syn-rift 2 package (BCU to Top Brent Group) shown in Figure 5-42 on the other hand is only affected by the Upper Jurassic rifting event and illustrates a thin covering of sediments over the structural highs such as the Cormorant Field and thick sediments in the opposing hangingwalls.

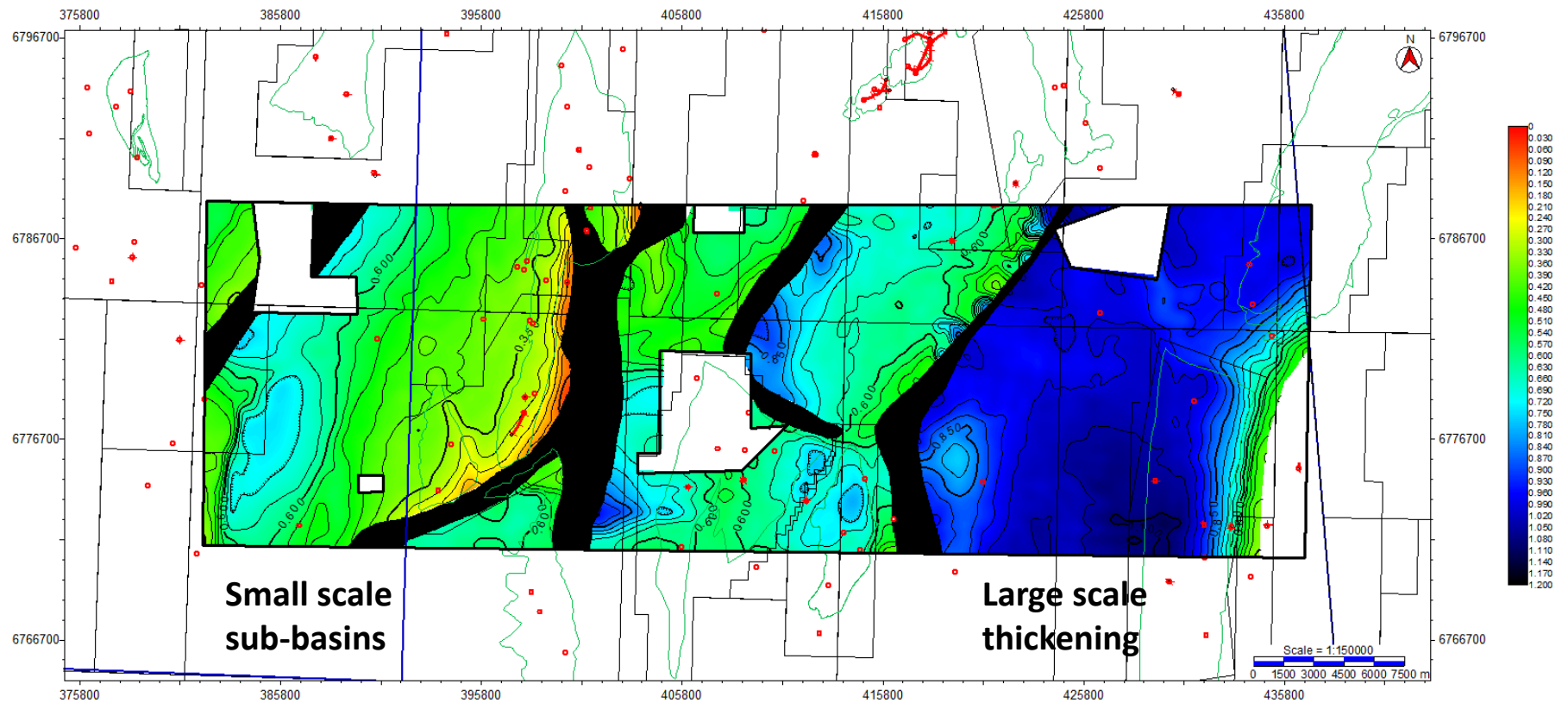


Figure 5-40. Complete thickness isochron from BCU to Permo-Triassic illustrating a significant thickness in the tectonostratigraphic megasequence package under the Brent Field.

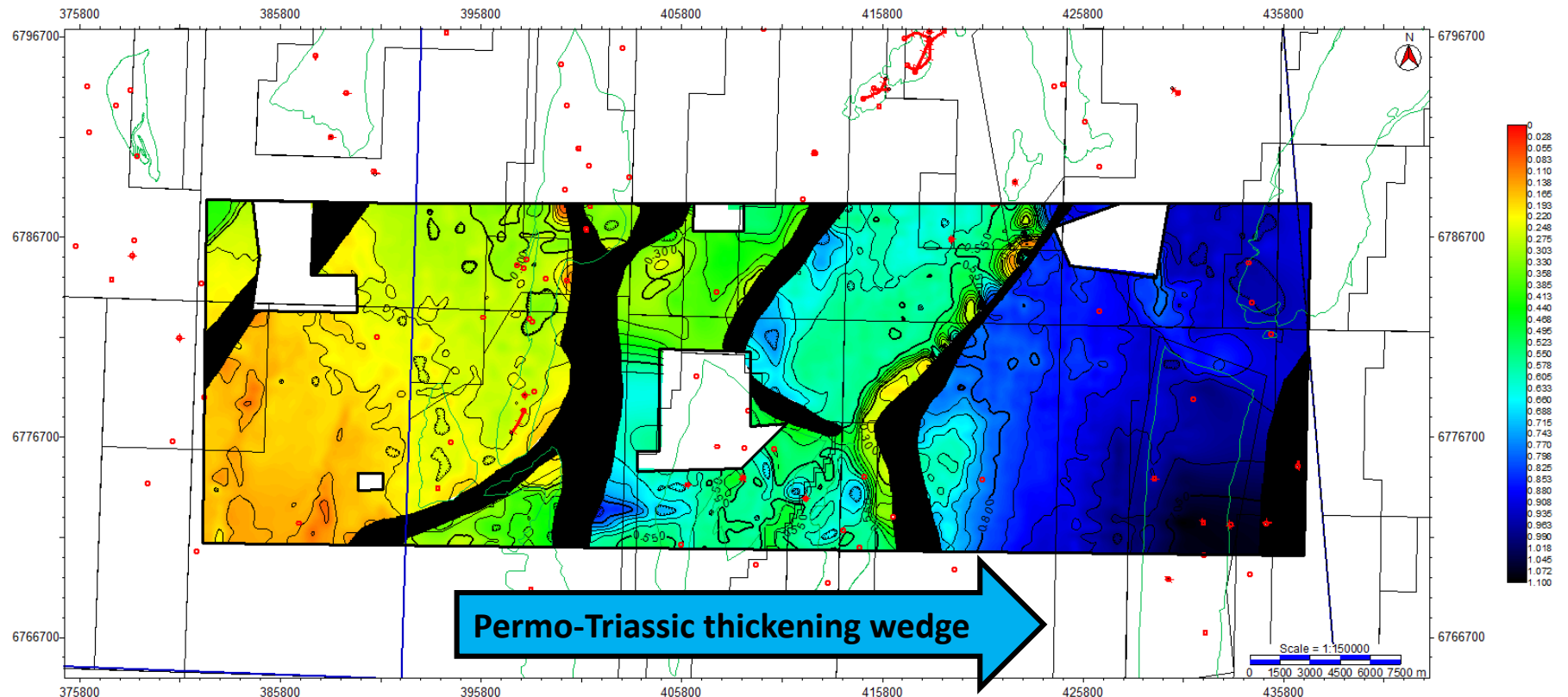


Figure 5-41. Top Brent Group to Top Permo-Triassic isochron map illustrates an easterly thickening wedge.

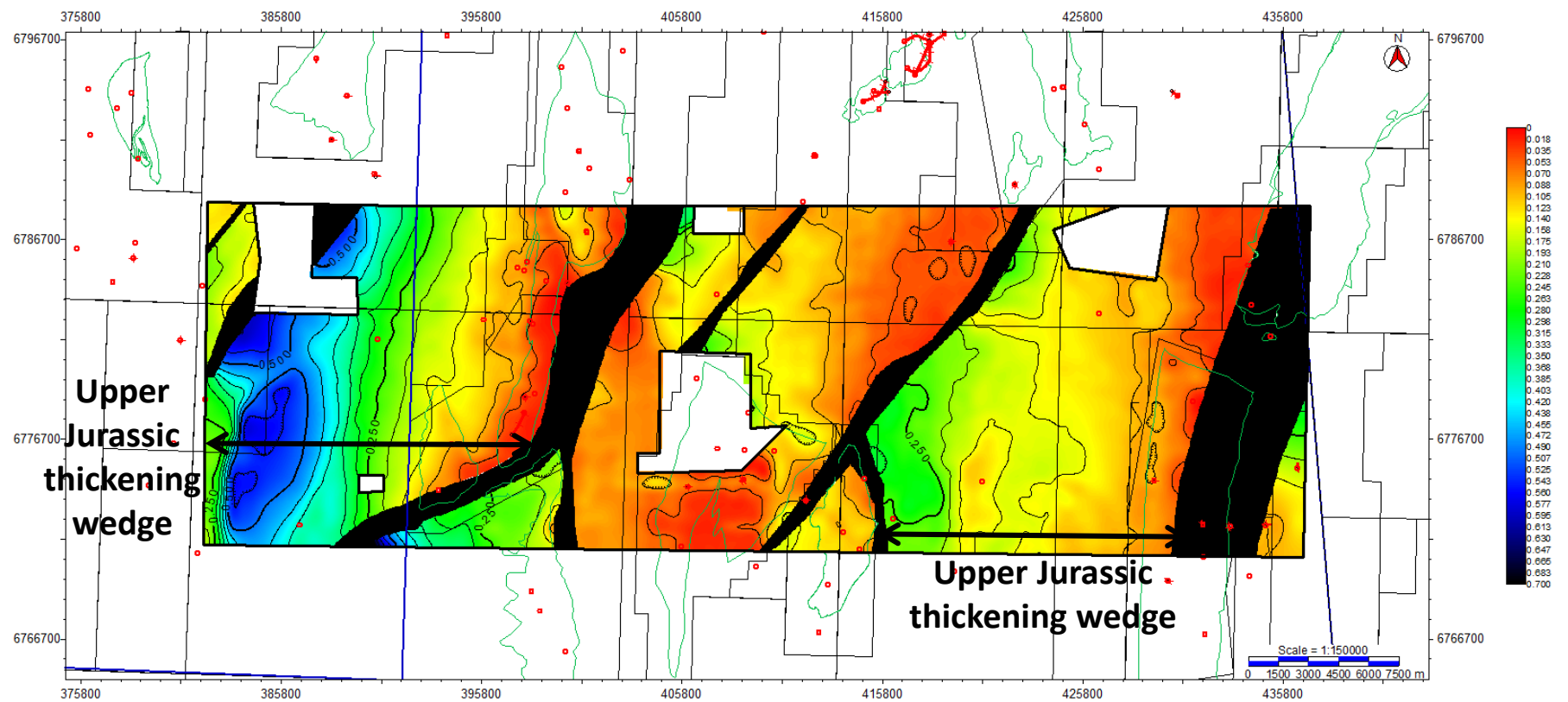
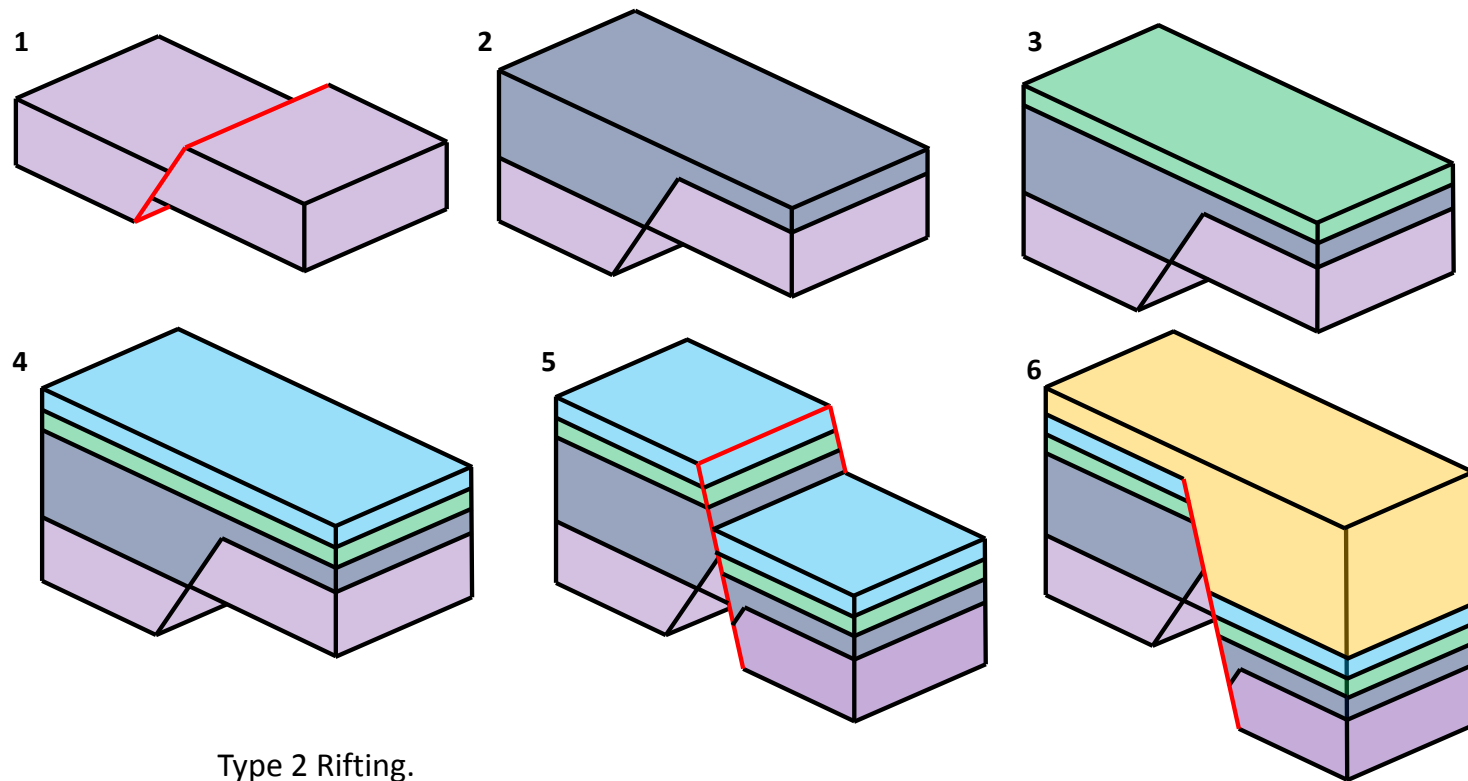


Figure 5-42. Top BCU to Top Brent Group isochron map shows westerly thickening wedges of the Upper Jurassic (Syn-Rift 2) sequences.

This is clearly seen in the Cladhan area in the west, where a series of N-S oriented depo-centres are located down-dip of the Cormorant Field bounding fault. By comparing the syn-rift 1 and syn-rift 2 packages in this location, a stark contrast in thickening direction is highlighted. In the Permo-Triassic the general thickening trend is to the west, whereas in the Upper Jurassic it is to the east. This switch in orientation of thickening sediments can be related directly to the orientation and polarity (dip) of normal faults during separate rifting events. As noted earlier any Permo-Triassic faults may be almost impossible to detect as they are completely overwritten by the Upper Jurassic rifting event. Unlike the Tern-Eider Ridge area, the old Permo-Triassic faults are not reactivated as such but the old liniments still have an important role to play.

Previous work by Tomasso et al. (2008) showed that in the Ninian and Alwyn North Fields, which are directly to the south of this study area, have older Permo-Triassic sediments which exhibit an east to west thickening pattern into old Permo-Triassic faults. In both areas it is extremely difficult to identify the exact location of the initial faults except in the Ninian Horst where the original westerly dipping Permo-Triassic fault plane was identified (Figure 5-26). It is most likely that the initial faults are in the same location of the later Upper Jurassic faults. By analysing the Triassic sediments found in the wells Tomasso et al. (2008) were able to identify Permo-Triassic highs and the conglomerate rich associated to high levels of erosion, as well as the fine grained mudstones located down-dip in ancient depo-centres associated to the Permo-Triassic rifting event.



Type 2 Rifting.

1. Permo-Triassic faulting
2. Triassic Sedimentation
3. Early Jurassic Sedimentation
4. Middle Jurassic Sedimentation
5. Upper Jurassic Faulting
6. Cretaceous Sedimentation

pre-rift 1
syn-rift 1
post-rift 1
pre-rift 2
syn-rift 2
post-rift 2

Figure 5-43. Schematic illustration of the evolution of Type two multiphase rifting.

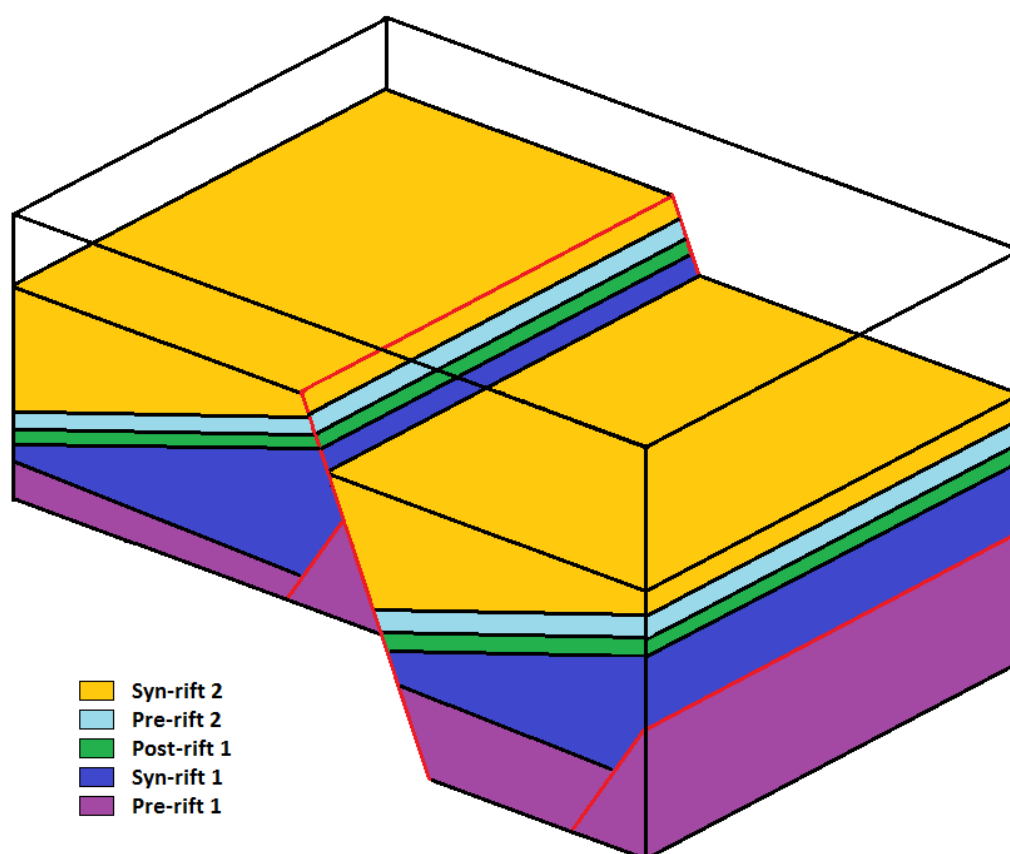


Figure 5-44. Box diagram for the structural evolution of Type 2 rifting.

The initial westerly dipping normal faults in the Permo-Triassic although they are of a different polarity to that of the Upper Jurassic faults will leave lineaments of weakness for the younger sediments to exploit in a future rifting event. Thus, during the Upper Jurassic rifting event the N-S weakness relic lineaments were identified and utilised in generating a series of easterly dipping normal faults. It is generally accepted that the Upper Jurassic rifting event was of a greater magnitude than that of the Permo-Triassic rifting event. This would have destroyed any trace of the underlying faults, meaning only the syn-rift packages are left to identify the initial fault location of orientation.

Due to the thick post rift successions of the North Sea in the Cretaceous and Tertiary, the initial Permo-Triassic faults are now buried at depths of some 4-

5 seconds deep in the seismic sections making interpretation of any remnant structures extremely difficult. As imaging is reduced in the deepest sections of seismic data, accompany this with the complex overwriting of structural lineaments the Permo-Triassic faults may be almost impossible to identify within seismic data. But, the structural trend generated by the initial Triassic rifting event has influenced the location of the Upper Jurassic faults but not the polarity of the faults. It appears that the Triassic faults in this study area tip out vertically in the Lower Jurassic sediments. When the second phase of rifting is initiated these weakness trends are then utilised even if they are in an opposed direction of throw. This rifting and Type 1 rifting both lead themselves to vertical relay ramping of normal fault. Type 1 is pure vertical relay-ramping of two normal faults, whereas; Type 2 rifting uses the underlying weakness trends as a guideline to where new faults nucleate and grow in three dimensions.

The overall pattern of structural feedback that can be identified in the Cormorant to Brent area is that faulting between the two rifting events have the same fault strike (N-S), opposed fault polarity (Permo-Triassic westerly dipping and Upper Jurassic easterly dipping) with some re-use of the original fault plane, which identifies this as a separate rifting type (Type 2 rifting) to that explained earlier in the Tern-Eider Ridge location. This location has a similar structural feedback to that of Type 1 rifting apart from the polarity of the second phase of faults. This rifting type shows that both sets of rifting have the same fault strike and there is some re-use of fault planes from the initial rifting phase but not to the same extent as that in the TER. The evidence from the Cormorant to Brent Fields illustrates significant Triassic depo-centres located under the footwalls of Upper Jurassic normal faults. The structural evolution of Type 2 rifting is influenced by the initial underlying rift and the structural lineation generated by the Triassic rifting.

This style of multi-phase rifting (Figure 5-43 and Figure 5-44) can also form laterally continuous features as seen in the Cormorant and Brent Fields, where large Upper Jurassic structures have formed over underlying depocentres. The effect this rifting has on the petroleum system is that reservoir quality is a function of position in a half graben environment which is highly contrasting between Triassic and Brent Group.

5.3.3 Type 3 Rifting; oblique fault strike, partial fault plane reactivation and variable fault polarity

The Pobie Platform area is located to the SW of the Tern-Eider Ridge and directly to the west of the Cormorant Field (Figure 5-45). The study undertaken within this area allows the remnants of the NE-SW Caledonian faults to be observed along with the N-S oriented Upper Jurassic normal faults where they emerge from the ESB and transect the neighbouring platform area. This study area shows the interaction and reactivation of these two fault lineaments and the potential structures that form by multi-phase rifting.

This study area is roughly 375Km² and is covered by two 3D seismic volumes and calibrated by 17 boreholes. Within the study area, three seismic sections have been generated and well tied by synthetic seismograms (Figure 5-46) to illustrate the structures created in this area. As this area is obliquely cross cut by multiple rifting events it is difficult to identify dip and strike lines, so three arbitrary seismic lines have been generated to best show the evolution of the Pobie Platform area.

All three seismic lines run from the NW to SE and are termed dip lines as they run perpendicular to the underlying Caledonian orientation and oblique to the Upper Jurassic rifting event. Seismic line 3-1 (Figure 5-47 and 5-48) is

located across the southern part of the study area and illustrates a structural high known as the Pobie Platform. This Pobie Platform has one well (210/29a-3) that penetrates the structure and encounters Gneissose Basement at 850m. The Pobie Platform is the western limit of the East Shetland Basin. The fault that makes up the east limit of the structural feature is the western rift shoulder of the East Shetland Basin. A half graben can be observed to the west of the Pobie Platform which represents the Unst Basin. The sediment cover over the Pobie Platform is relatively thin, but a full Brent Group is recorded which suggests that the structural high was not in place prior to the Upper Jurassic rifting event. Over the Pobie Platform, no Cretaceous sediments are found; they have either been deposited then eroded away or were never deposited over the structural high in the Cretaceous. The Upper Jurassic normal faults that are identified in the south-easterly section of the seismic line relate to terrace areas which form within the East Shetland Basin.

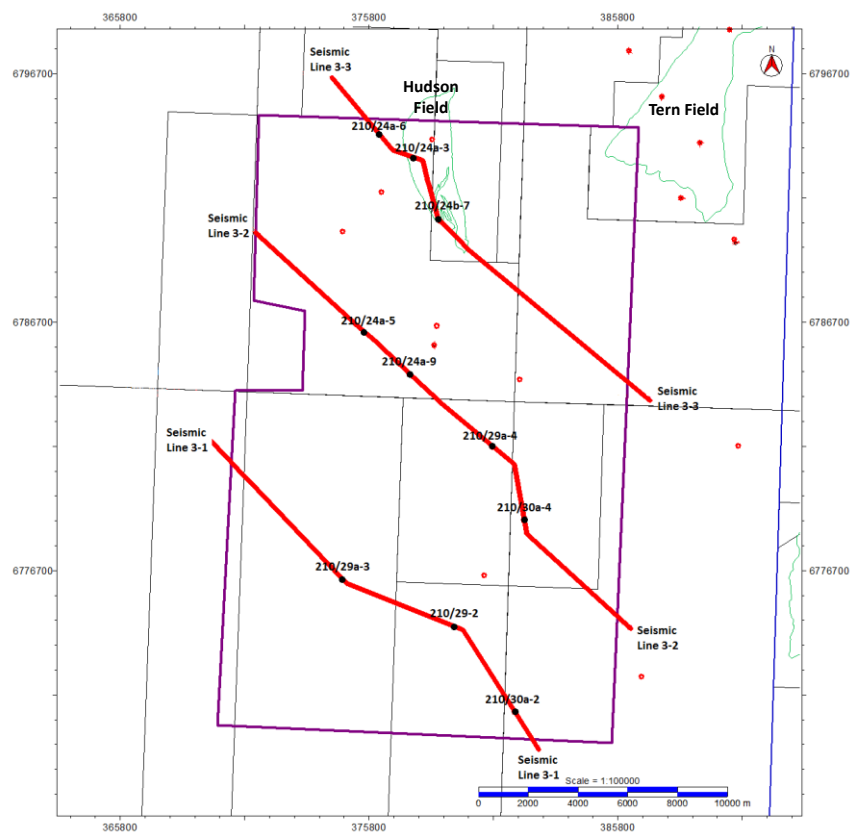


Figure 5-45. Study area 3 outline and orientation of seismic lines used in the study.

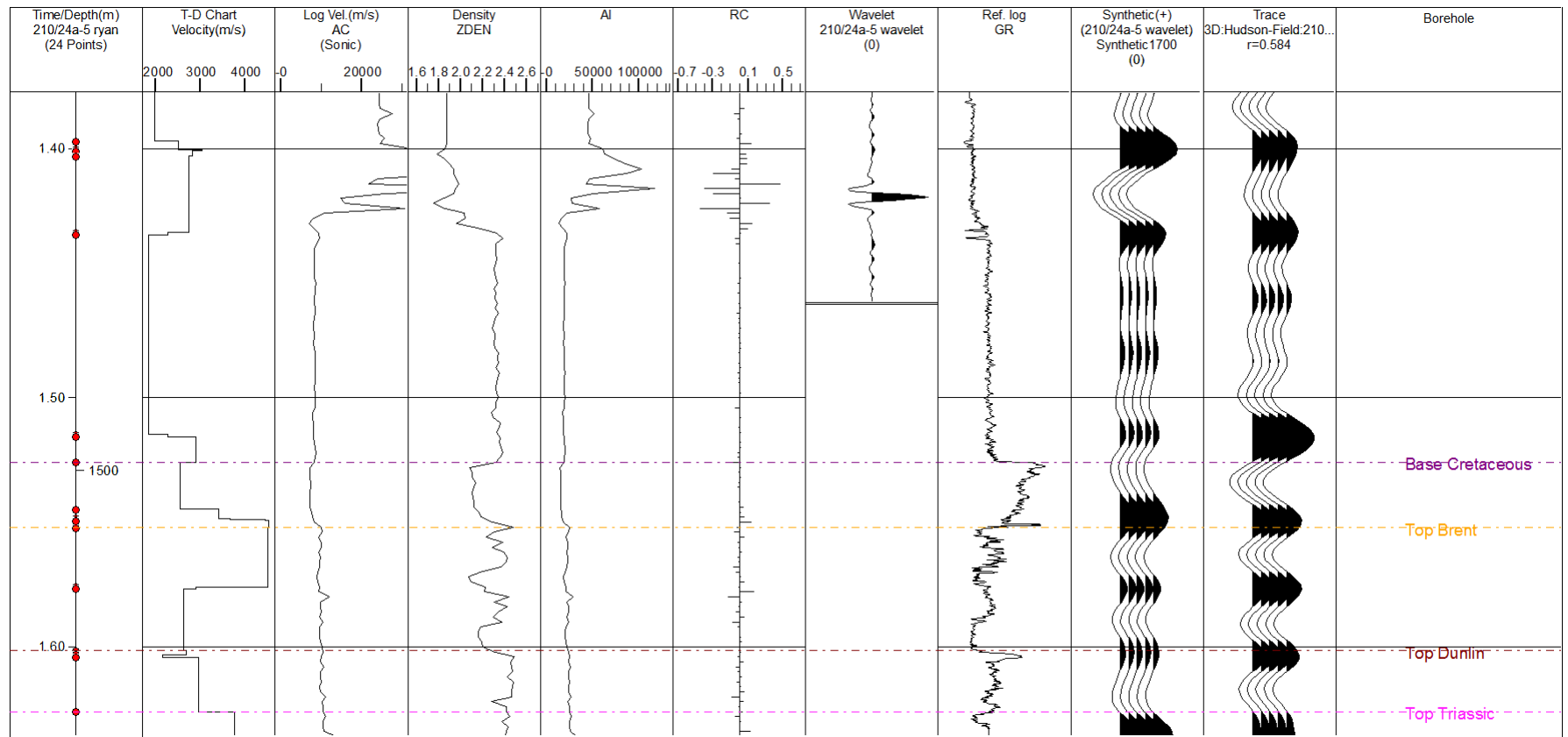


Figure 5-46 synthetic seismogram for well 210/24a-5

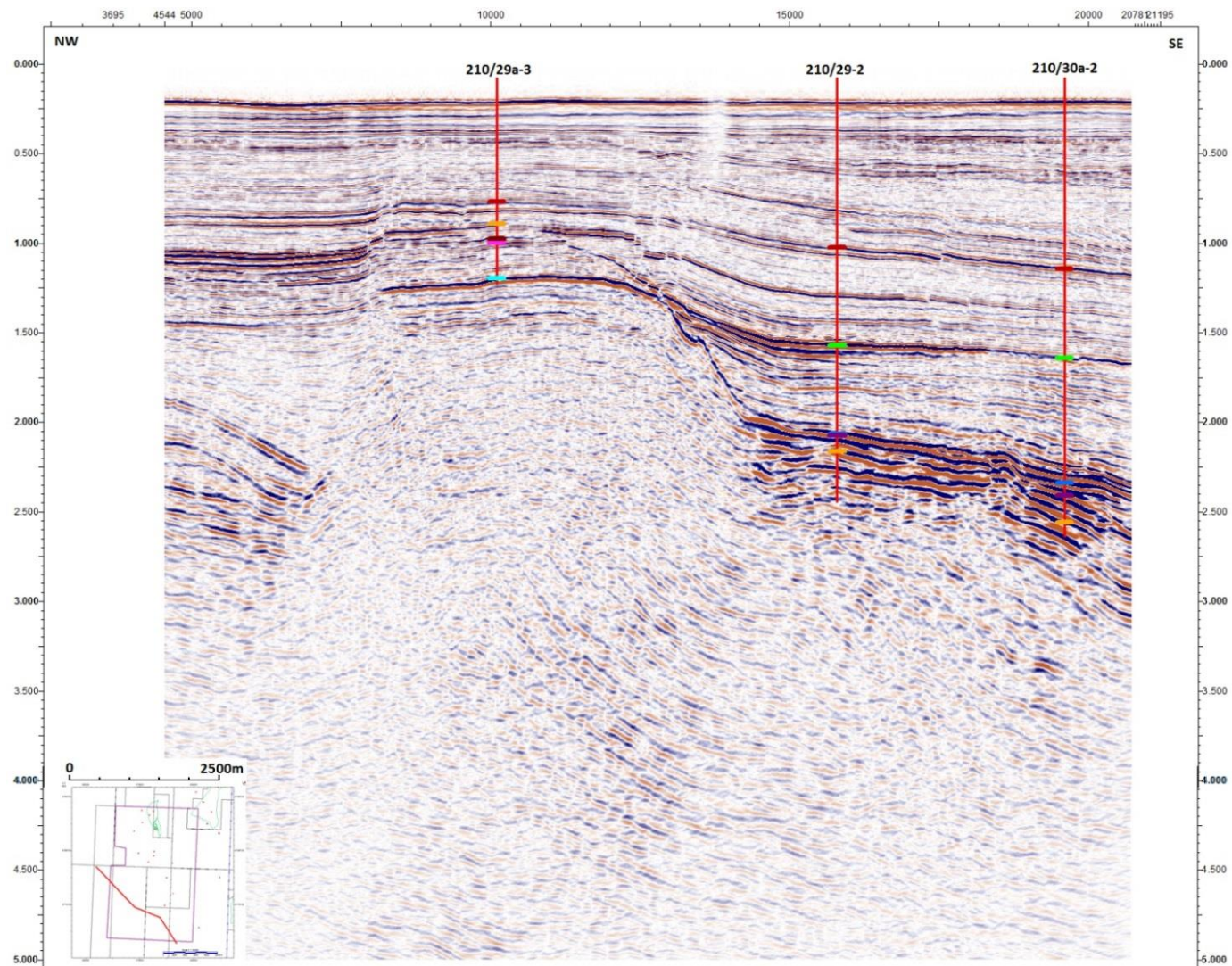


Figure 5-47 Seismic Line 3-1 is the furthest south of the three seismic lines, here the Pobie Platform can be imaged along with the terrace areas to the NE and SW.

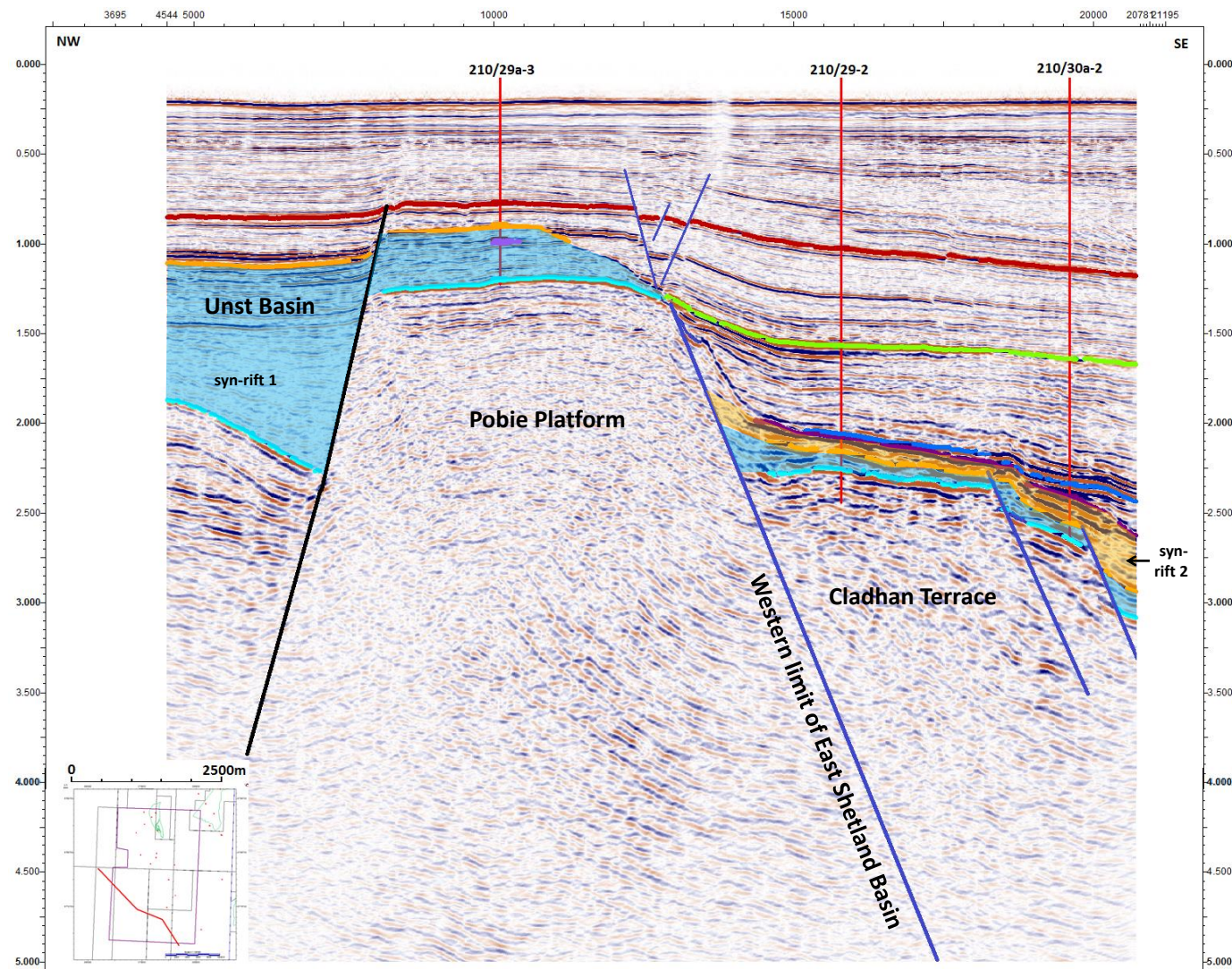


Figure 5-48 Seismic Line 3-1
the reactivation of the old
Caledonian trending Pobie
Fault can be observed
although it is in the footwall to
the Upper Jurassic normal
fault

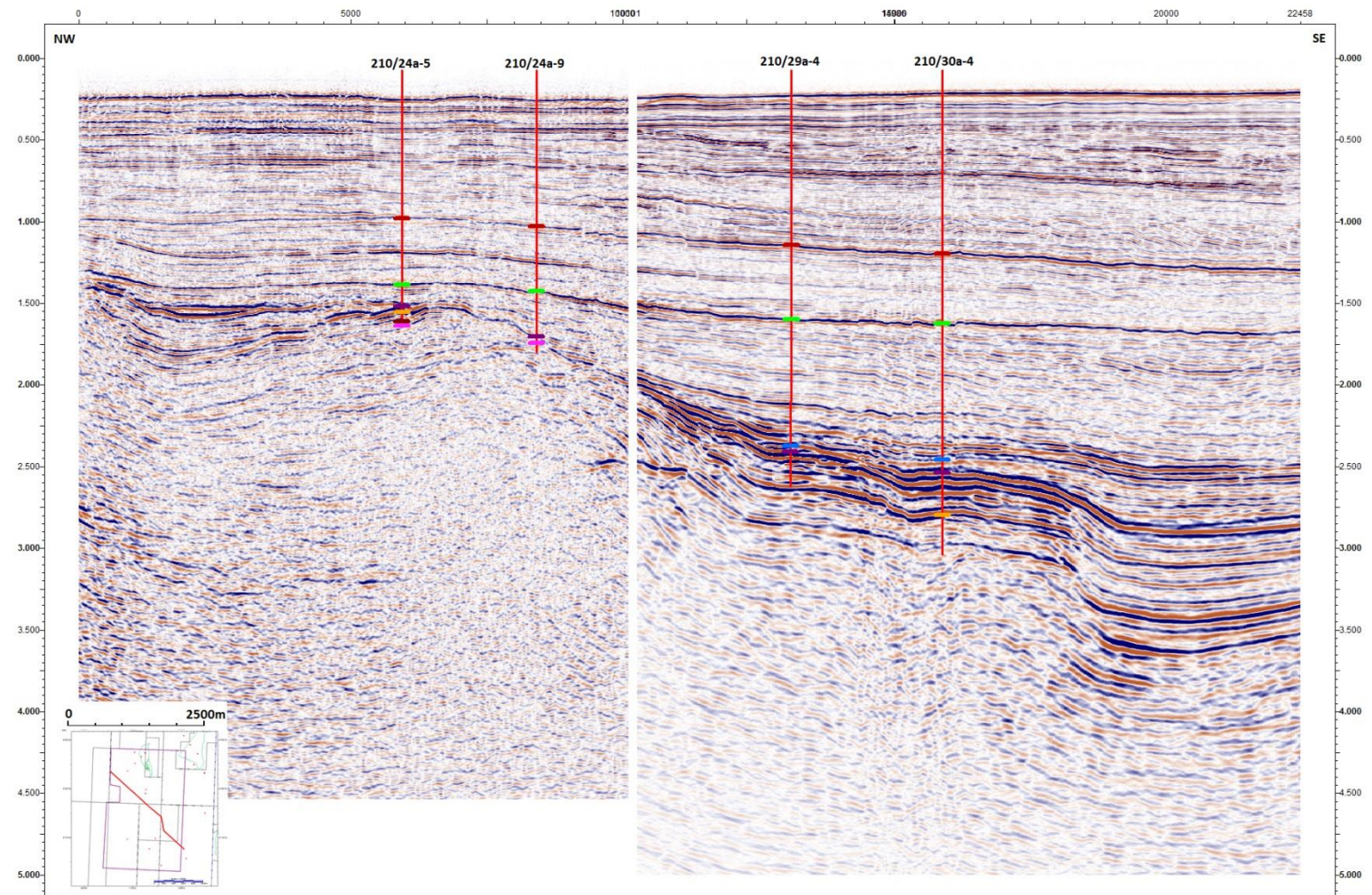


Figure 5-49 Seismic Line 3-2 is located within the central location of the three seismic sections, here the Pobie Platform is not present but the rift shoulder is located further to the NW.

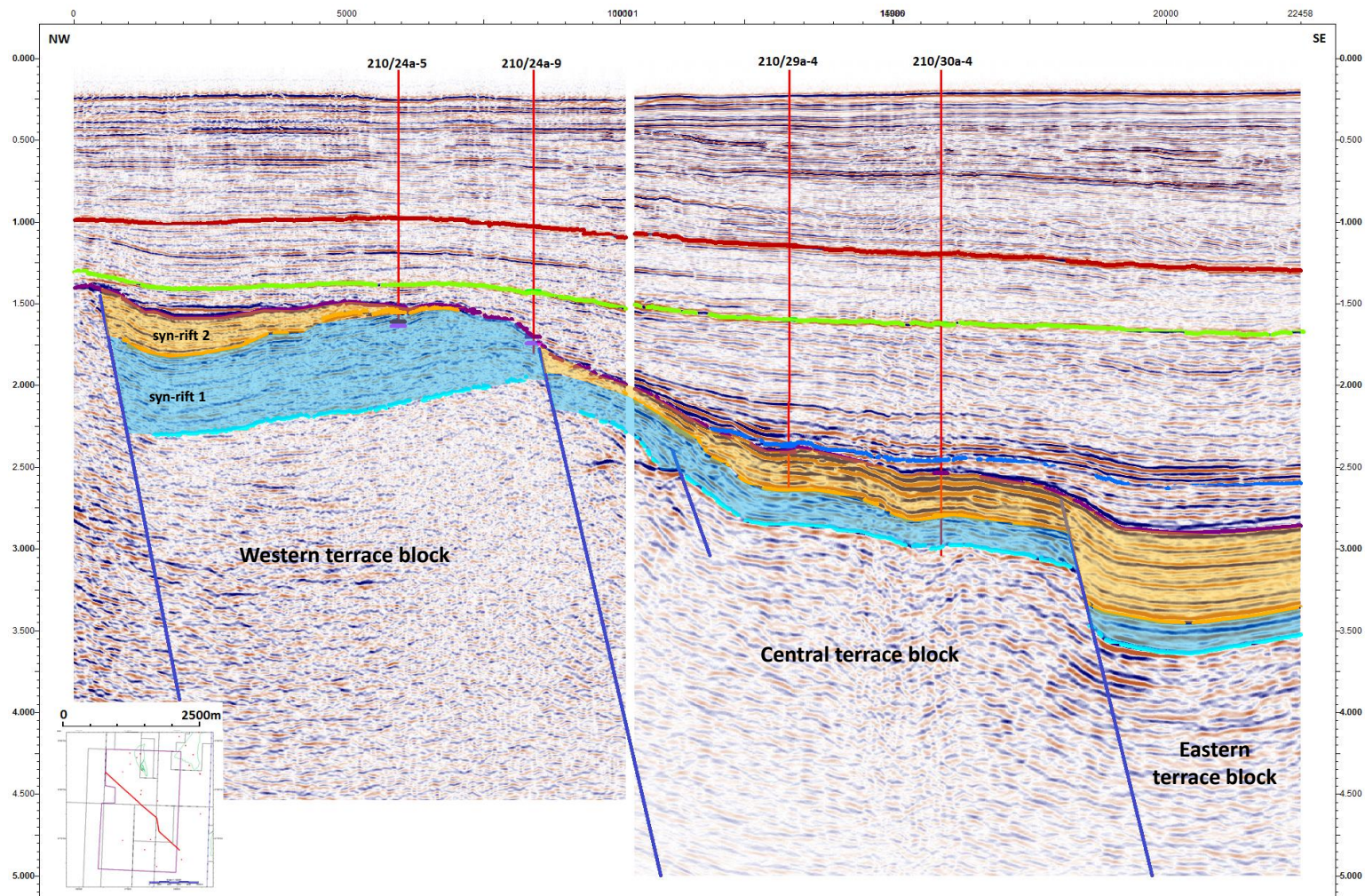


Figure 5-50 Seismic Line 3-2 illustrates two large terrace blocks that have formed in the Upper Jurassic. The terrace block to the NW has a significantly larger section of Mesozoic sediments within it as this was a hangingwall location during the initial Permo-Triassic rifting event.

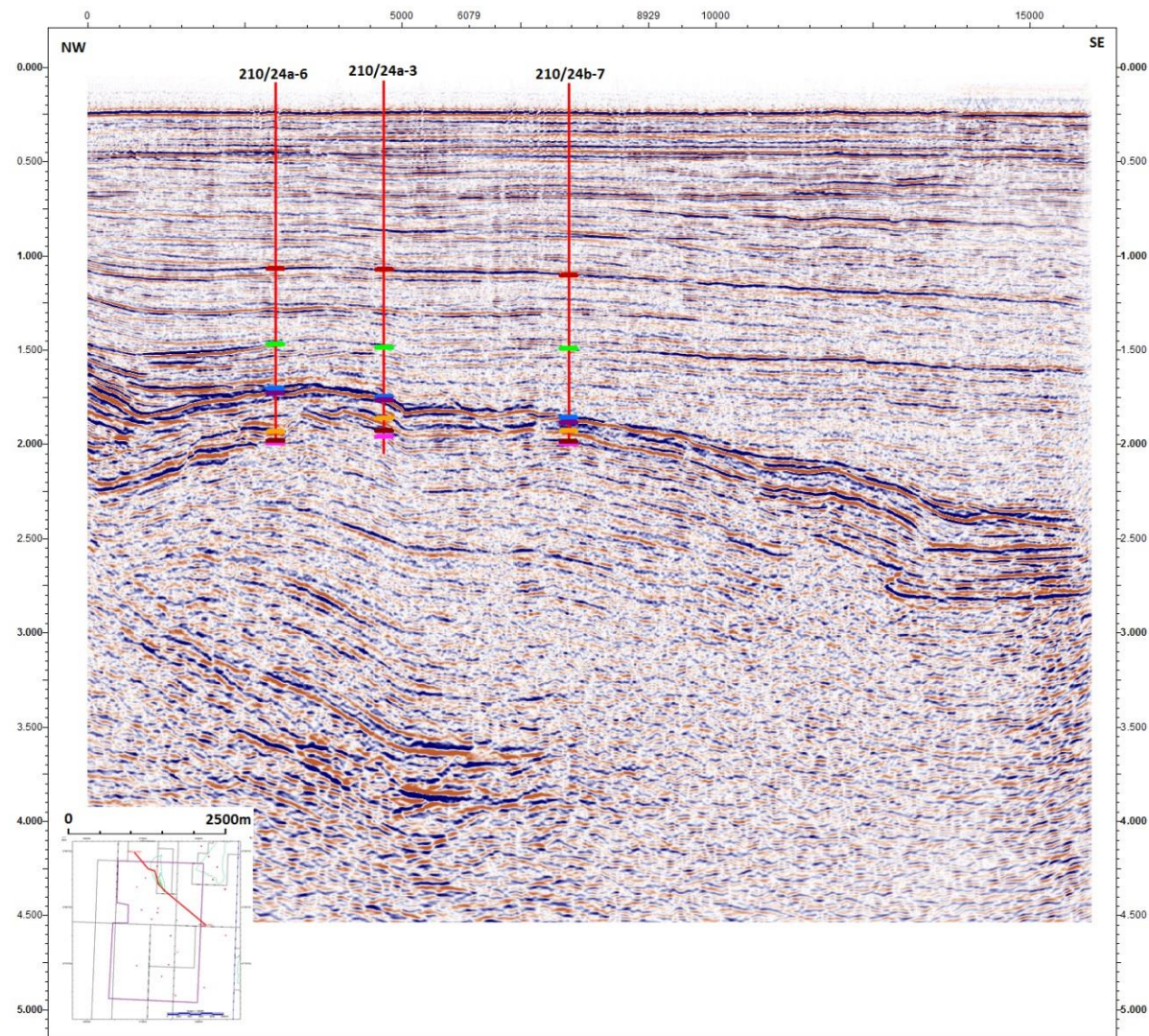


Figure 5-51 Seismic Line 3-3 is furthest north of the three sections and illustrates reactivation of an initial fault plane.

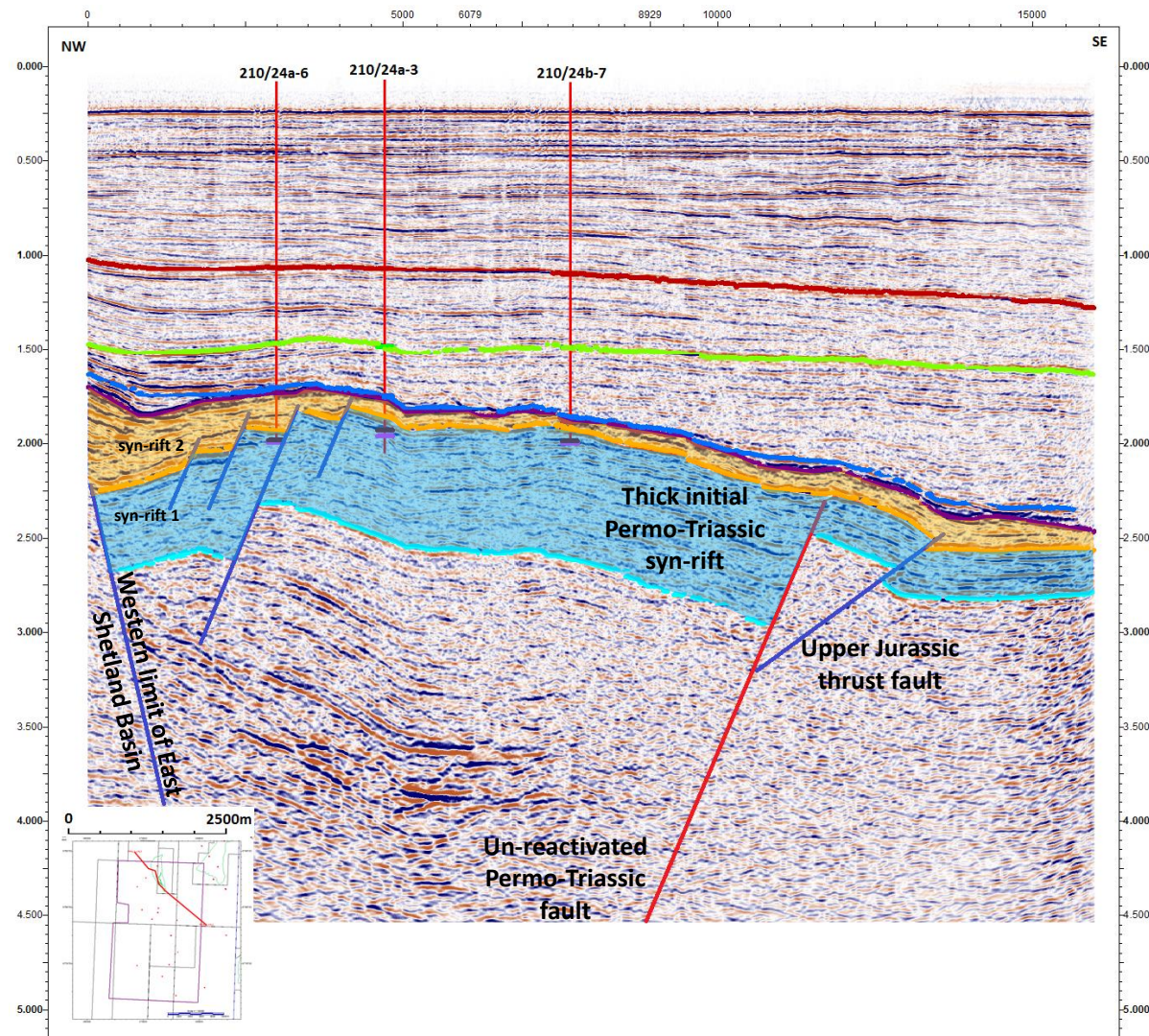


Figure 5-52 Seismic Line 3-3 highlights the Upper Jurassic thrust fault that forms as a result of a space issue due to the western bounding and Tern-Eider Ridge extensional faults.

Seismic line 3-2 (Figure 5-49 and 5-50) further illustrates the generation of the Upper Jurassic terrace blocks from the western rift shoulder (Pobie Platform). From this seismic section, it is clear to see that the thickness to syn-rift package 1 varies across the Upper Jurassic fault plane. This is similar to Type 2 rifting and could be the location of an underlying Permo-Triassic fault that is not visible within the seismic data. This thickness variation is also observed in seismic line 3-1 and is explained by the presence of the Pobie Fault, which is thought to have initially moved in the Permo-Triassic.

The final seismic line 3-3 (Figure 5-51 and 52) is located through the northern section of the study area and is a similar location of seismic line 1-3 which indicates a Permo-Triassic fault that has not reactivated in the Upper Jurassic. To the south east of the Permo-Triassic high is a thrust fault that was identified in section 5.3.1. This thrust fault it thought to have formed as a direct result of a space issue within the western edge of the East Shetland Basin. As the western rift shoulder causes an eastern extension and the Tern-Eider Ridge a westerly extension, this purely extension regime causes internal compression. As the west rift shoulder is the dominant fault it is the Tern-Eider Ridge fault that buckles and generates a small scale thrust fault and rollover anticline to accommodate the localised compression in a purely extensional setting. The top structure maps generated over this area are the Top Jurassic, Top Brent Group and the Top Basement. As little to no Cretaceous sediments are deposited over the Pobie Platform it was not possible to create a BCU horizon. To replace this horizon a Top Jurassic horizon was interpreted and accounts for any Upper Jurassic Humber Group sediments that were deposited over the Middle Jurassic Brent Group.

The Top Upper Jurassic horizon (Figure 5-53) shows a significant low has developed in the eastern section of the study area which represents the East Shetland Basin. The south-eastern tip of the Tern-Eider Ridge can also be

imaged in the north east corner of the dataset. The primary feature that is evident throughout the Top Jurassic structure map is the presence of the Pobie Platform and the edge of the Unst Basin which are significant highs throughout the map.

These structural highs are also imaged in the Top Brent Group structure map (Figure 5-54) along with a relay ramp to the east of the Pobie Platform. These Upper Jurassic relay ramps can play a crucial role in transporting coarse clastic material from the rift shoulders to the deeper sections of the rift basin. The thrust fault that was identified in the seismic data can also be imaged north of this relay ramp. It may also be possible to see how little subsidence has occurred in the Brent Group along the Tern-Eider Ridge (TER) in the Upper Jurassic rifting event.

The Permo-Triassic structure map (Figure 5-55) on the other hand shows a significant depo-centre that is in placed along the TER lineation. This is further evidence to the idea of Type 1 rifting that was discussed earlier. This map is the first opportunity in which it is possible to say that the Pobie Fault and the TER were once one structure. Both faults have the same orientation and dip, but are separated by the N-S oriented Upper Jurassic basin bounding fault. It is possible that this fault was once one but has since been cut into two separate strands that may move independently in a second rifting event. It is also important to note that the Upper Jurassic thrust fault and relay ramp structures are also imaged on this map but are in fact imposed on this map as the Basement top structure map responds to all rifting events that has occurred within the study area that effect the horizon. As the Basement is relatively shallow at these locations and the sediment cover is thin, the Upper Jurassic faulting is able to affect the horizon and therefore be imaged in the Basement map.

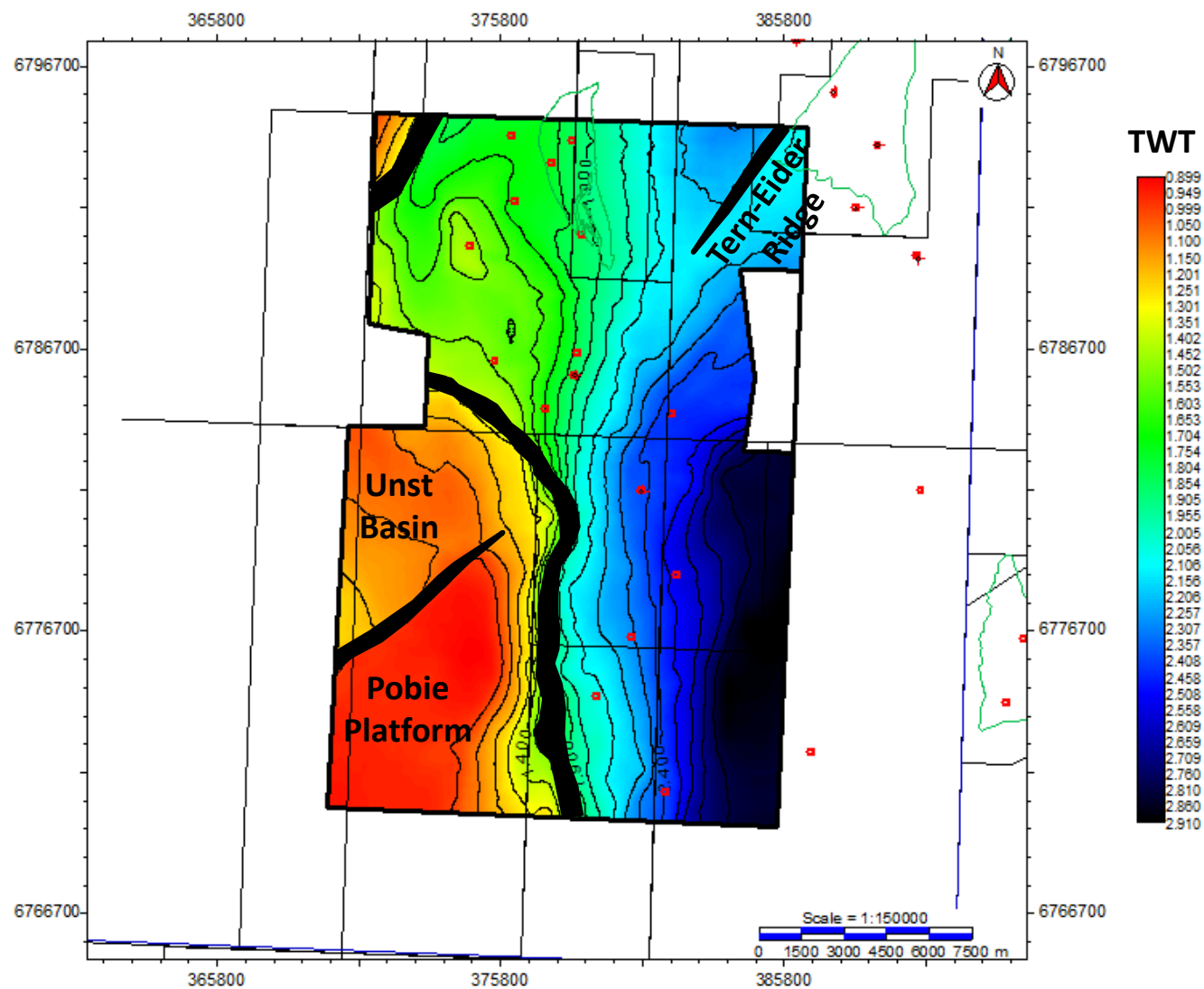


Figure 5-53. Top Jurassic top structure map illustrating the structural high relating to the western limit of the East Shetland Basin which also contains the Unst Basin.

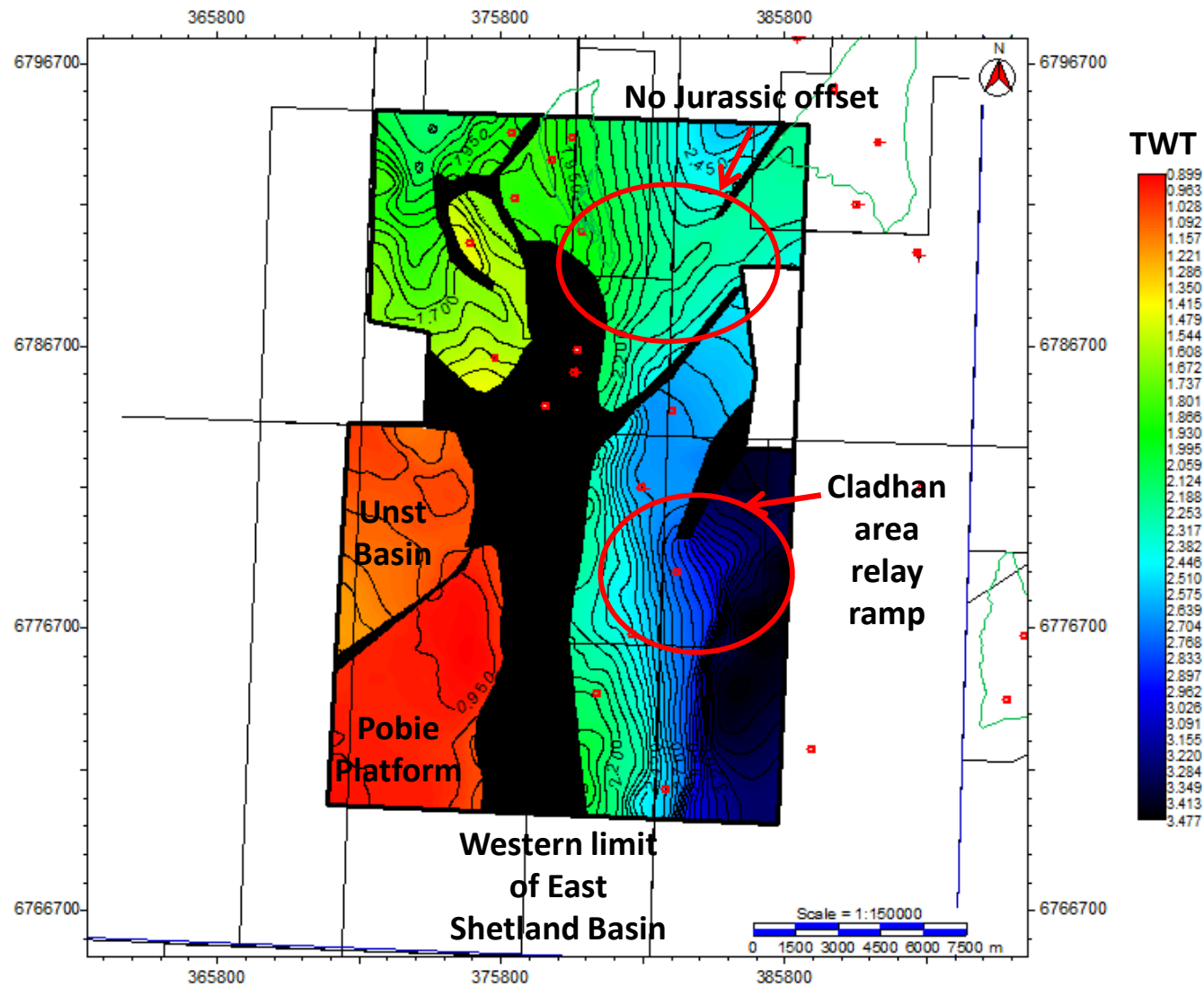


Figure 5-54. Top Brent Group structure map illustrates the Cladhan area relay ramp to the east of the Pobie Platform. The thrust fault highlighted in earlier seismic lines can also be imaged to the north of the Cladhan area.

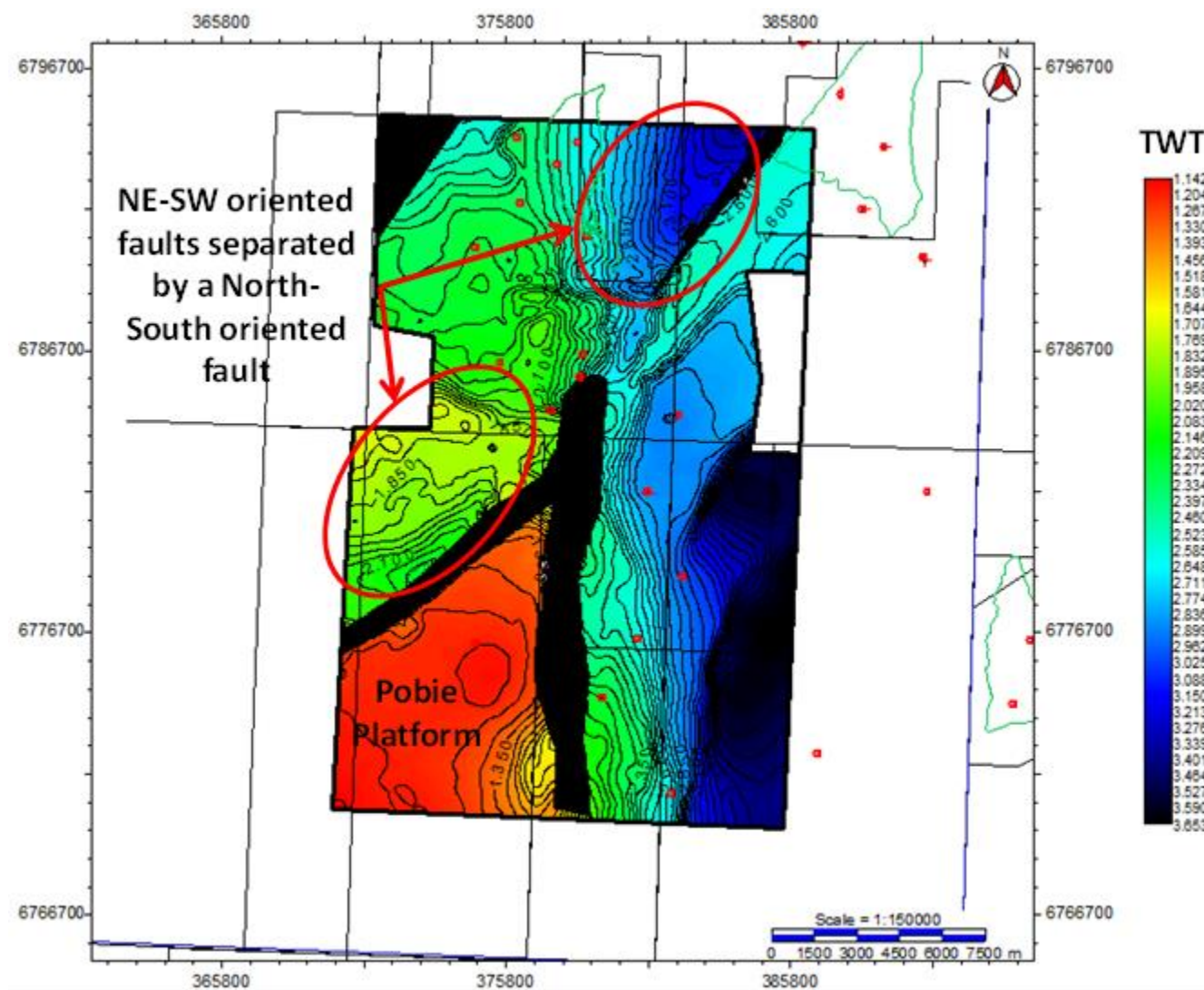


Figure 5-55. Top Basement structure map highlights two Permo-Triassic basins which appear to be cross cut by the Upper Jurassic rift bounding fault.

As in Type 2 rifting (Cormorant to Brent), the N-S oriented Upper Jurassic rifting event has over written the underlying NE-SW lineated Permo-Triassic faults, thus dominating the structural patterns. But, in areas where no N-S faults are found the NE-SW faults are prominent. This is illustrated in the NE and SW striking sections, which is represented by the Tern-Eider Ridge and the Pobie Platform. As these two fault trends (Caledonian and Upper Jurassic) have an influence on the structural features within the Pobie study area it is vitally important to analyse the isochron maps to identify if any reactivation has occurred along the Caledonian trending faults.

As the structural pattern of the maps is dominated by a large Upper Jurassic, easterly dipping N-S normal fault a series of thickness maps between the set horizons illustrates the timing of movement along the faults.

The thickness map between the Top Jurassic and the Top Basement (Figure 5-56) shows a mixed response to thickening trends. Within this map it is possible to see the large scale depo-centres that were created in the Permo-Triassic which align NE-SW in the TER and the Pobie Platform area. The smaller N-S striking depo-centres relating to the Upper Jurassic rifting event in the terrace area east of the Pobie Platform are also present.

These N-S striking normal faults can be better observed in the Upper Jurassic to Top Brent Group isochron (Figure 5-57). Although the entire area east of the basin bounding fault has undergone hangingwall subsidence it is the relay ramp area that has subsided more than anywhere else. Other Upper Jurassic features such as the TER and the thrust fault can also be observed along with the thin covering of Upper Jurassic sediments over the Pobie Platform. This thin sediment cover may be related to either a lack of deposition from the Brent through to the Paleocene or it has undergone high levels of erosion during the Cretaceous and Tertiary.

The isochron map between the Brent Group and the metamorphic Basement (Figure 5-58) measures the Syn-rift 1 package which the NE-SW faults are the only fault lineations present in this initial rifting event. This fault movement has resulted in creating a large depo-centre in the Pobie Platform and the TER. The areas directly to the SE of this fault lineament can be identified as the initial Permo-Triassic footwall high that has since been transected by the Upper Jurassic rifting event to create the structures we see today. The depo-centre that was created in the Permo-Triassic looks like it may have been a more laterally continuous feature that has been transected by a more recent phase of rifting. This would agree with the earlier suggestion that the depo-centre in the Pobie Platform and the TER was a singular fault related to the Unst Basin.

By showing that the Permo-Triassic faults have reactivated, it must be noted that the Pobie Fault has reactivated which is located in the footwall to the Upper Jurassic fault.

It was noted in the TER area that the largest offset along the Permo-Triassic depo-centre was located towards the southwest of the area. If this lineation is continued on the south-westerly trend it is possible to see it linking with the Pobie fault in the Pobie Platform as shown in Figure 5-56. This suggests a Permo-Triassic fault was initially in place prior to the Upper Jurassic rifting event. The reactivation of this NW dipping normal fault in the Upper Jurassic can be seen clearly in the Tern-Eider Ridge area to the northeast and is illustrated in Type 1 rifting, but, in the Pobie Platform area a separate map is needed to show this fault movement (primarily due to the scale of faulting on the Pobie Platform area is not of the same magnitude as in the basin).

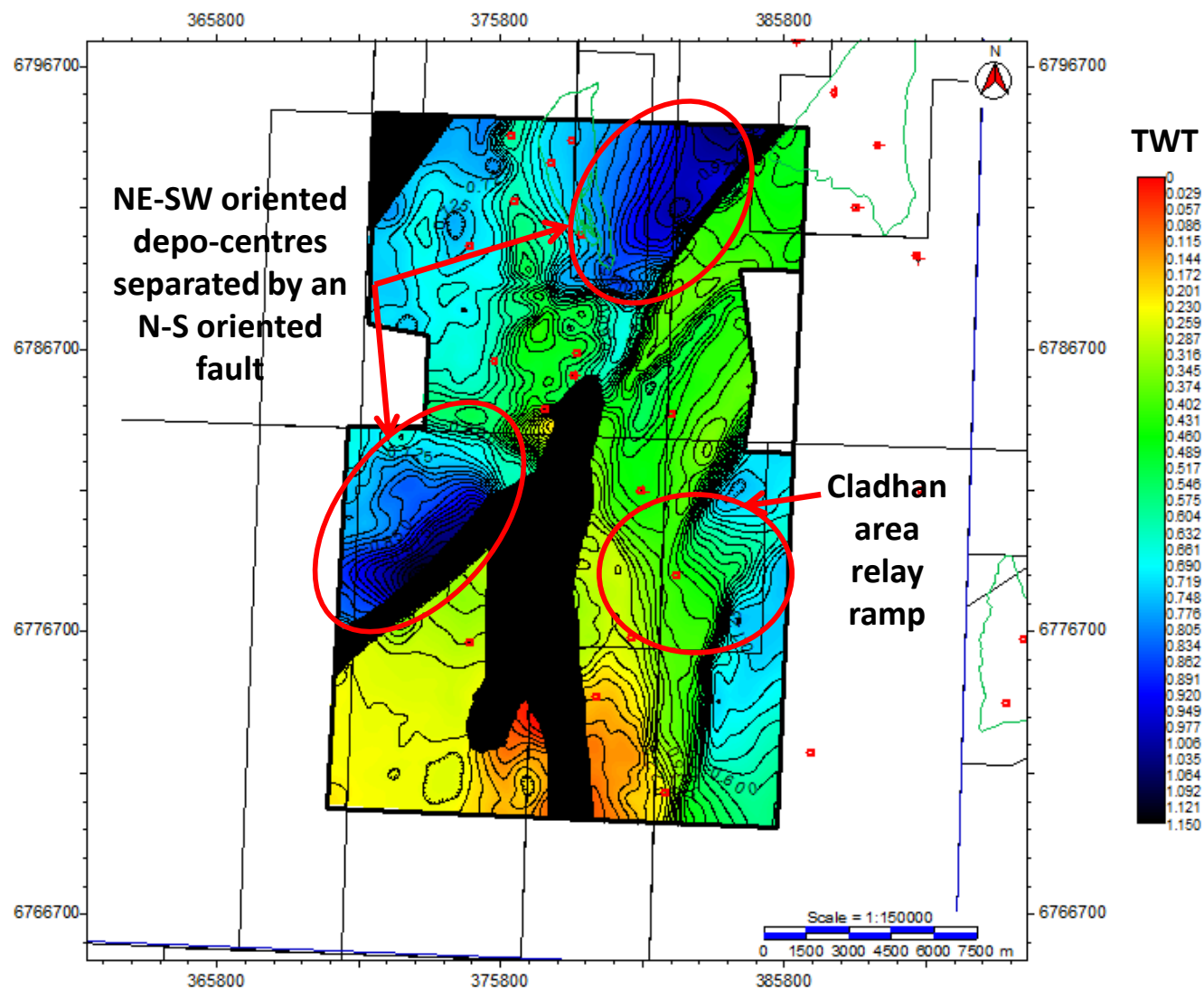


Figure 5-56. Top Upper Jurassic to Permo-Triassic isochron map highlighting the NE-SW oriented depocentres to the north and the N-S oriented depocentres relating to the Cladhan area to the south.

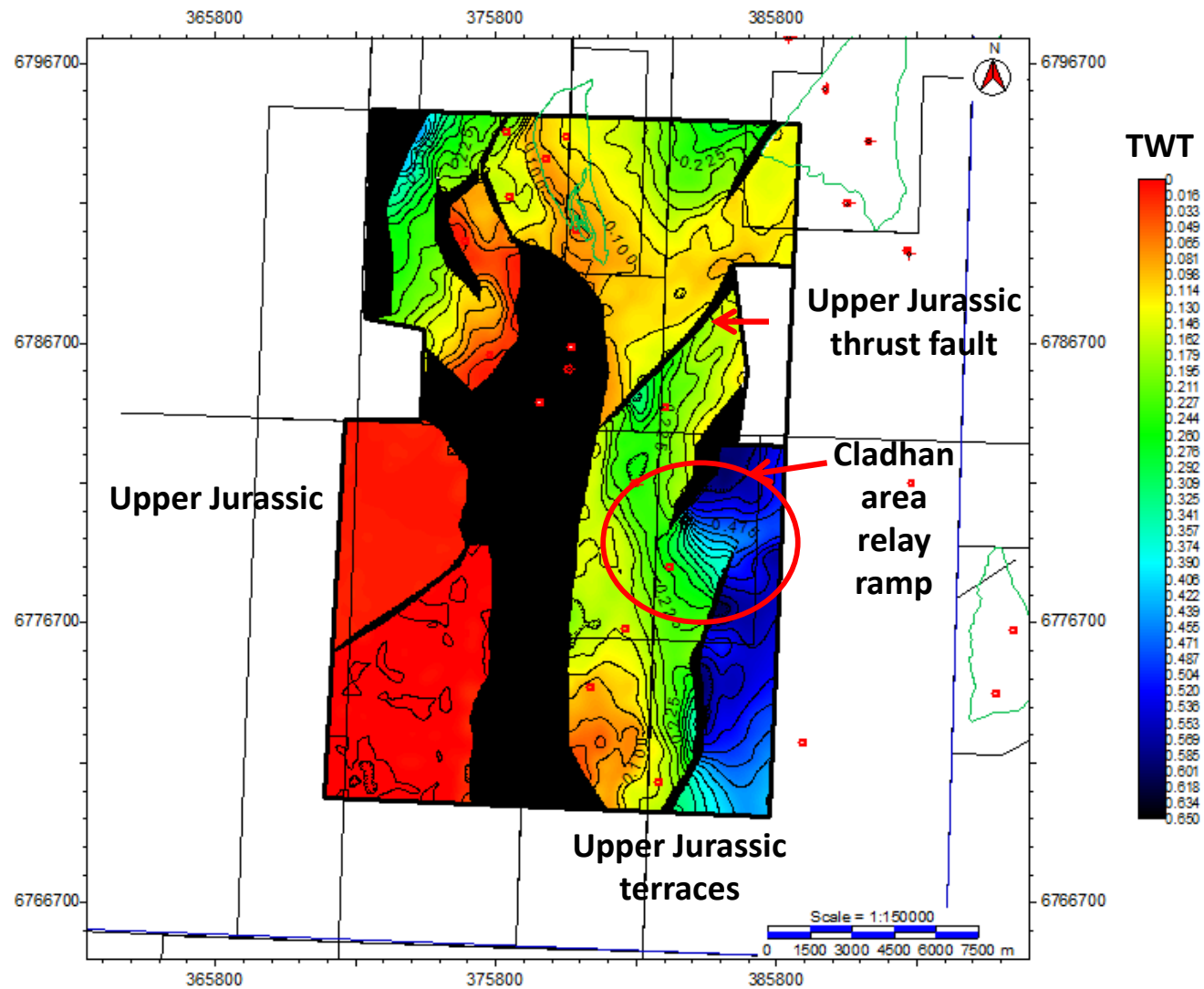


Figure 5-57. Top Upper Jurassic to Top Brent Group isochron shows the greatest amount of thickening to be found in the Cladhan relay ramp area and a thinning of section over the hangingwall of the upper Jurassic thrust fault.

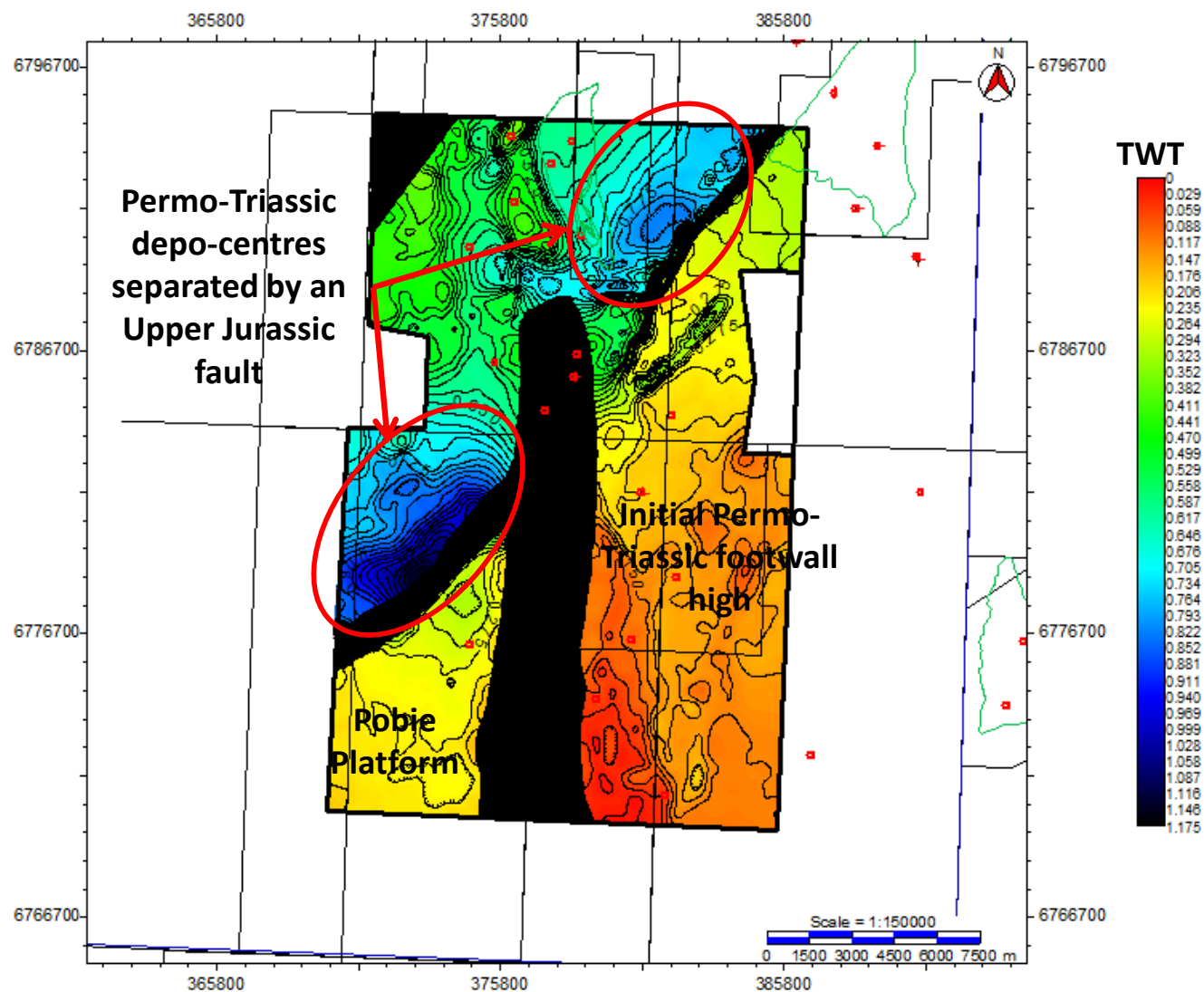


Figure 5-58. Top Brent to Permo-Triassic isochron map shows the thickest Permo-Triassic sediments to be located in the depo-centres that were highlighted in the Top basement structure map. It appears that the depo-centres seem to thicken to the SW and die out to the NE suggesting this initial fault could be further observed to the SW in to the Unst Basin.

This map (Figure 5-59) measures the thickness between the Top Balder Formation and the Top Brent Group as no Base Cretaceous pick and shows the movement of the fault more clearly. As noted earlier, no Cretaceous sediments were recorded over the Pobie Platform, but accommodation space was still created in the Upper Jurassic. Eventually, when sedimentation rates outstripped that of erosion over the Pobie Platform in the Tertiary, the Upper Jurassic accommodation space was filled, which allows the reactivation of the Permo-Triassic faults in the Upper Jurassic to be observed. This thickness map shows the thickening of sediments to the SW of the Pobie Fault. As noted above, the importance of this fault reactivation relates to the faults location. In Type 1 the reactivation, the fault plane was reactivated in the same environment in both rifting events, but in this case the Pobie fault is in a footwall location in the Upper Jurassic rifting event. In this elevated footwall location the extension stresses are significantly weaker than that of a basin area such as the TER area. This would account for the small level of faulting that is observed in the Pobie fault.

It is important to note that even if an initial fault is cross cut by a later rifting event, the separate fault strands still have the ability to reactivate as long as the stress align as observed along the Pobie Fault.

Further analysis of the Upper Jurassic to Top Brent map illustrates the importance of the N-S bounding fault in this area. It was noted in the TER area and earlier in this section that a thrust fault is present within seismic line 1-3 and 3-3. The cause of this thrust is related to the northward-propagating rift shoulder (basin-bounding) fault early in the Upper Jurassic rifting event and the reactivation of the Permo-Triassic NE-SW Tern-Eider Ridge fault.

As the easterly dipping Upper Jurassic normal fault became the prominent fault in the area and the north-westerly dipping Permo-Triassic fault became

more active in the Upper Jurassic, a space issue occurred where the two faults overlapped. With both faults extending in opposing directions it was inevitable that an area of localised compression would occur in this purely extensional environment. This localized compression is expressed as the thrust fault which is observed at the south-easterly tip of the TER. It must be noted that the thrust fault occurs through the footwall of the initial Permo-Triassic fault block. Figure 60 and 61 illustrates an arbitrary line that is taken through the study areas and best shows off this localised compression and the occurrence of a thrust fault.

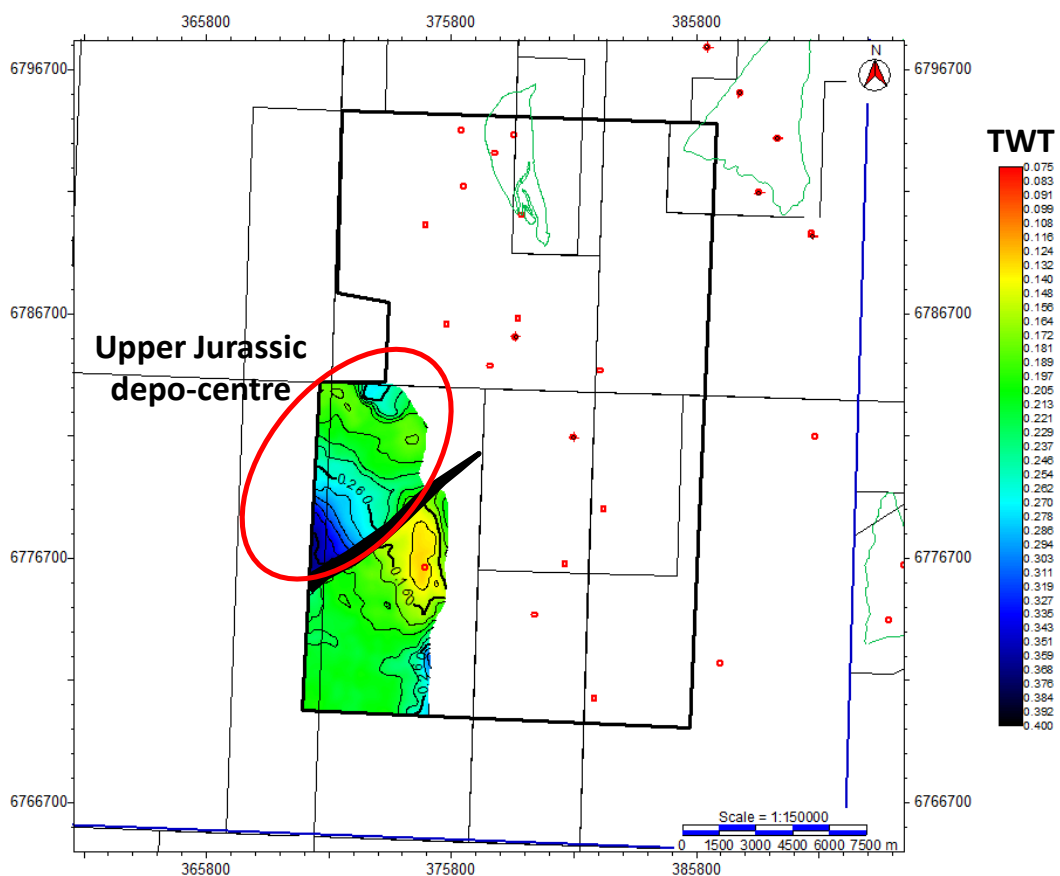


Figure 5-59. Isochron between the Top Balder and Top Jurassic over the Pobie Platform illustrating the accommodation space generated by the Upper Jurassic rifting event.

The proximity of the Permo-Triassic fault to the N-S bounding fault can also affect the location of reactivation in the Upper Jurassic. It has been noted in both this section and Type 1 rifting that the Permo-Triassic depo-centres

along the Tern-Eider Ridge and the Pobie Platform were once one structure. But the length of the Upper Jurassic NW dipping fault does not match up with that of the underlying Permo-Triassic fault in the TER area. In seismic line 1-3 and 3-3 it is possible to see Permo-Triassic offset but no Upper Jurassic fault movement. These areas also correspond to areas of localised compression and no Upper Jurassic can occur. Only when the compression stresses are nullified does the Permo-Triassic fault reactivate in the Upper Jurassic, as observed in seismic line 1-2, where thickening of syn-rift package 1 and 2 is observed.

Another faulting anomaly that is observed in the area relates to small scale N-S fault in the Pobie Platform that may relate to the N-S faults observed in the Tern-Eider Ridge. As the Tern-Eider Ridge and the Pobie Platform were once the same structure it is possible to use the Pobie Platform as an analogue for the TER, as it has undergone significantly less structural deformation.

The series of N-S normal faults observed in the Tern-Eider Ridge that was active in the Upper Jurassic which are responsible for defining the Tern and Eider Fields themselves. The timing of activity on these faults are directly associated to the Upper Jurassic rifting event, but it may be possible to relate them to older structural trends.

The evidence from Figure 5-62 suggest that the Pobie Platform has some internal deformation on the Top Basement level that is not related to the Upper Jurassic rifting. The age of these faults could range from Caledonian to Permo-Triassic, but are not related to the Upper Jurassic due to the undeformed sediments above the Basement horizon.

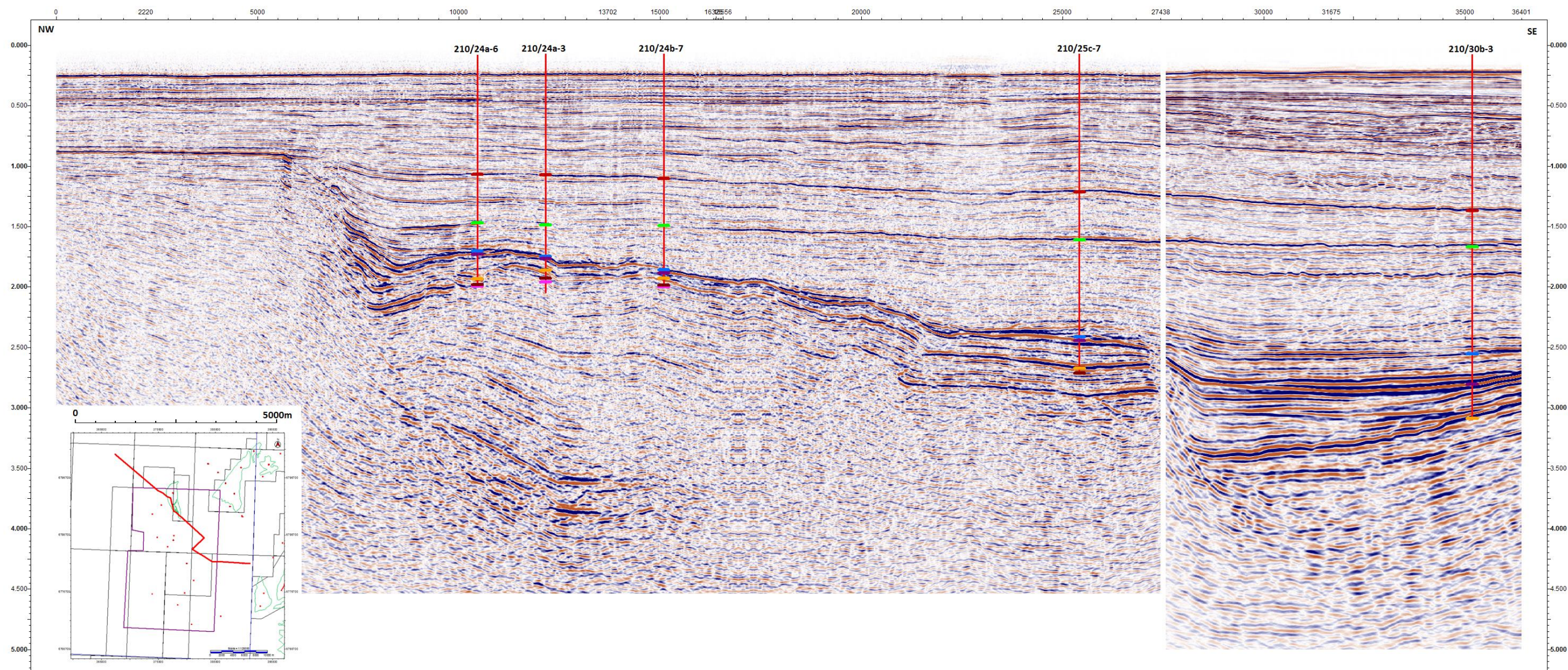


Figure 5-60. Uninterpreted section illustrating the extensionally derived thrust fault located to the SW of the Tern-Eider Ridge.

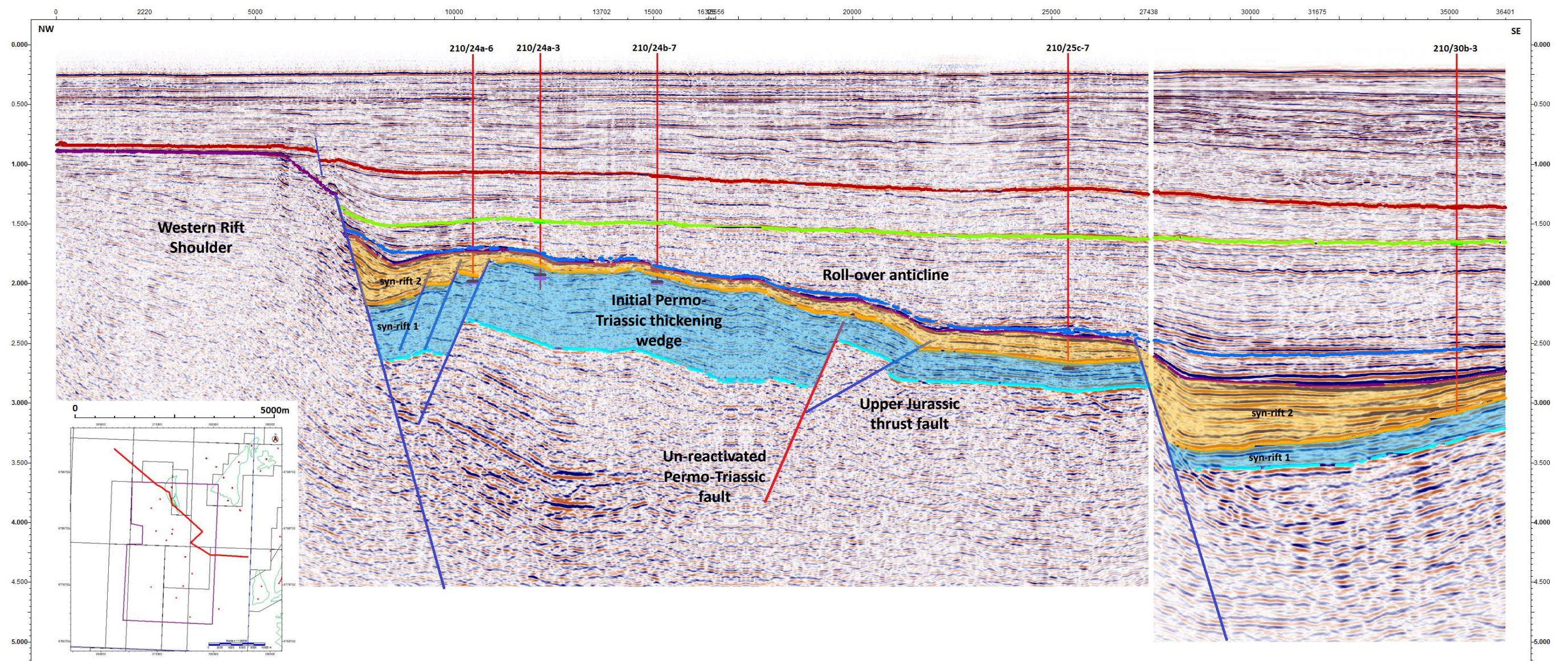


Figure 5-61 Seismic section illustrating the extensionally derived thrust fault which is located to the SW of the Tern-Eider Ridge.

Mapping out these potentially Caledonian or Permo-Triassic aged faults (Figure 5-63), results in the formation of a series of N-S oriented normal faults dipping to the west, similar to that of the Permo-Triassic faults observed in area 2 (Cormorant to Brent). Identification of these north-south lineaments in the Basement implies that these features are long lasting, but have the potential to reactivate in a later rifting event. It may be possible to say that these faults observed in the Pobie Platform may also have been observed in the Tern-Eider Ridge. With this in mind, it is plausible to suggest that the N-S faults in the Tern-Eider Ridge are not initially dated as Upper Jurassic faults, but are in fact older faults that have reactivated in the Upper Jurassic rifting event.

Whether it be due to reactivation and destruction of the initial structure or the deeper burial and poorer imaging quality, the initial Caledonian to Permo-Triassic structures are much more difficult to age date in the Tern-Eider Ridge compared to that of the better preserved Pobie Platform.

This study area is extremely complex as it contains localized Type 1 rifting along individual faults such as the Pobie Fault, an area of localized compression can be observed with a thrust fault and potential ancient Caledonian faults are located in the Pobie Platform all within a cross cutting multi-rift environment.

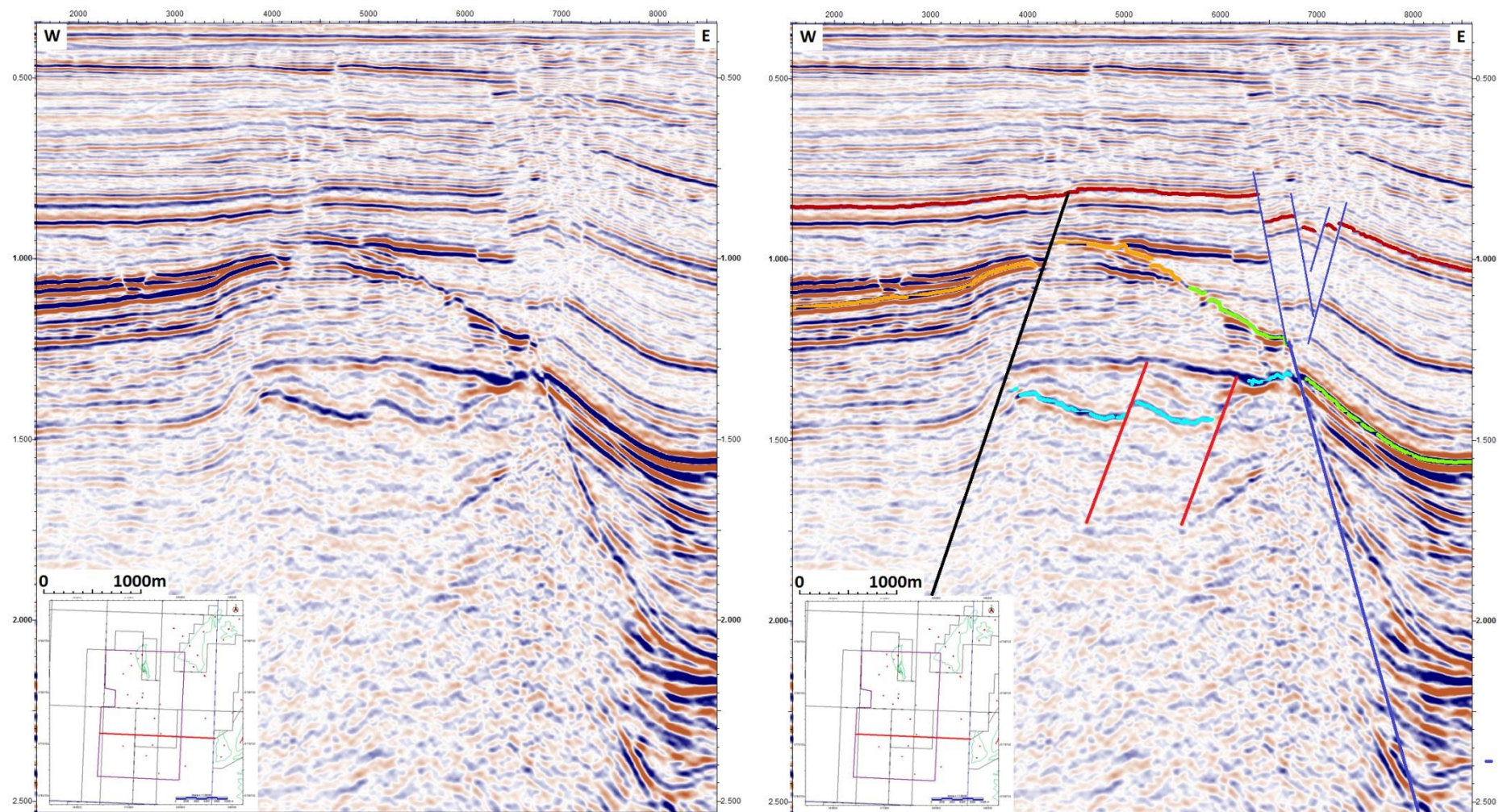


Figure 5-62 The East – West section shows a series of NNE-SSW oriented faults which are present within the basement material of the Pobie Platform. The strike of these faults is the same to that of the faults which create the hydrocarbon fields on the Tern-Eider Ridge.

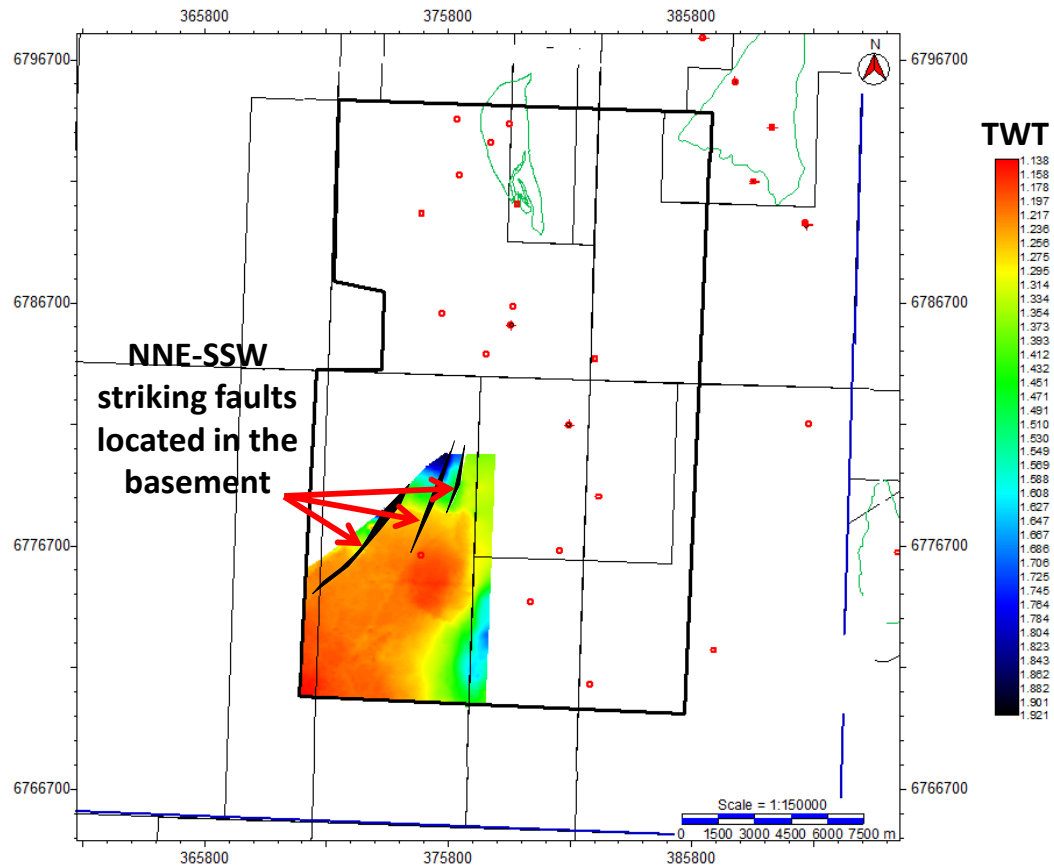


Figure 5-63. Top Structure map of ancient NNE-SSW oriented faults in the Pobie Platform.

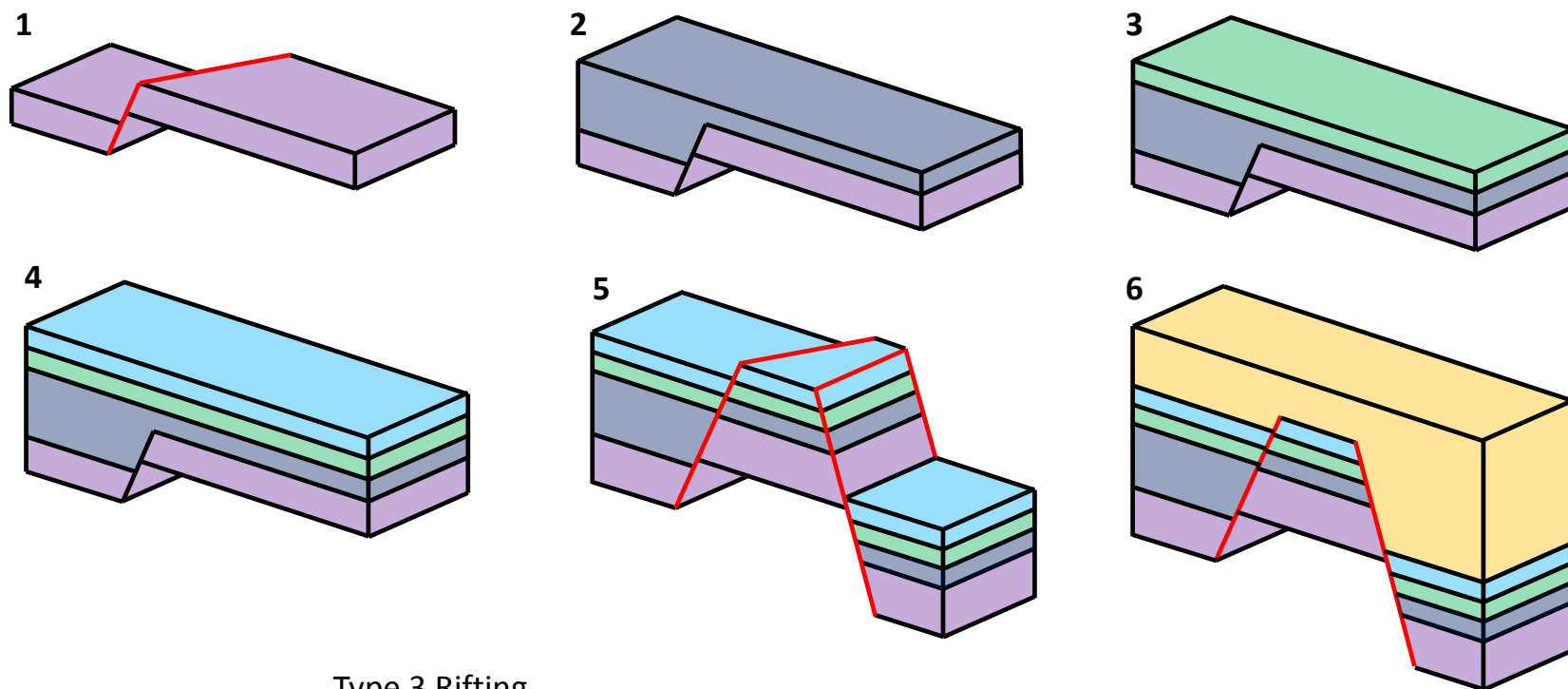
As some reactivation of the Permo-Triassic fault is observed in the Pobie Platform, this area must have been in net extension prior to being uplifted into the platform location. The growth of the basin-bounding fault through the Upper Jurassic is key to understanding the intricacies of the effects of multi-phase rift evolution. Effectively, the Pobie Platform area can be subdivided into 3 separate faulting periods. The first rifting period was the NE-SW oriented Permo-Triassic faults. The second phase of faulting relates to the reactivation of these faults in the Upper Jurassic as seen along the Tern-Eider Ridge and the Pobie Platform. The final stage of faulting is solely related to the Upper Jurassic rifting event and is illustrated by the generation of a series of N-S lineated easterly dipping normal faults.

In this final stage of faulting, the currently reactivating NE-SW faults that are distal to any N-S striking faults remain in net extension and continue to reactivate until the end of the Upper Jurassic rifting event. Areas that are in close proximity to large scale Upper Jurassic normal faults either cease to reactivate, as seen to the NE-SW striking fault on the Pobie Platform or go into localised compression where opposing polarity faults and form singular thrust faults in favour of the dominant fault stress.

This leads to a complex structural pattern that contains faults with multiple strike orientations (NW-SW striking Permo-Triassic and N-S striking Upper Jurassic), faults with varying fault polarity (westerly dipping Permo-Triassic faults and easterly dipping Upper Jurassic faults) and some reactivation and re-use of existing structural lineaments.

This third type of rifting which is observed here is the first to occur with a cross cutting nature (Figure 5-64, Figure 5-65 and Figure 5-66). Type 3 multi-phase rifting is observed in the Pobie Platform area, where the initial Permo-Triassic faults are obliquely cross-cut by Upper Jurassic rifting faults. This results in faults from the two rifting events having different fault strikes, although they are oblique to one another some fault planes are reused, if the polarity of the fault dip match up, as seen in the Pobie Fault on the Pobie Platform.

Areas that have a cross cutting nature are determined by the strength and obliquity of the faults. As seen in the Pobie Platform area the large easterly dipping normal fault is actually the western rift bounding fault and will cross cut all other faults. This fault has only ever moved in the Upper Jurassic, but, faults in the footwall of this platform area follow the NE-SW Caledonian fault trend and reactivate in both the Triassic and the Upper Jurassic.



Type 3 Rifting.

1. Permo-Triassic faulting
2. Triassic Sedimentation
3. Early Jurassic Sedimentation
4. Middle Jurassic Sedimentation
5. Upper Jurassic Faulting
6. Cretaceous Sedimentation

- pre-rift 1
syn-rift 1
post-rift 1
pre-rift 2
syn-rift 2
post-rift 2

Figure 5-64 Schematic illustration of the development of Type 3 rifting

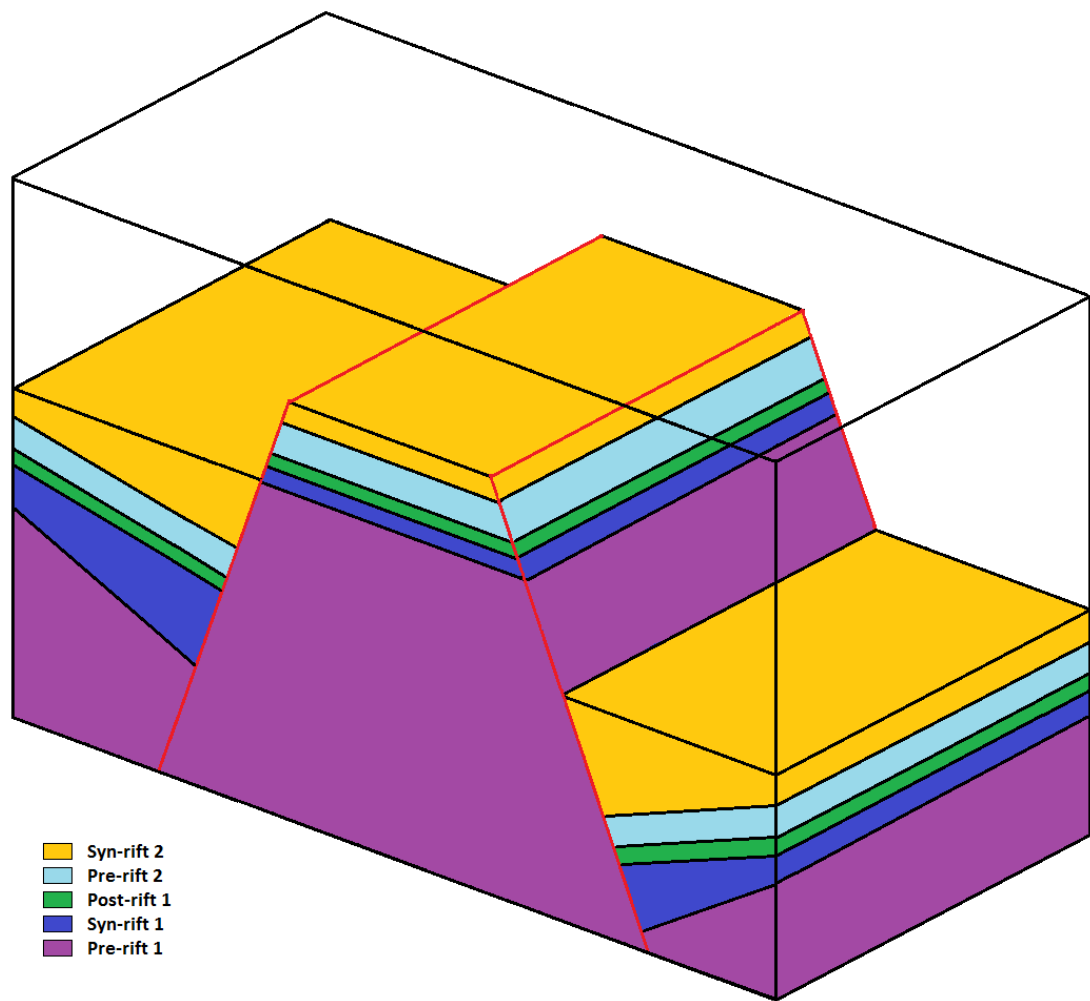


Figure 5-65. Box diagram for Type 3 rifting.

The reactivation of normal faults does occur in this study area, but mainly in the Pobie Platform area and the Tern-Eider Ridge area which was already covered in Type 1 rifting. The reason for reactivation in the platform area is related to the orientation of the regional stress field. As the north-south bounding fault propagates northwards the general stress field results in an east-west stretching orientation. Although the underlying faults do not follow this trend exactly, they are oblique enough to reactivate as long as the polarity (dip) of the faults matches up. It is easy for the Pobie Fault to reactivate as the polarity of the fault in the Triassic matches up roughly with the stretching polarity in the Upper Jurassic.

This fault is observed directly across the fault plane in the hangingwall of the bounding fault but has not reactivated. The primary reason being that the fault moved in the Triassic with a north-westerly dip, but in the Jurassic it would need to be the reverse of that in the hangingwall. This is why the southern tip of the eastern edge of the Tern-Eider Ridge reactivates as the fault polarity matches up enough for old fault planes to reactivate. This level of cross rifting can have a dramatic effect on the petroleum system by determining trap location and shape along with hydrocarbon kitchen location and burial depth.

As Type 3 faulting has faults of a cross cutting nature, it is possible to say areas such as the Pobie Platform have remained a high throughout both rifting events. This area can now be identified as a High-High due to its structural positioning during the two rifting events. The Unst Basin location to the west of the dataset was originally a hangingwall Low in the Triassic, but a footwall high in the Upper Jurassic, resulting in this area being identified as a Low-High. The relay ramp location directly to the east of the bounding fault was a high during the Permo-Triassic and a structural low in the Upper Jurassic and is called a High-Low. The final area to the north is the main basin area which moved in both the Triassic and the Jurassic and was a hangingwall low in both rifting events. This results in the area being identified as a Low-Low. The structural configuration of these fault blocks also reflects in the positioning of hydrocarbon elements. The Low-Low area is the most likely location of a kitchen area where hydrocarbons can enter the oil and gas windows, whereas the High-High area is the major trap location. The Low-High area and other areas that are High-Low are terrace areas which may also act as trap locations or hydrocarbon migration routes. This is seen throughout the Pobie Platform area, but, the platform itself which makes up the primary trap is so shallow the hydrocarbons found here are heavily biodegraded and unproducibile .

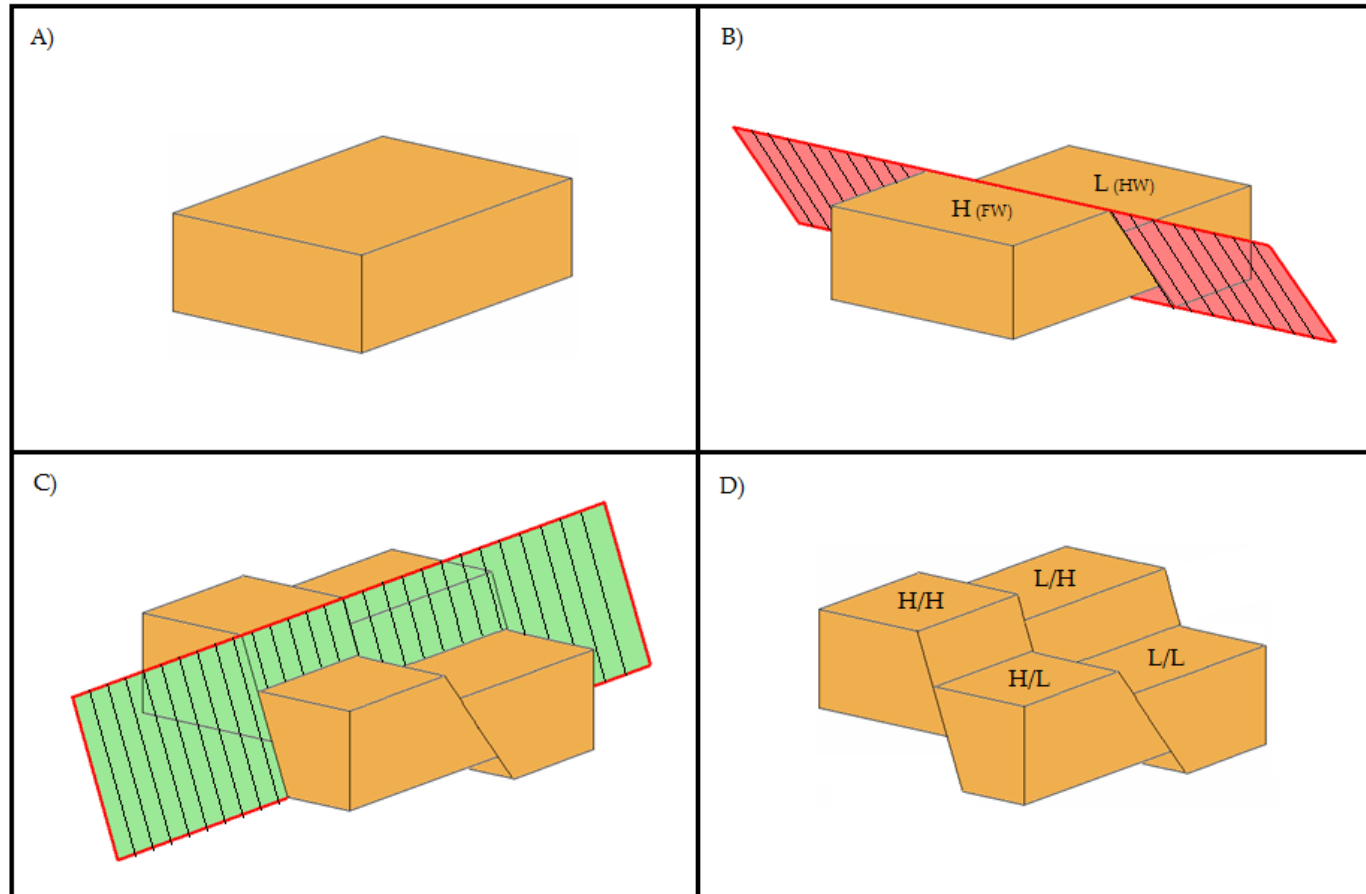


Figure 5-66. Box diagram evolution of a transected rift block. (A) Initial undeformed state. The initial fault (B) is identified with a red plane separating the block into an initial footwall and hangingwall scenario. The second rifting phase (C) identified in green cuts these two blocks into four and again forming a new relative footwall and hangingwall. By merging the two faults systems together it is possible to identify each of the blocks has a unique evolution

The location of this rifting type (Figure 5-61) is often reserved for the rift margins or basin bounding areas. These areas are subject of large scale extensional rifting in the second rift phase which over-prints and dominates the structural trend of the underlying fault pattern. This is observed in the Pobie Platform where the underlying Caledonian faults are cut at a perpendicular angle by the rift bounding Upper Jurassic fault.

5.3.4 Type 4 Rifting; perpendicular fault strike, partial fault plane reactivation and mixed fault polarity

The Causeway to Statfjord Nord area is aligned in a NE-SW orientation and is located within the eastern section of the study area (Figure 5-67). This localised study area contains the Causeway, Thistle, Osprey, Dunlin, Murchison and Statfjord Nord fields. The overall structural orientation is that of the Caledonian trend (NE-SW). Although the Caledonian trend is dominant, there is evidence that fault interaction has occurred with fault relating to Tornquist plate cycle (NW-SE), Permo-Triassic and Upper Jurassic rifting events.

This sub-area measures roughly 810Km² in area and is comprised of four individual 3D seismic volumes which cover the majority of the area. The only blank area is identified towards the bottom of the area but hold little or no importance to the structures observed throughout the area.

Throughout this location, eight arbitrary seismic sections have been created and well tied by synthetic seismograms (Figure 5-68) to best illustrate the structural evolution of the Causeway to Statfjord study area. Three of these lines are oriented NE-SW and are classified as strike lines, five other are oriented NW-SE and are called dip lines as they are aligned adjacent to the

major structures and illustrate their importance with a greater level of clarity. Throughout these sections a series of important horizons have been interpreted. The main horizons which are used to illustrate the multiple syn-rift packages in the study area are the Base Cretaceous Unconformity, the Brent group and Base Syn-rift 2. As in the Type 2 study area between the Cormorant and Brent Fields the Base Syn-rift 2 horizon is a marker horizon that is observed below an obvious syn-rift package. In shallower areas this has been interpreted as the top metamorphic Basement but here it is a horizon dated somewhere around the Permo-Triassic boundary.

The three strike lines all observe a horst structure towards the south-western edge of the section. Seismic lines 4-1 and 4-2 indicate this structure as the Thistle Field whereas; in section 4-3 this horst structure generates the Dunlin Field.

Seismic line 4-1 (Figure 5-69 and Figure 5-70) shows the prominent high that is the northern edge of the Thistle Field along with other smaller Upper Jurassic normal faults. This structural high is bounded by two NW-SE oriented faults that follow the old Tornquist trend. The other faults which are Upper Jurassic in age also follow this ancient orientation. This suggests that the Tornquist trend might have reactivated in the Upper Jurassic.

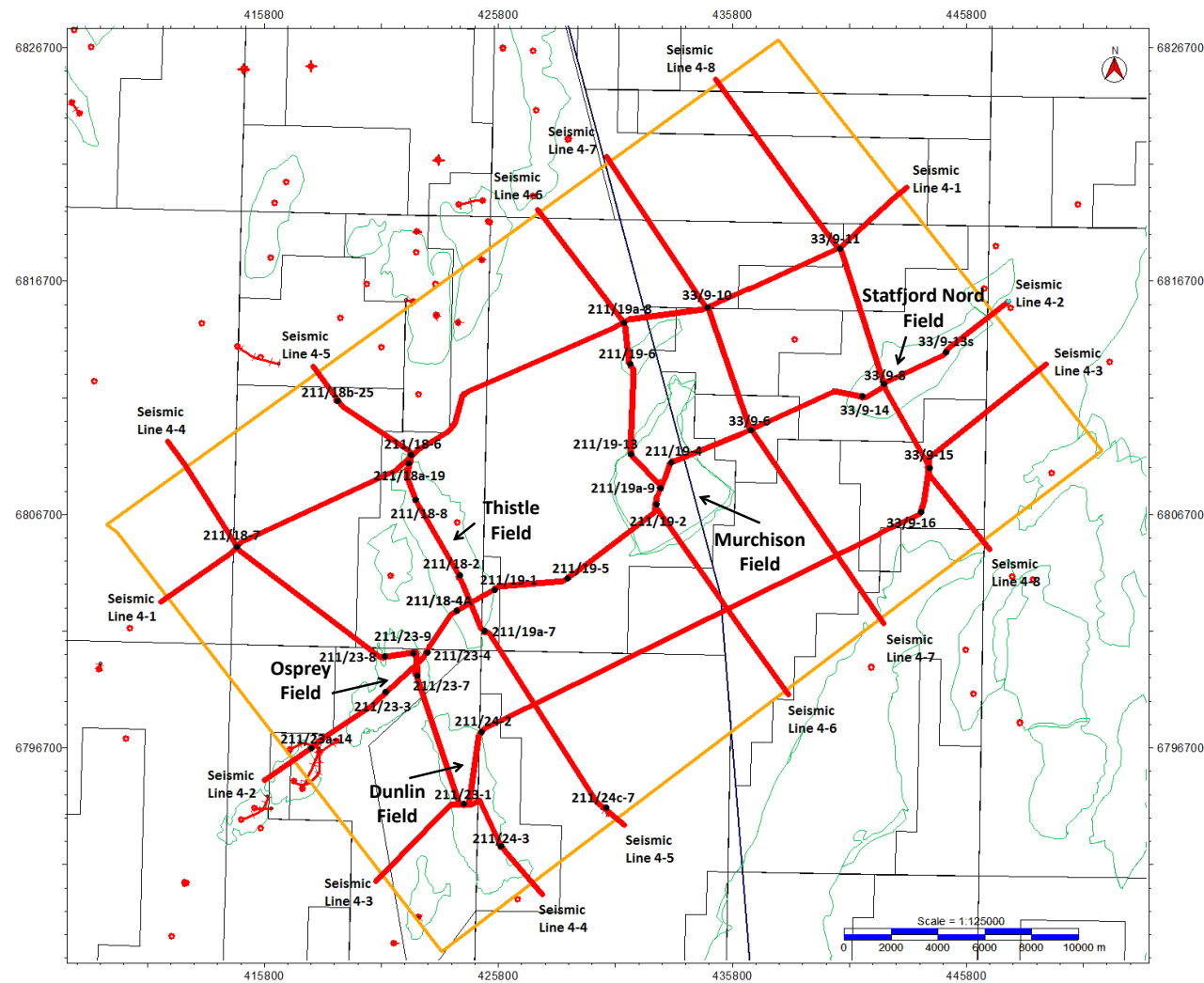


Figure 5-67. Map illustrating the localised study area and seismic lines used in this location.

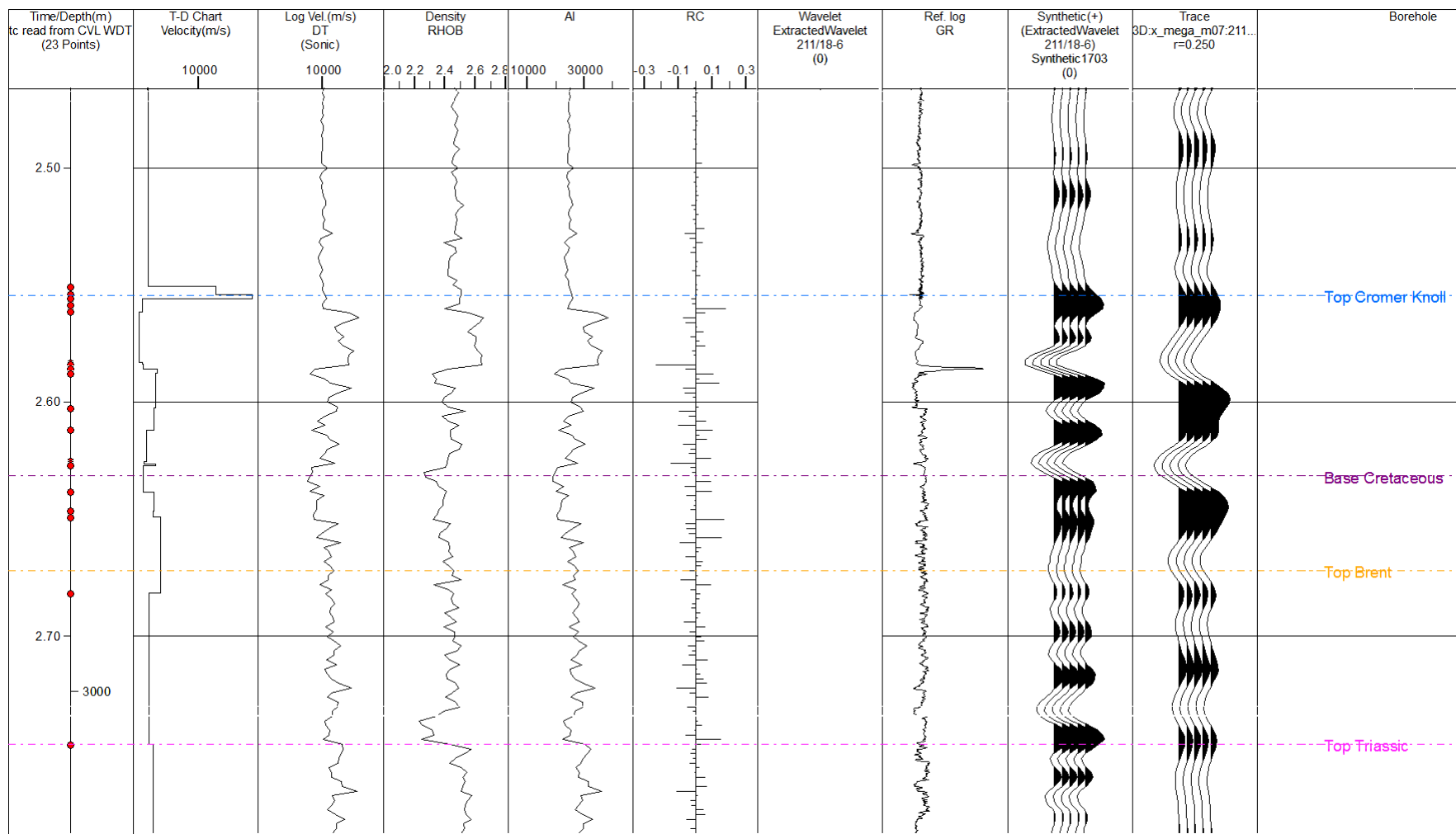


Figure 5-68 synthetic seismogram for well 211/18-6

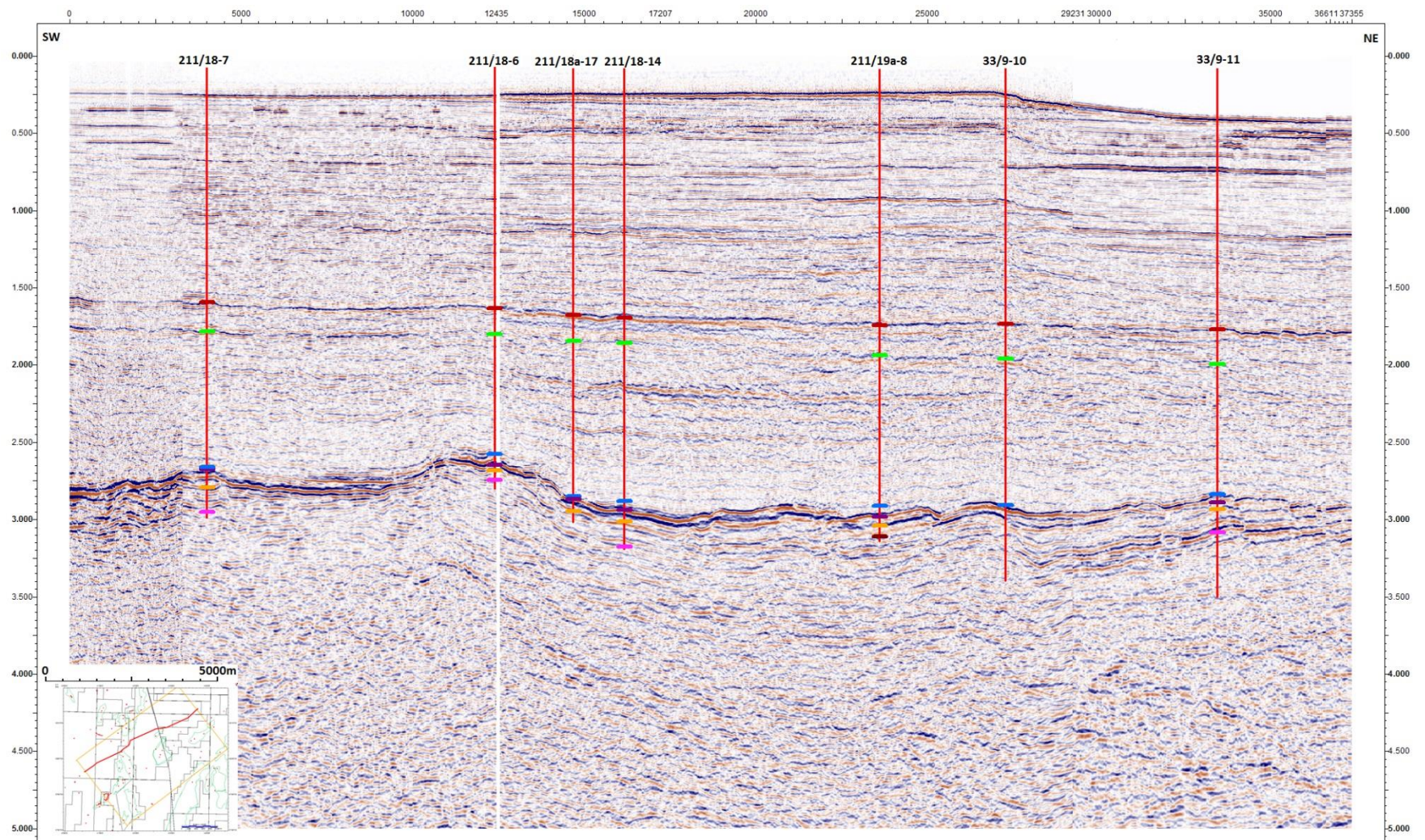


Figure 5-69. Seismic line 4-1 is the furthest NW of the three strike lines in this study.

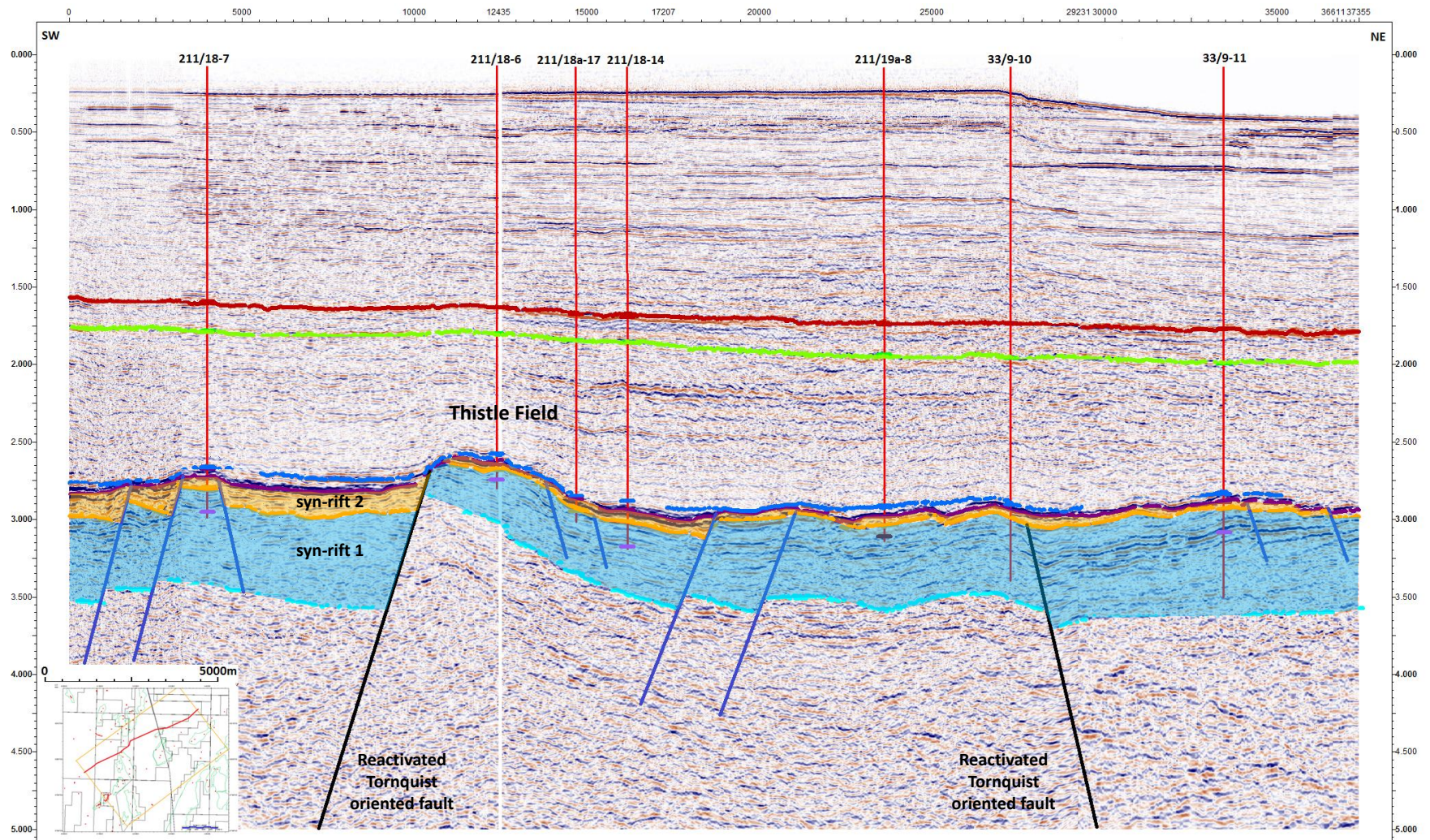


Figure 5-70. Seismic line 4-1 illustrates a series of NW-SE trending faults cross cutting into the footwall of an Upper Jurassic fault.

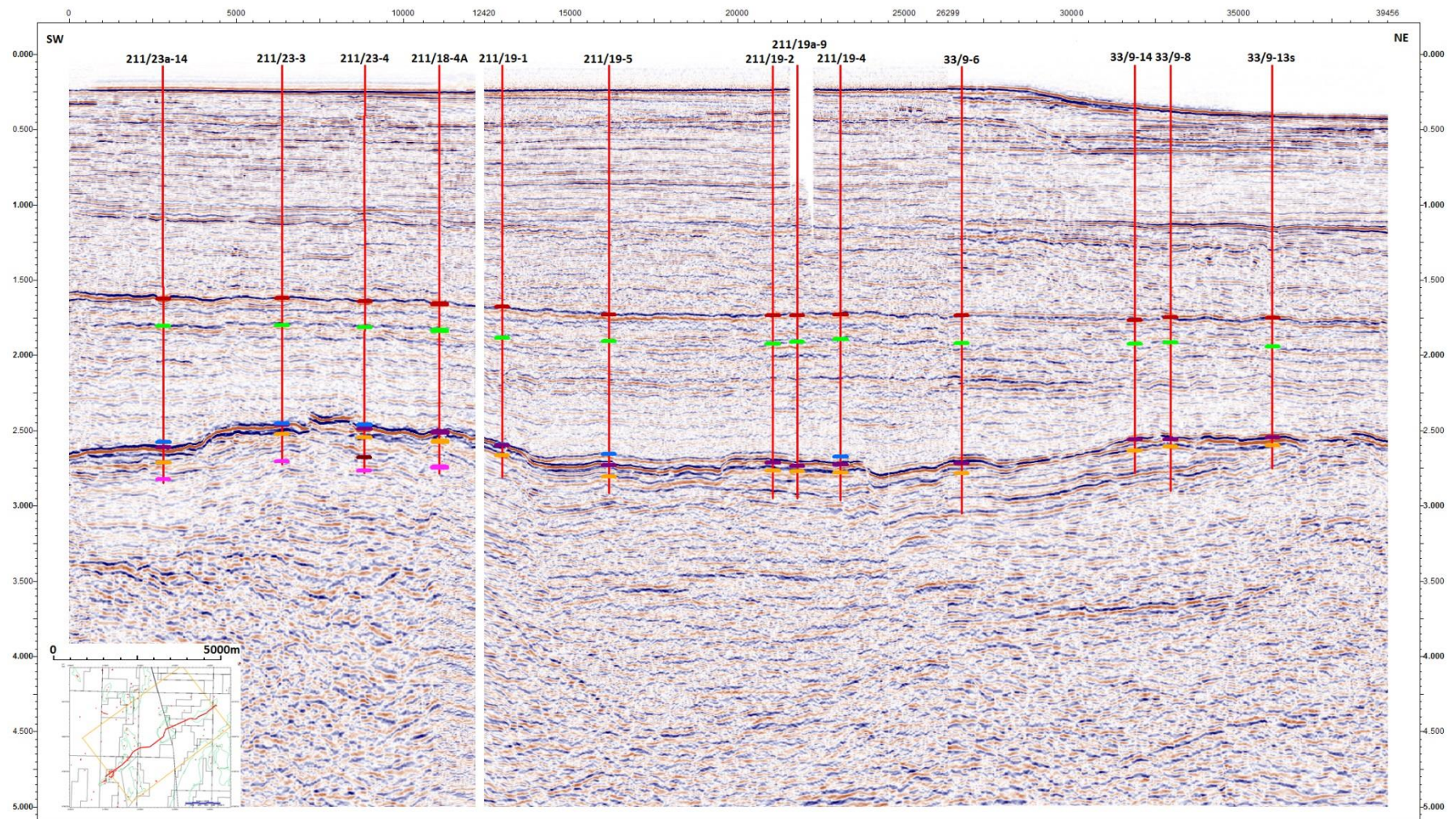


Figure 5-71. Seismic line 4-2 is a central strike line through the study area.

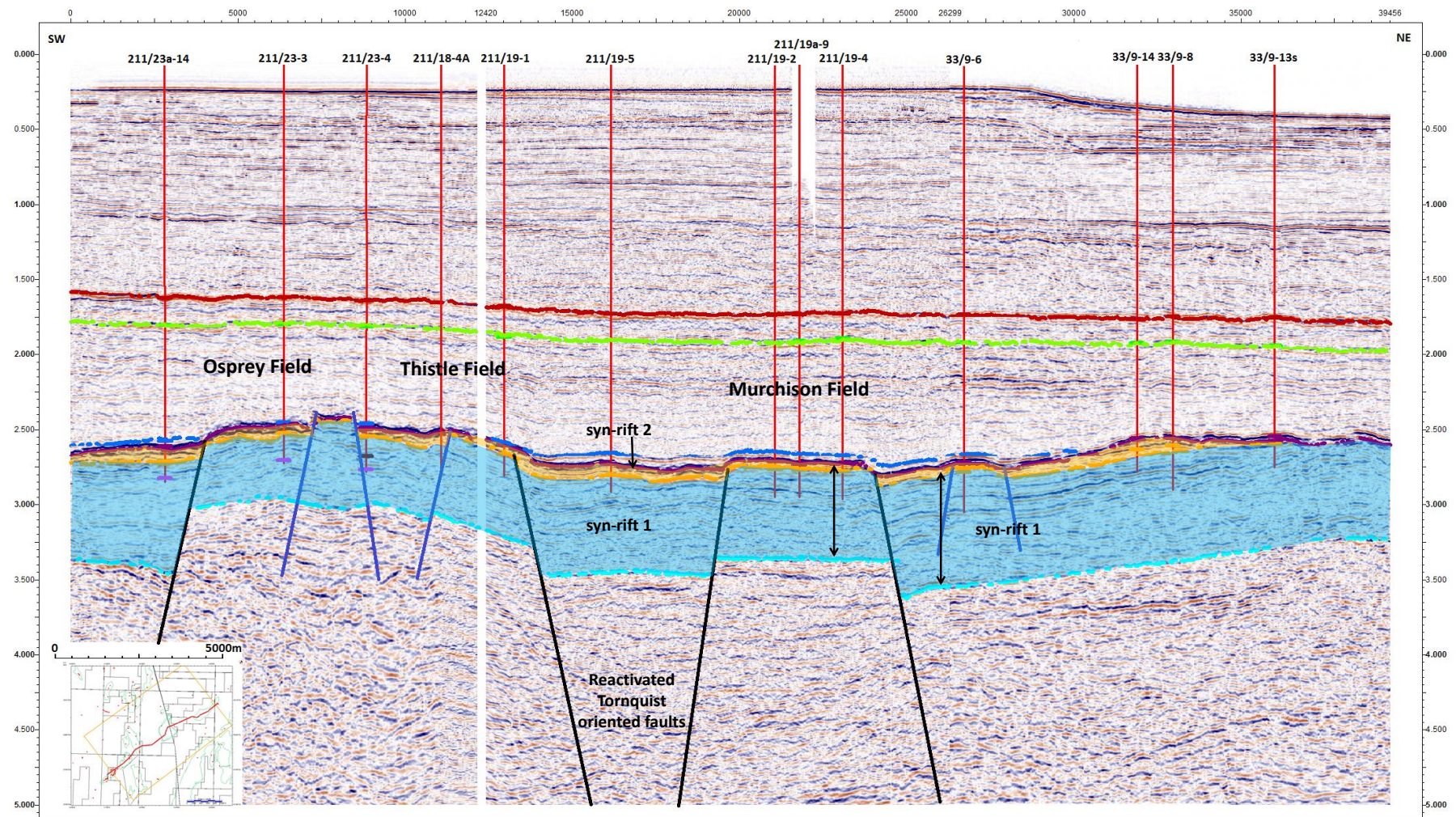


Figure 5-72. Seismic line 4-2 illustrates the large scale Tornquist trending faults cross cutting into the Caledonian trending Upper Jurassic footwall and is responsible for creating the Thistle (west) and the Murchison (east) Fields.

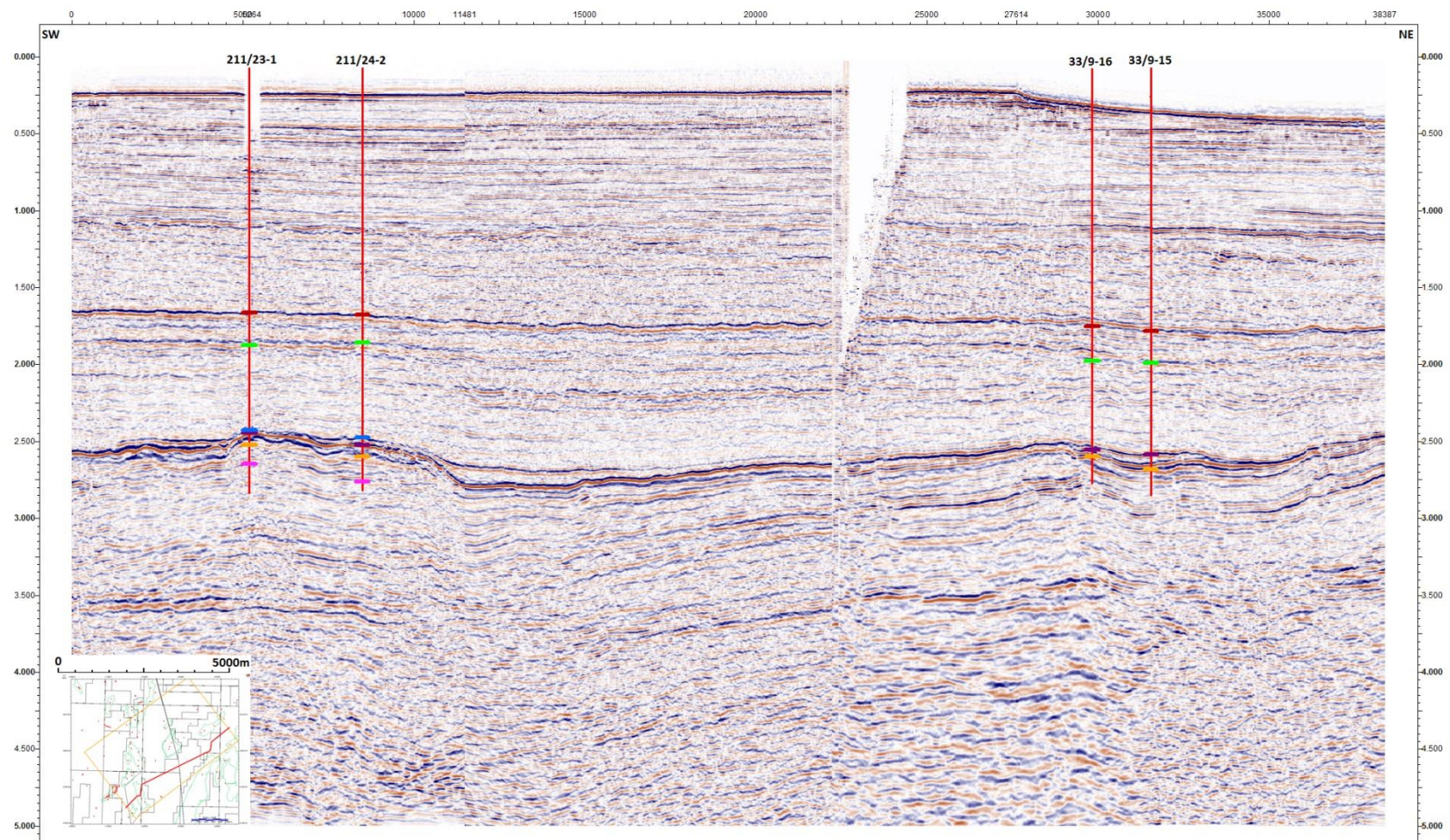


Figure 5-73. Seismic line 4-3 is the furthest southeast of the three strike lines with the majority of the section located in the hangingwall to the large scale Upper Jurassic Normal fault.

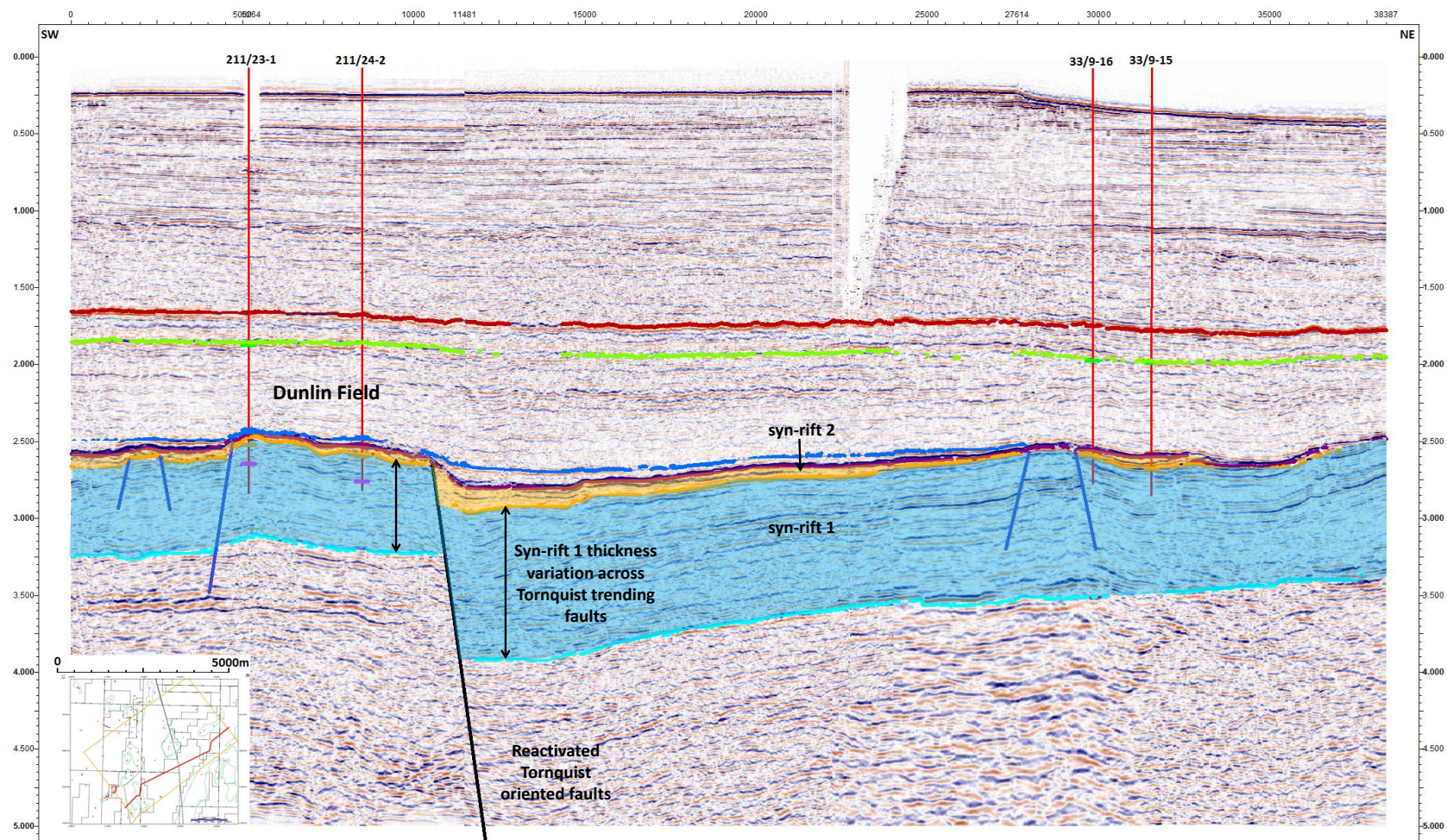


Figure 5-74. Seismic line 4-3 illustrates the large cross cutting fault of a Tornquist trend which has been cross cut by the Upper Jurassic Normal fault. This NW-SE trending fault would have originally been the same fault that bounds the Thistle Field to the NE, but as it is in the hangingwall it creates the Dunlin Field.

It is possible to identify other significant structural highs in Seismic Line 4-2 (Figure 5-71 and 72) such as the Murchison Field. This Upper Jurassic structure is also bound by older Tornquist structure faults. The area between the Thistle and Murchison Fields is a graben and is akin to being a piano key. The structural configuration of horst and graben structures is observed throughout the East Shetland Basin but not necessarily in seismic strike lines. This would suggest that an initial fault system would have been in place which has become dormant, until a later phase of stretching has occurred along a similar stress regime and caused reactivation of these faults.

Seismic line 4-3 (Figure 5-73 and 74) further illustrates the presence of the NW-SE oriented Tornquist faults. Within this region, it is possible to see the Dunlin Field which is bound to the west by a potentially reactivated fault, but is situated in the hangingwall of an NE-SW oriented Upper Jurassic normal fault. It appears that this horst structure that makes up the Thistle and Dunlin Fields may have once been a continuous structure and has since been cross cut by a the reactivation of another fault system in the Upper Jurassic. The orientation of the horst block is roughly NW-SE which is consistent with the Tornquist trend and appears to be cut by a Caledonian (NE-SW) trending fault between the two fields. The structures that are present along these strike lines suggest a combination of reactivation has occurred along two ancient plate systems. Within the Thistle, Dunlin and Murchison Fields it appears that some of the NW-SE trending Tornquist faults have reactivated. But, these faults have also been crosscut by the NE-SW oriented faults in the Upper Jurassic rifting event which follow the Caledonian lineation. The Murchison Field is a prime example of this as its north-eastern and south-western flanks are formed by a Tornquist faults which has reactivated in the Upper Jurassic, whereas the south eastern flank is composed of solely Upper Jurassic faults. The combination of these two fault trends generates the distinct cubic structure that is the Murchison Field.

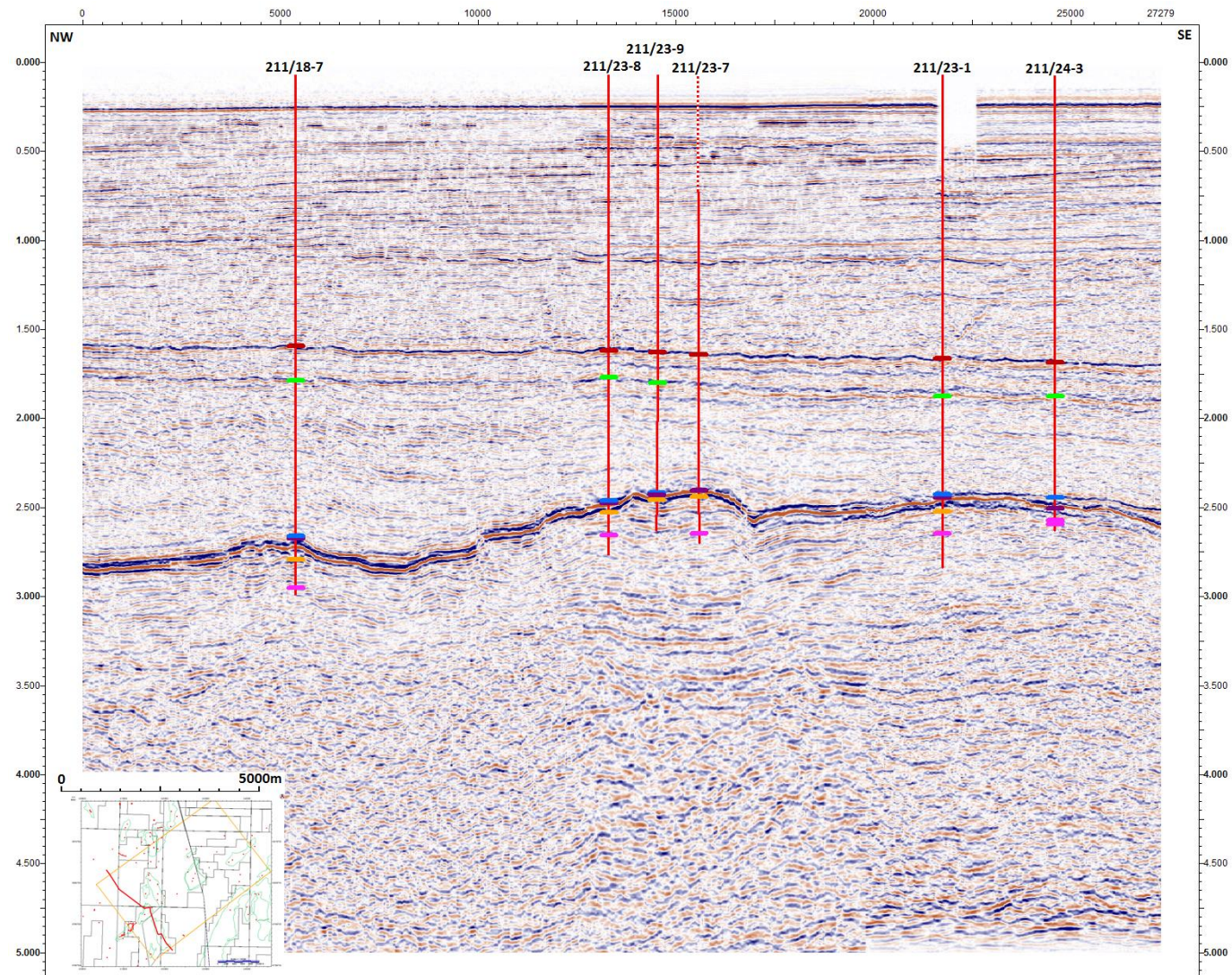


Figure 5-75 Seismic Line 4-4 is a dip line that is situated to the far SW of the study area and passes through the Osprey and Dunlin Fields. Here the Osprey Field can be observed in the centre of the seismic section forming an Upper Jurassic structural high.

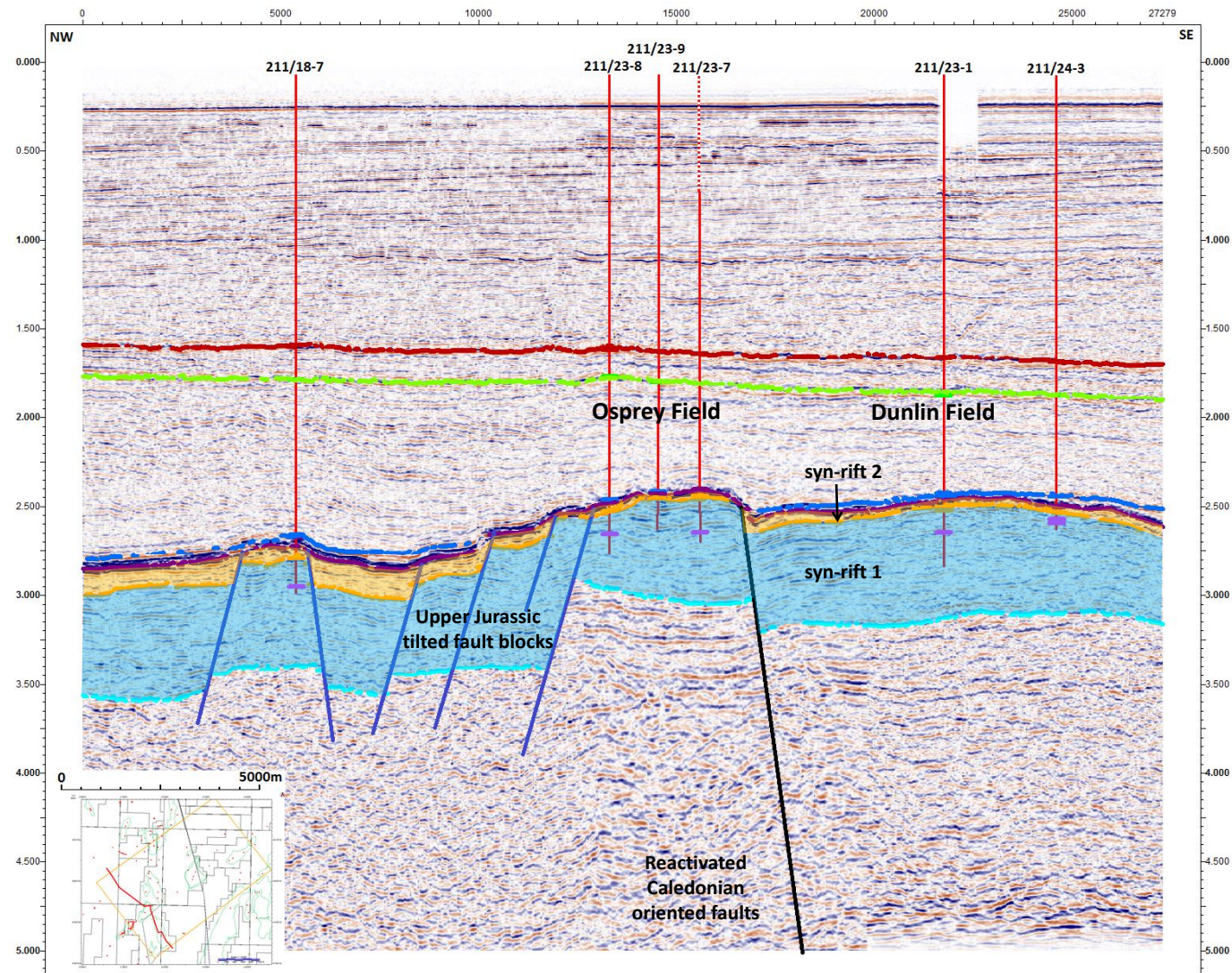


Figure 5-76 Seismic Line 4-4 highlights the syn-rift 1 thickness variation across the reactivated Caledonian oriented normal fault.

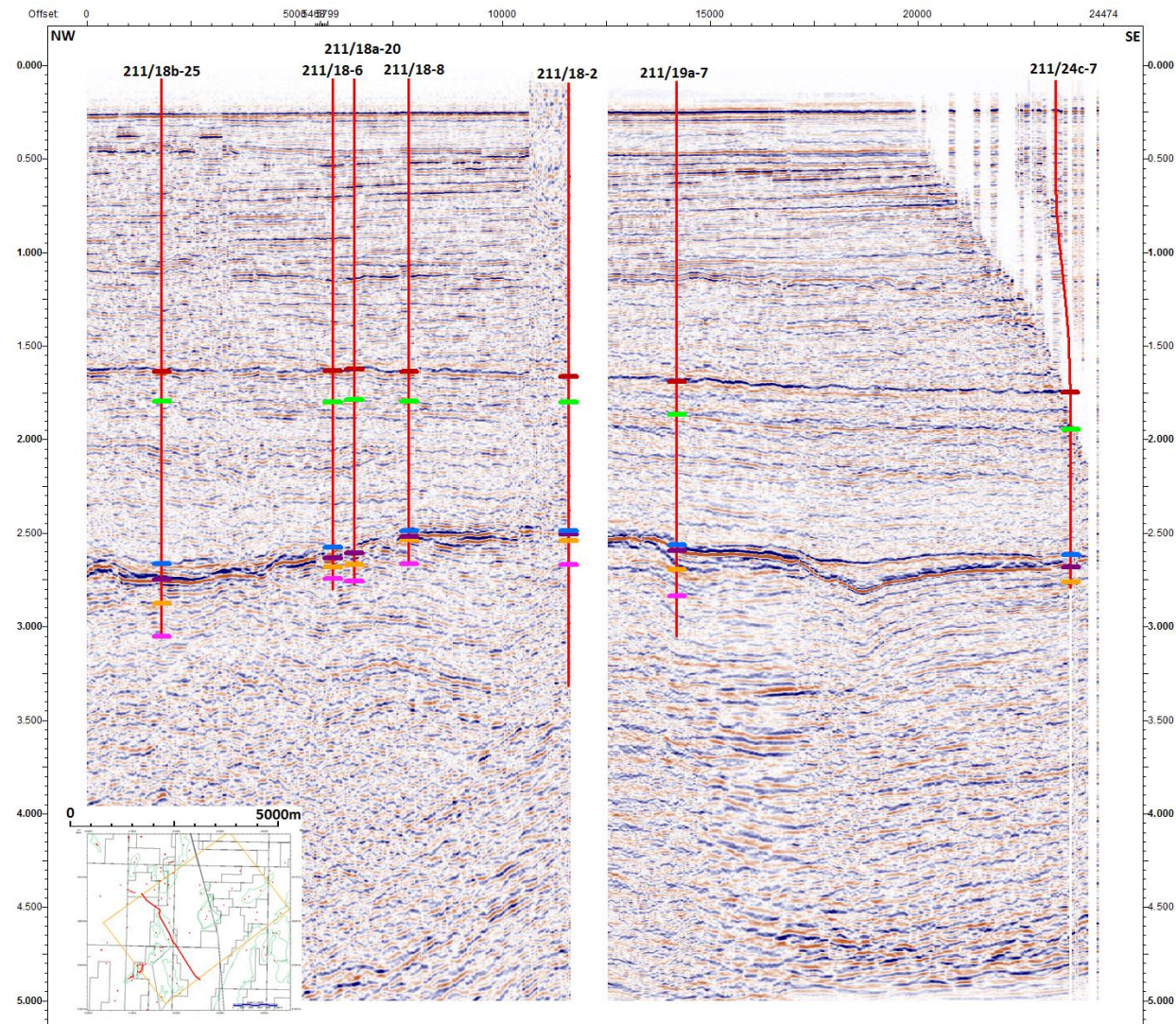


Figure 5-77 Seismic Line 4-5 is also situated to the SW of the dataset and passes through the Thistle Field.

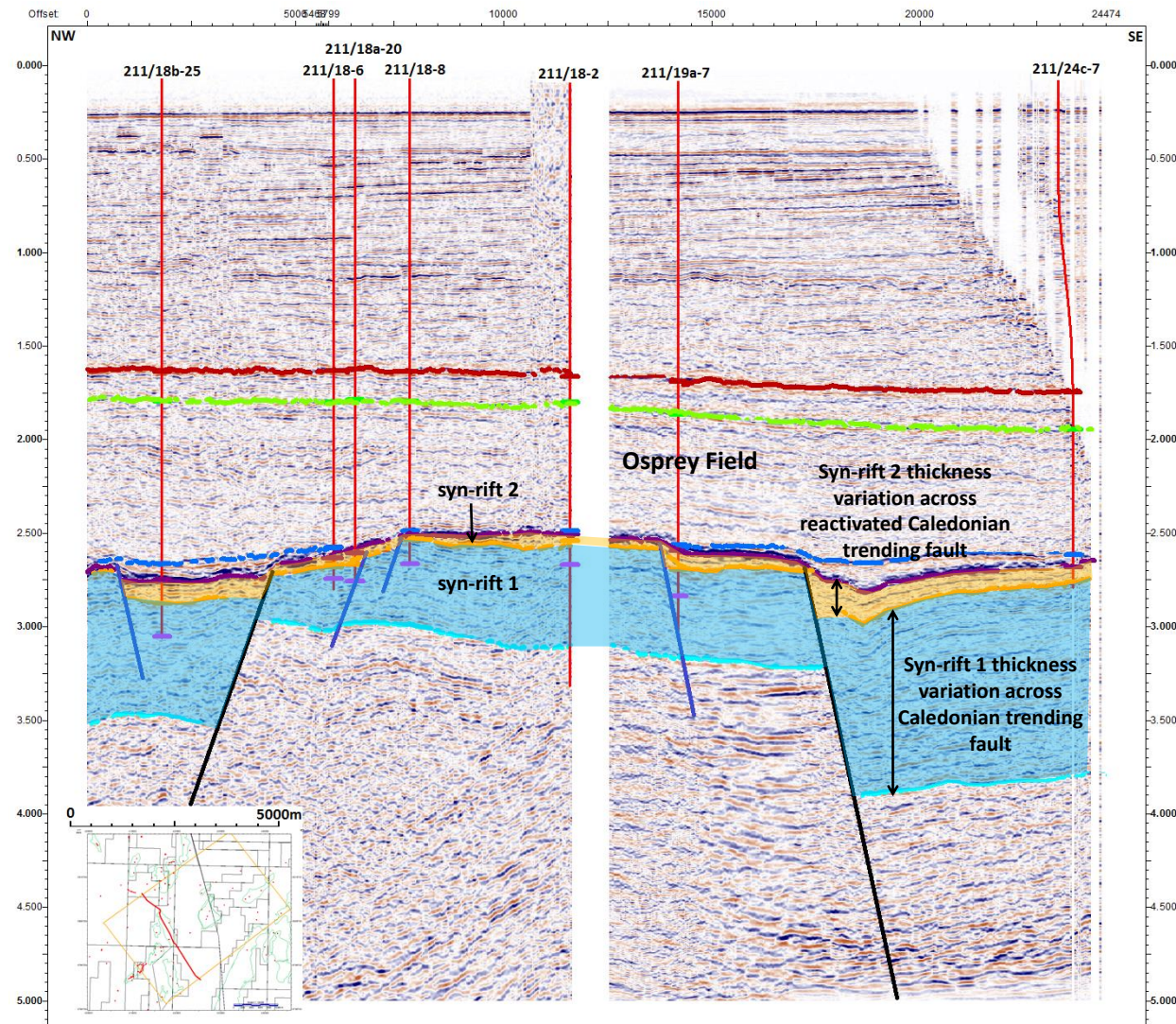


Figure 5-78 Seismic Line 4-5 illustrates that the Thistle location has been a structural high through both the Permo-Triassic and Upper Jurassic rifting events.

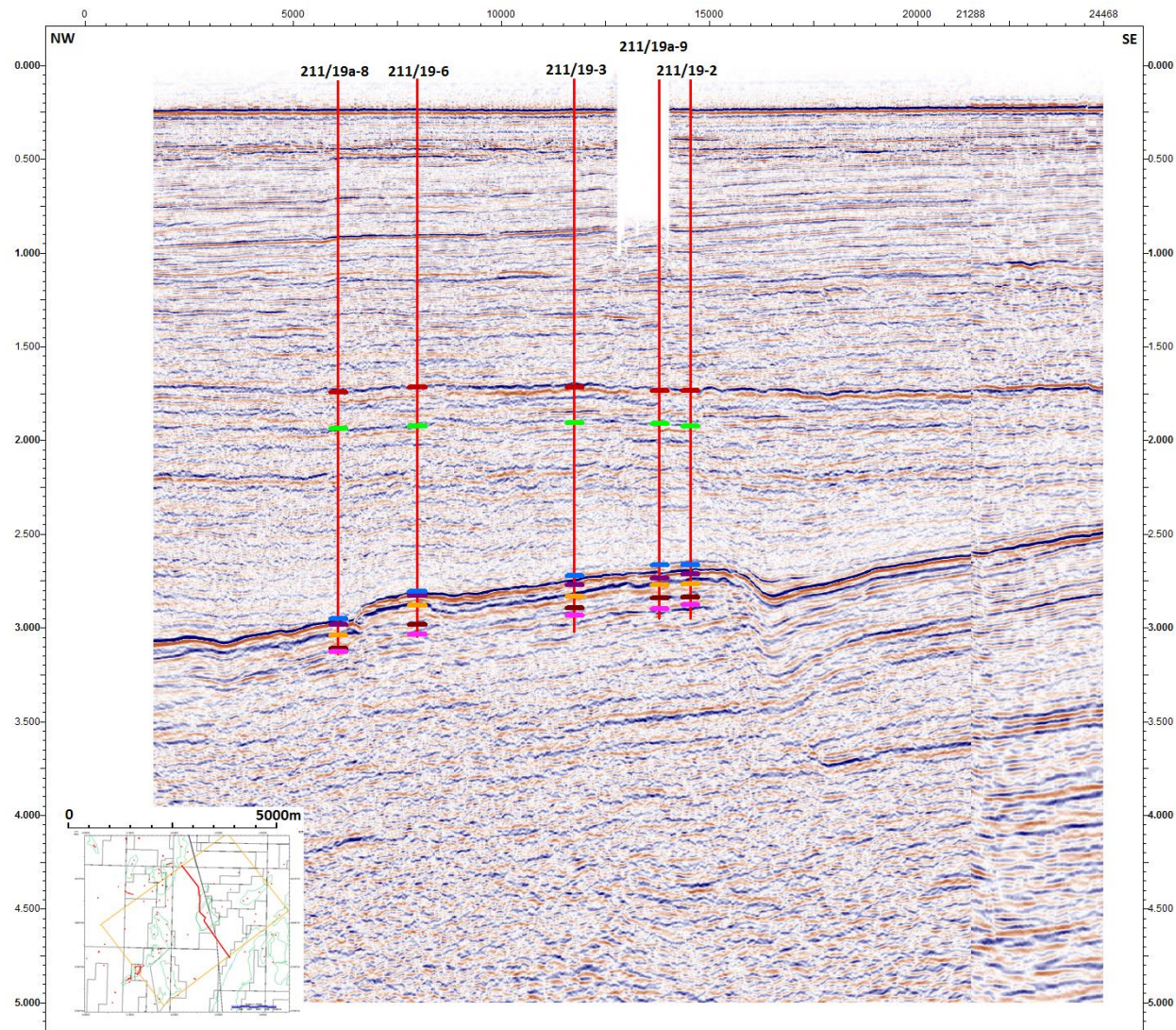


Figure 5-79 Seismic line 4-6 is a relatively central line that passes through the Murchison Field.

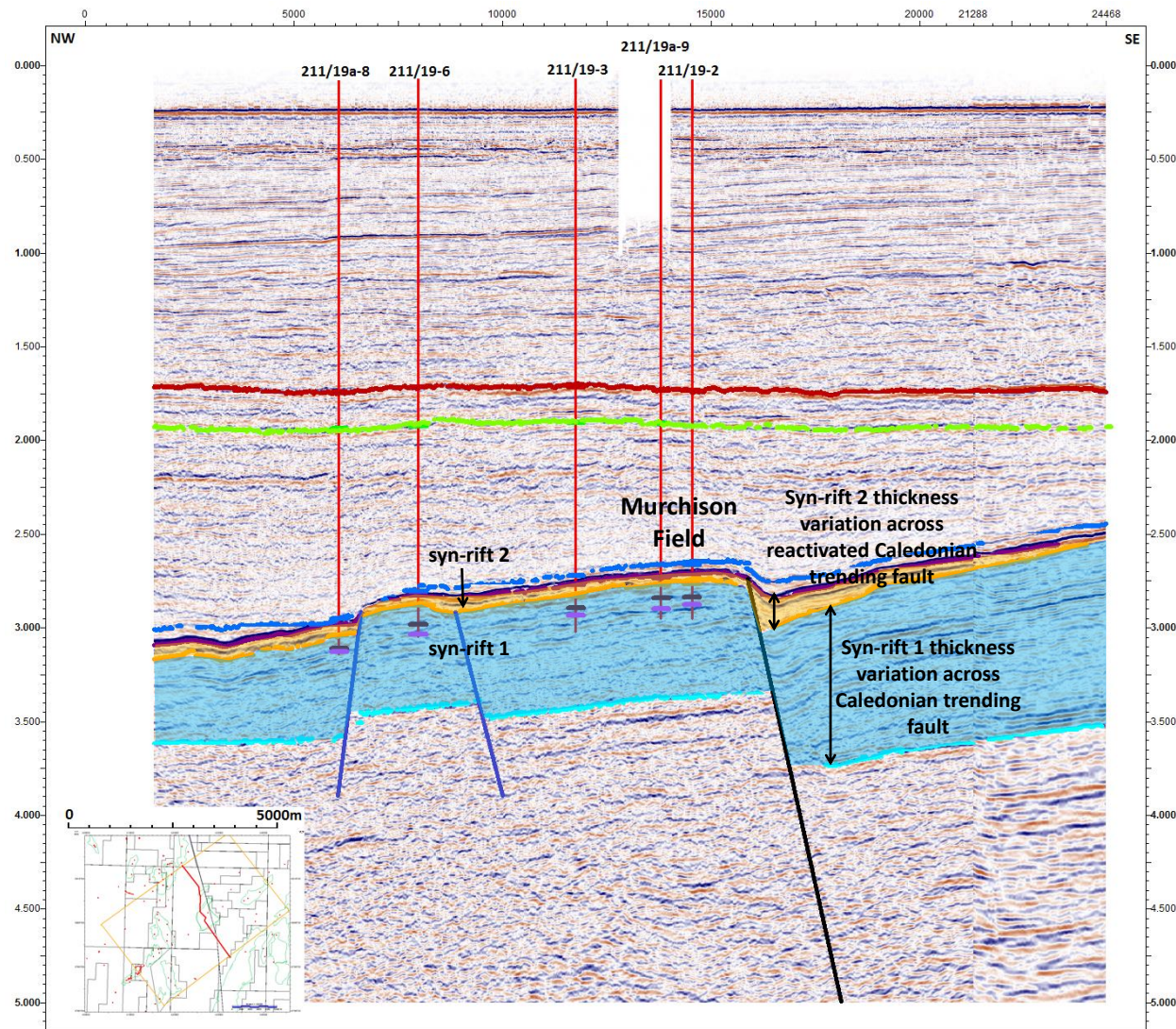


Figure 5-80 Seismic line 4-6 illustrates a large scale fault to the SE of the section is the Caledonian trending fault which bound the field. This structural feature was also a structural high through both the Permo-Triassic and Upper Jurassic rifting events.

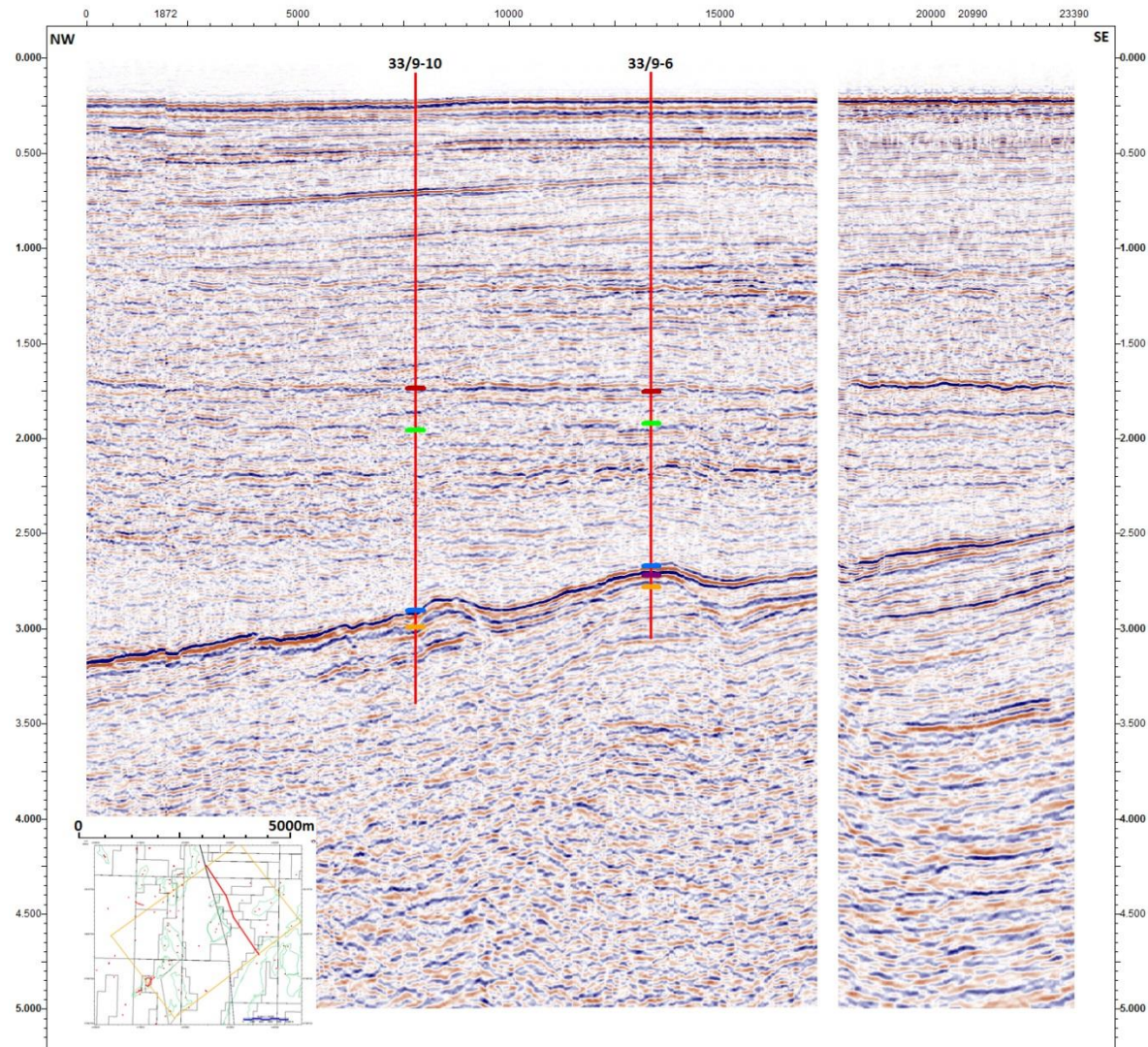


Figure 5-81 Seismic line 4-7 passes through the graben location between the Murchison Field and the Statfjord Nord Field to the NE.

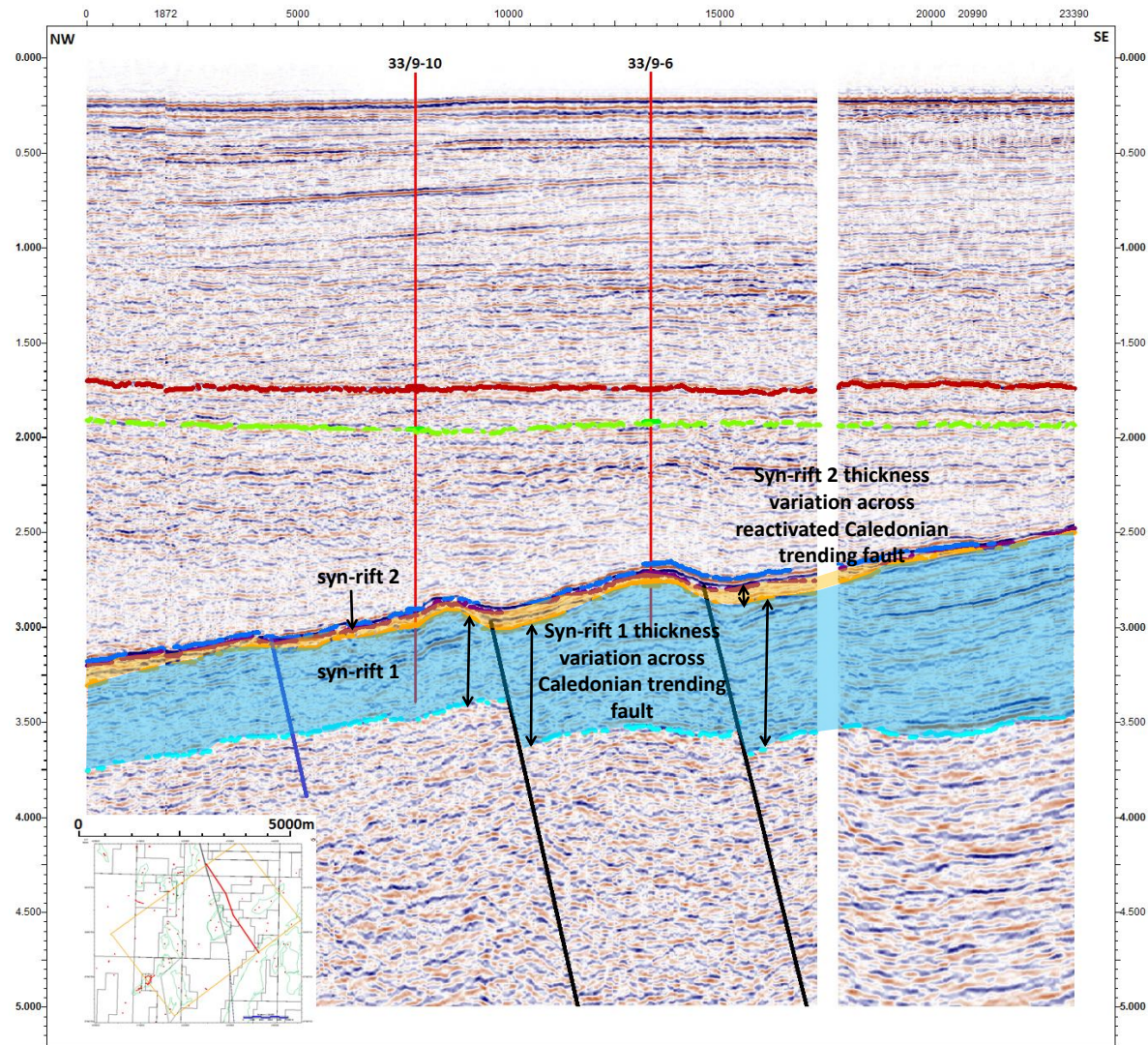


Figure 5-82 Seismic line 4-7 illustrates two sub-dividing sections of the multi-tiered fault block can be imaged in this section. Both of these sections were located in the hangingwall low to a Tornquist trending fault in the Permo-Triassic rifting event but the area to the NW with a thinner covering of Mesozoic sediments is situated in the footwall to the Upper Jurassic normal fault. The area to the SE on the other hand has been in the hangingwall location in both rifting event.

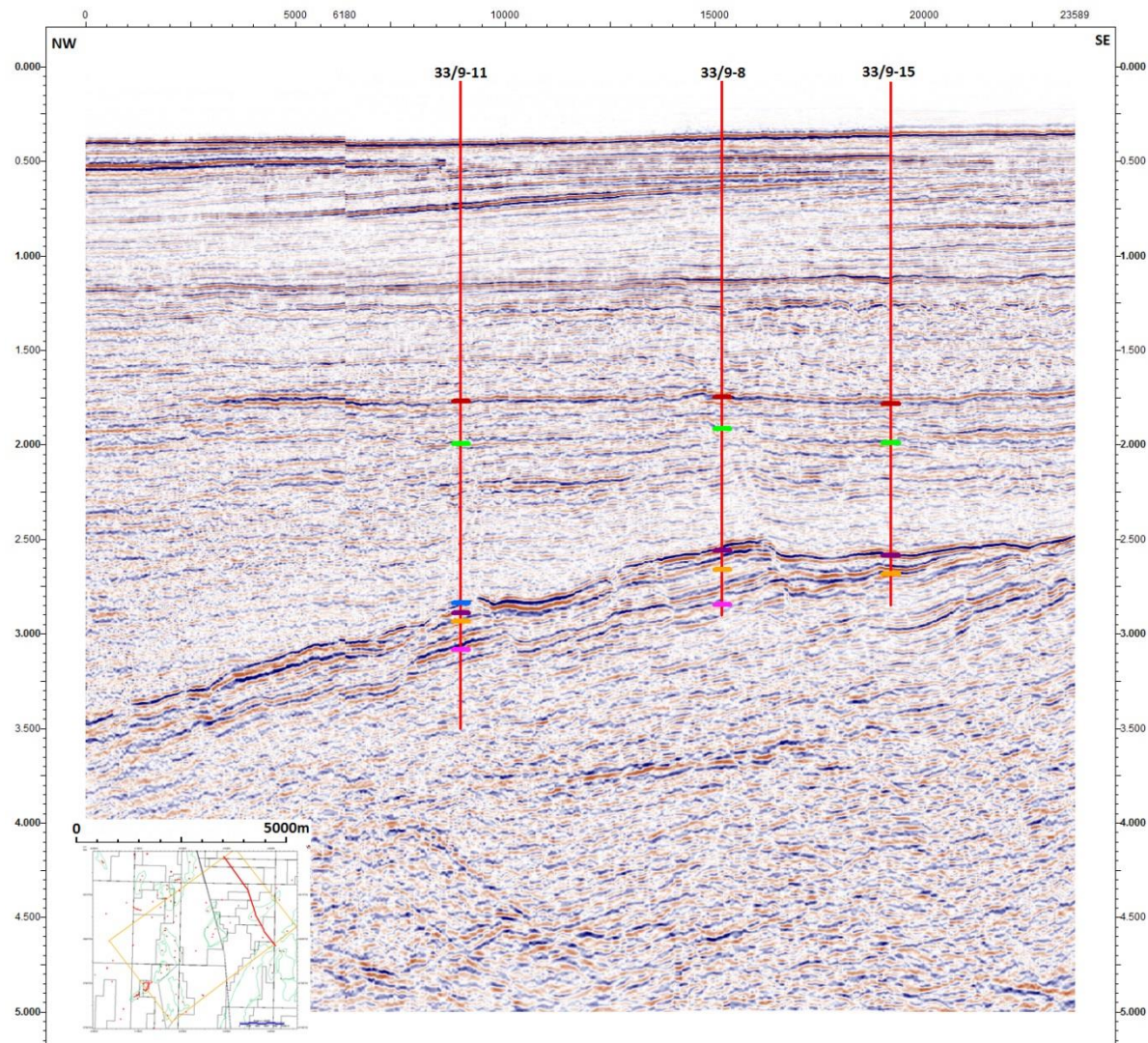


Figure 5-83 Seismic Line 4-8 is situated to the far NE of the study area and passes through the Statfjord Nord Field.

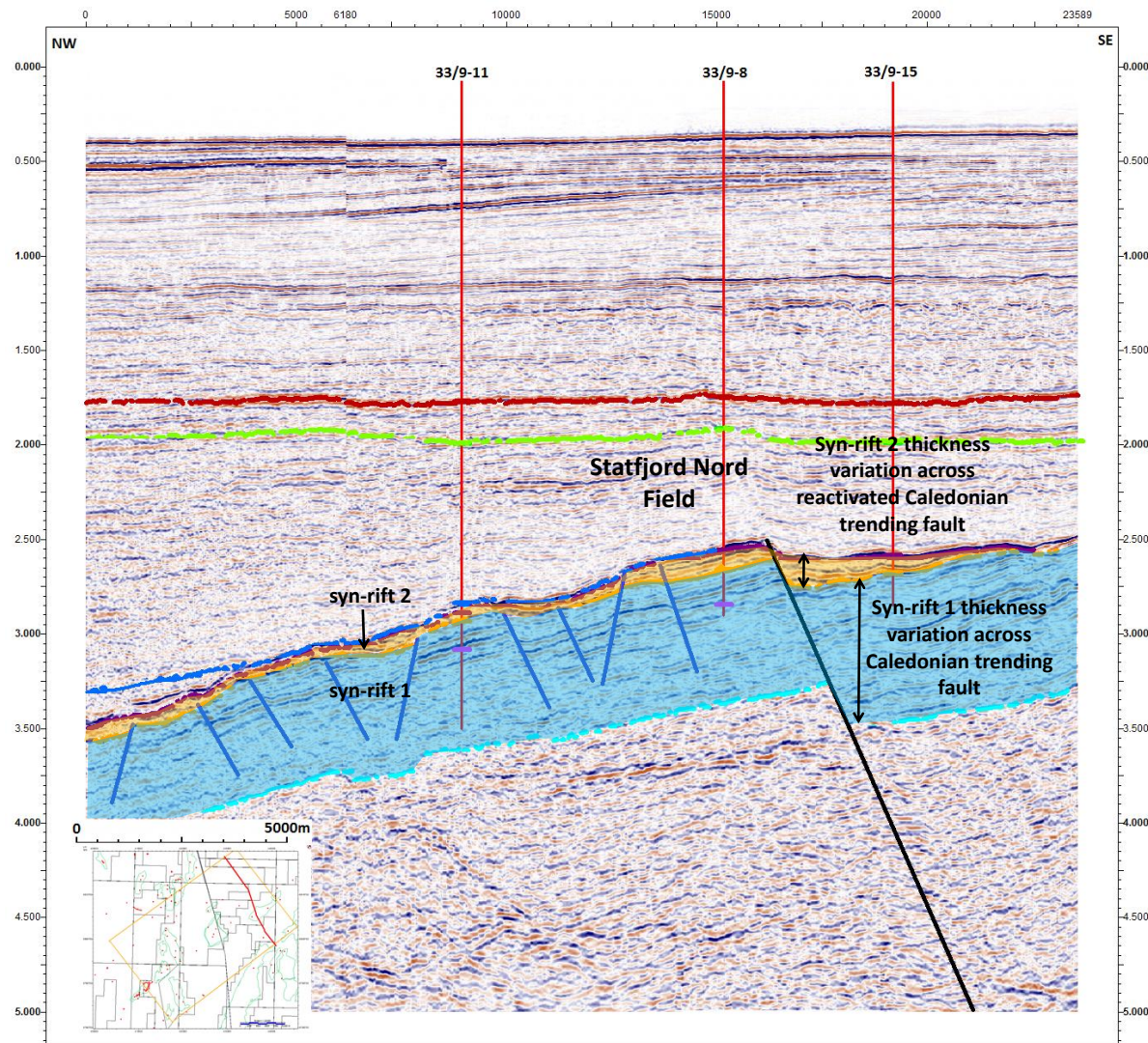


Figure 5-84 Seismic Line 4-8 illustrates that the Thistle and Murchison Fields was also a structural high through both rifting events.

The five dip lines that have been generated over the Causeway to Statfjord area best illustrate the result of the Upper Jurassic rifting and fault plane reactivation. Most of the seismic sections illustrate either a tilted fault block or horst block that generates a hydrocarbon trap in a three-way fault bound closure. In seismic line 4-4 the horst block resembles the Osprey Field. In sections 4-6 and 4-8 the horst block and tilted fault block form the Murchison and Statfjord Nord Fields respectively. These structural features formed due to the Upper Jurassic rifting phase and are bound to the south-west by large scale normal faults.

Seismic line 4-4 (Figure 5-75 and 76) is the south-westerly dip line of all through this area and travels over the Osprey and Dunlin Fields. The fault that separates these two hydrocarbon fields is oriented NE-SW and divided the fields into a footwall and hangingwall domains. The fact that the Dunlin field is a structural trap in the hangingwall location hints at multi-phase rifting. Although this is in a structural low in the Upper Jurassic rifting event, the fault block might not have always been a structural low. As identified in Type 3 rifting it is possible for old structural highs to be cross cut and subside in later rifting events.

The Thistle Field on the other hand is a fault block that has been in a footwall high through rifting on the perpendicular fault trends and such forms a footwall high to both sets (High-High). Seismic line 4-5 (Figure 5-77 and 78) illustrates this with reactivated faults bounding the structure. Within the structure it is also possible to identify some smaller scale Upper Jurassic faults which give structural relief to the high. A significant thickness variation of syn-rift 1 package is also observed across the south-easterly bounding fault. This fault is a NE-SW striking fault which may have initially been active in the Permo-Triassic.

Further structural highs that are located in potential High-High include the Murchison Field, which is illustrated in seismic line 4-6 (Figure 5-79 and 80) the Sigma discovery and the Statfjord Nord Field. A large reactivated NE-SW oriented fault bounds the field to the southeast, whilst smaller scale Upper Jurassic normal faults are located within the high. Unlike the Thistle and osprey Fields there is no structural trap found in the hangingwall to the Caledonian trending fault. This may be related to the lack of reactivation of the Tornquist fault in the Upper Jurassic.

The graben areas in-between these structural highs are illustrated in seismic line 4-7 (Figure 5-81 and 82) which has very little structural feedback. The only faults that are identified within this section are the reactivated faults that bound the Murchison Field. Smaller Upper Jurassic faults are also observed within the section but they have very little offset and occur parallel to the NE-SW trend.

Seismic line 4-8 (Figure 5-83 and 84) is the furthest NE of all the dip lines and passes over the Statfjord Nord Field. This field is similar to the Thistle and Murchison Fields as it too is found in a High-High environment. This field does however have more Upper Jurassic faulting within the tilted fault block which may cause some level of compartmentalisation of the hydrocarbon field. This arrangement of highs and lows as noted earlier can be described like a set of piano keys, where traps form in the uplifted horst structures.

The strike lines imply a fault reactivation of the NW-SE Tornquist trending faults and the dip lines show reactivation of NE-SW Caledonian trending faults. The combination of these two faulting orientations is key in understanding the structural evolution of the Causeway to Statfjord Nord area.

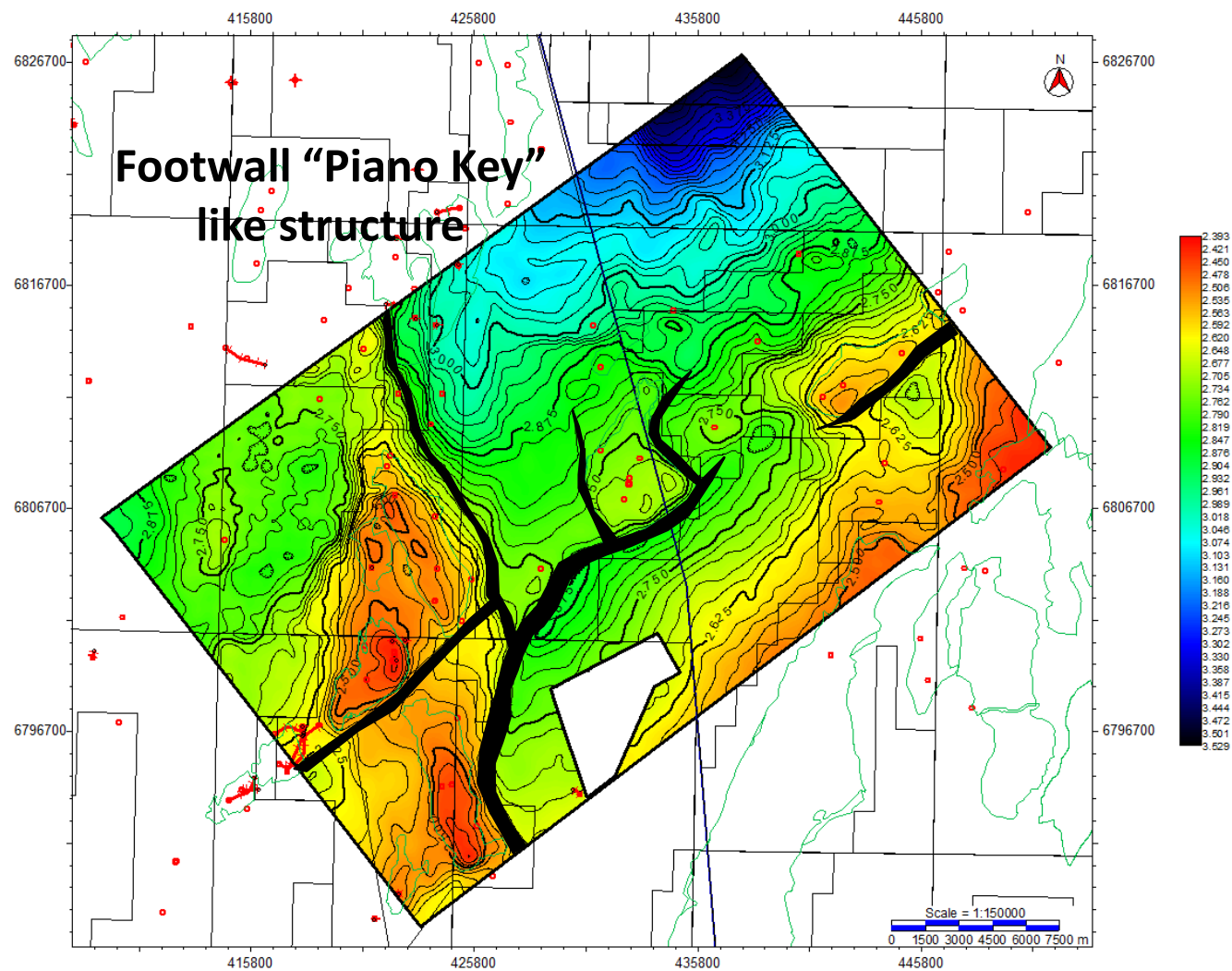


Figure 5-85. Base Cretaceous structure map illustrates a series of highs and lows relating to reactivated faults in the Upper Jurassic.

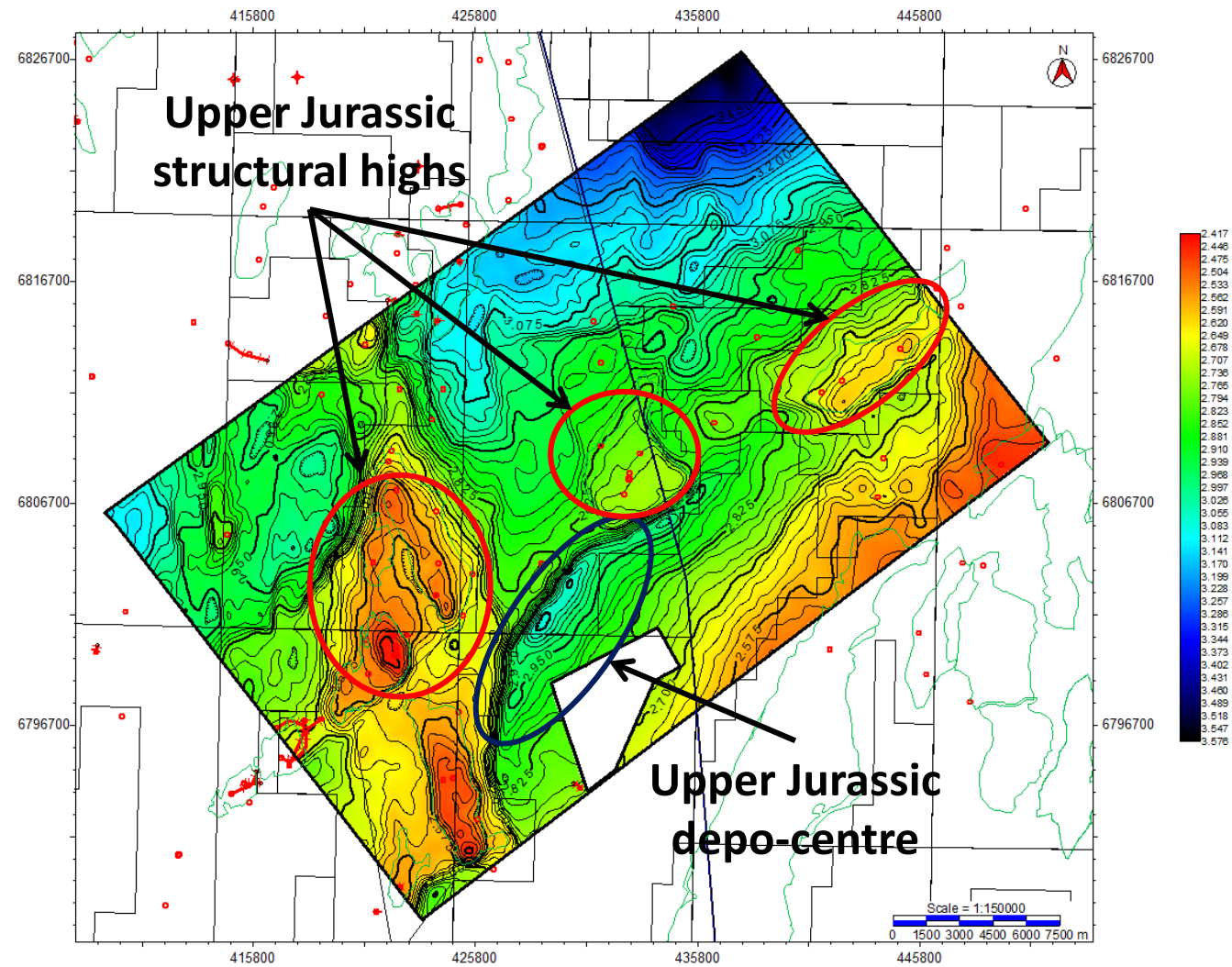


Figure 5-86. Top Brent Structure Map highlights the hydrocarbon fields that have formed as a result of Upper Jurassic faulting.

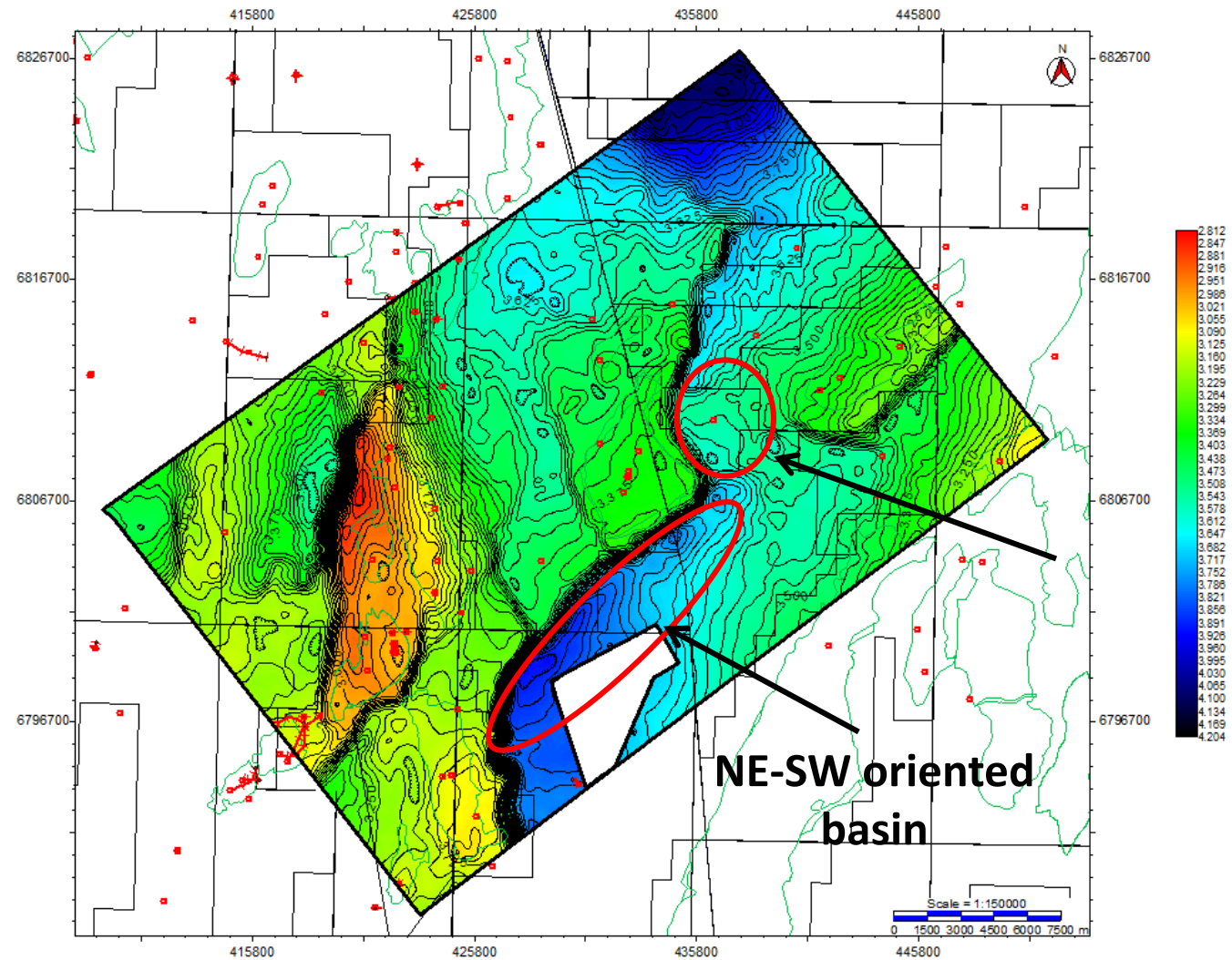


Figure 5-87. Base Syn-rift 1 structure map shows the initial Permo-Triassic depo-centres that were in place prior to Upper Jurassic rifting.

The evolution and reactivation of these fault systems can be seen in the top structure maps of the Base Cretaceous, Top Brent and Base Syn-Rift 1. Each of these maps and the resulting time thickness maps will be able to illustrate the timing of movement for each of these faults and whether or not these faults have reactivated through time.

The Base Cretaceous map (Figure 5-85) shows the full effect of all the rifting events and the effects of reactivated faults. The primary features that can be identified are the NW-SE trending faults that make up the NE limit of the Thistle and Dunlin Fields. This Tornquist trending horst block is however crosscut by a NE-SW Caledonian fault. Other features such as the Murchison Field can be seen along a similar NE-SW trending fault that has moved in the Jurassic, as too can the Statfjord North Field to the eastern part of the study area.

The evolution of faulting in this area can be further observed in the Top Brent and Base Syn-Rift 1 structure maps. The Top Brent structure map (Figure 5-86) further shows the importance of the NE-SW Caledonian and NW-SE trending faults and the role they play in determining the hydrocarbon traps. It has been noted that the Caledonian and Tornquist faults are aligned perpendicular to one another. But, the eastern edge of the Dunlin Field and southern limit of the Murchison Field are comprised from the same fault. These faults were initially separate and grew from the NW-SE Dunlin fault and the NE-SW trending Murchison fault to one singular fault. Although fault growth and linkage is a common occurrence in the East Shetland Basin it is rare that it happens between two faults with perpendicular fault alignments. This results in the dogleg shaped fault that runs from the southern tip of the Dunlin Field all the way through to the Murchison Field.

This dogleg fault can be observed more clearly in the Base Syn-rift top structure map and appears to have grown and linked all the way up to the northeast edge of the Murchison Field. This fault starts to die out after the Murchison Field but, it does show this zigzag fault linkage between multiple oriented faults is possible. Another major fault that is observed in the Top Triassic map is located on the western edge of the Thistle field. This relatively north-south trending fault appears to have initiated in the Triassic and reactivated in the Jurassic Rifting event. This fault is oriented N-S and could have initially formed in the Permo-Triassic, as illustrate in Type 2 rifting where N-S oriented Permo-Triassic fault play an important role in the fault evolution.

The Base Syn-Rift 1 structure map (Figure 5-87) also shows the effect of the NW-SE Tornquist trending normal faulting. The NE and SW edges of the Thistle and Murchison Fields illustrate the reactivation of this faulting trend although there is significantly more offset observed elsewhere in the study area. These faults appear to be cross cut by the zigzagging fault but still play an important role in determining important structural highs that can trap hydrocarbons.

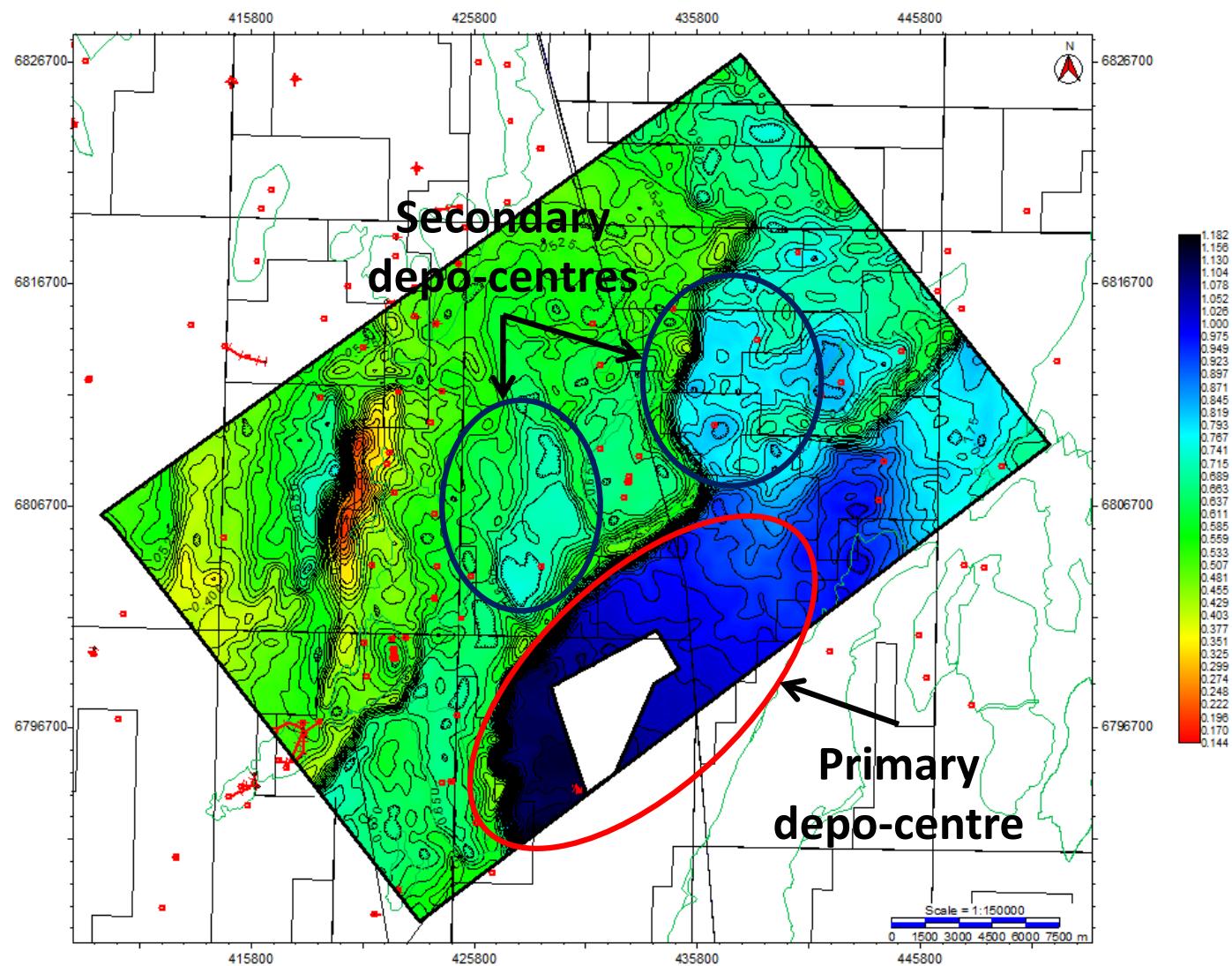


Figure 5-88. BCU to Base Syn-rift 1 isochron map shows the location of the depo-centres for both rifting events throughout the study area.

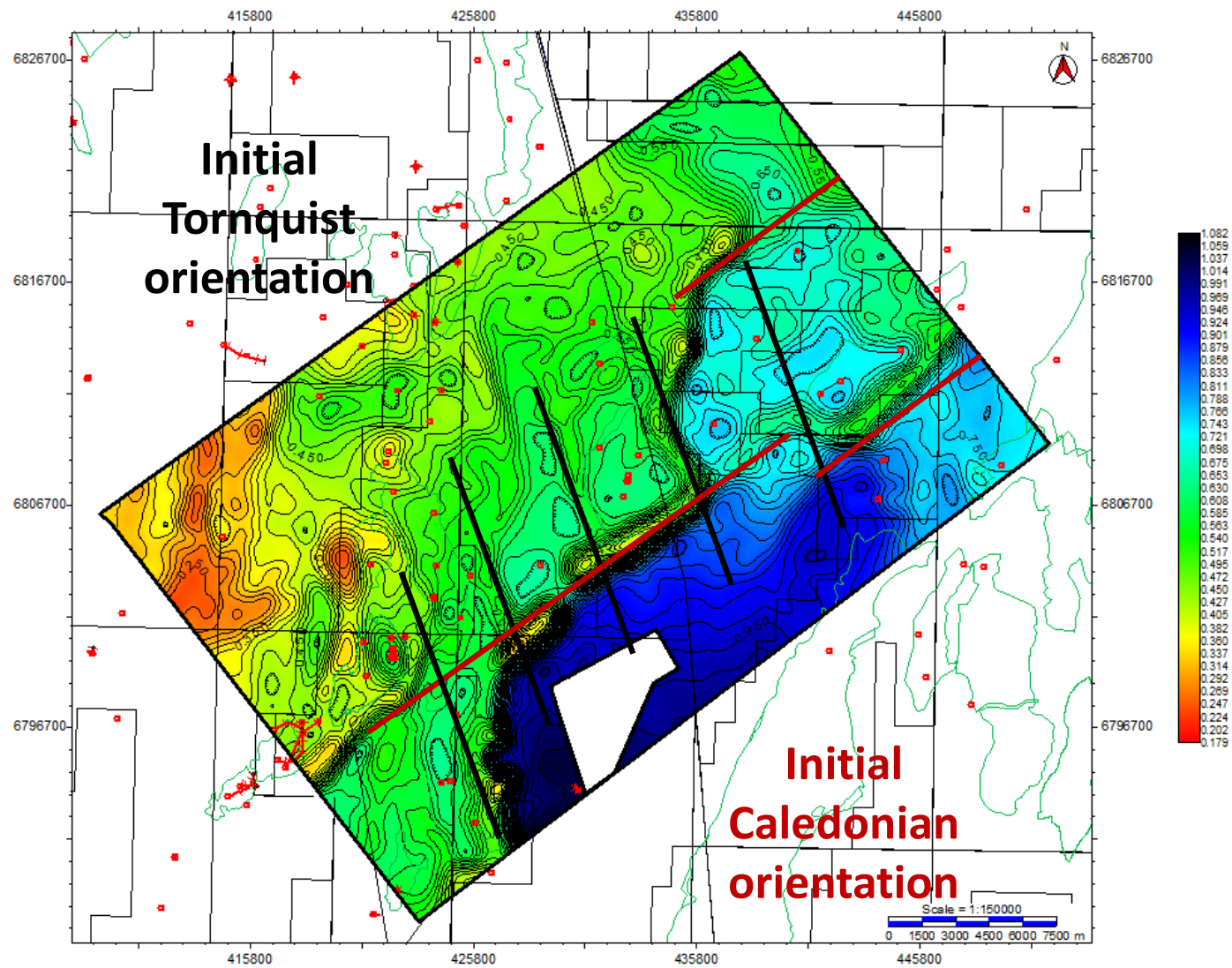
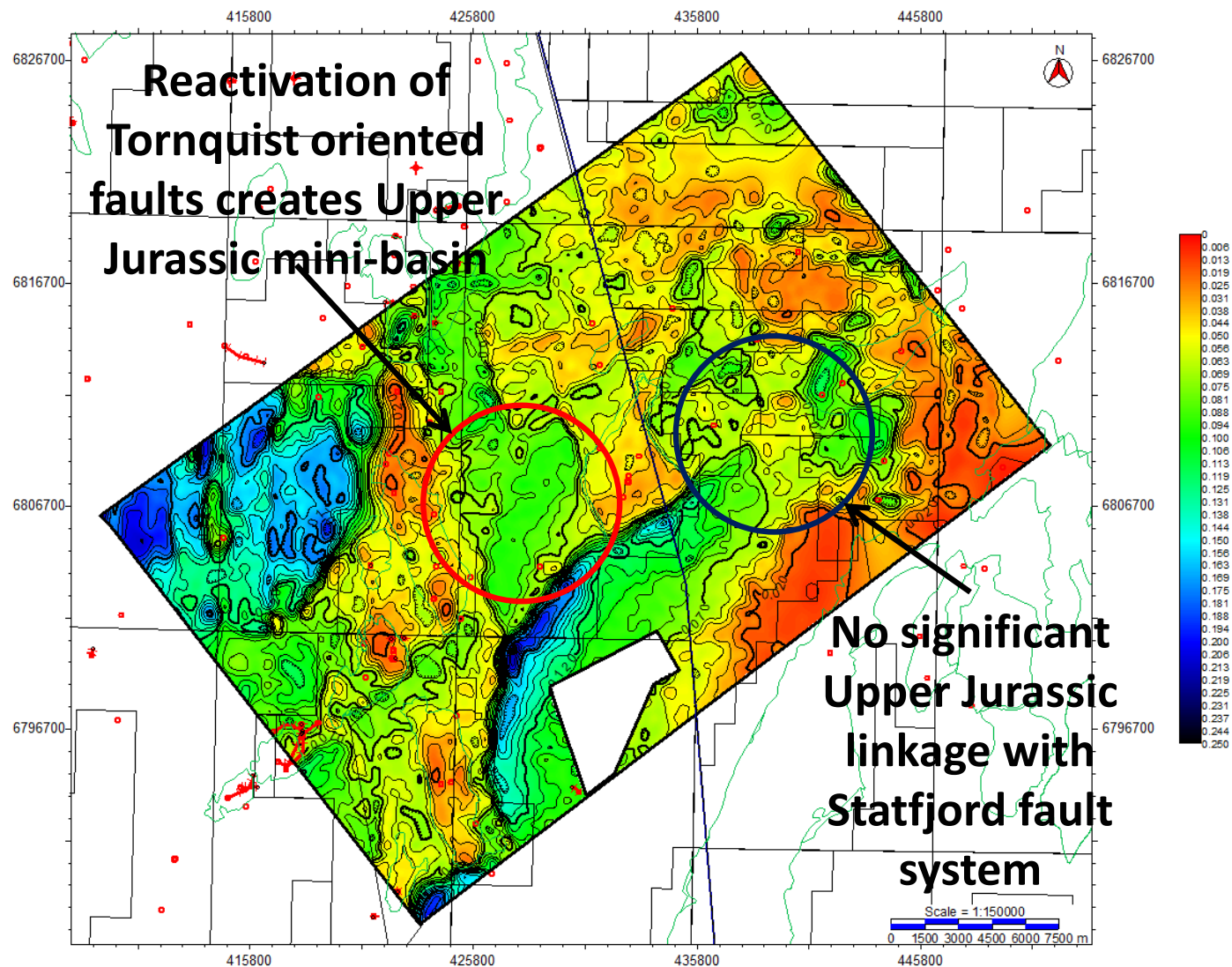


Figure 5-89. Brent Group to Base Syn-rift 1 isochron map illustrates the reactivation of the Caledonian and Tornquist faults in the Permo-Triassic.



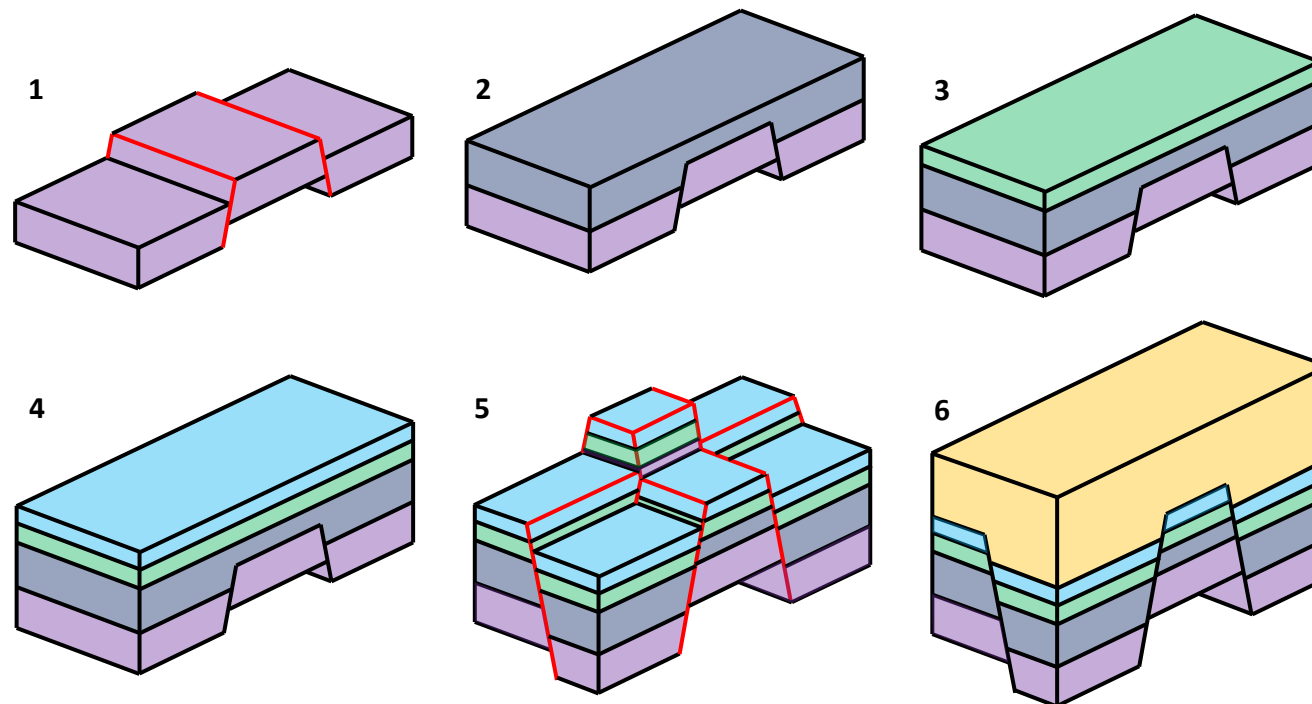
From each of these top structure maps a series of time thickness maps have been generated to illustrate thickening packages at separate rifting events. The overall thickness map from BCU to Base Syn-Rift 1 (Figure 5-88) shows the results of both rifting events and brings out the major faults in the study area. The main faults observed throughout the area are similar to those seen in the Triassic Top structure map. The largest of these faults is the zigzagging fault which runs from the Dunlin to Murchison Fields. It appears that this fault has been reactivated in both the Triassic and Upper Jurassic rifting events. This thickness map agrees with the idea of fault linkage between Caledonian and Tornquist trending faults. This linkage appears to depend upon the fault polarity and if the fault block would be subsiding or lifting in the same orientation from both faults. This fault system is heavily identified throughout the Top Brent Group to the Base Syn-Rift 1 thickness map (Figure 5-89). However, some features that are observed in this time map are artefacts of the map generation and not related to the underlying geology. These are ridges which form where there is inconsistent overlap between the two structure maps; an example is located on the south-eastern edge of the Statfjord Field.

The Base Cretaceous to Brent isochron map (Figure 5-90) illustrates the effects of faults that moved purely during the Upper Jurassic Rifting event. Here it is possible to see that the major zigzag fault identified in the previous thickness map has moved during Jurassic times, but not to the same extent. It is also possible to observe other faults surrounding the Thistle and Murchison Fields that have moved during this rifting period. Other large scale fault movement can be observed on the western edge of the Thistle fault. This would suggest that this fault has reactivated in a Type 1 style and moved in both the Permo-Triassic and Upper Jurassic. Smaller scale fault movement within the BCU-Brent time thickness map can be associated to the Caledonian trending fault which separates the Causeway, Osprey and

Thistle Fields in a footwall location to the Dunlin Field in a hangingwall location. Further footwall faults are observed between the Thistle and Murchison Fields which gives the piano key appearance that was noted in seismic line 4-2. The normal faults that are situated on the eastern edge of the Thistle Field and the western edge of the Murchison Field create a graben location between the two fields in the footwall of the major normal fault. These normal faults appear to have an underlying trend that has been cross cut by the major fault. This is illustrated by the presence of the major depocentre in the hangingwall of the major fault. It is possible that the depocentre location has been influenced by the underlying fault patterns.

This location therefore shows a complex level of reactivation, linkage and fault interaction. The way in which the lineations of two separate plate cycle and two rifting provinces interact is key into understanding the evolution of the East Shetland Basin. Where these faults reactivate large offsets can be observed, although it is possible for some faults to have moved in one rifting event and not another. This can be key into understanding the petroleum system and trap formation.

This is the fourth type of cross rifting (Figure 5-91 and 92) that can be observed in the East Shetland Basin. Within this area the greatest amount of structural feedback can be observed. The main feedback can be observed around the centre of this study area around the Murchison Field, where NE-SW Caledonian trending faults have been crosscut by NW-SE Tornquist trending faults. These faults are perpendicular to one another which results in a combination of reactivation and cross-cutting faults. This leads to the study area being described as a multi-rifting event in which fault strike is perpendicular, fault polarity is mixed and there is partial reactivation of existing faults.



Type 4 Rifting.

1. Permo-Triassic faulting
2. Triassic Sedimentation
3. Early Jurassic Sedimentation
4. Middle Jurassic Sedimentation
5. Upper Jurassic Faulting
6. Cretaceous Sedimentation

pre-rift 1
syn-rift 1
post-rift 1
pre-rift 2
syn-rift 2
post-rift 2

Figure 5-91 Schematic diagram of the evolution of Type 4 rifting.

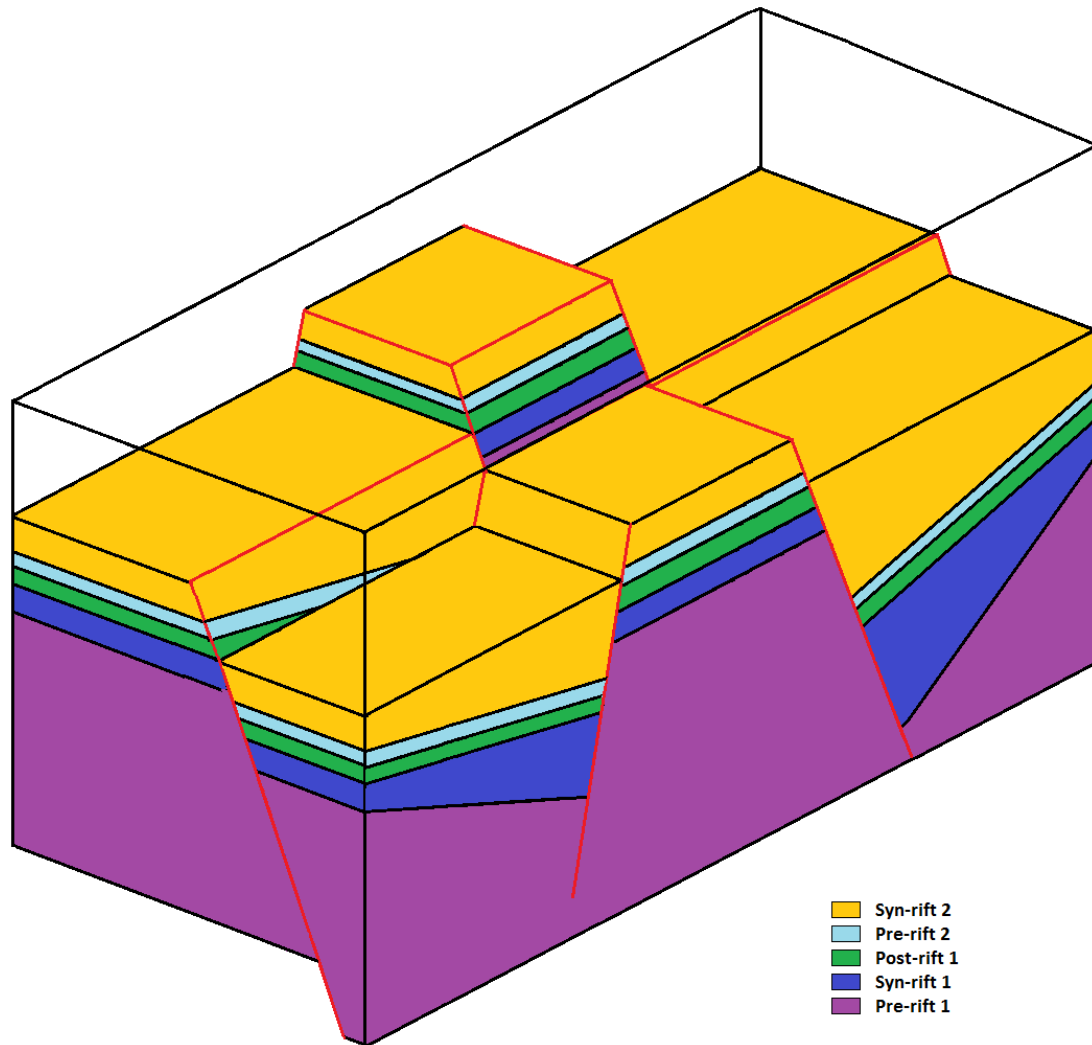


Figure 5-92. Box diagram of Type 4 rifting around the Murchison Field.

The Murchison Field has been the location of a structural study previously by Young et al (2001). Within this study the Murchison Field and the surrounding area were explained as an Upper Jurassic growth and linkage fault system.

Work around the Murchison Field led Young et al (2001) to propose a simple model of fault growth and segment linkage to explain that fault and subsidence patterns observed along the major fault systems between the Murchison and Statfjord Nord Fields. The model states that the NE-SW

oriented fault that bounds the Murchison Field to the southeast grows towards the Statfjord Field to the northeast. As faults that relate to the Statfjord Nord Field grow to the southwest a relay ramp forms between the two sets of faults and as the faults continue to grow a linking and relay breaching “jog fault” forms between the two faults to make the faults one. This new fault strand then continues to move as one through the Upper Jurassic.

The evolution of the Murchison Field has been earlier described as an example of Type 4 rifting (Chapter 5.3.4) and the evidence from the work undertaken by Young et al further supports the evidence for the multi-block theory. One of the seismic lines used in the paper is shown in Figure 5-93 and runs parallel to the NE-SW field bounding fault. This seismic line is located in the hangingwall wall to the main fault and the jog fault is positioned as the western boundary to the Statfjord Nord Field. It is possible to observe a thickening of Lower Jurassic Dunlin sediments across this NW-SE oriented fault thus demonstrating its role as a Triassic-Lower Jurassic extension precursor. It may further be possible from its disposition relative to other structures to say that this fault is located in the position of an older Permo-Triassic fault that follows the Tornquist trend. This would create a graben structure similar to that seen between the Thistle and Murchison Fields.

By superimposing the Permo-Triassic Tornquist trending fault onto Upper Jurassic thickness maps, it is possible to see that the underlying faults have influenced Upper Jurassic fault patterns. The Heather Formation appears to thicken along the complete length of the fault from Murchison Field all the way along to the Statfjord Field in the NE. However, the Draupne Formation time thickness map is slightly different. Here it is possible to demonstrate that the main depo-centre of the fault is located at the Murchison Field and

thins towards the Statfjord Field. This would suggest that the NW-SE oriented fault which makes up the NE edge of the Murchison Field has reactivated in the footwall. By the zig-zag fault reactivating in the Upper Jurassic footwall, the depo-centre that was located along the length of the NE-SW striking fault has been shifted to the NE edge of the Murchison.

A very subtle change in thickness also occurs along the NE-SW trending fault thus showing the effects of the under lying Tornquist faults. Like in the Thistle and Dunlin Fields where a Permo-Triassic horst has been cross cut by a NE-SW trending fault both locations remain a structural high. Although the Murchison Field and it opposed area is not on the same scale as the Thistle and Dunlin Fields, it is therefore possible to demonstrate the effects of a smaller scale horst block in this area. The Heather thickness map from the Young et al paper shows a thinning of sediment in the Upper Jurassic hangingwall where the cross cut horst structure would be located. This further illustrates the effects of the underlying faults and their implication on Upper Jurassic faulting.

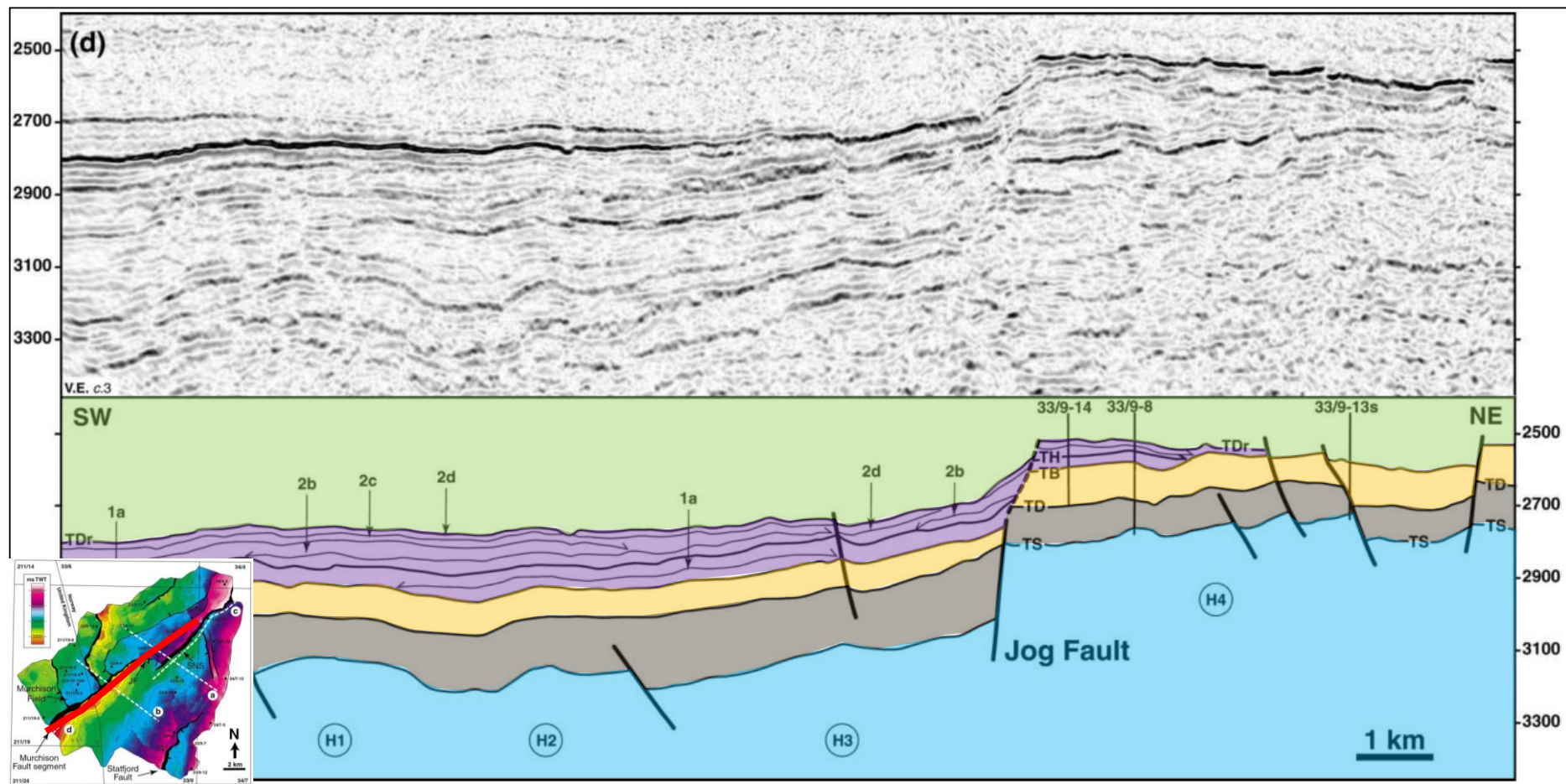


Figure 5-93 Seismic line from Young et al illustrating thickening of Lower Jurassic Dunlin sediments against the jog fault. This would suggest that an older Permo-Triassic fault is in place to cause this thickening (Young et al 2001).

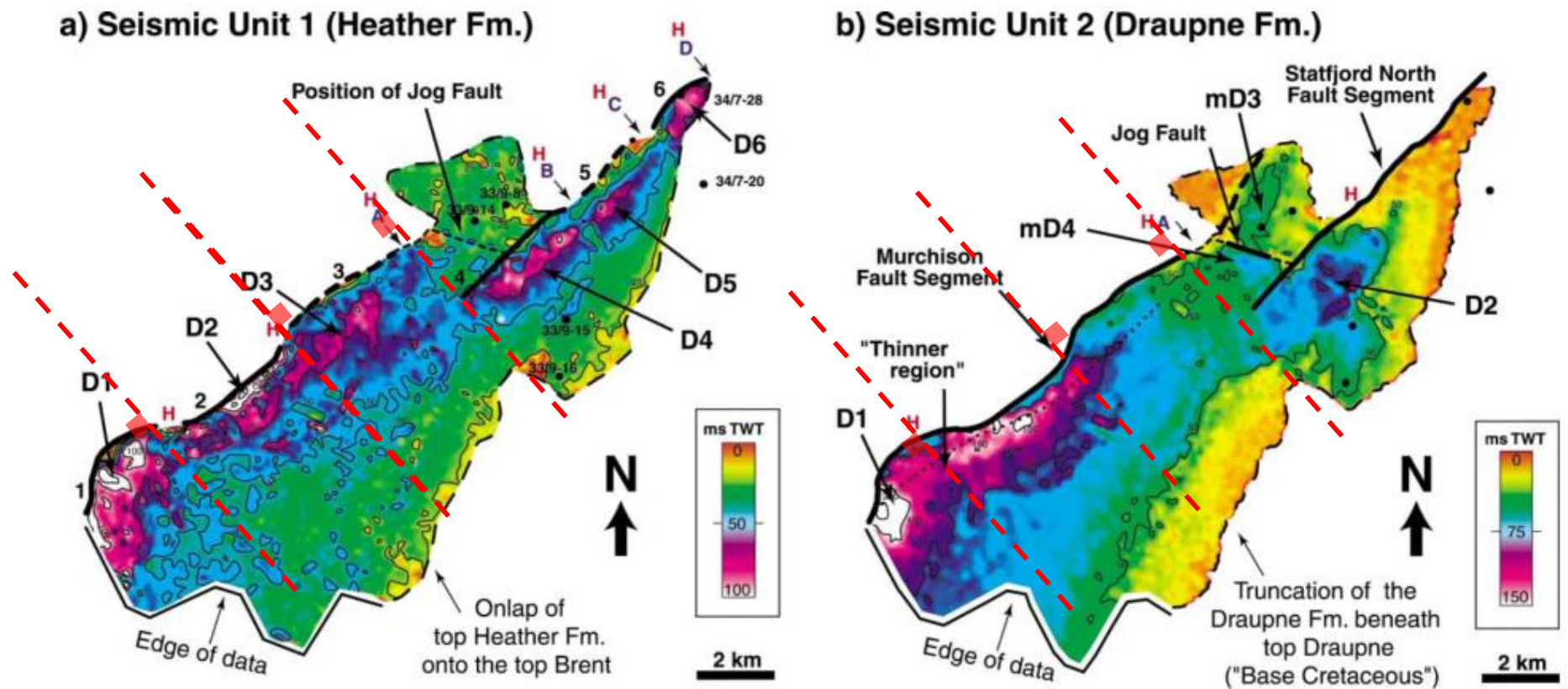


Figure 5-94 Illustrates two isochron maps used in the Young et al paper to explain the depocentre evolution through time. On these maps the underlying Permo-Triassic Tornquist trending faults have been superimposed on and match up with the Upper Jurassic depo-centre (Young et al 2001).

Although no thickness maps for the footwall location are shown in Young et al's paper, clear evidence of its occurrence and thickening can be clearly observed there (Figure 5-94). Its occurrence and thickening package can be related to the hard linking of normal faults along the Caledonian and Tornquist trends. By creating a well section from the Thistle Field through to the Statfjord Nord Field it is possible to observe the earlier identified piano key style of structures (Figure 5-95). This linkage area to the northeast of the Murchison field is key in understanding the evolution of the Murchison area. This location is subject to NW-SE oriented normal faulting in the Triassic, which leaves a trend of weakness that has the potential to reactivate in a later rifting event. As faults align vertically from rift to rift, if they have the same polarity it is highly likely that this fault trend has reactivated opposed to the formation of release faults.

The underlying structural trend as shown in Figure 5-93 shows a large northeasterly dipping normal fault where the fault in the Upper Jurassic fault is located. In the Triassic this fault is part of the master fault which determines the sediment distribution through the Permo-Triassic rifting phase. The reactivation of this fault in the Upper Jurassic could also be that of a Master fault and not a subsidiary fault. This would suggest that the NE-SW oriented normal fault would grow to the NE, but when the Permo-Triassic fault reactivates the orientation of the fault changes and a kink is created along the fault. This would suggest that the linkage area to the northeast of the field is a failed relay-ramp due to the relocation of the master fault. It may be plausible that the master fault started to form a relay ramp, but the reactivation of the Permo-Triassic fault shifted the location of subsidence and uplift. This would challenge the general idea of the Murchison Field formation pointed out by Young et al. (2001) which identifies the Murchison Upper Jurassic master fault to have hard linking with the Statfjord Nord master fault to the northeast.

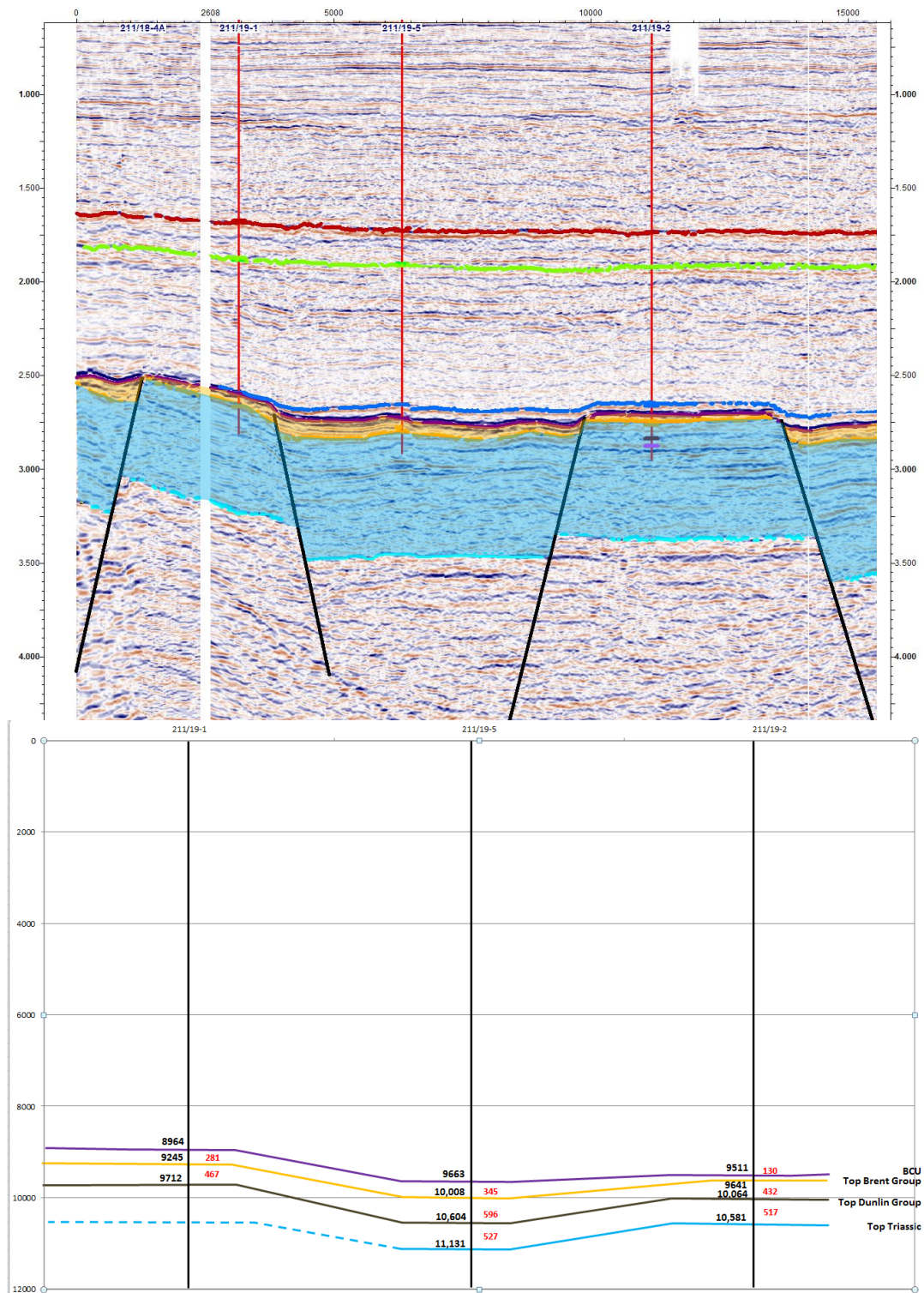


Figure 5-95. Well section through the Thistle and Murchison Fields show a subtle difference in thickness between the stratigraphic units corresponding to separate rift sequences. The numbers in black represent the depth (ft), whereas the figures in red represent thickness. Here it is possible to see a thickening within the footwall of these fields a thickening trend can be observed in the graben area, which suggests that faulting must have been active prior to the upper Jurassic.

This evolution of the Murchison area, which suggests that older faults are reactivating, as opposed to release fault forming can be further illustrated when looking along the master fault strike. The Thistle Field and Causeway Field to the southwest and the Statfjord Field to the northeast also show strong evidence that an underlying structural weakness is playing an important role in determining the location and orientation of normal faults in the footwall of Upper Jurassic master faults. The evidence of these underlying horst structures can also be observed in the hangingwall of a master fault in the Dunlin Field. Here a large horst structure is present in the hangingwall, but, if no Triassic faulting had occurred only upper Jurassic subsidence would be present, not a structural high.

It is also possible to see a distinct thickening package within the Statfjord Formation against the eastern edge of the Dunlin/Hutton Fields (Figure 5-96). Work from Johnson and Stewart (1985) analyse the way in which the Statfjord Formation is deposited within the North Viking Graben. Within this study a schematic section is generated from borehole data which clearly illustrates a Triassic thickening wedge up against the Dunlin/Hutton Fields. For this thickening wedge to occur there must have been an underlying structural relief generated by an earlier Permo-Triassic rifting event. This further supports the theory of fault reactivation throughout the East Shetland Basin.

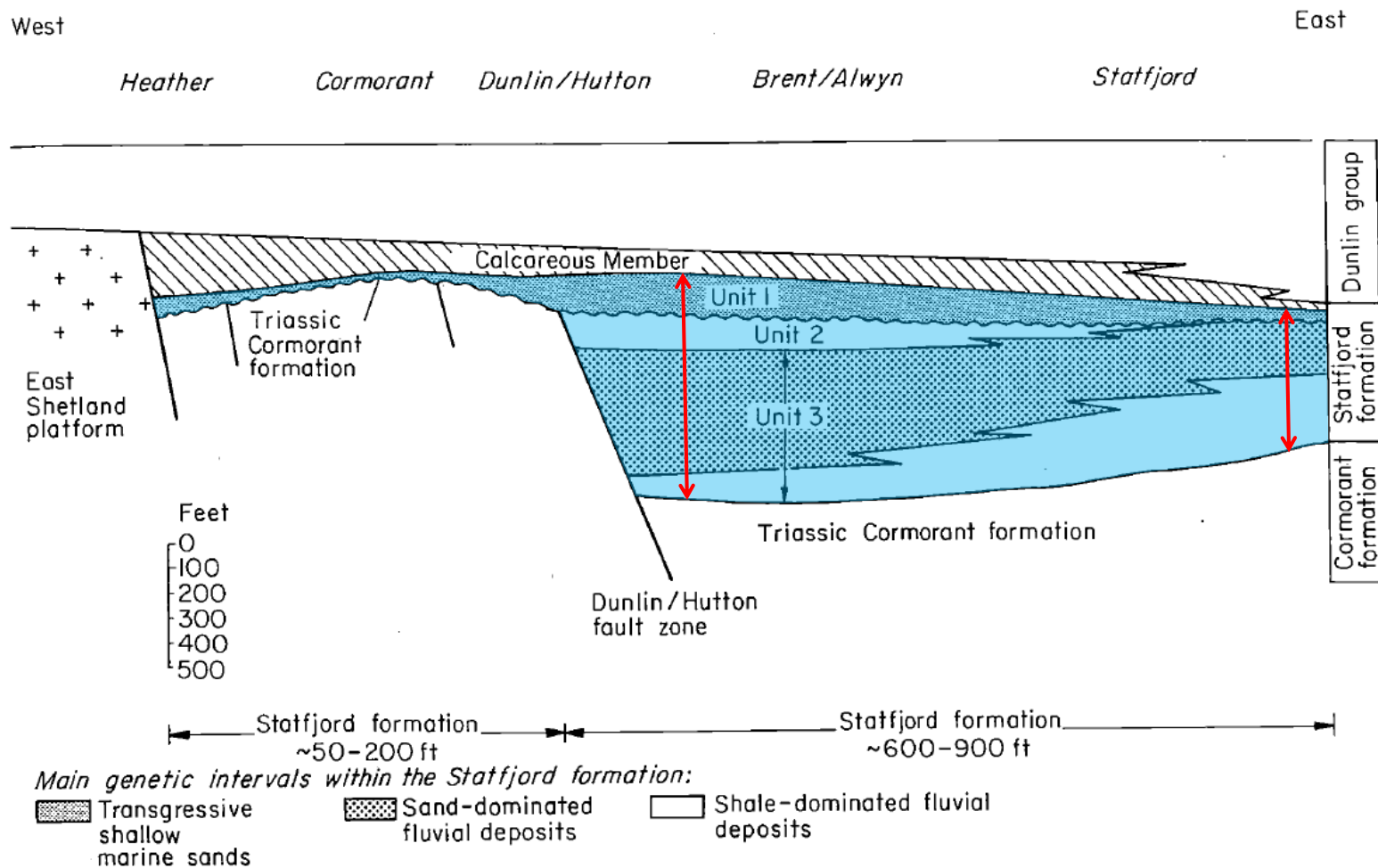


Figure 5-96 Illustrating Triassic thickening against the Dunlin/Hutton fault system (Johnson & Stewart 1985)

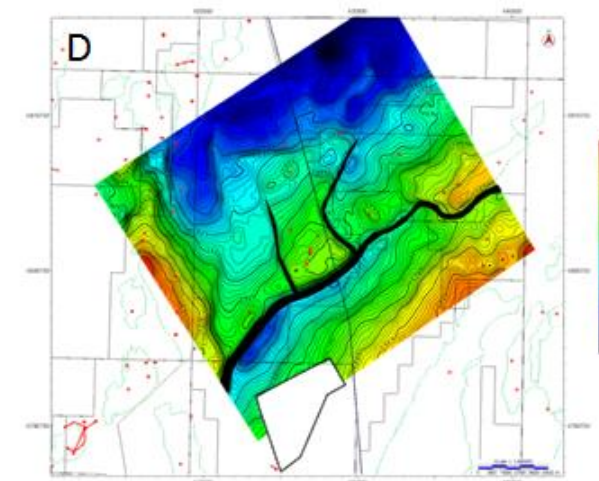
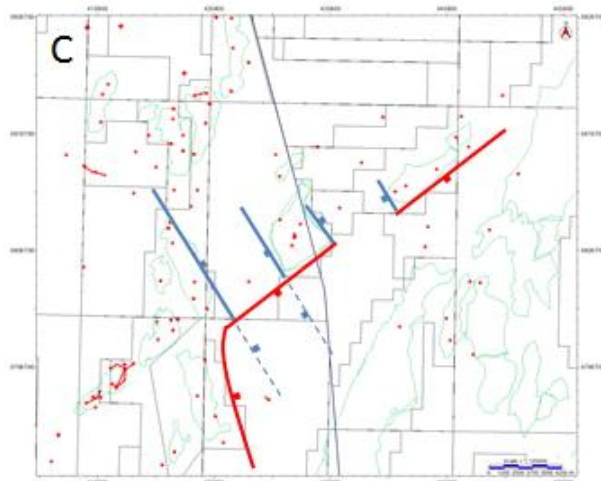
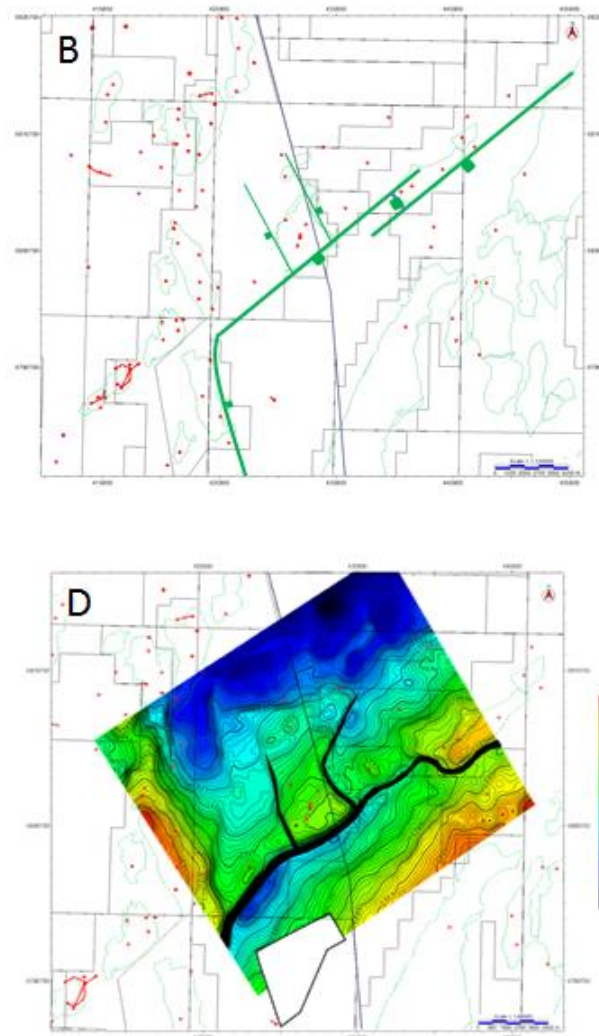
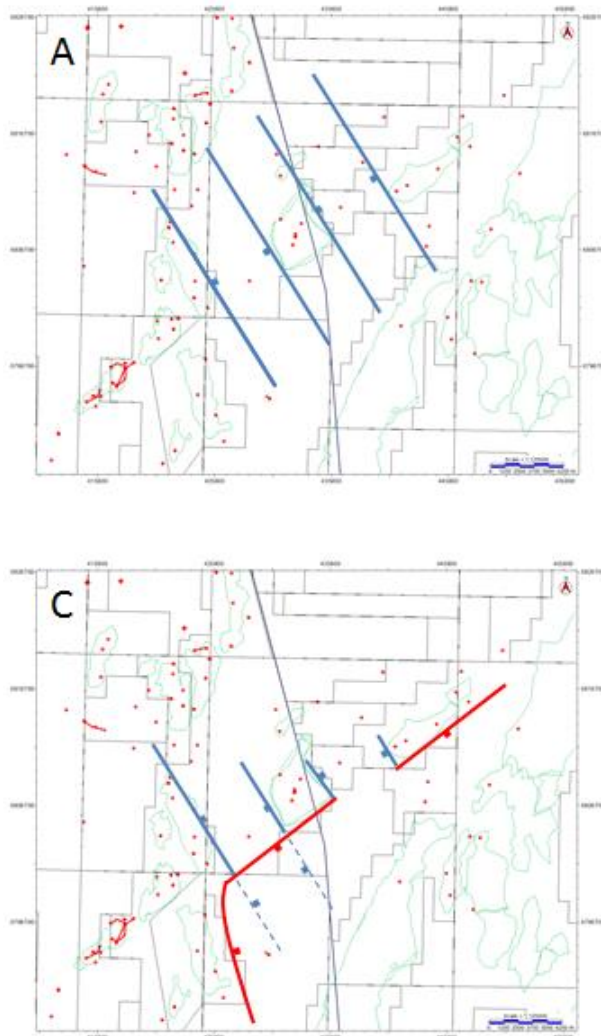


Figure 5-97. Structural evolution variables for the Murchison Field. A illustrates the underlying Tornquist trending Triassic faults (Blue). B illustrates the evolution of the Murchison Field by Young et al. (2001), with the field forming through relay-ramping of overlapping normal faults and subsequent release faults forming in the footwall of this new, longer fault. C illustrates the formation of the Murchison Field with the aid of reactivating the underlying Triassic faults. It may have been possible for the upper Jurassic fault to propagate past the NE edge of the Murchison Field, but once the Triassic fault began to move again the fault strand became abandoned. D highlights a top structure map of the Brent Group around the Murchison Field.

Unlike Type 3 rifting where the crosscutting faults are oblique to one another Type 4 rifting occurs where the faults are perpendicular to one another. As the faults are perpendicular it is more likely that an underlying trend can reactivate opposed to a new fault forming, as the alignment of an old trend will still align with one of the sigma values of the newer fault system (Figure 5-97).

As illustrated in Type 3 rifting a series of Triassic and Jurassic highs and their interaction and evolution over time can directly influence the prospectivity of a petroleum system. This can be further observed in this rifting type. The Murchison Field is an area that was a high in both Triassic and Upper Jurassic making it a High-High. The area directly opposite the Murchison Field down dip of the Caledonian fault is a High-Low which generates a structural high in the hangingwall of the normal fault. In other words a structural trap is generated in what is otherwise a structurally low lying position. This structural feedback can also be observed in the Dunlin Field, but the migration routes in this area must be present in the hangingwall for oil to fill the structural trap generated by the NW-SW striking Tornquist faults. This would suggest that Type 4 multi-phase rifting generates several structural traps, although not all of them may be filled depending on hydrocarbon migration routes. As in other multi-phase rifting types, a kitchen area can be defined by the interaction of faulting, in this instance structurally low areas can be identified although they may not be deep enough to generate hydrocarbons. The primary control on the hydrocarbon system that Type 4 rifting has is determining trap size, shape and location.

The locations of these rifting events are normally intra-basinal such as the Causeway to Murchison location. In these locations the reactivation of underlying structural trends can occur with almost an equal amount of

throw compared to the faults created in the second rifting phase. This is dominant in the intra-basinal areas where both structural trends are present and not one of the structural trends is dominant, as seen in Type 3 rifting.

5.4 *Effects of transecting rifts*

The East Shetland Basin is a complex structural domain where fault growth, linkage and interaction are observed in many different rifting types. Within this study area, up to four separate structural domains can be identified. Each of these domains has formed through the use of existing fault trends and linkage of them with new fault trends that formed during a new rifting phase. Table 5-3 has been generated to simplify the overall structural feedback from each of the four rifting types.

The resulting structural feedback varies in complexity from Type 1 to Type 4 rifting. In Type 1 rifting the reactivation of an existing fault plane with the same strike and polarity is fairly straight forward, whereas, Type 4 rifting is generated by reactivation and interaction of old fault trends within multiple rifting events. This perpendicular cross cutting of faults is crucial to understanding the structural evolution throughout the East Shetland Basin.

Extensional (normal) faulting creates two distinct areas across the fault plane, an uplifted footwall high and a subsiding hangingwall low. These areas have different sedimentological evolutions to one another primarily relating to the amount of accommodation space created. The footwall high areas are commonly associated with the reduction of accommodation space which results in a thin draping or erosion of sediments during the syn-rift phase of the rift. During the post-rift phase when the complete drowning of structures occurs, thick sediments packages occur over the footwall highs.

The hangingwall location on the other hand generates significant accommodation space during the syn-rift phase and results in thick sediment packages. This area then undergoes a similar sedimentation style to that of the footwall in the post-rift phase.

Table 5-3 illustrating the varying types of rifting observed in the East Shetland Basin and their principle characteristics.

	Fault Strike	Fault Plane reactivation	Fault Polarity	Location
Type 1	Parallel	Full	Same	Tern -Eider Ridge Troll Field
Type 2	Parallel	Partial	Opposite	Cormorant to Brent Fields
Type 3	Oblique	Partial	Variable	Pobie Platform (rift shoulders)
Type 4	Perpendicular	Partial	Mixed	Murchison Thistle Causeway

If however this structural event is cross cut by another with a different strike orientation, a separate footwall high and low will be generated relating to the most recent faulting event (Figure 5-66). This is what has occurred in the East Shetland Basin. The Permo-Triassic fault trend has been cross cut by the Upper Jurassic rifting event and in areas where Type 3 & 4 rifting is present a multi-tiered fault block system can be generated. The cross-cutting nature of a Type 4 rift will create four distinctive areas, which will play an important role in the petroleum system and in determining trap location and kitchen areas.

The most prospective area for hydrocarbon trap formation is reserved for the area which is located in the footwall high during both rift events, termed the High-High. These will generate fault-bounded three way dip closures relating to the cross cutting faults, as seen in the Murchison Field and the Pobie Platform. Within this location the Upper Jurassic Brent Group has been elevated into a structural high and is bound by three faults. The next structurally elevated level can be found in the footwall to the most recent rifting event but was in the hangingwall during the initial rifting event. This area is termed Low-High. This locality often acts as the carrier bed for the primary trap feature in the High-High. Although this location is not the structurally highest area it can be prospective as a terrace structure.

The two remaining locations are found in the hanging wall to the most recent rifting event. The area that was a structural high during the initial rifting event is called a High-Low and as illustrated in the Dunlin Field. This can also generate a structural trap in a currently structurally low position. Although this is a hangingwall low, the initial footwall high might still form a structural high for hydrocarbons in the newly formed basin to migrate into. The adjacent area which was a hangingwall low in both rifting events is termed a Low-Low and has the lowest possibility to form a structural trap. It is more likely that this area has the potential to form a localised kitchen area for the generation and migration of hydrocarbons. As in areas such as the Pobie Platform, the Low-Low areas preferentially preserve thickened sedimentary sequences than structurally higher areas and are the sites of greatest differential subsidence, something that might promote source rock maturation.

A detailed study of the Murchison area has already been undertaken, but another area close by also illustrates this Type 4 structural topography. This is observed in the Halibut High area of the Dons region (Figure 5-98 and a

well section through the area in Figure 5-99). Although no hydrocarbon fields have been identified in this Halibut High area, it still has the same structural evolution as the Murchison Type 4 location.

The Halibut High has been an area for exploration since 1974 with the drilling of well 211/18-5. Since then three other wells have been drilled in the plateau area. They have all been plugged and abandoned as they encountered nothing more than hydrocarbon shows. This can be explained by the Type 4 rifting event that has occurred throughout the area.

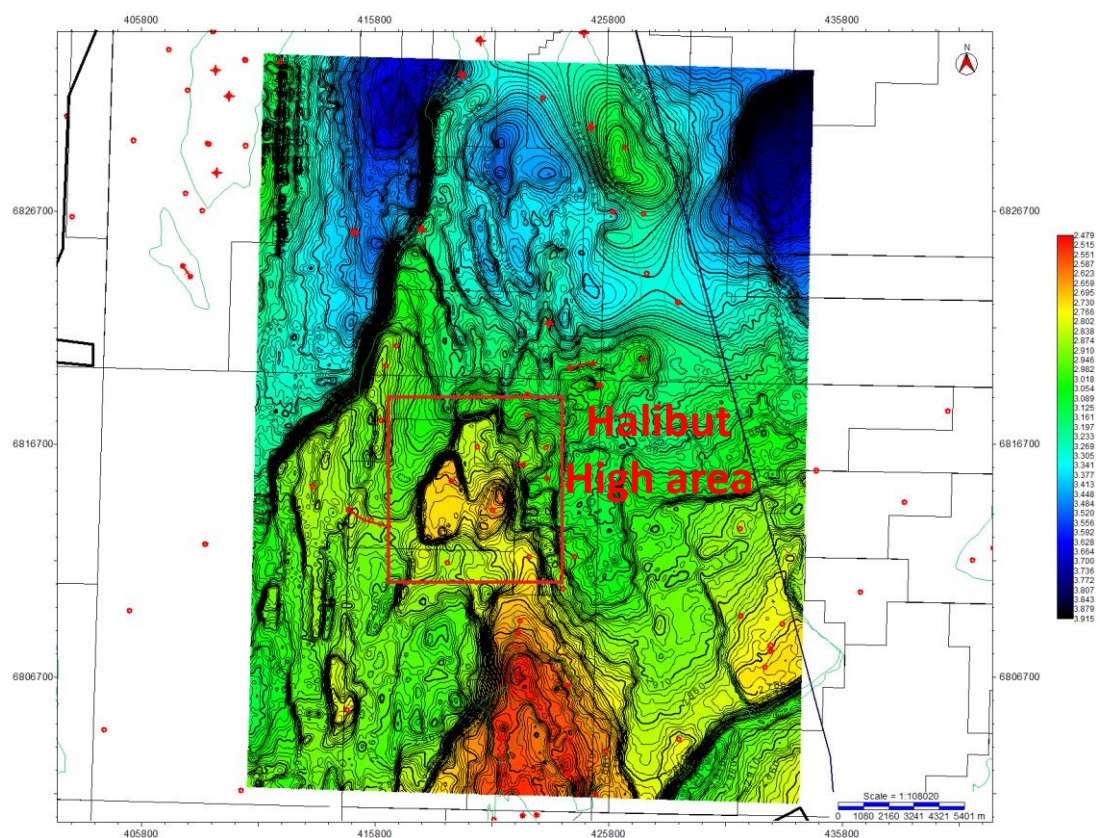


Figure 5-98. A Top Brent Group map illustrating the Halibut High study area highlighted in the red box.

Like the Murchison, Thistle and Dunlin Fields a strong NW-SE Permo-Triassic lineament is evident in the Halibut High area. This structural lineament can also be observed in the basin area directly to the north which may be responsible for the generation of hydrocarbons found in the West

Don and other fields of the Don Cluster. The evidence for Permo-Triassic faulting is not just evident in seismic mapping, but also in the borehole data acquired.

The southernmost well (211/18-25) has a thin section of Statfjord sediments, suggesting it originally lay in a footwall location during/ after the Permo-Triassic rift activity. This is also seen in the central well (211/18-5) further suggesting a footwall location. The well furthest north (211/18-16) on the other hand has a thicker Statfjord Formation section. The difference in sediment thickness between the two footwall location wells and the single hangingwall location is ~90ft. This difference in sediment thickness is related to the post-rift infill relating to the Permo-Triassic faulting, where the remaining under-filled basins were filled with sediment (Figure 5-89).

The identification of this underlying Permo-Triassic fault has a significant effect on the petroleum system. As the Halibut High area was a structural high during the first rifting event and was then subject to cross-cutting faults along with reactivation of the Permo-Triassic fault in the Upper Jurassic rifting event and created a multi-tiered fault block system.

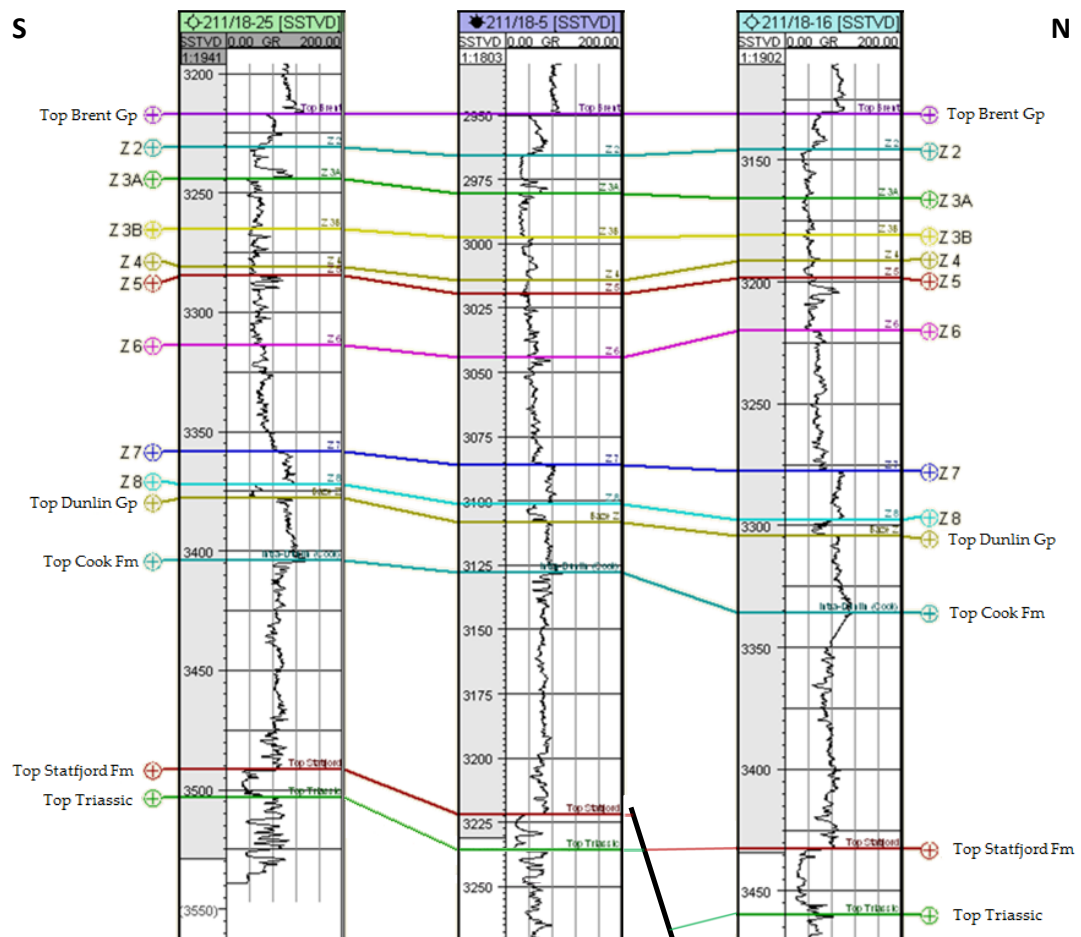


Figure 5-99. An S-N well correlation through the Halibut High area illustrating an increase in Statfjord Formation sediment thickness across the NW-SE Permo-Triassic fault.

As in the Murchison area, the Halibut High High-High area was of immediate interest and was the location of the first well, but like the other wells in the plateau, it was dry. The primary reason for this relates to the amount of uplift and subsidence that has occurred during the Upper Jurassic rifting event. The amount of offset that occurred during the second phase was so severe that the structural trap was removed from the hydrocarbon migration routes. The structural high was too elevated for carrier beds to connect to the top quality reservoir found over the structural high. This shows that the faults that generated the trap must be closed and do not act as conduits for hydrocarbon flow. This idea is further enhanced by the juxtaposition of the Brent Group sediments against the Kimmeridge Clay

Formation, making it hermetically sealed. In this instance the severity of the Upper Jurassic faulting was such that the flanking High-Low and Low-High areas were also removed from the migration routes leading the structure to be a migration black spot. Additional evidence of the cross-cutting nature of the Upper Jurassic faults can be observed in the area directly north of the Halibut High. Here the Permo-Triassic fault actually continues into the Upper Jurassic hangingwall and reactivates, as the fault has the same polarity, illustrating a small scale Type 1 rifting event. More of these NW-SE striking faults continue to the Penguin Ridge to the northeast.

The underlying NE-SW Caledonian trends which reactivated in both the Permo-Triassic and Upper Jurassic generated large structural features such as the Tern-Eider Ridge. It is plausible that this ridge feature is not the only structural high generated by the reactivation of this fault trend. Other structural highs such as the Tampen Spur in the Norwegian sector are a cross-cut extension of the Tern-Eider Ridge. Work undertaken by Lee & Hwang (1993), show how the Tern-Eider Ridge may have been a significantly larger extensional feature which has now been cross cut by the Upper Jurassic rifting event (Figure 5-100).

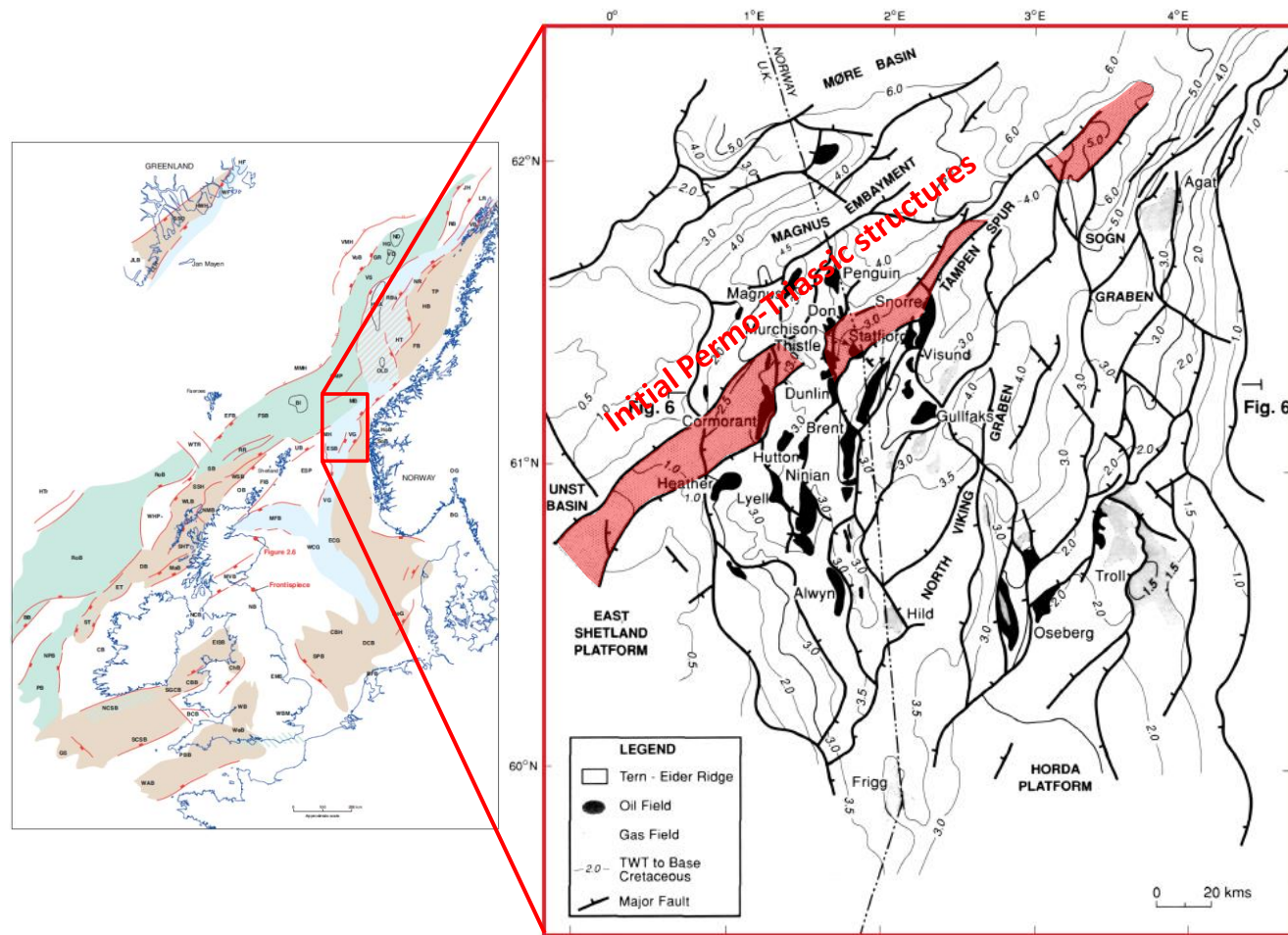


Figure 5-100. Maps illustrating the structure of the Northern North Sea and the effects of the underlying Caledonian trend. The highlighted box illustrates the possible extremity of the Tern-Eider ridge and associated structures (Lee and Hwang 1993; Coward 2003).

The cause of fault reactivation along the NE-SW striking structural lineament is a direct result of the orientation of the Northern Viking Graben. The southern section of the Viking Graben is oriented N-S and is responsible for generating several hydrocarbon traps. When the Viking Graben propagates north towards the East Shetland Basin the Viking has a slight shift in orientation. The alignment of the Northern Viking Graben is NNE-SSW, which is enough obliquity for the underlying Caledonian trending faults to reactivate and not become cross-cut.

Although the majority of the feedback from the cross rifting events is structural there is a more subtle sedimentological story to be told. This is covered in chapters 6 and 7, which talk about the generation of islands due to the extent of uplift in the footwalls of normal faults and what occurs to the eroded sediments over the footwall crest or platform areas.

When you zoom out of the East Shetland Basin and put the basin in the regional picture it is possible to see the total effects of the multi-phase rifting events. Figure 5-101 illustrates the large scale tectonic events that are at play throughout the history of the Basin. It is important to remember that although the East Shetland Basin is a postage stamp within the Northern Atlantic, it still adheres to the larger structural events that have happened in the past and these cannot be ignored no matter what scale you work on.

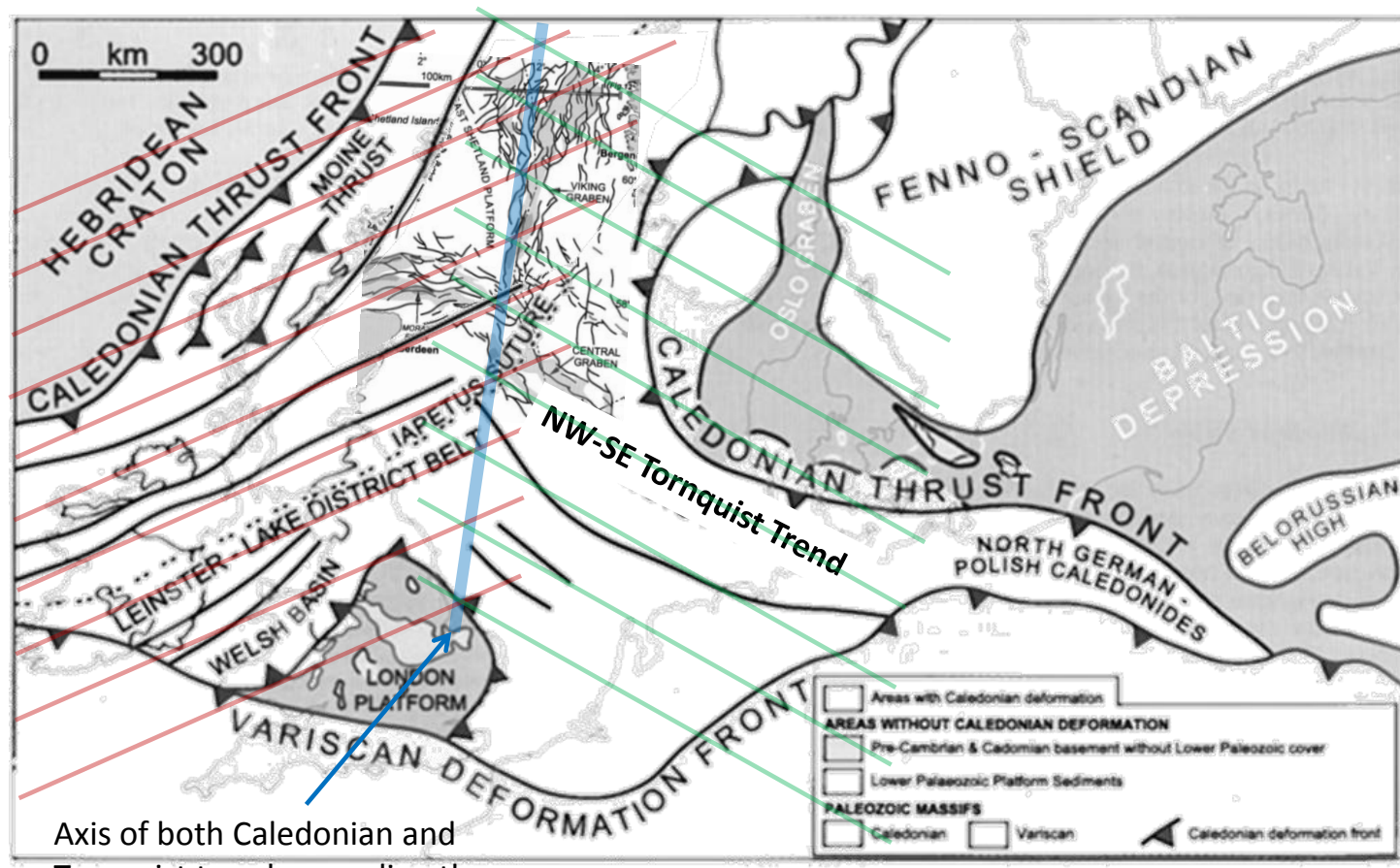


Figure 5-101. Map illustrating the overall structural trends observed throughout the whole of the Greater North Sea area. The Caledonian Trend (red) and the Tornquist Trend (green) cross and intercept over the East Shetland Basin, which results in the multiple styles of cross-rifting throughout the basin (edited after Underhill (1998)).

5.5 Conclusions

The four study areas illustrated highlight four separate incidents of fault growth and linkage through two separate rifting events and the interactions of these faults through time. It is clear to see that the underlying weakness trends of the Caledonian (NE-SW) and the Tornquist (NW-SE) plate cycles have a huge effect on the structural evolution of the East Shetland Basin through the Mesozoic.

Several faults within the basin have reactivated along these older trends at one or either of the Mesozoic rifting events. Some features may have only moved once and not reactivated later on or, visa-versa, no faulting in the initial rifting event but moving in the latter. The interaction of these faults and the cross cutting nature can determine key features of a petroleum system such as trap size and hydrocarbon kitchen location.

The simplest method of multi-phase rifting is the reactivation of the initial fault plane with the same strike and polarity (Type 1 rifting). This can be observed in the Tern-Eider Ridge, suggesting the ridge was a large structural feature in the Triassic and still is today.

The evolution of Type 2 rifting can be observed in the Cormorant to Brent area, where fault reactivation has occurred along the same strike but with an opposite polarity. This leads to the generation thick hangingwall sections from the initial rifting phase found in the more recent footwall. It may be possible to say that these faults are interlinked by a vertical relay ramping of initial antithetic faults and faults in the second phase of rifting.

The location of the rift bounding fault is key to some locations, as seen in the Pobie Platform area (Type 3 Rifting). In this location the first signs of cross-cutting faults are observed. The Pobie Fault is a perfect example of an initial fault which has been reactivated in a second phase of rifting along the same strike and polarity along the same fault plane, but has been cross cut by a larger rift bounding fault. This separates the initial fault into two separate strands, one that reactivates (Pobie Fault) and one that remains dormant.

The fourth type of rifting observed in the East Shetland Basin is observed between the Causeway to Statfjord area. This location illustrates cross-cutting fault area present in both rifting events, illustrating the effect of the underlying planes of weakness generated by the earlier plate cycles. The generation of structural highs and lows over two separate rift sequences has a large determining factor upon what role the fault block will play in the hydrocarbon system. If the fault block was a high throughout both rift sequences it is highly likely that this will form a trap location, but if the block was a low through both phases it is likely to have formed a kitchen area.

The ability to reactivate faults that have a cross cutting nature largely comes down to the polarity of the old faults and the orientation of the stretching phase during a set rifting event. If the polarity of the underlying fault matches up with a stretching phase, there is a good chance the fault will reactivate along the original plane, as seen in Type 1 rifting. If the polarity of the fault is opposed to that of the current stretching forces it may not reactivate along the same plane, but cross-cut. This fault will either cross-cut along the same strike with an opposed polarity (Type 2 rifting) or completely cross-cut the underlying trend with an opposed polarity and strike (Type 3 and 4 rifting).

The role of multi-phase rifting and its effects on the petroleum system in the East Shetland Basin control several key factors such as trap size, shape, formation, kitchen size and location along with determining migration routes, reservoir distribution and sealing quality, through time.

Chapter 6 Evidence for and Controls on Upper Jurassic Island Archipelago formation

6.1 *Introduction*

The Northern North Sea of the United Kingdom has been subjected to at least two (Permo-Triassic and Upper Jurassic) rift events which have resulted in the generation and trapping of hydrocarbons within the basin such as the Upper Jurassic Brent Group sand-prone sequences. The later of the two has overwritten the earlier and has created the majority of the large prospective structures observed in the North Sea today (Viking Graben), although some initial structures can also be observed (Penguin Ridge). Although the North Sea and surrounding marginal areas underwent extension throughout the Upper Jurassic, there are locations which illustrate more local shallowing and/ or uplift within the basins. This is commonly related to the shallow sea levels that were experienced throughout the Middle-Upper Jurassic accompanied with fault block rotation from the Upper Jurassic rifting event. Fault block rotation modelling (Yielding 1990) and the flexural cantilever model (Kusznir 1991) illustrates that if the top surface is level with a static sea level prior to rifting, the footwall surface has the potential to be uplifted above sea level by the time faulting has ceased. On average between 10 - 20% of the displacement across a normal fault relates to footwall uplift (Roberts & Yielding 1994). The amount of footwall uplift is directly related to the steepness of the normal fault, the steeper the fault the greater the amount of footwall uplift (Roberts and Yielding 1994).

The uplift and rotation of fault blocks in the Northern North Sea associated with normal faulting may be the driving force in generating an island

archipelago. It is well documented that the onset of seismic-scale rifting in the North Sea initiated in the Upper Jurassic, shortly after the deposition of the Middle Jurassic Brent Group sediments. Extensive studies of the Brent Group show how these sand prone units are part of a northward prograding delta system. The formation of a delta system generally occurs within relatively shallow depths, hence, the formation of lagoonal sediments in the Upper Brent, Ness formation. If the top pre-rift Brent Group sediments are close to sea level prior to faulting it would seem plausible that these sediments will be brought above sea level at some point through the Upper Jurassic and through to the Lower Cretaceous.

This being the case, it is plausible that the rifting in the Upper Jurassic can uplift the Middle and Lower Jurassic sediments above sea level and create an island archipelago. This could have major consequences for the petroleum system as the Middle Jurassic Brent Group sediments are the primary reservoir in the Northern North Sea. The location of these sediments and any post depositional anomalies could play a crucial role in the reservoir properties of one of the most prolific hydrocarbon reservoirs in the world, whether this being the erosion and re-deposition of the reservoir rock or the meteoric flushing of the Brent Group sediments.

If islands did form then, it is highly likely that they are to be found in the Upper Jurassic compared to the Lower Cretaceous. After a prolonged period of deposition and infill the initial islands may have been submerged by Lower Cretaceous time but were exposed during deposition of the Heather Formation and the Kimmeridge Clay Formation. Only the biggest of the islands will be present throughout the Lower Cretaceous. Evidence of the uplift and erosion relating to the Upper Jurassic rifting can be seen throughout the East Shetland Basin. It is in these locations where the greatest amount of uplift will have occurred and the most likely location to where an

island will have formed. With this in mind it is also the area in which the most erosion may be observed.

The aim of this chapter is to identify if it was possible to bring the Brent Group sediments above sea level to create a series of Upper Jurassic islands. If so what the geological consequences of these marine based sediments being sub-aerially exposed.

6.2 Study Area

As an Upper Jurassic island archipelago occurred throughout the basin in multiple locations the whole of the seismic dataset will be used, which covers the majority of the East Shetland Basin.

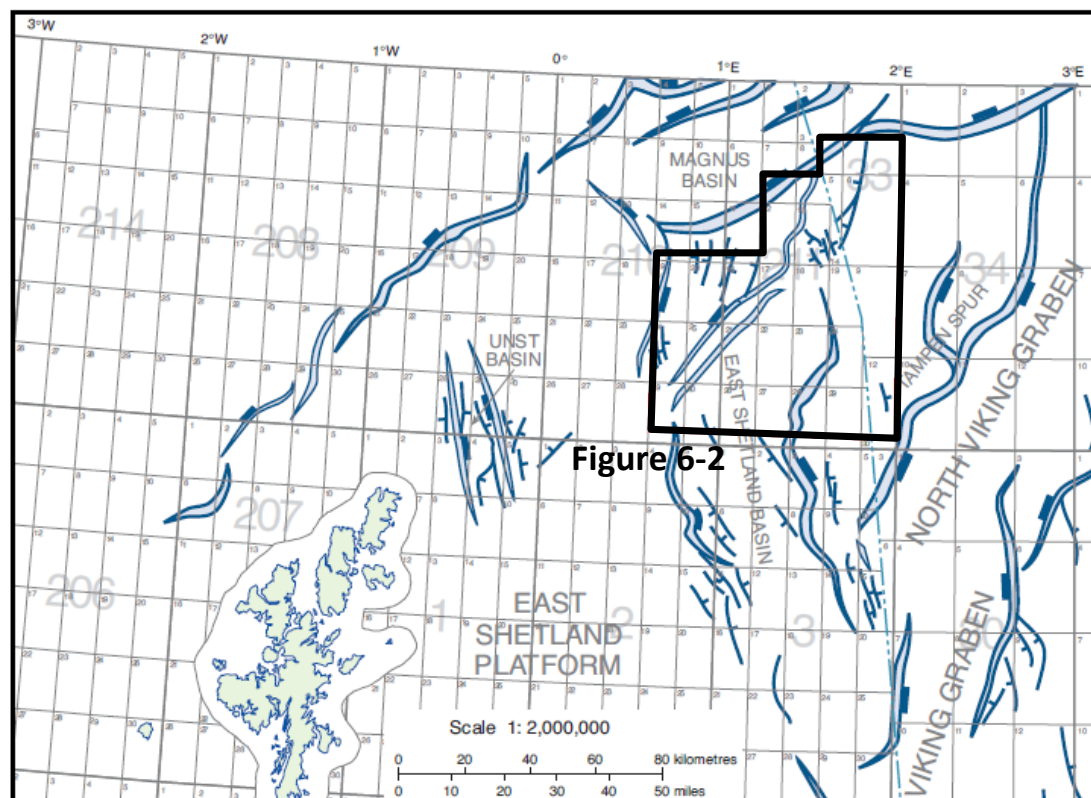


Figure 6-1. Map illustrating the location of seismic coverage and the regional structures affecting the area (Copestake 2003).

Figure 6-1 illustrates some of the regional structures that are observed throughout the seismic datasets, which have formed or reactivated in the Upper Jurassic. The extensive stretching phase in the Upper Jurassic is primarily responsible for the uplift and subsidence of sediments which form the structural traps and hydrocarbon kitchen areas in the East Shetland Basin. By analysing the way in which fault blocks are uplifted it may be possible to identify if the pre-rift Brent Group sediments were brought above sea level during the Upper Jurassic rifting event.

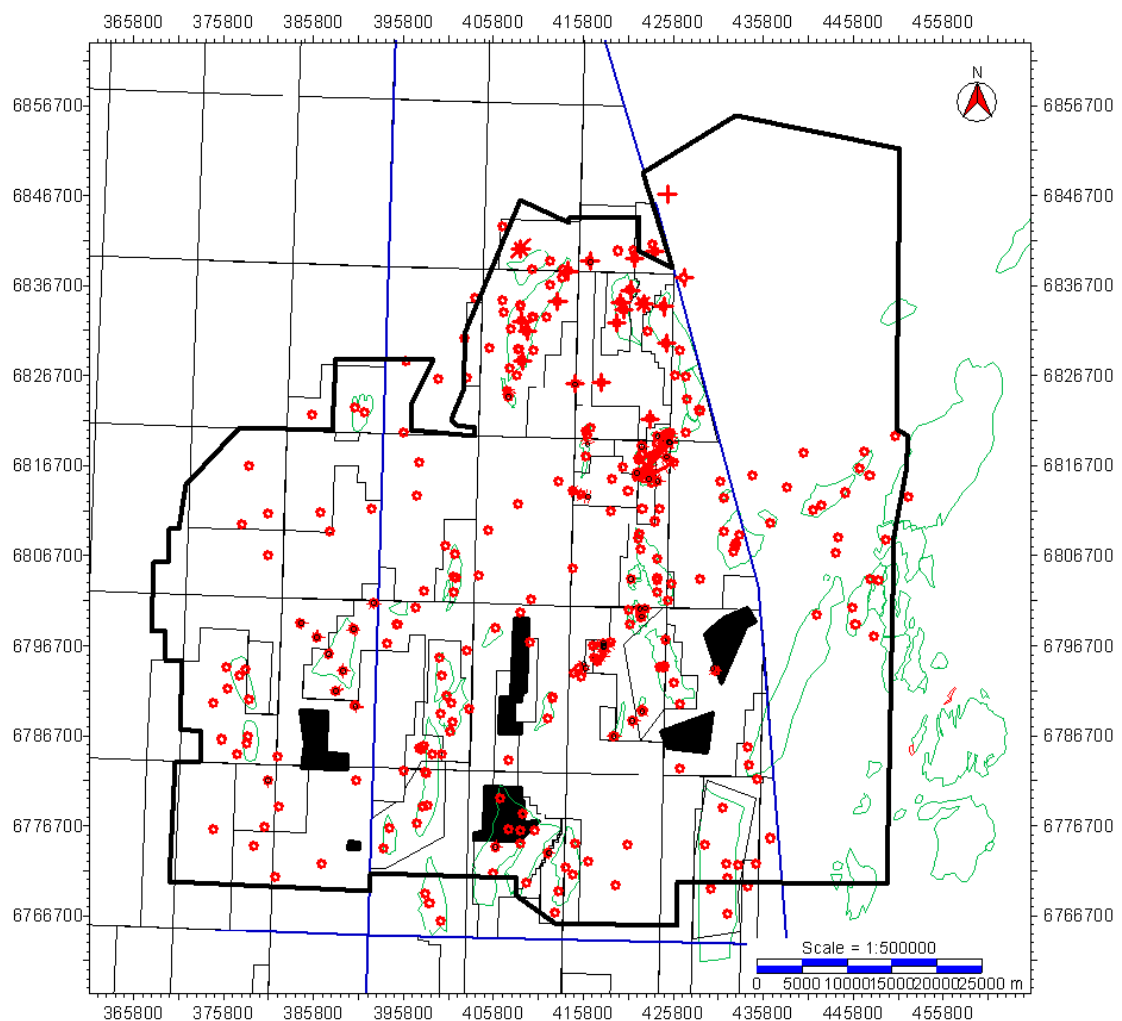


Figure 6-2. Study area for the study of an Upper Jurassic island archipelago

In total 12 different overlapping seismic volumes have been used in this study area. These seismic volumes cover an area of 5,500km² over the East

Shetland Basin, giving comprehensive data cover. Contained within this seismic acreage are over 250 wells in the UK sector alone which give valuable insights to the underlying subsurface (Figure 6-2).

With this concentration of boreholes, it has been possible to tie the seismic and wells together with great confidence and also use the boreholes for biostratigraphic analysis. The majority of these wells are drilled over the highs of tilted fault blocks, which could have formed part of the Upper Jurassic archipelago and some of the wells are targeting more subtle plays within the basin, thus, comparison between footwall highs and lows can be made.

Table 6.4. List of seismic data used in this study.

Seismic Data	
Renamed Seismic Survey	Actual Seismic Survey
Cladhan 3D Dataset	GE983F0002
Don SW+NE	BP933F0005
Hudson 3D Dataset	SH963F0002
Hutton 3D Dataset	CN903F0001 + CG963D2001
M07 3D Dataset	Mega Merge M07
N07 3D Dataset	Mega Merge N07
Murchison Small 3D Dataset	CG963D2004
Murchison Large 3D Dataset	
Tern-Eider Ridge 3D Dataset	SH953F0001
Tern-Spec 3D Dataset	WG973F0002
West Don-Thistle	ET893F0001
Western Geco 210/11 PreSTM 2008 3D Dataset	

Table 6.5. List of blocks in which boreholes will be used.

Well Data				
210/15	210/19	210/20	210/24	210/25
210/29	210/30	211/7	211/8	211/11
211/12	211/13	211/14	211/16	211/17
211/18	211/19	211/21	211/22	211/23
211/24	211/25	211/26	211/27	211/28
211/29	211/30			

Within this large dataset, specific locations have been highlighted to illustrate the occurrence of an Upper Jurassic island archipelago. Other areas such as the Brent Field can be used as examples to illustrate the role of biostratigraphic data. It may also be possible to compare and contrast areas against each other depending on their palaeo-environment during the island formation, to see if any of the sediment properties alter within the uplifted sediments.

A key reason why this study was undertaken within the East Shetland Basin relates to the Norwegian Trench (Figure 6-3). This is a large scale erosive unconformity which formed throughout the Quaternary due to glacial and fluvial processes. In some areas such as the Skagerrak Strait the seabed is located some +500m below sea level, whereas, the East Shetland Basin has very little seabed surface topography. The extent of this erosion plays a key role in seismic interpretation and could potentially make the identification of an island archipelago considerably more difficult.

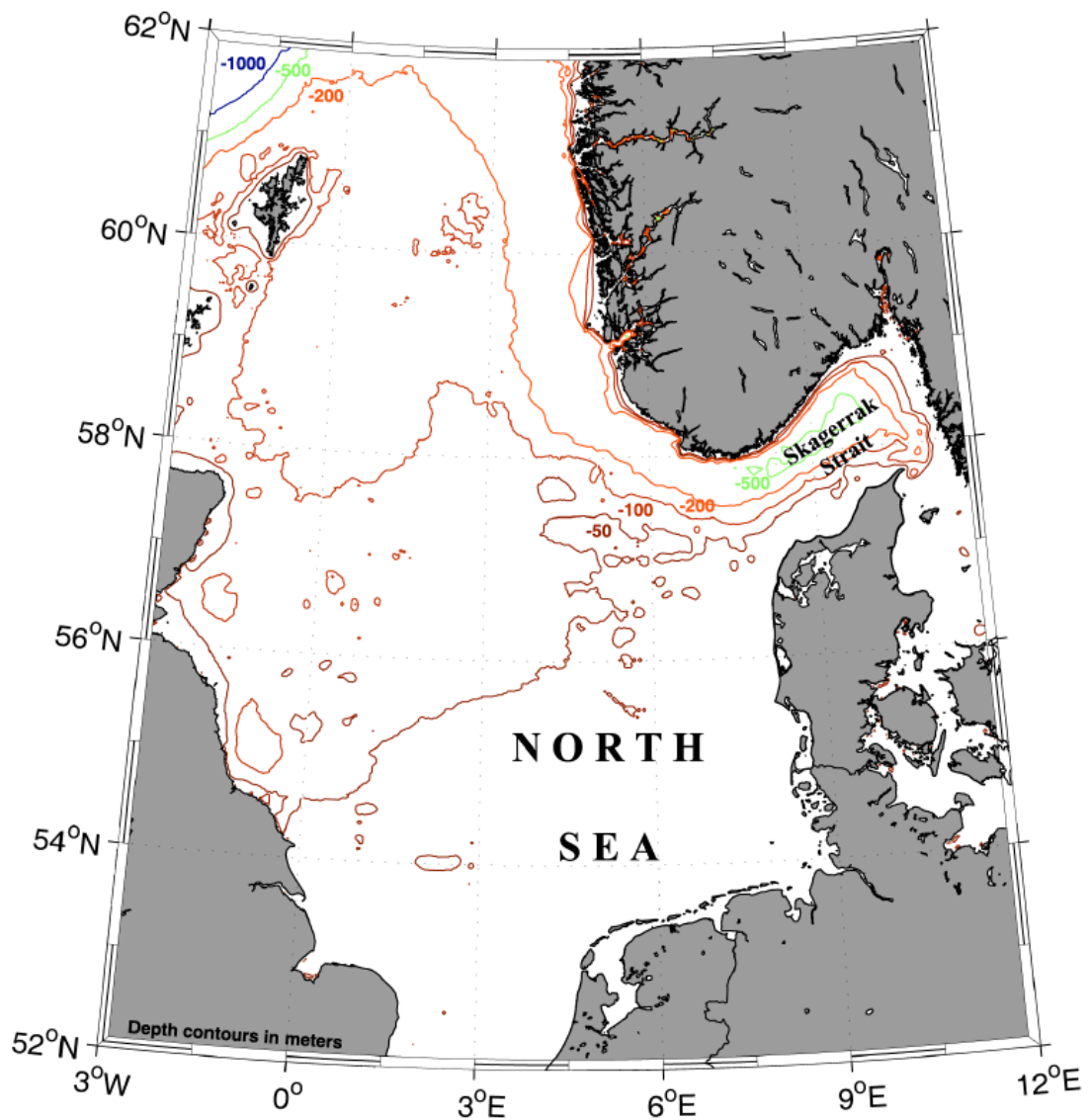


Figure 6-3. Map illustrating the effect of Quaternary erosion on the SW coast of Norway (Jackson 2004).

6.3 Effects of Jurassic Rifting

The Upper Jurassic rifting event can be observed by several different data types. Seismic data can be used to visually see the structures that are created by large scale normal faults and biostratigraphy can be used to date unconformities throughout the basin.

6.3.1 Seismic Interpretation

The vast amount of seismic data that is accessible throughout the East Shetland basin makes it possible to see the large scale tilted fault blocks that have been created by the Upper Jurassic rifting event (Figure 6-4). These large scale normal faults have structural traps that form the hydrocarbon fields such as Brent, Statfjord, Hutton and Cormorant South.

What is clear from the seismic data is the vast amount of erosion that has occurred over the crests of the tilted fault blocks. In some of the large fault systems such as the Strathspey-Brent-Statfjord system, the erosion in fact cuts down into the Lower Jurassic Dunlin Group (Figure 6-5). The greatest amount of erosion is reserved for the large scale faults where the greatest amount of uplift may have occurred.

The cause of this erosion could be related directly to the amount of uplift that has occurred along a fault. The scale of faulting also has an effect on the amount of accommodation space available in the subsiding hangingwalls. The erosion and the varying rates of accommodation space may also show eroding / thinning or condensing of the Heather Formation. The rest of the Upper Jurassic Humber Group can also be marked out using the same process as the sediments directly above the pre-rift Brent Group sediments will be heavily influenced by footwall uplift and the reduction in accommodation space and increase in erosion.

It is well documented that there was a significant sea level drop at the onset of the Cretaceous, which is marked by the Base Cretaceous Unconformity (BCU). This led to a change in depositional environment after the drowning of the Brent Group, to the relatively deep water deposition of the Humber Group. The shallowing of the East Shetland Basin sea level at Lower

Cretaceous time makes it possible to map the Lower Cretaceous Cromer Knoll Group on-laps onto the newly formed Upper Jurassic structures. As seen in Figure 6-4 the Cromer Knoll drapes and onlaps over and onto the structural highs. From this it is possible to see that the Cromer Knoll may or may not have been deposited over some of the fault crests, suggesting the fault crest were not in the marine realm during the Lower Cretaceous. This potentially illustrates a sub-crop and supra-crop relationship between the erosion of the pre-rift Brent Group sediments and the deposition of the late syn-rift Cromer Knoll sediments.

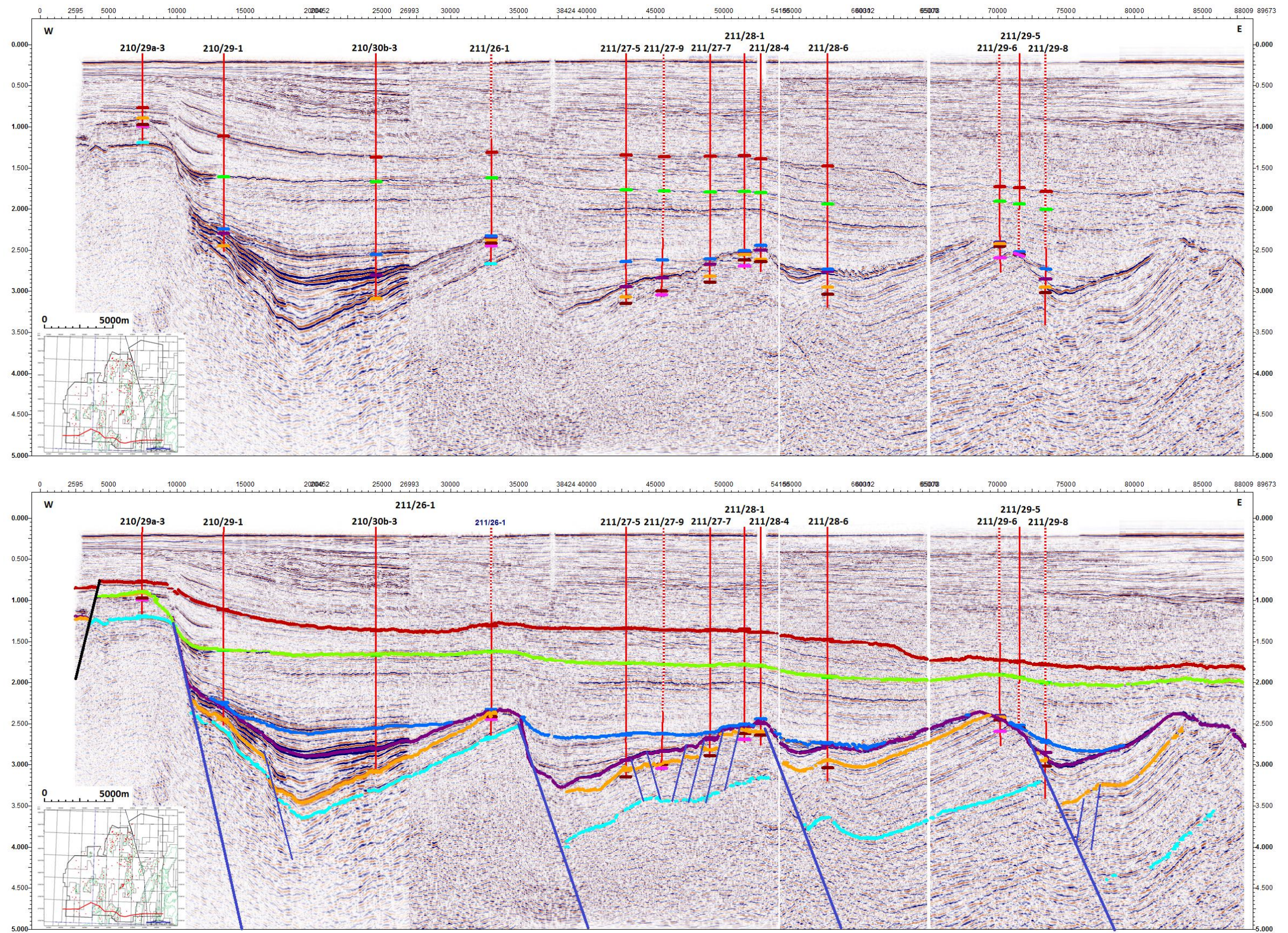


Figure 6-4. Interpreted seismic cross section of the East Shetland Basin illustrating a series of tilted fault blocks which form large hydrocarbon fields such as the Cormorant, Hutton and Brent Fields.

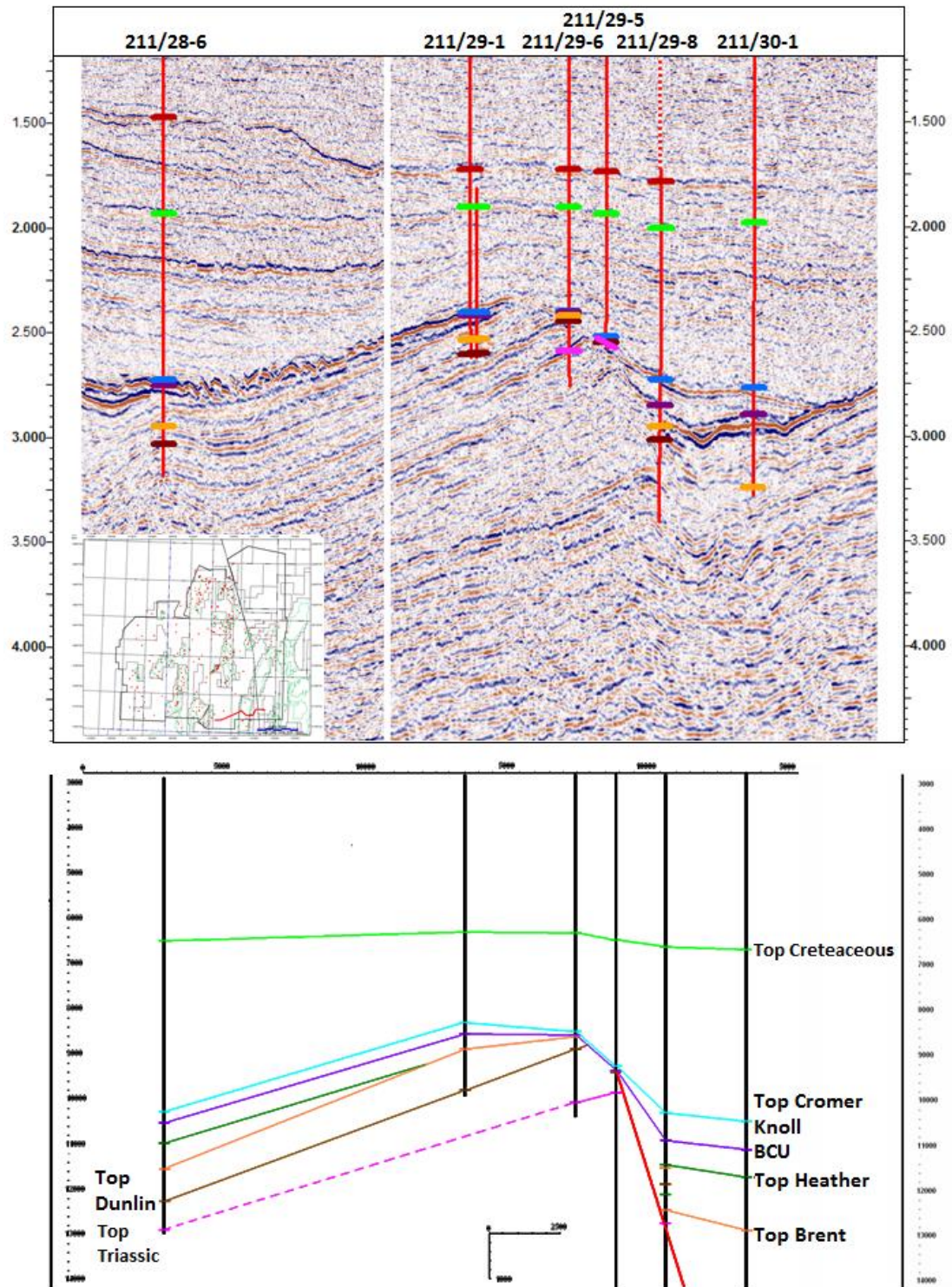


Figure 6-5. Well log cross section over the Brent Field. Possible to see the eroded section of the Brent Group sediments and image the sediments below seismic resolution.

As illustrated in Figure 6-5 and Figure 6-6, these erosion surfaces can play a huge role on the hydrocarbon prospectivity and the location of potential exploration wells. The removal of the pre-rift sediments can be estimated through seismic interpretation. This can be achieved by projecting the fault plane and the top of the pre-rift (Top Brent Group) sediments until they intercept as illustrated in Figure 6-6. By extrapolating the eroded sediment back to its initial position it is possible to anticipate the level of erosion that has occurred over a fault block. When the fault plane is also extrapolates there will come a point where the two surface will meet. This should occur at some point in the post-rift sediments but they are to be ignored for this analysis. This should now generate an image of what the pre-rift sediments would have looked like if no erosion had occurred (Figure 6-6).

Now that the initial structure has been restored it may be possible to map out the eroded section of a potential island with the use of the Base Cretaceous Unconformity. Although the Cromer Knoll sediments are the latest stages of syn-rift sedimentology they are not to be included in this analysis, but used later on to illustrate the late stage of syn-rift infill (supra-crop).

The generation of an isochron map between the top pre-rift (Brent Group) and top Kimmeridge syn-rift surface with the newly generated interpolated surface and fault planes, makes it possible to show the extent of erosion that has occurred over the fault crests. This will generate a time thickness map which will illustrate the thickness of the Upper Jurassic Humber Group, the on-lap and thinning of these sediments on to the structural highs and the presence of the structural highs. By mapping the eroded section of the top pre-rift it may also be possible to see how big of an island the footwall of the fault may have been.

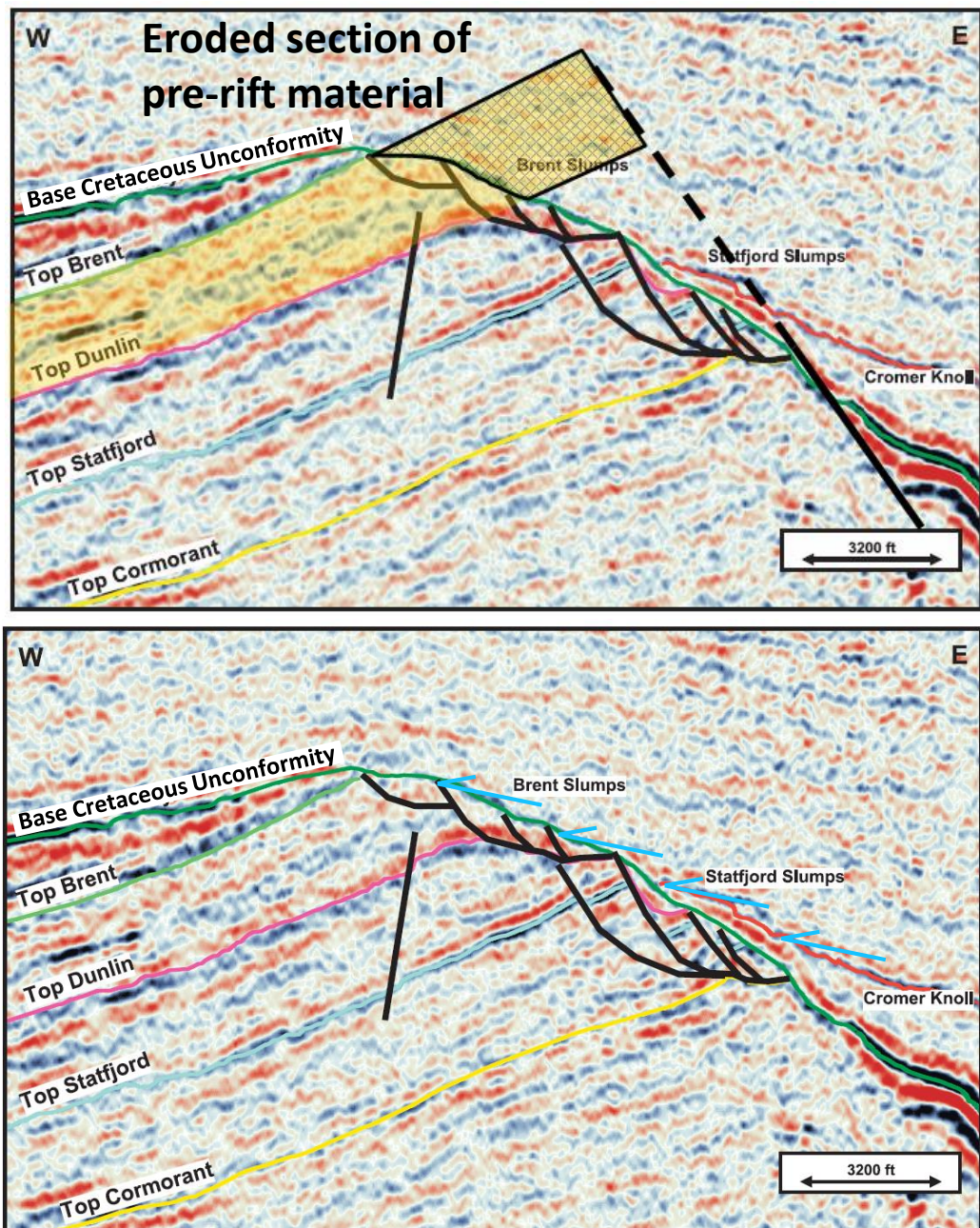


Figure 6-6. Brent field illustrating the erosion that can affect the up-dip location of the reservoir unit (edited from (Taylor 2003)). The crossed hatch Brent section is the areas that have been eroded away (sub-crop), whereas in the lower image the blue arrows indicate areas of onlap (supra-crop).

Figure 6-7 is the isochron map that illustrates the missing sedimentary sections over fault crests may have actually at one point been uplifted significantly above sea level and eroded away. The zero contour on the map is effectively where the current location of the top syn-rift pick is located

level with the original location of the top pre-rift prior to erosion. The areas in green on the map illustrate areas that are located above the Base Cretaceous Unconformity and the locations of extra sediment that has been removed during the erosion period.

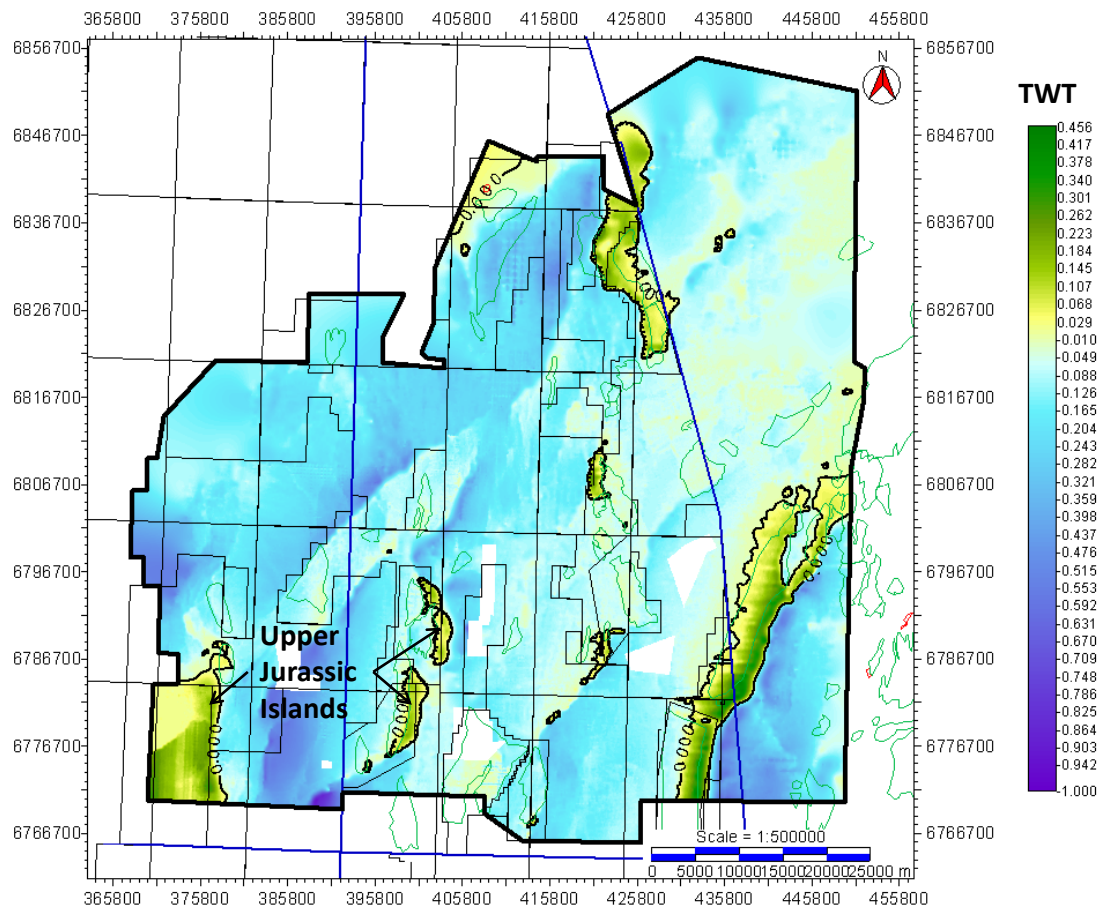


Figure 6-7. Map illustrating the possible location of islands by seismic mapping of a pre-rift and syn-rift isochron.

The map produced suggests that intense erosion only occurred over the large scale fault systems such as the Strathspey-Brent-Statfjord fault system. Other locations are the Cormorant Fields, Thistle Field, the Penguin Ridge and a location to the furthest south west which makes up part of the East Shetland Platform, known as the Pobie Platform. The isochron map also highlights several locations that are indicated in yellow, it may be possible that these areas may have been exposed to some erosion but only for a short period of

time before sedimentation continued in the Upper Jurassic/ Lower Cretaceous.

The evidence over the Brent Field and would suggest a time gap of almost 100Ma between active deposition over the structural high in some locations. It may well be that an island did not form for this period of time but the amount of erosion rates over the fault crests were so strong that they cut down so deep it appears to have formed for longer than it may have actually done.

Seismic interpretation can also be used to illustrate the late stage of sedimentary infill regarding the syn-rift packages, previously described as the supra-crop. The rifting phase which initiated in the Upper Jurassic terminated in the Lower Cretaceous. The figures above illustrate the effects of sediments within the Upper Jurassic Humber Group; it is also possible to show varying sedimentology in the Lower Cretaceous. One thing that must be noted on the Fig.6.5 is the lack of the Berriasian in the chronostratigraphy column. The interpretation of the Berriasian is extremely difficult as it is thought to straddle the boundary between the uppermost Jurassic and lowermost Cretaceous. The sediments that are deposited here are coarse clastics, deposited directly upon the marine organic rich Kimmeridge Clay Formation.

One problem that occurs with Berriasian sediments, is the preservation of sediments in the rock record. At this time, sea level fall led to mass erosion of sediments, hence, the clastic nature of any Berriasian sediments. It is most likely that these sediments are heavily cannibalised as erosion occurs deep into the upper Jurassic sediments in some areas, thus the Berriasian sediments are eroded shortly after deposition and re-deposited within the basin. The Humber Group on the other hand is relatively straightforward

and is generally separated into two major formations. The most upper unit is the Kimmeridge Clay Formation which acts as both seal and source for the hydrocarbon system. The lower unit is the Heather Formation which consists of predominantly silt and shale units.

The Kimmeridge Clay Formation was deposited during the Kimmeridgian in a relatively deep sea environment, which led to the generation of the primary source rock in the East Shetland Basin. At the end of the Jurassic there was a significant drop in sea level which led to the Base Cretaceous Unconformity. This unconformity can be observed throughout the whole basin. This resulted in a significant change in depositional environment from the start of the Cretaceous. The sediments found in the Lower Cretaceous are generally shallow marine silts and marls. By knowing the depositional environment at this time it is possible to infer the Top Cromer Knoll at a pseudo-sea level in Lower Cretaceous times. The Lower Cretaceous is the final stage of the syn-rift sediments and does not have the same infill pattern as the initial Upper Jurassic Humber Group sediments.

The initial syn-rift infill that occurs in a rifting event relates primarily to individual faults and the accommodation space they make. This would relate to the Humber Group, where thick sections of the Heather Formation and the lower units of the Kimmeridge Clay Formation would be deposited in the hangingwall of large normal faults. The majority of the Kimmeridge Clay Formation would have been deposited within the second phase of rifting, which relates to the linkage of normal faults and accommodation space being generated on a wider scale over the basin. This depositional pattern would then continue until the post-rift stage began and thermal subsidence takes over the role of creating accommodation space.

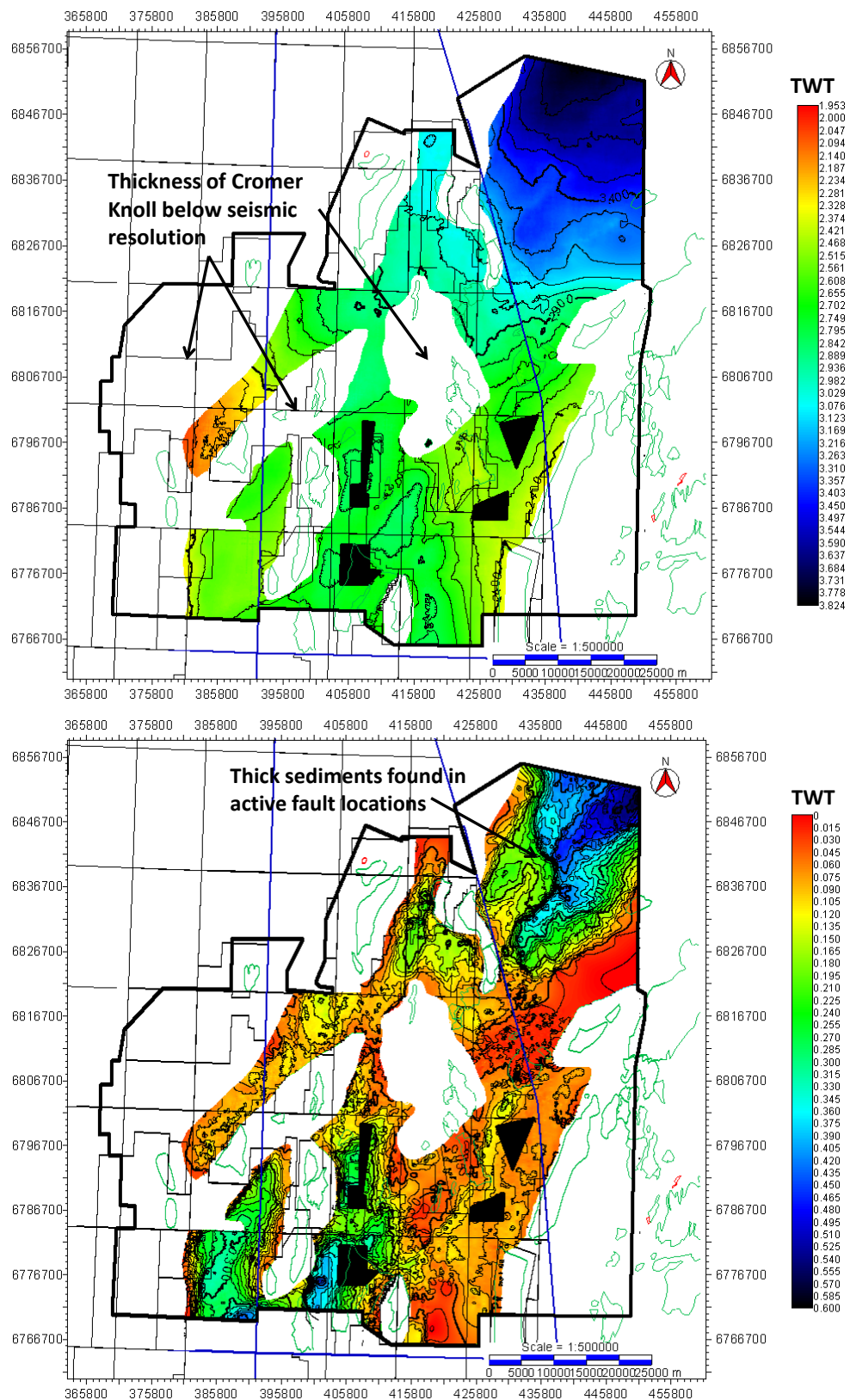


Figure 6-8. Top structure and time thickness (isochron) map of the Cromer Knoll Group. Here it is possible to identify thickening depo-centres in the late stage of the Upper Jurassic rifting event

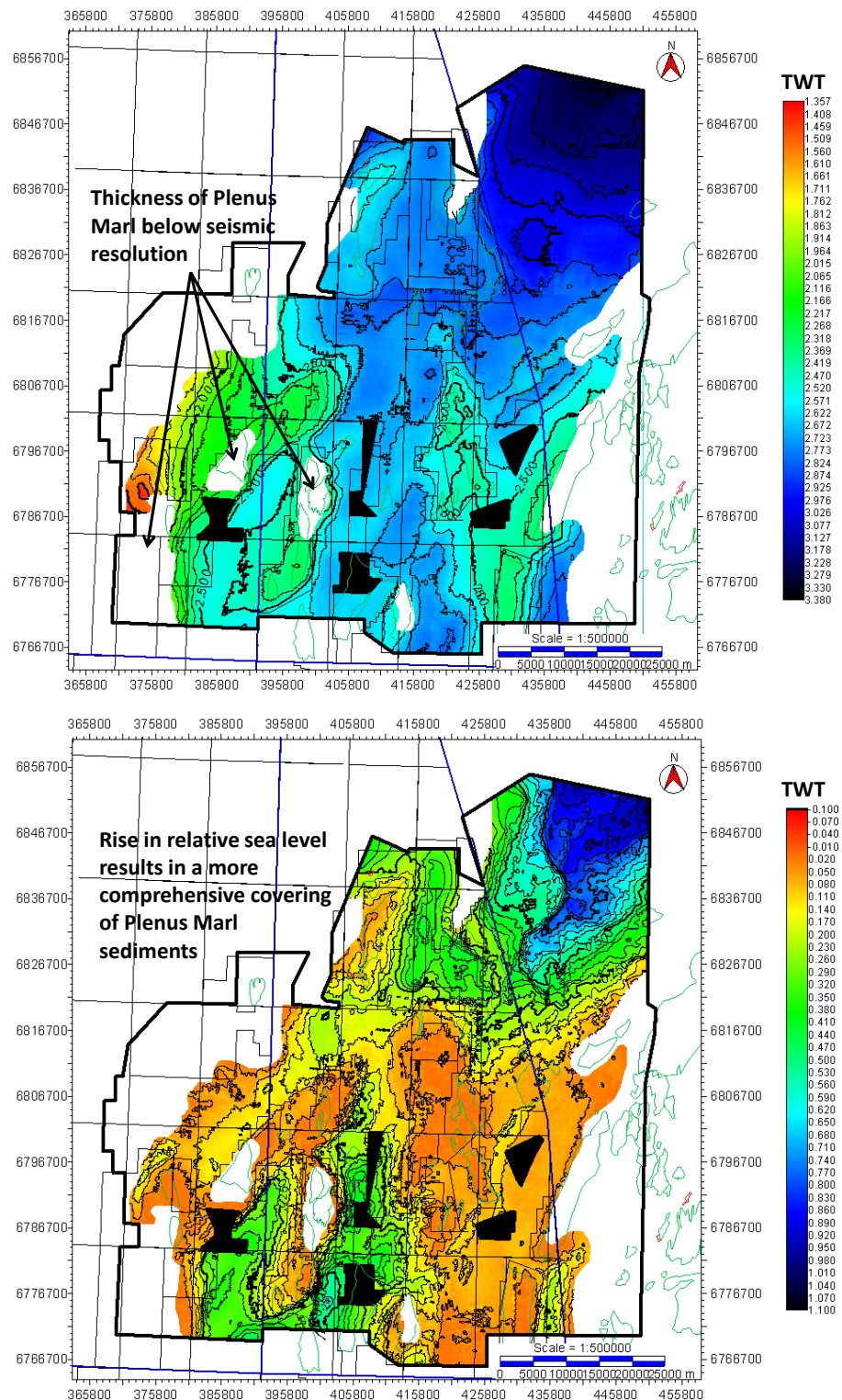


Figure 6-9. Map of the Top Plenus Marl. Areas in white are areas of non-deposition suggest either an erosive surface was present or that the surface is on-lapping to a structurally high feature, which may be above sea level. The lower map illustrating the thickness of the Plenus Marl and it thinning out onto the structural highs such as the Tern-Eider Ridge.

The main difference between this and what happened in the East Shetland Basin is the occurrence of the Base Cretaceous Unconformity (Figure 6-10). This dramatic unconformity which can be identified as a condensed section in basinal areas (Rawson 1982), makes it possible to accurately map syn-rift on-lap surfaces, such as the lower Cretaceous Cromer Knoll and Plenus Marl Formation. The erosion of the highs created in the Upper Jurassic and lowering of relative sea level results in the Cromer Knoll having a silty texture that fills in the remaining lows created by the rifting event. This Lower Cretaceous infill results in a saucer shape infill between the structural highs. Areas where the Cromer Knoll is not present can be inferred to as erosion or more likely a lack of deposition. It is unlikely that the Cromer Knoll has been eroded as the Northern North Sea has been subsiding since the Upper Jurassic rifting event.

The lack of natural uplift from rifting and deepening seas from the on-set of the Lower Cretaceous reduces the odds that the Cromer Knoll has been eroded post depositionally.

This enhances the idea that sediments belonging to the Cromer Knoll Group were not deposited over the structural highs. As the Cromer Knoll is a shallow marine sediment, for it not to have been deposited in the area in question, the region must not have been in the marine realm; thus above sea level. By mapping out the Cromer Knoll (Figure 6-8) and the Plenus Marl (Figure 6-9) onlaps it is possible to identify areas that may have been islands throughout the Lower Cretaceous.

The main difference between the two maps is the size of the supra-crop areas. These areas that may have been present throughout the Cromer Knoll are considerably larger than that of those at the time the Plenus Marl was

deposited. This is related to the drowning of the fault crests and the post-rift thermal subsidence which initiated in the Lower Cretaceous.

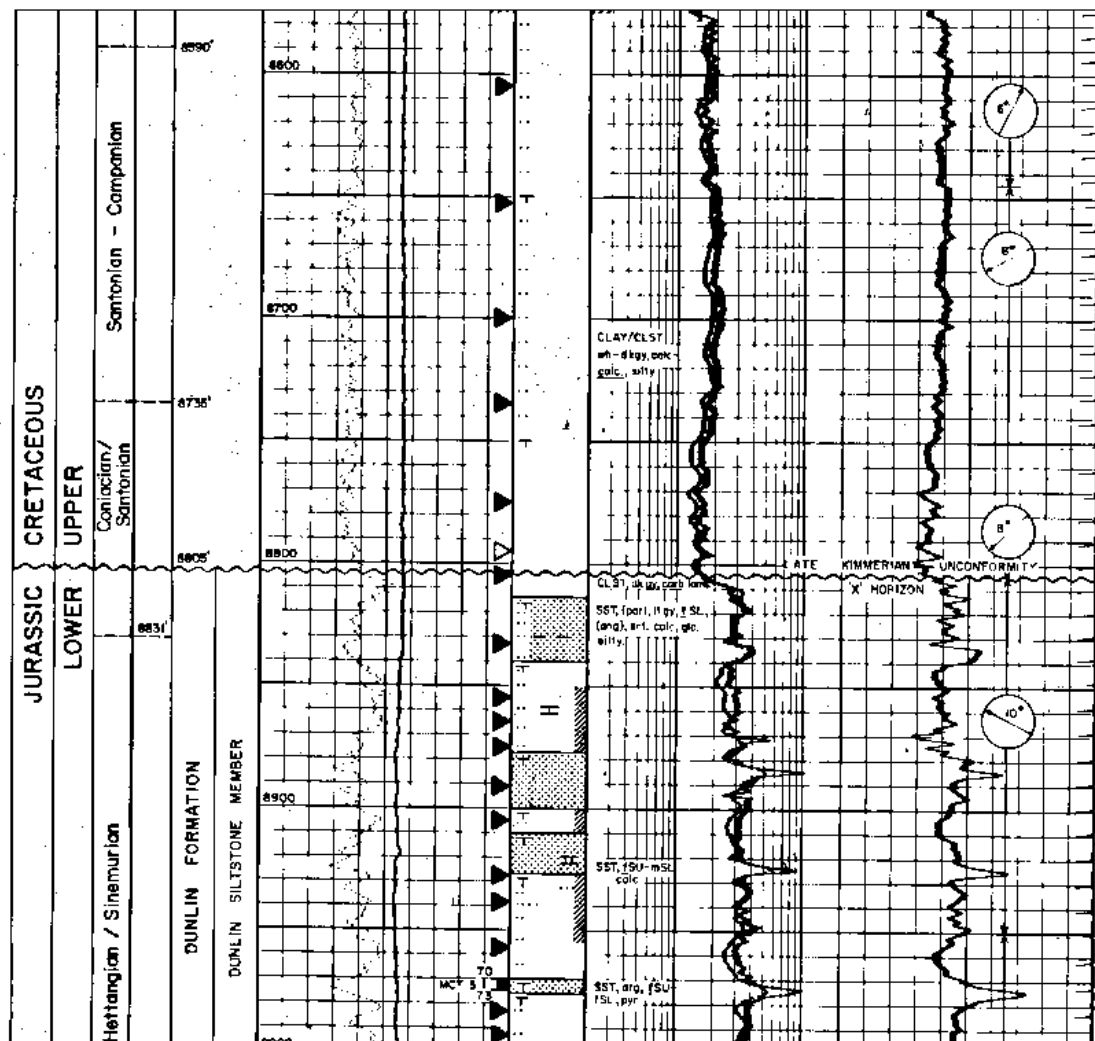


Figure 6-10. Well 211/29-4 illustrates an erosion surface between the Lower Jurassic Dunlin Group and Upper Cretaceous sediments, suggesting an island formed during the Upper Jurassic and eroded sediments of Middle and Lower Jurassic age and prevented deposition through the Upper Jurassic and Lower Cretaceous.

One issue with interpreting the Cromer Knoll Group relates to a tuning effect in the seismic data. In many of the well logs, there is evidence of the Cromer Knoll Group, but, not enough for it to be defined on the seismic data. This may lead to some pitfalls within the interpretation over the structural highs, although the sheer volume of well data makes it possible to pick the correct trace over and around structural highs. Thus it is only possible to interpret a

maximum possible extent of supra-crop throughout the Lower Cretaceous, rather than define specific limitations in the Lower Cretaceous.

This is where well log data can be used to tie together the seismic interpretation to the sub-seismic analysis. By tying all the vast amount well data together over an eroded section it may be possible to more accurately tie down the areas of intense erosion that seismic cannot. This has been previously undertaken over the Brent Field by Struijk & Green (1991) in Figure 6-11 and clearly illustrates the fine detail that can be generated using the well logs alongside the seismic data for sub-seismic analysis. Wells such as 211/29-4 show the subcrop sediments relate to the Lower Jurassic Dunlin Group and the supra-crop sediments being the Upper Cretaceous Coniacian sediments.

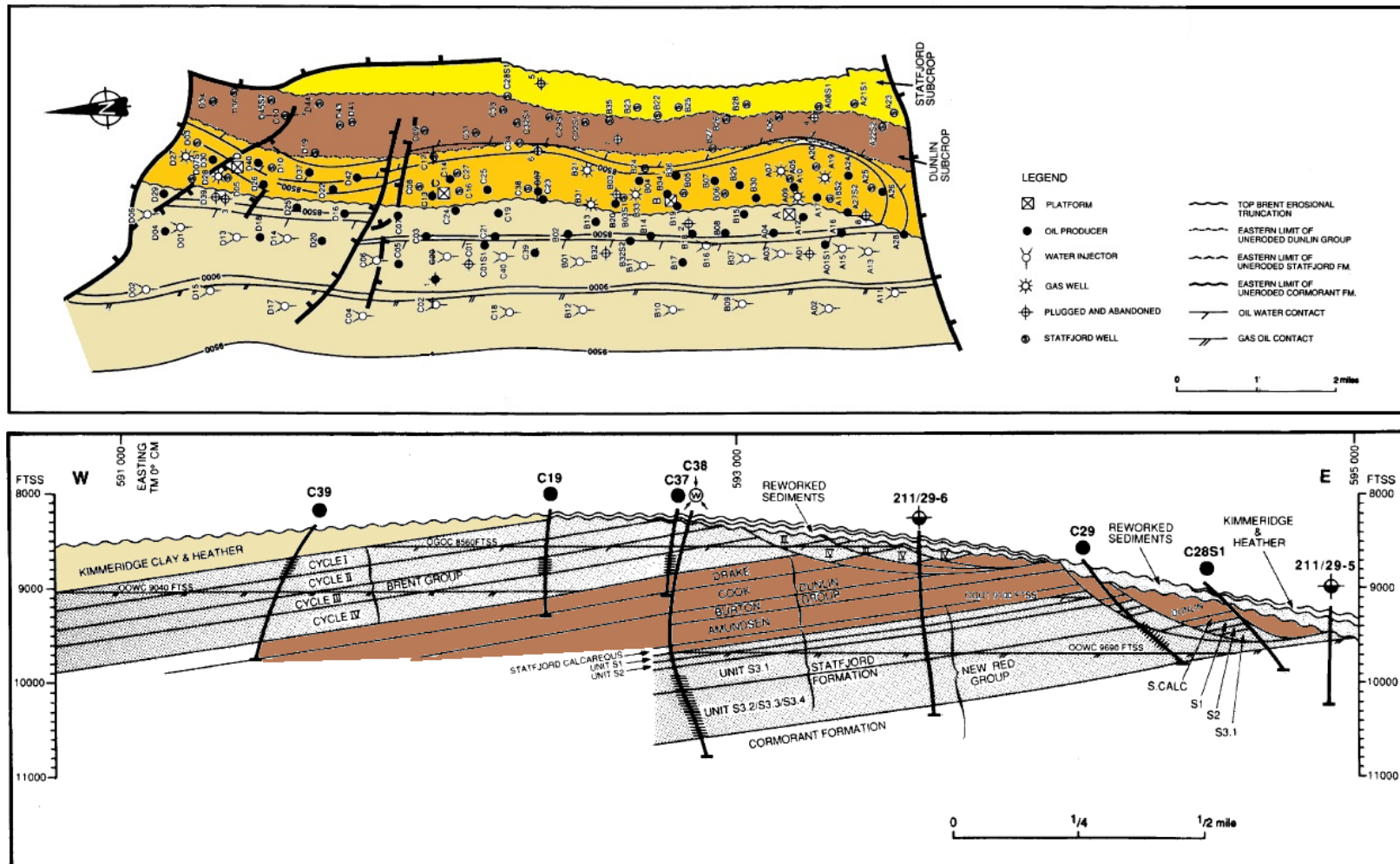


Figure 6-11. Illustration of the sub-crop over the Brent Field (Struijk and Green 1991).

6.3.2 Biostratigraphic Analysis

The greatest asset of seismic data is that it visually illustrates what has occurred on a regional scale. By looking at the East Shetland Basin as a whole it is now possible to identify select locations in which anomalies such as extensive erosion and onlapping Lower Cretaceous sediments can be analysed in greater detail with biostratigraphy. The biggest issue with seismic data is the resolution of information ~15m, this is where biostratigraphy can be used not only to identify sediments below this resolution but also to put an accurate date to the horizons and illustrate any breaks within the geological record. Being able to correctly identify the timing of these breaks in sedimentation can be key in determining the structural and sedimentological evolution of the East Shetland Basin.

Biostratigraphic reports undertaken on wells within the study area can be used to illustrate breaks within the sedimentary record. These breaks exist primarily due to erosion and the removal of previously deposited sediments. The East Shetland Basin in the Upper Jurassic – Lower Cretaceous is predominantly a marine rift-basin, where thick deposits of Upper Jurassic sediments can be observed within the hangingwalls of normal faults. The Middle Jurassic Brent Group is dated as Bajocian with the onset of rifting occurring in the Bathonian. As the Bathonian sediments represent syn-rift material it has been possible to date individual packages and colour code them according to their age as shown in Figure 6-12. The basin wide Base Cretaceous Unconformity which occurs at the end of the Jurassic removes the majority of any Portlandian sediments deposited. Although in some basinal areas where erosion rates were low, some Portlandian sediment has been preserved, but they have not been classified in this analysis. The footwall highs on the other hand are exposed to much higher erosion rates and may

cut down into the underlying stratigraphy. One of the factors that determine erosion rates over the structural highs is uplift; the larger the fault, the greater the uplift, thus, a greater erosional potential.





System	Series	Stage			Colour code
JURASSIC	UPPER JURASSIC	TITHON- IAN	VOLGIAN	PORTLANDIAN	
		KIMMERIDGIAN			
		OXFORDIAN			
	MIDDLE JURASSIC	CALLOVIAN			
		BATHONIAN			
		BAJOCIAN			
		AALENIAN			

Figure 6-12. Chronostratigraphic break down of the Middle and Upper Jurassic (Cox 1990).

The onset of rifting occurred in the Bathonian (Upper Middle Jurassic) and as rifting continued the relative depth of the sea increased with it (i.e. shallow marine in the Bathonian through to deep marine by the Portlandian). This uplift meant that any island formation could have formed as early as the Bathonian and lasted through to the Lower Cretaceous, when rifting ceased. By using the biostratigraphic logs it is possible to see what sediments are present within the boreholes.

With the logs it may be possible to identify unconformities that may be related to the uplift of individual normal faults and when faults may have hard linked together. Wells that appear to have sections missing back the theory that during these times of missing sediments the well location may have been brought up above sea level and heavily eroded.

Figure 6-13 illustrates four maps each of which highlight which wells contain missing sections due to the uplift and erosion relating to the footwall uplift. Each map in Figure 6-13 relates to an individual time frame, such as the light blue map, which indicates all the wells that have an erosion surface in the Bathonian dates sediments. Figure 6-13 illustrates that there is a change in erosion rates throughout the syn-rift as much more erosion has been observed in the Bathonian, Callovian and Oxfordian than there has in the Kimmeridgian.

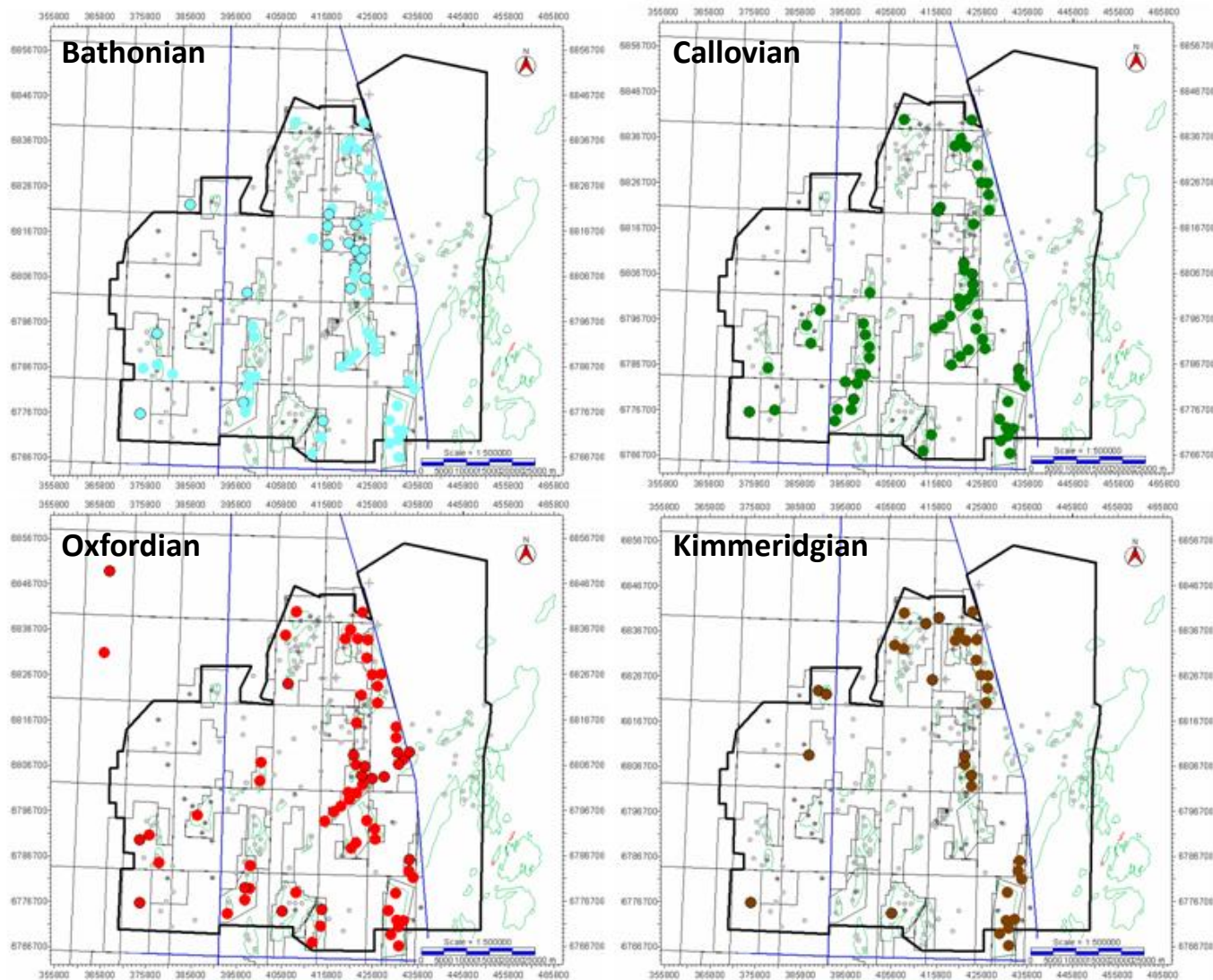


Figure 6-13. Maps illustrating the erosion surfaces observed within biostratigraphic and composite logs throughout the study area. Only the significant structural highs such as the Pobie Platform, Penguin Ridge and Brent Field show erosion in Kimmeridgian times, whereas erosion was observed throughout the basin in the Bathonian Callovian and Oxfordian times.

Areas such as the Pobie Platform, Penguin Ridge and Brent Field are all structures that have erosion throughout all four stages. Erosion rates must have been extremely high over these structural features and in the Brent Field some wells illustrate no Middle Jurassic sediments what so ever. This means meaning the primary reservoir (Brent Group) unit is missing, and erosion has occurred down in to the Lower Jurassic Dunlin Group. The lack of Lower Cretaceous sediments over this high also illustrates that the high was not submerged until the Upper Cretaceous meaning this would have been a long lasting structural high throughout the rifting phase.

Other areas such as the Penguin Ridge, Cormorant Field and the Thistle Field also show strong signs of prolonged erosion which could relate to island formation. One major trend that appears from this map is the large amount of erosive surfaces that have formed during the Bathonian, Callovian and Oxfordian. This would lead to the idea that these areas would have been uplifted during the early stages of rifting, but the uplift associated to their respective faults could not keep up/ overtake relative sea level rise, leading the areas to become submerged in the Kimmeridgian.

One key feature that is observed in the individual maps is the effects of fault growth and linkage on island formation, which can be observed around the Causeway area. Within this area a full sequence of Bathonian sediments are observed, but erosion has occurred within the Callovian and the Oxfordian. This would suggest that in the Bathonian when rifting was in its infancy the individual faults did not have enough uplift to raise the sediments above sea level.

The fault growth and linkage evolution can be best observed in Figure 6-14 which is a combination of all four maps. This figure collaborates all the individual well data from each stage and highlights when and where erosion

was occurring and for how long. A well that has erosion purely in the Bathonian will remain light blue, but if erosion is observed in the Bathonian and Callovian the well symbol will be cut in half and be shaded in light blue and dark green. If a well indicates erosion through all four stages then the well symbol will be divided into four quarters and shaded in with each of the representing colours.

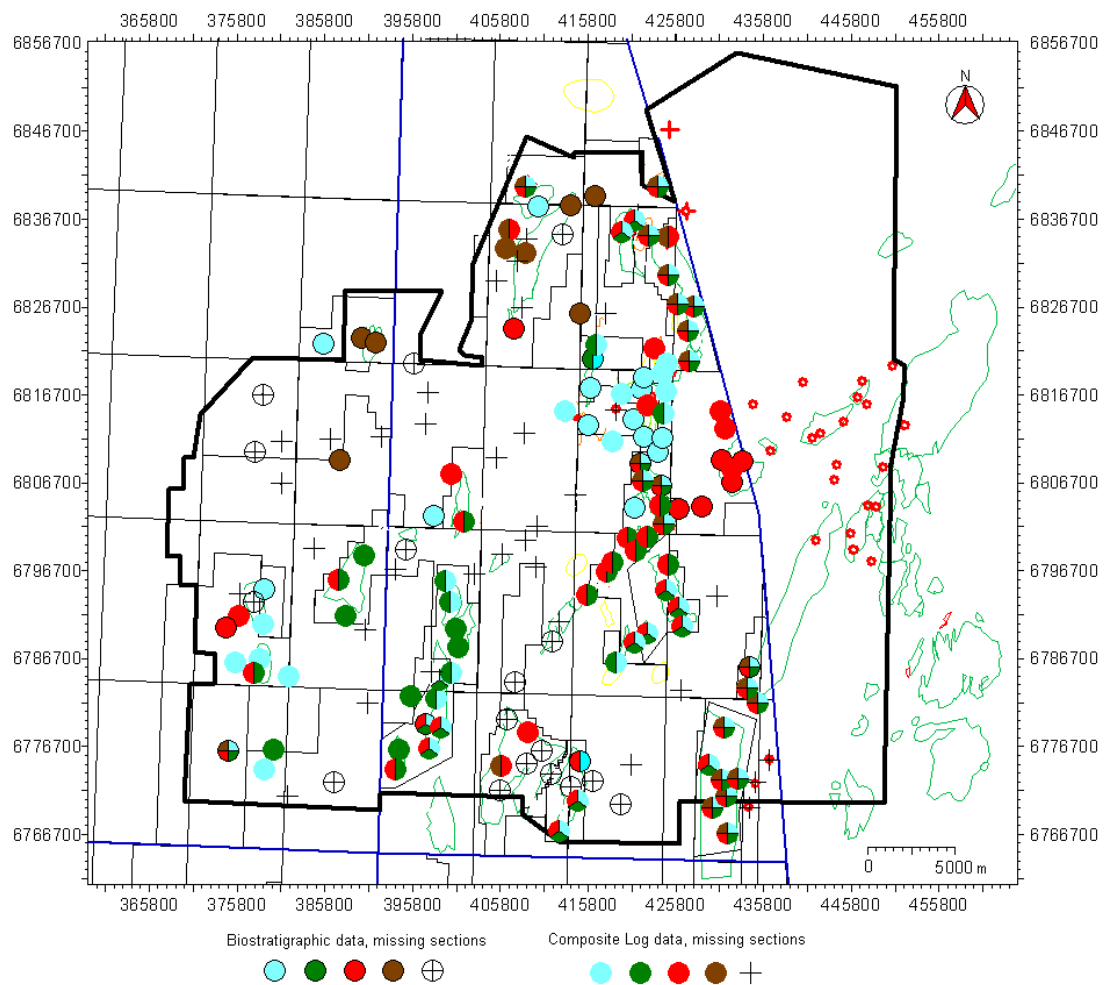


Figure 6-14. Map illustrating the biostratigraphic breaks in the sedimentary record due to erosion in the East Shetland Basin

As the faults continued to grow and hard link through the Callovian and Oxfordian, the uplift along this now larger fault may have been enough to lift the sediments above the sea level and become eroded. It must be noted that

the Causeway area is towards the south-western tip of the larger fault system and thus does not have as much uplift compared to that of the Thistle Field. The Thistle field as a result shows evidence of erosion through all four of the measured time periods. But, as shown in Causeway the individual faults did not have enough uplift to raise the sediments above sea level in the Bathonian, but here Bathonian erosion is present. Could it be that the amount of uplift and erosion through the Callovian and Oxfordian in the Thistle area was enough to cut down and remove the underlying Bathonian sediments from the sedimentological record?

It is not just the Thistle Field that shows this pattern of uplift and erosion. It may be possible that this style of uplift and erosion occurred throughout the basin and is exaggerated in the Brent Field, where uplift was considerably greater than that of other faults, which has led to higher rates of erosion. The erosion is so intense over the Brent Field crest that no Upper Jurassic sediments are present in some wells, which led to Upper Cretaceous sediments being deposited directly on top of the Lower Jurassic Dunlin Group.

Is it possible then that in the upper-most Middle Jurassic that there were very few or no islands present as the uplift created by individual faults was not enough to create an island archipelago. It wasn't until the Upper Jurassic, predominantly in the Callovian and Oxfordian, where fault growth and linkage became the uplift driving force and brought sediments above sea level, where they could have been eroded away. This would suggest that the size of the island would determine the erosive rates. The size of the field is a direct result of faulting and thus the larger the fault the greater the uplift. The larger islands would also have a greater altitude. This increase in altitude and size will have a higher rate of erosion compared to that of a smaller island. Areas that are predicted to have increased erosion could

dramatically reduce the amount of sediment preserved in the deeper, underlying Brent Group.

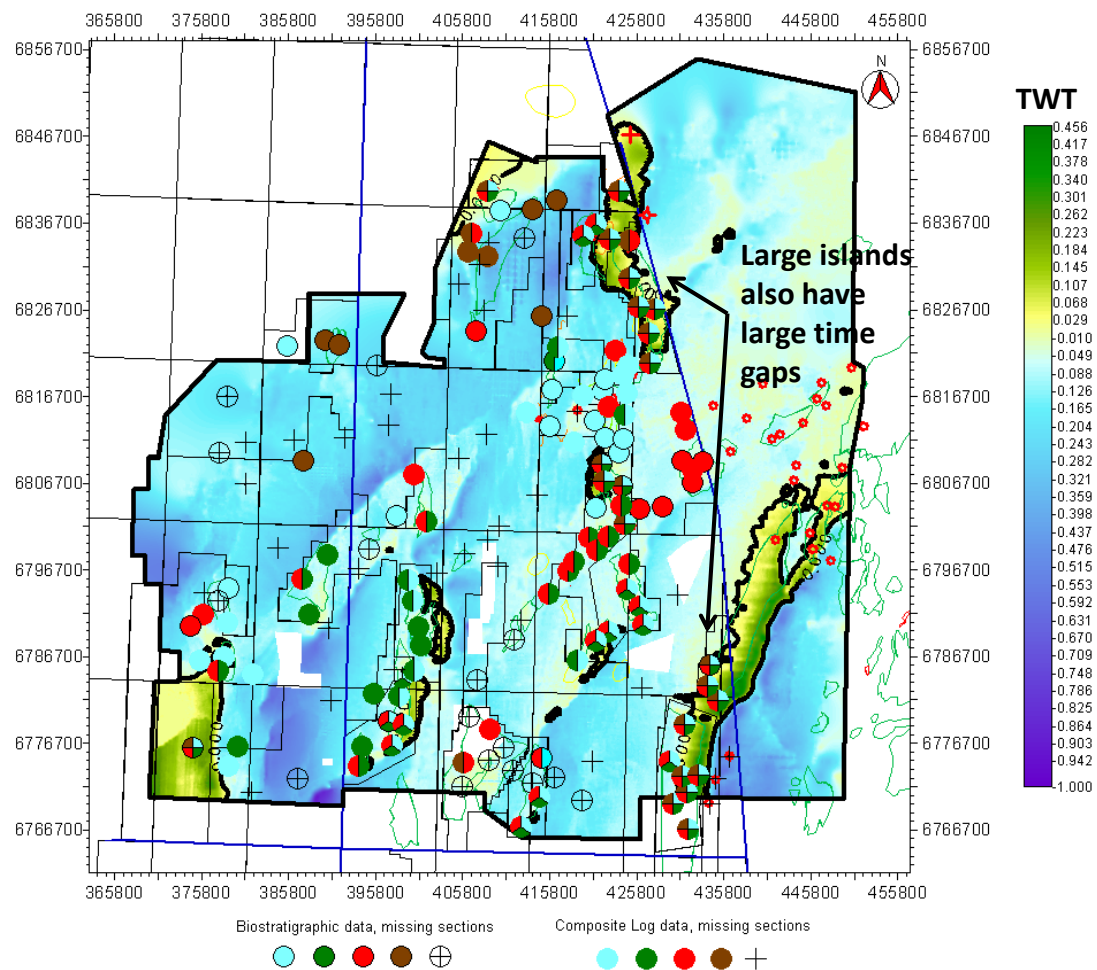


Figure 6-15. Overlaying the biostratigraphic data on top of the Base Cretaceous Unconformity to top Brent isochron map illustrates the potential location for island locations.

By comparing the well data and seismic interpretation against one another in Figure 6-15 it is possible to see that areas that are missing on the seismic correspond with the biostratigraphic data. These two sets of data give a strong indication of where it is possible to predict where islands may have formed within the Upper Jurassic. Areas that are to have predicted large amounts of erosion over the structural highs also have large gaps within the sedimentological record, emphasising the theory of island formation and their possible location. By analysing the biostratigraphy of well logs and

reconstructing the structural features pre-erosion is possible to anticipate island location.

The regional cross section (Figure 6-4) shows the tilted fault block geometry associated with the Upper Jurassic rifting event. The western edge of the cross section is situated over the Pobie Platform and forms one of the rift shoulders to the Viking Graben. The crests of these tilted fault blocks are locations of the hydrocarbon fields Cormorant, Hutton, Brent and Gullfaks (west to east). Each one of these areas has undergone a period of erosion, some greater than others, such as Hutton, which is heavily faulted and has minor erosion whereas the Brent fault block has a large scale unconformity, which in areas separated the Lower Jurassic Dunlin Group with Upper Cretaceous sediments.

It is further clear to see the thickening packages relating to the syn-rift sediments, such as the Heather Group, Kimmeridge Clay Formation and Cromer Knoll Group. The deposition of the Heather and the Kimmeridge Clay Formation can be clearly seen within the depocentres of the large scale normal faults. Whereas, the Lower Cretaceous Cromer Knoll sediments drape over the underlying Upper Jurassic stratigraphy. In the case of the Brent and Gullfaks Fields there are very little or no Cromer Knoll sediments present over the high, suggesting they were sub-aerial during the Lower Cretaceous.

6.3.3 Sedimentological Analysis

The final sedimentological analysis that was undertaken over the study area, relates to the deeper, non-island locations. Within these locations, it is difficult to identify directly the presence of an island, but it may be possible

to identify the effects of an island archipelago. If an island archipelago formed and the Upper Jurassic sediments were eroded, as illustrated above, these predominantly sand prone units must have been re-deposited, either down dip of the fault or shed back from the fault crest. The erosion of the uplifted sediments would have occurred within the Upper Jurassic, where mud sediments dominate. With this noted, it is possible to identify within the Humber Group, sand prone members which relate to the erosion of the Middle Jurassic Brent Group over the fault crest.

The amount of sand deposited around the fault crest is ultimately determined by the amount of time the fault block formed an island, but other key factors such as gradient and climate are also important. The longer the fault block formed an island would result in a longer period of erosion and greater amounts of the Brent group being eroded. This could also lead to the generation of beach sedimentation around the fault crests. These additional sand prone areas could become important in determining secondary reservoirs as the hunt for hydrocarbons in a mature basin continues. Wells within the East Shetland Basin, over these structural highs such as the Penguin Field, contain marine generated oolitic sediments. Oolites can form in more than one way, ranging from aeolian to marine conditions. The sediments found over the Penguin Ridge and other areas suggest that these sediments were formed by inorganic precipitation of calcium carbonate (CaCO_3) in a high energy shallow environment, such as a beach. For oolites to form the precipitation of calcium carbonate needs a host rock for the CaCO_3 to precipitate on, these grains can be sourced back to the fault crest. It is difficult to illustrate the location of these sands using the well data as the majority of the wells are drilled over structural highs whereas wells required to illustrate this evidence needs to be located down-dip of the crest on the footwall block. Wells that are located within these areas all show an increase

in sandy material within the Heather Formation, which could relate to the erosion of the eroded footwall crests.

An important process which relates to the formation of these secondary reservoir sediments is uplift rates. When islands form it is important to know how quickly the islands are emerging and how long they are going to form for. Using analogues from the Greek islands, an uplift rate of 1.5mm/yr can be applied to footwall uplift rates (Stewart 1996). As the Brent Group sediments were deposited close to/at sea level, this continuous uplift over a prolonged period of time could create significant island features. The Upper Jurassic rifting event in the Northern North Sea lasted for approximately 5Ma and is sufficient time for the sediments to surface above sea level, even though there is an apparent increase in sea level due to the rifting event in the Upper Jurassic during the deposition of the deep marine Kimmeridge Clay Formation.

The presence of these near-shore sediments in a marine dominated location, along with evidence from biostratigraphic reports, seismic volumes and geophysical well data strongly suggest that an island archipelago formed within the East Shetland Basin in the Upper Jurassic.

6.4 *Effects and Consequences of Island Formation*

Now that an island archipelago can be defined within the East Shetland Basin, it is important to see what effects this has on sediments and sediment dispersal. As noted above, the depositional environment of the Upper Jurassic island archipelago would have been during the syn-rift stage of the Upper Jurassic rifting event. The primary effect associated to this depositional stage is the generation of accommodation space in the

hangingwalls of normal faults and the erosion and re-deposition of footwall sediments. A secondary effect of the island archipelago formation is related to meteoric leaching in the sand prone units that are brought up close to or above sea level.

6.4.1 Island Archipelago Erosion in the East Shetland Basin

With the formation of an island archipelago, sediment dispersal patterns change. Prior to the formation of an island archipelago the primary sediment dispersal patterns were fairly straight forward with the thickest sediments found in the hangingwall areas of normal faults where accommodation space is at its greatest, and relatively thin sediments found over the footwalls where accommodation space is reduced. Now that some of the sediments in the footwall of these large scale normal faults have been brought up above sea level, a potential shore line can develop around the uplifted areas. This in turn leads to areas of non-deposition and areas of pinch out and erosion. In a sense, the sediments are filling in around the uplifted areas in the saucer shaped depressions created by hangingwall subsidence, and being eroded over the structural highs.

This can have an enormous effect on the petroleum system within the East Shetland Basin. As the primary reservoir unit within the East Shetland Basin, the Brent Group, which is now thought to have been brought up above sea level in some areas of the East Shetland Basin, any potential erosion and re-deposition of this sand prone unit can be crucial in the exploration for hydrocarbons. This is illustrated in the Brent Field, where the crest of the footwall has been heavily eroded and re-deposited either down dip or back shed from the structural high. If this is the case then there is potentially as

secondary reservoir deposited within the Upper Jurassic strata of the Humber Group.

The re-deposition of the Brent Group sediments in the Upper Jurassic may create a secondary reservoir, potentially, a smaller localised version of the Magnus Field. The Magnus Field generated a series of Upper Jurassic sub-marine fans which were back-shed from the Magnus High Boundary Fault (Figure 6-16). The footwall uplift of the Upper Jurassic fault block caused the erosion of the up Middle and Upper Jurassic sediments that were previously deposited over the high. These sediments are then back-shed down the fault block as sub-marine fans (Figure 6-17). This influx of clastic material within a predominantly mud based environment will be well capped to prevent any leakage if the sediments are charged by hydrocarbons.

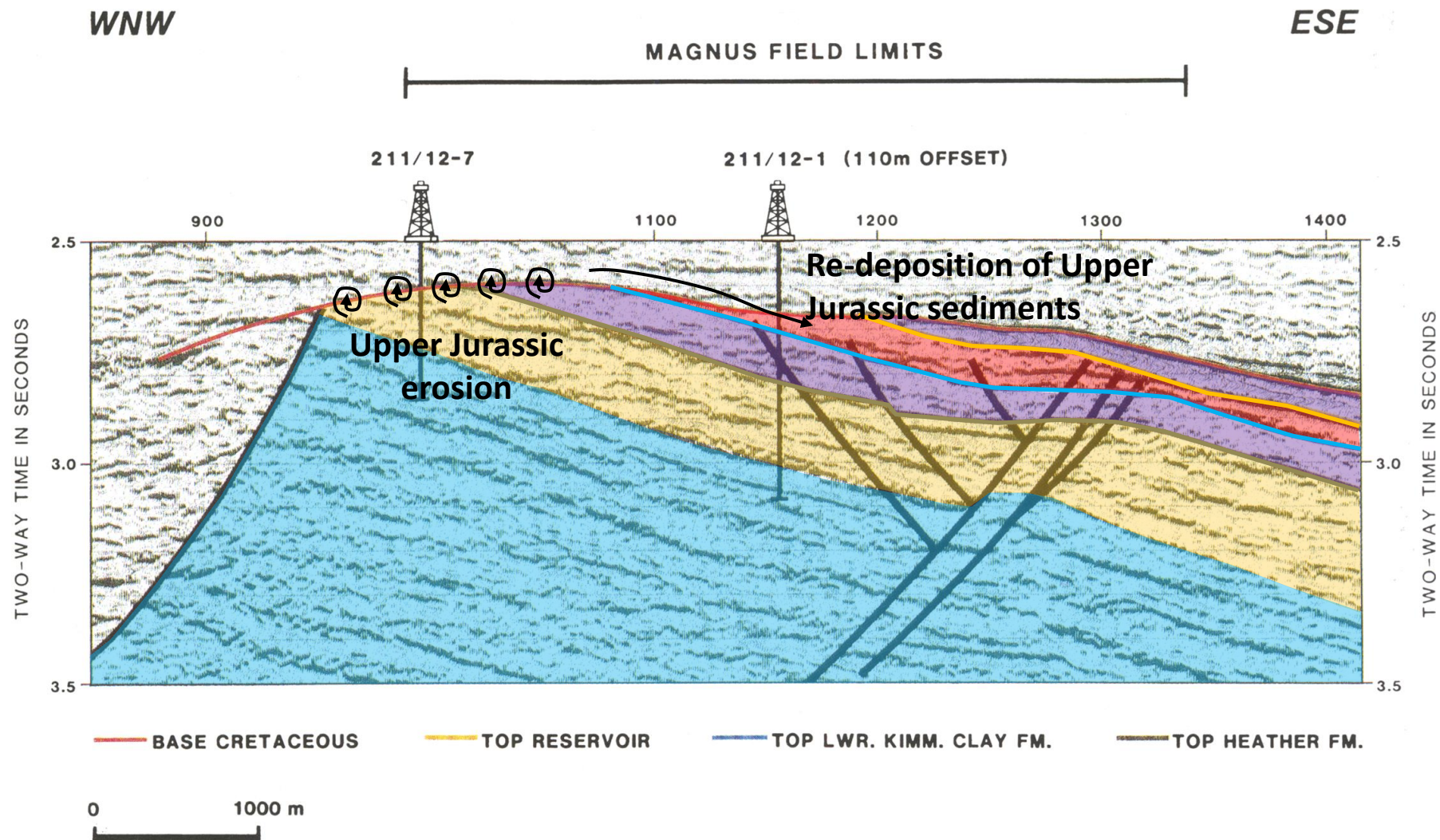


Figure 6-16 highlighting the development of the Magnus Sandstones Formation (Shepard 1991).

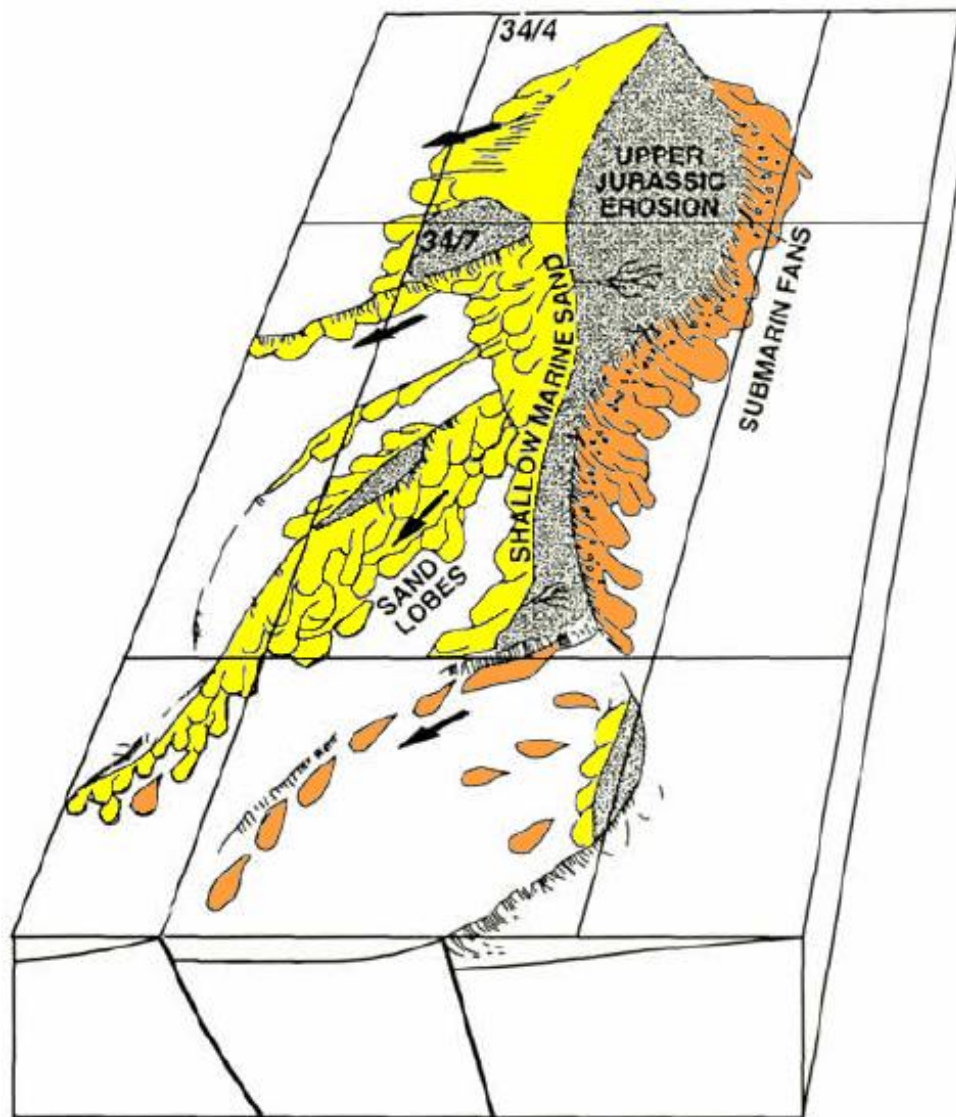


Figure 6-17. Illustration of two types of secondary reservoirs over the Snorre Field. Generation of down-dip detached sands (orange) and back shed attached sands, which could possibly for oolitic sediments (yellow) (Dahl and Solli 1993).

Although these secondary reservoirs may not be on the scale of the structural traps (Figure 6-18) formed by the rifting event, but, the erosion and re-distribution of the Middle Jurassic Brent sands are directly related to the formation of an Upper Jurassic island archipelago. As a result, the Upper Jurassic sediments do not conform to a normal syn-rift sediment dispersal pattern, due to the localised uplift and erosion of footwall crests, which may have been brought above sea level.

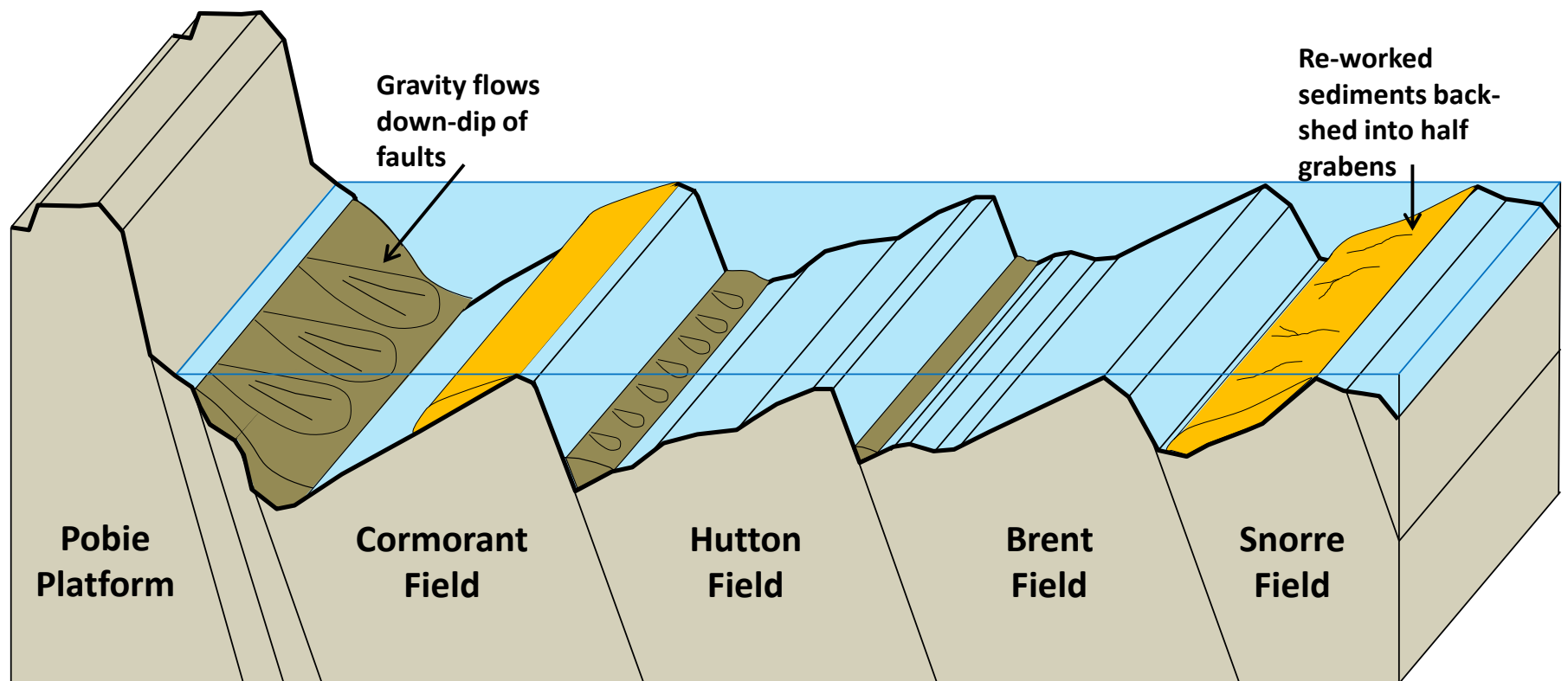


Figure 6-18 schematic diagram of the varying environments created by the Upper Jurassic rifting.

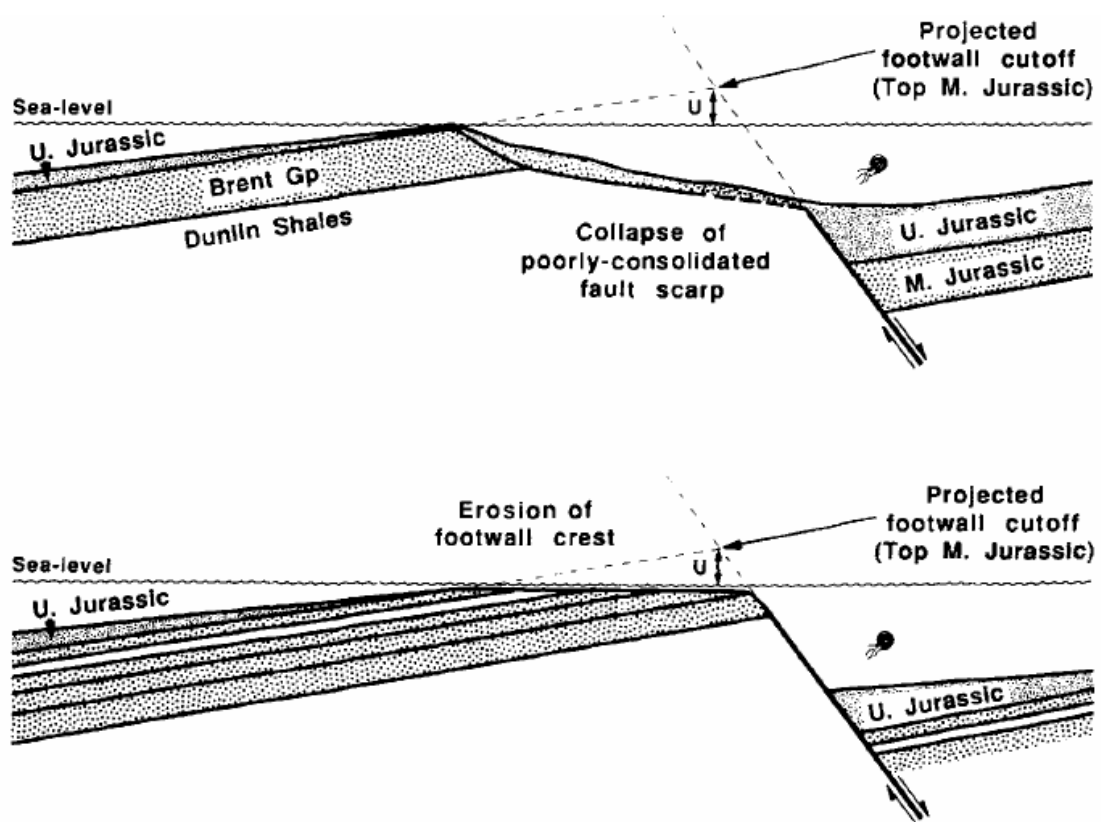


Figure 6-19. Illustration of the erosion that may occur to the Upper Jurassic sediments as a result of footwall uplift close to or above sea level (Yielding 1992).

The angle of a fault plane and the amount of uplift is a determining factor in the amount of erosion that a fault crest may undergo. In areas such as Causeway where the uplift is not as high as the Brent field area the amount of erosion observed is considerably less. This can be a key feature to determine what sediments are re-deposited and the quality of sediment deposited. This is seen over the Snorre Field (Figure 6-17) where the rate of uplift and erosion is so high that erosion cuts down into the Triassic sediments (Figure 6-19). This means that not only has the sand prone Brent Group sediments been eroded and redistributed, so has the sandy Upper Triassic – Lower Jurassic Statfjord Sandstone Formation. This results in the deposition of two sand prone sequences within the Humber Group separated by the more mud prone sediments of the Dunlin Group (Figure 6-20). Although there are some sandstone formations within the Dunlin Group, it is a predominantly mud based section and as it is deposited within the

Humber Group, which is also mud prone, the likelihood of prospective sequences of reworked Dunlin sediments is low.

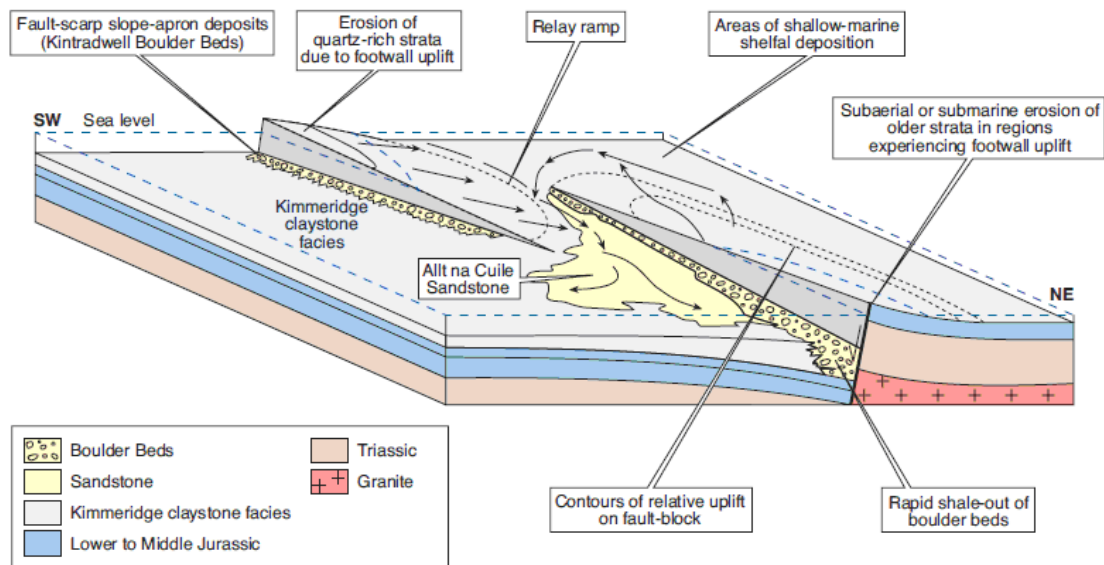


Figure 6-20. Illustration of sediment dispersal patterns as a result of footwall uplift segmentation and fault propagation (Underhill 1994).

6.4.2 Meteoric leaching

As the Middle Jurassic Brent Group sediments were uplifted up above sea level during the rifting event, the uplift subsequently led to erosion to the Brent Group and the overlying Humber Group. This is observed over several tilted fault blocks throughout the East Shetland Basin. What has also been noted is an increase in the amount of altered feldspars and vermiform kaolin minerals within the Brent Group sandstones and in some areas (such as the Penguin Ridge) the underlying Triassic Statfjord Sandstone Formation. These are direct products of meteoric leaching, which would have occurred when the sediments were brought up above sea level.

It has been shown by Glasmann (1992) that framework grain dissolution of feldspars is present within Brent Group sediments and by Emery et al in the

Magnus Sandstone Formation. This is the partial dissolution or complete removal of feldspar minerals within a sandstone body. This is a direct process of meteoric leaching. Framework grain dissolution can be defined as the sweeping of acidic waters through a feldspar rich sandstone body. Meteoric waters are naturally acidic as they contain carbon dioxide (CO_2) and sulphur dioxide (SO_2) which can produce carbonic acid (H_2CO_3) and sulphuric acid (H_2SO_4) (Bjørkke and Jahren 2010). These acidic waters are capable of dissolving aluminium-silicates such as K-feldspar over a prolonged period of meteoric flushing (Siebert 1984). These acids are then flushed through underlying sandstone formations by meteoric waters (Figure 6-21).

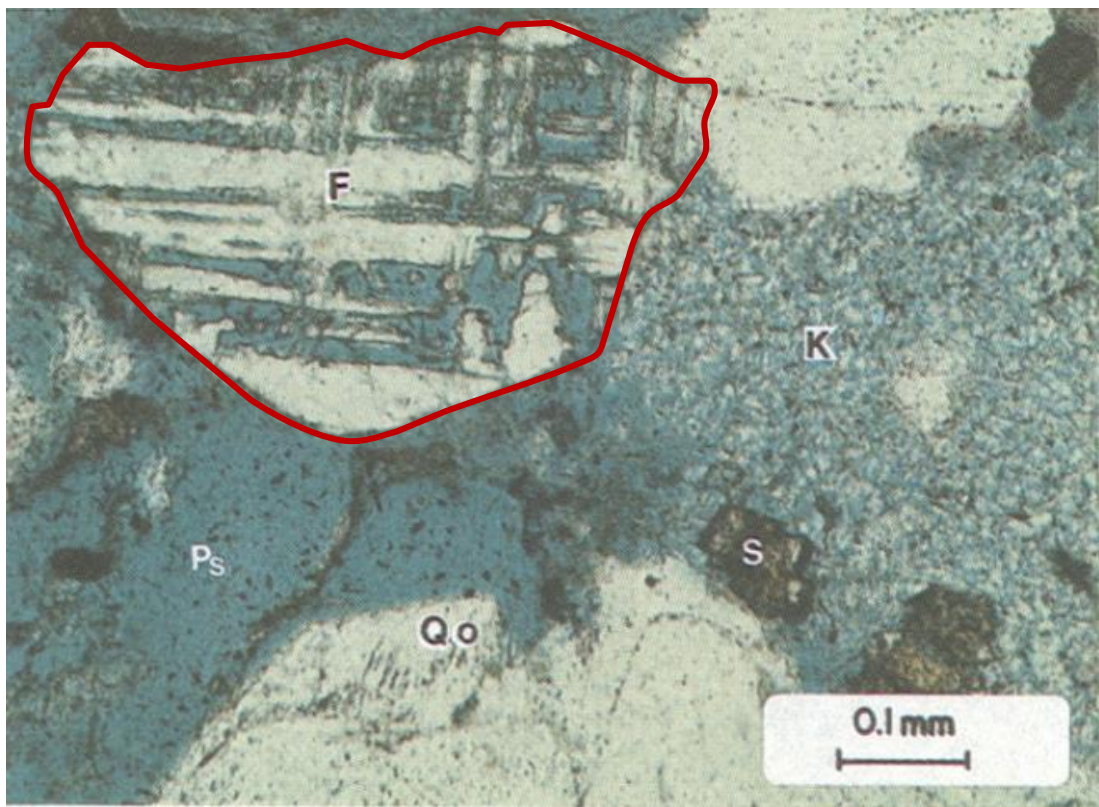


Figure 6-21 Illustrating feldspar grain dissolution. Evidence from well 211/27-A28 located within the Hutton Field highlight a feldspar grain (F) has been partially dissolved due to meteoric leaching (Scotchman et al 1989).

The dissolution of K-feldspar only occurs where the acids are flushed through the sandstone stratigraphy (Figure 6-22). This flushing is going to occur over the crests of tilted fault blocks, where the water head pressure of

the meteoric waters are high enough to penetrate down through the sand bodies. As the feldspars go into dissolution, the meteoric fluids became less saturated with respect to minerals such as feldspars and thus the leaching and dissolving capacity of the meteoric waters will diminish. As a result, only the fault crest may exhibit grain dissolution, other areas further down dip may remain the same or may have an increased amount of K-feldspars. The increased K-feldspars may come as the precipitation of potassium due to the large quantities of it being produced and washed away by the up-dip leaching process.

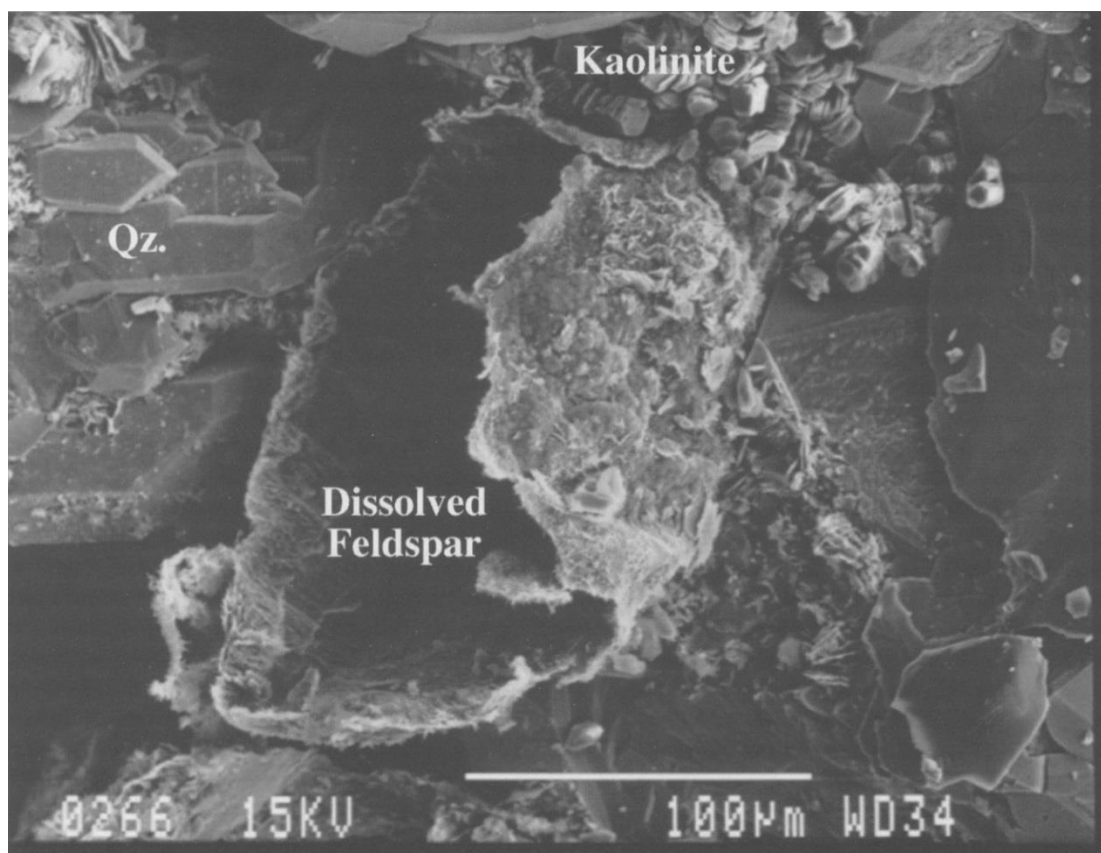


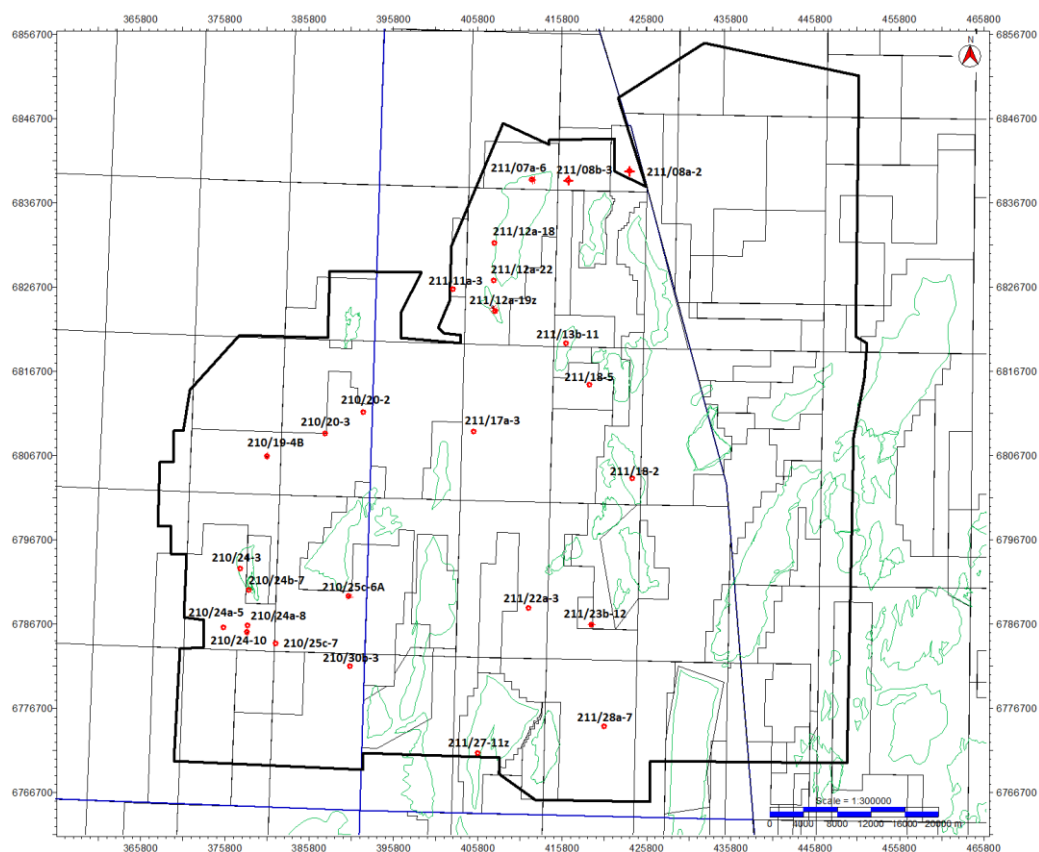
Figure 6-22 Evidence of feldspar grain dissolution in the Huldra Field, Northern North Sea (Bjørlykke 1998). The dissolution of feldspar grains can significantly increase porosity within reservoir units.

The timing of this mineral dissolution is directly related to the timing of uplift and exposure of the sediments above sea level and the amount of time spent above sea level. It will not be possible for meteoric flushing to occur

unless the sediments have been brought up above sea level. The earliest point at which dissolution can occur relates directly to the timing at which meteoric waters can enter the sandstone prone layers. The longer the sandstones are exposed to these conditions the “cleaner” the sands may become, with more feldspars being dissolved. If an area remains above sea level for a prolonged period of time, erosion will start to have an effect on the exposed areas. The removal of the overburden will result in a deeper penetration of the acidic fluids, thus, a greater zone of grain dissolution.

The data presented in this chapter strongly supports an environment in which influx of meteoric waters in the Brent Group sandstones has resulted in the dissolution of K-feldspars. It has also been suggested that that removal of these grains actually “clean” the sandstone units and improve the porosity of the sandstone unit. The one down side to the meteoric flushing is the generation of the clay mineral kaolin. Although the presence of a clay mineral such as kaolin is not necessarily a good thing, kaolin is generally a porosity filling clay rather than a permeability reducing clay mineral such as illite. The kaolin minerals are created by increasing porosity from the feldspar dissolution and the amount of porosity that the kaolin grains are reducing is minimal compared to the amount of porosity created.

It has been suggested by Taylor et al. (2010) that the overall impact of meteoric flushing is not that great and that it only creates 2-5% more porosity depending on how much leaching has occurred. But, considering the porosity of a Northern North Sea ranges generally from 18-22% a variation of 2-5% on top of these values can improve the porosity value by anything from 9 to 28 percent in an individual formation, something that has the potential to change whether or not a prospect is producible or economically viable.



210/19-4B	210/20-2	210/20-3	210/24a-3	210/24a-5	210/24a-7
210/24a-8	210/24a-10	210/25-6A	210/25c-7	210/30b-3	211/07a-6
211/08a-2	211/08a-3	211/11-3	211/12a-18	211/12a-19z	211/12a-22
211/13b-11	211/17a-3	211/22a-3	211/23-4	211/23b-12	211/27-11Z
211/28a-7					

Figure 6-23. Map illustrating boreholes which have potassium concentration logs and can be used for the study of meteoric leaching.

The analysis of well data (Figure 6-23) through the study area makes it possible to highlight the potential that meteoric leaching has on reservoir enhancement in the Northern North Sea. By producing a series of seismic sections (Figure 6-24) which have been well tied to wells with sufficient well data it is possible to analyse the change in porosity along a structure and compare areas that are anticipated to have formed islands to those which have not. The well logs used within this study are Gamma Ray (GR), Potassium Concentration (POTA), Porosity (PHID) and Bulk Density (RHOB). The porosity value was generated using the Bulk Density value

form the log data. To measure the porosity a set of values are needed regarding the density of fluid and grain matrix.

$$\text{Porosity (PHID)} = \frac{(\text{Bulk Density matrix} - \text{Bulk Density log})}{(\text{Bulk Density matrix} - \text{Bulk Density Fluid})} \times 100\%$$

Within this study the bulk density recording for the matrix and the fluid remained constants throughout. The Bulk Density of the matrix was measured at 2.65g/cm³ (sandstone), whereas, the Bulk Density of fluids was 1g/cm³ (water).

Seismic line A-A' is located over the Cormorant Field and illustrates the importance of meteoric flushing in the East Shetland Basin. Through this section (Figure 6-25) three well sections are used to illustrate the change in porosity along the tilted fault block. Well 210/25c-6A is located in the hangingwall low to the Tern-Eider Ridge and the average porosity within the Brent Group sediments is 10%. This location is not expected to have been exposed above sea level and would have seen no improvement in reservoir quality. Wells 211/26-5A and 211/26b-10 are located further up-dip and have significantly different porosity values. Well 211/26-5A has an average porosity of 20% whereas well 211/26b-10 has an average porosity of 35%. Both of these environments are anticipated to have undergone some level of meteoric leaching. Well 211/26b-10 is located over the crest of the structure and is anticipated to have undergone a greater level of "cleaning" compared to the other wells, which is shown through the porosity logs. No potassium concentration logs were present over the two up-dip wells, so no comparison between potassium concentration can be undertaken.

Seismic line B-B' (Figure 6-26) measures a similar set of data over the Brent Field. The Brent Field has a similar structural architecture. Five wells are situated within this section, but, wells 211/29-5 and 211/29-6 have no

Gamma Ray or Bulk Density logs available for this analysis. The most westerly of the three wells (211/28a-7), is located down-dip of the structural high and has a porosity value of 10%. The same to that of the corresponding well in the Cormorant Field study. Well 211/29-1 located further up-dip has a greater porosity value of 20%. The furthest east well (211/29-8) has a porosity value of 10% but is located in the hangingwall to the Brent Field and is not expected to have undergone any meteoric leaching.

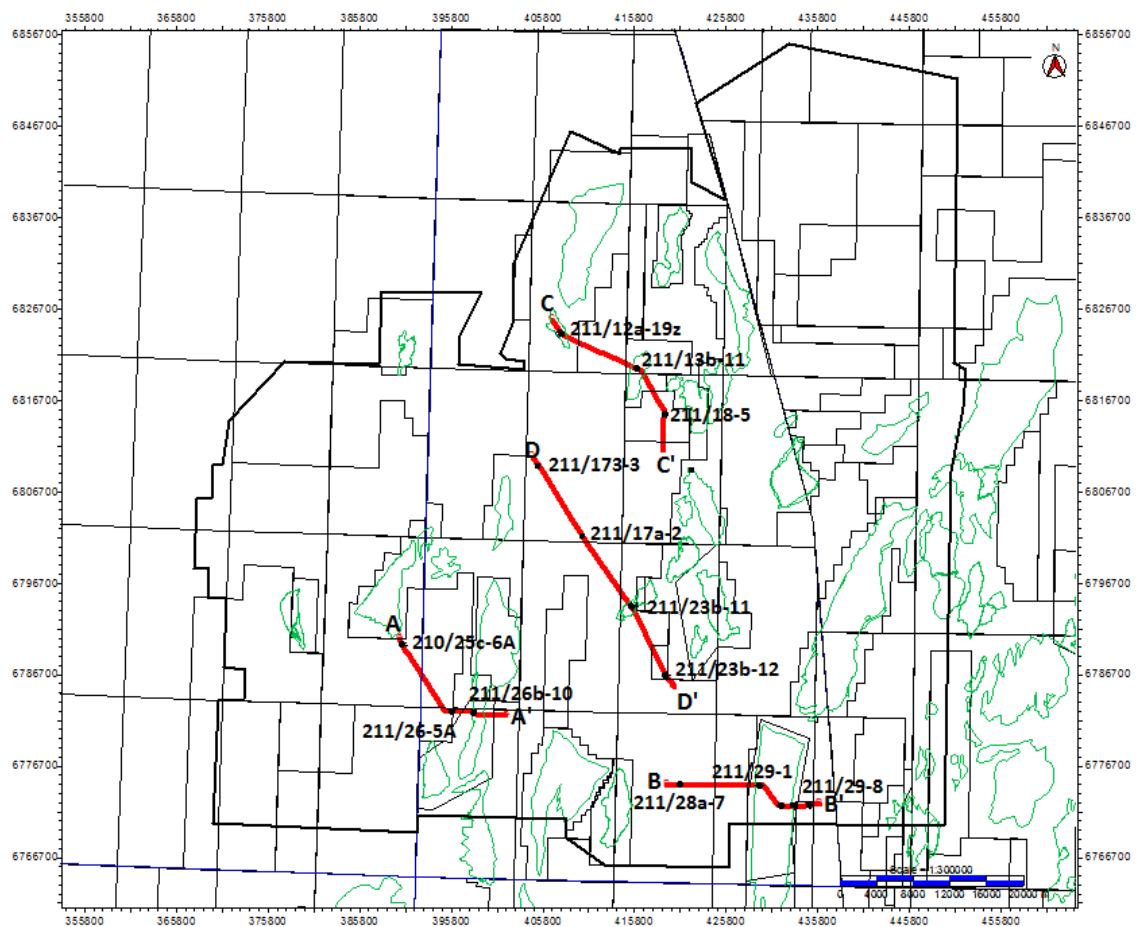
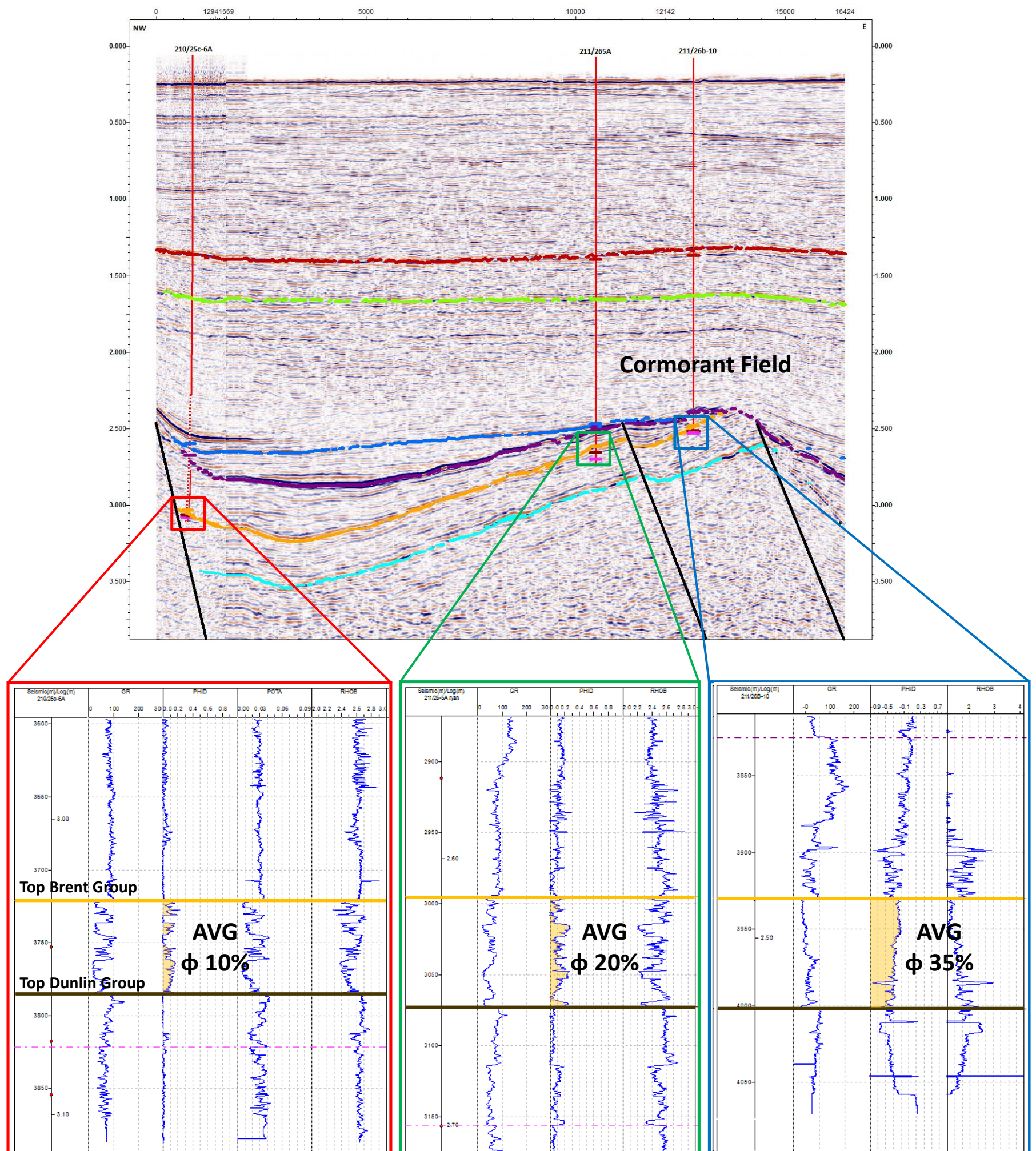


Figure 6-24 A series of seismic lines have been generated to illustrate the effects of meteoric leaching in the East Shetland Basin. By using a suite of well logs which include Gamma Ray, Potassium Concentration and Bulk Density it is possible to see the change in porosity depending upon the location of each well.



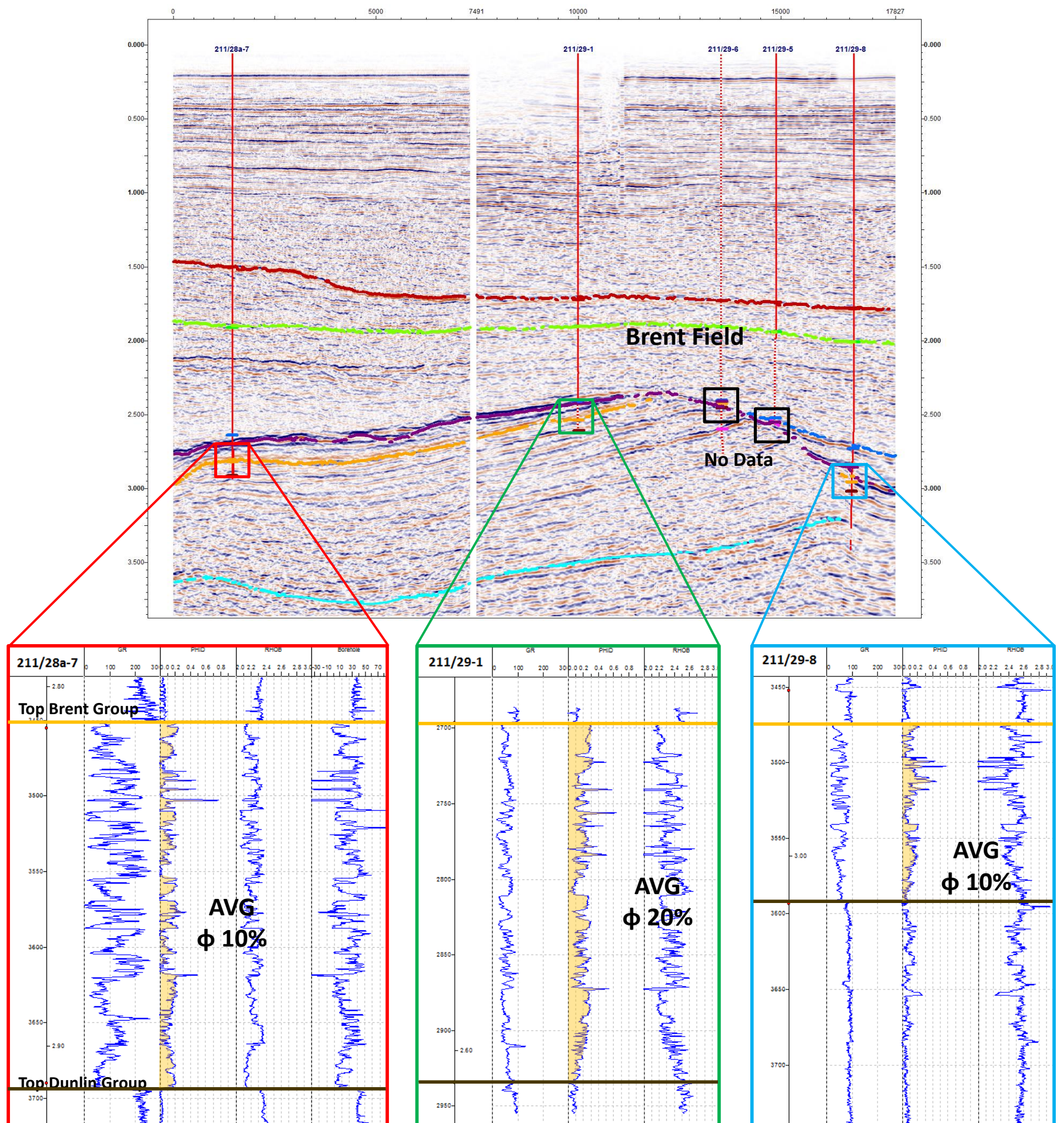


Figure 6-26 Seismic and well section through the Brent Field. The improvement of reservoir quality in the up-dip locations of a tilted fault block are again observed here.

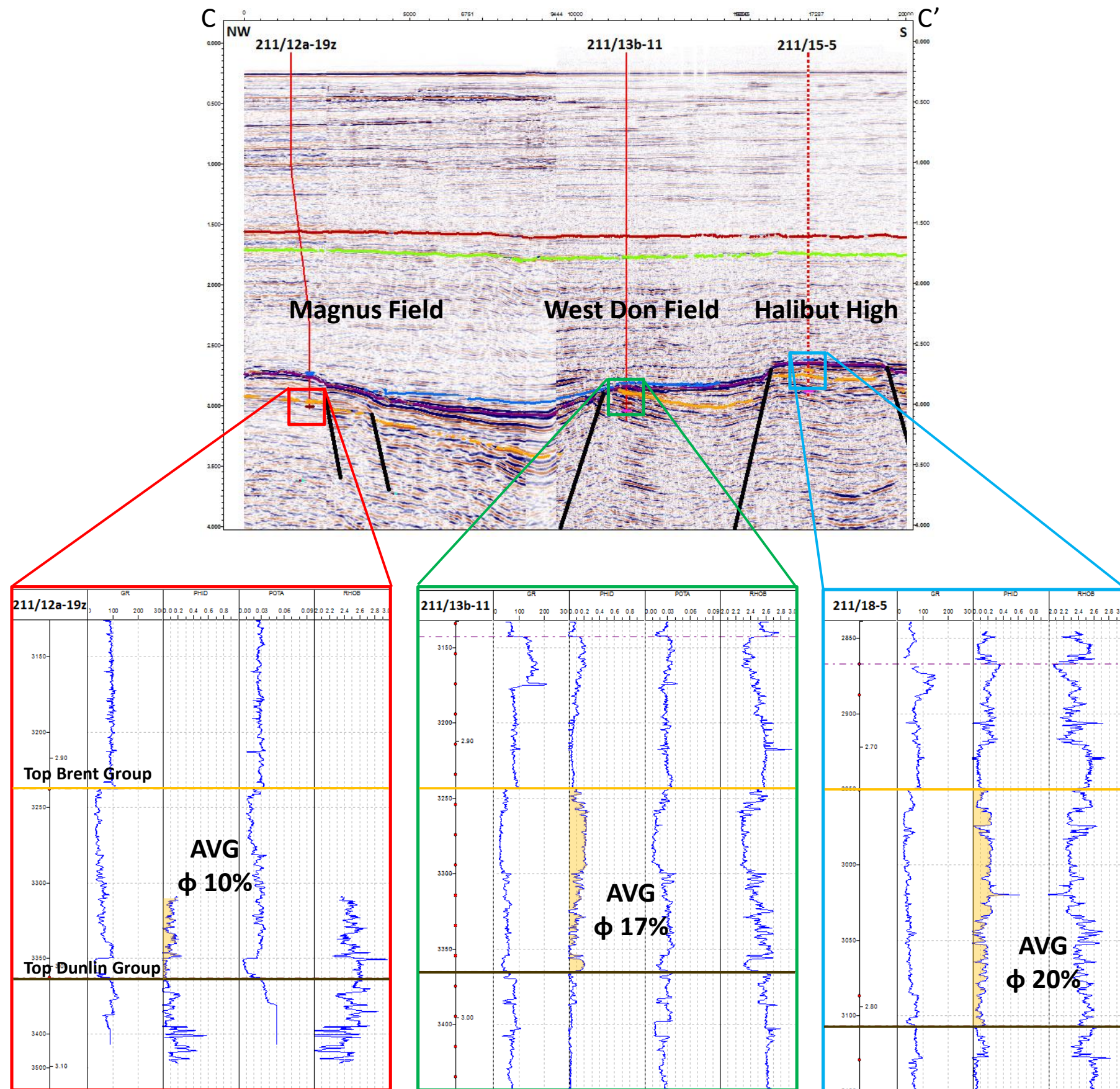


Figure 6-27 Seismic and well section through the Magnus and West Don Fields and also through the structure known as the Halibut High.

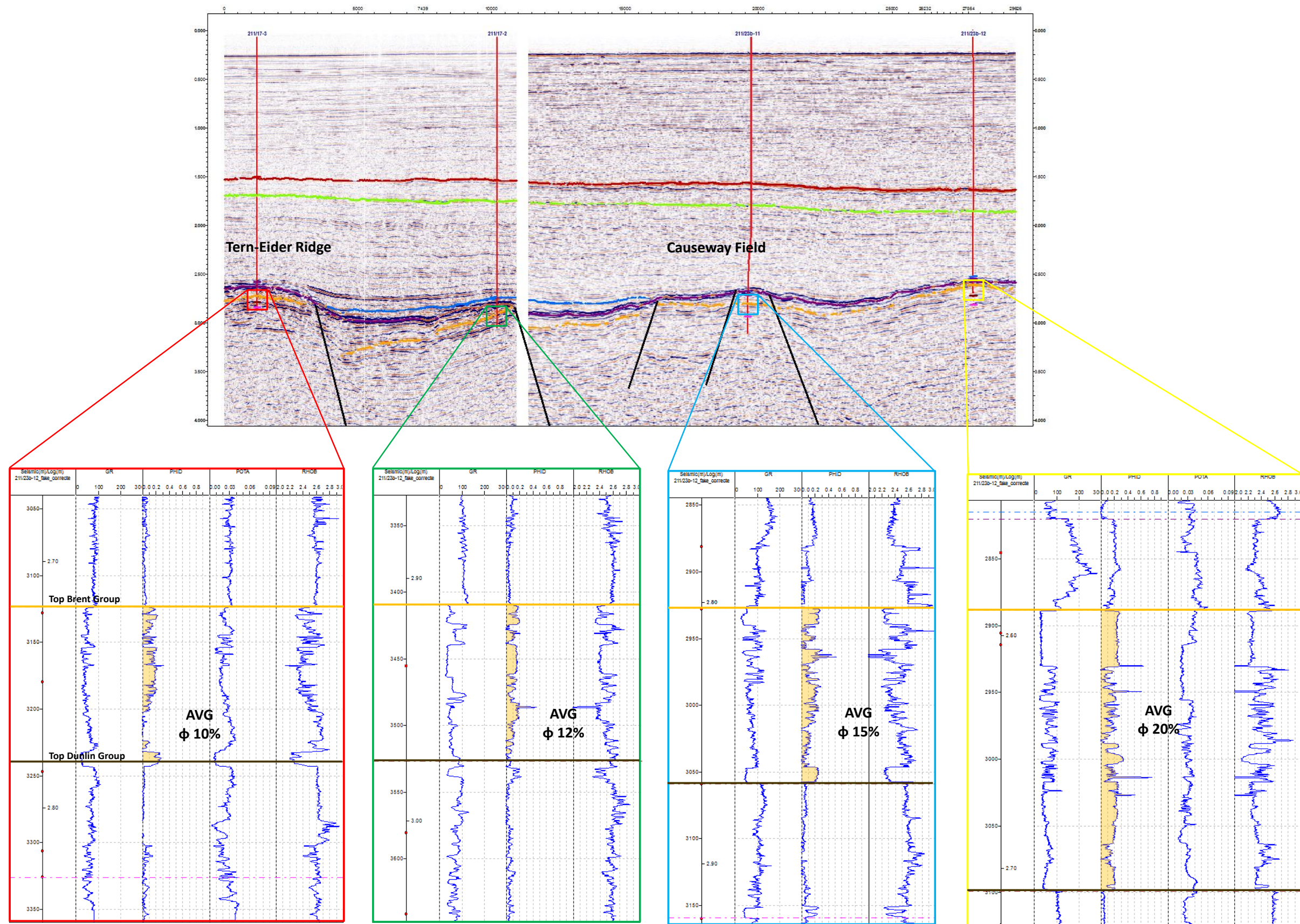


Figure 6-28 seismic and well section illustrating the change in porosity values from the northern edge of the Tern-Eider Ridge to the Causeway Field

The third seismic section C-C' (Figure 6-27) is located to the north of the study area and covers the Magnus Field, West Don Field and the Halibut High structures. Well 211/12a-19z, which is located within the Magnus Field, has an average porosity of 10% and is located down dip of the main structural high situated west of the section. This agrees with the pattern identified in the two previous sections of down-dip locations have a low porosity value. The wells located over the West Don Field (211/13b-11) and Halibut High (211/18-5) are situated in more structurally elevated locations and are more likely to have undergone a some level of meteoric leaching. The Halibut High is a more elevated than the West Don structure is likely that this feature has undergone a greater level of leaching. This is represented within the porosity values and within the Potassium Concentration logs.

Within this section Potassium Concentration logs are present within wells 211/12a-19z (Magnus Field) and 211/13b-11 (West Don Field). Although both wells have a similar response to Potassium Concentration within the Brent Group, a subtle difference can be identified. The Potassium Concentration in the more structurally elevated 211/13b-11 well is on average 0.01ppm lower than that of the value found in well 211/12a-19z. This decrease in porosity can be related to the meteoric leaching effect of bringing the West Don area close to or above sea level in the Upper Jurassic rifting event. Whereas the Magnus Field well did not undergo the same level of leaching, due to the inability of the fresh meteoric water to penetrate down deeply enough to effect the well location.

Seismic section D-D' (Figure 6-28) focuses upon the area surrounding the Causeway Field. Within this section four boreholes have been selected to

further illustrate the effect of meteoric leaching and the subsequently improvement in reservoir properties.

All four wells are located in the highs of structural traps and thus, comparison to down-dip location can only be achieved with wells in other sections. Well 211/17a-3 is the most north-westerly borehole and has an average porosity of 10%. This borehole is located in the north-easterly limit of the Tern-Eider Ridge, but is not a major structural high. The Causeway Field is located within the centre of the seismic section and an increase in porosity is observed. Within well 211/23b-11 the porosity has raised to 15% on average. The largest porosity within the Brent Group is located in the south-easterly location of the seismic section. Well 211/23b-12 is located to the south west of the Dunlin Field, which is a structural high and may have undergone a level of meteoric leaching as this location has a thin covering of Upper Jurassic sediments.

The generation of secondary porosity would be welcomed within the East Shetland Basin. However, its effects of this early diagenetic process may be overwritten in a deeper stage diagenesis. It may be possible that all of the porosity that is created by the leaching process may be filled by later stage quartz overgrowths or clay minerals. This all depends on when and if the areas are charged by hydrocarbons and the quartz grains in particular are coated by hydrocarbons rather than water, which would restrict quartz overgrowths from forming. As shown in the figures above (Figure 6-25 to 6-28) areas such as the Cormorant Field retain this increase in porosity that was generated by the meteoric flushing.

One aspect that must be considered when talking about grain dissolution and the possibility of increasing porosity is whether the structure is an open

or closed system. There is a significant difference in reservoir quality depending upon the type of system applied.

When the sandstone unit is described as a closed system, the grain dissolution associated to the feldspar grains must act as a linear equation. If the grains go into solution within up-dip areas then they will precipitate down-dip when the waters become overly concentrated in dissolved minerals. This can have the adverse effect to that seen in the up-dip locations. In up-dip locations where porosity values increase it is likely that the porosity values in the down-dip location will decrease due to the precipitation of feldspar minerals. But, if the system is acting as an open system then this reduction in down-dip porosity is unlikely to occur. In this case the fluids may exit the sandstone unit after dissolution and take the dissolved feldspars out of the system. If this occurs it is likely that the up-dip porosity will increase and the down-dip porosity will not be altered.

Within the East Shetland Basin it is likely that the fault blocks have acted as a closed system. This is best shown in the Cormorant Field example (Figure 6-25). Within this location the up-dip porosity is over double that of the porosity found in the down-dip location. Here, it is possible that the feldspars which have dissolved over the crest of the fault block and created porosity have precipitated in the down-dip location and thus reduced porosity in this location.

It has been widely accepted that kaolin forms within shallow acidic ground waters, preferably at low temperatures, which suggests meteoric waters. Wilkinson et al. (2006) noted the presence of vermiform kaolin within the Brent Group sandstones in the Cormorant Field forms from a direct result of fresh water input into the Brent Sandstone units (Figure 6-29). It is possible

to see regular blocky kaolin, which is thought to post-date the vermiform kaolin and forms during burial of the sandstone units (Wilkinson 2006). Vermiform kaolin is a worm like shaped version of the Kaolin clay group which is thought to primarily form in shallow meteoric conditions.

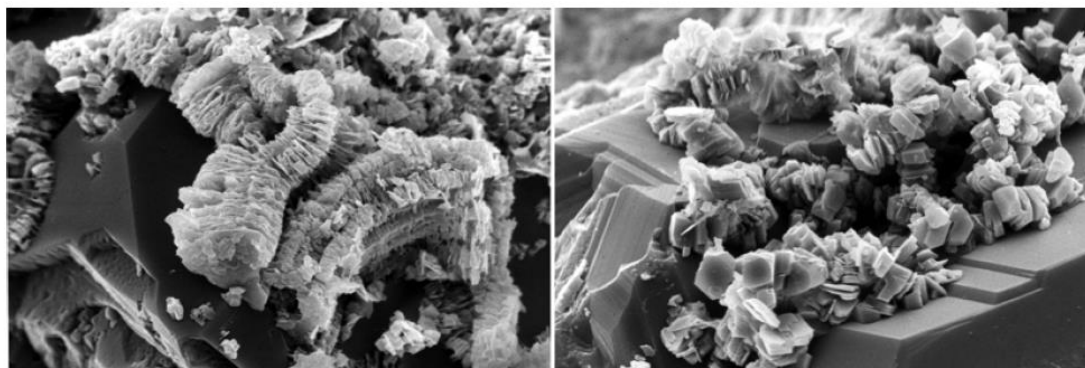


Figure 6-29. Illustration of kaolin morphologies over the Cormorant Field. Left: illustrates vermiform kaolin. Right: regular blocky Kaolin found down dip of the Cormorant Field (Wilkinson 2006).

For the vermiform kaolin to grow it must have formed before burial and in close proximity to a regular source of meteoric water. It has been suggested that these early kaolin minerals formed directly after deposition when the Brent delta was still having an influence of the depositional environment. The source of the kaolin is thought to be the direct result of K-feldspar dissolution. For this dissolution to occur there must have been a process of leaching from meteoric waters. Thus, the sediments had to have been penetrated by meteoric waters, either directly after deposition or when the sediments were uplifted during the Upper Jurassic rifting event.

For the growth of kaolin to have occurred directly after deposition the supply of fresh water must come from fluvial channels that created the Brent delta itself. The supply of fresh water will have reduced significantly after the Ness Formation due to a rise in sea level and the deposition of the regressive Tarbert Formation. The supply of meteoric waters later in the Upper Jurassic may be more sporadic in terms of location but the areas that

do endure meteoric leaching will have prolonged influx of meteoric waters. This leaching will also cause dissolution of K-feldspars which is needed to create the ingredients to form the kaolin. The leaching would have occurred when the sediments were uplifted during the Upper Jurassic rifting event. This uplift would have exposed the Middle Jurassic Brent Group sandstones either in the fault scarp or by erosion of the overlying sediments and the waters migrating through the remaining Humber Group sediments. This flushing and erosion would also generate the broken fragments of mica that is needed as the nucleation point of any kaolin mineral.

The presence of vermiform kaolin in a potentially uplifted area such as the Cormorant Field, gives further evidence that these areas were once uplifted and flushed with meteoric waters. The flushing of meteoric waters could have come through either erosion or exposure through fault scarps. For the leaching of meteoric waters to occur the sediments themselves must have been brought up above sea level, otherwise the vermiform kaolin could not have formed.

6.5 Conclusions

The work undertaken on seismic, geophysical well logs and biostratigraphic logs over the full study area has illustrated that there was an Upper Jurassic island archipelago in the East Shetland Basin.

The interpretation of key horizons in several 3D seismic blocks makes it possible to map out large sections of eroded pre-rift and syn-rift sediments that were meant to be within a predominantly marine environment. The erosion of these sediments is located directly over the crest of tilted fault

blocks. This erosion could have only occurred by the footwalls of normal faults being uplifted above sea level and eroded in a terrestrial environment.

These erosion surfaces can be mapped out with the use of biostratigraphic data. The majority of wells within the East Shetland Basin are tied together with biostratigraphic analysis. The biostratigraphic data is used to illustrate any unconformities or breaks in stratigraphy. It has been made clear to see here that over the projected island locations there are significant breaks in the stratigraphy. Over the Brent Field alone there is a time gap of almost 100Ma. Although the island will not have been exhumed for this period of time, it proves that the area has been brought up to an area of high erosion, much greater than that expected just below sea level. Thus, suggesting that these areas have been brought up above sea level where erosion rates are considerably higher, and would have been great enough to cut down deep into the pre-rift sediments, as seen over the Brent Field.

As there has been a large amount of erosion over the footwall crests and of the Brent Group sediments, the redistribution of these sediments is key in identifying any secondary reservoir units that may form in the syn-rift Humber Group sediments.

It has been shown that the uplifting of the Middle Jurassic Brent Group sediments in the Upper Jurassic by the flexural-cantilever model have been eroded over the footwall crests, but more than just erosion has occurred in these areas. It has been possible to illustrate that these areas have been flushed by meteoric waters and what response this has on the sand prone sediments.

It can be seen that in the areas of uplift and flushing of the Brent Group has caused a significant reduction in potassium. This potassium reduction is directly related to the framework grain dissolution of K-feldspars that are present within the Brent Group sandstones. The removal of these potassium rich minerals from the fault crests illustrates a significant influx of meteoric waters into the system.

Further evidence of meteoric waters can be seen by the increased amounts of vermiform kaolin, which is a direct result of feldspar dissolution in a shallow, meteoric environment. The removal of these feldspars may also lead to the generation of secondary porosity, which could result in improved reservoir properties and performance.

The study of the fault growth and linkage in determining the Upper Jurassic island archipelago illustrates that the petroleum system is affected by determining the location of secondary reservoirs and the reservoir properties of the primary reservoir the Brent Group.

With the theory of an island archipelago now provable it is possible to role this interpretation out into other areas where large scale Quaternary erosion may have occurred such as the Norwegian sector and see the implications this has for creating secondary syn-rift reservoirs in the Upper Jurassic. Many of these Upper Jurassic deposits occur as turbidites such as the Magnus Sandstone Formation, but do smaller more intricate flows occur and if so are they able to trap and accumulate hydrocarbons?

Chapter 7 Role of Basement Structure and Normal Fault Propagation in Governing syn-rift Sediment Dispersal

7.1 Introduction

Throughout the East Shetland Basin there are several examples of structural reactivation between the initial Permo-Triassic rifting event and the more recent Upper Jurassic rifting event. In areas such as the Penguin Ridge, old Permo-Triassic faults reactivate along the initial fault plane in the Upper Jurassic to accentuate large precursor structural highs. In other areas' such as around Ninian and Alwyn North fields, it is possible to identify precursor and successor faults with a similar strike but with opposed dip polarity. The older westerly dipping Permo-Triassic faults become cross-cut by easterly dipping Upper Jurassic faults. In yet other areas the two fault trends are oblique. What this section will try to show is the effect that this rift obliquity can have on development and evolution of structural styles and consequent dispersal pathways as highs were eroded and the subsequent sediment is transported down into the basin areas through relay ramps. The presence of channelized systems detected by mapping amplitudes allows subtle stratigraphic plays to be recognised. The drowning of these large scale rift structures form a top seal to the reservoir on and subsequently also led to the smaller scale (compactional) faulting in the Paleogene.

The Cladhan area lies on the western margin of the North Viking Graben (Figure 7-1), the northern arm of the North Sea trilete rift system. It is situated at the boundary between the East Shetland Platform and East Shetland Basin. The latter is dominated by a series of SW-NE and N-S

striking normal fault segments formed during two (Permo-Triassic and Upper Jurassic) rift events.

The main effects of the superimposition of two rift events is that SW-NE striking structures formed during the Permo-Triassic have been transected by N-S faults formed during the Upper Jurassic.

The Cladhan area is ideally situated for understanding the consequences of Upper Jurassic transection of Triassic precursor structures and the effect that syn-rift normal fault propagation has on relay ramp development and sediment dispersal. The interpretation of which is made possible by the occurrence of five strategic, high fidelity 3-D seismic volumes (Figure 7-2) calibrated by 110 exploration and development wells (Table 1 & 2).

7.2 *Cladhan and Tern-Eider Ridge*

Two main structural trends can be observed in the study area (Figure 7-1), the Unst Basin and the Tern-Eider Ridge show evidence of a NE-SW fault orientation; whereas the majority of the East Shetland Basin has more of an N-S fault orientation. Each of these structural trends has smaller scale faults which play an important role in determining the structural evolution of the area.

Highlighted in Figure 7-1 is the NE-SW oriented Pobie fault, which generated a Triassic structural high, known as the Pobie Platform. This continued to form a component of the East Shetland Platform in the Upper Jurassic. Other faults relating to the Upper Jurassic rifting are the N-S oriented terrace faults. These form a series of structural terraces along the edge of the East Shetland Platform.

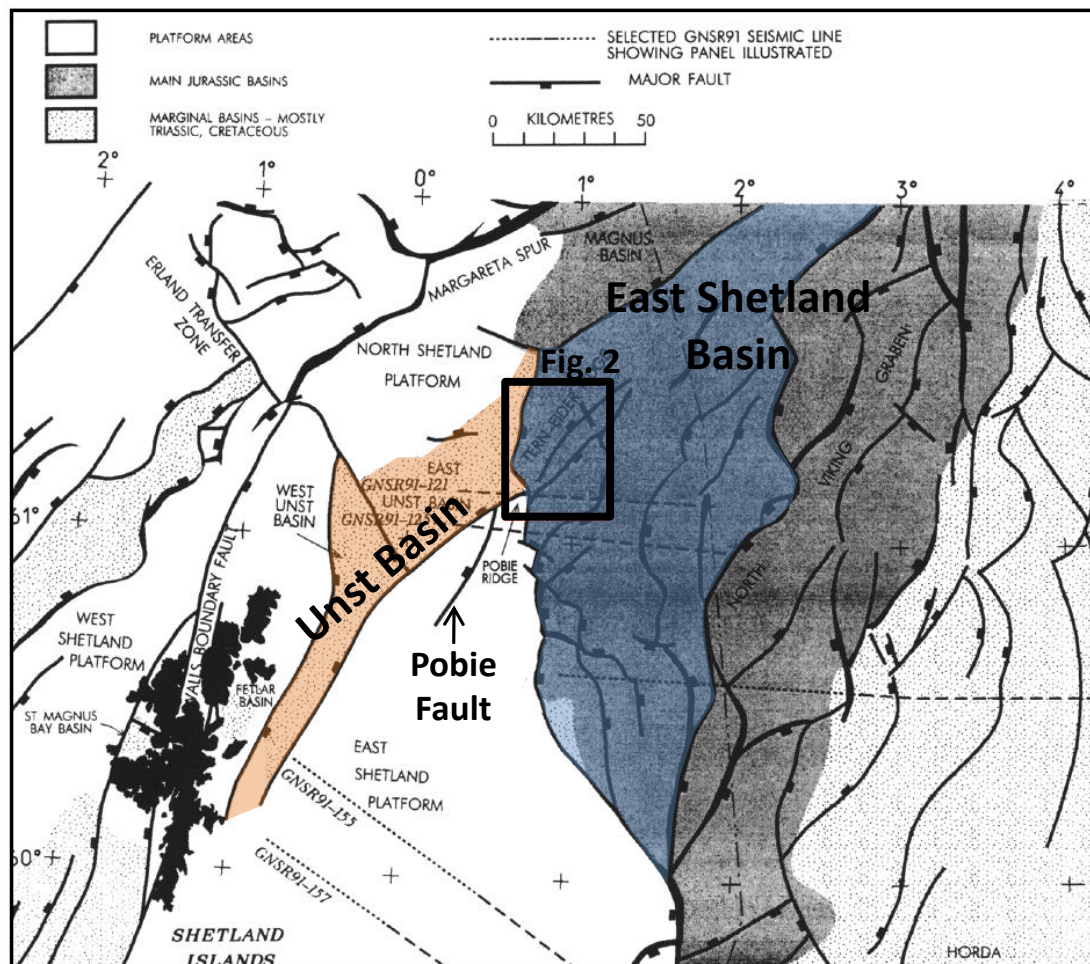


Figure 7-1. Semi-regional basin map showing the locations of the Unst and East Shetland Basins along with large scale normal faulting. Highlighted in black is the study area which is covered by a series of 3D seismic datasets and the insert in red highlights the location of the Cladnan Field (Platt 1995, Sterling Resources, 2012).

7.2.1 Seismic data and well calibration

Five separate seismic volumes were used in undertaking this study. The Cladnan area is located to the south and is highlighted in red. Other seismic volumes are used to illustrate both Permo-Triassic and Upper Jurassic faults, such as the Tern-Eider ridge and the East Shetland Platform.

Table 6. List of seismic data used in the study around the Cladhan area.

Seismic Data	
Used Survey Name	Actual Survey Name
Cladhan Dataset	GE983F0002
Hudson Dataset	SH963F0002
M07 Dataset	Mega Merge M07
Tern-Eider Ridge Dataset	SH953F0001
Tern-Spec Dataset	WG973F0002

Table 7. List of Exploration and Development wells available within the seismic coverage of the Cladhan area.

Well Data				
210/19	210/20	210/24	210/25	210/29
210/30	211/16	211/21	211/26	

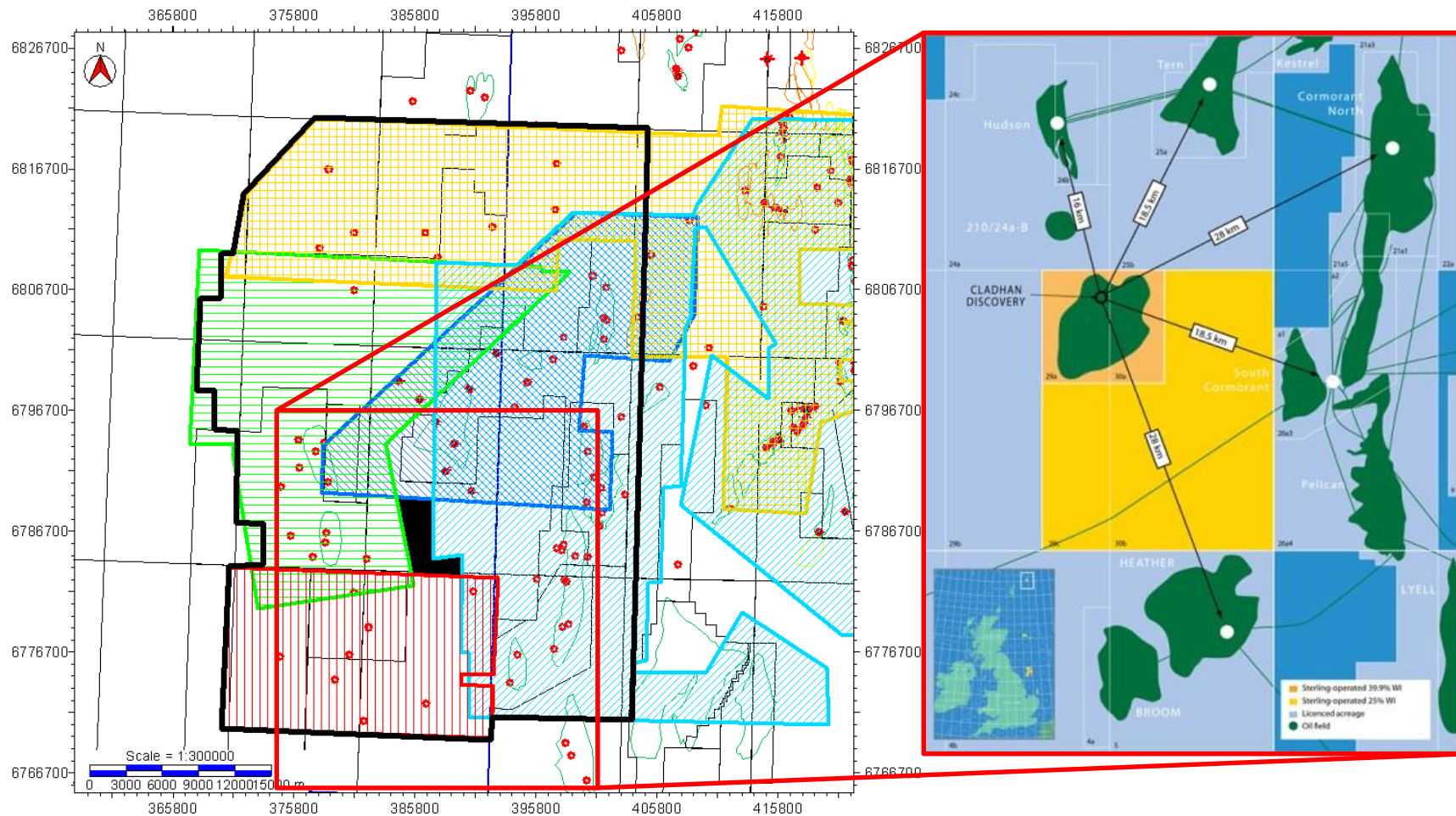


Figure 7-2 Highlighted in red is the Cladhan 3D seismic data volume and in blue is the Tern-Eider Ridge 3D seismic data volume extent

The 110 exploration and development wells that are located within the study area, highlighted in Figure 7-2 are tied to the seismic data by synthetic seismograms. The synthetic seismogram for well 210/29a-3 is illustrated in Figure 7-3, by generating these seismograms it is possible to accurately tie the seismic data to the well data.

Further well analysis shows the development of the platform-terrace-basin relationship that dominates the Cladhan area (Figure 7-4). By generating a seismic section through the wells in Figure 7-4 it is possible to compare the two sets of data. What can be seen in Figure 7-5 and 7-6 which cannot be picked up by the well data is the heavily eroded section on the eastern edge of the Pobie Platform. This is a perfect example of the strength of combining the two sets of data. Well data can be used to infer large scale features such as the structural elements that can be observed in the Cladhan area, but the seismic data can bring out more subtle pieces of information that are located away from the wells.

The Cladhan seismic dataset (Figure 7-2 highlighted in red) is roughly 300km² in size and contains 8 wells which can be used to calibrate the seismic volume and aid interpretation of key horizons within the volume. These wells range in location from over the structural high identified as the Pobie Platform or the East Shetland Platform to the much deeper East Shetland basin location. The Tern-Eider Ridge seismic volume (Figure 7-2 highlighted in dark blue) is larger than the Cladhan volume and has a surface area around 440km². As there are two existing hydrocarbon fields located within this seismic volume, which are the Tern field and the Eider field, which lend their name to the horst structure they are found on. There is as a result, a greater concentration of well data over this seismic volume compared to the Cladhan data, which further aids interpretation along the ridge and the surrounding graben areas to the SE and NW.

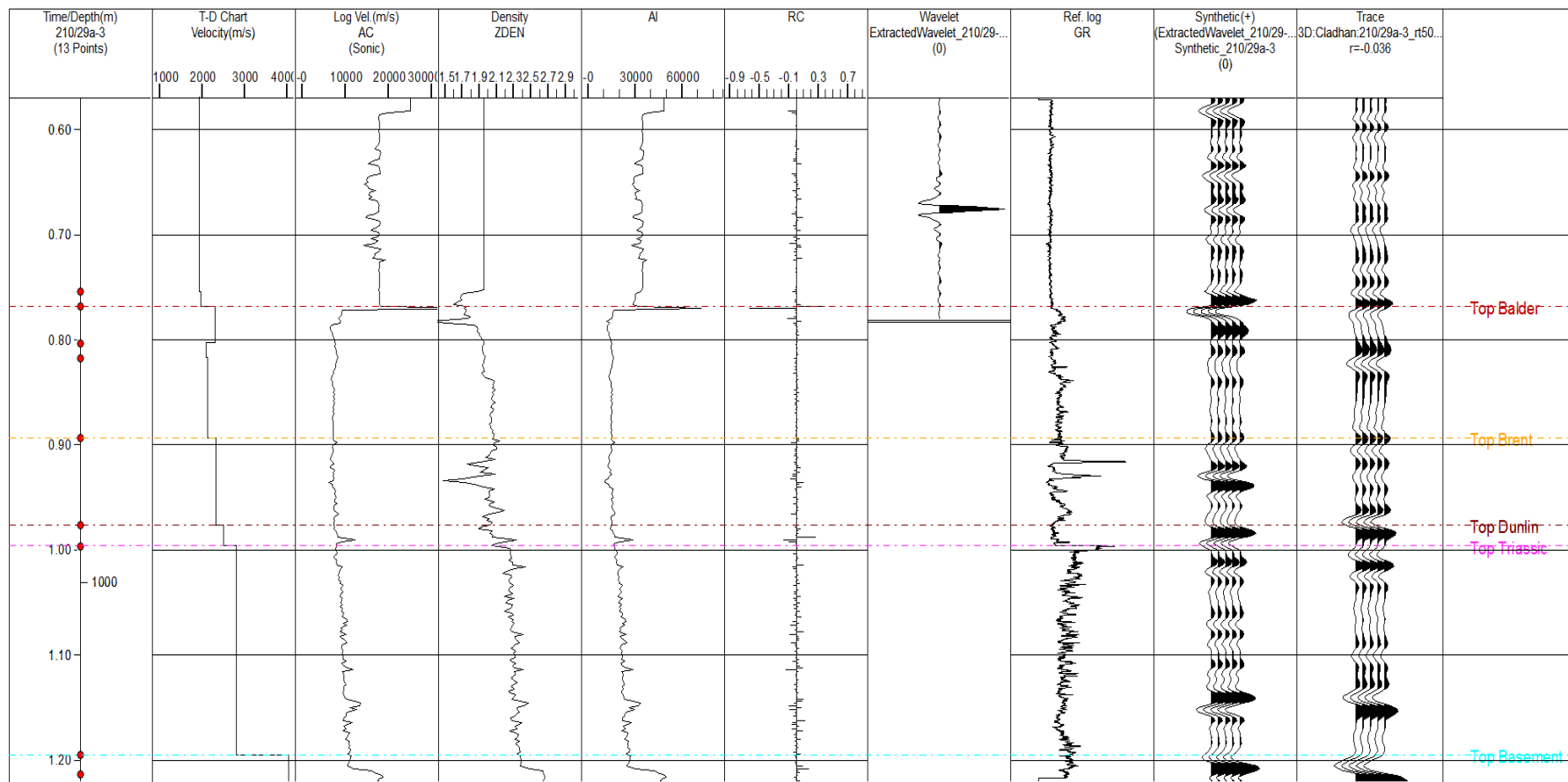


Figure 7-3 Synthetic seismogram for well 210/29a-3 illustrating the tie from the borehole to the seismic data within the Cladhan study area.

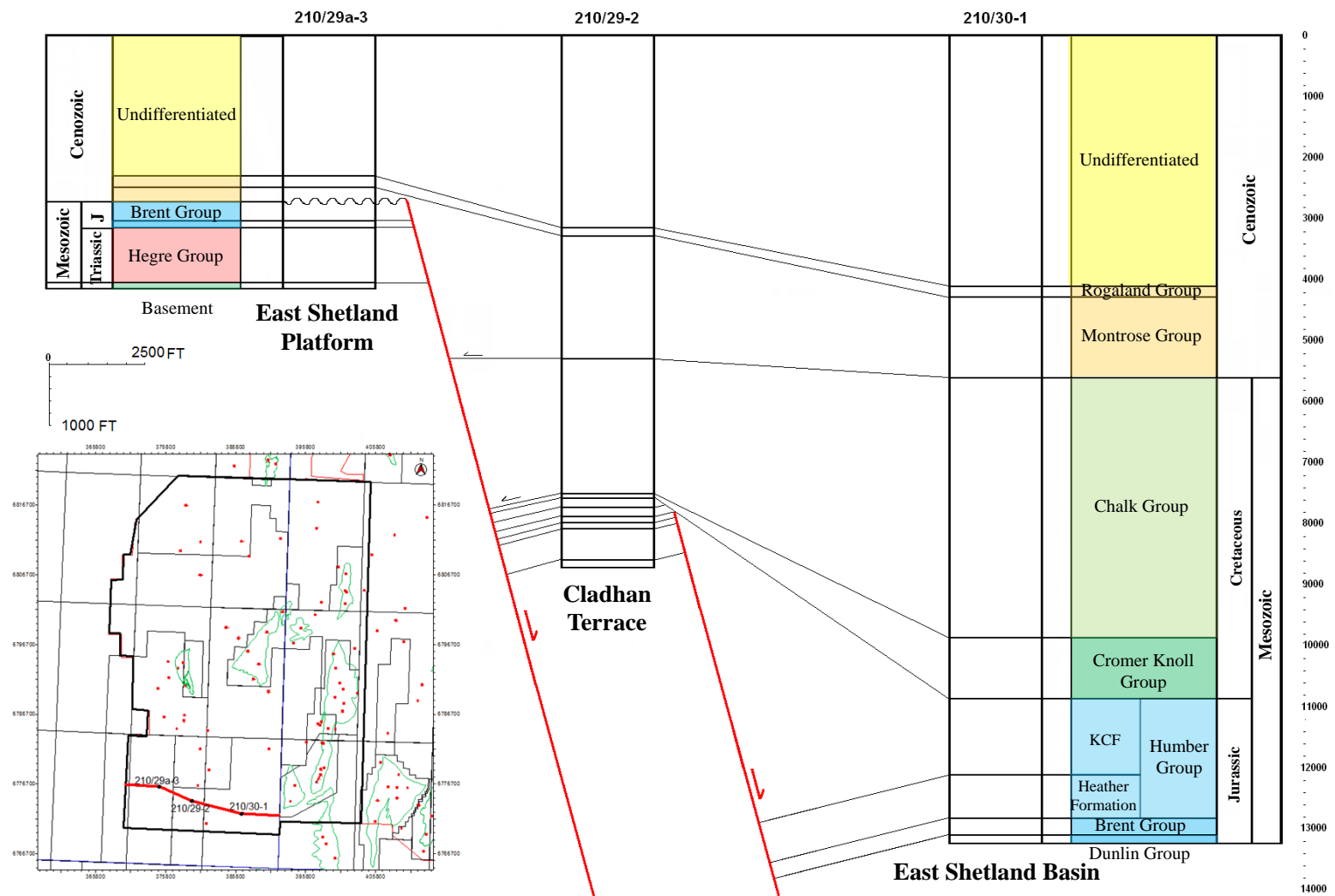


Figure 7-4. Well correlated section through the Cladhan seismic dataset

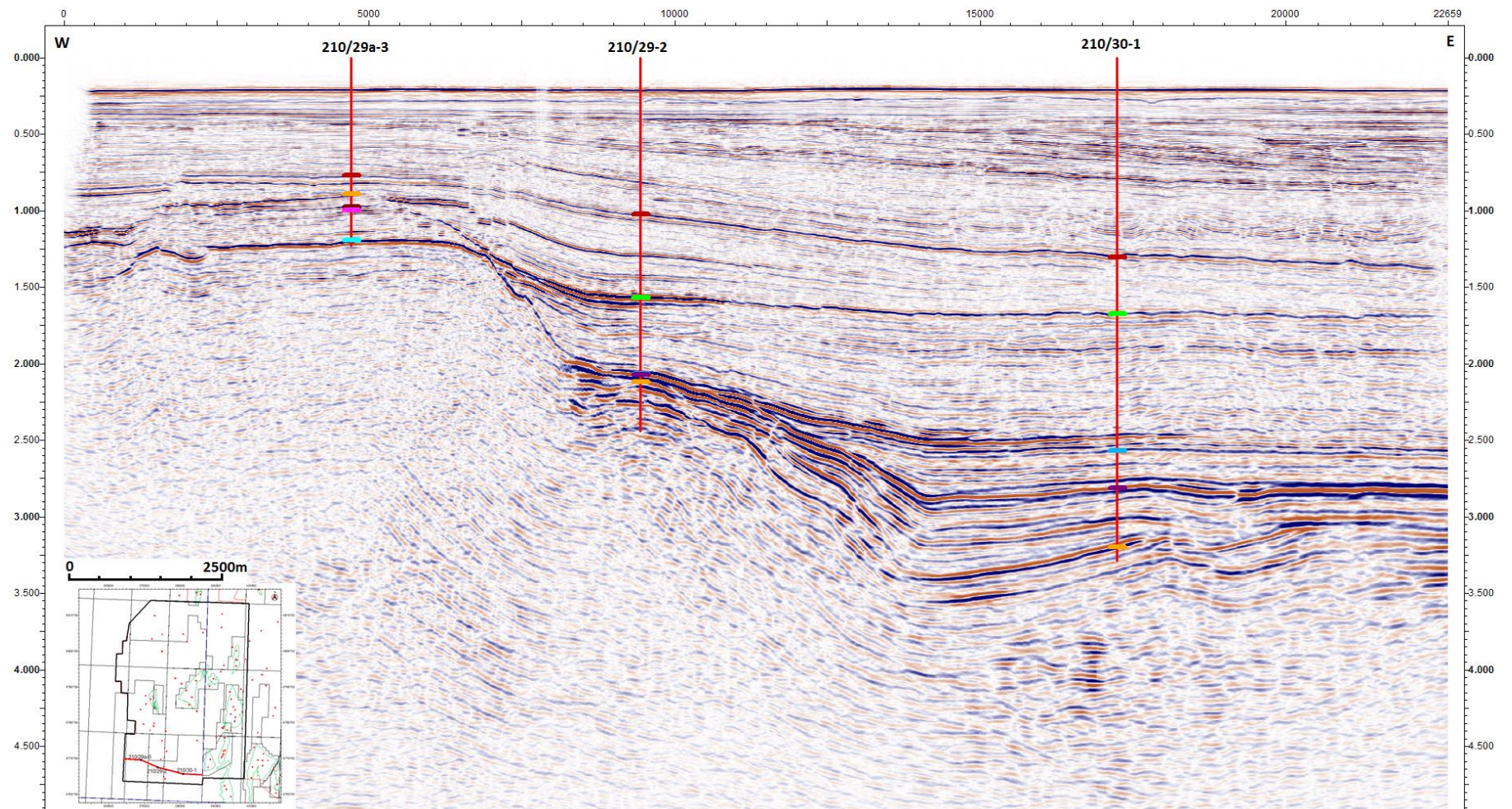


Figure 7-5. Seismic line from the Pobie Platform (west) through to the basinal area to the east.

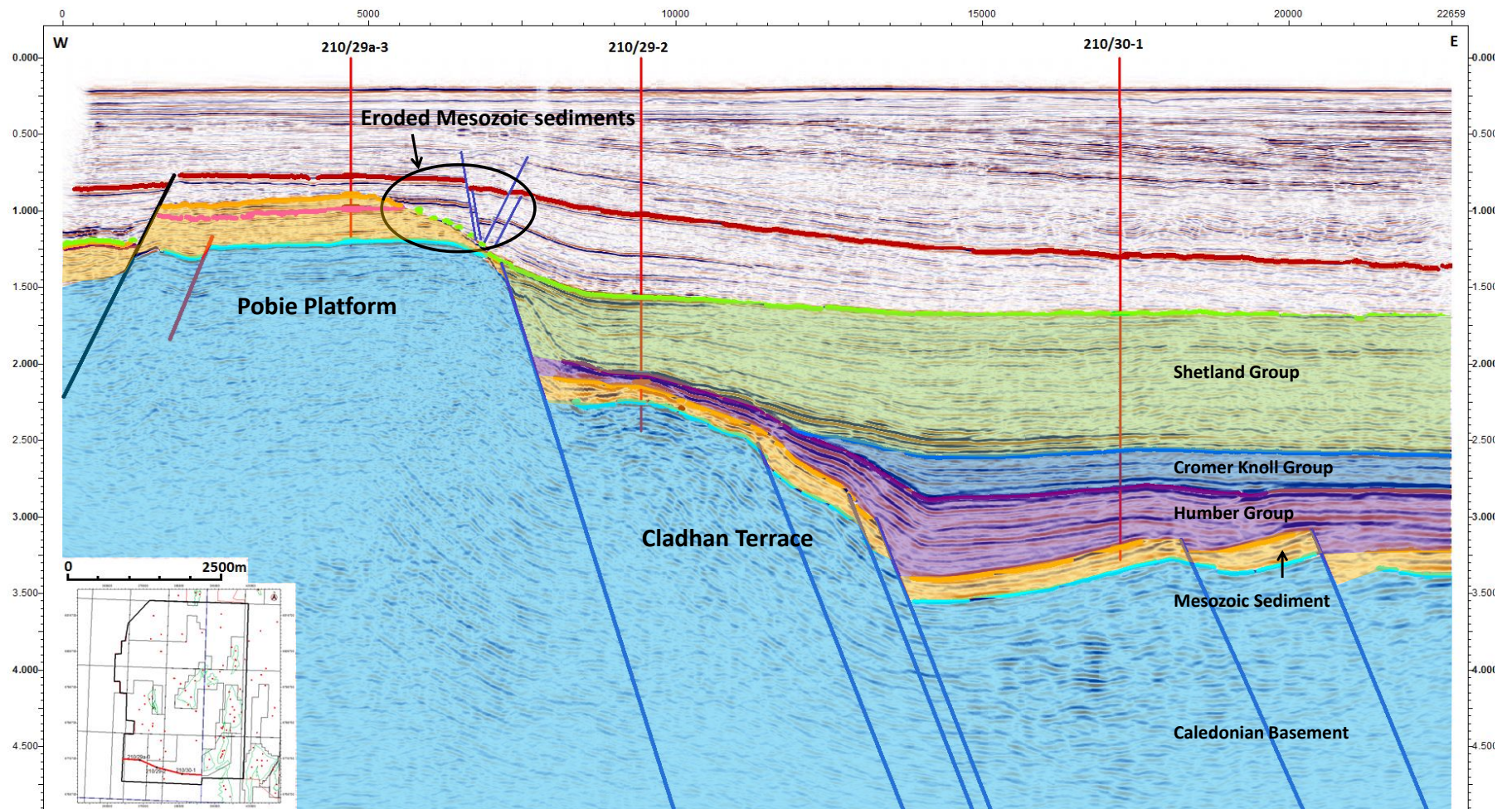


Figure 7-6. The seismic line illustrates a large terrace area to the east of the Pobie Platform. The eastern edge of the Pobie Platform has been heavily eroded; it is possible that the eroded material may have been re-deposited down-dip of the large scale normal fault.

7.3 *Permo-Triassic Rifting*

The first phase of stretching in the Northern North Sea relates to Permo-Triassic rifting. The faults which form as a result of this stretching phase orientate NE-SW and form significant structures throughout what is now the East Shetland Basin. This initial faulting forms a series of basins such as the Unst Basin and Magnus Basin and highs such as the Pobie Platform and North Shetland Platform, all of which are highlighted in Figure 7-7.

Another structure which formed in the Permo-Triassic rifting is the Tern-Eider Ridge. This horst structure is located in the East Shetland basin and is also orientated NE-SW. When analysing the Pobie Platform, it is possible to identify a large scale normal fault orientated NE-SW, called the Pobie fault. This too was active during the Permo-Triassic. It may be possible that these two faults were initially one which has been transected by the more recent Upper Jurassic rifting event. It has been suggested by Lee and Hwang (1993) that the Tern-Eider Ridge was in fact a much larger structure that ran throughout the whole of the East Shetland Basin, illustrated in Figure 7-8. They also suggest that the Pobie fault and the western edge of the Tern-Eider Ridge was one much large fault. If this is the case then the Unst Basin was a much larger structure than it is it is assumed to be by current interpretation, as the basin was sub-divided by the Upper Jurassic rifting event (Figure 7-9). The Tern-Eider Ridge and the Pobie fault are both observed in the Cladhan area and the Permo-Triassic faults can be mapped out. With the aid of the seismic datasets mentioned above, it is possible to see how the Pobie fault and the Tern-Eider Ridge were once the same structure prior to Upper Jurassic rifting. By using the 3D seismic volumes along with the well data available it is possible to identify important horizons in these structures such as the gneissose basement in the Cladhan area.

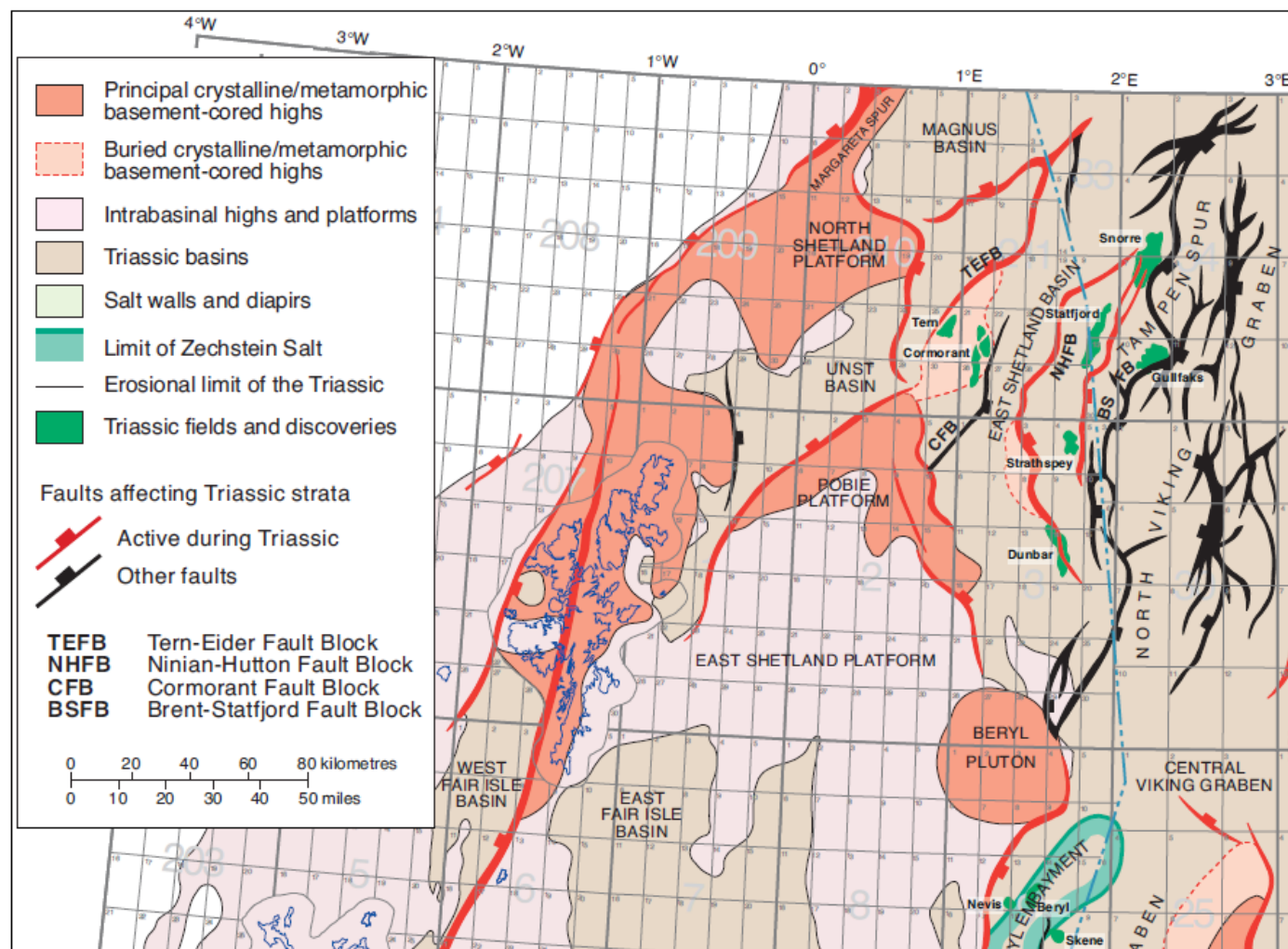


Figure 7-7. Platforms and basins created by Permo-Triassic rifting (Goldsmith 2003).

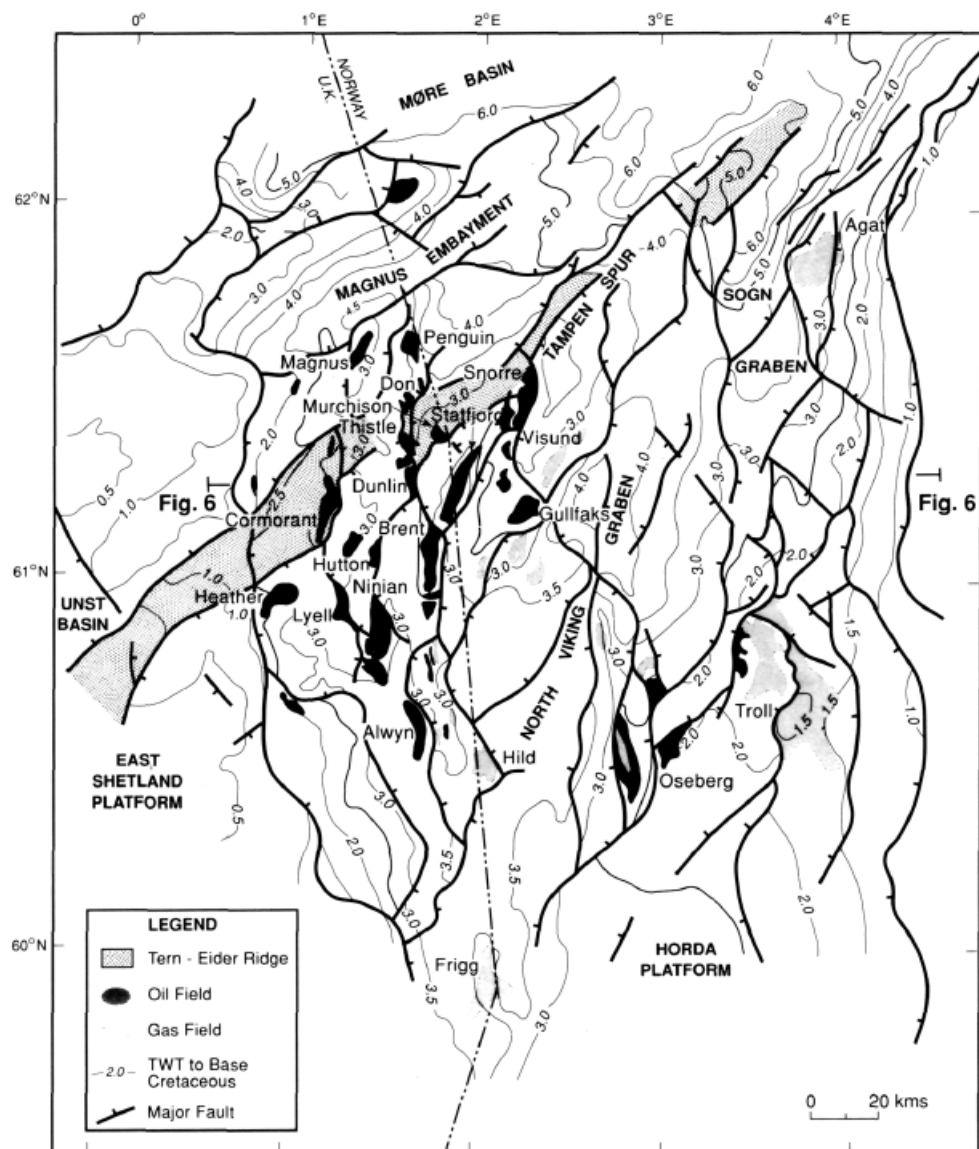


Figure 7-8 Previous research illustrate the Tern-Eider Ridge may have once been a much larger laterally continuous structural feature (Lee and Hwang 1993).

These can be used to aid the interpretation in the Tern-Eider Ridge area where wells do not penetrate deep enough to enter the gneissose basement. The ability to identify the basement throughout these sections is crucial in determining structural patterns which occurred in the initial Permo-Triassic rifting event. Where basement is relatively shallow it is plausible to say that the area in question was a structural high during the Permo-Triassic rifting event, as the structural high has only recently been covered by sediments.

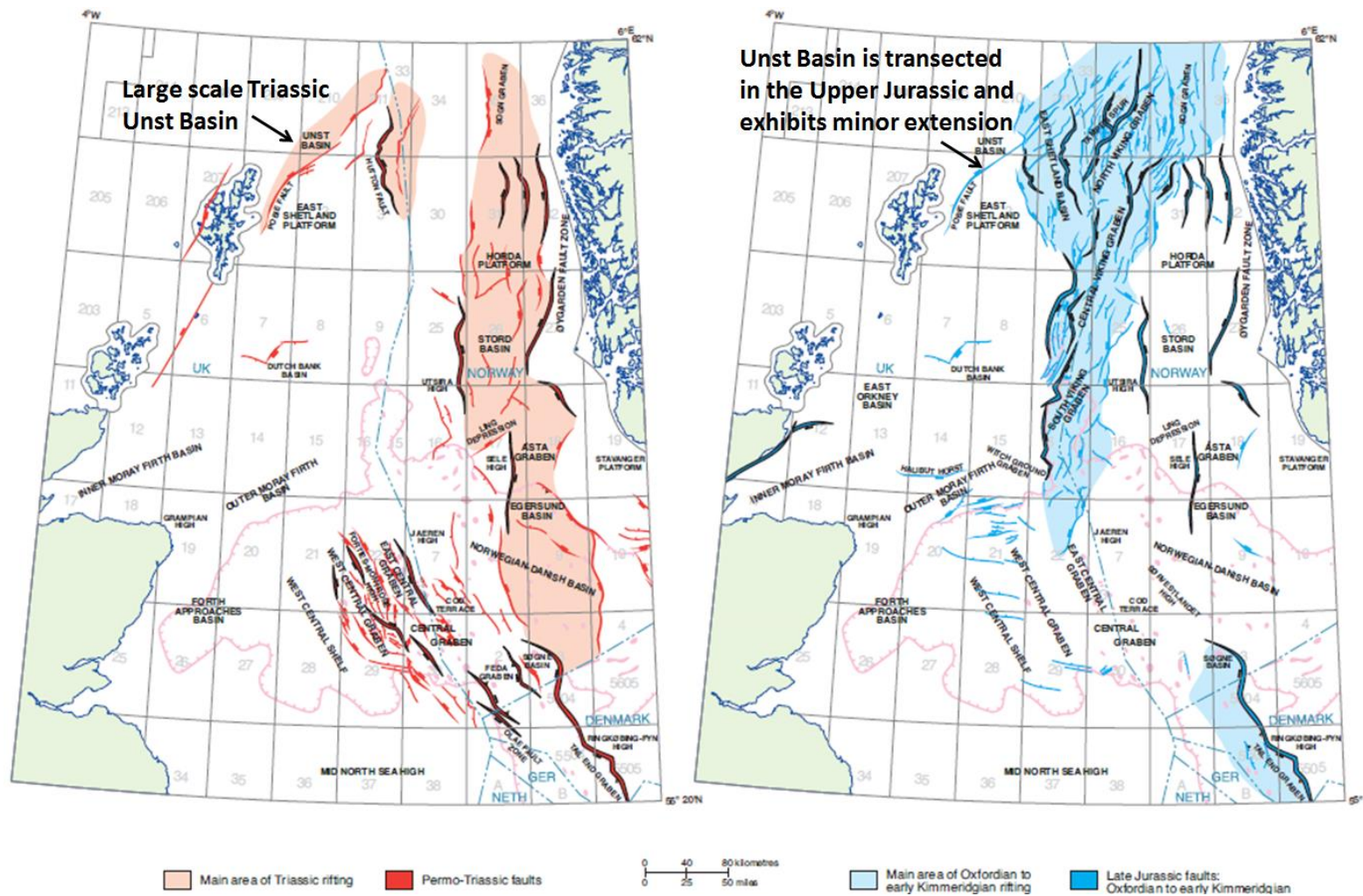


Figure 7-9. Initial shape and size of the Unst Basin in the Triassic compared to what it looks like after the Upper Jurassic rifting event (Zanella 2003).

The hangingwall located on the north-western edge of the Tern-Eider Ridge and in the hangingwall of the Pobie fault (Figure 7-10), a section of thickening in what must be Triassic sediments can be observed. These sediments are inferred as Triassic as the top and base Brent Group can be identified with the use of wells throughout the seismic. The thickening patterns observed in Figure 7-11 illustrate that Permo-Triassic faulting was indeed active within this area and play a crucial role in determining structural patterns and petroleum prospectivity.

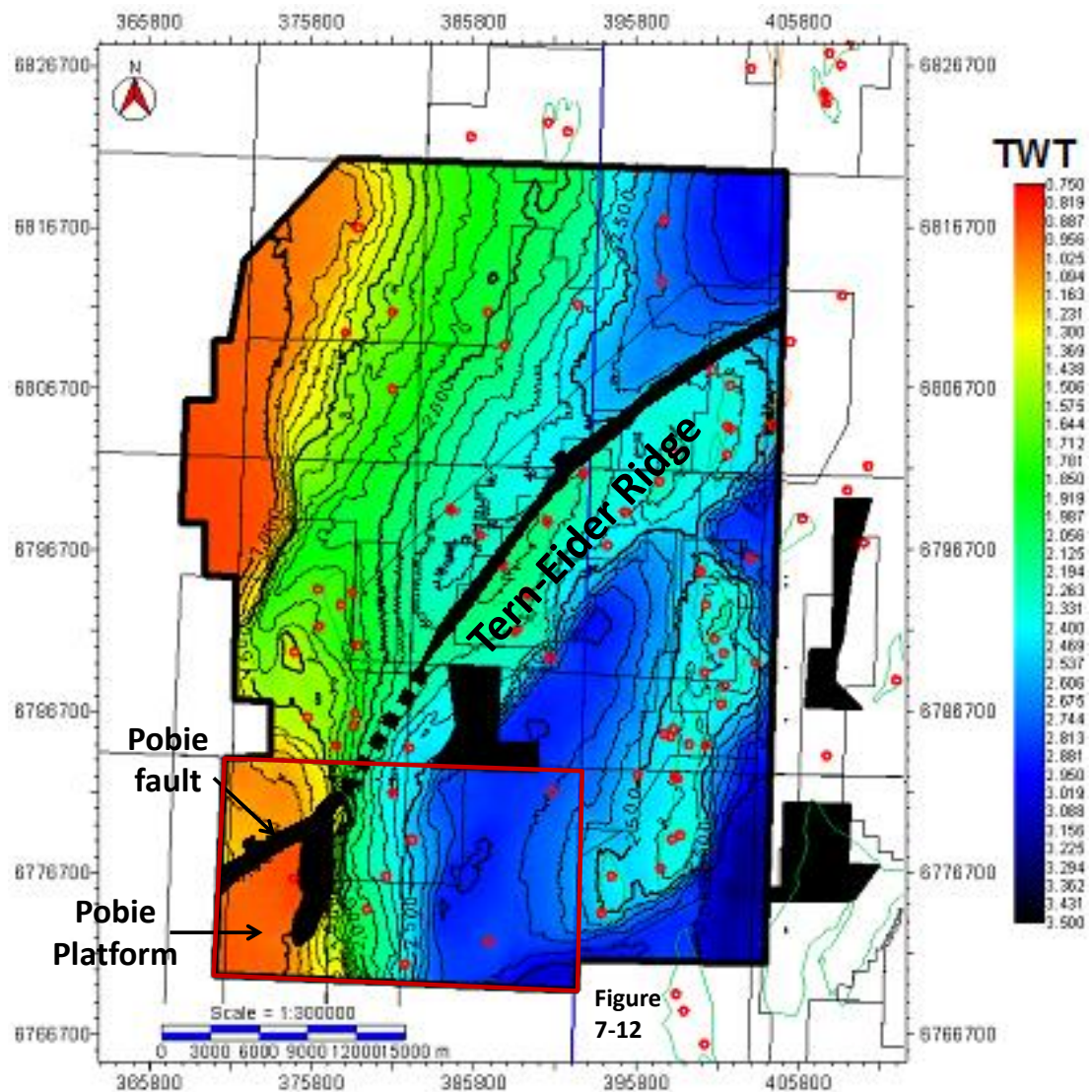


Figure 7-10. Top Cretaceous map illustrating the NE-SW orientation of the Tern-Eider Ridge and Pobie fault.

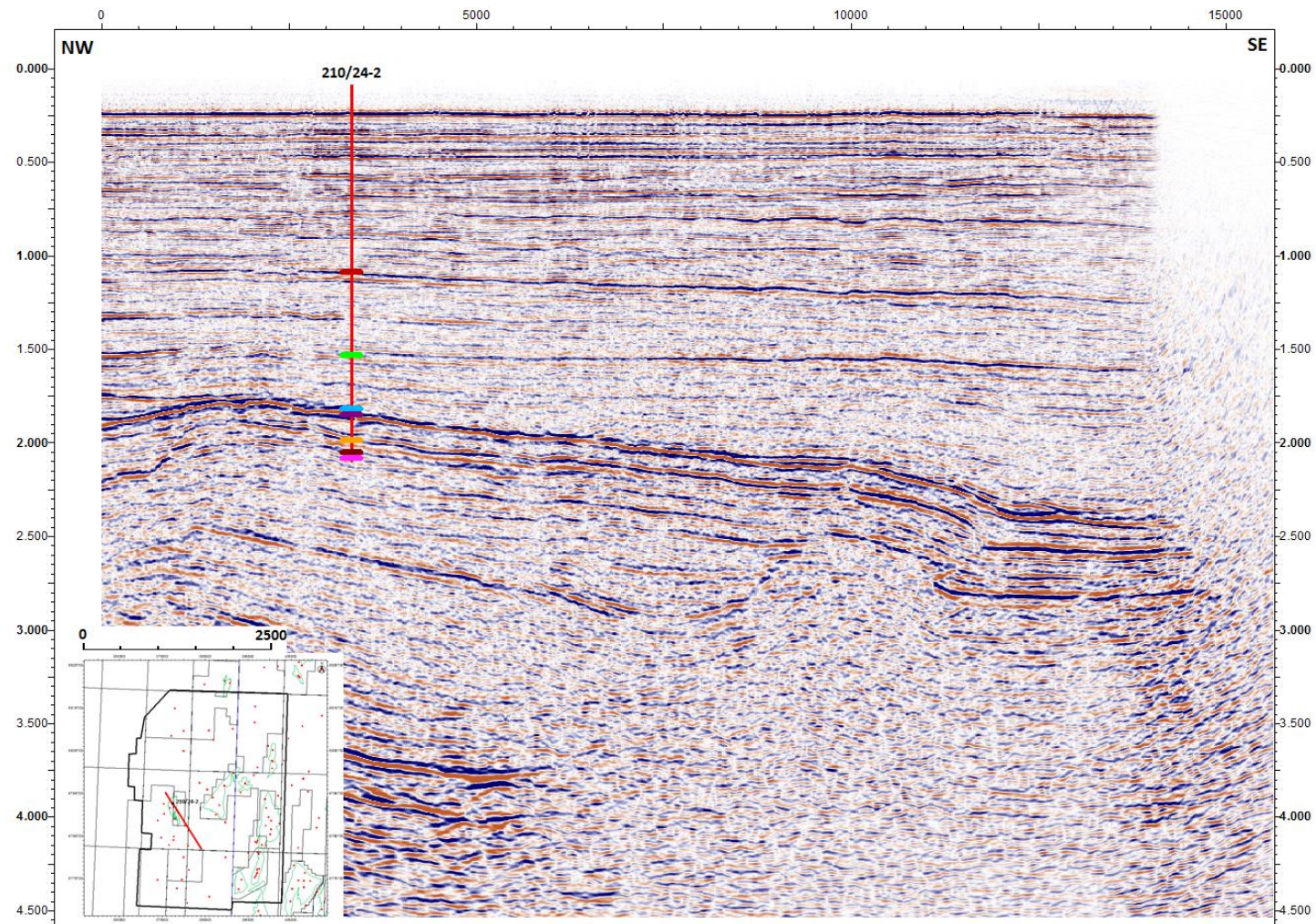


Figure 7-11 Uninterpreted seismic section through the southern limits of the Tern-Eider Ridge.

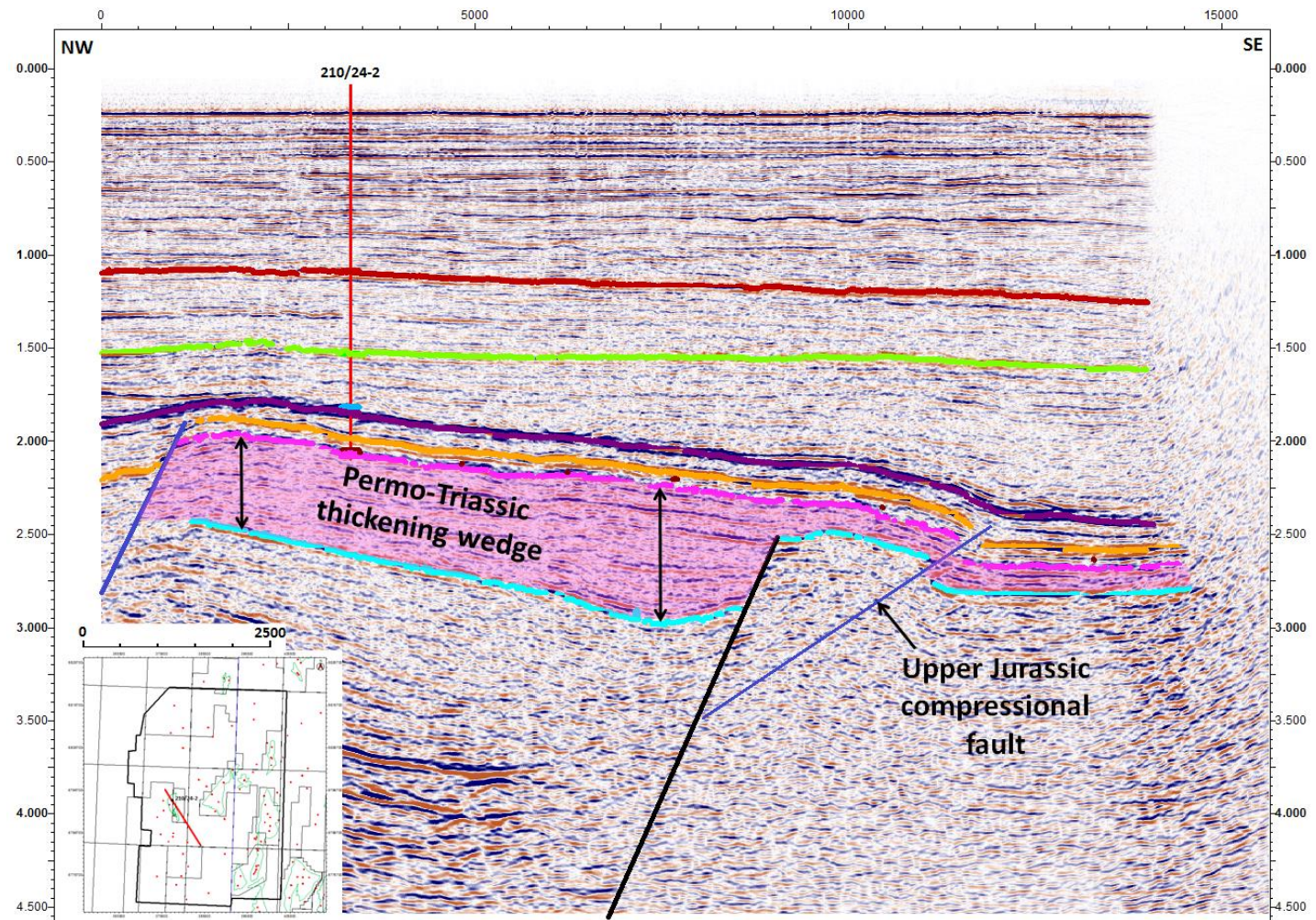


Figure 7-12. Seismic cross section illustrating a thickening package of Permo-Triassic sediments in the hangingwall to the western edge of the Tern-Eider Ridge.

7.4 *Jurassic Rifting*

The formation of the East Shetland Basin is generated by the stretching event in the Upper Jurassic. The overall orientation of the Upper Jurassic rifting in the Northern North Sea (Viking Graben) is North-South, although in the neighbouring East Shetland Basin some faults are orientated more NNW-SSE. The result of this rifting phase generates a series of structural traps and features which makes the North Sea one of the most prolific hydrocarbon basins in the world. Upper Jurassic rifting is also observed in the Cladhan area. One of the major structures that exist in the Cladhan area is the Pobie Platform. The platform as shown in Figure 7-12 was formed by the Permo-Triassic rifting. The Platform was then dissected by the north-south Upper Jurassic rifting event. One of the Jurassic faults evident within the Cladhan dataset is the East Shetland bounding fault, which generates the western rift shoulder to the Upper Jurassic rifting event. It is this fault which keeps the Pobie Platform as a structural high throughout the Jurassic and Lower Cretaceous. Other normal faults are found within the Cladhan area. Directly to the east of the East Shetland Platform Fault, two smaller easterly dipping normal faults form a relay ramp, which can control sediment supply to the basin. These two faults have not linked together, meaning both of them move independent of one another. The northern most one of these faults is the eastern limit of the Tern-Eider Ridge, illustrating the propagation of the normal faults in the Upper Jurassic. The formation of these smaller scale faults forms a series of terraces throughout the East Shetland Basin as shown in Figures 7-13 and 7-14. As hydrocarbons are expelled from the source rock, these structural highs may eventually become filled and form significant hydrocarbon fields. Directly to the north of the Cladhan area, this terrace area has been explored and resulted in the discovery of the Rinnes prospect.

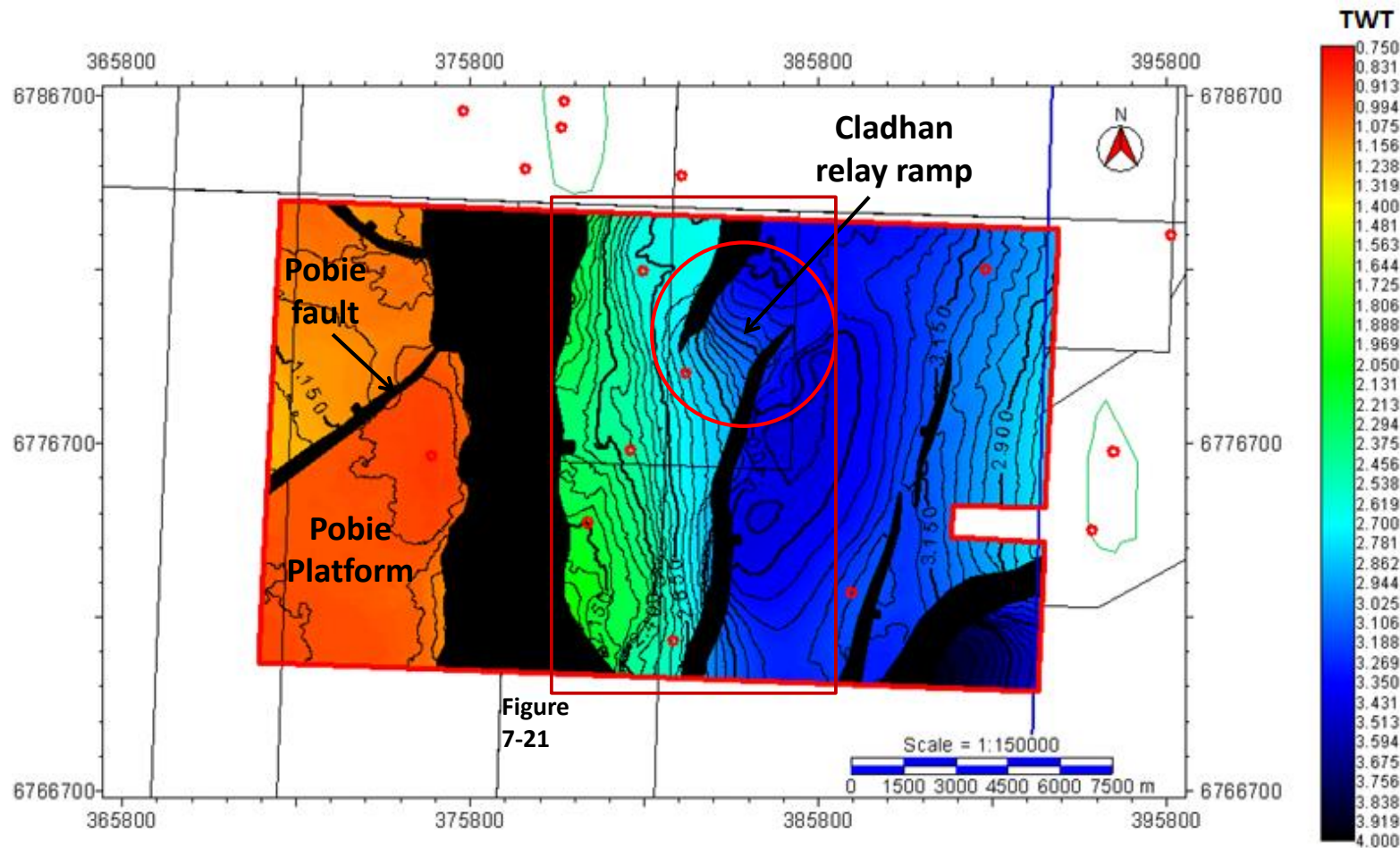


Figure 7-13. Top Brent Group structure map illustrating the north-south orientation of the Upper Jurassic faults and some of the structural features that form as a result. Over the Cladhan area a relay ramp forms where two Upper Jurassic North-South orientated normal faults overlap and do not link through faulting. This creates a terraced area, which separates the Pobie Platform high with the East Shetland Basin area.

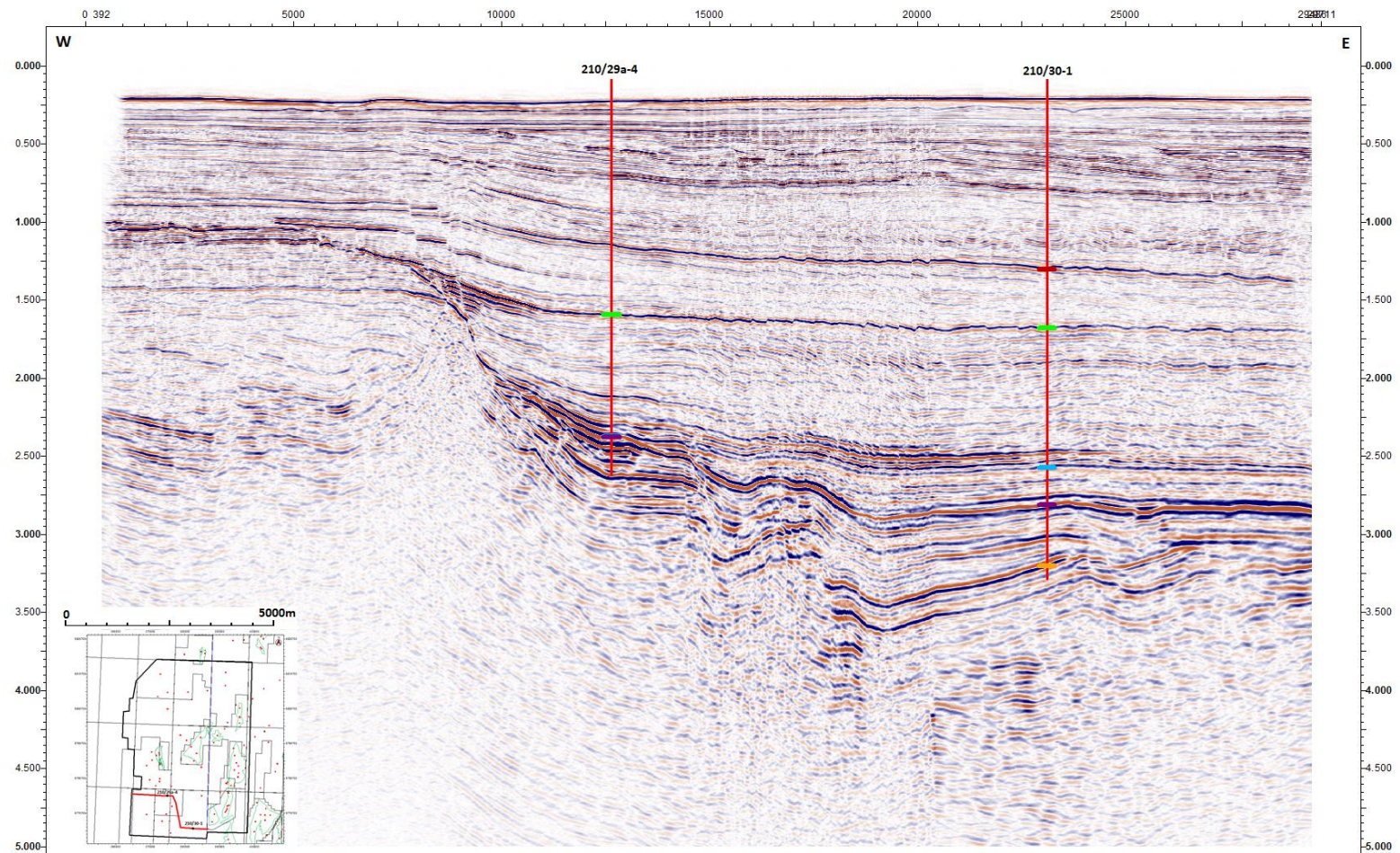


Figure 7-14. West-East seismic section through the Cladhan study area.

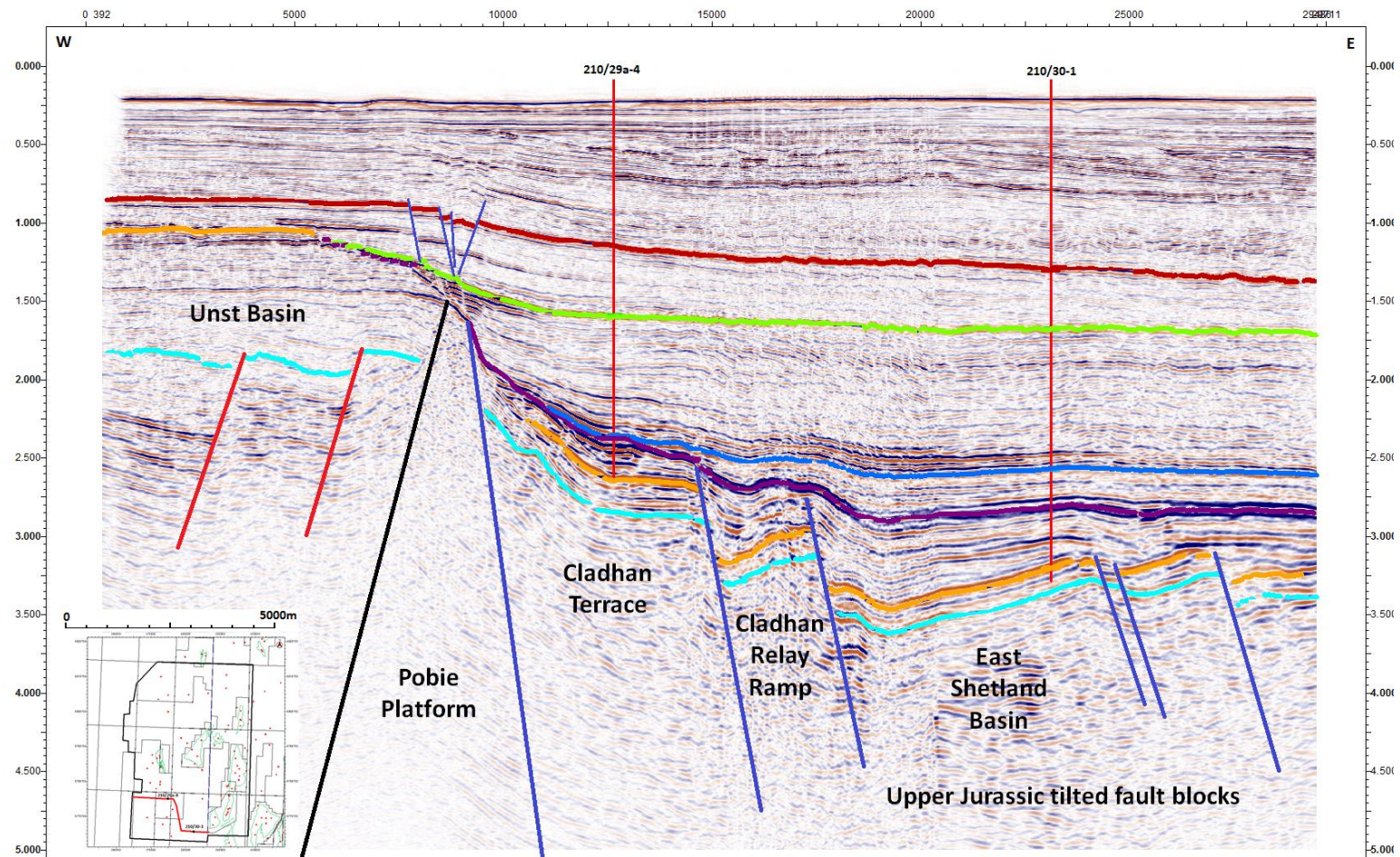


Figure 7-15. Seismic line illustrating the role of N-S orientated Upper Jurassic faults. This seismic line illustrates how the seismic volume can be sub-divided in to different structural domains. From West to East the section can be divided into the Unst Basin – Pobie Platform– Cladhan Terrace – Cladhan Relay-Ramp – East Shetland Basin. The faults highlighted in red are the Permo-Triassic faults including the reactivated Pobie Fault.

The relay-ramp structure which defines the terrace area in the Cladhan area may play an important role in sediment distribution. Relay-ramps have been shown to act as conduits for the transportation of coarse clastic material into basin areas (Gawthorpe and Hurst 1993; Gupta et al 1999), which can be investigated in the Cladhan area by inferring the high amplitude anomalies as a change of thin bed lithology. This can directly influence the location of any potential deep-water fans that may occur during the rifting event in the Upper Jurassic. These gravity-flows may act as secondary reservoirs for more subtle petroleum plays within the basin. This can be extremely important in the Upper Jurassic as the deposition of the Humber Group which consists of the Heather Formation and Kimmeridge Clay Formation is predominantly silt or mud based. These may act as very good seals for the underlying Brent Group, but any other potential reservoirs deposited within the Humber Group would also be well sealed vertically and laterally by the mud dominated sediments.

The role of Jurassic faulting in the Cladhan area plays a direct role in controlling the modern day structural relief in and around the Cladhan area. The generation of rift shoulders and terraced areas within the East Shetland Basin is crucial in determining a petroleum system.

7.5 Reactivation of Permo-Triassic faults in the Upper Jurassic

The presence of two rift systems within the same area can be differentiated quite simply, if, like in this area the rifts have different orientations. As illustrated in Figure 7-9 the Permo-Triassic rifting has a NE-SW orientation and the Upper Jurassic rifting is orientated N-S. The easiest way to see if

reactivation of the older faults has occurred in the Upper Jurassic is to see if any NE-SW orientated faults are present.

Highlighted in Figure 7-15 is the Pobie fault, a NE-SW orientated fault that was active during the Upper Jurassic, whereas the rest of the faults associated to Upper Jurassic rifting are orientated more N-S. Other faults that are orientated in this direction relate to the Tern-Eider Ridge. As illustrated in Figure 7-11 the Tern-Eider Ridge and the Pobie Fault were both active during the Permo-Triassic and from the above maps it is possible to see that they were also active during the Upper Jurassic.

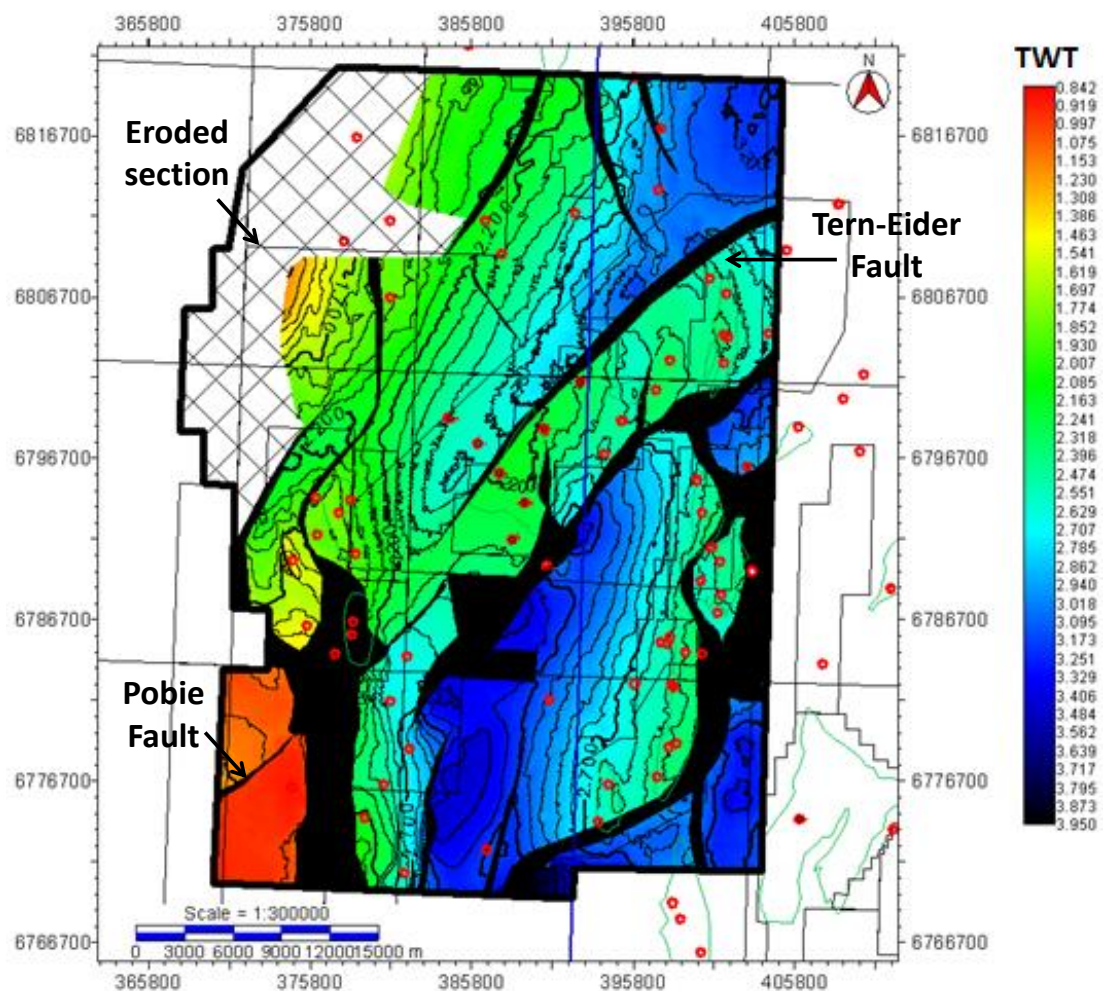


Figure 7-16. Top Brent Group structure map illustrating the reactivation of the NE-SW faults in the Upper Jurassic. The Pobie Fault and the Tern-Eider Ridge illustrates major fault movements in the Upper Jurassic which do not have an orientation N-S, but retains their NE-SW orientation from the older Permo-Triassic rifting event.

Further evidence that these older faults have reactivated in the Upper Jurassic can be observed in the seismic dataset. It is possible to identify two separate thickening sections relating to two separate stretching phases along the same fault plane. Although no well data can be used to directly date the reflectors in the Permo-Triassic rifting wedge to the west of the Tern-Eider Ridge, the seismic reflectors show enough evidence to illustrate thickening did occur along this fault in the Permo-Triassic rifting event (Figure 7-16).

A similar thickening package set can be observed on the western edge of the Tern-Eider Ridge (Figure 7-11). It is anticipated that these two faults may have at one time been the same fault. Analysis of the fault-plane however and the juxtaposition of set horizons along the fault confirm the twin movement along this fault. On initial inspection, the overall displacement along the Tern-Eider Ridge looks fairly constant.

There is the occasional increase in displacement which could be inferred as fault linkage and the relocation of fault depo-centres. As mentioned earlier, the Tern-Eider Ridge is an area that has undergone reactivation of the Permo-Triassic faults in the Upper Jurassic. With this noted, an analysis of pre-rift sediments was undertaken along the fault plane to identify potential depocentres, and reactivation of faults (Figure 7-17). The two pre-rift horizons used are the Top Brent Group and the Top Basement. As noted above, the overall displacement along the fault is fairly constant. When the Top Brent displacement is analysed and it is clear to see that towards the SW, where it is closest to the East Shetland Platform Fault, the displacement of the fault is nil. As the displacement analysis moves NE along the fault it is possible to see that the displacement of the Brent Group increased. This shows that the fault was defiantly active during the Upper Jurassic, as the Brent Group went from being undeformed to having a large displacement.

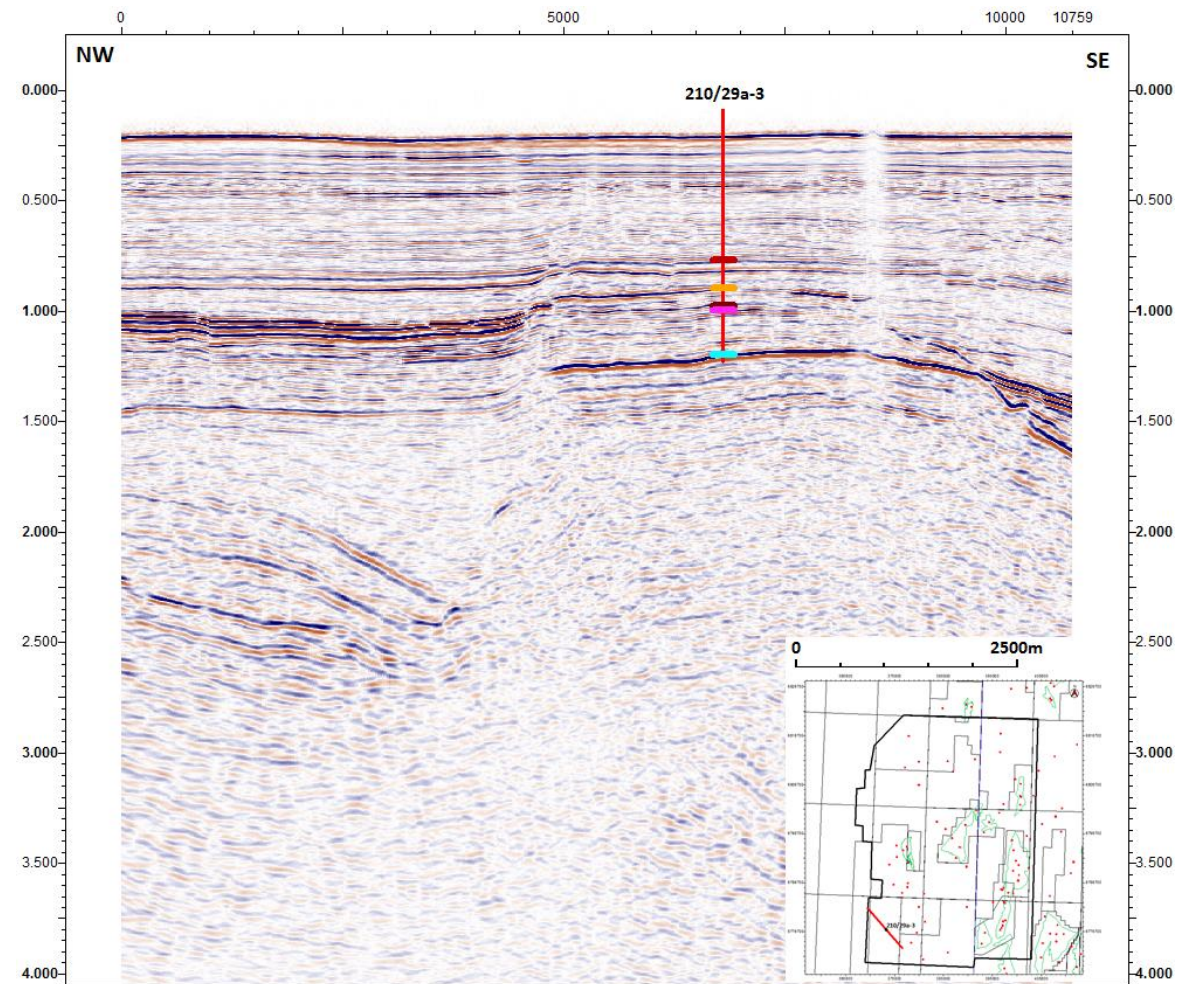


Figure 7-17 Uninterpreted seismic section through the Pobie fault.

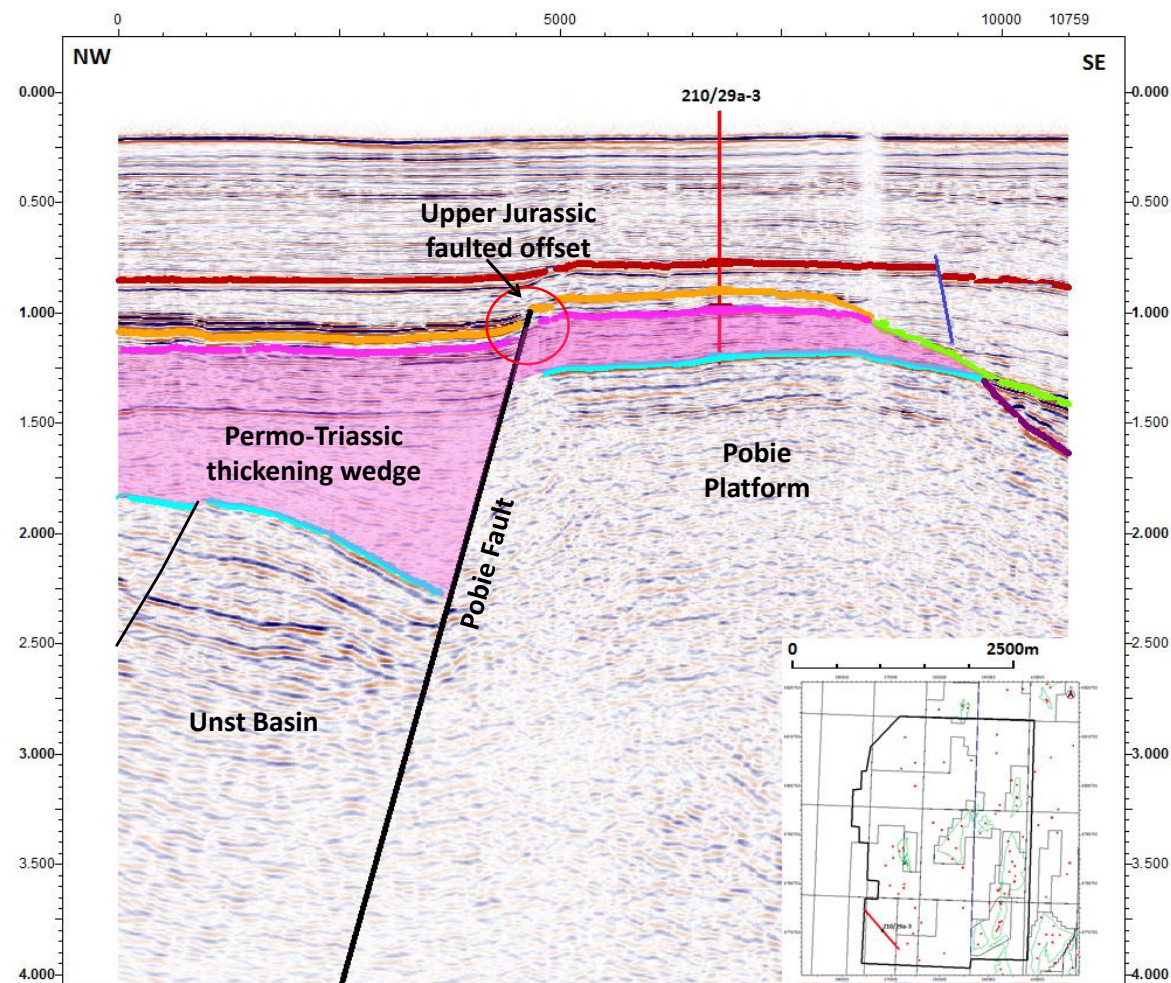


Figure 7-18. Cross section through the Pobie Fault and on to the Pobie Platform. It is possible to identify two separate thickening packages, relating to the two individual rifting events (Pink relates to Permo-Triassic faulting and the orange wedge to the fault reactivating in the Upper Jurassic).

The mapping of the Upper Jurassic rifting event has made it possible to quantify displacement along the fault plane along with the displacement of the basements movement in the initial Permo-Triassic rifting. The current mapping of the Basement will illustrate the overall movement along the fault, as the initial Permo-Triassic faulting will have been over-written by the Upper Jurassic rifting event. By subtracting the Brent Group displacement away from the overall displacement it is possible to accurately observe the initial Permo-Triassic rifting.

With the overprint of the Upper Jurassic rifting removed, it is clear to see that a large scale fault was present during the Permo-Triassic within the area. Both faults have roughly the same amount of displacement although there is a slight difference in their lateral positioning. The central depocentre for the Permo-Triassic faulting is towards the SW of the study area, which is close to the current location of the East Shetland Platform Fault. Whereas, the depocentre location for the Upper Jurassic faulting is further towards the NE of the section. The difference in displacement could be related to the generation and the northwards propagation of the rift shoulders to the west. It is also possible to observe the linkage points of the initial Permo-Triassic faults in Figure 7-17 between the individual fault segments.

With the generation of a rift-defining fault which is expected to cut through the entire seismogenic layer the stresses relating to the underlying fault may have been drastically reduced over the relic depocentre. As the East Shetland Basin grew throughout the Upper Jurassic, the underlying fault will have begun to shift and become active again. With the original depocentre now a structural high, a new depocentre location was formed along the same fault trend. As mentioned earlier the Tern-Eider Ridge has been interpreted as just part of a larger structure that was present in the Permo-Triassic rifting.

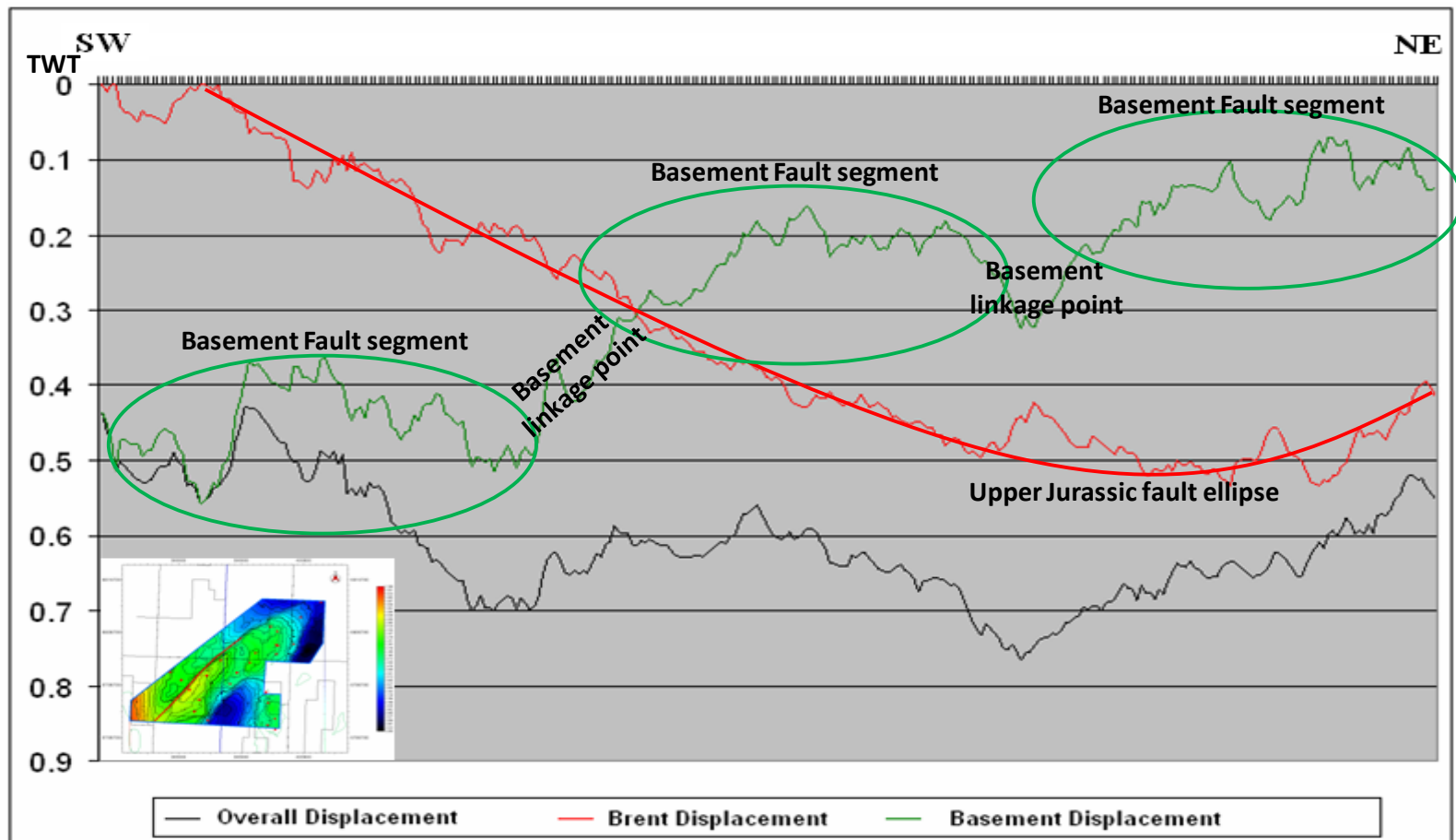


Figure 7-19. Graph showing the displacements between the Permo-Triassic and Upper Jurassic pre-rift sediments along the western edge of the Tern –Eider Ridge. The black line represents the overall displacement of both rifting events and relates to the economic basement. The red line illustrates the displacement of the top Brent Group sediments, which are the pre-rift to the Upper Jurassic rifting event and records fault movement solely for this stretching event. By subtracting the Upper Jurassic faulting from the overall displacement it is possible to generate the initial Permo-Triassic Displacement, this is illustrated here by the green line.

Reactivation of the fault was an inevitability, the only difference between this fault and the original would be the location of the structural high and relating depocentre. In the Permo-Triassic the high was located around the Pobie Platform and the basin being the Unst Basin. Whereas, in the Upper Jurassic the structural high was the Tern-Eider Ridge and the basin became part of the greater basin that is the East Shetland Basin. This illustrates that reactivation of faults can occur in both the basin (Tern-Eider Ridge) or within the surrounding platform areas (Pobie fault).

7.6 *Upper Jurassic sedimentary dispersal patterns*

Although the primary response to a transected rift is structural, there is a more subtle response relating to the sedimentology. The potential erosion and reworking of sediments in the uplifted areas could form secondary reservoirs. The reservoir rocks in this case will be deposited as either footwall sourced alluvial fans or back-shed hangingwall sourced alluvial cones, as shown in Figure 7-18. If the basin area has axial drainage the reservoir sandstones are deposited in axial channel facies and hangingwall and footwall sourced alluvial cones. The primary difference between these two areas is dependent upon the climate of the areas. The internally drained area has a much lower flux of water which results in the lack of channel sediments and the formation of a playa lake and alluvial fans. Areas which are drained by river channels are generally wetter and have a greater flux of water passing through the basin area. In both of these areas footwall sourced fans and cones form close to the fault plane and are found along with the back-shed sediments. The primary difference is the generation of laterally continuous axial channel sands in the wetter through drained area. This is vitally important in determining the location of secondary reservoir sandstones that have been affected by a secondary rifting event.

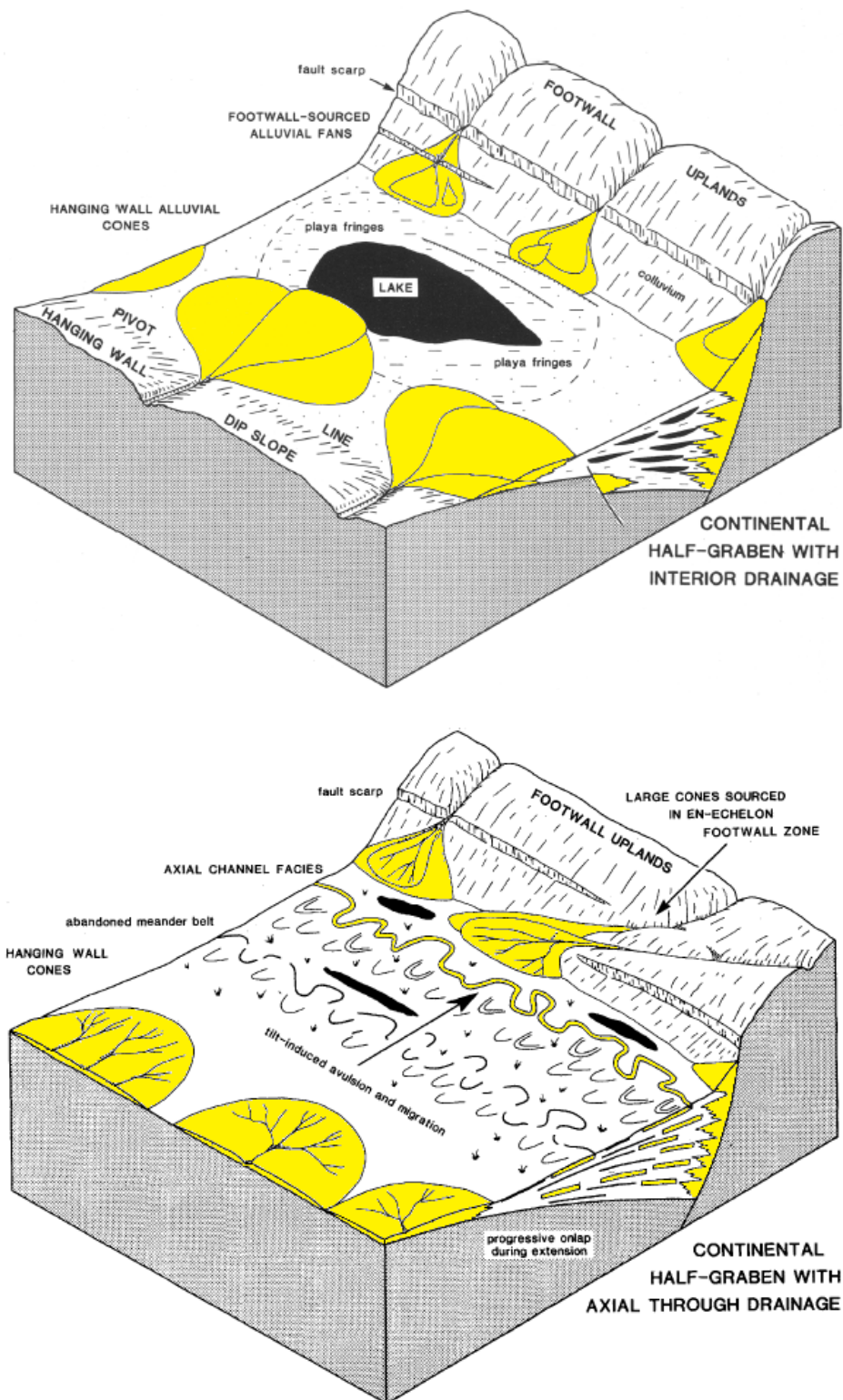


Figure 7-20. Varying sediment responses relating to the development of a half graben system in the Permo-Triassic rift system (Leeder and Gawthorpe 1987).

An understanding of where the reservoir rocks are in relation to the initial rifting event can play a huge role in determining and syn-rift play opportunities. When the second phase of rifting occurs in the Upper Jurassic it may elevate the reservoir units currently located in a hangingwall location to a structurally high footwall environment and generate a potential secondary reservoir target.

The onset of rifting in the Upper Jurassic resulted in the creation of accommodation space and a subtle change in sedimentary deposition patterns. The Middle Jurassic is dominated by the Brent Group, which was laid down in a deltaic environment; whereas the Humber Group is dominated by the silty marine Heather Formation and overlaid by the deep marine Kimmeridge Clay Formation. This rise of sea levels throughout the Upper Jurassic results in the lack of coarse clastic deposited within the Cladhan area. The resultant rifting as noted above also created a series of highs such as the Pobie Platform, which may have been brought up above sea level during the rifting event. The uplift of Middle Jurassic sediments and subsequent erosion of these sediments play an important role in the influx of clastic reservoir material into the Cladhan Terrace and neighbouring basinal areas. The extent of this erosion can be observed in Figure 7-19 where Late Paleocene sediments are deposited directly upon Upper Jurassic Brent Group sediments. As shown in Figure 7-20, the Cladhan area is separated into three defining areas. To the west is the platform location, to the east is the East Shetland Basin and in between is the Cladhan terraced area. The terraced area is separated from the basin by a series of Upper Jurassic normal faults that form a relay ramp in the central Cladhan area. This relay ramp could aid the supply of clastic material into a predominantly mud based environment. Analysis of well 210/29a-3 (Figure 7-19) shows a large erosive unconformity between the Middle Jurassic Brent Group sediments and the Late Paleocene, Lista Formation.

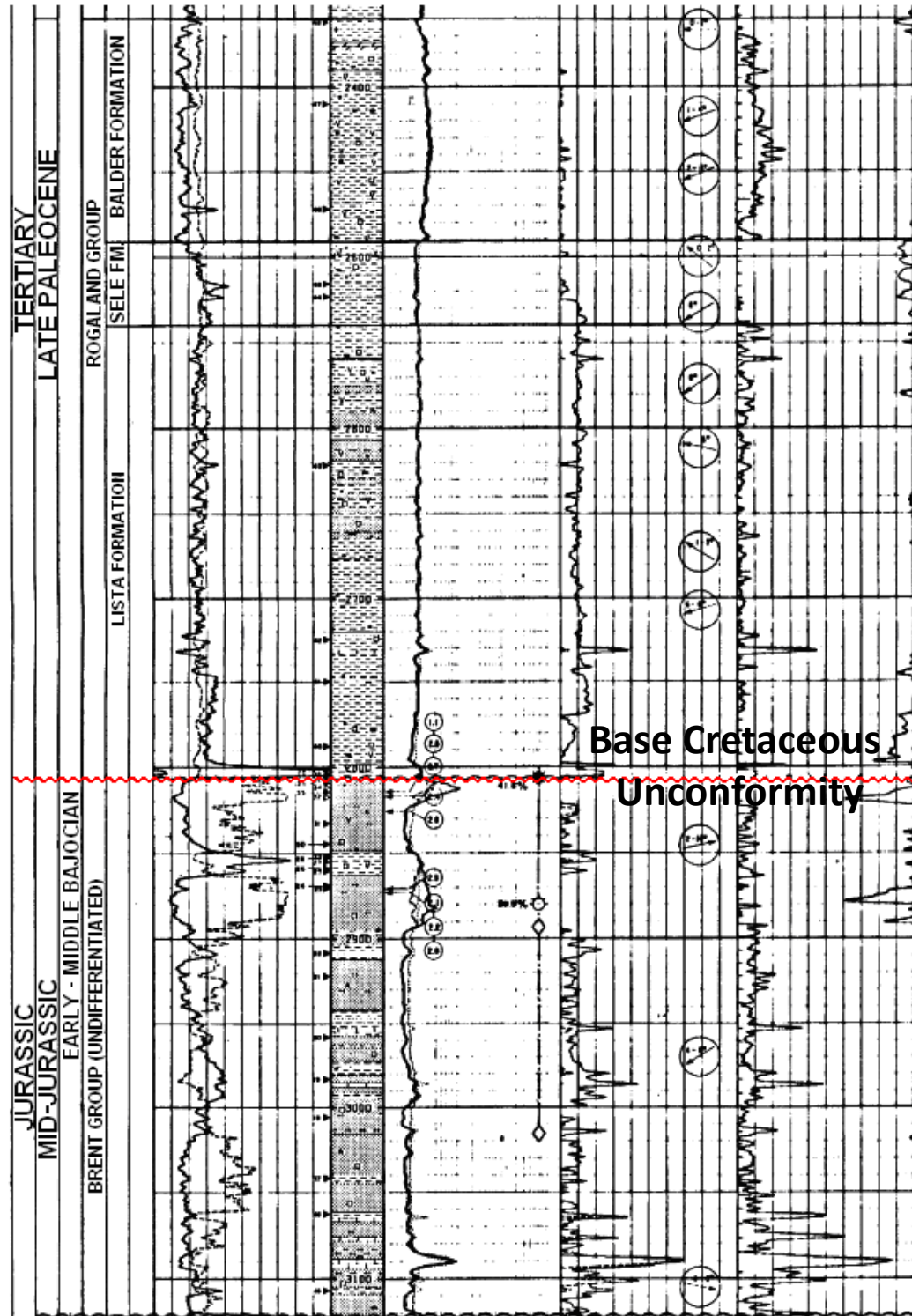


Figure 7-21. Well Log 210/29a-3 illustrating the erosional unconformity (highlighted in red) over the Pobie Platform and the lack of Cretaceous sediments deposited over the Middle Jurassic Brent Group sediments.

The lack of any Cretaceous sediment here demonstrates that a major time gap of almost 100Ma. This has either formed through the lack of deposition of sediments whilst the Pobie Platform was a structural high or as a direct result of the high being eroded whilst it was brought up above sea level.

What is clear to see in the seismic cross-sections over the Pobie Platform in Figure 7-20, is that large amounts of the eastern edge of the platform have been eroded away. In some areas the erosion cuts down into Triassic sediments. The erosion and potential re-deposition of the Brent Group sand based sediments are crucial in determining the location of any potential secondary reservoirs within the Cladhan area.

As the Brent Group is predominately sand prone and it is likely to be eroded away during the early stages of the Upper Jurassic rifting event, it is likely to be re-deposited within the Upper Jurassic Humber Group. As noted earlier the Humber Group is predominantly mud prone. It acts as an effective seal to the underlying Brent sandstone reservoir. So the formation of a sandy secondary reservoir in a mud based host rock could prove an exciting prospect in terms of petroleum prospectivity. If the sandy Brent Group has been re-deposited within the mud based Humber group it may be possible to identify potential bright spots where these sand based sediments have been laid down. It is possible to identify bright spots within the seismic data and they are found around the relay ramp location within the Cladhan area which is shown in Figure 7-21. It is further possible to see lobes of these bright spots which indicate the sediments have flowed down the relay ramp from the terraced area to the mud prone, basin area of the Cladhan dataset.

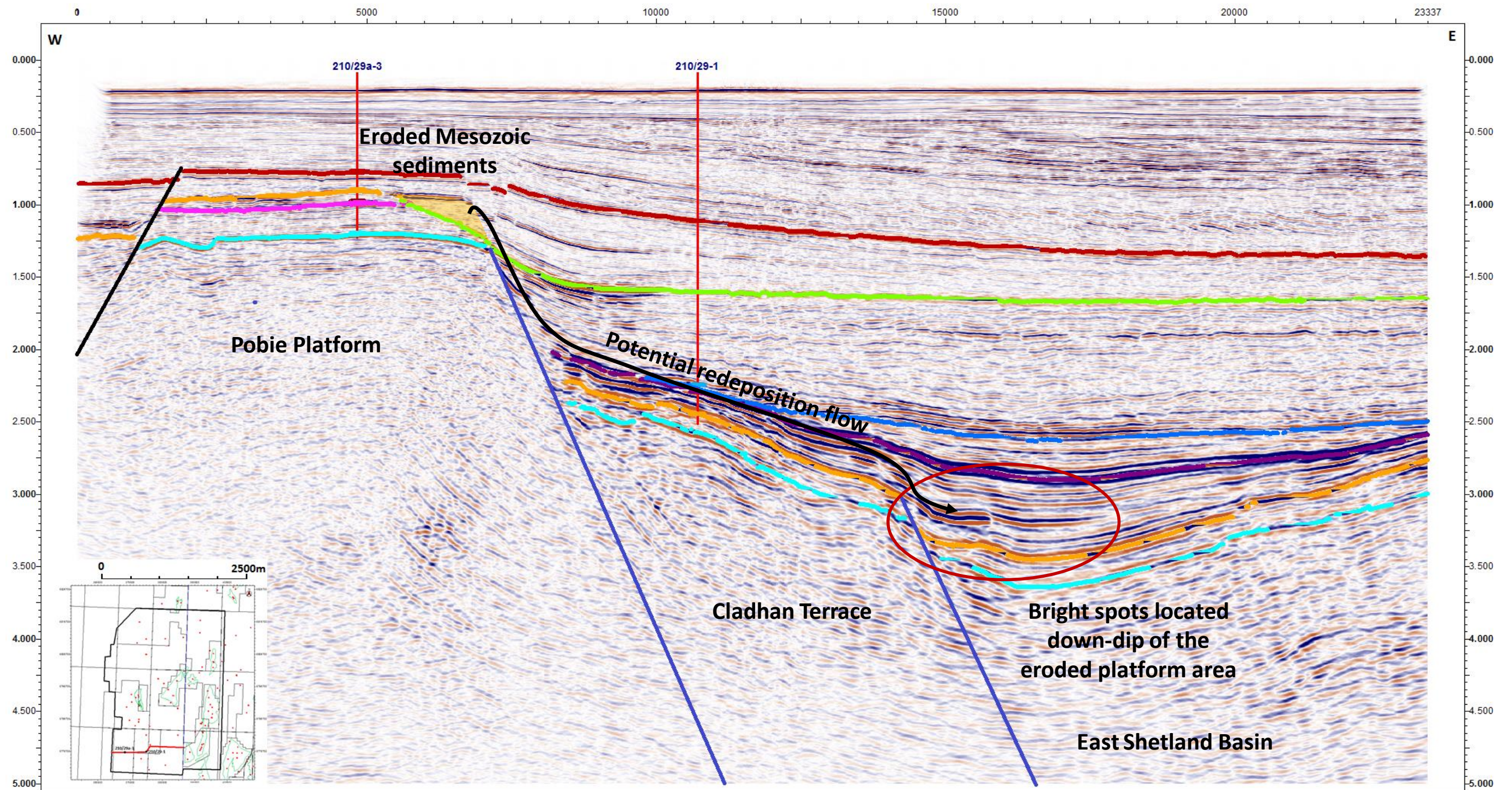


Figure 7-22. Diagram illustrating the erosion of the Brent Group sediments on the Pobie Platform and potential re-deposition into the terraced and basin areas in the Cladhan area.

Although these bright spots can be inferred to as the eroded and reworked sediments of the Brent Group over the Pobie Platform, more evidence is needed to tie them back to and demonstrate a platform itself. This is why once the bright spot horizon was picked, a series of amplitude extractions were undertaken to try and identify any other potential bright spots or bright zones that appear with the Cladhan dataset. These amplitude extraction maps were generated by creating a continuous horizon through the bright spots. This horizon then had the z-values converted from time to the corresponding amplitude value present within the horizon interpretation.

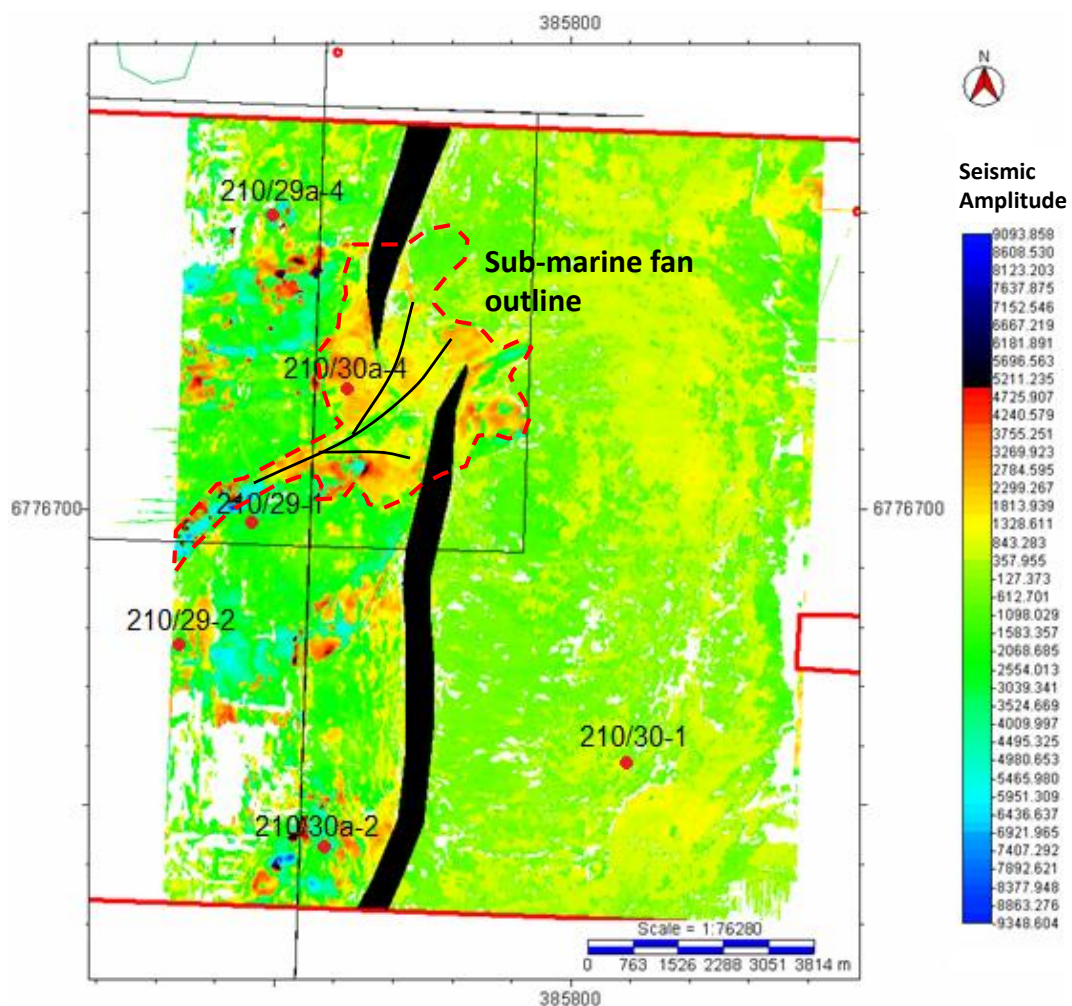


Figure 7-23. Mapping of the amplitudes identified within the seismic data and undertaking amplitude extraction on the horizon makes it possible to identify a potential submarine fan, sourced from the SW, towards the Pobie Platform.

What is clear to see in Figure 7-21, the bright spots are part of a greater submarine fan system, which seems to source itself from the south-west towards the Pobie Platform. The appearance of this submarine fan system and the orientation from which it is sourced indicates that this flow system is in fact sourced from the Pobie Platform. It is most likely that the sediments that make up the flow are sand based as to account for the amplitude anomalies that is the fan system. These sand prone units which have been deposited in the Upper Jurassic must have been the eroded material of recently deposited Middle Jurassic sediments. The bright spots that are present in the Cladhan Field can be easily mistaken for a direct hydrocarbon indicator (DHI), but it is extremely likely that this brightening effect could in fact be caused by the sandstone units themselves. As is the case with thin bedded sandstone formations such as the units in the Cladhan area a brightening effect may be generated by a tuning effect (Figure 7-22). It is possible that the thinly bedded sandstone units may just be below seismic resolution but are still having an enough of an effect to cause and over brightening of amplitudes and may be misinterpreted as a DHI.

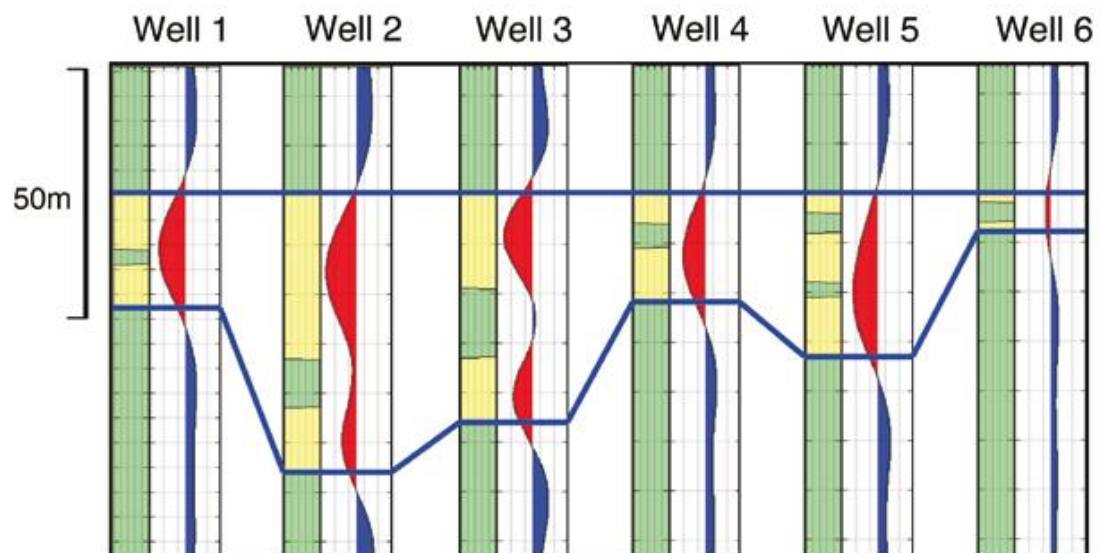


Figure 7-24. Basic illustration of how thinly bedded sediments can influence the seismic response of the surrounding sediment (Simm, 2009)

There is however evidence that the down-dip fan locations contain hydrocarbons. As illustrated in Figure 7-20 significant bright spots can be observed in the basin area of the section. It is also possible to identify a 180° polarity reversal in the same seismic section. This could be an indicator that something has changed the properties of the sandstone unit, potentially hydrocarbons. This led to the generation of a sandstone confidence map (Figure 7-23) which is constrained by both well and seismic data

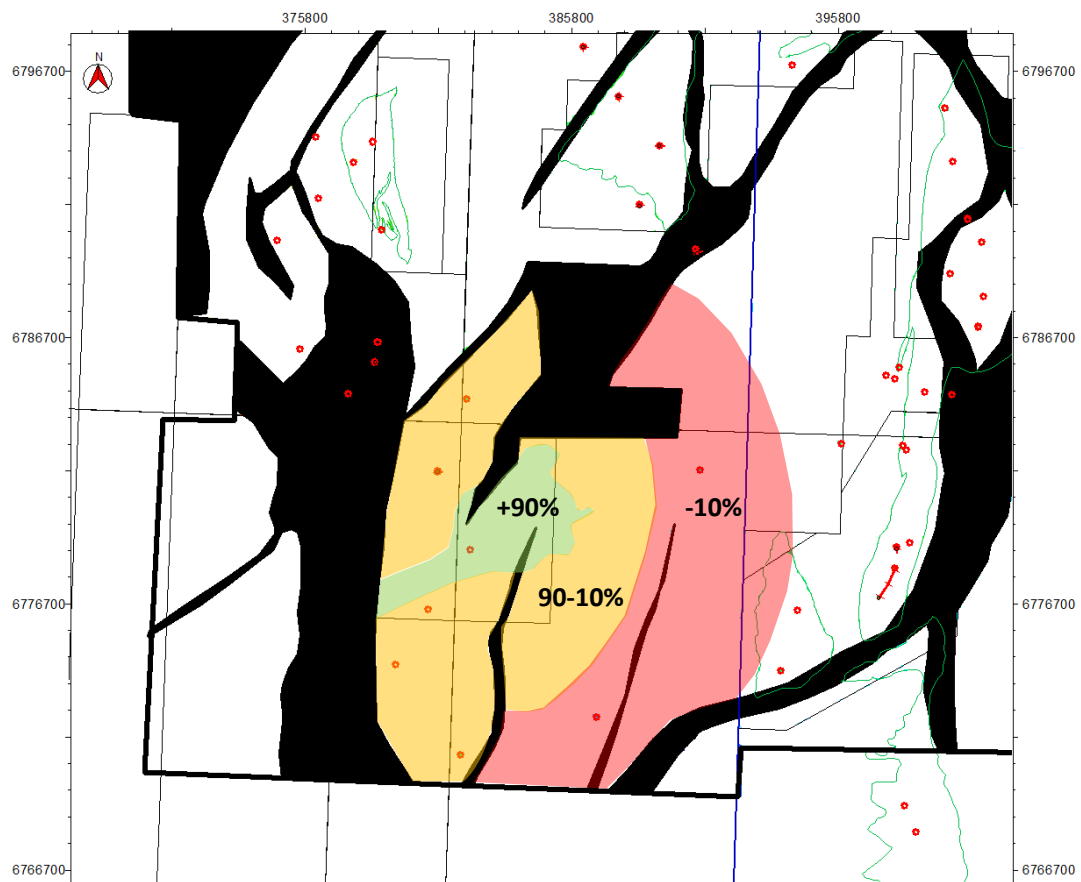


Figure 7-25. Cartoon illustrating a reservoir confidence map. Areas in green illustrate a 90% chance of finding effective reservoir, orange ranging from 90-10% and red below 10%. The evidence for this is determined by well logs and distance from the source area, which in this case is the Pobie Platform.

7.6.1 Cause of the anomalies

The occurrence of linear amplitude anomalies at the site of a relay ramp is highly suggestive of channelized inflow into the basin. Proof that the anomalies were not only channels but moreover sandy and oil prone caused the drilling of well 210/29-a in 2009.

The evolution of the sand channels found in the Cladhan relay ramp area is very delicate, as a singular sand prone gravity flow is not the only channel present. Although the seismic data and amplitude maps indicates a clear image of a distinct fan shape deposit over relay ramp location (Figure 7-21), it is possible to infer a series of smaller channels at lower stratigraphic levels.

Seismic line 7-26 highlights the main channel sand as the bright spot, but, it is possible to identify smaller bright spots at lower levels which may coincide with smaller debris flows. This can be further supported by analysing the composite log to well 210/30a-4 which targeted both of these bright spots. The two separate bright spots are related to a series of channel sequences observed within the Cladhan relay ramp area (Figure 7-24 and Figure 7-25).

The well and seismic data make it possible to define three major sand sequences; Sequence 1, Sequence 2A and Sequence 2B, separated by the Mid-Magnus Shale Formation (Figure 7-24). As these units are split by the shale unit the channels have been separated into Lower (Sequence 1) and Upper (Sequence 2A + 2B) channels. These have been the study of biostratigraphic analysis to identify when the sediments were deposited.

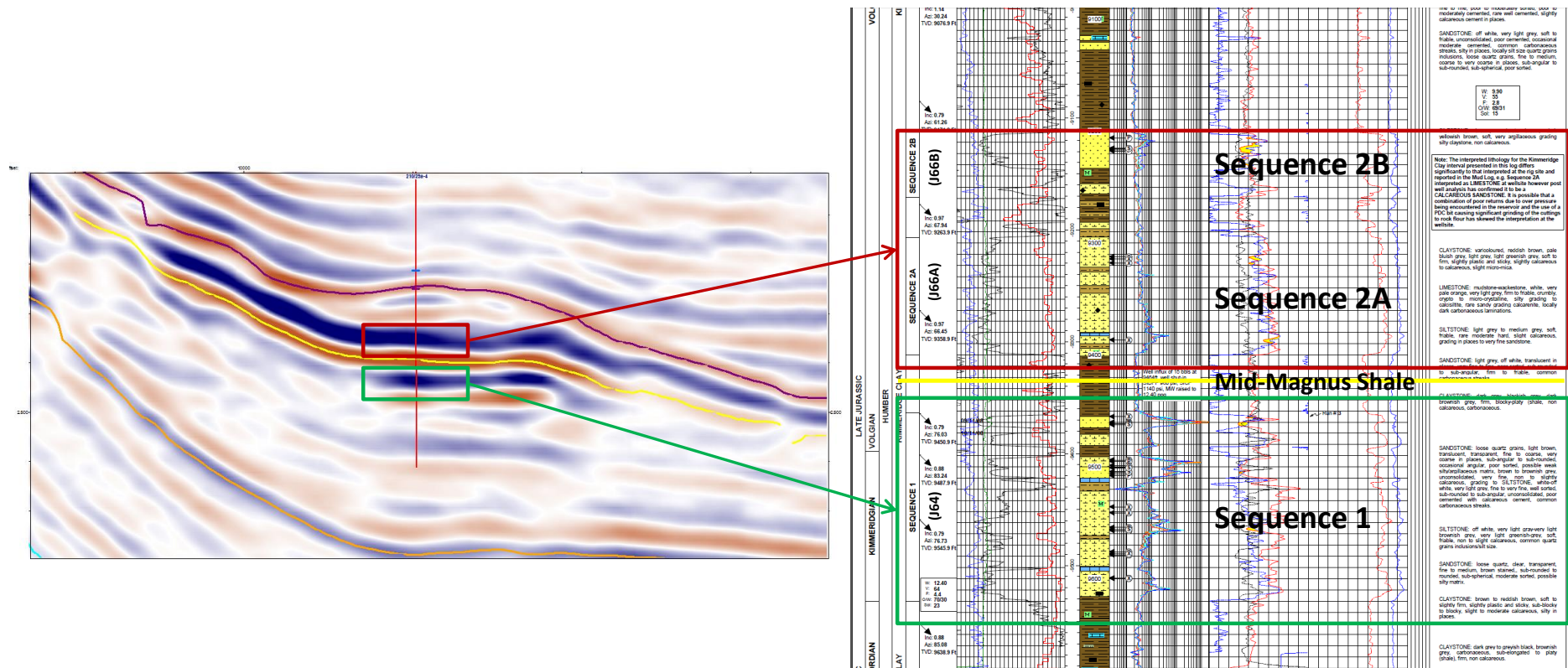


Figure 7-26 zoomed in section illustrating the two bright spots that can be correlated to two separate channel sands found in well 210/29a-4

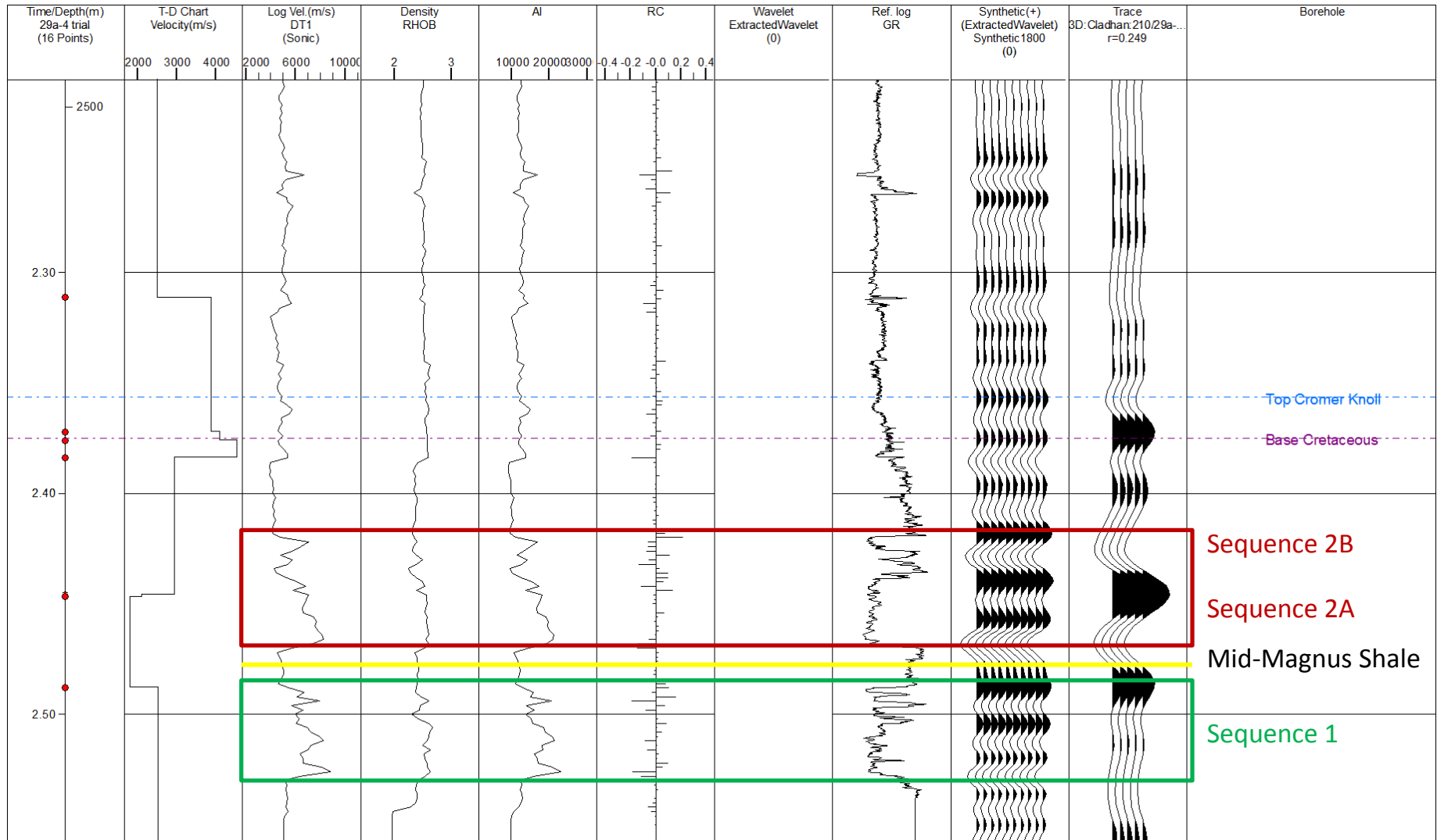


Figure 7-27 The synthetic seismogram for well 210/29a-4 further illustrates the effect of the channel sediments

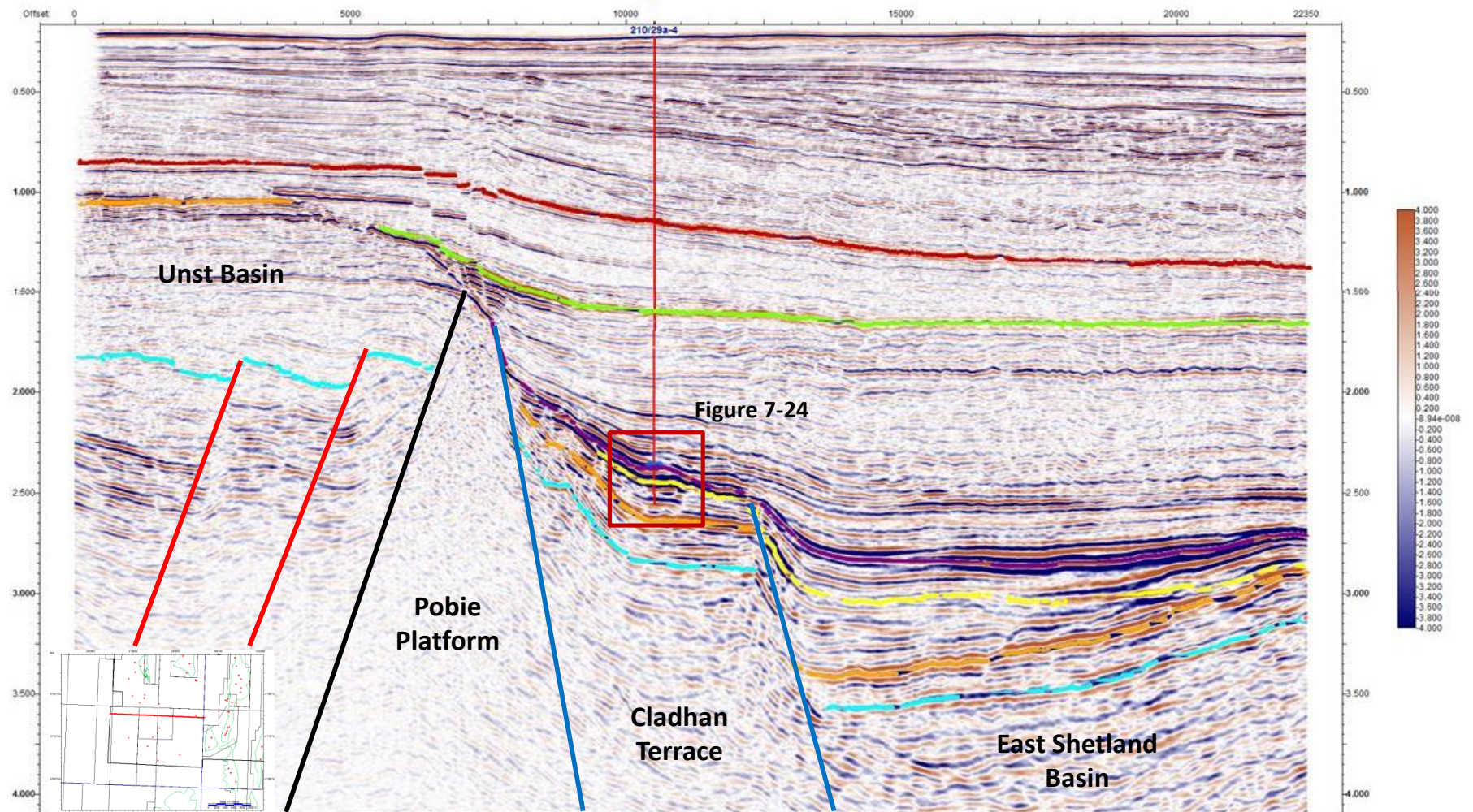


Figure 7-28 Seismic section highlighting the bright-spots that are indicative of the Upper Jurassic channel sediments.

Wellsite Tops (provisional only)	Prognosis		Uncert. +/- (ft)	Actual		Difference TVDRT (ft) -high /+ low
	MDRT (ft)	TVDSS (ft)		MDRT (ft)	TVDSS (ft)	
RT	0	+87	0	0	+87	0
Seabed-Recent/Paleogene Undifferentiated	592	-505	3	623	-536	+31
Balder formation-Eocene/Paleocene	3652	-3565	40	3630	-3543	-22
Upper Cretaceous	5407	-5320	65	5364	-5277	-43
Upper Cretaceous Undifferentiated	-	-	-	-	-	-
Cenomanian-Upper/Lower Cretaceous – Cromer Knoll Group	8537	-8450	145	8557	-8469	+19
Kimmeridge Clay formation-Upper Jurassic	8943	-8855	145	9029	-8941	+86
Sand D-MGS	9057	-8970	160	-	-	-
Sand C-MGS	9232	-9145	240	-	-	-
Sand B-MGS	9430	-9343	240	-	-	-
Sequence 2B				9201	9113	
Sequence 2A				9295	9207	
Sequence 1				9452	9364	
3 rd order cycle – J76 <i>Kochi</i>				9050	8962	
3 rd order cycle - J73B				9071	8983	
3 rd order cycle - J71 <i>Fittoni</i>				9139	9051	
3 rd order cycle - J66C				9159	9071	
3 rd order cycle – J66B <i>Pectinatus</i>				9181	9093	
3 rd order cycle – J66A <i>Hudlestoni</i>				9280	9192	
3 rd order cycle – J64 <i>Autissiodorensis</i>				9450	9362	
3 rd order cycle – J63 <i>Eudoxus</i>				9486	9398	
3 rd order cycle – J62 <i>Baylei</i>				9517	9429	
3 rd order cycle – J56 <i>Rosenkrantzi</i>				9591	9503	
3 rd order cycle – J54A <i>Glosense</i>				9735	-9647	
TD	9587	-9500		9735	-9646.9	+146.9

Figure 7-29 Biostratigraphic analysis undertaken by Sterling resources to date the sand channel sequences.

The resulting biostratigraphic analysis (Figure 7-27 and Figure 7-28) identified that Sequence 1 channel sediments were deposited in the Early Kimmeridgian and can be placed within the J Sequence system at the J64 maximum flooding surface “Autissiodorensis” and is dated at ~140Ma. The Sequence 2A channels however, are placed in the Late Kimmeridgian and are part of the J66a maximum flooding surface “Hudlestoni” which is dated at ~138Ma. The Sequence 2B sediments are similar to the 2A channels but can also be identified as a separate system. The 2B sediments are the Latest Kimmeridgian sediments and are placed in the J66b sequence. These sediments are dated at ~137.5Ma and are equivalent to the Brae Formation sands found in the Brae Complex located in the Viking Graben (Partington et al 1993).

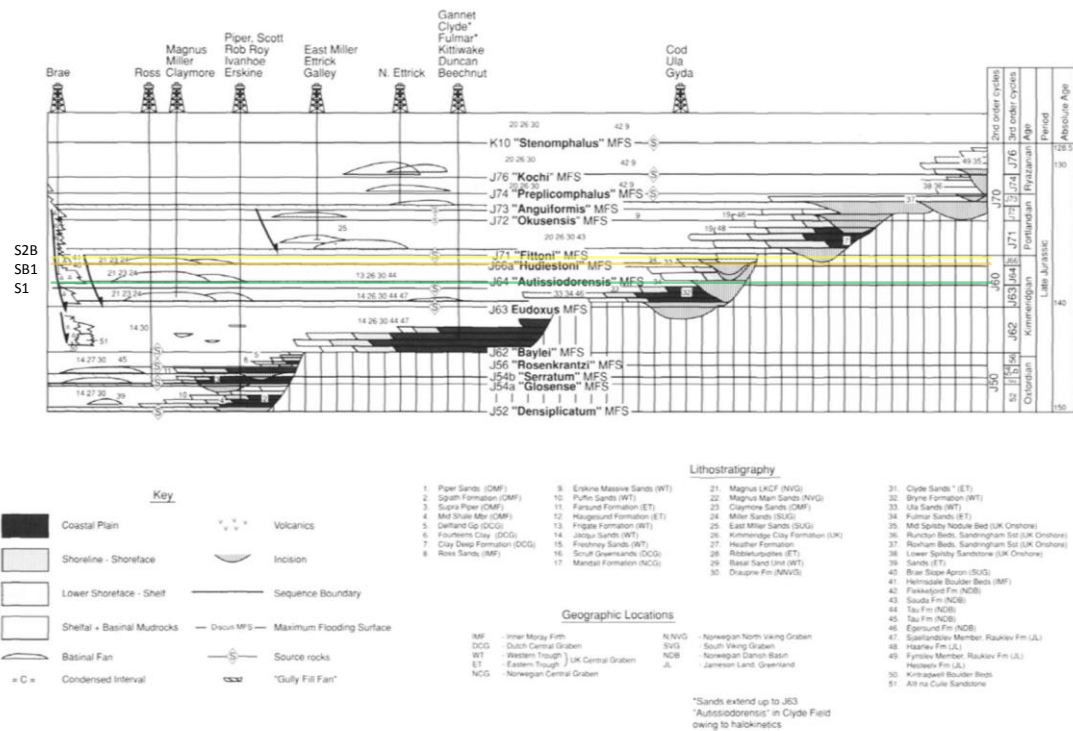


Figure 7-30 A stratigraphic template for the North Sea highlighting where the Sequence 1, 2A and 2B sands fit into the depositional environment (Partington et al 1993)

The combination of the seismic data and the well data shows that when amplitude extraction maps are generated it is extremely important to know the sedimentological evolution of the area, so that it is possible to target specific units or flows. In the Cladnan area it should be possible to undertake two separate amplitude maps, one for the lower sands and one for the upper channel systems, as illustrated in Figure 7-29.

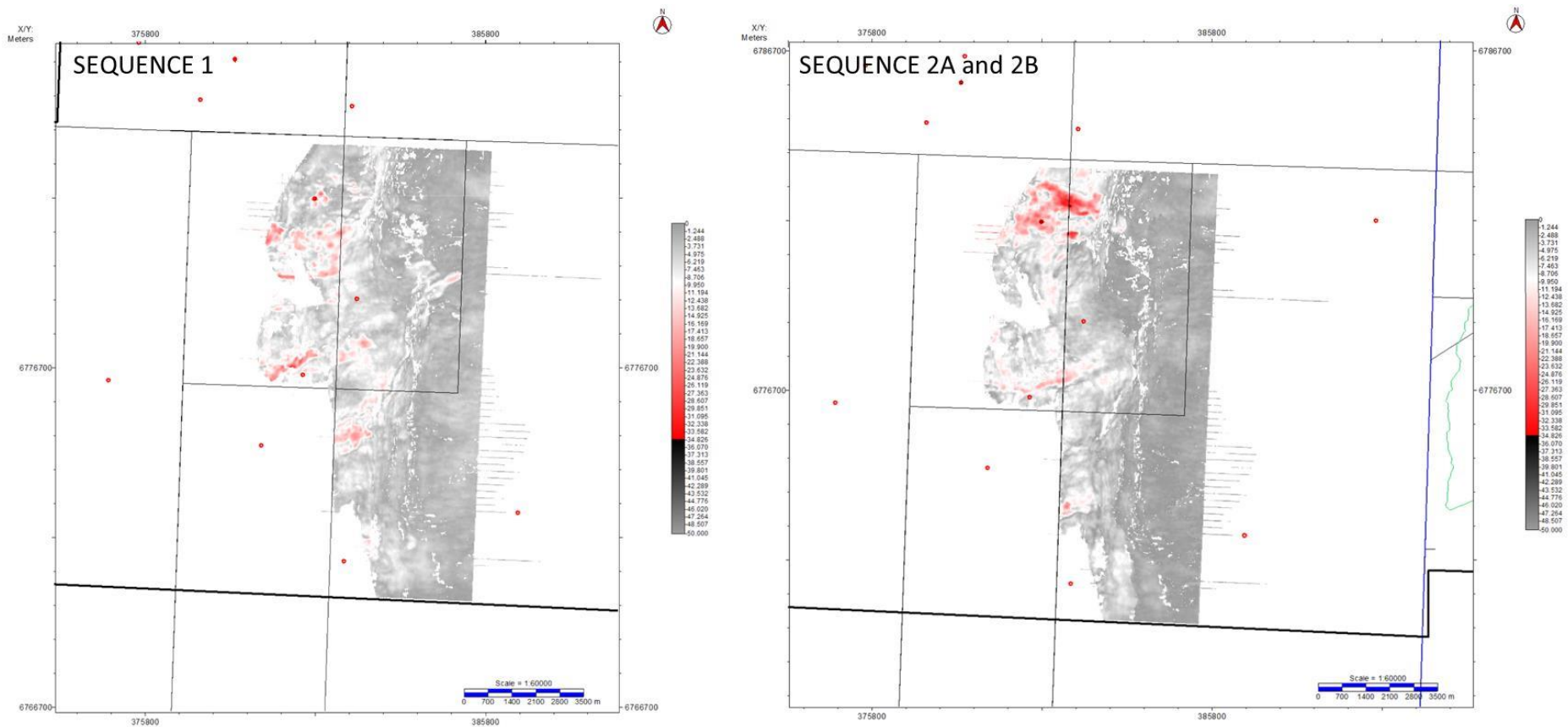


Figure 7-31 Amplitude extraction maps of the Lower (S1) and Upper (S2A+B) channel sands. The amplitude extraction map for the Sequence 1 sand channels was undertaken by creating a measurement window below the Mid-Magnus Shale of 20ms, where the largest negative reflection is measured. A similar window of 20ms was created above the Mid-Magnus shale to measure the Sequence 2A and 2b channel sands..

The Upper and Lower amplitude maps from the Cladhan area now tell a more complete story to that of the overall amplitude map highlighted in Figure 7-21. By separating out the channels into Lower and Upper sequences it is possible to identify a change in depositional nature of the sediments through time. In the Lower channel sequence, it is possible to see a swarm of thin NE-SW striking channels that reach out beyond the Cladhan area, into what has been defined as the East Shetland Basin. The Upper sediments on the other hand illustrate a shift in deposition as only two sand channels are identified. The central channel is in a similar location to that of the Lower sand channels which may be related to an underlying trend. More importantly the large amplitude response identified to the north of the area at the 210/29a-4 location shows a ponding of sediment. This ponding may have occurred as the Upper Jurassic relay ramp faults developed and the subtle uplift and change in topography made it difficult for any sediment to reach the East Shetland basin and remain stranded on the Cladhan Terrace.

As noted above it is possible to see two separate flow systems. The Lower debris flows are smaller in size but greater in number, whereas, the Upper section illustrates a larger flows that pond on the Cladhan terrace. This change in sedimentation has been previously documented by Surlyk (1987), where his study of onshore Greenland sand channel sequence can be illustrated here.

Within the Surlyk study, it is possible to identify that the development of thin sand channel sediments are derived from a laterally continuous shelf environment (Figure 7-30). In the Cladhan area the source area would be the Pobie Platform and the depositional area the Cladhan Terrace. When the sand channels are sourced from a singular point, it is possible for larger sand bodies to form. In the case of the East Shetland Basin, the source would still be the Pobie Platform but the depositional area would be the Cladhan relay

ramp area. As little topographic relief would have been present in this early channel formation, the Lower sand channels would not have been influenced by the Cladhan relay ramp and its associated features. As the faults further developed through the Jurassic the accompanying footwall uplift from the faults would have deflected the Upper sand channels to the relay ramp location forming a larger channel sequence.

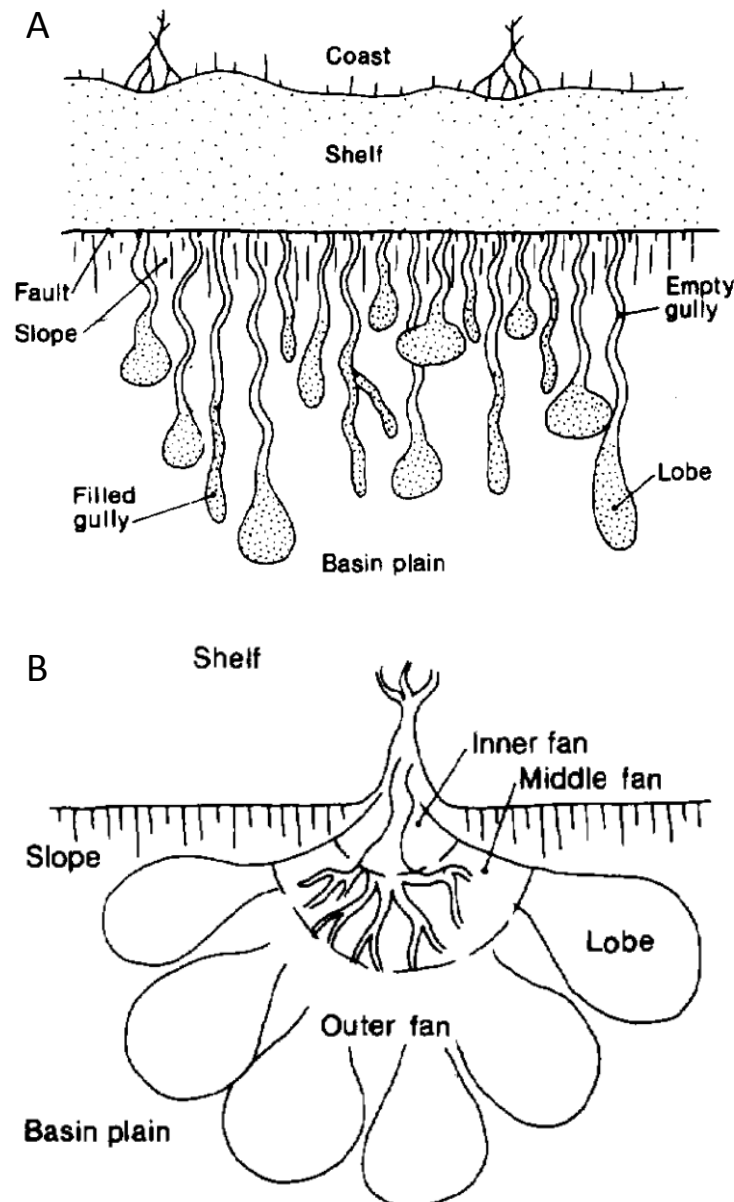


Figure 7-32 case study from onshore Greenland illustrating the different deposition style deepening on varying source points (Surlyk 1987).

As the Upper Jurassic faults grow through time and their footwalls uplift, they will act as a natural funnel to the relay ramp area for any debris flows that occur from the Pobie Platform (Figure 7-31). This is shown in the above amplitude extraction maps (Figure 7-29), which show the Upper sequence of channels do not extend in to the basin area due to the increasing gradient of the footwall location. This increase in angle causes the Upper channel sequences to pond in the footwall location and generates a potential large sand body. As illustrated by the drilling of well 210/29a-4, which targeted one of these Upper sand channels when drilling commenced in 2008.

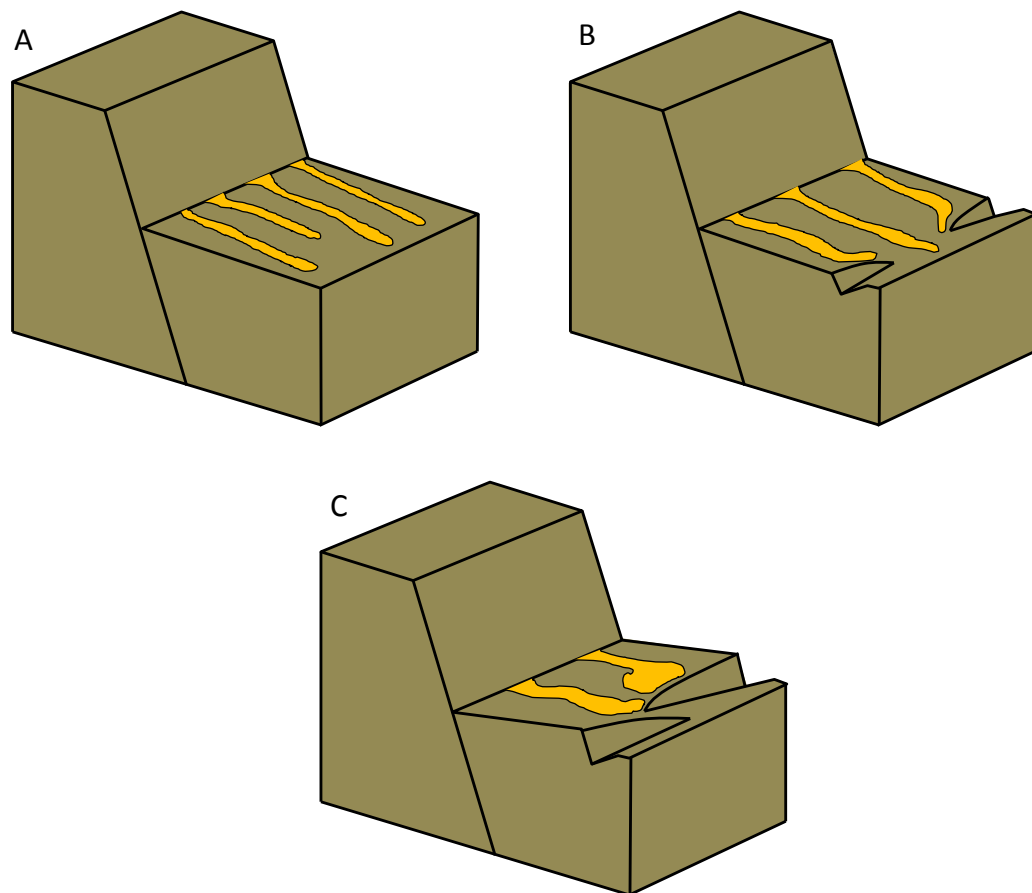


Figure 7-33 Schematic diagram illustrating the evolution of the channel sediment distribution over the Cladhan relay ramp due to fault growth. A – Illustrates the ribbon like channel sands which formed in the early stages of the Cladhan Terrace. B – As the Cladhan faults grew, the footwall uplift deflected the channel sands down a relay ramp. C – The final stage of channel development relates to the ponding of sediment in the footwall highs. Here the channels were unable to reach the basin area and ponded over the footwall.

More evidence from the well data suggests that these debris flow units are individual events that have occurred at separate times. Pressure data from well 210/29a-4 shows that the Upper and Lower sand channels are not in communication and are separated by the shaley (J64) Mid-Magnus shale (Figure 7-32). The Mid-Magnus Shale must therefore act as a localised seal and plays a crucial role in the petroleum system in the Cladhan Terrace. Figure 7-32 shows the pressure data plotted against True Vertical Depth and illustrate a significant change in pressure regime along the well.

Three pressure regimes are identified in this well; the first is that of the upper water leg found from sea level down to the Mid-Magnus Shale. This shows that the Upper sequence of sand units are in full communication with the overburden. A significant pressure increase is observed however across the Mid-Magnus Shale, showing that the shale unit is in fact acting as a localized seal and causing the Lower sequence of sand units to become over pressured. The final pressure regime is located below the hydrocarbon bearing sands and follows a similar trend to that of the initial overburden regime. This section of the well can be identified as the water leg beneath the reservoir units. The sudden change in pressure is typical of a cap rock sediment in this case it must be the Mid-Magnus Shale.

The change in pressure from one sand unit and the sealing nature of the Mid-Magnus Shale unit may be identified due to the sediment source of the sand channels and a case of inverted stratigraphy from the Pobie Platform. It has been illustrated through this chapter that the primary sediment source area for the channel sands is the Pobie Platform. It has also been identified that the eastern edge of the Pobie Platform has been heavily eroded, to the extent that Triassic sediments have been cut into. This erosion and reworking of the Jurassic and Triassic sediments can be illustrated throughout the channel formation history (Figure 7-33).

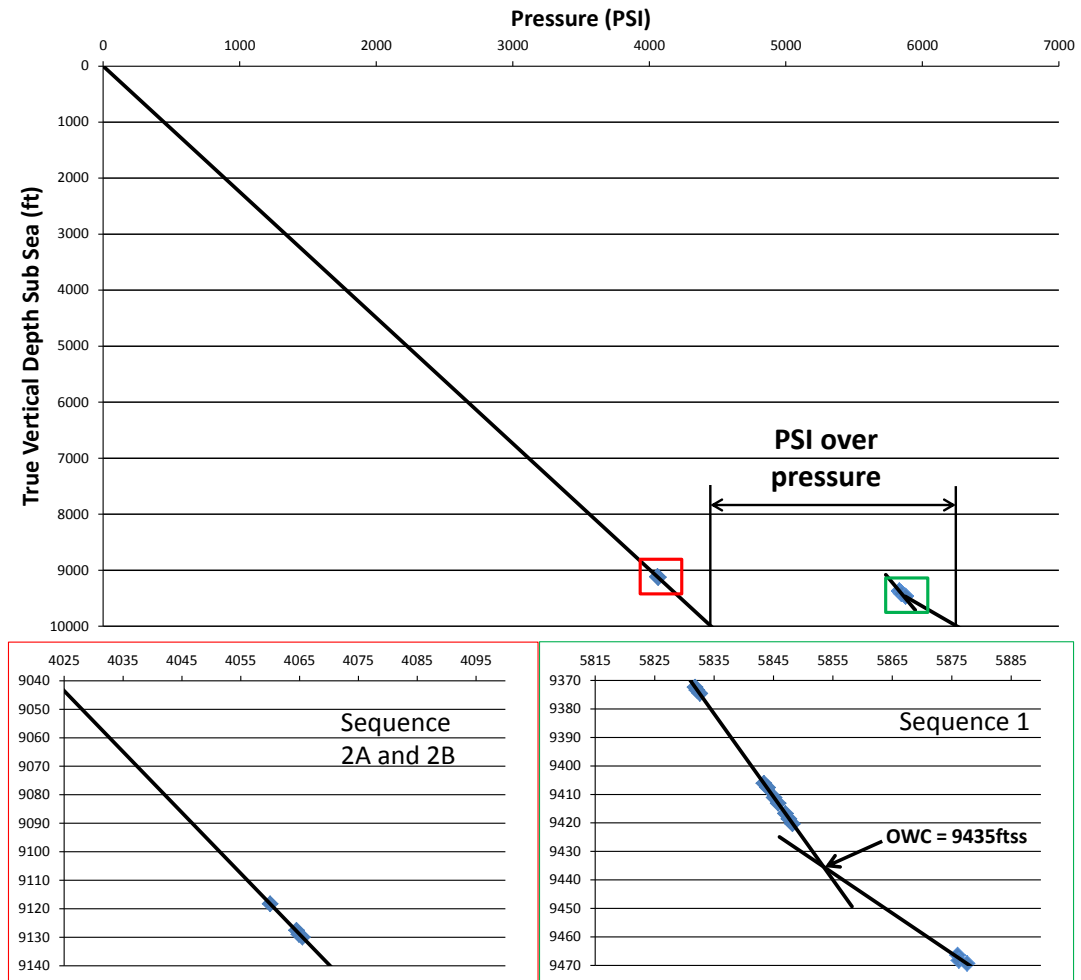


Figure 7-34 Pressure data from well 210/29a-4. Two separate pressure trends can be observed within the two sandstone sequences. The pressure system identified in sequence 2A and 2B appears to be in communication to the sea level and increase steadily with depth. But, the pressure system identified in Sequence 1 sandstones is significantly over-pressured.

The Brent sediments would have been the first to have been eroded during the uplifting of the Pobie Platform. The redistribution of these sediments would form the Sequence 1 Lower sand channels found over the Cladhan Terrace. As the Pobie Platform continued to be uplifted and further erosion occurred, the Lower Jurassic Dunlin Group sediments would have been reworked into the terrace area. Although no major sand units are located within the Dunlin Group the reworking of the mud prone Dunlin sediments into the already mud prone Humber Group sediments could generate a localised seal to the underlying sediments.

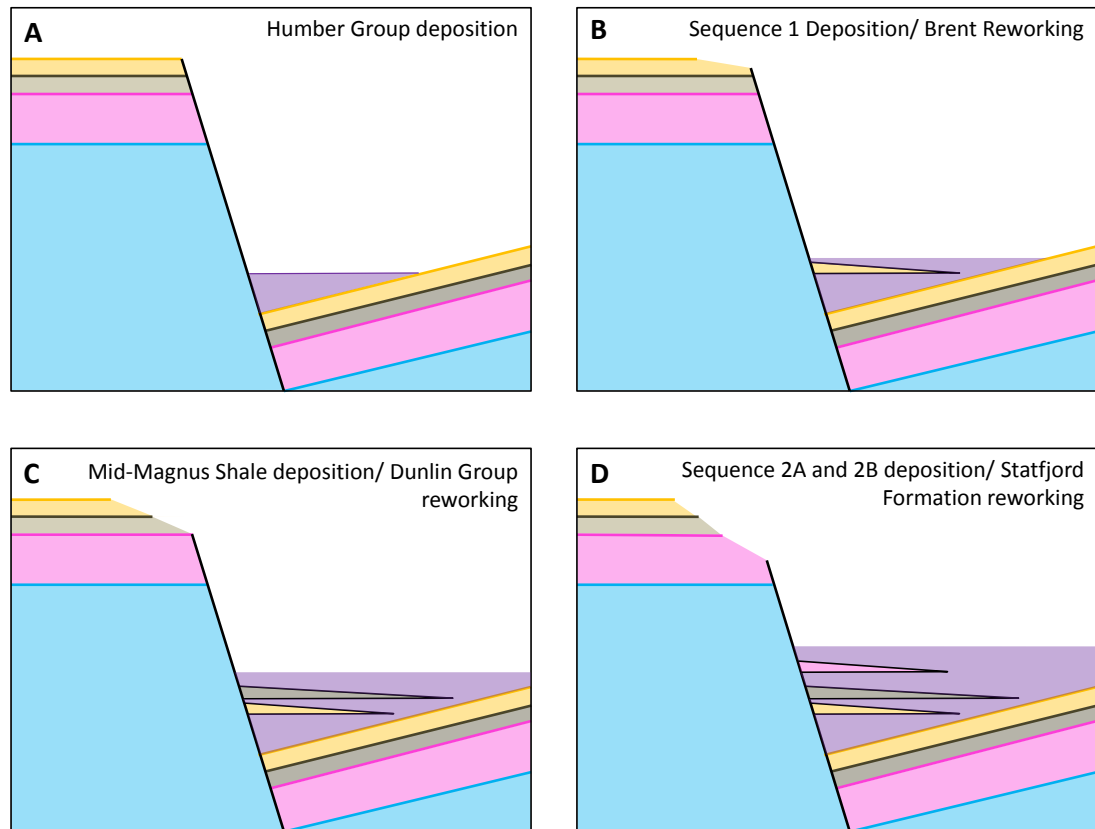


Figure 7-35 Schematic diagram illustrating the inverted clast stratigraphy of the Jurassic and Triassic sediments from the Pobie Platform on to the Cladhan Terrace through the Upper Jurassic.

The Reworking of the Dunlin Group may have a role to play in the petroleum system in the Cladhan area but the redistribution of sediments is not finished from the Pobie Platform. As the erosion continued to cut down through the Lower Jurassic sediments eventually the Upper Triassic – Lower Jurassic Statfjord Formation would have been reworked. The Statfjord Formation has already been identified as a prospective reservoir in the East Shetland Basin. So the reworking of this sand prone from the Pobie Platform to the Cladhan Terrace could result in generating the Sequence 2A and 2B sand prone channels found in the Upper Humber Group. This would show that the Lower sequence of sand channels are sourced from a completely different host rock to that of the Upper sediments, but from the same location.

So, by the reworking of the Lower Jurassic Dunlin Group in the Kimmeridgian, the Mid-Magnus Shale acts as a local seal for the Cladhan area. This has a large impact on the petroleum system surrounding the Cladhan area. What is key in determining a successful petroleum system is the sediment distribution and the migration routes to the Cladhan Terrace. If the Mid-Magnus Shale is a localised seal, and is not buried deeply enough in the terrace area to produce hydrocarbons, where are the hydrocarbons migrating from to reach the Lower sequences? When analysing the individual (Lower and Upper) amplitude extraction maps it is possible to see that the Lower units extend down into the East Shetland Basin where the relay ramp is situated. This is not the case for the Upper sequences. It is probable that the Kimmeridge Clay Formation has been buried deeply enough in the Basin area and is feeding the Lower units which just manages to reach this kitchen area. As the Upper units are separated by the Mid Magnus Shale and do not reach laterally as far in to the basin area as the Lower units, the Upper units remain dry whereas the Lower units may be hydrocarbon prone.

7.6.2 Sedimentary dispersal analogues

The re-distribution of sediment from a structural high across a fault plane has been analysed in several areas of the North Sea. The Miller and Brae Fields are examples of submarine fans forming stratigraphic traps. Evidence from the Helmsdale area and the resultant Allt na Cuille Sandstone Formation also looks at the distribution of sediments around a relay ramp location. The deposition of the Brae Formation in the Miller and Brae Fields has a similar pattern to that of the Cladhan Field (Figure 7-34). The Miller Field reservoir sediments are sourced from the structurally high Fladen Ground Spur to the west and form part of the Brae complex submarine fan

systems (Rooksby, 1991). This is further evidence that understanding the structural and sedimentological evolution can lead to the identification of subtle hydrocarbon bearing submarine fans.

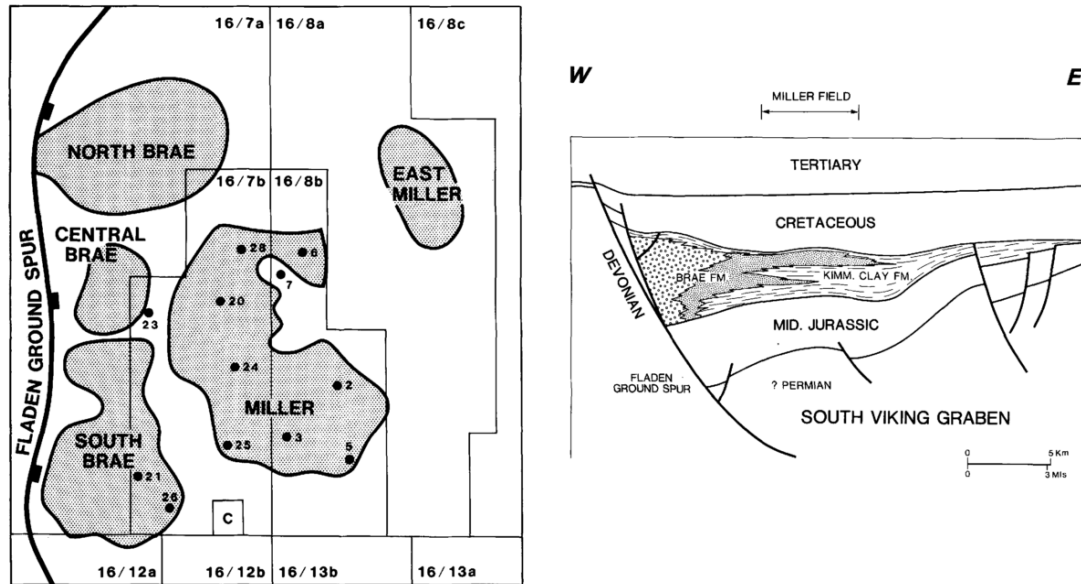


Figure 7-36 Illustration of the Brae and Miller Fields accompanied with a generalized cross section of the fields (Rooksby 1991).

Although the Miller and Brae Fields prove the concept of a hydrocarbon bearing submarine fan system, further analysis of the Cladhan Field must be undertaken to determine the fields potential.

The Allt na Cuille Sandstone Formation in the Helmsdale area is a prime example of how a relay ramp location in the North Sea has a determining factor on sediment distribution (Figures 7-35 and 7-36). The deposition model of alluvial fan or conglomerate sediments in near the fault plane with the development of channel sandstones later can be inferred here.

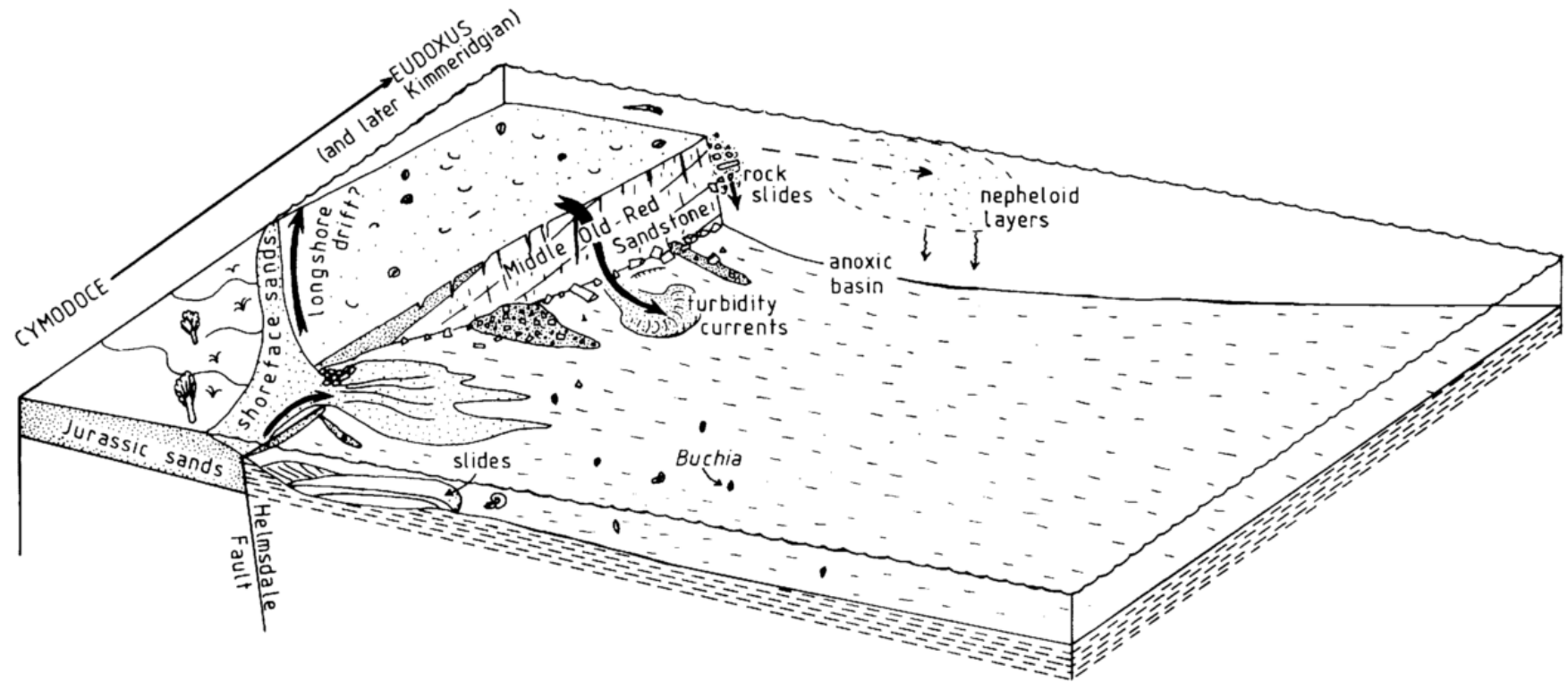


Figure 7-37 Diagrammatic illustration of the varying types of sedimentation that can occur around a fault plane location in the Helmsdale area (Wignall & Pickering, 1993).

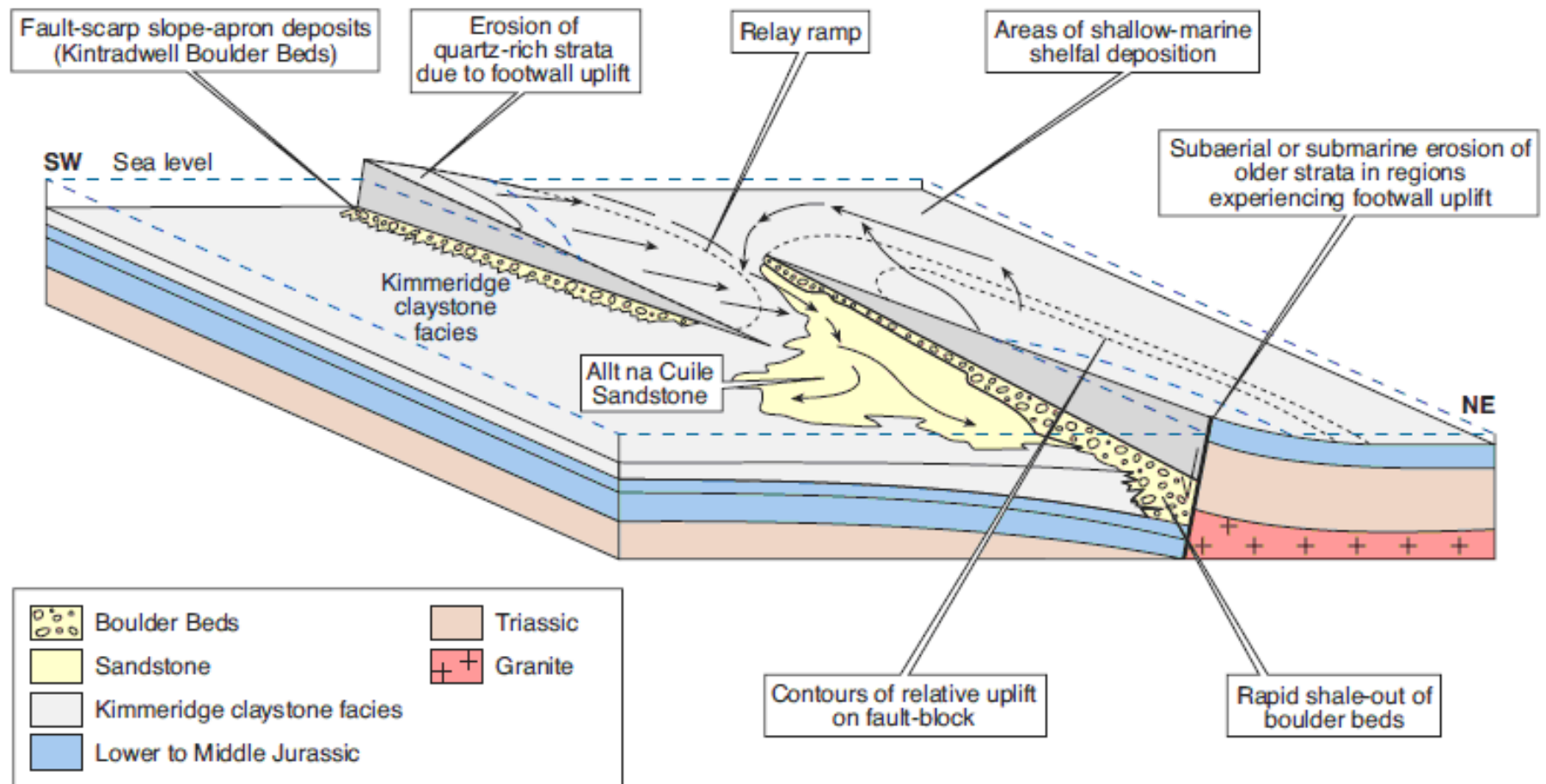


Figure 7-38. Illustration of sediment dispersal patterns as a result of footwall uplift segmentation and fault propagation (Underhill 1994).

The generation of a relay ramp as seen in Figure 7-36 can act as a conduit for coarse clastic sediments to be deposited in what would normally be a mud or silt prone environment. The source of these sand prone units as observed in the Cladhan area come from adjacent structurally high areas. These sediments can be deposited in a variety of sedimentary processes, ranging from turbidite flows, alluvial fans and fluvial sediments. The sedimentary process seen in the Cladhan area is that of a turbidity current that is deposited over a relay ramp location. This in a sense is a combination of sedimentary processes that are observed in the Helmsdale area.

A simple restoration model for the Cladhan area again illustrates the eroded section missing from the eastern Edge of the Pobie Platform (Figure 7-37). With the use of a basic depth conversion model and measuring the area that has been eroded it is possible to estimate the amount of sediment that has been eroded from the platform edge. In total nearly 3 million cubic meters of sediment has been removed from the Pobie Platform, which has either been deposited down dip or back shed into the Unst Basin. This volume of sand prone material could become an attractive prospect if its constraints were known. The Pobie Platform has indicated that to the eastern edge of the platform the Middle Jurassic Brent Group has been heavily eroded, meaning there is a high possibility that this is a submarine fan composed of reworked Brent sandstone material, from the Pobie Platform. Identifying sand prone submarine fans encased within the mud dominated Humber Group, could lead to exploration in the Upper Jurassic sediments in and around the edges of the terraced areas. The ability to predict where these fan systems are is crucial in terms of petroleum basin evolution. The understanding of secondary reservoir source material and formation is crucial in determining petroleum prospectivity. With this in mind the flow direction of this submarine fan is along a familiar orientation.

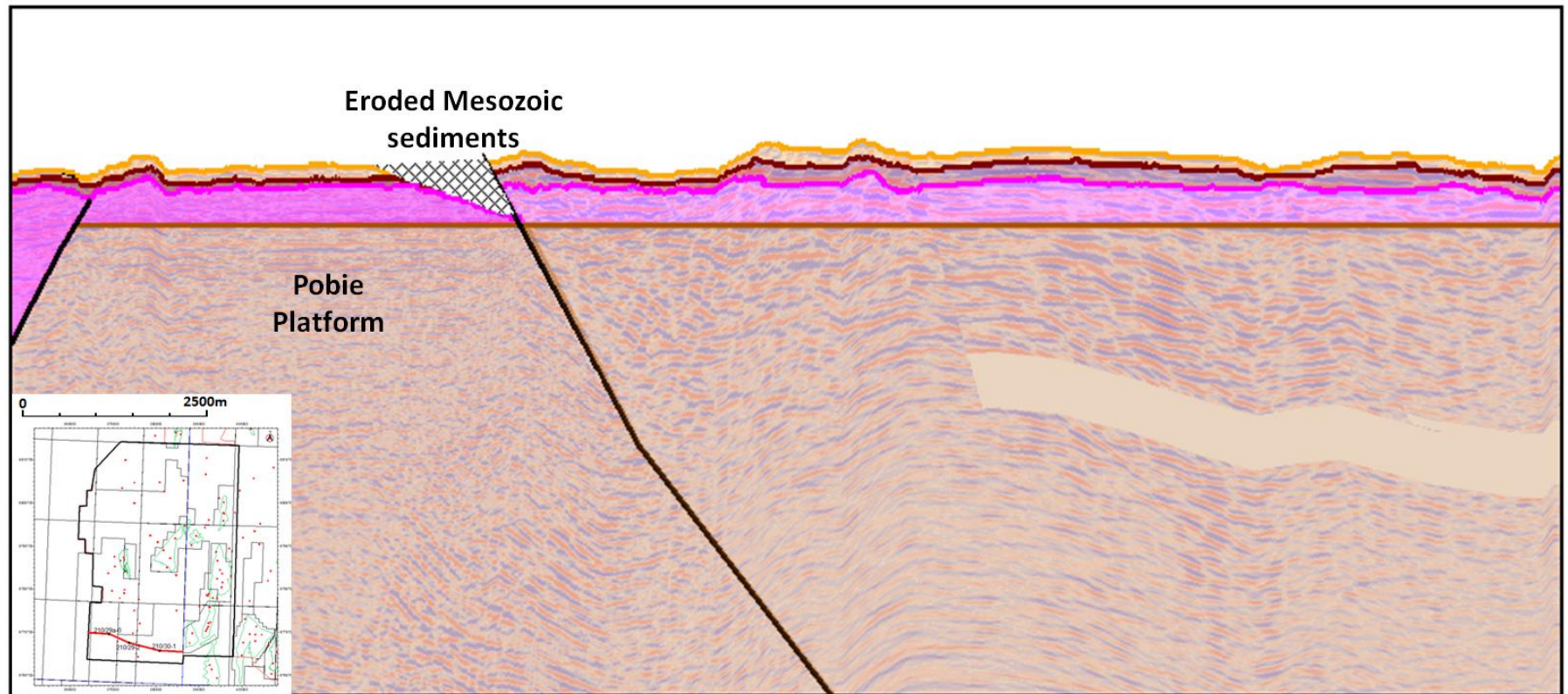


Figure 7-39. Restoration work upon the Top Brent horizon illustrates a missing section of Brent Group sediments over the Pobie Platform. An estimated 3 million cubic meters of sediment has been eroded from the eastern edge of the Pobie Platform. This figure was generated by measuring the eroded area and applying a simplified depth conversion model to the missing section to generate a depth of scour. The volumes also took into consideration the shape of the eroded area which in this case was triangular.

7.7 *Influence of underlying structural patterns*

The orientation of the submarine fan identified by amplitude extraction and subsequently verified by drilling of well 210/29-4 is NE-SW. This is the same orientation of the initial Permo-Triassic rifting event. Does this mean that there are underlying Permo-Triassic faults that have influenced the deposition of the Upper Jurassic submarine fan systems?

To analyse the prospect of underlying Permo-Triassic faulting, seismic lines were generated perpendicular to the flow direction of the sedimentary submarine fan (Figure 7-38). Another note on the flow direction relates to other potential flows, although one fan system is clear to see, directly to the south is a similar oriented grouping of bright spots. Upon analysis of the areas around the submarine fan, it is possible to identify an underlying fault from the Permo-Triassic rifting event. These NE-SW orientated faults are not on the same scale as the Tern-Eider Ridge faults, but are still important in determining the deposition of reworked Middle Jurassic sediments. The location of the faults is the most important factor in determining the orientation of Upper Jurassic submarine fans. The submarine fans are located above the hangingwalls lows of the Permo-Triassic faults. The first thing to point out here is that these older Permo-Triassic faults have not been reactivated in the Upper Jurassic rifting event. It is clear to see the Permo-Triassic pre-rift block and the on-lapping syn-rift sediments. The overlying post/intra -rift sediments have been eroded away to leave an unconformity close to the base Brent horizon. The sediments expected to have been deposited in this half graben structure relate to the Triassic Herge Group and the Lower Jurassic Dunlin Group. The overlying Brent group looks relatively undeformed by the older faults, which backs up the theory that these faults remained dormant during the Upper Jurassic rifting event.

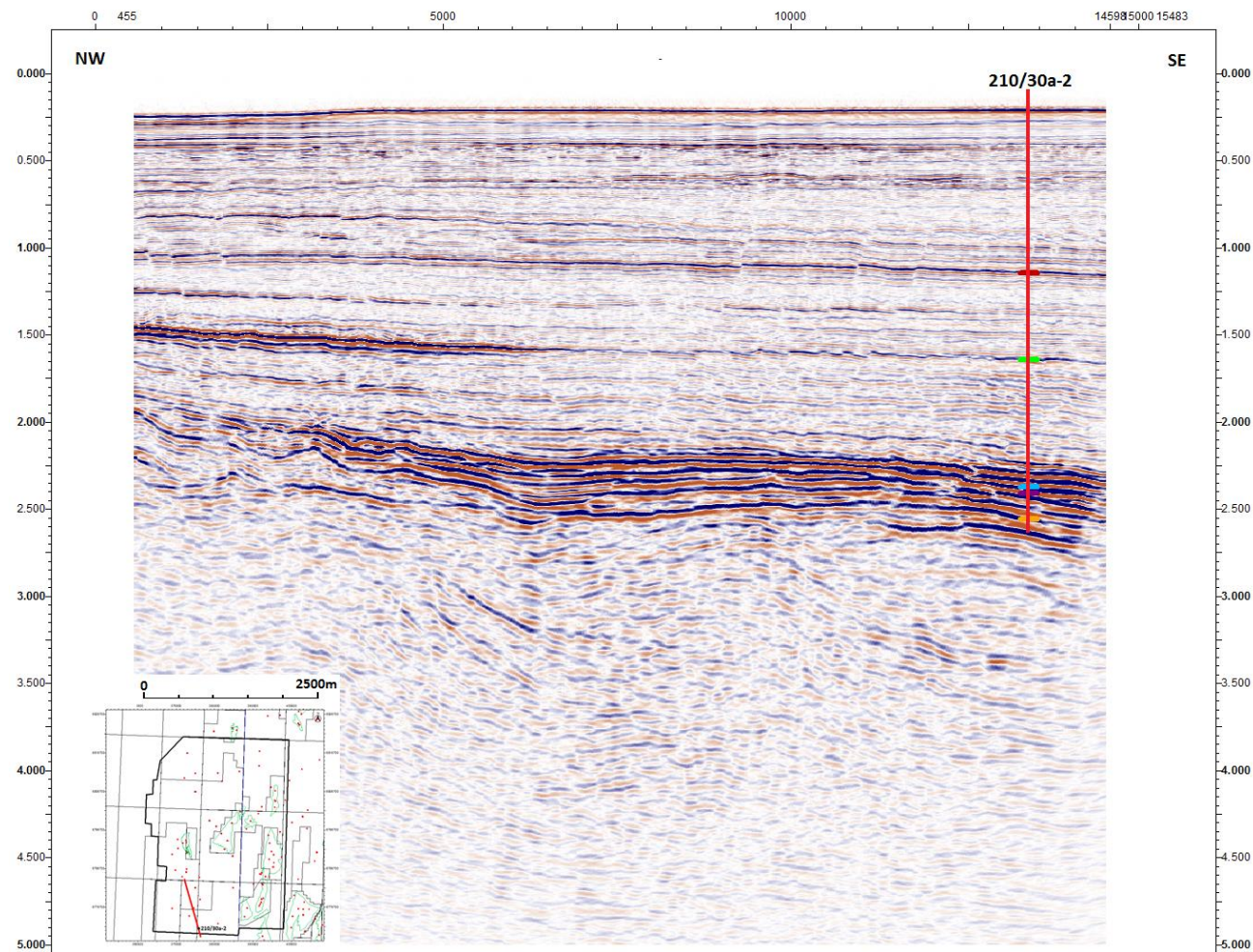


Figure 7-40 Uninterpreted seismic section in the hangingwall of the Cladhan Terrace.

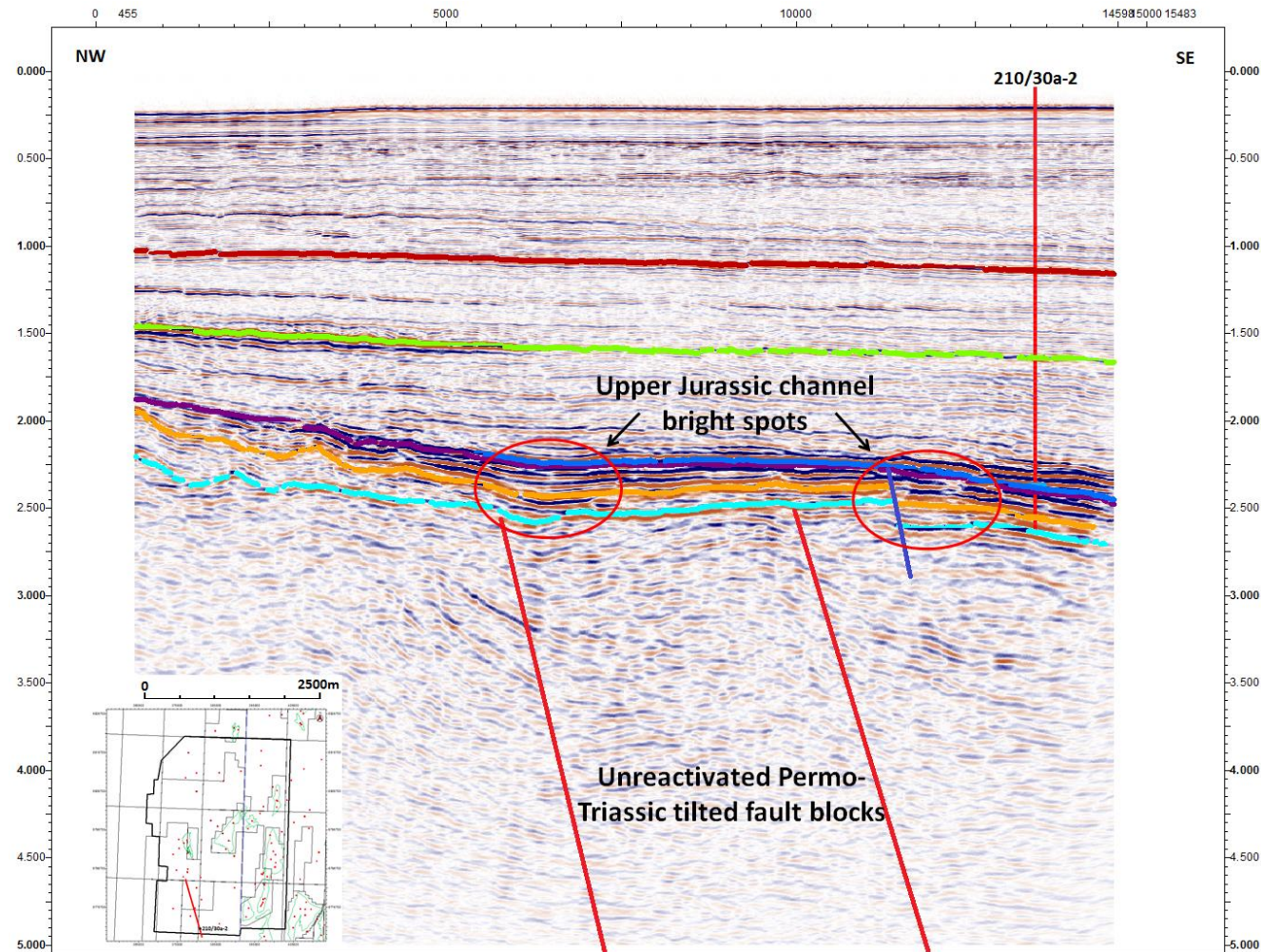


Figure 7-41 Seismic cross-section illustrating the generation of compaction driven lows in the Triassic sediments to aid the direction of flow for Upper Jurassic submarine fans.

It is plausible that the Triassic faults even though they did not reactivate in the Upper Jurassic still directly affected the deposition of the submarine fans. The effects the faults may have had on the Upper Jurassic sedimentation patterns will solely relate to compaction driven accommodation space. The greatest compaction rates of the mud based sediments found in the hangingwall, will occur where the sediments are thickest. These areas of increased compaction will generate a series of subtle lows directly above the hangingwall lows in the Permo-Triassic faults.

The subtle lows will in turn aid will the flow direction of submarine fans, funnelling sediment in a NE-SW orientation towards the basin area. This will account for the flow direction of the Upper Jurassic submarine fan that is sourced from the eastern edge of the Pobie Platform. The compaction driven lows are seen in each of the fault block hangingwalls. The hangingwall to the fault block (furthest SE) identified in the Figure 7-28 also illustrates this compaction driven accommodation space and the active deformation of the Brent group sediments. This results in the formation of the second potential flow observed in the amplitude extraction map above. It is possible to track one of these faults into the basin area by using a dip map (Figure 7-39) and the seismic data (Figures 7-40).

A dip map is created by measuring the change in angle between two points on a set horizon. In Figure 7-39 a dip map is created by measuring the change in dip along the top Brent Group horizon. The darker areas illustrate an increase in dip from location to location. These maps can be used for fault identification as it would highlight areas where sharply dipping beds are present.

The fault which is responsible for the primary channel sand seems to have reactivated. The location of this fault is crucial to its reactivation. This

underlying Permo-Triassic fault is cross-cut by an Upper Jurassic fault at the relay-ramp area. For the relay ramp to become breached a fault perpendicular to the Permo-Triassic trend must form. But, with an underlying trend in place the old fault reactivates rather than link to the fault propagating from the north. This may have occurred due to the stress needed to create a breaching relay ramp fault was greater than that of reactivation of the Permo-Triassic fault. This illustrates the role of fault growth and linkage of two different faults relating to two separate rifting events, with different orientations.

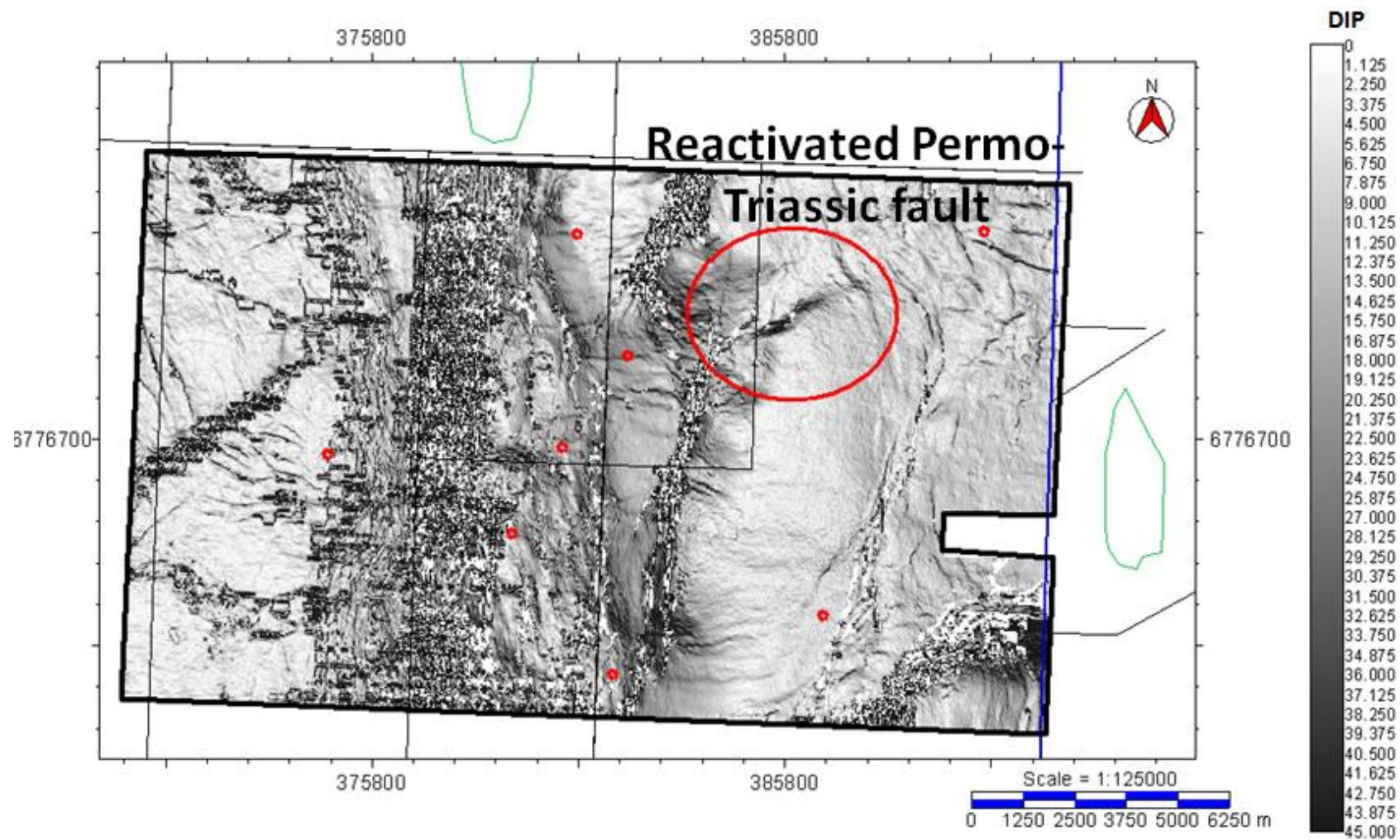


Figure 7-42. Top Brent Group dip map, illustrating the reactivation of an underlying Permo-Triassic fault in the hangingwall area of Cladhan.

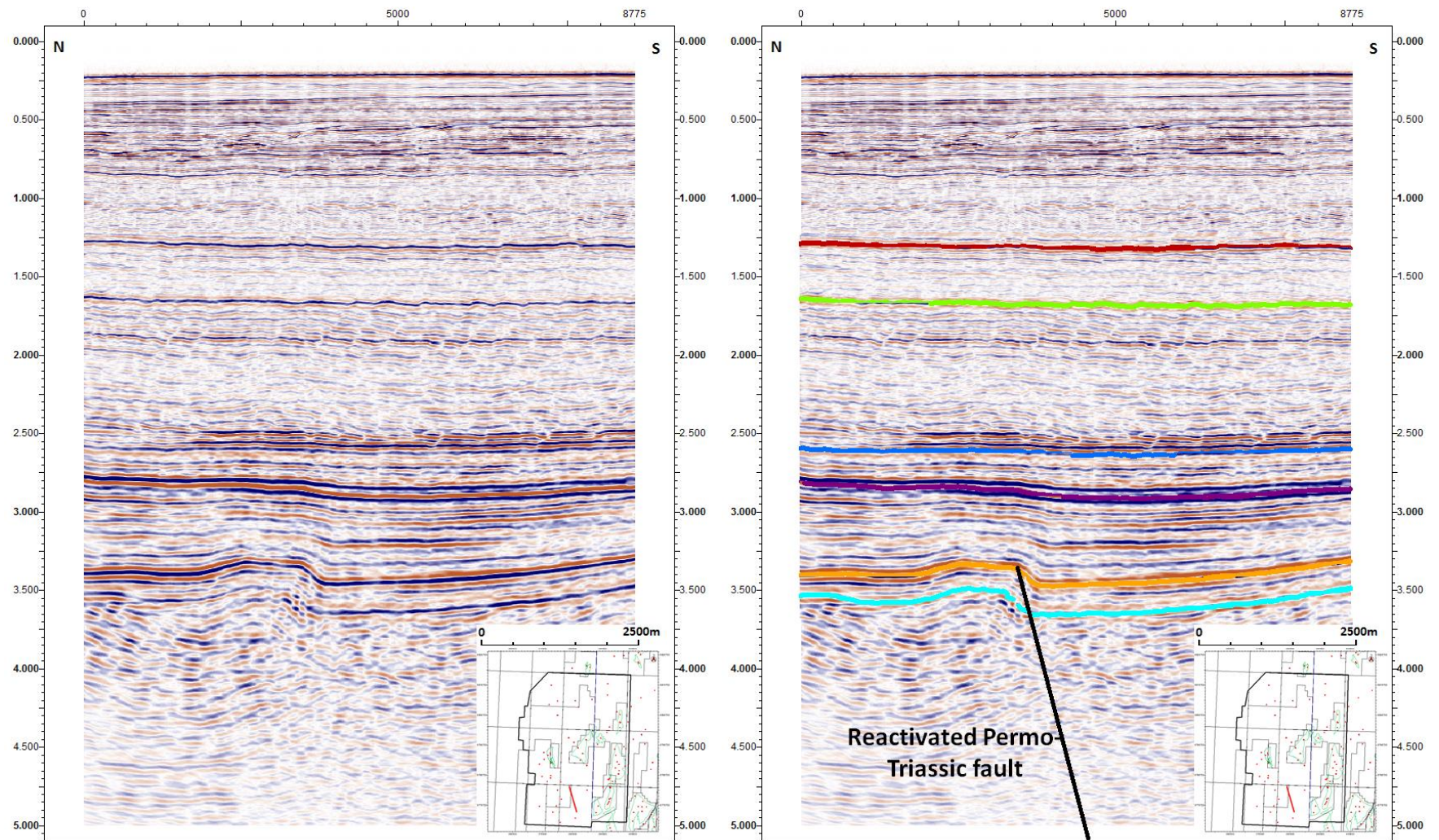


Figure 7-43. Seismic cross section illustrating the reactivation of an old Permo-Triassic fault in the basin area of Cladhan.

The identification of potential sedimentary/ stratigraphic traps and petroleum plays in a mature basin is crucial in a basins discovery lifetime. There has been an increase in the exploration of subtle plays in the East Shetland Basin as most of the major hydrocarbon fields have been discovered and developed. Areas like Cladhan are a prime example of future field types in the mature East Shetland Basin.

7.8 *Drowning of the Pobie Platform*

As mentioned in earlier chapters it is possible for islands to form during the Upper Jurassic and through to the Lower Cretaceous. The formation of an island in the archipelago can thus be extended into the Cladhan area and a large island is generated in the shape of the Pobie Platform.

As illustrated earlier, the NE-SW Permo-Triassic faults generated such structures as the Pobie Platform and the Tern-Eider Ridge. With the reactivation of faults in the Upper Jurassic and the position of the East Shetland Platform fault the Pobie Platform remained a structural high throughout most of the Cretaceous, whereas the Tern-Eider Ridge was submerged during the early stages of the Shetland Group sedimentation.

Seismic and well data over the Pobie Platform indicate that the first sediments to completely cover the eroded Brent Group sediments belong to the Late Paleocene, Lista Formation. This would suggest that the Pobie Platform was sub aerially exposed for almost 100Ma. It is clear to see from the seismic data that the Pobie Platform was not completely submerged by water until the mid-late Paleocene. The well reports on the other hand suggest a slightly different pattern of drowning.

The well logs that are not situated on the structural high show the deposition of Danian limestone. The formation of this sediment is generally assumed as the erosive debris from the upper most part of the Upper Cretaceous. The upper most part of the Cretaceous period is the Maastrichtian, which also coincided with the period of maximum sea level rise in the North Sea. The increase in sea level could have actually resulted in the drowning of the Pobie Platform enough for a thin draping of Maastrichtian sediments to be deposited. With the fall of this sea level high the newly deposited sediments would have been eroded and redeposited down dip of the Pobie Platform. This would account for the presence of the Danian sediments found in some of the well logs (Figure 7-41). It is interesting to note that well 210/30a-3, which is furthest away from the Pobie Platform, does not record any Danian sediments at the Upper Cretaceous/ Cenozoic boundary.

This is further supported in the seismic data by a series of bright spots in and around the Upper Cretaceous boundary horizon close to or against the East Shetland Platform fault. This would suggest that sediments are being shed off the platform top to form talus slopes in the basin.

This shedding of sediment can be observed in maps of the Top Cretaceous. The Cretaceous sediments of the Northern North Sea are considerably different to that of the Southern North Sea. To the south the Chalk Sea is present where thick deposits of chalk and limestone's are present, but to the north the presence of chalk slowly grades out into mudstones and siltstones. The later compaction of these sediments forms a series of polygonal faults which can be observed through seismic interpretation.

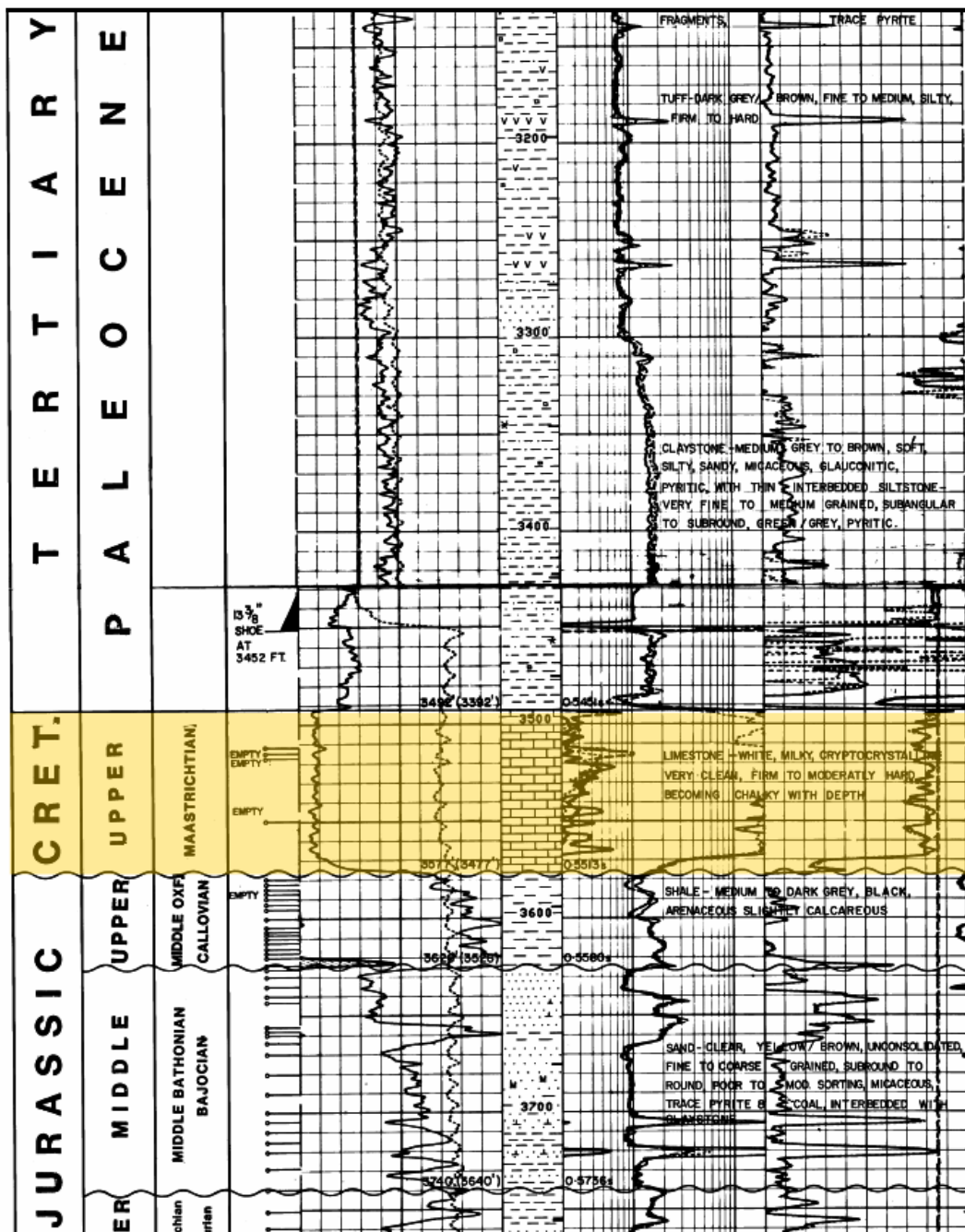


Figure 7-44 well 210/19-3 illustrating the presence of Upper Cretaceous (draping) sediments over the East Shetland Platform.

In the Cladhan area these polygonal faults are present in the basin, but are not observed in the terraced area. Here the talus slopes drape over the polygonal faults, masking their presence.

This suggests that the Pobie Platform was in fact covered during the Upper Cretaceous and the subsequent sediments were eroded away shortly after deposition (Figure 7-42). This potential semi-drowning of the Pobie Platform has played an important role in the preservation of the Brent Group. Further evidence of this initial drowning phase is observed in well 211/19-3. Within this well, deposits of the Upper Cretaceous Shetland Group are found, suggesting the platform was drowned pre-Paleocene.

These sediments remained preserved as this structural high which makes up part of the East Shetland Platform is not as high as the Pobie Platform, which was a structural high within the East Shetland Platform, thus, a greater amount of sediment accommodation space was generated during this initial drowning period. When sea level fell again, these thicker sediments recorded over the East Shetland Platform were eroded but not to the same extent as the sediments deposited over the Pobie Platform. The thin sediment covering over the structural highs were completely eroded off and redeposited down dip (Figure 7-43), whereas, the thicker sediment covering over the platform were eroded but some covering was preserved when the eventual drowning of the Platform occurred in the Paleocene. As noted earlier (Figure 7-19), well 210/29a-3 shows a large scale erosive unconformity. The unconformity time gap between these two layers is 100Ma.

If the Upper Cretaceous Maastrichtian sediments were not deposited on top of the Brent Group then the underlying Middle Jurassic sands themselves would have been eroded away even more after the fall in sea level towards the end of the Maastrichtian. Although this would be positive for exploration in the basement it would be less so for the exploration in the Pobie Platform, as no secondary reservoirs would be present.

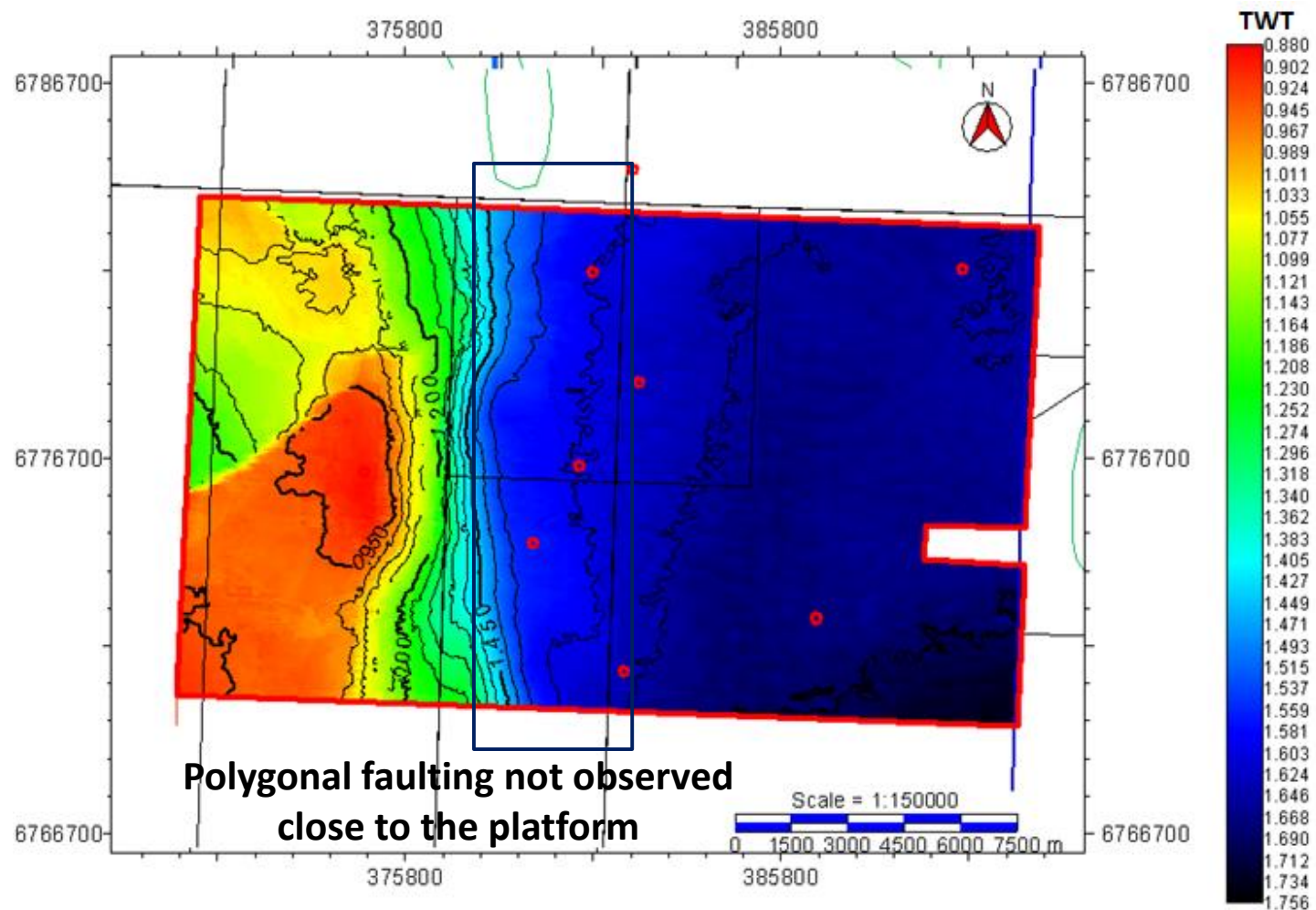


Figure 7-45. Base Tertiary map illustrating the existence of the Pobie Platform at Cretaceous times and the partial covering of polygonal faulting at this layer by redeposited sediments from the structural high to the west.

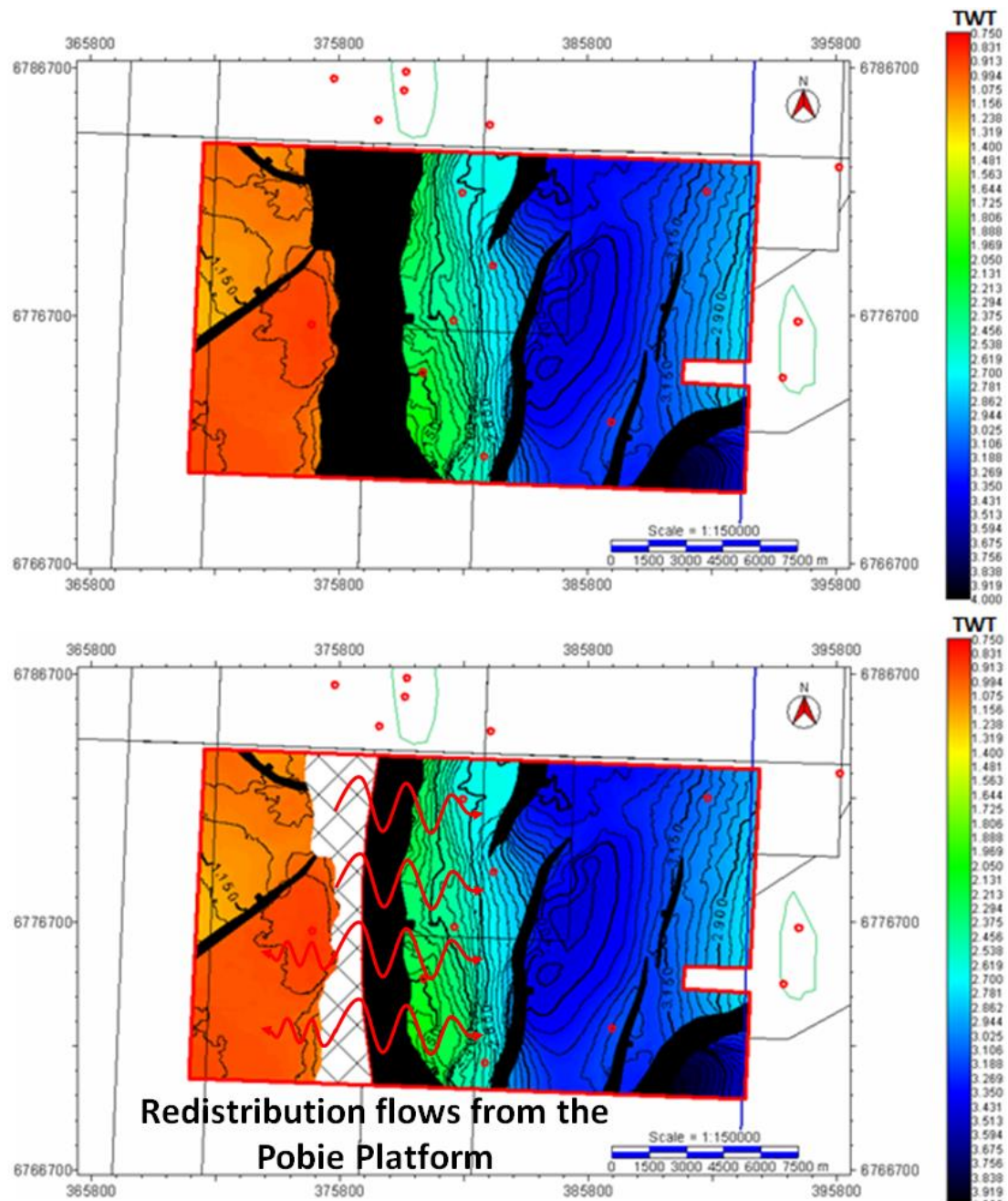


Figure 7-46. Top Brent time structure map, illustrating areas which have been eroded down through the Brent Group on the footwall high that is the Pobie Platform. The cross-hatched area is where Brent Group sediments are not present over the platform.

It is clear to see that on the eastern edge of the Pobie Platform the Brent Group succession has been totally eroded away. This could be due to a combination of erosion and footwall slumping and degradation through time. If the covering of the Maastrichtian sediments did not occur, it is highly likely that the extent and thickness of the Brent group over the Pobie

Platform would be considerably lower than what it is now. This would drastically reduce the prospectivity of the structural high. The high on the Pobie Platform was in fact drilled in October 1990 and targeted the Jurassic Brent sands and the Triassic Cormorant Formation. The resultant well tests identified zones of oil staining and oil shows in the Brent Group and gas shows in both Jurassic and Triassic formations. The oil found in the Brent Group sediments were heavily biodegraded, due to the relative shallowness of the structural high and the well was abandoned.

7.9 Eocene Fault Reactivation

Although most of the faulting in the East Shetland Basin is contained to the two rift phases (Permo-Triassic and Upper Jurassic), it is, however, possible to identify some small scale faulting in the Paleocene. These faults are best observed in the Balder Formation (Figure 7-44). These faults do not affect an active petroleum system, as the 210/29a-3 well located on the Pobie Platform contains heavily biodegraded heavy oil in the Brent Group, which makes the Pobie Platform non-prospective. All of these Balder level faults terminate at the top Cretaceous (Top Shetland Group) and are located above the fault bounding the East Shetland Platform and are clearly identified with the use of a horizon dip map (Figure 7-45). It is inferred that these faults have formed as a direct result either of differential compaction over the fault plane or by fault reactivation in response to Atlantic plate margin forces. This is inferred as the footwall has a thin covering of Mesozoic sediments which is under-pinned by Pre-Cambrian basements, whereas, the hangingwall has a thick Mesozoic sedimentary section. As the basin area has a greater amount of sediment thickness compared to the platform area, it is expected that compaction will play some role in determining the post-rift depositional pattern, such as the late Paleocene Lista and Balder Formations.

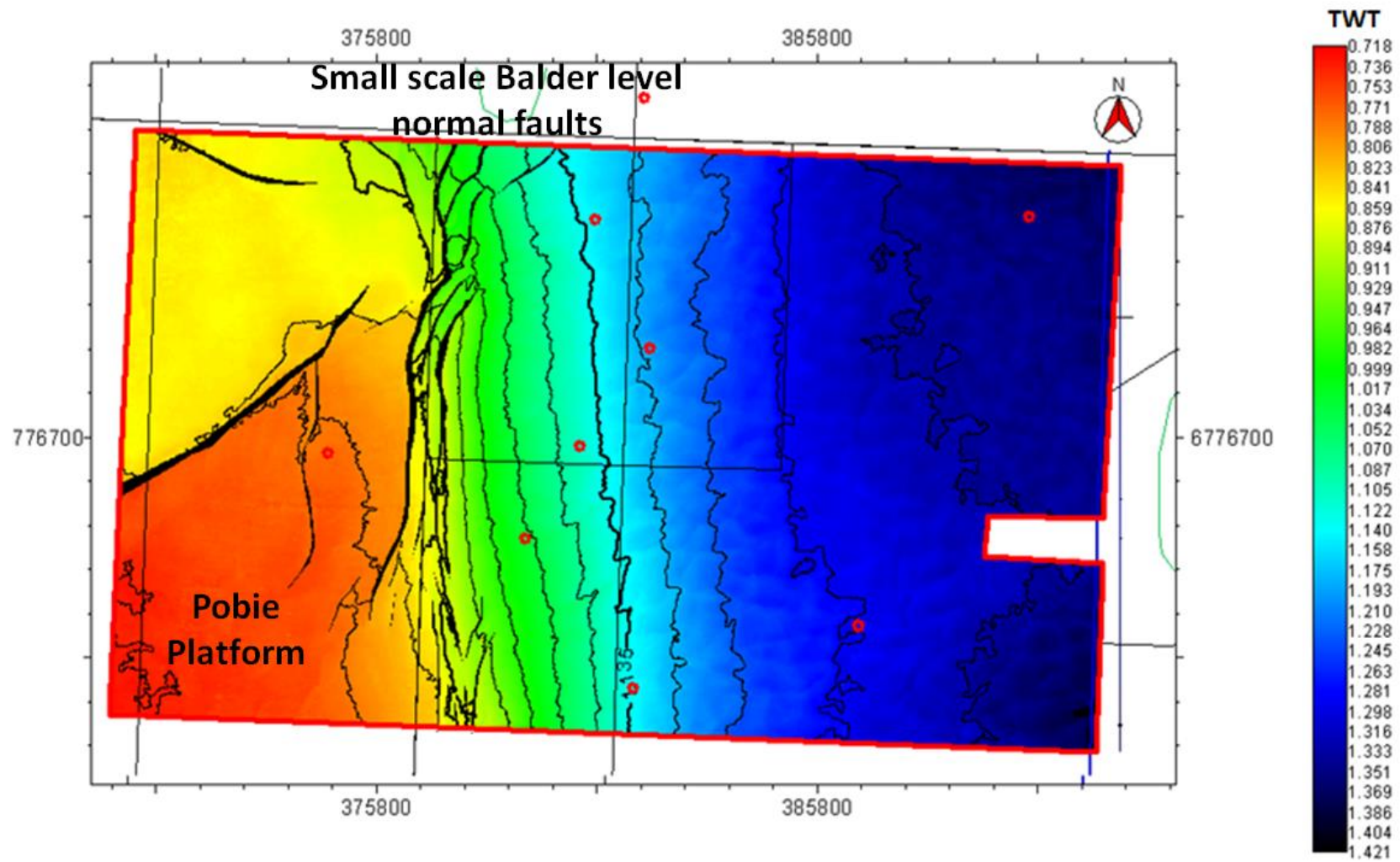


Figure 7-47. Top Balder Formation. Identification of small scale faulting (Black) above the East Shetland Platform fault.

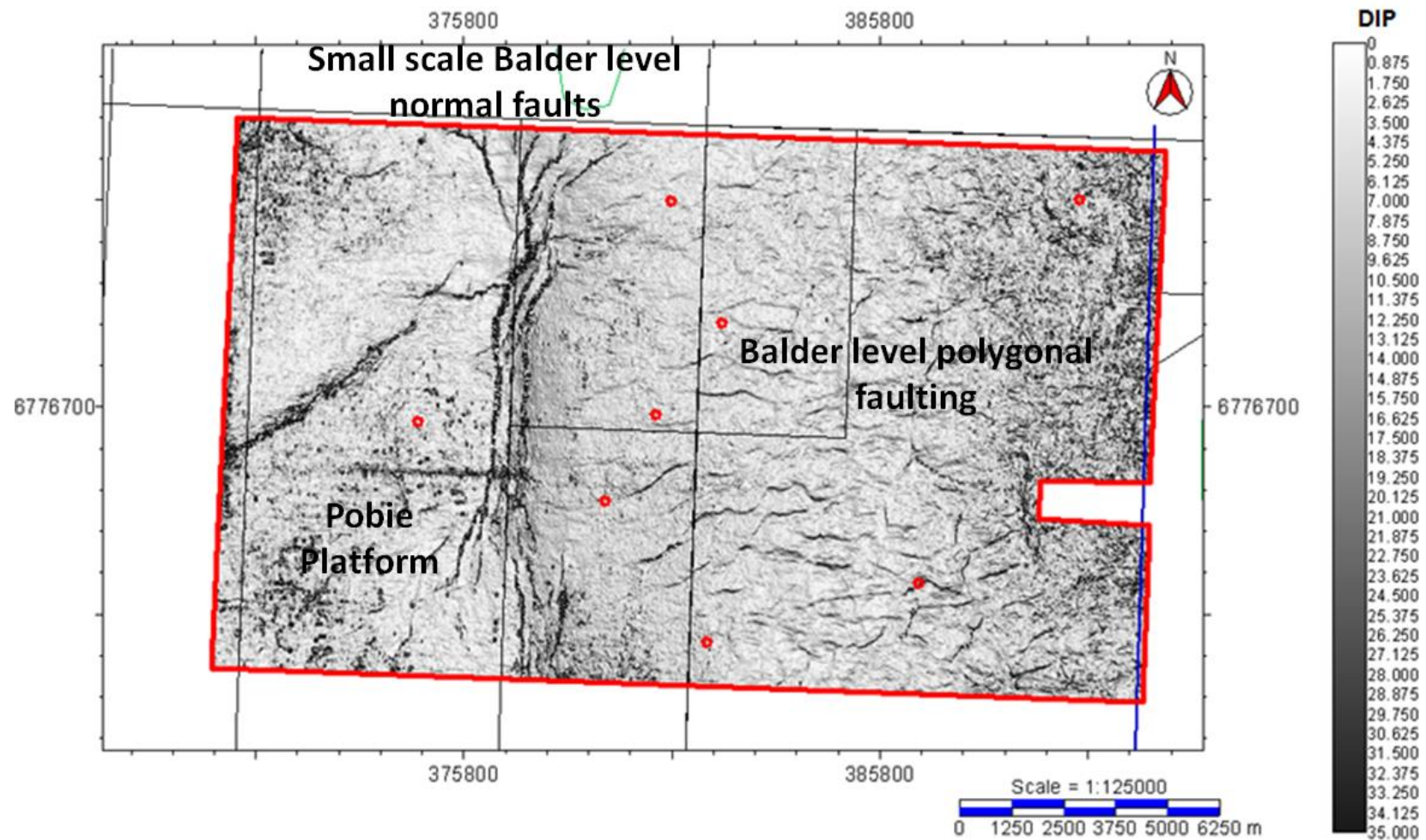


Figure 7-48. Top Balder dip map illustrating faults within the Balder level. The faults orientated E-W are compaction related polygonal faults, whereas the N-S faults are related to the slipping of Paleogene sediments.

If these faults were related to compaction of the Mesozoic and Cenozoic sediments, the faults would penetrate further down than the top Cretaceous level. These faults would then link with the underlying structural trend created by the Upper Jurassic rifting event. As mentioned earlier the Top Cretaceous, Shetland Group has a covering of eroded Danian sediments, which was eroded off the top of the Pobie Platform in the very Upper Cretaceous. It is possible that this unconsolidated limestone material has formed a potential slip-surface for overlying sediments to slump on.

The faulting and associated slumping and slipping of sediments could conceivably also be related to the opening of the Northern Atlantic. When the Northern Atlantic opening occurred in the Tertiary, this resulted in uplift and tilting of the marginal areas. The United Kingdom and North Sea were two of these marginal areas which were affected by the uplift and illustrate an easterly tilt as a direct result of the ocean opening. This easterly uplift and tilting of the Pobie Platform may have resulted in recently deposited Paleogene sediments slumping down-dip. The slipping of these sediments could also form the small scale faulting observed at the Balder level (Figure 7-46). These types of sedimentary structures are observed in the Southern North Sea basin, where salt layers such as the Zechstein Super Group and Triassic Röt Halite aid slipping and slumping along a tilted paleoslope. This could indicate the formation of an easterly dipping paleoslope over the Pobie Platform and Upper Cretaceous basin sediments in the Tertiary, upon which sediments could slump. As compaction and sedimentation continue to modern day these slump-derived faults remain active in to Oligocene times.

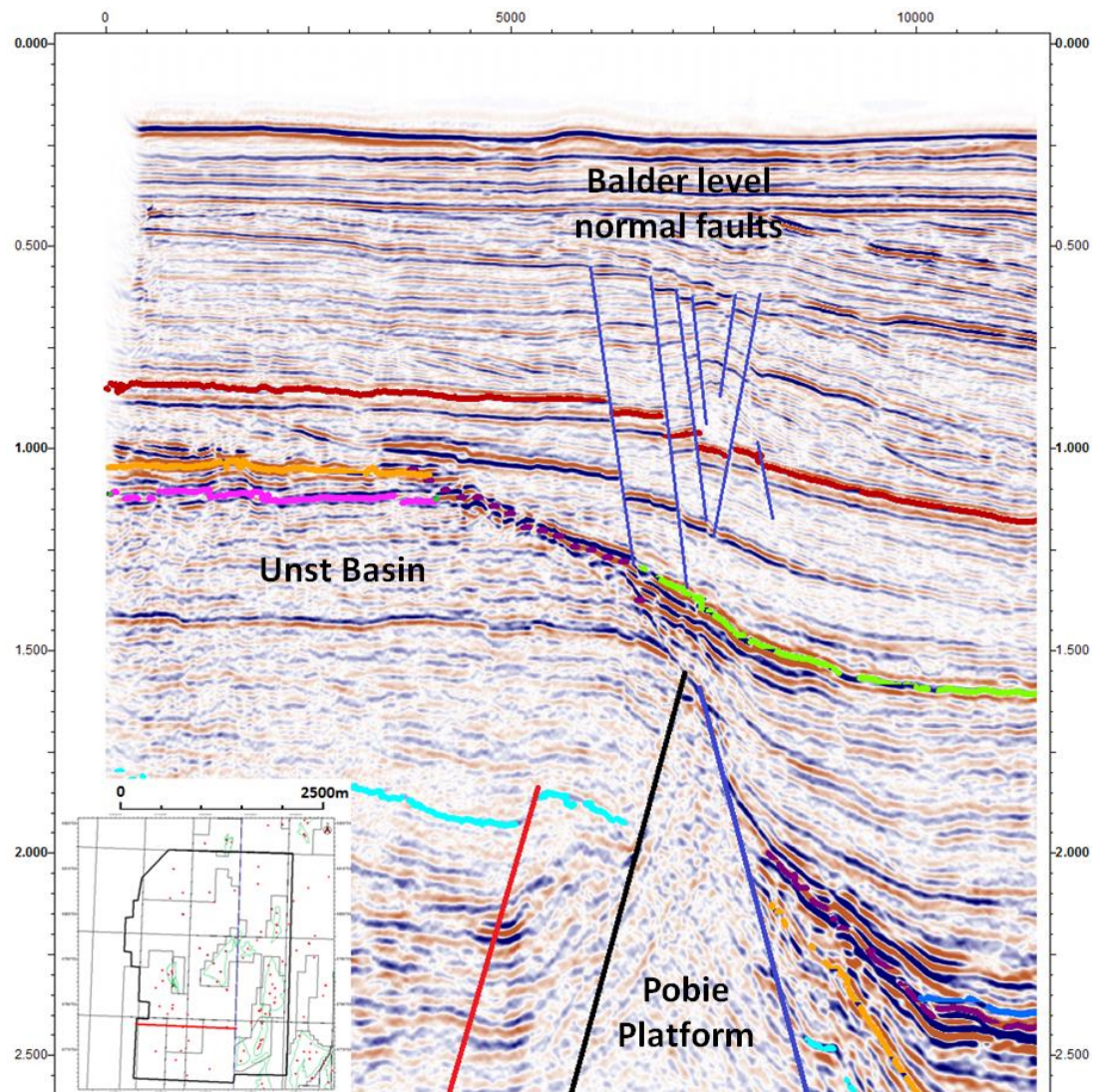


Figure 7-49. Seismic section showing the lack of linkage between of the two sets of faults and the decollement of the Balder level faults in the Base Tertiary/ Upper Cretaceous.

7.10 Conclusions

The work undertaken over the Cladhan and Tern-Eider Ridge areas make it possible to see the resulting effects of Permo-Triassic reactivation and cross rifting in the Upper Jurassic Rifting event. The reactivation of the Pobie fault and the Tern-Eider Ridge along older Permo-Triassic faults forms a series of structural highs which play an important role in determining petroleum prospectivity. The generation of the structural highs leads to the erosion of

Middle Jurassic Brent Group sediments, which may then be re-deposited to form a secondary reservoir within the Upper Jurassic, which is observed in the Cladhan area.

The presence of a sand prone submarine fan within the mud dominated Humber Group could lead to increased exploration within the basin area parallel to the Upper Jurassic rift shoulders. The deposition of these sand units can be influenced by compaction driven lows which are formed by the underlying Permo-Triassic rifting faults, which have not reactivated.

Although the drowning of the Pobie Platform does not appear to affect the petroleum system the timing of complete submergence is important in determining the structural evolution of the area. The partial drowning and then erosion of the Upper Cretaceous Maastrichtian sediments plays a key role in generating a slip surface for Paleocene faulting. The regional westerly uplift generated by the opening of the North Atlantic formed an easterly dipping palaeoslope for which recent sediments could slip and slump along. The slipping of these sediments over the basement under-pinned Pobie Fault to the sediment dominated basin area results in small scale faulting which is terminates in the slip surface that is the Upper Cretaceous.

The direct effects of compaction and/or multi-phase rifting events associated with the far away effects of the North Atlantic opening, illustrate the role of fault growth and linkage is key in understanding these structural complexities observed throughout the study areas.

Chapter 8 Discussion and Implications

8.1 *Introduction*

The study of multiple rifting events and their interaction can have a significant impact upon basin development. The influence of underlying trends of structural weakness and their impact upon future rifting event can be critical in developing a petroleum system

Normal faulting is observed throughout the whole of the North Sea and plays a crucial role in determining petroleum systems at every level. Whether it is involved in trap formation, sealing, reservoir distribution, kitchen generation or migration, normal faulting evidently played a part, either basin wide or on a field scale. Each element of a petroleum system can be affected by multiple phases of rifting but the general principle that applies is that trap formation predates source rock maturity, an outcome optimal for petroleum prospectivity. If an area undergoes multiple rifting events it is possible for the overlapping of key petroleum system events and multiple critical moments, as observed in Figure 8-1. This can lead to increase prospectivity but also increase in structural complexity.

Large scale extensional fault block rotation results from basin stretch is effective in the creation of closures due to footwall uplift, which in the case of this study area has created a series of islands throughout the Northern North Sea. The generation of the fault-controlled islands caused fault blocks to undergo much higher levels of erosion than that of the sediments in the marine realm. The erosion and re-distribution of these sediments into neighbouring hangingwall depocentres can be key in understanding the quality of reservoirs and the distribution of secondary syn-rift reservoirs that

are sourced and sealed by the Kimmeridge Clay Formation in the East Shetland Basin.

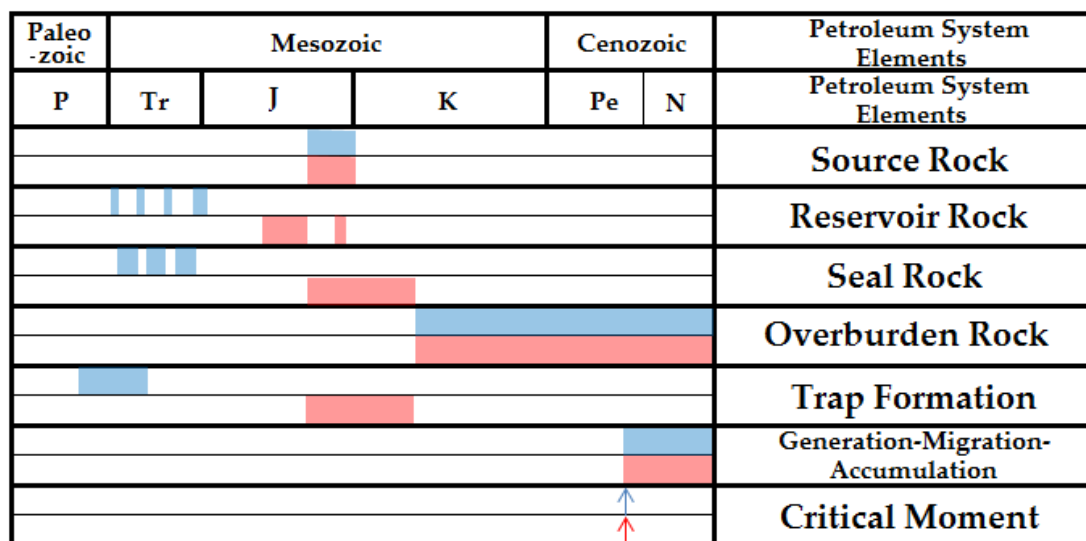


Figure 8-1. Schematic illustration of the petroleum systems in the East Shetland Basin. The bars in blue are the timing of the petroleum elements in the initial Permo-Triassic rifting event where the red blocks are illustrating the Upper Jurassic rifting event and the resulting petroleum system elements (Buley 1993; Jones 2003).

Although the interaction of cross rifting due to a later rift transecting an older one has previously been inferred to be a consequence from release faulting (Gill, 2005), new evidence obtained through better imaging of the underlying structures in the East Shetland Basin (presented herein) suggests that release faulting does not occur and the faulting can be explained by cross faulting due to rift transection. Locations where cross-rifting has occurred can further determine potential island locations along with hydrocarbon kitchen location and burial. As illustrated in the Northern North Sea areas that were in the hangingwall in both sets of rifts will have effectively undergone two phases of subsidence, which can transport potential source rocks into the oil and gas windows. If the source rocks are brought into either of these windows then migration will occur through a reservoir carrier bed or via the fault which may act as a conduit to flow. On the other hand, the increased level of faulting may actually hamper fluid

flow and significantly alter hydrocarbon migration fairways or compartmentalize a reservoir rock. Although these effects are demonstrable in the East Shetland Basin of the Northern North Sea similar events can be observed in other areas of the North Sea along with other basins around the World.

8.2 *Release Faulting vs. Reactivation*

The primary result of a rifting phase is the generation of normal faults which are aligned perpendicular to the stretching direction. These faults are generally termed master faults, which often have a series of other normal faults with a similar orientation.

Release faults can be located in both the footwall and hangingwall to the master fault. When the subsidiary fault has the same polarity as the master fault it is termed a synthetic fault, when the fault has an opposing polarity it is called an antithetic fault. The greatest throw of these faults I found at the branch point with the master fault.

Other subsidiary faults can form and have a perpendicular orientation; these splay faults can also form in the footwall and hangingwall of the master faults to aid in the uplift or subsidence of the master faults. In general subsidence is the greater of these two forces and the footwall uplift is relative to the amount of hangingwall subsidence created. These faults are often termed release faults, but evidence from the East Shetland Basin surrounding the Murchison Field, illustrates that these perpendicular faults may be the result of reactivation.

Initially transfer faults were the proposed model for large scale extensional faults throughout the North Sea. Detailed publications (Beach 1984; Gibbs 1984) attempted to illustrate the role of listric faults had in the structural development of the North Sea. Evidence from seismic data demonstrates that the North Sea is dominated by large scale planar normal faults that formed through rifting, thus countering the argument of a basin and range type locality. Initial listric faults were interpreted in seismic data, but, this was an imaging issue relating to time migration, once the data was depth converted the faults became planar in appearance. This led to the transfer fault theory to have a diminishing role in describing the evolution of the North Sea. The release faults theory appeared to be an attractive alternative until the interaction of underlying rift system through fault linkage and reactivation of faults proved more substantial.

The Murchison Field in the East Shetland Basin has the appearance of a rotated cube and is located in the footwall of a large scale south-easterly dipping normal fault. The master fault to this field is oriented NE-SW with a pair of NW-SE faults bounding the field to the northeast and south west. It strongly infers that the NW-SE faults that bound the field to their branch point against the master fault are release faults that form in the footwall to aid the uplift of the master fault. Evidence from Destro (1995, 2003), suggest that the majority of the release faults form in the hangingwall where subsidence and hence, line stretch was greatest. It is possible for release faults to form in the footwall but it is normally in areas of large amount of uplift. It is common that the release faults form in the centre of the master fault where the largest amount of uplift and subsidence are evident. In the Murchison area no hangingwall release faults are present, which is surprising as it is more common for them to form there as the amount of subsidence normally outweighs the amount of uplift, thus encouraging faults in the hangingwall (Gill, 2005).

The evidence from the Murchison Field (Figure 8-2) does not quite agree with the theory of release faulting as the position of the faults are solely in the footwall and there is a lateral offset between the structural high and the hangingwall low. As noted earlier, release faults in the hangingwall have a smaller spacing than that of the faults in the hangingwall. This is primarily related to subsidence rates being significantly greater than footwall uplift. Whereas, transected faulting would align with each other in both the footwall and hangingwall. This is observed here where the deepest section of the hangingwall (deep blue) is to the southwest of the structural high.

Another issue with the Murchison Field forming through release faulting is the location of the faults relating to the fault tip. Although the master fault is continuous to the northeast, the offset between the footwall and hangingwall decreases significantly. It is possible that this occurs due to the fault growth and linkage history of the area. It has been generally thought that the master fault grows to the northeast and links with another fault with the same lineation that generates the Statfjord Nord Field (Young 2001)

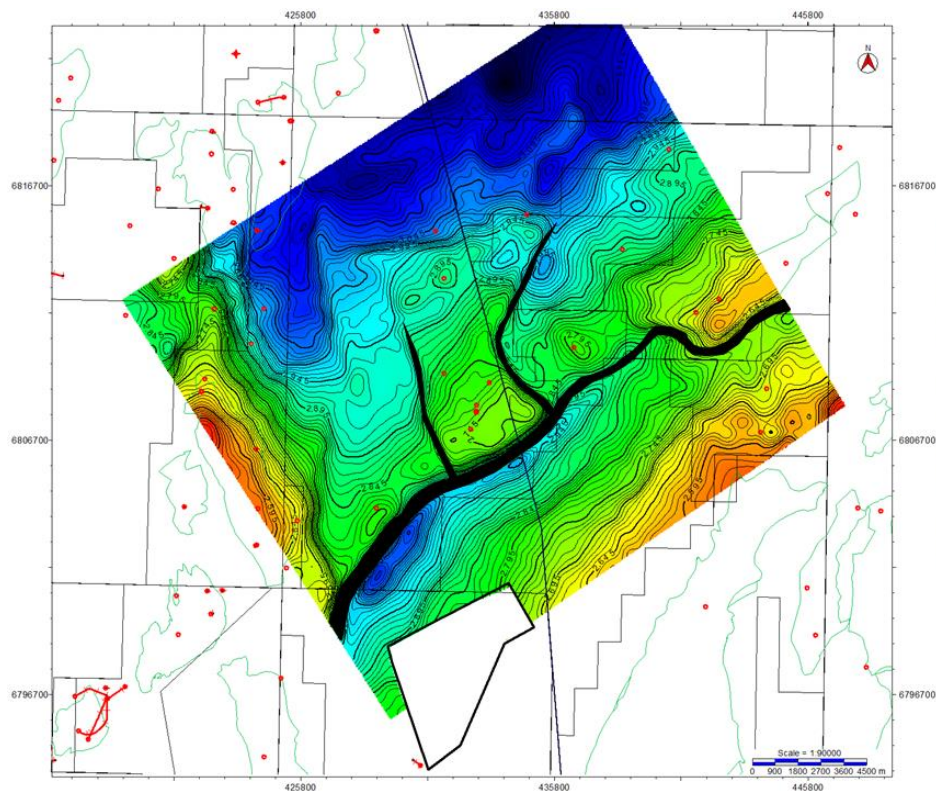


Figure 8-2. Fault polygons indicating the orientation of faults that generate the Murchison Field.

As the offset of the fault decreases as the fault dies out, the stress within the footwall and hangingwall also decreases. If this is the case, how and why do the faults that bound the Murchison Field form, as it is unlikely that they formed by release faulting.

The evidence from the Murchison Field and surrounding areas suggests that reactivation of existing normal faults plays a crucial role in determining Upper Jurassic fault locations (Figure 5-97). The evidence further suggests that due to the lack of structural feedback in the hangingwall where release faults are more commonly found and the specific location of the normal faults to the areas of uplift and subsidence it is unlikely that these faults formed by release faulting. This can be observed throughout the structural lineament from the Causeway Field in the southwest to the Statfjord Nord Field in the northeast.

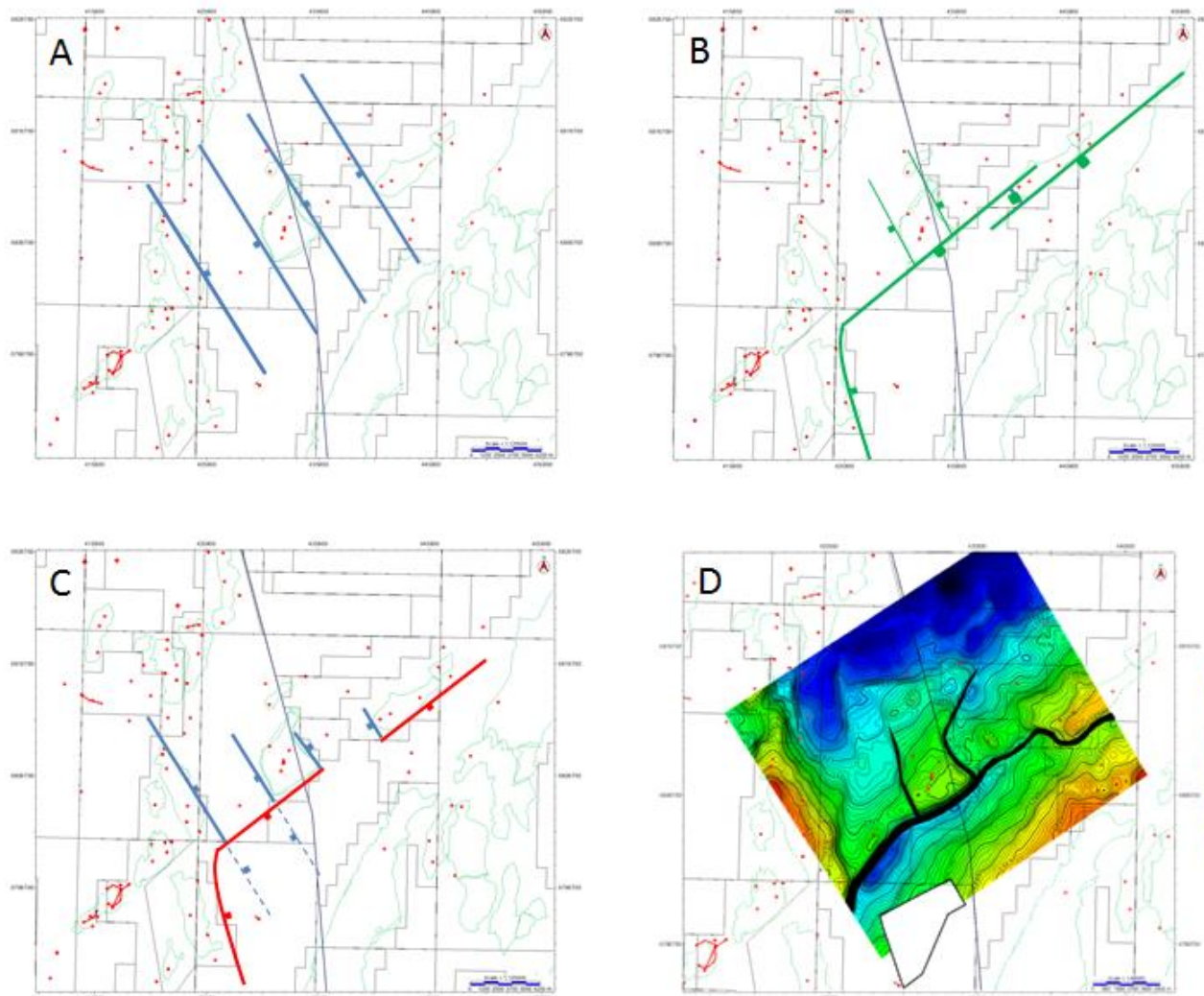


Figure 8-3. Structural evolution variables for the Murchison Field. A illustrates the underlying Tornquist trending Triassic faults (Blue). B illustrates the evolution of the Murchison Field by Young et al. (2001), with the field forming through relay-ramping of overlapping normal faults and subsequent release faults forming in the footwall of this new, longer fault. C illustrates the formation of the Murchison Field with the aid of reactivating the underlying Triassic faults. It may have been possible for the upper Jurassic fault to propagate past the NE edge of the Murchison Field, but once the Triassic fault began to move again the fault strand became abandoned. D highlights a top structure map of the Brent Group around the Murchison Field.

8.3 *Regional Responses*

8.3.1 East Shetland Basin Response

The structural configuration that is observed in the East Shetland Basin affects hydrocarbon exploration on exploration and field development levels. As the East Shetland Basin is a mature hydrocarbon basin, the majority of the structures are well defined and their structural evolution is deeply understood. It is possible to challenge some of the existing theories as exemplified by the Murchison Field, where it was initially thought that the field was defined by release faulting where in fact it has been defined by reactivated cross-rifting faults. This structural feedback can then be inferred to other structures along a similar structural trend, such as the Causeway Field.

The Causeway Field is situated to the SW of the Murchison Field, but it is along the same structural trend. It is also formed by the same trending faults that define the Murchison Field, it may be possible that the reactivation of older faults has also occurred in this location and resulted in the formation of the Causeway Field.

Areas to the north of the Causeway and Murchison Fields also show this underlying fault configuration such as the Halibut High (Figure 8-4). Although the structure is dry of hydrocarbons the formation of the structure occurred through cross rifting. Evidence has been shown through well logs where up to 30m of extra intra-rift sediment is located in an Upper Jurassic footwall high which was once a Permo-Triassic hangingwall low.

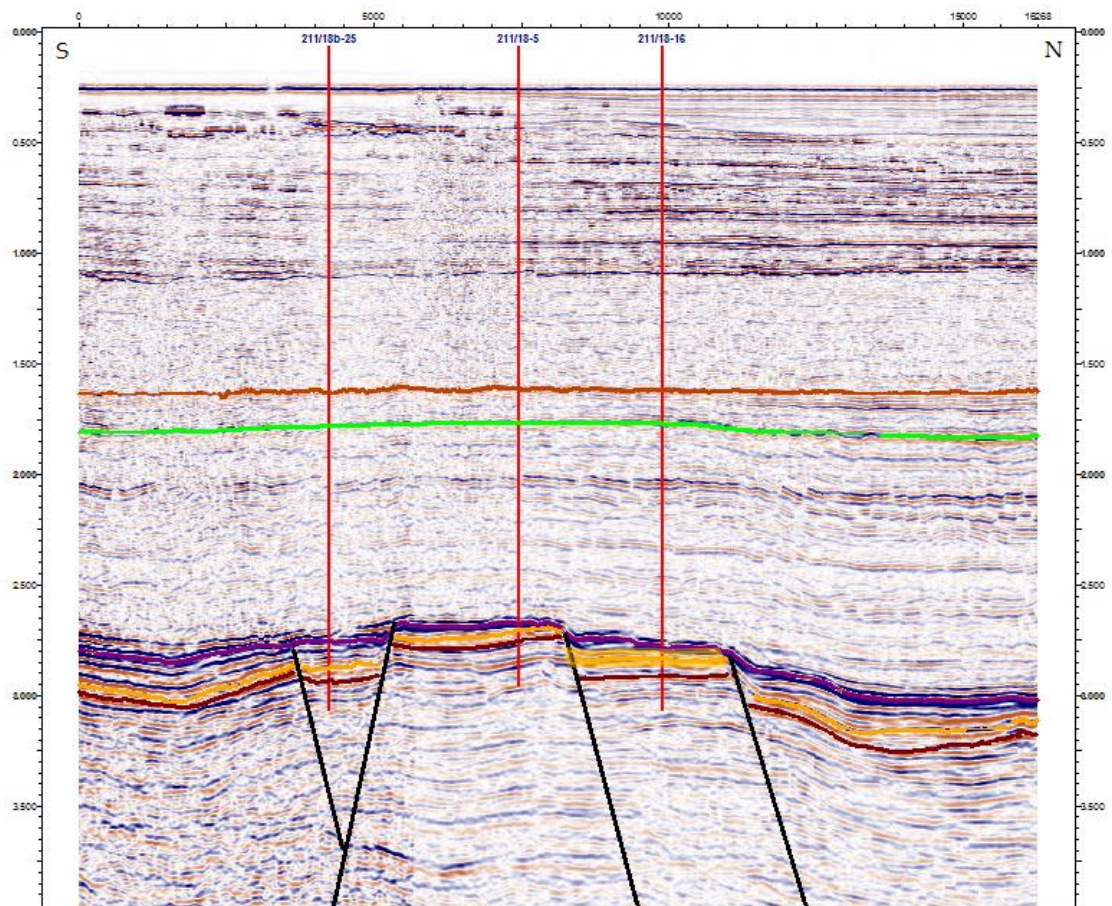


Figure 8-4. Seismic section over the Halibut High illustrating the thickness variation over the structural high that is related to the interaction of underlying fault systems that have been cross cut by a later rifting event.

When observing the East Shetland Basin as a whole, it is possible to detect the areas where reactivation and linking of multiple rift phases has occurred on a regional scale (Figure 8-5). A prime example of this can be observed from the Hutton Field to the Murchison Field. Here fault linkage has occurred on a regional scale with the linkage of Caledonian (NE-SW) trending faults with the use of Tornquist trending fault (NW-SE) as the relay ramps (Figure 8-6). By this method of fault growth and linkage, large scale faulting and reactivation has resulted in the creation of three significant structural highs that have been filled with and trapped hydrocarbons to become significant fields in the East Shetland Basin.

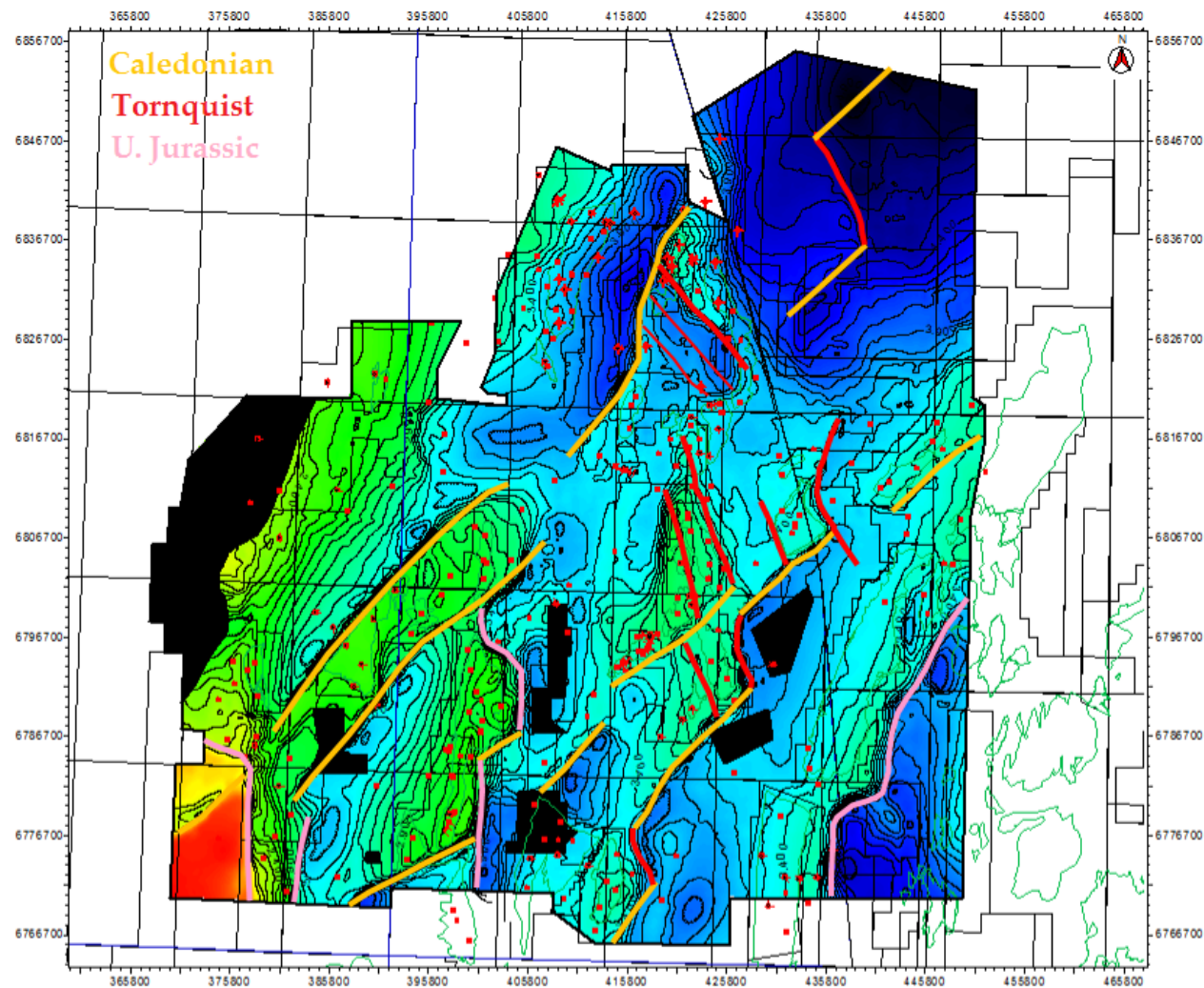


Figure 8-5. Illustration of the Top Basement structure map within the East Shetland Basin. This map encapsulates the effects of faulting in all of the rifting events that has occurred in the basin from the Permo-Triassic through to the Upeer Jurassic rifting event. Within this area Caledonian trending faults are illustrated in yellow, Tornquist trending faults in red and purely Upper Jurassic faults in pink.

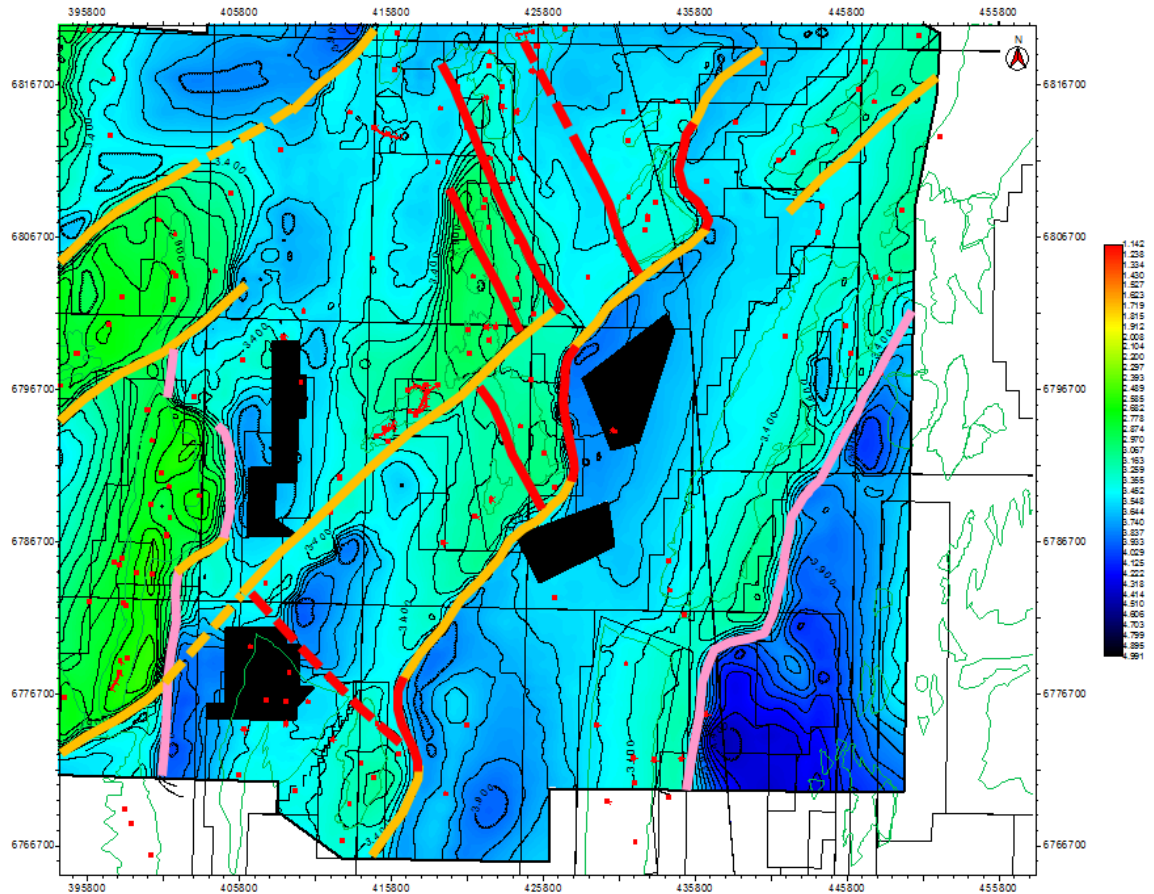


Figure 8-6. Top Basement structure map illustrating the breached relay ramp locations due to the interaction of the Caledonian (orange) and Tornquist (red) faults.

Breached relay ramps are commonly observed on within a rift system and results in the hard linking of multiple faults. By utilising the underlying weakness trends that belong to the Tornquist trend it has been possible to demonstrate that the linkage of fault relating to two separate plate cycles within the Permo-Triassic and Upper Jurassic rifting events. This type of fault linkage is crucial in determining several components to a petroleum system such as trap and kitchen area, along with more subtle effects relating to reservoir deposition and migration routes.

8.3.2 North Sea Response

The North Sea as a whole is still the site for exploration even though it is a mature basin. Exploration in the North Sea has been undertaken for over 70 years which results in the majority of the large scale structures have been found, meaning more subtle or complicated traps and structures are needed.

This philosophy has been applied in the Norwegian sector of the Central North Sea, where the Johan Sverdrup Field which is estimated to be the third largest Norwegian oil field has recently been discovered. Situated south of the East Shetland Basin the Utsira High is a long standing structural high, which follows the old Tornquist and Caledonian structural lineaments. The field is situated in the hangingwall to a NE dipping normal fault which has reactivated through multiple rifting events, including the most recent Upper Jurassic rifting event. Multiple syn-rift packages can be observed in the hangingwall of this fault, which including Upper Jurassic, Permo-Triassic and Paleozoic rifting packages. This location makes up the eastern limb of a longstanding horst structure which is bound to the east by a Caledonian (NE-SW) trending fault which cross-cuts the Tornquist trending fault to the north.

The Johan Sverdrup Field (Figure 8-7) illustrates Type 3 & 4 rifting where old structural trends have been reactivated and cross cut by subsequent rifting events. The structural configuration of the Johan Sverdrup Field would place the primary reservoir in a Permo-Triassic hangingwall but an Upper Jurassic footwall. This is extremely similar to the Pobie Platform area in more ways than one. In both of these instances the H/H area is not the location of the primary reservoir, as the Johan Sverdrup and Cladhan Fields are both found in the structurally lower flanks (Figure 8-8). Within these locations the Pobie Platform and the Ragnarrock High are both structural highs dominated by

basement material. The erosion observed in the high to the west of the Johan Sverdrup Field is so severe that the economic basement is on-lapped by Cretaceous sediments. In Jurassic times the NE-SW trending fault in the primary fault which creates the dominant feature, but some fault reactivation does occur on the eastern flank of the structure where the Johan Sverdrup Field is located. This is similar to the reactivation of the Pobie fault observed over the Pobie Platform in the East Shetland Basin.

The Upper Jurassic syn-rift sediments form the primary reservoir for the Johan Sverdrup Fields which are found in the hangingwall of the reactivated normal fault. No Jurassic sediments are found in the footwall of the normal fault, which implies that this structural high could have been an island location during the Upper Jurassic rifting phase, it is also possible that it was an island at other rifting events, but further well data would be required. If older sediments were deposited they will have been eroded away during the next rift phase, which could generate a secondary reservoir or secondary stratigraphic trap in lower sequences, as observed in the Cladhan area of the East Shetland Basin.

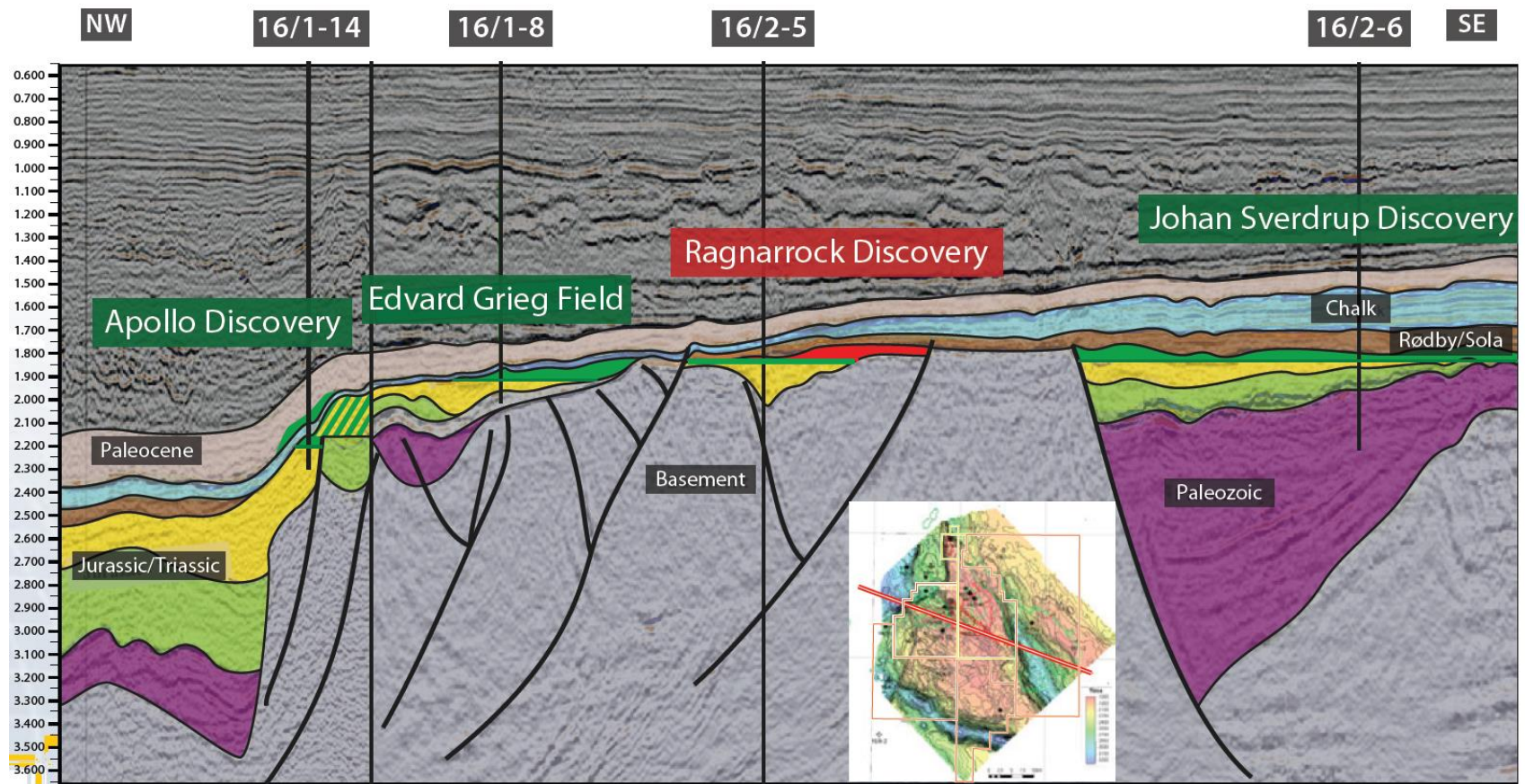


Figure 8-7. Geological cross section through the Norwegian Johan Sverdrup Field which is found in the hangingwall to a normal fault which has reactivated through multiple rift phases. Evidence from this geological section shows thickening packages in the hangingwall to the major fault in the Upper Jurassic, Triassic and the Permian Rotliegend sections suggesting the fault has been active in more than one phase of rifting. This fault is oriented NW-SE and aligns with the Tornquist trend suggesting that it is a long lasting trend of weakness (Lundin 2012).

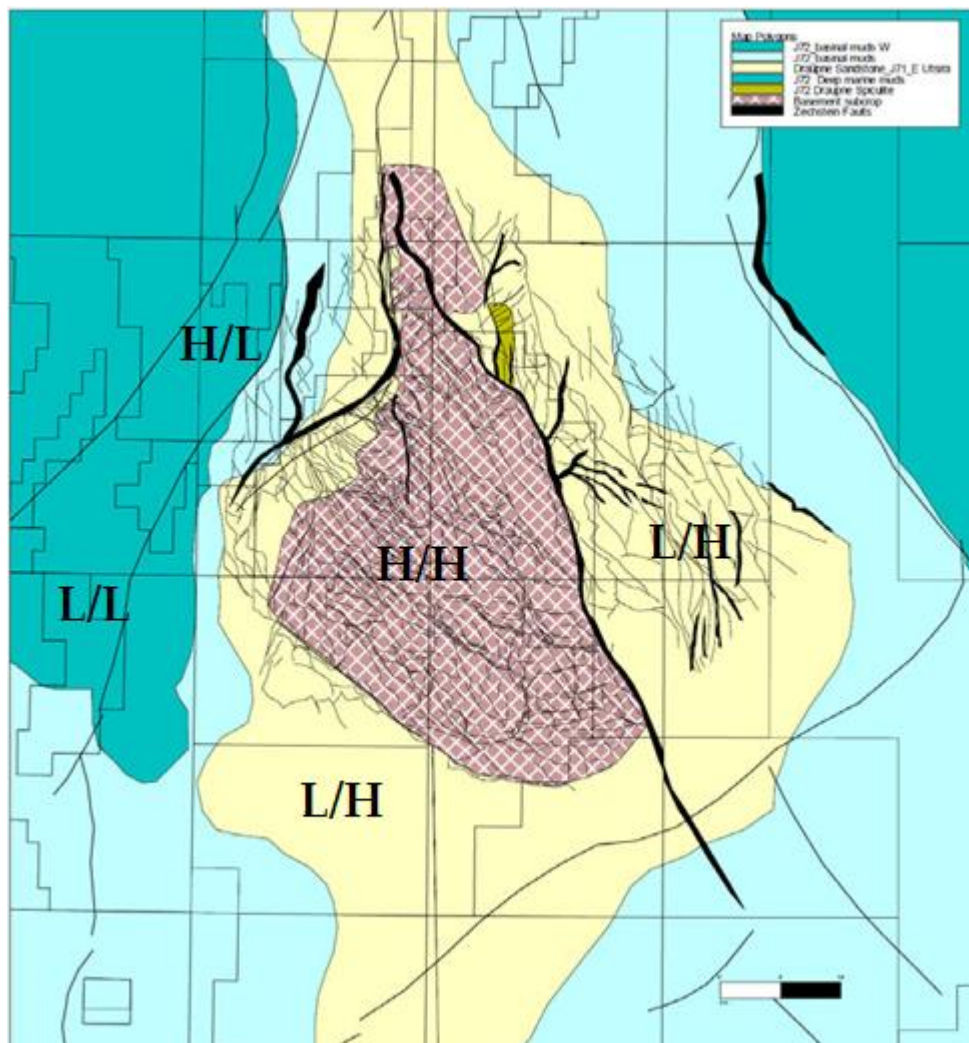


Figure 8-8. Illustrates the structural configuration of the multi-tiered fault block system around the Johan Sverdrup Field (Lundin 2012).

The recent discovery of the Johan Sverdrup Field illustrates that even in a mature basin it is possible to find significantly large fields in structurally complex areas. The understanding of cross-rifting as a whole could aid in the identification of new fields where old lineament trends have reactivated or influenced the active rifting event.

Further evidence of cross rifting around the North Sea can be found as far north as the northern coast of Norway in the Heidrun Field (Figure 8-9). Within this hydrocarbon field an initial Permo--Triassic rifting event can be situated below the Jurassic horst structure.

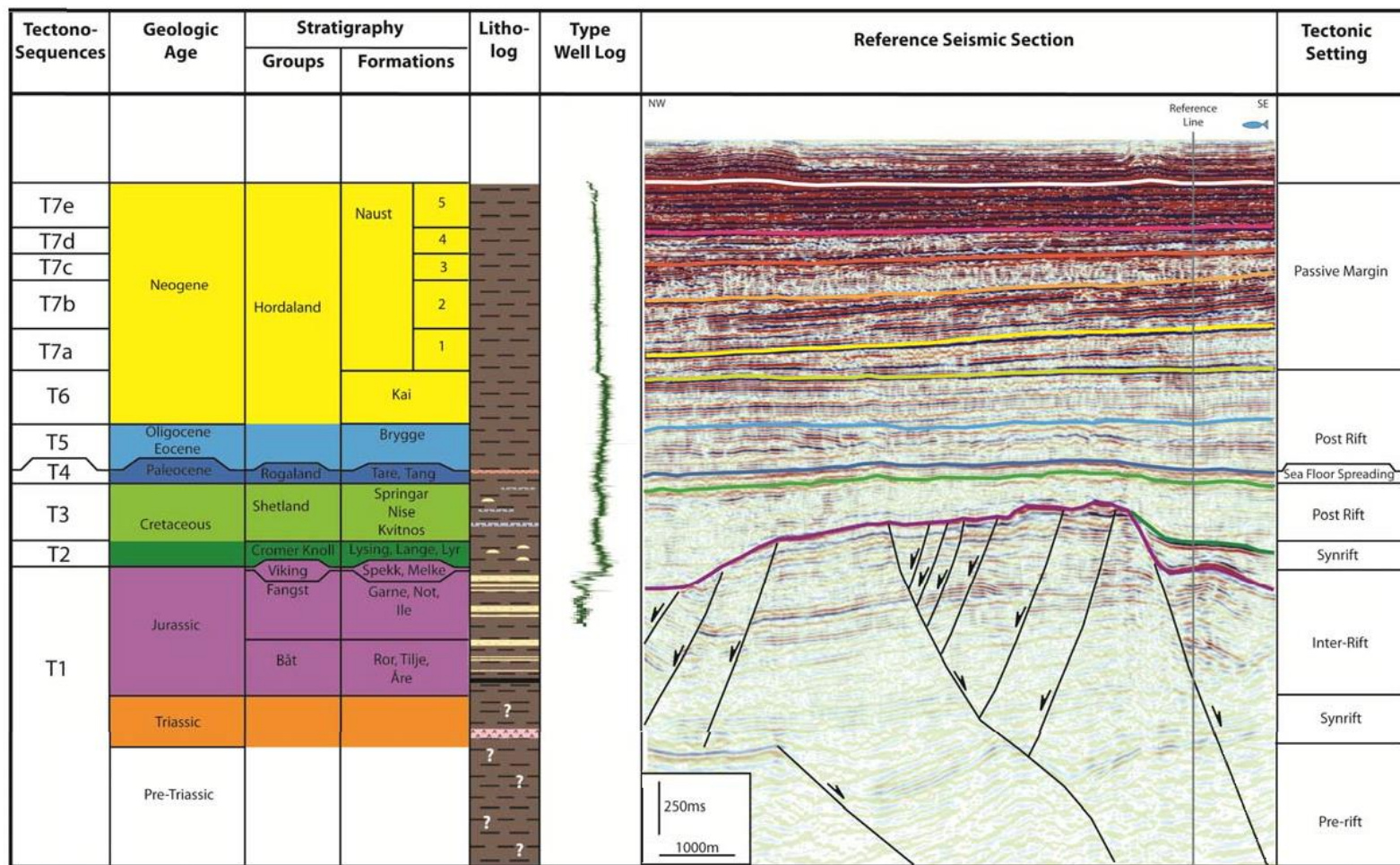


Figure 8-9. Diagram illustrating the tectonic setting of the Heidrun Field, which illustrates at least two rifting events separated by an intra-rift section (Ramnarine 2011).

Within this area a deep seated structural configuration can be illustrated as a Permo-Triassic rifting event. The occurrence of the underlying faults which are separated by an intra-rift section containing thin salt sections is detached from the overlying Jurassic rifting in many areas. The reactivation of Permo-Triassic faults in the Jurassic is purely determined by the strike and polarity of the faults in both rifting event s matching up. This is seen in the Tern-Eider Ridge of the East Shetland Basin and can be inferred as Type 1 transected rifting. Within this area the salt plays a determining factor on fault reactivation. In areas where the fault polarity of the Jurassic faulting is opposite to that of the underlying fault it is common for the faults to detach within the salt layers. This detachment of faults results in no communication between the two rift systems.

It has been illustrated in Tomasso et al. (2008) that the underlying basin fill is also of great importance when considering transecting faults. Depending upon the depositional environment the deposition location of reservoir material in the syn-rift may be structurally altered after multiple phases of rifting. Locations that were initial hangingwall lows and contained potential reservoir material have been uplifted in a secondary rifting event the sand prone sediments may become charged with hydrocarbons. This is illustrated in Figure 3-11.

8.4 Generic Consequences

The cross-cutting nature of normal faults in this manner is not restricted solely to the North Sea. The literature review suggests that the phenomenon may be observed around the World and that it may be more common than generally realised and affect different petroleum systems, such as Offshore

Newfoundland where the Labrador and North Atlantic meet and in the Sudan and Kenyan areas of the East African Rift where that Late Cenozoic structures crossed the Mesozoic Anza Graben. As in the North Sea the delicate interaction of underlying basement lineations and multiple rift phases determine hydrocarbon systems.

8.4.1 Offshore Newfoundland

The southeast offshore area of Canada surrounding eastern Newfoundland has undergone a similar structural evolution to that of the North Sea. An initial basement trend was in place by Paleozoic orogenies, to the extent that the Charlie Gibbs fracture zone could be traced from the Great Glen in Scotland to onshore Newfoundland in the early Jurassic as seen in Figure 8-10 (Hubbard 1985). As in the North Sea this underlying weakness trend reactivates during multiple rifting events. It can also be observed that faults in the initial rifting system reactivate in the second rifting phase and determine the petroleum system.

The initial rifting event that occurred in the Offshore Newfoundland area is thought to have initiated in the Late Triassic, lasted for ~90Ma and terminated in the Early Jurassic and is known as the Atlantic rifting event (Hubbard 1985). The bounding fracture zones for this rifting event were orientated NW-SE which generated a series of NE-SW to form along the basement trend. These reactivated faults are thought to have formed major deposition areas such as the Avalon and Gabriel Grabens. The second rift phase initiated in the Berriasian and ended in Early Cenomanian 50Ma later and is known as the Labrador rifting event. The Labrador rift was bounded by NE-SW trending fracture zones which created a series of NW-SE oriented normal faults in the Lower Cretaceous. The cross-cutting nature of the

Offshore Newfoundland normal faults follows the type of rifting observed in the North Sea. The initial Triassic-Jurassic rifting observed here follows the example the Type 1 and 2 rifting observed in the Ten-Eider Ridge and Cormorant to Brent locations. In all of these locations normal faults in a phase have reactivated along an older fault trend with both the same strike and polarity (Type1) and in other areas the same strike but opposite polarity (Type 2). These faults form the large graben basins earlier mentioned with a NE-SW orientation. The Lower Cretaceous rifting event however is adjacent to the Triassic-Jurassic trend with most of the major normal faults and follows the Type 3 and Type 4 rifting observed in the Pobie Platform and Causeway to Statfjord areas of the North Sea. Both of these locations have faults cross-cutting one another from different rifting phases along with some fault reactivating depending upon the fault polarity. The major faults that have reactivated are the Charlie Gibbs Fracture Zone and the Avalon Graben (Sinclair 1999). Both of these faults have reactivated as fracture zones, such as the bounding rift shoulders seen in the Pobie Platform and limit the extent of any internal major lineament of the Lower Cretaceous rifting event.

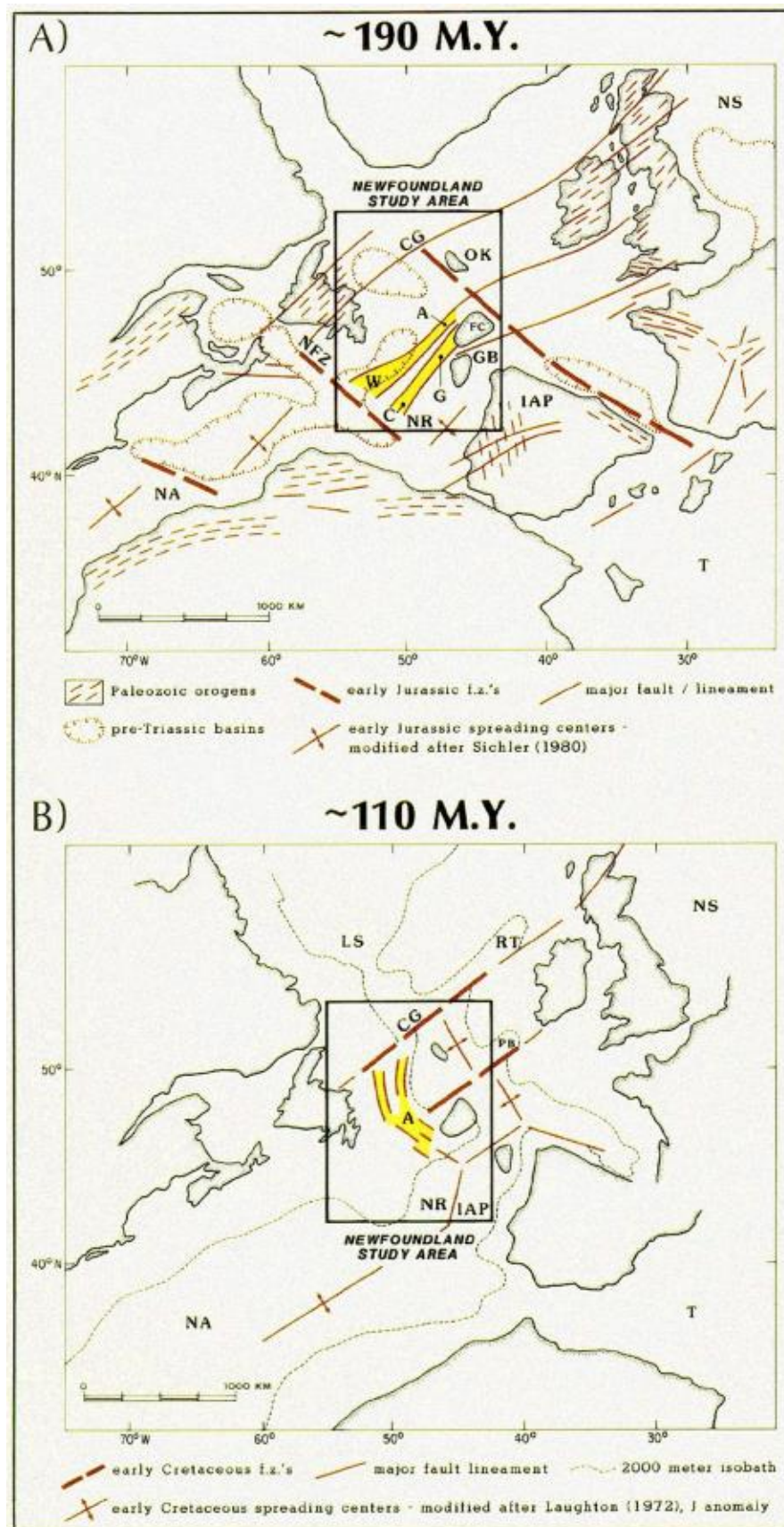


Figure 8-10. Structural history of the Offshore Newfoundland area (Hubbard 1985).

The majority of the large scale Lower Cretaceous lineaments are oriented NW-SE and reactivate with any underlying faults with a strongly correlated strike and polarity. The Lower Cretaceous in the Newfoundland faults have a more cross-cutting nature than those of the North Sea Upper Jurassic faults as they were formed as a result of a propagating rift arm from a R-R-R Triple Point Junction to the southwest. This rift arm continued to the northwest to create the Labrador Sea, to which the rifting megasequences and rifting have gained their names (Hubbard 1985).

The largest field discovered in the Offshore Newfoundland area is the Hibernia Field, which was discovered in 1979 (Arthur 1982). This field was discovered in the Hibernia and Avalon Lower Cretaceous sediments which are located in the Avalon Graben, which is the central cross rifting area (Sinclair 1999). In this location both Triassic-Jurassic faults have been overwritten by the Lower Cretaceous sediments. The architecture of the Type 3 and Type 4 cross-rifting can be observed throughout this area, although there is a subtle difference between the North Sea and the Newfoundland areas.

The main structural traps observed in the North Sea are found in the locations that were a high in both rifting events (Murchison Field/High-High). The High-High areas located in the Offshore Newfoundland area have a relatively thin sedimentary covering in the Lower Cretaceous and are dominated by basement sediments. This results in the terrace areas becoming more prospective (Figure 8-11). This is seen within the type 3 rifting where the Pobie Platform is too shallow and the migrated hydrocarbons are heavily biodegraded. These terrace areas are likely to be termed Low-High or High-Low, depending upon the orientation of fault block (footwall/ hangingwall) to the current fault.

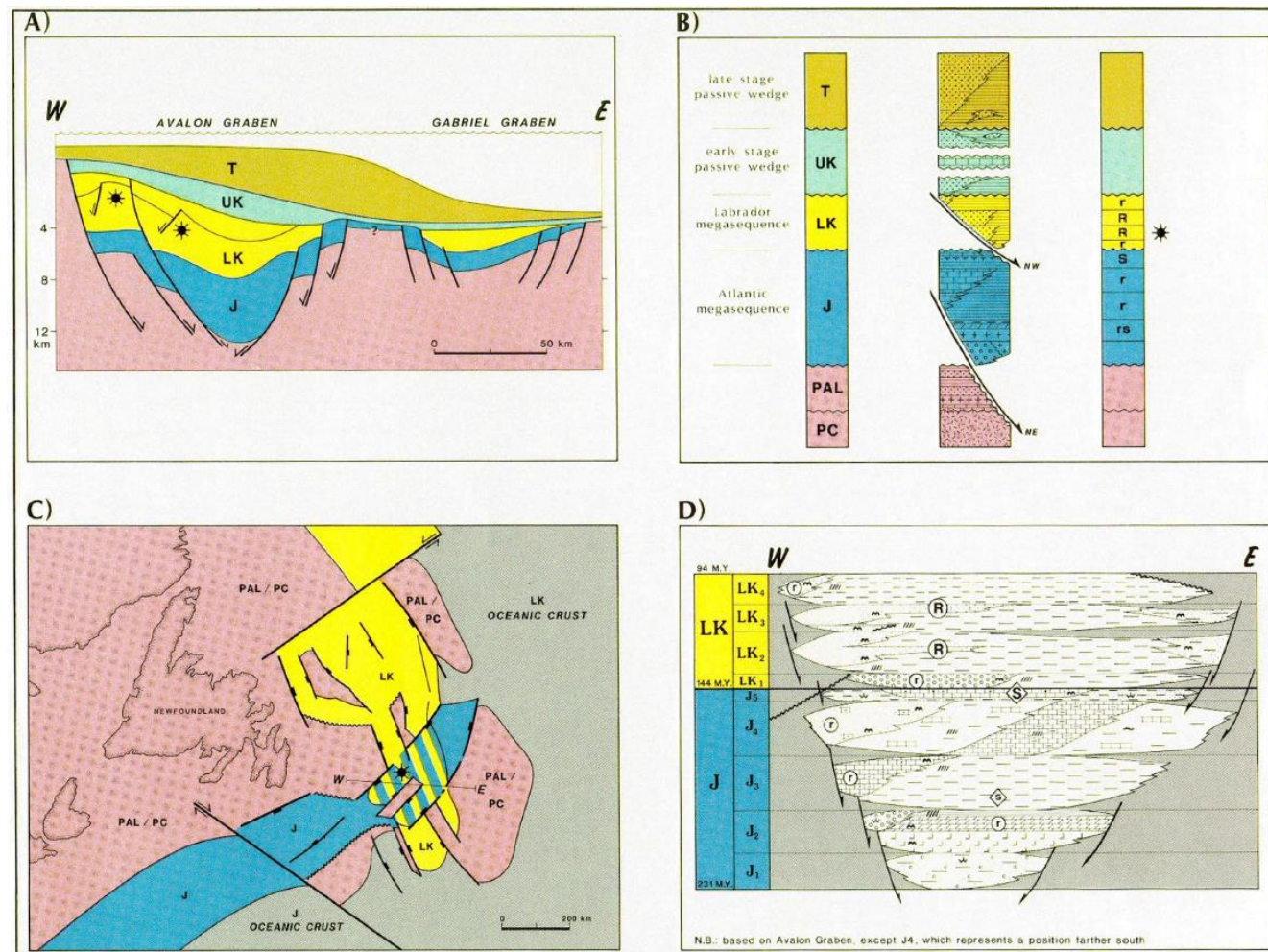


Figure 8-11. Localised study of the faulting linkage and evolution through the Mesozoic (Hubbard 1985).

The major problem with this fault block set-up is the potential of reservoir compartmentalization. Although this maybe an issue in terms of migration it is also a factor in terms of a hydrocarbon seal. This again depends upon reservoir thickness and the size of a faults throw. If a fault is reactivating it is possible that it may generate a greater throw to that of a new fault, thus offsetting the reservoirs across fault planes due to the existing weakness in the subsurface. Well data from the Hibernia area suggest that reservoir compartmentalisation exists in this field which illustrates the effects of multi-rift faulting has on the hydrocarbon system as a whole and is not just in determining rap size, shape and location.

8.4.2 Kenya-Sudan, East African Rift

The North Sea and the Offshore Newfoundland areas are both examples of cross rifting with the rifting events in the second post-rift phase of rift evolution. The Kenya-Sudan area of the East African Ridge is an area that is currently in the second phase of syn-rift development. With the second phase of rifting currently occurring, it may be possible to anticipate potential structures for future petroleum systems and aid the understanding of multiphase rift evolution.

The continent of Africa has undergone several individual rifting events and can be separated into a series of shear zones, which creates a series of basement lineaments that can effect subsequent rifting events, as seen in Figure 8-12 (Gass 1977). The north eastern edge of Africa is currently the location of an active triple junction with the western limb located onshore (Ebinger 1989). This is known as the Ethiopian Rift arm and has a NE-SW orientation which is thought to have initiated in the Miocene (Chorowicz 2005). Underlying this trend an older rifting trend can be identified in

northwest Kenya and south-east Sudan. The Kenyan rifting can be identified by the Anza Rift, while the Sudan area has two rift locations which are named the Blue Nile and White Nile Rifts (Bosworth 1992; Bosworth 1994; Dou, Xiao et al. 2007). All of these rift sections have a NW-SE lineation and form large graben structures, which are thought to have formed in the Early Cretaceous and ceased movement in the Late Cretaceous (Schull 1988).

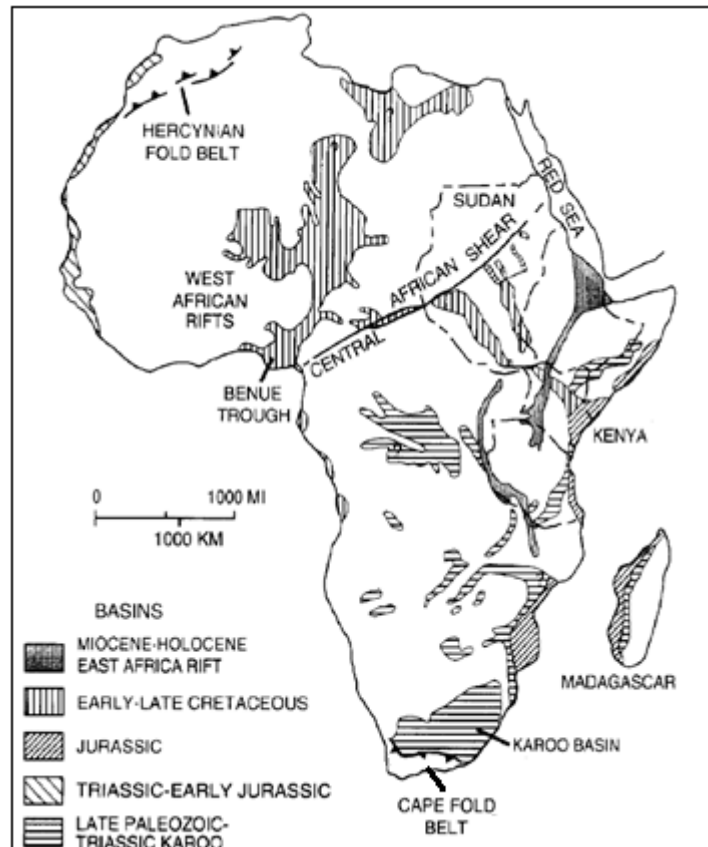


Figure 8-12. Regional map of Africa illustrating the location of the mobile belts located within the basement of the continent (Ebinger 1994).

Within the three rift systems found within the Kenyan and Sudan areas, active hydrocarbon production is evident. All of these fields are formed by the structures generated by the initial Cretaceous rifting (Figure 8-13). Most of these fields are located some distance away from the Ethiopian Rift Arm, as any structures that formed by the initial rifting event have been overwritten by the Miocene faults which leads to migration timing issues.

Although structures may have been generated and filled by the initial Cretaceous faulting, it is possible that the second phase of rifting may actually breach the trap and seal and causing the hydrocarbons to leak away. The generation of these dry highs due to the over-printing of the secondary rifting faults effectively hampers the current petroleum system that is emplaced and working to areas north and south of the Ethiopian rift arm (Figure 8-14 and Figure 8-15). Although the initial structures are being compromised by the Miocene faulting, the interaction of these faults will however generate structures that will become prospective in the future. One issue with the formation of these new traps is the migration and filling of the newly formed traps.

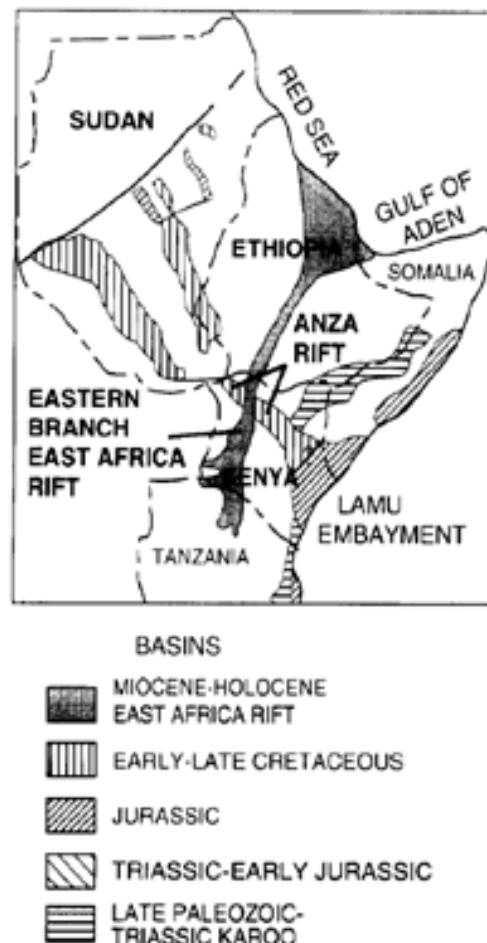


Figure 8-13. Structural evolution of the Eastern limb of the East African Ridge western limb (Ebinger 1994).

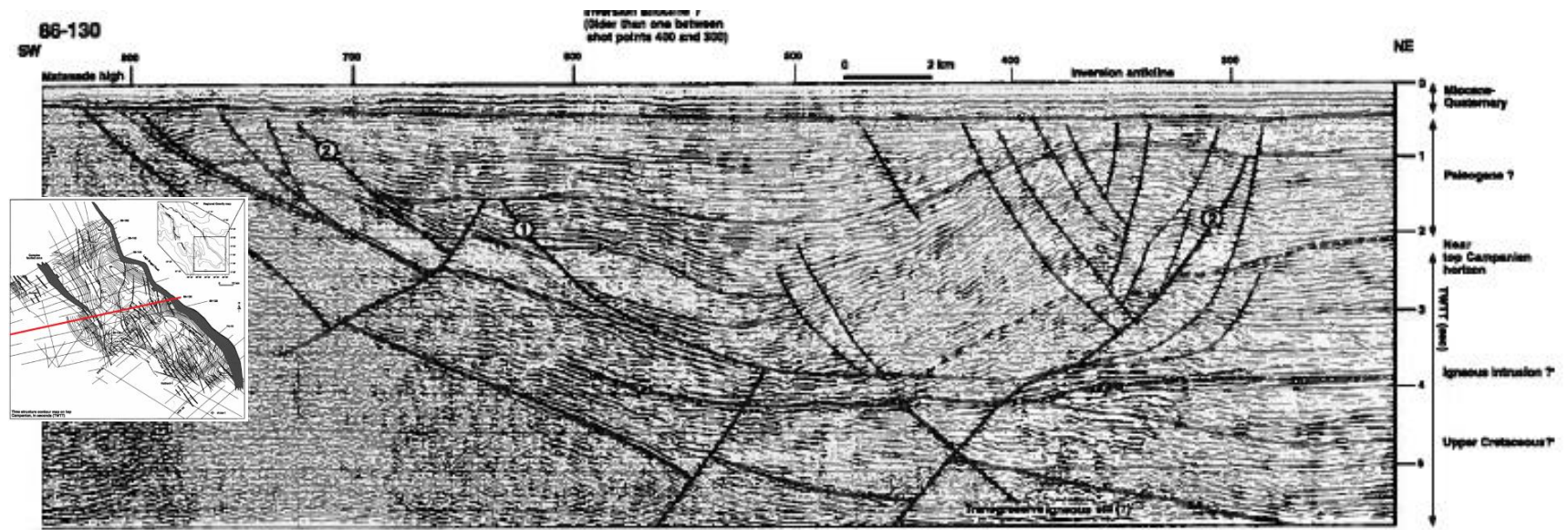


Figure 8-14. Seismic interpretation across the southern Anza Graben illustrating a series of structural features that range from shallow to deep within the seismic. The deep structures are related to older Basement and Cretaceous stretching events. The shallow events relate to the Holocene rifting, although some reactivation of faults has occurred in this most recent stretching phase (Morley 1999).

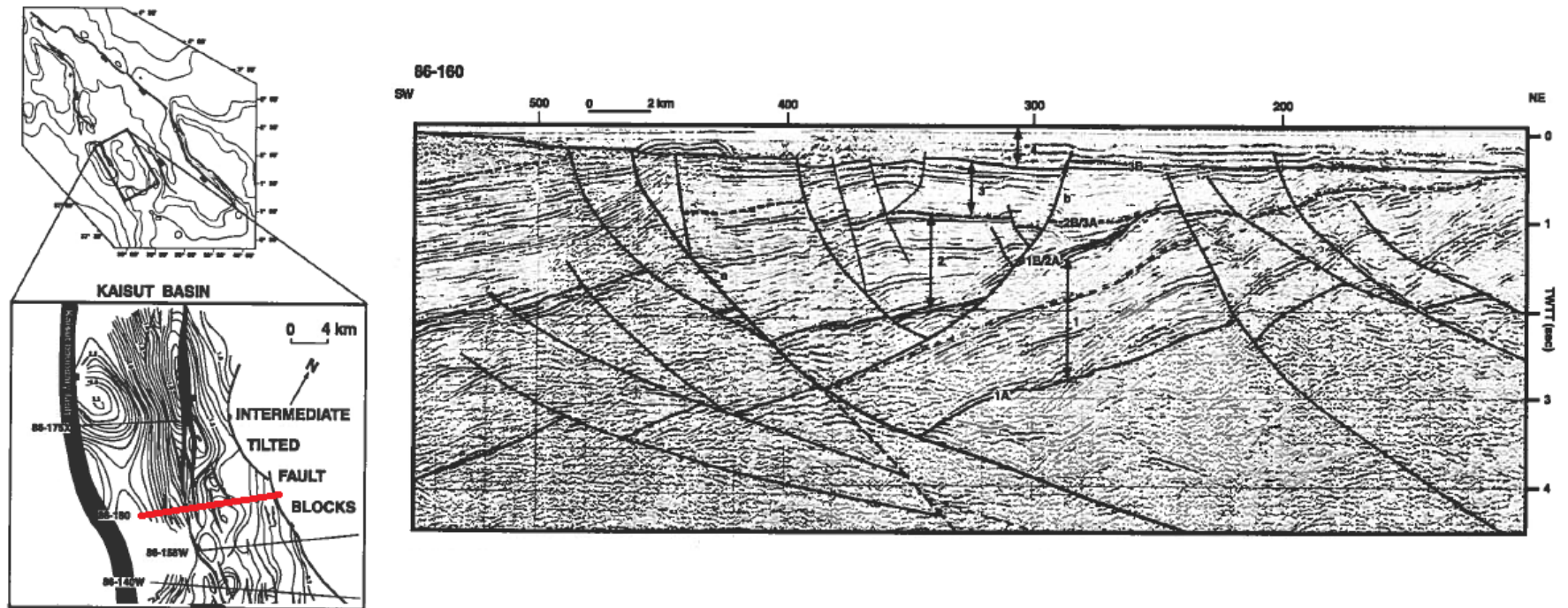


Figure 8-15. Seismic section oriented SW-NE through the southern Anza graben illustrating a combination of cross cutting faults (Morley 1999).

The current traps that will be conceded by the second phase of rifting will result in the remigration of any hydrocarbons that are currently emplaced. As the traps for the secondary traps are yet to fully form, it is possible that the fault planes act as conduits to flow for the hydrocarbons. This could lead to the filling of traps in higher stratigraphic levels. If this is the case, a new source rock may be required to fill the new traps created by the multiphase cross rifting.

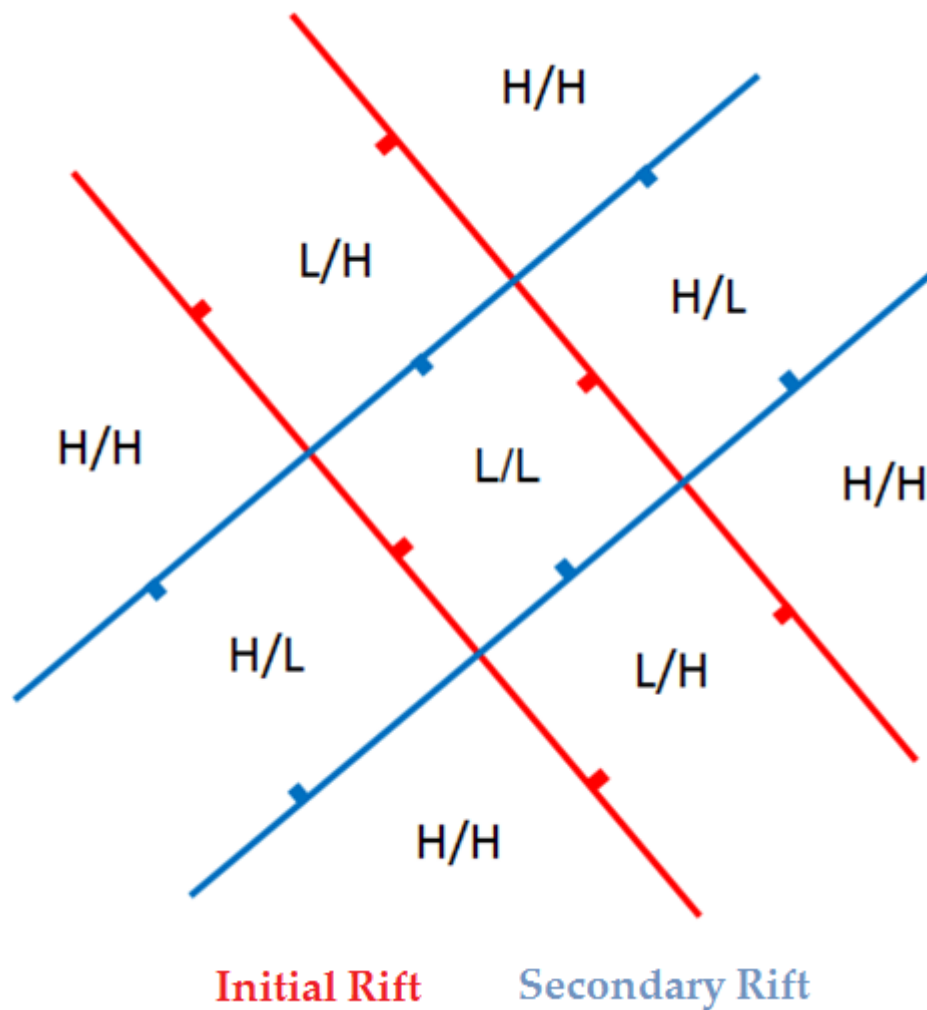


Figure 8-16. Cartoon illustrating the structural configuration that can be generated by the interaction of two perpendicular rift systems. The Tertiary Ethiopian Rift arm faults are illustrated in blue and the Cretaceous Anza Graben faults are depicted in red. By simplifying the model down it illustrates the locations of primary traps which were highs in both rifting events (H/H).

As noted earlier, the two rift systems have a perpendicular strike to one another, with the underlying Cretaceous rift oriented NW-SE and the Miocene rift aligned NE-SW. This perpendicular arrangement will lead to the generation of Type 3 & 4 rifting as seen in the North Sea. This will result in generating a series of structural highs that will form high quality traps, with a series of lower level terrace fault blocks, which may also form a series of traps (Figure 8-16).

This faulting will also influence hydrocarbon generation and migration. The generation of Low-Low fault blocks could be significant enough to emplace an alternative source rock into the oil or gas windows, and be a secondary source rock for the new structures.

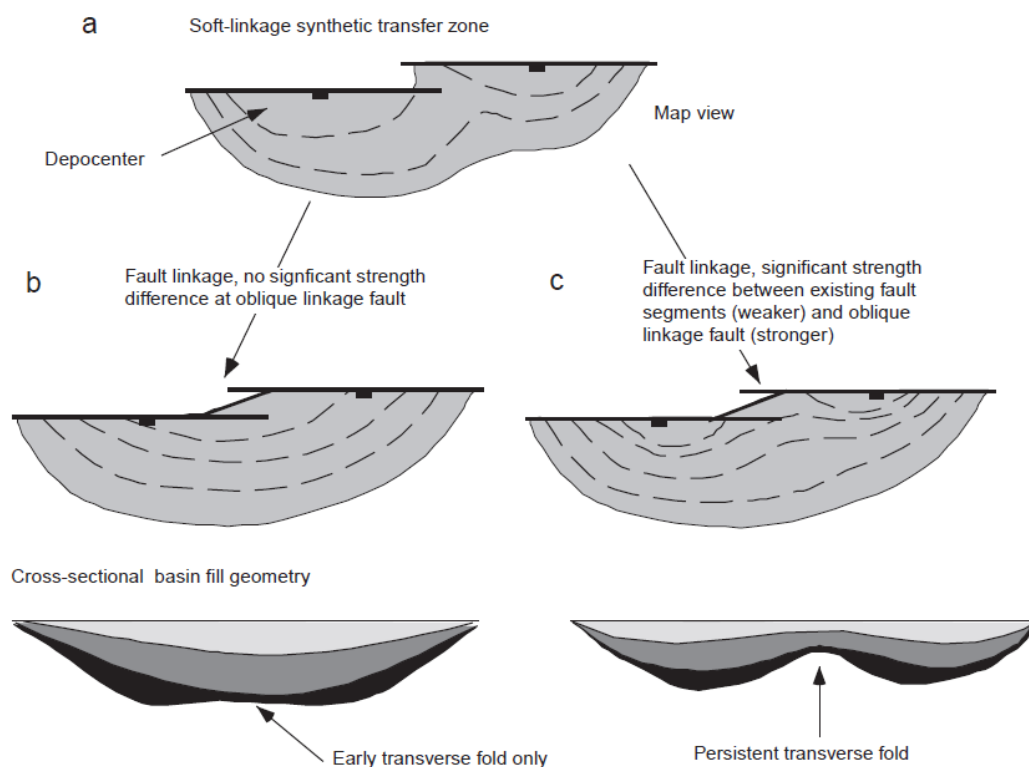


Figure 8-17. Diagram illustrating the formation of a transverse fold as seen in the South Lokichar Basin (Morley 2002).

With this complex arrangement of fault blocks, new migration route may have been generated which could either fill traps that were outside initial migration routes, or influence the migration route to the new structures and dry up the initial Cretaceous structures. It may also be noted that these new faults may act as barrier/ baffles to flow which could either enhance compartmentalization within a reservoir or act as a sealing fault for a major structural trap, as seen in several fields in the North Sea. All of these examples illustrate how multi-phase rifting can play a determining factor in an existing petroleum system and the future of new hydrocarbon systems.

As illustrated in Figure 8-16, the generation of multi-tiered fault blocks can create multiple structural traps as illustrated throughout the North Sea. Although the major tilted fault blocks are observed it may be possible to identify more subtle structures within the fault blocks.

Areas to the northwest of Kenya in the South Lokichar Basin also illustrate the underlying NW-SE structural lineament beneath the Anza Graben. By the process of fault linkage a series depo-centres can be created that have their own individual hangingwall topography, by linking two or more of these structures together a transverse fold can be generated (Figure 8-17). These folds can then become structural traps as seen in the South Lokichar Basin. These folds are also observed in the Anza Graben as illustrated in Figure 8-18.

Within the depo-centres of these folds it may be possible to identify sandstone units derived from either debris flows from the adjacent footwall high or channel complexes that drain the surrounding area. These sand prone sediments may prove to be hangingwall reservoir materials.

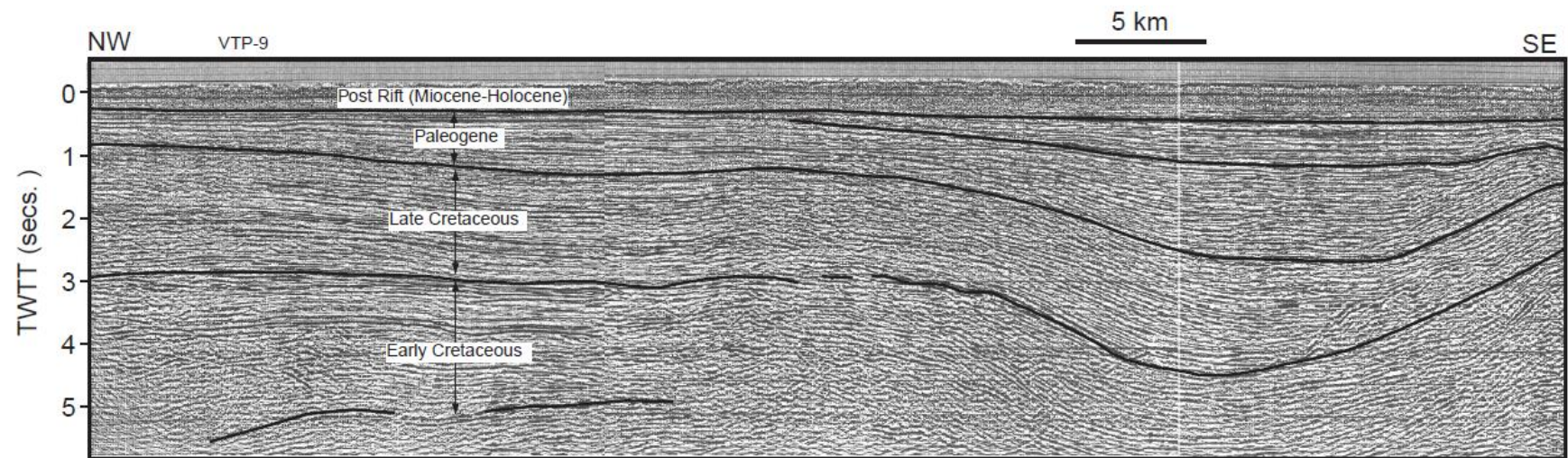


Figure 8-18. Seismic line parallel to the Anza Graben illustrating the formation of a transverse fold in the hangingwall to a Cretaceous normal fault (Morley 2002).

The filling of these structural traps, be they tilted or multi-tiered fault blocks or hangingwall transverse folds it is highly likely that the source area is linked to the evolution of the transected faulting. Figure 8-16 not only illustrates the formation of structural highs but the generation of significant hangingwall lows. The deepest of which is commonly situated in the centre of the overlying rifts. This L/L area has been subjected to subsidence in both rifting phases and thus the greatest opportunity to reach either the gas or oil window. As this location has been subjected to two phases of hangingwall subsidence it is possible that it can have two major source rocks, one from each of the rifting phases. This being the case it could produce significant hydrocarbons to fill the surrounding traps. As the H/H locations are located adjacent to this potential kitchen area the migration routes are not too complicated and charge proves possible.

If two source rocks do exist it may be possible for the initial Cretaceous source rock to enter the oil window if it has been located within a hangingwall low. If this is true, the generation of hydrocarbons from the Cretaceous source rock could be a direct source for the transverse folds created in the hangingwalls by the linkage of faults. As no major faults are in the direct path of hydrocarbon flow and the migration pathway fairly simple it may be plausible that each of the H/L and L/H blocks has its own self-contained kitchen area located within in structural block. This could be a major factor in the migration and filling of traps throughout the basin as a whole.

The effects of cross-rifting as a whole in the East African Rift are significant in every aspect of the petroleum system. The timing of the faults and the generation of a multi-tiered fault block can create both structural traps and kitchen source areas. The migration from which can vary from a simple up-

dip migration to a more complicated across fault plane migration, depending upon the nature of the faults (open or closed). The generation of sandstone reservoirs is directly related to cross-rifting in the form of debris flows or channel sandstones located in the hangingwall lows. This once again illustrates that a strong understanding of the structural geology and evolution of a basin is vital in determining not only the simple hydrocarbon structures but essential in determining the location of potentially massive reserves in more subtle down-dip locations.

Chapter 9 Conclusions

The Northern North Sea has undergone multiple phases of stretching and rifting, the result of which can be imaged in the East Shetland Basin where the lack of Tertiary erosion (seen on the Norwegian margin) gives a better insight into the evolution of one of the most prolific hydrocarbon basins in the World. New perceptions of the structural evolution have been illustrated and can be inferred to have generic significance for other transected rift basins, such as the Newfoundland Atlantic Margin and the Ethiopian rift arm of the East African Rift.

The role of fault interaction between Upper Jurassic extension and rifting phases in the Permo-Triassic is revealed in the new interpretation. The oldest trend of structural weakness that is observed in the East Shetland Basin relates to the formation of the precursor plate margin processes related to the development and evolution of the Iapetus Ocean and Tornquist Sea in the Lower Paleozoic. Other deep-seated fault trends are also found in the Paleozoic and relate to the closing of the Iapetus Ocean that was once situated in the Southern uplands. These predominately NE-SW trending faults were created during the oceans closure during the Silurian and early Devonian. A series of NW-SE faults were created as a result of the Tornquist Sea closing in the Ordovician and these are particularly prevalent in the Central and Southern North Sea out with the immediate study area encompassed in this Ph.D.

Although these underlying trends are observed in the basement formations it does not mean that they are exclusively active during the individual plate cycles. Evidence from the Tern-Eider Ridge illustrates the reactivation of a

Caledonian trending fault in both the Permo-Triassic and the Upper Jurassic rifting events.

The reactivation of old fault trends is dependent upon two vital components of the active rift system. These are the strike of the new fault to the older fault and the polarity of the faults between the two rift phases. If the strike and the polarity of the two faults overlap it is highly likely that there will be reactivation of the old fault in the active rifting event. If the strike of the two faults is perpendicular it is extremely likely that the faults will cross-cut one another. This may still result in reactivation of the old faults but only in a small scale environment, which may define the structural limits of a field, as exemplified by the Murchison Field.

This interaction and reactivation of normal faults over rifting periods of geological time will create series of multi-tiered fault blocks. The generation of a multi-tiered fault block system can determine trap location, kitchen location and migration pathways on both a regional and localised scale.

The greatest effects of the cross-rifting is observed in the Upper Jurassic where four varying type of cross rifting have been described;

- 1 - Same strike, same polarity and full fault plane reactivation.
- 2 - Same strike, opposed polarity, partial fault plane reactivation.
- 3 - Oblique strike, variable polarity, partial fault plane reactivation.
- 4 - Perpendicular strike, mixed polarity partial fault plane reactivation.

Type 1 cross rifting generally creates a series of linear structures that are bound on at least one side that has undergone several episodes of rifting. The other bounding fault on the other hand may have only reacted in the most recent stage of rifting but can still have significant offset. The type example of this location is the Tern-Eider Ridge.

Type 2 rifting also creates a series of linear structures although they will not have the same amount of structural topography as seen in Type 1 cross rifting. Within this fault system pattern reactivation of old fault planes is more subtle and is related to vertical relay-ramping. Although no hard linkage occurs between the new and old faults, the old faults act as a general plane of weakness for the new faults to move in stratigraphically higher levels. The exemplar for this rifting is between the Cormorant and Brent Fields.

Type 3 rifting has a higher level of structural complexity to it as it is the first situation where old and new fault trends are cross cutting one another. The cross-cutting nature of these faults in this structural environment occurs at oblique angles and generally relates to the formation of large scale, basin bounding faults. This combination of faults and fault reactivation creates a multi-tiered fault block system. The area that remained a structural high in both of the rifting events has undergone high level of uplift and erosion and is usually responsible for economic basement situated in a relatively shallow location within the Basin. This type of fault linkage and reactivation often occurs at rift or basin margins, with the second phase of rifting identified by a major bounding fault. The case example for this type of rifting is the Pobie Platform, although it is also seen in the Johan Sverdrup Field.

Type 4 cross rifting generally occurs within the basin area of a rift phase and illustrates the reactivation and interaction of new and old faults in a perpendicular alignment. This again creates a multi-tiered fault block the highest of which often creates a structural trap. It has also been proven that the structural high within the newly formed hangingwall may also form a structural trap (as seen in the Dunlin Field). The generation of this multi-tiered fault block may also be responsible for the generation of localised

kitchen areas, which may subsequently charge the adjacent highs. This is often observed in intra-basinal areas where the underlying structural configuration can be fully activated, as seen in the Causeway to Murchison area.

Evidence from the Norwegian Sea, Newfoundland Basin and the East African Rift illustrate that the underlying deep seated basement structural trends are a decisive factor in controlling the structural configuration within a rift basin. This in turn determines primary structural traps, primary kitchen areas and has a major influence on migration routes.

The initial fault growth and linkage of faults from one rift to another may also generate subtle structures within both footwalls and hangingwalls of a multi-tiered fault block. The generation of transverse folds in the hangingwall of a multi-tiered fault block will further enhance the exploration of topographic highs situated within structurally lower fault blocks.

Another effect of transected rifting in the Upper Jurassic is the creation of an archipelago island system. The generation of an island system shortly after deposition of the deltaic Brent Group, which is the primary reservoir has a pivotal role in the hydrocarbon system.

The uplift of marine sediments into a sub-aerial environment results in the sediments being flushed by meteoric waters. This flushing effect has resulted in large quantities of K-feldspar and plagioclase feldspars going into dissolution and essentially cleaned the fault crest of tilted fault blocks. The resulting loss of grains from the sandstone units increases the porosity of the already relatively high porosity reservoir sandstone.

The generation of these structural highs also creates a series of secondary reservoirs. The most common of which relates to the eroded back shed sediments of the Middle Jurassic Brent Group. As the tilted fault blocks were uplifted they were exposed to high levels of erosion that cut down into the underlying stratigraphy. In areas of extreme uplift as seen over the Brent Field erosion occurs down into the Lower Jurassic Dunlin Group.

In some areas where the eroded Brent Group sediment is deposited down-dip of the normal fault, the resulting density flow may become prospective, such as the Cladhan Field. Here, the sand prone sediments have been eroded and re-deposited in the predominantly mud-based Humber Group and generates a series density flow bright spots.

The occurrences of bright spots are often a direct hydrocarbon indicator, but in this instance it is more relating to the presence of a clean sandstone unit surrounded by mud prone units. Although hydrocarbons have migrated to the sands, the porosity is too tight for production in the Cladhan Field.

The results of a transecting rift affect all aspects of a petroleum system from trap size, reservoir deposition and kitchen area generation. By understanding the controls and effects that multi-phase rifting has upon a rift basin can be crucial in the development and evolution not only of a field but as a basin as a whole. This has been recently observed in the Norwegian sector of the Northern North Sea, where as recent as 2010 the third largest oil field in Norway was discovered in a multi-tiered fault block location. The discovery of the Johan Sverdrup Field illustrates that even in a mature basin, new methods of exploration can be found if you look deep enough for them.

Chapter 10 References

Ahmadi, Z., Sawyers, M., Keynon-Roberts, S., Stanworth, B., Kugler, K., Kristensen, J. & Fugelli, E. (2003). "Paleocene." The Millennium Atlas: petroleum geology of the central and northern North Sea.

Alexander, J. (1992). "A discussion of alluvial sandstone body characteristics related to variations in marine influence, Middle Jurassic of the Cleveland Basin, UK, and the implications for analogous Brent Group strata in the North Sea Basin." Geological Society, London Special Publication, **61**: 149-167.

Allan, U. S. (1989). "Model for hydrocarbon migration and entrapment within faulted structures." AAPG Bulletin **73**(7): 803-811.

Arthur, K. R., Cole, D.R., Henderson, G.G., & Kushnir, D.W. (1982). "Geology of the Hibernia discovery, In:Halbouty, M.T. (ed.) *The Deliberate search for the subtle Trap*." AAPG Bulletin **32**: 181-195.

Badley, M. E., Price, J. D., Rambech Dahl, C. & Agdestein, T. (1988). "The structural evolution of the northern Viking Graben and its bearing upon extensional modes of basin formation." Journal of the Geological Society **145**(3): 455-472.

Beach, A. (1984). "Structural evolution of the Witch Ground Graben." Journal of the Geological Society **141**(4): 621-628.

Becquey, M., Lavergne, M., & Willm, C. (1979). "Acoustic impedance logs computed from seismic traces." Geophysics **44**(9): 1485-1501.

Bosworth, W. (1992). "Mesozoic and early Tertiary rift tectonics in East Africa." Tectonophysics **209**(1-4): 115-137.

Bosworth, W., & Morley, C. K. (1994). "Structural and stratigraphic evolution of the Anza rift, Kenya." Tectonophysics **236**(1-4): 93-115.

Bowman, M. B. J. (1998). "Cenozoic." In. Glennie, K. (Eds) Introduction to the Petroleum Geology of the North Sea: 350-375.

Brennand, T. P., van Hoorn, B., James, K. H. & Glennie, K. W. (1998). "Historical Review of North Sea Exploration." In: Glennie, K.W (ed)

Introduction to Petroleum Geology of the North Sea. 4th Edition. Blackwell Scientific Publications: 1-41.

Bretan, P., Yielding, G. & Jones, H (2003). "Using calibrated shale gouge ratio to estimate hydrocarbon column heights." *AAPG Bulletin* **87**(3): 397-413.

Brown, S., Richards, P. C., & Thomson, A. R. (1987). "Patterns in the deposition of the Brent Group (middle Jurassic), UK North Sea." In: Brooks, J., & Glennie, K. (Eds.) *Petroleum Geology of Northwest Europe*: 899-913.

Burke, K. and J. F. Dewey (1973). "Plume Generated Triple Junctions: Key Indicators In Applying Plate Tectonics To Old Rock." *Journal Of Geology* **81**: 406-433.

Burley, S. D. (1993). "Models of burial diagenesis for deep exploration plays in Jurassic fault traps of the Central and Northern North Sea." *Geological Society, London, Petroleum Geology Conference* **4**: 1353-1375.

Cannon, S. J. C., Giles, M. R., Whitaker, M. F., Please, P. M. & Martin, S. V. (1992). "A regional reassessment of the Brent Group, UK sector, North Sea." In: Brooks, J. (Eds) *Geological Society, London, Special Publications* **61**(1): 81-107.

Chauvian, A. L., & Valachi, L.Z (1980). "Sedimentology of the Brent and Statfjord formations of the Statfjord Field. *In: The sedimentation of the North Sea reservoir rocks.*" *Norwegian Petroleum Society* **16**: 1-17.

Chorowicz, J. (2005). "The East African rift system." *Journal of African Earth Sciences* **43**(1-3): 379-410.

Cohen, S. C. (1981). "Postseismic rebound due to creep of the lower lithosphere and asthenosphere." *Geophysical Research Letters* **8**: 493-496.

Copestake, P., Sims, A., Crittenden, S., Hamar, G., Ineson, J., Rose, P. & Tringham, M. (2003). "Lower Cretaceous." *The Millennium Atlas: petroleum geology of the central and northern North Sea*.

Coward, M. P., Dewey, J.F., Hempton, M. & Holroyd, J. (2003). "Tectonic evolution." *The Millennium Atlas: petroleum geology of the central and northern North Sea*.

Cowie, P. A. G., S. & Dawers, N.H. (2000). "Implications of fault array evolution for synrift depocentre development: insights from a numerical fault growth model." *Basin Research* **12**: 241-261.

Cox, B. M. (1990). "A review of Jurassic chronostratigraphy and age indicators for the UK." Geological Society, London, Special Publications **55**(1): 169-190.

Dahl, N. and T. Solli (1993). "The structural evolution of the Snorre Field and surrounding areas." Geological Society, London, Petroleum Geology Conference, series **4**: 1159-1166.

Davies, S. J., Dawers, N. H., McLeod, A. E., & J. R. Underhill (2000). "The structural and sedimentological evolution of early synrift successions: the Middle Jurassic Tarbert Formation, North Sea." Basin Research **12**: 343-365.

Dawers, N. H. and J. R. Underhill (2000). "The Role of Fault Interaction and Linkage in Controlling Synrift Stratigraphic Sequences: Late Jurassic, Statfjord East Area, Northern North Sea." AAPG Bulletin **84**(1): 45-64.

Dean, K., McLachlan, K., & Chambers, A. (1999). "Rifting and the development of the Faeroe-Shetland Basin." Geological Society, London, Petroleum Geology Conference **5**: 533-544.

Deegan, C. E., and Scull, J. B., (1977). "A proposed standard lithostratigraphic nomenclature for the Central and Northern North Sea." Report of the Institute of Geological Sciences **77/25**.

Destro, N. (1995). "Release fault: A variety of cross fault in linked extensional fault systems, in the Sergipe-Alagoas Basin, NE Brazil." Journal of Structural Geology **17**(5): 615-629.

Destro, N., Szatmari, P., Alkmim, F.F. & Magnavita, L.P. (2003). "Release faults, associated structures, and their control on petroleum trends in the Reconcavo rift, northeast Brazil." AAPG Bulletin **87**(7): 1123-1144.

Donato, J. A., and Tully, M. C. (1981). "A regional interpretation of North Sea gravity data. ." In. L. V. Illing, and G. D. Hobson (Eds.) Petroleum Geology of the Continental Shelf of North-West Europe: 65-75

Dou, L., K. Xiao, et al. (2007). "Petroleum geology of the Melut Basin and the Great Palogue Field, Sudan." Marine and Petroleum Geology **24**(3): 129-144.

Ebinger, C. J. (1989). "Tectonic development of the western branch of the East African rift system." Geological Society of America Bulletin **101**(7): 885-903.

Ebinger, C. J., & Ibrahim, A. (1994). "Multiple episodes of rifting in Central and East Africa: A re-evaluation of gravity data." *Geologische Rundschau* **83**(4): 689-702.

Erratt, D., Thomas, G. M. & Wall, G. R. T. (1999). "The evolution of the Central North Sea Rift. In: Fleet A. J., Boldy S. A. R. (eds) *Petroleum Geology of Northwest Europe: Proceedings of the 5th Conference*." Geological Society, London, : 63-82.

Færseth, R. B. (1996). "Interaction of Permo-Triassic and Jurassic extensional fault-blocks during the development of the northern North Sea." *Journal of the Geological Society* **153**(6): 931-944.

Færseth, R. B., & Gabrielsen, R.J., & Hurich, C.A. (1995). "Influence of basement in structuring of the North Sea basin, offshore southwest Norway." *Norsk Geologisk Tidsskrift* **75**: 105-119.

Færseth, R. B., & Ravnås, R. (1998). "Evolution of the Oseberg Fault-Block in context of the northern North Sea structural framework." *Marine and Petroleum Geology* **15**(5): 467-490.

Færseth, R. B., Knudsen, B. E., Liljedahl, T., Midbøe, P. S., & Søderstrøm, B. (1997). "Oblique rifting and sequential faulting in the Jurassic development of the northern North Sea." *Journal of Structural Geology* **19**(10): 1285-1302.

Fisher, M. J., Mudge, D.C. (1998). "Triassic." In: Glennie, K. (Eds) *Introduction to the Petroleum Geology of the North Sea*: 212-244.

Fitton, G. J. (1983). "Active versus passive continental rifting: Evidence from the West African rift system." *Tectonophysics* **94**(1-4): 473-481.

Fordham, AM., North, CP., Hartley, AJ., Archer, SG. & Warwick, GL. (2010). 'Dominance of lateral over axial sedimentary fill in dryland rift basins'. *Petroleum Geoscience*, vol 16, no. 3, pp. 299-304.

Fraser, S., Robinson, A., Johnson, H.D., Underhill, J. R. & Kadolsky, D. (2003). "Upper Jurassic." *The Millennium Atlas: petroleum geology of the central and northern North Sea*.

Frostick, L. E., Linsey, T. K. & Reid, I. (1992). "Tectonic and climatic control of Triassic sedimentation in the Beryl Basin, northern North Sea." *Journal of the Geological Society* **149**(1): 13-26.

Fyfe, A., Gregersen, U., Jordt, H., Rundberg, Y., Eidvin, T., Evans, D., Stewart, D., Hovland, M & Andersen, P. (2003). "Oligocene to Holocene." *The Millennium Atlas: petroleum geology of the central and northern North Sea*.
Gass, I. G. (1977). "The evolution of the Pan African crystalline basement in NE Africa and Arabia." *Journal of the Geological Society* **134**(2): 129-138.

Gawthorpe, R. L., & Hurst, J.M. (1993). "Transfer zones in extensional basins: their structural style and influence on drainage development and stratigraphy." *Journal of the Geological Society* **150**(6): 1137-1152.
Gawthorpe, R. L. and M. R. Leeder (2000). "Tectono-sedimentary evolution of active extensional basins." *Basin Research* **12**(3-4): 195-218.

Gawthorpe, R. L., I. Sharp, et al. (1997). "Linked sequence stratigraphic and structural evolution of propagating normal faults." *Geology* **25**(9): 795-798.

Gibbons, K. A., Jourdan, C. A. & Hesthammer, J. (2003). "The Statfjord Field, Blocks 33/9, 33/12 Norwegian sector, Blocks 211/24, 211/25 UK sector, Northern North Sea." *Geological Society, London, Memoirs* **20**(1): 335-353.

Gibbs, A. D. (1984). "Structural evolution of extensional basin margins." *Journal of the Geological Society* **141**(4): 609-620.

Glennie, K. W. (1995). "Permian and Triassic rifting in northwest Europe." *Geological Society, London, Special Publications* **91**(1): 1-5.

Glennie, K. W., Higham, J. & Stemmerik, L. (2003). "Permian." *The Millennium Atlas: petroleum geology of the central and northern North Sea*.
Goldsmith, P. J., Hudson, G. & Van Veen, P (2003). "Triassic." *The Millennium Atlas: petroleum geology of the central and northern North Sea*.

Graue, E., Helland-Hansen, W., Johnsen, J. R., Lømo, L., Nødtvedt, A., Rønning, K., Ryseth, A. & Steel, R. J. (1987). "Advance and retreat of Brent Delta System, Norwegian North Sea." In: Brooks, J. and Glennie, KW (Eds) *Petroleum Geoscience of North West Europe*: 915-937.

Hampson, G. J., Sixsmith, Peter J. & Johnson, Howard D. (2004). "A sedimentological approach to refining reservoir architecture in a mature hydrocarbon province: the Brent Province, UK North Sea." *Marine and Petroleum Geology* **21**(4): 457-484.

Helland-Hansen, W., Ashton, M., Lømo, L., & Steel, R. (1992). "Advance and retreat of the Brent delta: recent contributions to the depositional model." *Geological Society, London, Special Publications* **61**(1): 109-127.

Høimyr, Ø., Amund, K. & Nystuen, J.P. (1993). "Effects of heterogeneities in a braided stream channel sandbody on the simulation of oil recovery: a case study from the Lower Jurassic Statfjord Formation, Snorre Field, North Sea." Geological Society, London, Special Publications **69**(1): 105-134.

Hubbard, R. J., Pape, J., & Roberts, D.G. (1985). "Deposition Sequence Mapping to Illustrate the Evolution of a Passive Continental Margin. In: Berg, O.R., & Woolverton, D. (eds) *Seismic stratigraphy II: An Integrated Approach to Hydrocarbon Exploration*." AAPG Bulletin **39**: 93-115.

Husmo, T., Hamar, G., Høiland, O., Johannessen, E.P., Rømuld, A., Spencer, A. M. & Titterton, R. (2003). "Lower and Middle Jurassic." The Millennium Atlas: petroleum geology of the central and northern North Sea.

Jackson, C. R. (2004). An Atlas of Internal Solitary-like Waves and their Properties, 2nd edn. Global Ocean Associates, Alexandria, VA.

Jolley, S. J., Dijk, H., Lamens, J. H., Fisher, Q. J., Manzocchi, T., Eikmans, H. & Huang, Y. (2007). "Faulting and fault sealing in production simulation models: Brent Province, northern North Sea." Petroleum Geoscience **13**(4): 321-340.

Jones, E., Jones, B., Ebdon, C., Ewen, D., Milner, P., Plunkett, J., Hudson, G. & Slater, P. (2003). "Eocene." The Millennium Atlas: petroleum geology of the central and northern North Sea.

Jordt, H., Faleide, J., Bjørlykke, K. & Ibrahim, M.T. (1995). "Cenozoic sequence stratigraphy of the central and northern North Sea Basin: tectonic development, sediment distribution and provenance areas." Marine and Petroleum Geology **12**(8): 845-879.

Jordt, H., Thyberg, Brit I. & Nøttvedt, Arvid (2000). "Cenozoic evolution of the central and northern North Sea with focus on differential vertical movements of the basin floor and surrounding clastic source areas." Geological Society, London, Special Publications **167**(1): 219-243.

Kent, P. E. (1975). "Review of North Sea Basin development." Journal of the Geological Society **131**(5): 435-468.

Kirk, R. J. (1980). "Statfjord Field: a North Sea giant. In: Halbouty, M.T. (eds) Giant oil and gas fields of the decade 1968-78." American Association of Petroleum Geologists Memoir **30**: 95-116.

Knipe, R. J. (1997). "Juxtaposition and seal diagrams to help analyze fault seals in hydrocarbon reservoirs." AAPG Bulletin **81**(2): 187-195.

Knipe, R. J., Jones, G. & Fisher, Q. J. (1998). "Faulting, fault sealing and fluid flow in hydrocarbon reservoirs: an introduction." In: Jones, G., Fisher, Q.J. & Knipe, R.J (Eds) Geological Society, London, Special Publications **147**(1): vii-.

Kusznir, N. J., Marsden, G. & Egan, S. S. (1991). "A flexural-cantilever simple-shear/pure-shear model of continental lithosphere extension: applications to the Jeanne d'Arc Basin, Grand Banks and Viking Graben, North Sea." Geological Society, London, Special Publications **56**(1): 41-60.

Kyrkjebø, R., Gabrielsen, R.H. & Faleide, J.I. (2004). "Unconformities related to the Jurassic-Cretaceous synrift-post-rift transition of the northern North Sea." Journal of the Geological Society **161**(1): 1-17.

Lambiase, J. J. B., W. (1995). "Structural controls on sedimentation in continental rifts." Geological Society, London, Special Publications **80**(1): 117-144.

Larter, S. and I. Horstad (1992). "Migration of petroleum into Brent Group reservoirs: some observations from the Gullfaks field, Tampen Spur area North Sea." In: Brooks, J. (Eds) Geological Society, London, Special Publications **61**(1): 441-452.

Latin, D. M., Dixon, J.E., White, N. & Fitton, G.F. (1990). "Mesozoic magmatic activity in the North Sea Basin: implications for stretching history." Geological Society, London, Special Publications **55**(1): 207-227.

Leckie, G. G. (1982). "Lithology and Subsidence in the North Sea." Philosophical Transactions of the Royal Society of London. Series A, Mathematical and Physical Sciences **305**(1489): 85-99.

Lee, M. J. and Y. J. Hwang (1993). "Tectonic evolution and structural styles of the East Shetland Basin." Geological Society, London, Petroleum Geology Conference , series **4**: 1137-1149.

Leeder, M. R. and R. L. Gawthorpe (1987). "Sedimentary models for extensional tilt-block/half-graben basins." Geological Society, London, Special Publications **28**(1): 139-152.

Leveille, G. P., Knipe, R., More, C., Ellis, D., Dudley, G., Jones, G., Fisher, Q.J. & Allinson, G (1997). "Compartmentalization of Rotliegendes gas reservoirs by sealing faults, Jupiter Fields area, southern North Sea." Geological Society, London, Special Publications **123**(1): 87-104.

Leveille, G. P., Primmer, T.J., Dudley, G., Ellis, D. & Allinson, G.J. (1997). "Diagenetic controls on reservoir quality in Permian Rotliegendes sandstones, Jupiter Fields area, southern North Sea." Geological Society, London, Special Publications **123**(1): 105-122.

Lundin (2012). "Confronting Energy Paradoxes." 30-08-2012, from <http://www.ons.no/index.cfm?event=downloadfile&famid=308947>.

MacGregor, A. G., Trussell, P., Lauver, S., Bedrock, M., Bryce, J. & Mounlds, T. (2005). The Magnus Field: extending field life through good reservoir management and enhanced oil recovery. In Doré, A.G. & Vining, B.A. (Eds) Petroleum geology: North-West Europe and Global Perspectives- Proceedings of the 6th Petroleum Geology Conference: 469-475.

McKenzie, D. (1978). "Some remarks on the development of Sedimentary basins." Earth and Planetary Science Letters, **40**: 25-32.

McLeod, A. E., Dawers, N. H. & Underhill J. R. (2000). "The propagation and linkage of normal faults: insights from the Strathspey-Brent-Statfjord fault array, northern North Sea." Basin Research **12**: 263-284.

Milne, A. D. and A. M. Brown (2003). "The Don Field, Blocks 211/13a, 211/14, 211/18a, 211/19a, UK North Sea." In. Gluyas, J.G. & Hitchens (Eds) Geological Society, London, Memoirs **20**(1): 257-263.

Morley, C. K. (2002). "Evolution of Large Normal Faults: Evidence from Seismic Reflection Data." AAPG Bulletin **86**(6): 961-978.

Morley, C. K., Bosworth, W., Day, R.A., Lauck, R., Bosher, R., Stone, D.M., Wigger, S.T., Wescott, W.A., Haun, D., & Bassett, N. (1999). "Geology and Geophysics of the Anza Graben." In: Morley, C.K. (eds) *Geoscience of Rift Systems - Evolution of East Africa*. AAPG Studies in Geology **44**: 67-90.

Morris, P. H., Payne, S. N. J. & Richards, D. P. J. (1999). "Micropalaeontological biostratigraphy of the Magnus Sandstone Member (Kimmeridgian-Early Volgian), Magnus Field, UK North Sea." In. Jones, R.W. & Simmons, M.D. (Eds) Geological Society, London, Special Publications **152**(1): 55-73.

Morton, N. (1993). "Potential reservoir and source rocks in relation to Upper Triassic to Middle Jurassic sequence stratigraphy, Atlantic margin basins of the British Isles." Geological Society, London, Petroleum Geology Conference **4**: 285-297.

Nadin, P. A., Kusznir, N. J., & Toth, J. (1995). "Transient regional uplift in the Early Tertiary of the northern North Sea and the development of the Iceland Plume." *Journal of the Geological Society* **152**(6): 953-958.

Nettleton, L. L. (1971). "Elementary gravity and magnetics for geologists and seismologists." Society of Exploration Geophysicists.

Nettleton, L. L. (1976). "Gravity and Magnetism in Oil Prospecting." International series in the Earth & Planetary Sciences.

Oakman, C. D., & Partington, M.A. (1998). "Cretaceous." In: Glennie, K. (Eds) *Introduction to the Petroleum Geology of the North Sea*: 294-349.

Odinsen, T., Reemst, P., Beek, P.V.D., Faleide, J.I. & Gabrielsen, R.H. (2000). "Permo-Triassic and Jurassic extension in the northern North Sea: results from tectonostratigraphic forward modelling." In: Nøttvedt, A., Larsen, B.T., Gabrielsen, R.H., Olaussen, S., Brekke, H., Tørudbakken, B., Birkeland, Ø., Skogseid, J. (Eds.), *Dynamics of the Norwegian Margin*. Geological Society, London, Special Publications **167**(1): 83-103.

Olsen, K. H. M., P. (1995). Chapter 1 Introduction: Progress in understanding continental rifts. *Developments in Geotectonics*, Elsevier. **Volume 25**: 3-26.

Partington, M. A., Copestake, P., Mitchener, B.C. & Underhill, J.R. (1993). Biostratigraphic calibration of genetic stratigraphy sequences in the Jurassic-lowermost Cretaceous (Hettangian to Ryazanian) of the North Sea and adjacent areas. In: Parker, J.R. (Eds) *4th Petroleum Geology of Northwest Europe*, Geological Society, London: 371-386.

Platt, N. H. (1995). "Structure and tectonics of the northern North Sea: new insights from deep penetration regional seismic data." Geological Society, London, Special Publications **80**(1): 103-113.

Prosser, S. (1993). "Rift-related linked depositional systems and their seismic expression." Geological Society, London, Special Publications **71**(1): 35-66.

Purvis, K. (1995). "Diagenesis of Lower Jurassic sandstones, Block 211/13 (Penguin Area), UK northern North Sea." *Marine and Petroleum Geology* **12**(2): 219-228.

Ramnarine, S. K. (2011). Late Cretaceous turbidites, Heidrun field, Norwegian Continental Shelf. Energy and Earth Resources, University of Texas at Austin. **Masters**.

Ravnås, R., Nøttvedt, A., Steel, R. J. & Windelstad, J. (2000). "Syn-rift sedimentary architectures in the Northern North Sea." Geological Society, London, Special Publications **167**(1): 133-177.

Rawson, P. F., & Riley, L. A. (1982). "Latest Jurassic-Early Cretaceous events and the "late Cimmerian unconformity" in North Sea area." AAPG Bulletin **66**(12): 2628-2648.

Richards, P. C. (1990). "The early to mid-Jurassic evolution of the northern North Sea." Geological Society, London, Special Publications **55**(1): 191-205.

Richards, P. C. (1991). "Evolution of Lower Jurassic coastal plain and fan delta sediments in the Beryl Embayment, North Sea." Journal of the Geological Society **148**(6): 1037-1047.

Richards, P. C. (1992). "An introduction to the Brent Group: a literature review." In: Brooks, J. (Eds) Geological Society, London, Special Publications **61**(1): 15-26.

Richards, P. C., Lott, G.K., Johnson, H., Knox, R.W.O'B. & Riding, J.B. (1993). "Jurassic of the Central and Northern North Sea." In: Knox, R.W.O'B & Cordey, W.G, Lithostratigraphic nomenclature of the UK North Sea

Rider, M. H. (1996). The Geological Interpretation of Well Logs, Whittles Publishing.

Ritchie, J. S. (2003). "The Dunbar, Ellon and Grant Fields (Alwyn South Area), Blocks 3/8a, 3/9b, 3/13a, 3/14, 3/15, UK North Sea." Geological Society, London, Memoirs **20**(1): 265-281.

Roberts, A. M. and G. Yielding (1994). "Continental extensional tectonics." In: Hancock, P.L. (eds) Continental Deformation, Pergamon Press, Oxford. : 233-250.

Roberts, A. M., Yielding, G., Kusznir, N. J., Walker, I. M. & Dorn-Lopez, D. (1995). "Quantitative analysis of Triassic extension in the northern Viking Graben." Journal of the Geological Society **152**(1): 15-26.

Røe, S.-L. and R. Steel (1985). "Sedimentation, sea-level rise and tectonics at the Triassic-Jurassic boundary (Statfjord Formation), Tampen Spur, Northern North Sea." Journal of Petroleum Geology **8**(2): 163-186.

Schlische, R. W., & Withjack, M.O (1999). "Rift Basin Architecture and Evolution." International Workshop for a Climatic, Biotic, and Tectonic, Pole-to-Pole Coring Transect of Triassic-Jurassic Pangea.

Schull, T. T. (1988). "Rift Basins of interior Sudan: Petroleum Exploration and Discovery." AAPG Bulletin **72**: 1128-1142.

Shepherd, M. (1991). "The Magnum Field, Block 211/7a, 12a, UK North Sea." In: Abbots, I.L. (Eds) Geological Society, London, Memoirs **14**(1): 153-157.

Sheriff, R. E., & Geldart, L.P. (1982). "Exploration Seismology Vol. 1. History, Theory and Data Acquisition." Cambridge University Press, Cambridge, UK.

Sheriff, R. E., & Geldart, L.P. (1983). "Exploration Seismology Vol. 2. Data-processing and interpretation." Cambridge University Press, Cambridge, UK.

Siebert, R. M., Moncure, G.K., & Lahann, R.W. (1984). "A theory of framework grain dissolution in sandstones, *in* McDonald, D.A., and Surdam, R.C., eds., Clastic diagenesis." AAPG Memoir **37**: 163-175.

Sinclair, I. K., Evans, J. E., Albrechtsons, E. A., & Sydora, L. J. (1999). "The Hibernia Oilfield – effects of episodic tectonism on structural character and reservoir compartmentalization." Geological Society, London, Petroleum Geology Conference **5**: 517-528.

Skarpnes, O., Hamar, G.P., Jakobson, K.H. & Ormaasen, D.E. (1980). "Regional Jurassic setting of the North Sea north of the central highs. *In*: the sedimentation of the North Sea reservoir rocks." Norwegian Petroleum Society **13**: 1-8.

Smith, C. and I. R. Hatton (1998). "Inversion tectonics in the Lyme Bay-West Dorset area of the Wessex Basin, UK." Geological Society, London, Special Publications **133**(1): 267-281.

Sonder, L. J., & Jones, C.H. (1999). "WESTERN UNITED STATES EXTENSION: How the West was Widened." Annual Review of Earth and Planetary Sciences **27**(1): 417-462.

Spencer, A. M. and V. B. Larsen (1990). "Fault traps in the Northern North Sea." Geological Society, London, Special Publications **55**(1): 281-298.

Steel, R. and A. Ryseth (1990). "The Triassic - early Jurassic succession in the northern North Sea: megasequence stratigraphy and intra-Triassic tectonics." Geological Society, London, Special Publications **55**(1): 139-168.

Steel, R. J. (1993). "Triassic-Jurassic megasequence stratigraphy in the Northern North Sea: rift to post-rift evolution." Geological Society, London, Petroleum Geology Conference **4**: 299-315.

Stewart, J. H. (1971). "Basin and Range Structure: A System of Horsts and Grabens Produced by Deep-Seated Extension." *Geological Society of America Bulletin* **82**(4): 1019-1044.

Stewart, S. A. (2001). "Displacement Distributions on Extensional Faults: Implications for Fault Stretch, Linkage, and Seal." *AAPG Bulletin* **85**(4): 587-599.

Struijk, A. P. and R. T. Green (1991). "The Brent Field, Block 211/29, UK North Sea." *Geological Society, London, Memoirs* **14**(1): 63-72.

Surlyk, F., Dons, T., Clausen, C.K. & Higham, J. (2003). "Upper Cretaceous." *The Millennium Atlas: petroleum geology of the central and northern North Sea*.

Taylor, J. C. M. (1998). "Upper Permian - Zechstein." In: Glennie, K. (Eds) *Introduction to the Petroleum Geology of the North Sea*: 174-211.

Taylor, S. R., Almond, J., Arnott, S., Kemshell, D. & Taylor, D. (2003). "The Brent Field, Block 211/29, UK North Sea." *Geological Society, London, Memoirs* **20**(1): 233-250.

Tomasso, M., Underhill, J.R., Hodgkinson, R.A. & Young, M.J. (2008). "Structural styles and depositional architecture in the Triassic of the Ninian and Alwyn North fields: Implications for basin development and prospectivity in the Northern North Sea." *Marine and Petroleum Geology* **25**(7): 588-605.

Trewin, N. H., Fryberger, S.G. & Kreutz, Helge (2003). "The Auk Field, Block 30/16, UK North Sea." *Geological Society, London, Memoirs* **20**(1): 483-496.
Underhill, J. R. (1994). "Discussion on palaeoecology and sedimentology across a Jurassic fault scarp, NE Scotland." *Journal of the Geological Society* **151**(4): 729-731.

Underhill, J. R. (1998). "Jurassic." In: Glennie, K. (Eds) *Introduction to the Petroleum Geology of the North Sea*: 245-293.

Underhill, J. R., & Hunter, K. L. (2008). "Effect of Zechstein Supergroup (Z1 cycle) Werrahalit pods on prospectivity in the southern North Sea." *AAPG Bulletin* **92**(Article): 827-851.

Underhill, J. R., & Partington, M.A. (1994). "Use of maximum flooding surfaces in determining a regional tectonic control on the Intra-Aalenian ("Mid Cimmerian") Sequence Boundary: Implications for North Sea basin

development and Exxon's Sea-Level Chart." In Posamentier, H.W. & Wiemer, P. (Eds.). *Siliciclastic Sequence Stratigraphy*. AAPG Memoir **58**: 449-484.

Underhill, J. R. and M. A. Partington (1993). "Jurassic thermal doming and deflation in the North Sea: implications of the sequence stratigraphic evidence." In: J.R. Parker, Editor, *Petroleum Geology of Northwest Europe: Proceedings of the Fourth Conference*, Geological Society, London (1993), pp. 337-345.

Underhill, J. R. and R. Stoneley (1998). "Introduction to the development, evolution and petroleum geology of the Wessex Basin." Geological Society, London, Special Publications **133**(1): 1-18.

Warren, E. A. and P. C. Smalley (1994). "Part 1: Compendium of North Sea Oil and gas fields." In: Warren, E.A. & Smalley, P.C. (Eds) Geological Society, London, Memoirs **15**(1): 3-77.

Warrender, J. (1991). "The Murchison Field, Block 211/19a, UK North Sea." Geological Society, London, Memoirs **14**(1): 165-173.

Watterson, J. (1986). "Fault dimensions, displacements and growth." *Pure and Applied Geophysics* **124**(1): 365-373.

Wernicke, B. (1985). "Uniform-sense normal simple shear of the continental lithosphere." *Canadian Journal of Earth Sciences* **22**(1): 108-125.

Wignall, P and Pickering, KT (1993) *Palaeoecology and sedimentology across a Jurassic fault scarp, NE Scotland*. Journal of the Geological Society, London, **150** 323 - 340.

Whitmeyer, S.J., Fichter, L.S., and Pyle. E.J. 2007. New directions in Wilson Cycle concepts: Supercontinent and Tectonic Rock Cycles *Geosphere*, December 2007, v. 3, p. 511-526.

Wilkinson, M., Haszeldine, R. S., & Fallick, A. E. (2006). "Jurassic and Cretaceous clays of the northern and central North Sea hydrocarbon reservoirs reviewed." *Clay Minerals* **41**(1): 151-186.

Yielding, G. (1990). "Footwall uplift associated with Late Jurassic normal faulting in the northern North Sea." *Journal of the Geological Society* **147**(2): 219-222.

Yielding, G., Badley, M.E. & Roberts, A.M. (1992). "The structural evolution of the Brent Province." In: Brooks, J. (Eds) *Geological Society, London, Special Publications* **61**(1): 27-43.

Yielding, G., Freeman, B. & Needham, T.D. (1997). "Quantitative fault seal prediction." *AAPG Bulletin* **81**(6): 897-917.

Young, M. J., Gawthorpe, R.L., & Hardy, S. (2001). "Growth and linkage of a segmented normal fault zone; the Late Jurassic Murchison-Statfjord North Fault, northern North Sea." *Journal of Structural Geology* **23**(12): 1933-1952.

Zanella, E., & Coward, M.P (2003). "Structural framework." *The Millennium Atlas: petroleum geology of the central and northern North Sea*.

Zervos, F. (1987). "A compilation and regional interpretation of the northern North Sea gravity map." In: Coward, M., Dewey, J., & Hancock, P. (Eds) *Geological Society, London, Special Publications* **28**(1): 477-493.

Ziegler, P. (1982). "Triassic rifts and facies patterns in Western and Central Europe." *Geologische Rundschau* **71**(3): 747-772.

Ziolkowski, A., Underhill, J.R., & Johnston, R.G.K. (1998). "Wavelets, well ties, and the search for subtle stratigraphic traps." *Geophysics* **63**(1): 297-313.

Chapter 11 Appendixes

Appendix 1 - Regional Top Structure and Isochron Maps

Appendix 1 - Regional Surfaces

Time Top Structure Maps

Sea Bed Structure Map

Top Balder Formation Structure Map

Top Cretaceous Structure Map

Top Plenus Marl Structure Map

Top Cromer Knoll Formation Structure Map

Base Cretaceous Unconformity Structure Map

Top Brent Group Structure Map

Top Dunlin Group Structure Map

Base Syn-Rift 1 Structure Map

Time Thickness Maps (Isochrons)

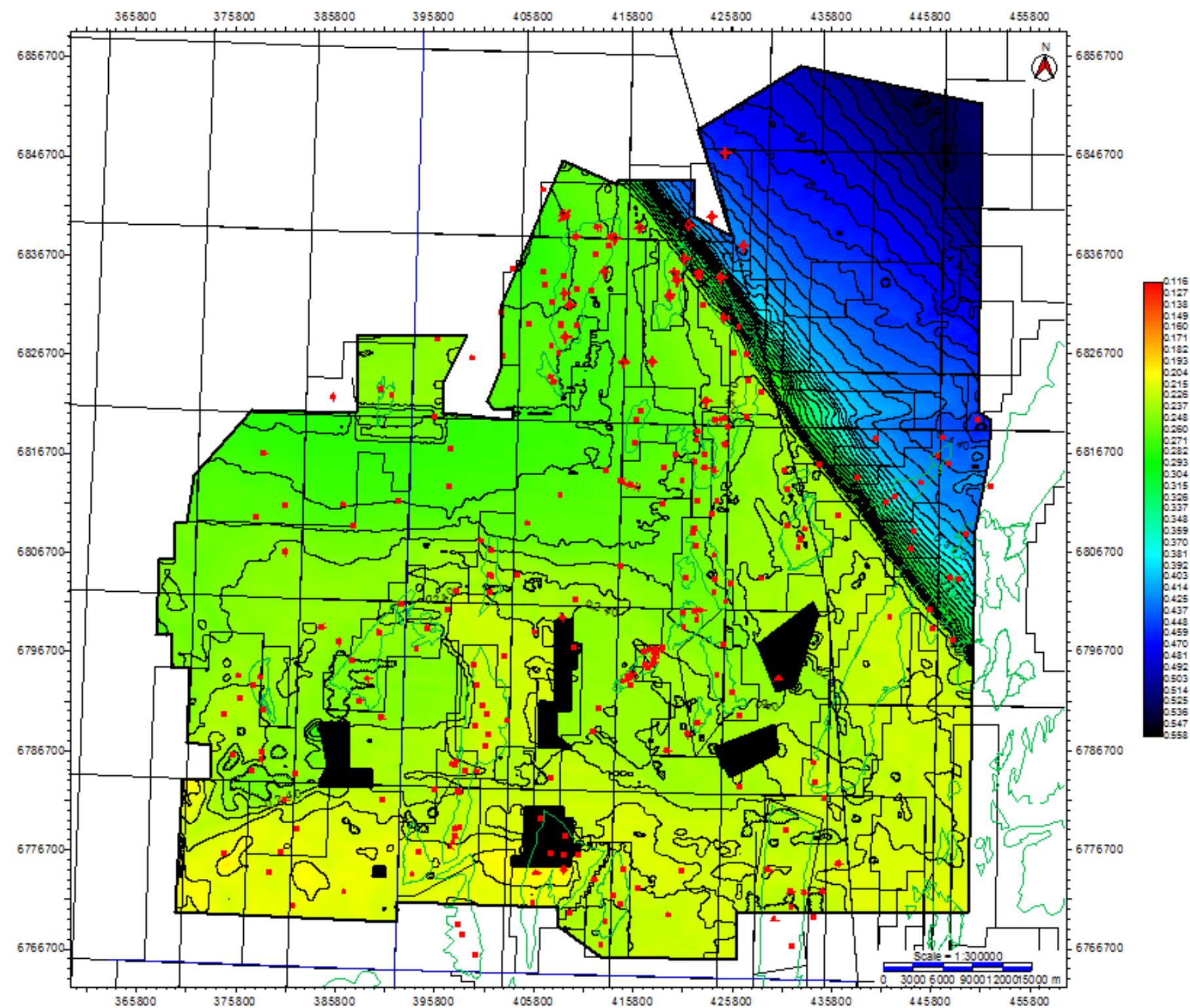
Post-Rift Package 2; Sea Bed to Base Cretaceous Unconformity Isochron

Syn-Rift Package 2; Base Cretaceous Unconformity to Top Brent Group
Isochron

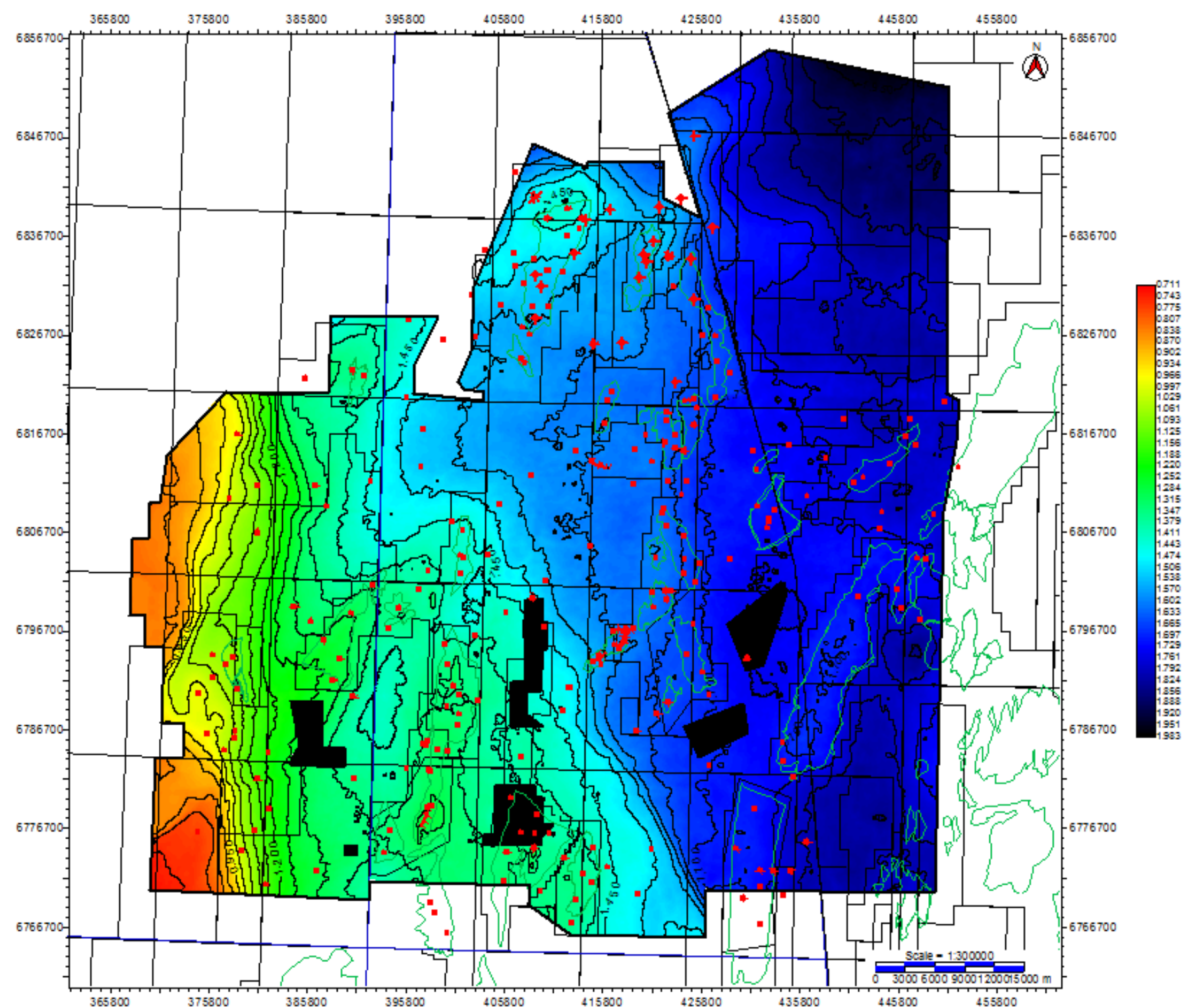
Intr-Rift; Top Brent Group to Dunlin Group Isochron

Rift Package 1; Top Dunlin to Base Syn-Rift 1 Isochron

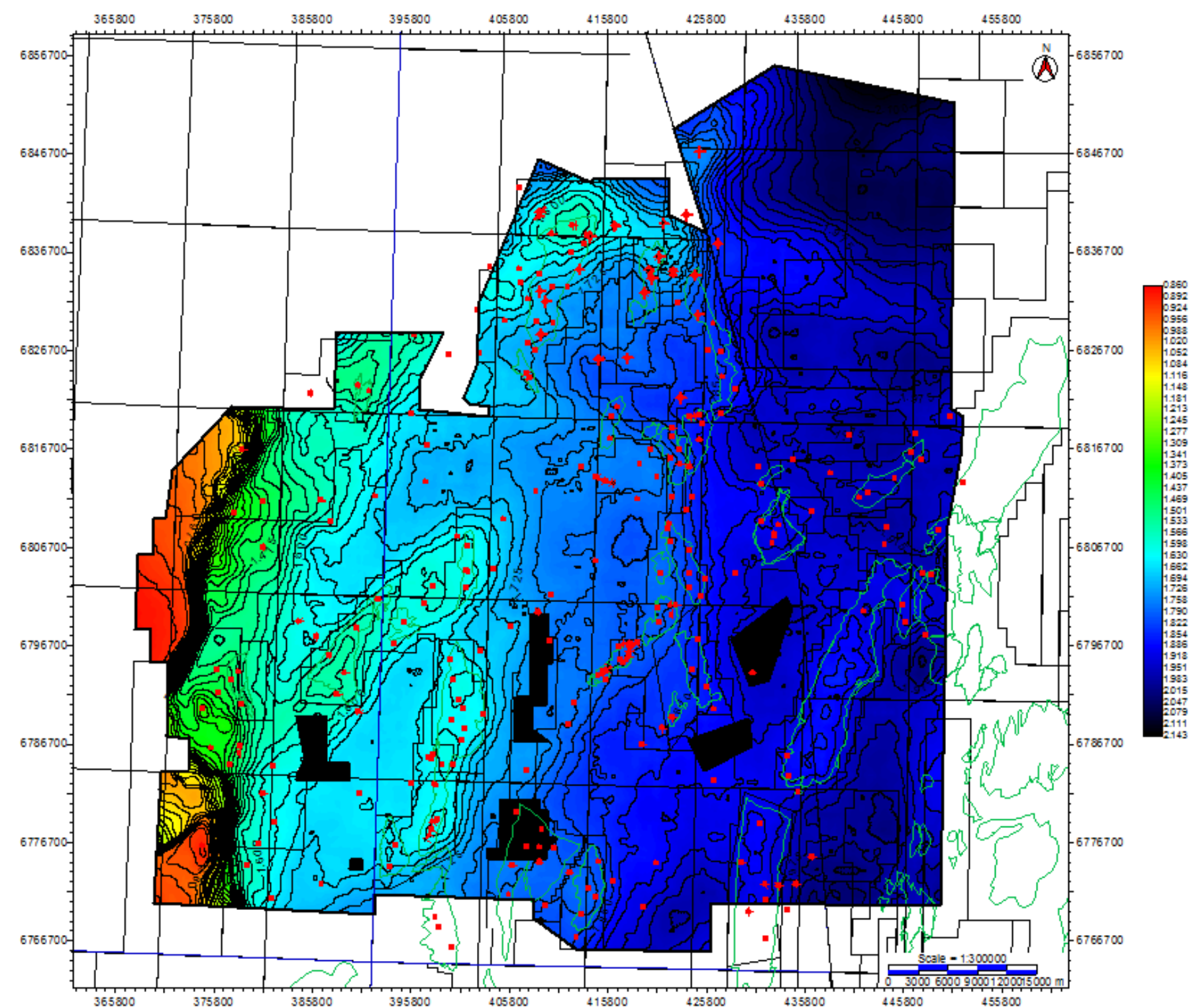
Sea Bed Structure Map



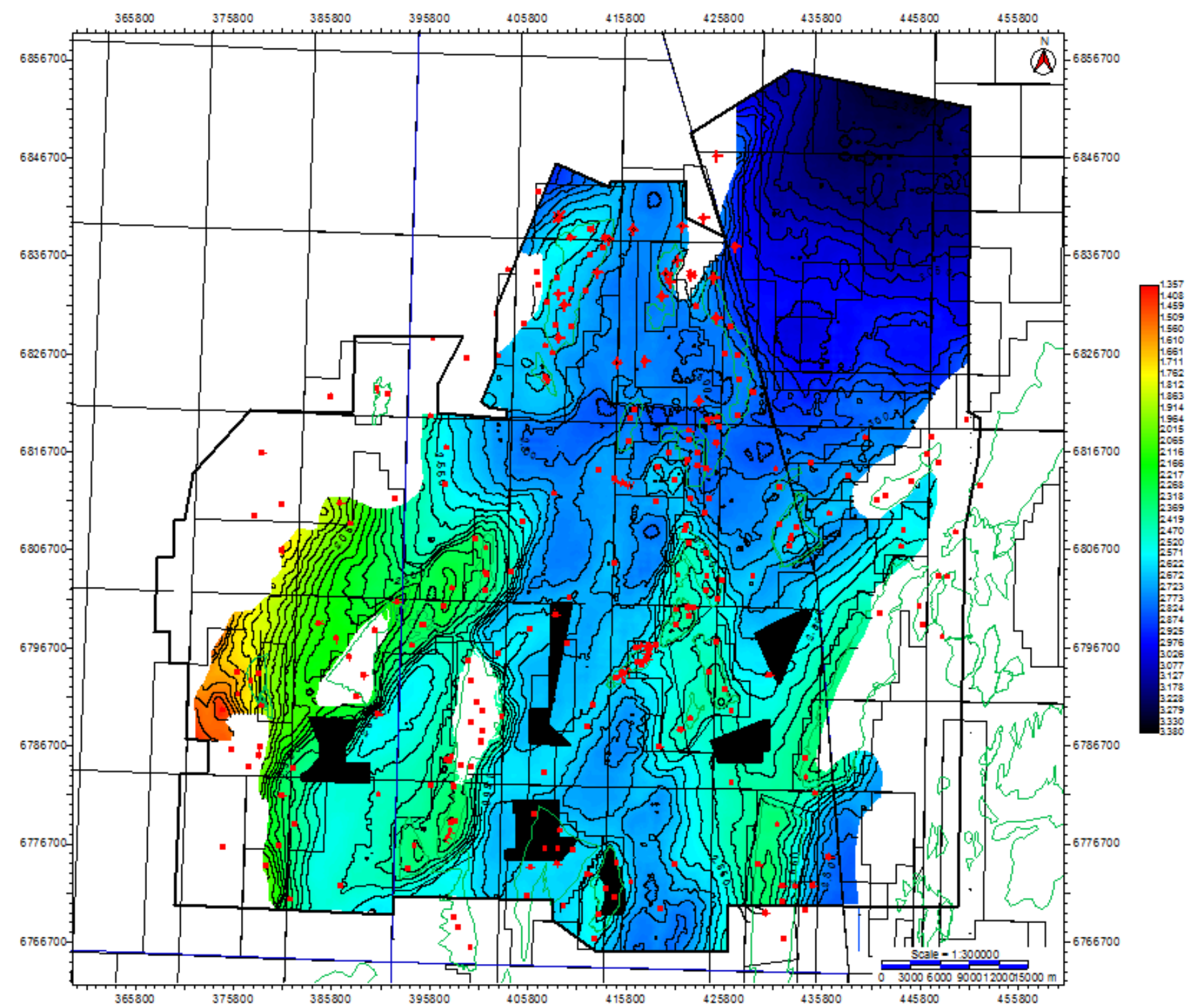
Top Balder Formation Structure Map



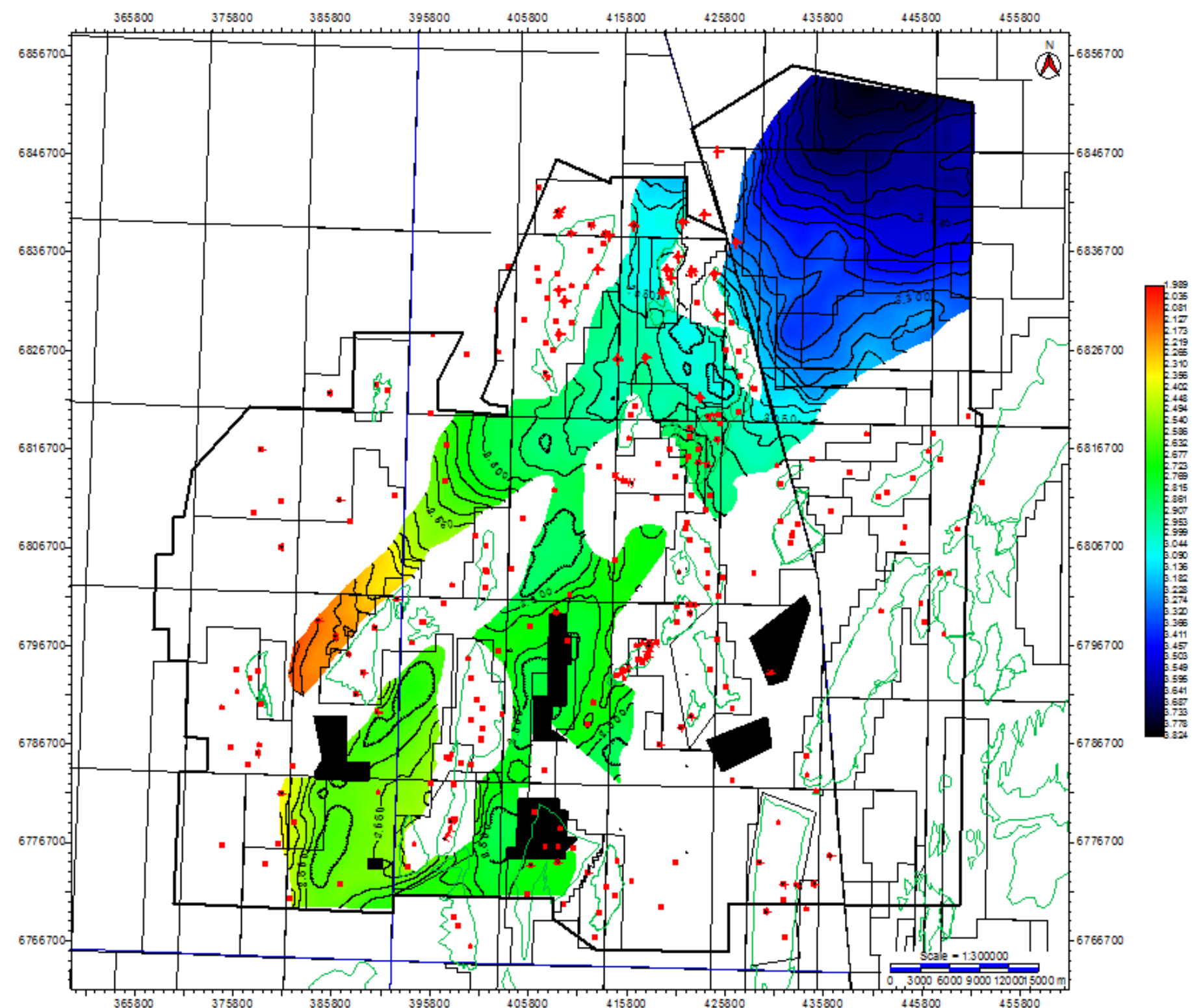
Top Cretaceous Structure Map



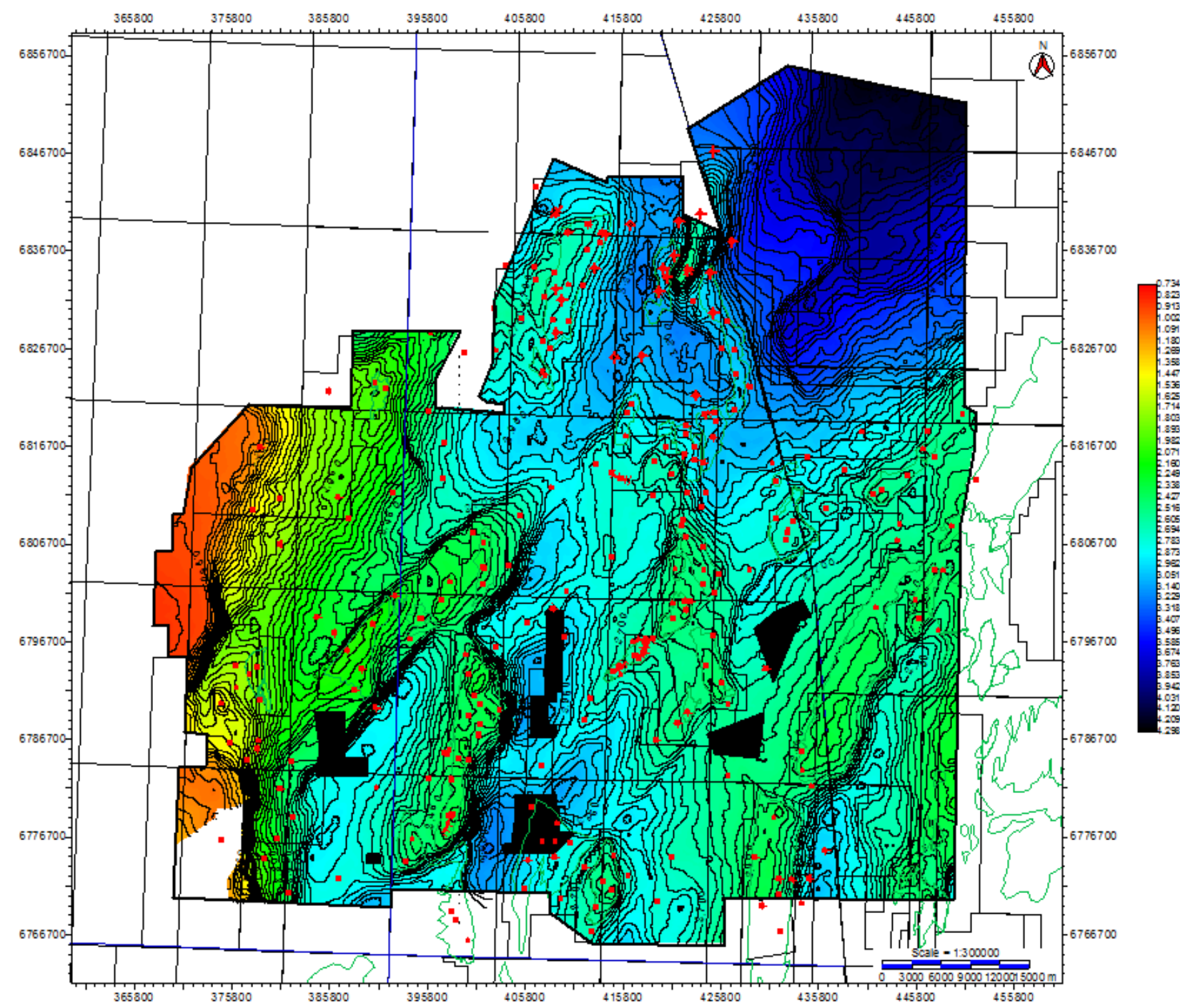
Top Plenus Marl Structure Map



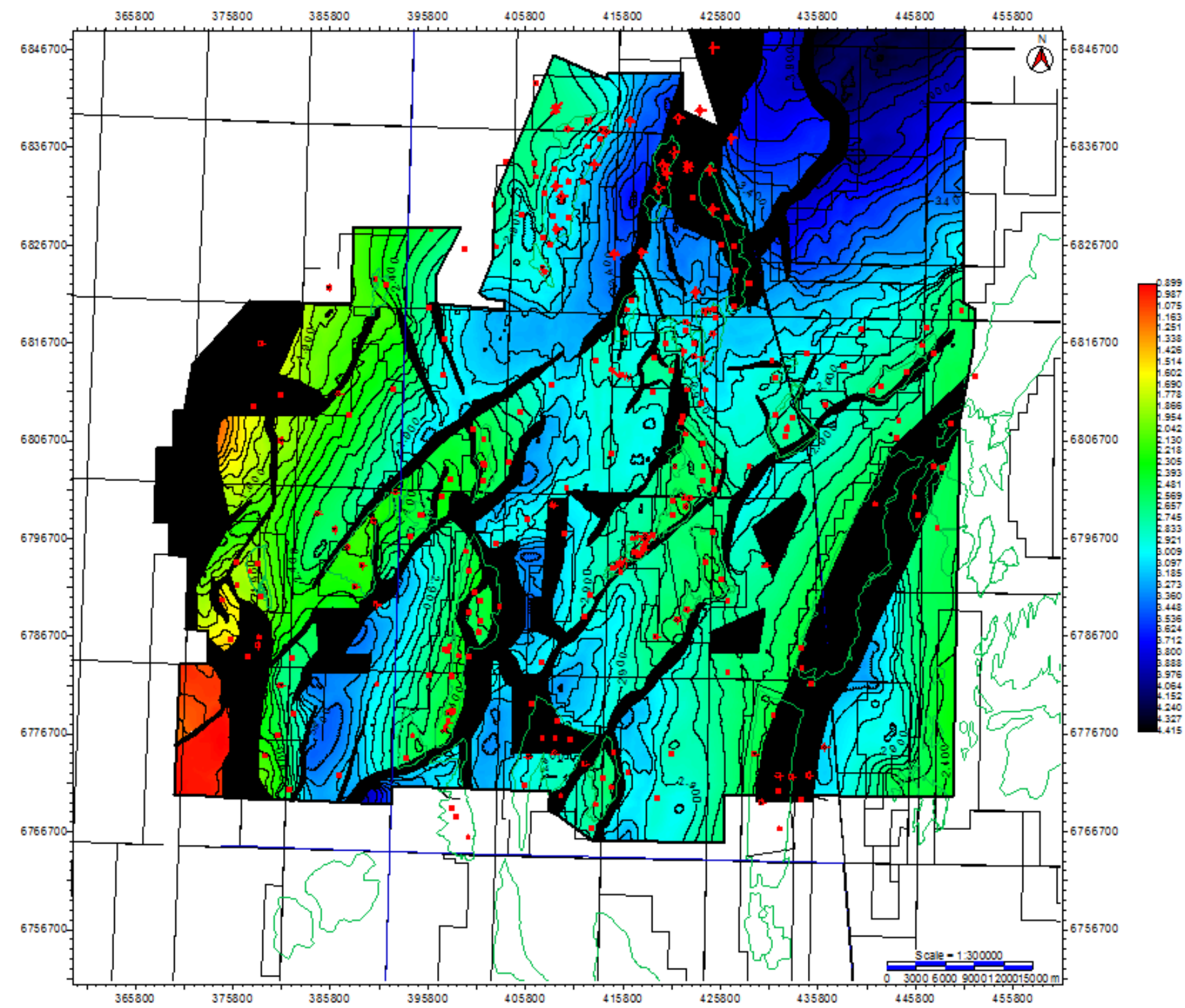
Top Cromer Knoll Formation Structure Map



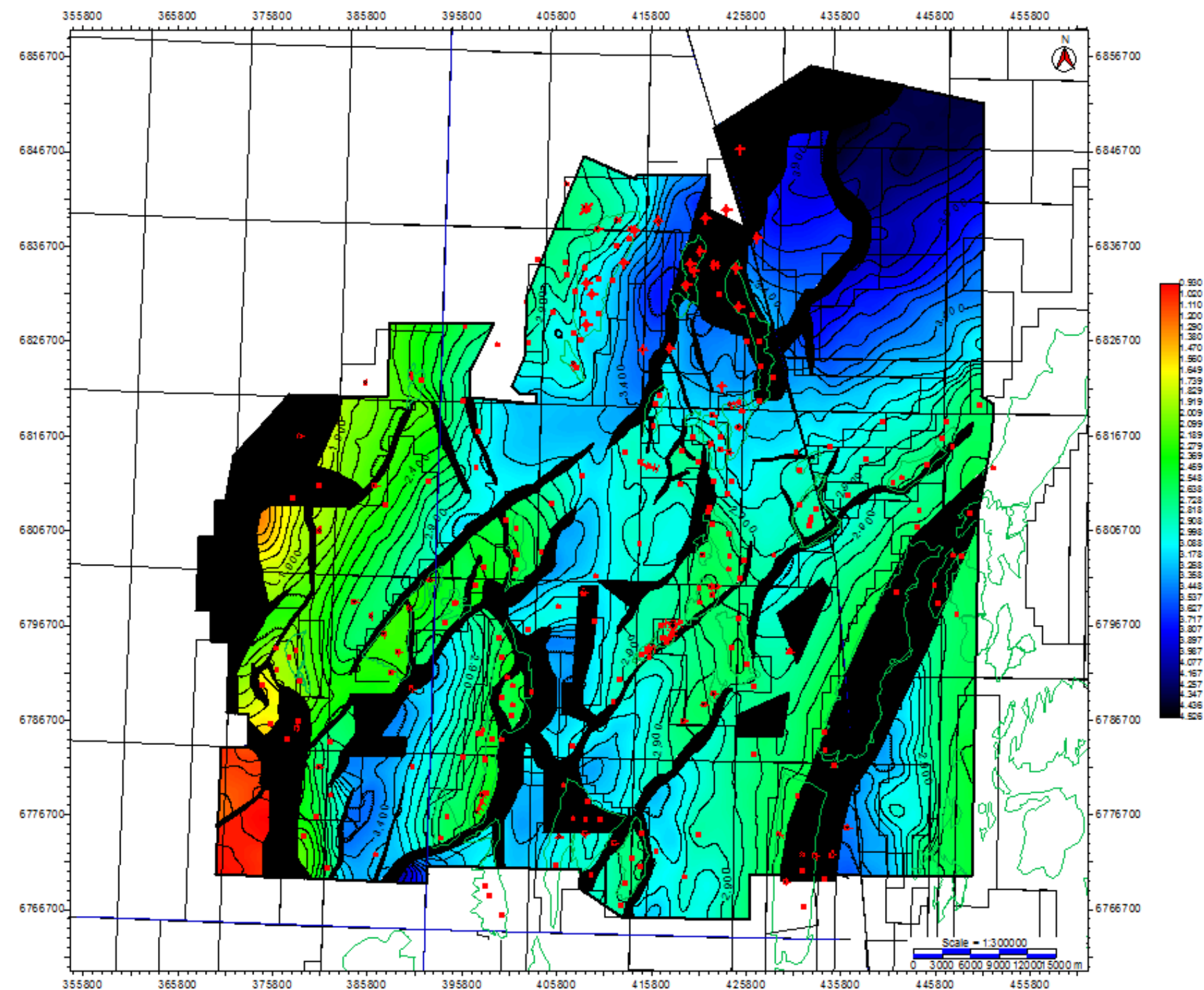
Base Cretaceous Unconformity Structure Map



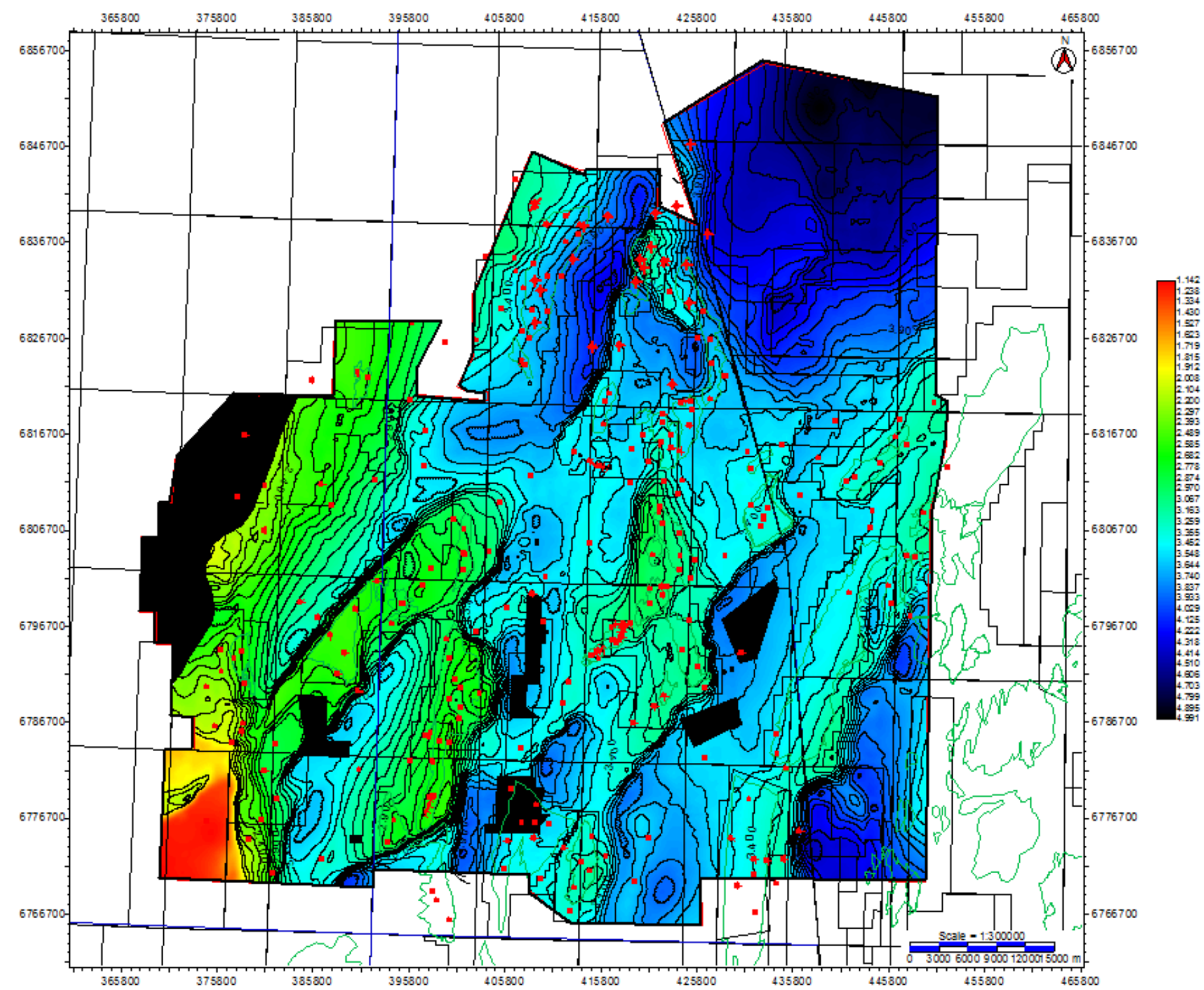
Top Brent Group Structure Map



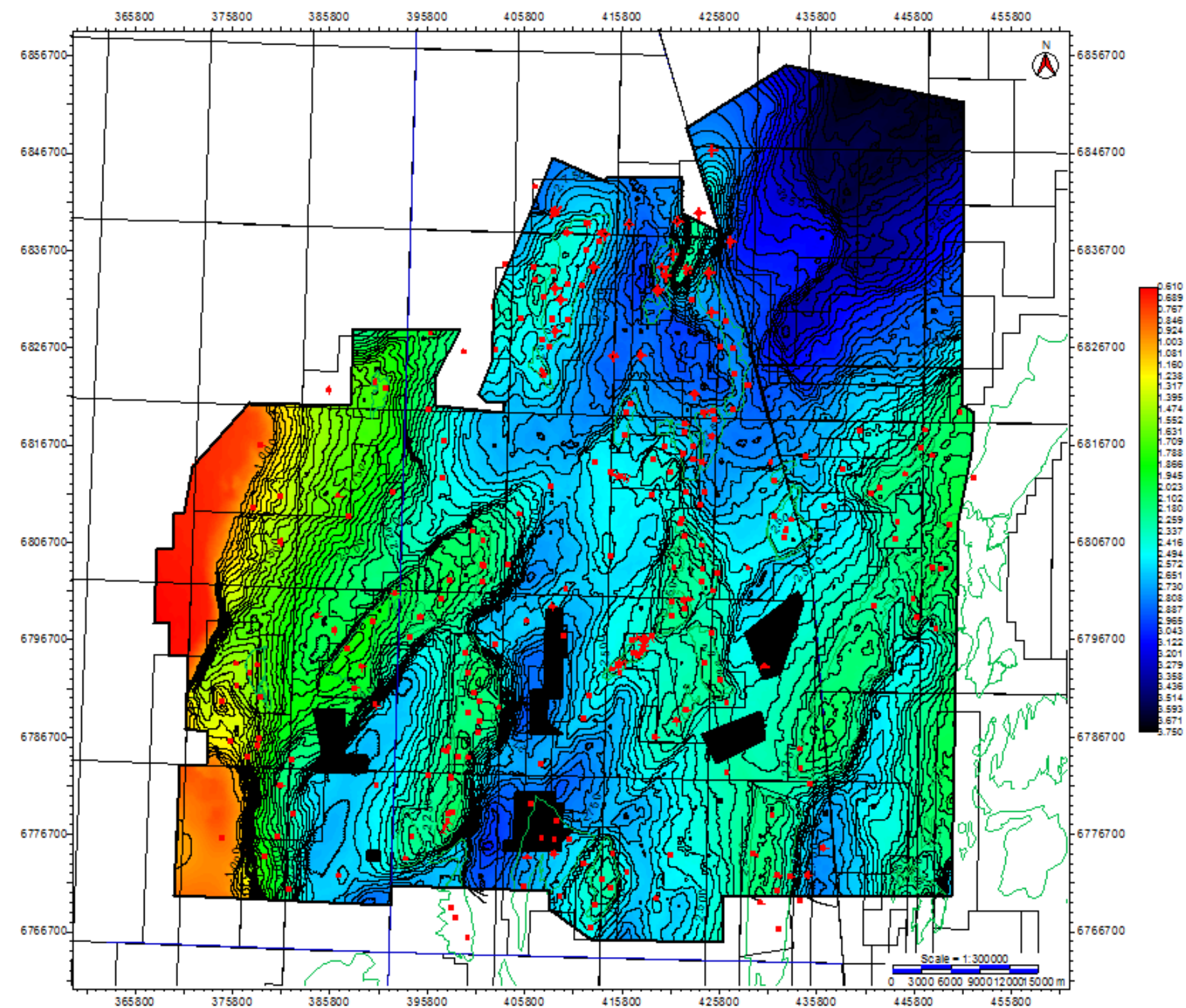
Top Dunlin Group Structure Map



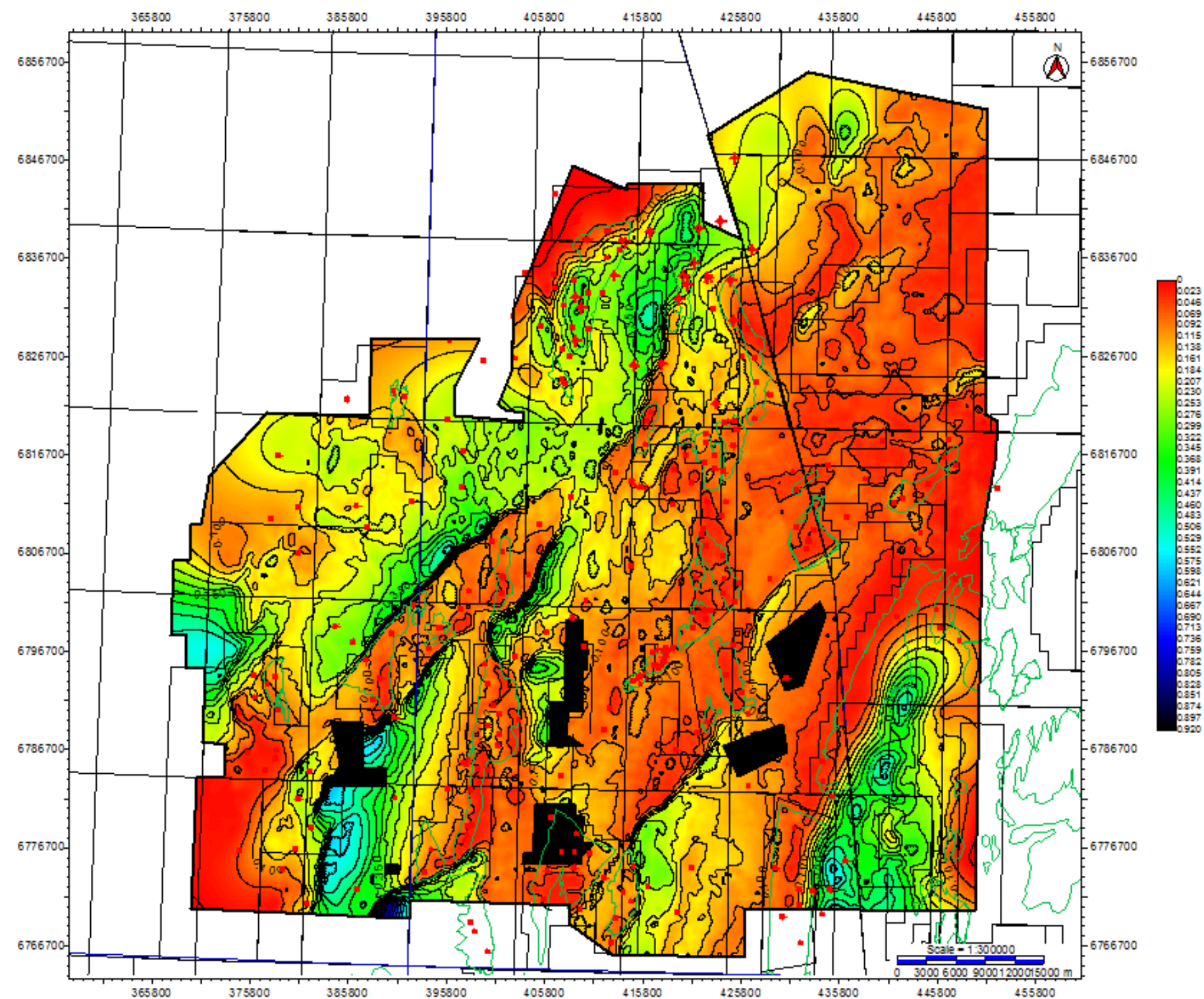
Base Syn-Rift 1 Structure Map



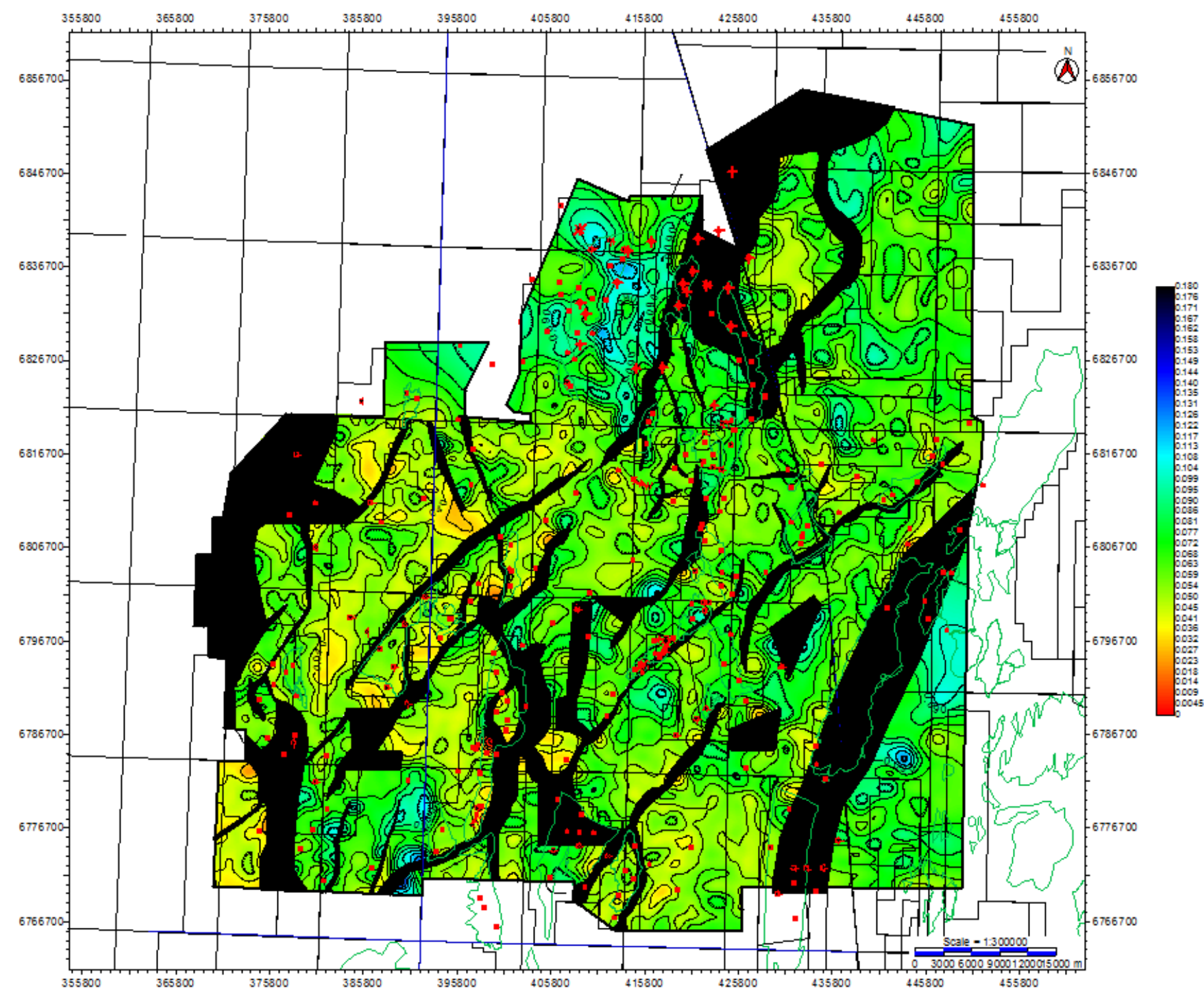
Post-Rift Package 2; Sea Bed to Base Cretaceous Unconformity Isochron



Syn-Rift Package 2; Base Cretaceous Unconformity to Top Brent Group Isochron



Intra-Rift; Top Brent Group to Top Dunlin Group Isochron



Rift Package 1; Top Dunlin Group to Base Syn-Rift 1 Isochron

